

**CONSTRUCTION AND DETAILING METHODS OF HORIZONTALLY CURVED  
STEEL I-GIRDER BRIDGES**

by

Brandon William Chavel

B.S., University of Pittsburgh, 1999

M.S., University of Pittsburgh, 2001

Submitted to the Graduate Faculty of  
Swanson School of Engineering in partial fulfillment  
of the requirements for the degree of  
Doctor of Philosophy

University of Pittsburgh

2008

UNIVERSITY OF PITTSBURGH  
SWANSON SCHOOL OF ENGINEERING

This dissertation was presented

by

Brandon William Chavel

It was defended on

March 24, 2008

and approved by

Dr. J.S. Lin, Associate Professor, Civil and Environmental Engineering

Dr. M.A.M. Torkamani, Associate Professor, Civil and Environmental Engineering

Dr. P. Rizzo, Assistant Professor, Civil and Environmental Engineering

Dr. P. Smolinski, Associate Professor, Mechanical Engineering and Materials Science

Dissertation Director: Dr. K.A. Harries, Assistant Professor, Civil and Environmental  
Engineering

Copyright © by Brandon W. Chavel

2008

# **CONSTRUCTION AND DETAILING METHODS OF HORIZONTALLY CURVED STEEL I-GIRDER BRIDGES**

Brandon W. Chavel, Ph.D.

University of Pittsburgh, 2008

The present research extends the state-of-the-art in understanding the important physical phenomena that impact the constructability and behavior of horizontally curved steel I-girder bridges. The steel erection procedure of a horizontally curved and skewed steel I-girder bridge is examined through the use of a nonlinear finite element model. The behavior of the structure is studied for each stage of steel erection by observations of girder stresses, displacements and reactions.

The eccentric application of gravity load resulting from horizontal curvature results in torsional forces being applied to the girder sections of a horizontally curved bridge. Due to the relative torsional flexibility of the steel I-girders, these forces can result in a marked girder rotation quantified in this work as web out-of-plumbness. The present research quantifies the effect and importance of girder web out-of-plumbness on primary member stress response in steel I-girders, both individually and as part of an assembly. Girder flange stresses and vertical and lateral displacements are presented for single straight and curved beam models and a curved two-girder system model all subject to up to 5 degrees of out-of-plumbness. Through a parametric study the effects of changes to radius or horizontal curvature, girder spacing, cross frame spacing, and web depth on the behavior of the curved two-girder system having initially out-of-plumb webs are investigated.

The effects of “inconsistent detailing” – an approach to designing bridge cross frames to mitigate girder web out-of-plumbness - are presented. Specifically, the structural behavior in terms of resulting “locked-in” girder flange stresses and displacements are discussed. The research work reported herein is primarily analytical in nature, employing detailed non linear finite element models to investigate the steel erection and web-plumbness issues associated with horizontally curved steel I-girder bridges.

Based on the analytical studies conducted, it is proposed that the effects of web out-of-plumbness need to be specifically considered for the effects on flange stresses in design, as an alternative to the practice of inconsistent detailing. Consideration of these effects during design and conventionally detailing girders and cross frames for the web-plumb position at no-load, in lieu of specifying inconsistent detailing to control web out-of-plumbness, will reduce construction problems that typically result from the practice of inconsistent detailing.

However, if inconsistent detailing is employed to mitigate web out-of-plumbness, it must be recognized by bridge designers that this approach has complex effects on “locked-in” stresses and constructability of curved I-girder bridges. These “locked-in” stresses and constructability issues need to be considered by bridge designers and steel erectors, respectively.

## TABLE OF CONTENTS

<b>ACKNOWLEDGEMENTS .....</b>	<b>XXVIII</b>
<b>1.0 INTRODUCTION.....</b>	<b>1</b>
<b>1.1 LITERATURE REVIEW .....</b>	<b>4</b>
<b>1.2 SCOPE OF RESEARCH .....</b>	<b>12</b>
<b>1.3 DISSERTATION ORGANIZATION .....</b>	<b>14</b>
<b>2.0 CURVED I-GIRDER BRIDGE BEHAVIOR .....</b>	<b>16</b>
<b>2.1 SINGLE CURVED I-GIRDER .....</b>	<b>17</b>
<b>2.2 CURVED I-GIRDER BRIDGE SYSTEM .....</b>	<b>18</b>
<b>2.2.1 Vertical Bending Effects.....</b>	<b>19</b>
<b>2.2.2 Lateral Flange Bending Effects .....</b>	<b>22</b>
<b>2.2.3 Displacements.....</b>	<b>26</b>
<b>2.3 NO-LOAD, STEEL AND FINAL DEAD LOAD CONDITIONS.....</b>	<b>27</b>
<b>2.4 DETAILING METHODS .....</b>	<b>28</b>
<b>2.4.1 Detail Method 1 – Girders and Cross Frames Detailed to be Web-Plumb at No-load.....</b>	<b>29</b>
<b>2.4.2 Detail Method 2 – Girders and Cross Frames Detailed to be Web-Plumb at Steel Dead Load (or Final Dead Load) Condition .....</b>	<b>31</b>
<b>2.4.3 Detail Method 3 – Inconsistent Detailing of Girders and Cross Frames</b>	<b>35</b>
<b>3.0 ERECTION STUDY S.R. 8002 RAMP A-1.....</b>	<b>36</b>
<b>3.1 SR 8002 RAMP A-1 FINITE ELEMENT MODEL .....</b>	<b>40</b>

3.1.1	Verification Study .....	40
3.1.2	SR 8002 Ramp A-1 Finite Element Model.....	44
3.2	INCONSISTENT DETAILING AND SR 8002 RAMP A-1 .....	47
3.2.1	Steel Dead Load Effects.....	48
3.2.2	Cross Frame Member Lengths .....	52
3.2.3	Consequences of Inconsistent Detailing.....	55
3.3	ANALYTICAL STUDY OF SR 8002 RAMP A-1 STEEL ERECTION.....	56
3.3.1	As-built Erection Sequence Study .....	57
3.3.2	Construction Stage 2e and 2e1.....	64
3.3.3	Construction Stage 3c.....	66
3.3.4	Construction Stage 3c1 .....	68
3.3.5	Construction Stage 3e1 .....	69
3.3.6	Construction Stage 4c1 .....	72
3.3.7	Construction Stage 5c1 .....	74
3.3.8	Construction Stage 5c2.....	75
3.3.9	Construction Stage F6c1.....	77
3.3.10	Construction Stage F6f1 .....	78
3.3.11	Summary of Analytical Study.....	80
4.0	STRUCTURAL BEHAVIOR OF OUT-OF-PLUMB CURVED I-GIRDERS ....	83
4.1	STRAIGHT I-GIRDER INVESTIGATION.....	84
4.1.1	Verification Study .....	84
4.1.2	Behavior of Straight I-Girder Rotated Out-of-Plane .....	88
4.1.3	Theoretical Calculation of Flange Stresses.....	91
4.1.4	Straight I-Girder Results Discussion .....	93
4.2	CURVED I-GIRDER INVESTIGATION.....	94

4.2.1	Verification Study .....	95
4.2.2	Behavior of Curved I-Girder Rotated Out-of-Plane .....	97
4.2.3	Single Curved I-Girder Results Discussion .....	100
4.3	<b>CURVED TWO I-GIRDER SYSTEM INVESTIGATION .....</b>	<b>101</b>
4.3.1	Base Model.....	103
4.3.2	Finite Element Modeling .....	105
4.3.2.1	Artificially induced out-of-plumbness.....	108
4.3.3	Radius Variation .....	111
4.3.3.1	Flange Stresses.....	112
4.3.3.2	Girder Displacements .....	125
4.3.3.3	Results Discussion .....	130
4.3.4	Girder Spacing Variation.....	131
4.3.4.1	Flange Stresses.....	132
4.3.4.2	Girder Displacements .....	139
4.3.4.3	Results Discussion .....	142
4.3.5	Cross Frame Spacing Variation .....	143
4.3.5.1	Flange Stresses.....	146
4.3.5.2	Girder Displacements .....	152
4.3.5.3	Results Discussion .....	155
4.3.6	Web Depth Variation.....	156
4.3.6.1	Flange Stresses.....	157
4.3.6.2	Girder Displacements .....	160
4.3.6.3	Results Discussion .....	162
5.0	<b>LOCKED-IN STRESSES DUE TO INCONSISTENT DETAILING .....</b>	<b>163</b>

<b>5.1</b>	<b>TOTAL DEAD LOAD BEHAVIOR.....</b>	<b>164</b>
<b>5.2</b>	<b>CROSS FRAME MEMBER LENGTHS.....</b>	<b>167</b>
<b>5.2.1</b>	<b>Inconsistently Detailed FEM.....</b>	<b>172</b>
<b>5.3</b>	<b>ANALYSIS RESULTS .....</b>	<b>172</b>
<b>5.3.1</b>	<b>Girder Displacements .....</b>	<b>172</b>
<b>5.3.2</b>	<b>Flange Stresses .....</b>	<b>175</b>
<b>5.3.3</b>	<b>Results Discussion .....</b>	<b>177</b>
<b>6.0</b>	<b>CONCLUSIONS .....</b>	<b>180</b>
<b>6.1</b>	<b>RECOMMENDATIONS .....</b>	<b>184</b>
<b>6.2</b>	<b>FUTURE RESEARCH NEEDS .....</b>	<b>185</b>
	<b>APPENDIX A.....</b>	<b>187</b>
	<b>APPENDIX B .....</b>	<b>189</b>
	<b>APPENDIX C.....</b>	<b>278</b>
	<b>APPENDIX D.....</b>	<b>323</b>
	<b>BIBLIOGRAPHY.....</b>	<b>327</b>

## LIST OF TABLES

Table 3-1 SR 8002 Ramp A-1 Girder Dimensions for Figure 3.5.....	39
Table 3-2 SR 8002 Ramp A-1 Girder Dimensions for Figure 3.5.....	40
Table 3-3 Differences in Diagonal Member Lengths at Cross Frame Line 6.....	54
Table 3-4 As-built Analytical Erection Sequence Naming Convention.....	59
Table 3-5 Reactions – Construction Stage 1 to Stage 2e1 .....	66
Table 3-6 Reactions – Construction Stage 3 to Stage 3e1 .....	72
Table 3-7 Reactions – Construction Stage 4c1 .....	74
Table 3-8 Reactions – Construction Stage 5c2.....	77
Table 3-9 Reactions – Construction Stage 5c2.....	80
Table 4-1 Straight I-Girder Ultimate Load Summary.....	91
Table 4-2 Maximum Top Flange Compressive Stress due to Concentrated Load of 50 kips .....	91
Table 4-3 Top Flange Compressive Stress Comparison.....	92
Table 4-4 Bottom Flange Tensile Stress Comparison .....	93
Table 4-5 Curved I-Girder Ultimate Load Summary .....	100
Table 4-6 Maximum Bottom Flange Stress due to Concentrated Load of 20 kips.....	100
Table 4-7 Girder Cross-Sections for Base Model.....	104
Table 4-8 G2 Maximum Bottom Flange Tip Stress at 0.5L Center Span.....	115

Table 4-9 G2 Maximum Inner-Edge Top Flange Tip Stress near 0.5L Center Span .....	118
Table 4-10 G2 Maximum Outer-Edge Top Flange Tip Stress at 0.0L Center Span .....	121
Table 4-11 G2 Maximum Inner-Edge Bottom Flange Tip Stress at 0.0L Center Span.....	124
Table 4-12 G2 Top Flange Vertical Displacement at 0.5L Center Span .....	126
Table 4-13 G2 Flange Lateral Displacements at 0.5L Center Span .....	128
Table 4-14 G2 Out-of-Plane Rotation at 0.5L Center Span.....	128
Table 4-15 G2 Maximum Outer-Edge Bottom Flange Tip Stress at 0.5L Center Span.....	133
Table 4-16 G2 Maximum Inner-Edge Top Flange Tip Stress near 0.5L Center Span .....	135
Table 4-17 G1 Maximum Outer-Edge Bottom Flange Tip Stress at 0.5L Center Span.....	137
Table 4-18 G2 Out-of-Plane Rotation at 0.5L Center Span.....	141
Table 4-19 Cross Frame Spacing Variation.....	144
Table 4-20 G2 Maximum Outer-Edge Bottom Flange Tip Stress near 0.5L Center Span.....	147
Table 4-21 G2 Out-of-Plane Rotation at 0.5L Center Span.....	154
Table 4-22 Girder Section Properties .....	157
Table 4-23 G2 Maximum Outer-Edge Bottom Flange Tip Stress at 0.5L Center Span.....	158
Table 4-24 G2 Inner-Edge Top Flange Tip Stress at 0.5L Center Span.....	160
Table 4-25 G2 Vertical Displacement at 0.5L Center Span .....	161
Table 4-26 G2 Out-of-Plane Rotation at 0.5L Center Span.....	162
Table 5-1 Cross Frame Diagonal Member Lengths for Web-Plumb at Total Dead Load.....	171
Table B-1 As-Built Erection Sequence Naming Convention .....	190
Table B-2 Intended Erection Sequence Naming Convention .....	263

## LIST OF FIGURES

Figure 1.1 Ford City Veteran’s Bridge Steel Superstructure (Chavel 2001).....	9
Figure 2.1 Single Curved Girder (Coletti and Yadlosky 2005).....	17
Figure 2.2 Shear Stresses Which Can Occur in a Curved I-Girder (Coletti and Yadlosky 2005)	18
Figure 2.3 Longitudinal Flange Stress Components (Hall et al. 1999) .....	20
Figure 2.4 Plan View of a Curved Girder Bridge .....	22
Figure 2.5 Lateral Flange Bending Diagram (Hall et al. 1999).....	23
Figure 2.6 Radial Flange Force Component (Poellet 1987).....	24
Figure 2.7 Radial Distributed Flange Force (Poellet 1987).....	24
Figure 2.8 Hoop Tension Analogy (Poellet 1987).....	25
Figure 2.9 Girder Rotation Due to a Given Loading .....	26
Figure 2.10 Girders and Cross Frames Detailed for Method #1.....	30
Figure 2.11 Displaced Position (Steel Dead Load) of Cross-Section Detail Method #1.....	31
Figure 2.12 Girders Rotated to Web-Plumb - New Cross Frame Member Lengths Determined.	33
Figure 2.13 Starting Points of Bridge Erection for Methods #1 and #2 .....	34
Figure 3.1 SR 8002 Ramp A-1 Design Drawing Framing Plan .....	36
Figure 3.2 SR 8002 Ramp A-1 Naming Convention.....	37
Figure 3.3 SR 8002 Ramp A-1 Type I Cross frame .....	38

Figure 3.4 SR 8002 Ramp A-1 Type II Cross frame .....	38
Figure 3.5 SR 8002 Ramp A-1 Girder Elevation.....	39
Figure 3.6 CSBRP Experimental Bridge (Linzell 1999) .....	41
Figure 3.7 CSBRP ES1-4 Experimental Results (Linzell 1999) and Analytical Results .....	43
Figure 3.8 SR 8002 Ramp A-1 FEM .....	45
Figure 3.9 SR 8002 Ramp A-1 FEM Mesh Density.....	46
Figure 3.10 MPC LINEAR constraint ( <i>ABAQUS</i> 2001) .....	46
Figure 3.11 Direction of Positive Out-of-Plane Rotation .....	49
Figure 3.12 Ramp A-1 FEM Out-of-Plane Rotation due to Steel Dead Load.....	50
Figure 3.13 Ramp A-1 FEM Out-of-Plane Displacement due to Steel Dead Load.....	51
Figure 3.14 Ramp A-1 FEM Vertical Displacement due to Steel Dead Load.....	51
Figure 3.15 Comparison of Diagonal Cross Frame Members for Different Detailing Methods..	52
Figure 3.16 Cross Frame Line A – Difference in Diagonal Member Lengths due to Detailing ..	54
Figure 3.17 Construction Stage 2e1 .....	65
Figure 3.18 Construction Stage 3c.....	67
Figure 3.19 Construction Stage 3c1 .....	69
Figure 3.20 View of Construction Stage 3c1 .....	69
Figure 3.21 Construction Stage 3e1 .....	71
Figure 3.22 Construction Stage 3e1 – von Mises Stresses .....	71
Figure 3.23 Construction Stage 4c1 .....	73
Figure 3.24 Construction Stage 5c1 .....	75
Figure 3.25 Construction Stage 5c2.....	76
Figure 3.26 Construction Stage 5c2 – von Mises Stresses .....	77

Figure 3.27 Construction Stage F6c1 .....	78
Figure 3.28 Construction Stage F6f1 .....	79
Figure 4.1 “S” Specimen Cross-Section (Morcos 1988) .....	85
Figure 4.2 “S” Specimen Elevation View (Morcos 1988).....	85
Figure 4.3 Straight Girder FEM Verification – Load-Deflection Response.....	87
Figure 4.4 Straight Girder FEM Verification – Modal Manifestations in Plan View .....	87
Figure 4.5 Straight Girder FEM Verification – Modal Manifestations in Elevation View .....	88
Figure 4.6 Straight Girder Out-of-Plane Rotations.....	89
Figure 4.7 Straight Girder Load-Deflection Response .....	90
Figure 4.8 CB1 Beam Plan View.....	95
Figure 4.9 Curved I-Girder FEM Verification.....	97
Figure 4.10 Curved I-Girder Load-Vertical Deflection Response.....	99
Figure 4.11 Curved I-Girder Load-Lateral Deflection Response .....	99
Figure 4.12 Chelyan Bridge Approach Ramp – Plan View.....	102
Figure 4.13 Curved Two-Girder System in Plan View (Base Model).....	103
Figure 4.14 Curved Two-Girder System Finite Element Model .....	106
Figure 4.15 Local Coordinate System for Support Locations .....	107
Figure 4.16 Base Model Steel Dead Load Analysis .....	109
Figure 4.17 Base Model – 5 Deg. Web Out-of-Plumb – Artificial Top Flange Displacement ..	110
Figure 4.18 Monitored Flange Stress Locations (Plan View).....	112
Figure 4.19 Flange Tip Stress Locations .....	113
Figure 4.20 G2 Bottom Flange Tip Stresses at 0.5L Center Span (R=509.3 ft).....	113
Figure 4.21 G2 Maximum Bottom Flange Tip Stresses at 0.5L Center Span .....	116

Figure 4.22 G2 Inner-Edge Top Flange Stresses at 0.5L Center Span (R=509.3 ft) .....	117
Figure 4.23 G2 Maximum Top Flange Tip Stresses at 0.5L Center Span .....	119
Figure 4.24 G2 Top Flange Outer-Edge Stresses at 0.0L Center Span (R=509.3 ft) .....	120
Figure 4.25 G2 Maximum Outer-Edge Top Flange Tip Stresses at 0.0L Center Span .....	122
Figure 4.26 G2 Bottom Flange Inner-Edge Stresses at 0.0L Center Span (R=509.3 ft) .....	123
Figure 4.27 G2 Maximum Inner-Edge Bottom Flange Tip Stresses at 0.0L Center Span .....	124
Figure 4.28 Girder Vertical Displacements (R=509.3 ft) .....	126
Figure 4.29 G2 Top Flange Lateral Displacement.....	129
Figure 4.30 G2 Outer-Edge Bottom Flange Tip Stresses at 0.5L Center Span .....	134
Figure 4.31 G2 Inner-Edge Top Flange Tip Stresses Near 0.5L Center Span.....	136
Figure 4.32 G1 Outer-Edge Bottom Flange Tip Stresses at 0.5L Center Span .....	138
Figure 4.33 Girder G1 Vertical Displacements at 0.5L Center Span .....	140
Figure 4.34 Girder G2 Vertical Displacements at 0.5L Center Span .....	140
Figure 4.35 G2 Top Flange Lateral Displacement.....	142
Figure 4.36 Cross Frame Spacing Arrangements .....	145
Figure 4.37 G2 Outer-Edge Bottom Flange Tip Stresses at 0.5L Center Span .....	148
Figure 4.38 G2 Bottom Flange Tip Stresses at 0.5L Center Span.....	149
Figure 4.39 G2 Inner-Edge Top Flange Tip Stresses at 0.5L Center Span .....	151
Figure 4.40 G2 Top Flange Tip Stresses at 0.5L Center Span .....	152
Figure 4.41 Girder G2 Vertical Displacements at 0.5L Center Span .....	153
Figure 4.42 Girder G2 Top Flange Lateral Displacements.....	155
Figure 4.43 G2 Bottom Flange Maximum Tip Stresses at 0.5L Center Span .....	159
Figure 5.1 Base Model Total Dead Load Vertical Displacement.....	165

Figure 5.2 Total Dead Load Displaced Position.....	166
Figure 5.3 G2 Lateral Displacement and Rotation due to Total Dead Load .....	167
Figure 5.4 Cross Frames Detailed for Web-Plumb at Total Dead Load.....	168
Figure 5.5 Cross Frames Detailed for Web-Plumb at Total Dead Load.....	169
Figure 5.6 Cross Frame Diagonal Member Misalignment .....	170
Figure 5.7 G2 Lateral Displacement and Rotation Comparison.....	173
Figure 5.8 Vertical Displacement Comparison.....	174
Figure 5.9 Outer-Edge Bottom Flange Tip Stresses at Mid-span of Center Span .....	175
Figure 5.10 Bottom Flange Tip Stresses at Mid-span of Center Span.....	176
Figure 5.11 Inner-Edge Top Flange Tip Stresses at Mid-span of Center Span .....	177
Figure B.1 Construction Stage 1 – Girder Vertical Displacement.....	191
Figure B.2 Construction Stage 1 – Girder Lateral Displacement .....	191
Figure B.3 Construction Stage 1 – Girder Out-of-Plane Rotation.....	192
Figure B.4 Construction Stage 2 – Girder Vertical Displacement.....	192
Figure B.5 Construction Stage 2 – Girder Lateral Displacement .....	193
Figure B.6 Construction Stage 2 – Girder Out-of-Plane Rotation.....	193
Figure B.7 Construction Stage 2a – Girder Vertical Displacement.....	194
Figure B.8 Construction Stage 2a – Girder Lateral Displacement .....	194
Figure B.9 Construction Stage 2a – Girder Out-of-Plane Rotation .....	195
Figure B.10 Construction Stage 2b – Girder Vertical Displacement.....	195
Figure B.11 Construction Stage 2b – Girder Lateral Displacement .....	196
Figure B.12 Construction Stage 2b – Girder Out-of-Plane Rotation.....	196
Figure B.13 Construction Stage 2c – Girder Vertical Displacement.....	197

Figure B.14 Construction Stage 2c – Girder Lateral Displacement .....	197
Figure B.15 Construction Stage 2c – Girder Out-of-Plane Rotation .....	198
Figure B.16 Construction Stage 2d – Girder Vertical Displacement.....	198
Figure B.17 Construction Stage 2d – Girder Lateral Displacement .....	199
Figure B.18 Construction Stage 2d – Girder Out-of-Plane Rotation.....	199
Figure B.19 Construction Stage 2e – Girder Vertical Displacement.....	200
Figure B.20 Construction Stage 2e – Girder Lateral Displacement .....	200
Figure B.21 Construction Stage 2e – Girder Out-of-Plane Rotation .....	201
Figure B.22 Construction Stage 2e1 – Girder Vertical Displacement.....	201
Figure B.23 Construction Stage 2e1 – Girder Lateral Displacement .....	202
Figure B.24 Construction Stage 2e1 – Girder Out-of-Plane Rotation .....	202
Figure B.25 Construction Stage 3 – Girder Vertical Displacement.....	203
Figure B.26 Construction Stage 3 – Girder Lateral Displacement .....	203
Figure B.27 Construction Stage 3 – Girder Out-of-Plane Rotation.....	204
Figure B.28 Construction Stage 3a – Girder Vertical Displacement.....	204
Figure B.29 Construction Stage 3a – Girder Lateral Displacement .....	205
Figure B.30 Construction Stage 3a – Girder Out-of-Plane Rotation .....	205
Figure B.31 Construction Stage 3b – Girder Vertical Displacement.....	206
Figure B.32 Construction Stage 3b – Girder Lateral Displacement .....	206
Figure B.33 Construction Stage 3b – Girder Out-of-Plane Rotation.....	207
Figure B.34 Construction Stage 3c – Girder Vertical Displacement.....	207
Figure B.35 Construction Stage 3c – Girder Lateral Displacement .....	208
Figure B.36 Construction Stage 3c – Girder Out-of-Plane Rotation .....	208

Figure B.37 Construction Stage 3c1 – Girder Vertical Displacement.....	209
Figure B.38 Construction Stage 3c1 – Girder Lateral Displacement .....	209
Figure B.39 Construction Stage 3c1 – Girder Out-of-Plane Rotation.....	210
Figure B.40 Construction Stage 3d – Girder Vertical Displacement.....	210
Figure B.41 Construction Stage 3d – Girder Lateral Displacement .....	211
Figure B.42 Construction Stage 3d – Girder Out-of-Plane Rotation.....	211
Figure B.43 Construction Stage 3d1 – Girder Vertical Displacement.....	212
Figure B.44 Construction Stage 3d1 – Girder Lateral Displacement .....	212
Figure B.45 Construction Stage 3d1 – Girder Out-of-Plane Rotation.....	213
Figure B.46 Construction Stage 3e – Girder Vertical Displacement.....	213
Figure B.47 Construction Stage 3e – Girder Lateral Displacement .....	214
Figure B.48 Construction Stage 3e – Girder Out-of-Plane Rotation .....	214
Figure B.49 Construction Stage 3e1 – Girder Vertical Displacement.....	215
Figure B.50 Construction Stage 3e1 – Girder Lateral Displacement .....	215
Figure B.51 Construction Stage 3e1 – Girder Out-of-Plane Rotation.....	216
Figure B.52 Construction Stage 4 – Girder Vertical Displacement.....	216
Figure B.53 Construction Stage 4 – Girder Lateral Displacement .....	217
Figure B.54 Construction Stage 4 – Girder Out-of-Plane Rotation.....	217
Figure B.55 Construction Stage 4a – Girder Vertical Displacement.....	218
Figure B.56 Construction Stage 4a – Girder Lateral Displacement .....	218
Figure B.57 Construction Stage 4a – Girder Out-of-Plane Rotation .....	219
Figure B.58 Construction Stage 4b – Girder Vertical Displacement.....	219
Figure B.59 Construction Stage 4b – Girder Lateral Displacement .....	220

Figure B.60 Construction Stage 4b – Girder Out-of-Plane Rotation.....	220
Figure B.61 Construction Stage 4c – Girder Vertical Displacement.....	221
Figure B.62 Construction Stage 4c – Girder Lateral Displacement .....	221
Figure B.63 Construction Stage 4c – Girder Out-of-Plane Rotation .....	222
Figure B.64 Construction Stage 4c1 – Girder Vertical Displacement.....	222
Figure B.65 Construction Stage 4c1 – Girder Lateral Displacement .....	223
Figure B.66 Construction Stage 4c1 – Girder Out-of-Plane Rotation .....	223
Figure B.67 Construction Stage 4d – Girder Vertical Displacement.....	224
Figure B.68 Construction Stage 4d – Girder Lateral Displacement .....	224
Figure B.69 Construction Stage 4d – Girder Out-of-Plane Rotation.....	225
Figure B.70 Construction Stage 4d1 – Girder Vertical Displacement.....	225
Figure B.71 Construction Stage 4d1 – Girder Lateral Displacement .....	226
Figure B.72 Construction Stage 4d1 – Girder Out-of-Plane Rotation.....	226
Figure B.73 Construction Stage 4e – Girder Vertical Displacement.....	227
Figure B.74 Construction Stage 4e – Girder Lateral Displacement .....	227
Figure B.75 Construction Stage 4e – Girder Out-of-Plane Rotation .....	228
Figure B.76 Construction Stage 4e1 – Girder Vertical Displacement.....	228
Figure B.77 Construction Stage 4e1 – Girder Lateral Displacement .....	229
Figure B.78 Construction Stage 4e1 – Girder Out-of-Plane Rotation .....	229
Figure B.79 Construction Stage 4f – Girder Vertical Displacement .....	230
Figure B.80 Construction Stage 4f – Girder Lateral Displacement.....	230
Figure B.81 Construction Stage 4e1 – Girder Out-of-Plane Rotation .....	231
Figure B.82 Construction Stage 4f1 – Girder Vertical Displacement .....	231

Figure B.83 Construction Stage 4f1 – Girder Lateral Displacement.....	232
Figure B.84 Construction Stage 4f1 – Girder Out-of-Plane Rotation .....	232
Figure B.85 Construction Stage 5a – Girder Vertical Displacement.....	233
Figure B.86 Construction Stage 5a – Girder Lateral Displacement .....	233
Figure B.87 Construction Stage 5a – Girder Out-of-Plane Rotation .....	234
Figure B.88 Construction Stage 5b – Girder Vertical Displacement.....	234
Figure B.89 Construction Stage 5b – Girder Lateral Displacement .....	235
Figure B.90 Construction Stage 5b – Girder Out-of-Plane Rotation.....	235
Figure B.91 Construction Stage 5c – Girder Vertical Displacement.....	236
Figure B.92 Construction Stage 5c – Girder Lateral Displacement .....	236
Figure B.93 Construction Stage 5c – Girder Out-of-Plane Rotation .....	237
Figure B.94 Construction Stage 5c1 – Girder Vertical Displacement.....	237
Figure B.95 Construction Stage 5c1 – Girder Lateral Displacement .....	238
Figure B.96 Construction Stage 5c1 – Girder Out-of-Plane Rotation .....	238
Figure B.97 Construction Stage 5c2 – Girder Vertical Displacement.....	239
Figure B.98 Construction Stage 5c2 – Girder Lateral Displacement .....	239
Figure B.99 Construction Stage 5c2 – Girder Out-of-Plane Rotation .....	240
Figure B.100 Construction Stage 5d – Girder Vertical Displacement.....	240
Figure B.101 Construction Stage 5d – Girder Lateral Displacement.....	241
Figure B.102 Construction Stage 5d – Girder Out-of-Plane Rotation.....	241
Figure B.103 Construction Stage 5d1 – Girder Vertical Displacement.....	242
Figure B.104 Construction Stage 5d1 – Girder Lateral Displacement .....	242
Figure B.105 Construction Stage 5d1 – Girder Out-of-Plane Rotation.....	243

Figure B.106 Construction Stage 5d2 – Girder Vertical Displacement.....	243
Figure B.107 Construction Stage 5d2 – Girder Lateral Displacement .....	244
Figure B.108 Construction Stage 5d2 – Girder Out-of-Plane Rotation.....	244
Figure B.109 Construction Stage F6a – Girder Vertical Displacement.....	245
Figure B.110 Construction Stage F6a – Girder Lateral Displacement .....	245
Figure B.111 Construction Stage F6a – Girder Out-of-Plane Rotation.....	246
Figure B.112 Construction Stage F6b – Girder Vertical Displacement .....	246
Figure B.113 Construction Stage F6b – Girder Lateral Displacement.....	247
Figure B.114 Construction Stage F6b – Girder Out-of-Plane Rotation.....	247
Figure B.115 Construction Stage F6c – Girder Vertical Displacement.....	248
Figure B.116 Construction Stage F6c – Girder Lateral Displacement .....	248
Figure B.117 Construction Stage F6c – Girder Out-of-Plane Rotation.....	249
Figure B.118 Construction Stage F6c1 – Girder Vertical Displacement.....	249
Figure B.119 Construction Stage F6c1 – Girder Lateral Displacement .....	250
Figure B.120 Construction Stage F6c1 – Girder Out-of-Plane Rotation.....	250
Figure B.121 Construction Stage F6d – Girder Vertical Displacement .....	251
Figure B.122 Construction Stage F6d – Girder Lateral Displacement.....	251
Figure B.123 Construction Stage F6d – Girder Out-of-Plane Rotation.....	252
Figure B.124 Construction Stage F6d1 – Girder Vertical Displacement .....	252
Figure B.125 Construction Stage F6d1 – Girder Lateral Displacement.....	253
Figure B.126 Construction Stage F6d1 – Girder Out-of-Plane Rotation.....	253
Figure B.127 Construction Stage F6e – Girder Vertical Displacement.....	254
Figure B.128 Construction Stage F6e – Girder Lateral Displacement .....	254

Figure B.129 Construction Stage F6e – Girder Out-of-Plane Rotation.....	255
Figure B.130 Construction Stage F6e1 – Girder Vertical Displacement.....	255
Figure B.131 Construction Stage F6e1 – Girder Lateral Displacement.....	256
Figure B.132 Construction Stage F6e1 – Girder Out-of-Plane Rotation.....	256
Figure B.133 Construction Stage F6f – Girder Vertical Displacement.....	257
Figure B.134 Construction Stage F6f – Girder Lateral Displacement.....	257
Figure B.135 Construction Stage F6f – Girder Out-of-Plane Rotation.....	258
Figure B.136 Construction Stage F6f1 – Girder Vertical Displacement.....	258
Figure B.137 Construction Stage F6f1 – Girder Lateral Displacement.....	259
Figure B.138 Construction Stage F6f1 – Girder Out-of-Plane Rotation.....	259
Figure B.139 Construction Stage 6d2 – Girder Vertical Displacement.....	260
Figure B.140 Construction Stage 6d2 – Girder Lateral Displacement.....	260
Figure B.141 Construction Stage 6d2 – Girder Out-of-Plane Rotation.....	261
Figure B.142 Construction Stage 6e2 (Final) – Girder Vertical Displacement.....	261
Figure B.143 Construction Stage 6e2 (Final) – Girder Lateral Displacement.....	262
Figure B.144 Construction Stage 6e2 (Final) – Girder Out-of-Plane Rotation.....	262
Figure B.145 Construction Stage 5e2 – Girder Vertical Displacement.....	264
Figure B.146 Construction Stage 5e2 – Girder Lateral Displacement.....	264
Figure B.147 Construction Stage 5e2 – Girder Out-of-Plane Rotation.....	265
Figure B.148 Construction Stage 5f2 – Girder Vertical Displacement.....	265
Figure B.149 Construction Stage 5f2 – Girder Lateral Displacement.....	266
Figure B.150 Construction Stage 5f2 – Girder Out-of-Plane Rotation.....	266
Figure B.151 Construction Stage 6a2 – Girder Vertical Displacement.....	267

Figure B.152 Construction Stage 6a2 – Girder Lateral Displacement .....	267
Figure B.153 Construction Stage 6a2 – Girder Out-of-Plane Rotation .....	268
Figure B.154 Construction Stage 6b2 – Girder Vertical Displacement.....	268
Figure B.155 Construction Stage 6b2 – Girder Lateral Displacement .....	269
Figure B.156 Construction Stage 6b2 – Girder Out-of-Plane Rotation.....	269
Figure B.157 Construction Stage 6c2 – Girder Vertical Displacement.....	270
Figure B.158 Construction Stage 6c2 – Girder Lateral Displacement .....	270
Figure B.159 Construction Stage 6c2 – Girder Out-of-Plane Rotation .....	271
Figure B.160 Construction Stage 6c3 – Girder Vertical Displacement.....	271
Figure B.161 Construction Stage 6c3 – Girder Lateral Displacement .....	272
Figure B.162 Construction Stage 6c3 – Girder Out-of-Plane Rotation .....	272
Figure B.163 Construction Stage 6d2 – Girder Vertical Displacement.....	273
Figure B.164 Construction Stage 6d2 – Girder Lateral Displacement .....	273
Figure B.165 Construction Stage 6d2 – Girder Out-of-Plane Rotation.....	274
Figure B.166 Construction Stage 6d3 – Girder Vertical Displacement.....	274
Figure B.167 Construction Stage 6d3 – Girder Lateral Displacement .....	275
Figure B.168 Construction Stage 6d3 – Girder Out-of-Plane Rotation.....	275
Figure B.169 Construction Stage 6e3 (Final) – Girder Vertical Displacement.....	276
Figure B.170 Construction Stage 6e3 (Final) – Girder Lateral Displacement .....	276
Figure B.171 Construction Stage 6e3 (Final) – Girder Out-of-Plane Rotation .....	277
Figure C.1 Outer-Edge Bottom Flange Tip Stresses at 0.5L of Center Span .....	279
Figure C.2 Inner-Edge Top Flange Tip Stresses at 0.5L of Center Span .....	279
Figure C.3 G2 Flange Tip Stresses at 0.4L of End Span .....	280

Figure C.4 Inner-Edge Bottom Flange Tip Stresses at 0.0L of Center Span.....	280
Figure C.5 Outer-Edge Top Flange Tip Stresses at 0.0L of Center Span.....	280
Figure C.6 Top Flange Vertical Displacement .....	281
Figure C.7 G2 Flange Lateral Displacement .....	281
Figure C.8 Outer-Edge Bottom Flange Tip Stresses at 0.5L of Center Span.....	282
Figure C.9 Inner-Edge Top Flange Tip Stresses at 0.5L of Center Span .....	282
Figure C.10 G2 Flange Tip Stresses at 0.4L of End Span .....	283
Figure C.11 Inner-Edge Bottom Flange Tip Stresses at 0.0L of Center Span.....	283
Figure C.12 Outer-Edge Top Flange Tip Stresses at 0.0L of Center Span.....	283
Figure C.13 Top Flange Vertical Displacement .....	284
Figure C.14 G2 Flange Lateral Displacement .....	284
Figure C.15 Outer-Edge Bottom Flange Tip Stresses at 0.5L of Center Span.....	285
Figure C.16 Inner-Edge Top Flange Tip Stresses at 0.5L of Center Span .....	285
Figure C.17 G2 Flange Tip Stresses at 0.4L of End Span .....	286
Figure C.18 Inner-Edge Bottom Flange Tip Stresses at 0.0L of Center Span.....	286
Figure C.19 Outer-Edge Top Flange Tip Stresses at 0.0L of Center Span.....	286
Figure C.20 Top Flange Vertical Displacement .....	287
Figure C.21 G2 Flange Lateral Displacement .....	287
Figure C.22 Outer-Edge Bottom Flange Tip Stresses at 0.5L of Center Span.....	288
Figure C.23 Inner-Edge Top Flange Tip Stresses at 0.5L of Center Span .....	288
Figure C.24 G2 Flange Tip Stresses at 0.4L of End Span .....	289
Figure C.25 Inner-Edge Bottom Flange Tip Stresses at 0.0L of Center Span.....	289
Figure C.26 Outer-Edge Top Flange Tip Stresses at 0.0L of Center Span.....	289

Figure C.27 Top Flange Vertical Displacement .....	290
Figure C.28 G2 Flange Lateral Displacement .....	290
Figure C.29 Outer-Edge Bottom Flange Tip Stresses at 0.5L of Center Span .....	291
Figure C.30 Inner-Edge Top Flange Tip Stresses at 0.5L of Center Span .....	291
Figure C.31 G2 Flange Tip Stresses at 0.4L of End Span .....	292
Figure C.32 Inner-Edge Bottom Flange Tip Stresses at 0.0L of Center Span.....	292
Figure C.33 Outer-Edge Top Flange Tip Stresses at 0.0L of Center Span.....	292
Figure C.34 Top Flange Vertical Displacement .....	293
Figure C.35 G2 Flange Lateral Displacement .....	293
Figure C.36 Outer-Edge Bottom Flange Tip Stresses at 0.5L of Center Span .....	294
Figure C.37 Inner-Edge Top Flange Tip Stresses at 0.5L of Center Span .....	294
Figure C.38 G2 Flange Tip Stresses at 0.4L of End Span .....	295
Figure C.39 Inner-Edge Bottom Flange Tip Stresses at 0.0L of Center Span.....	295
Figure C.40 Outer-Edge Top Flange Tip Stresses at 0.0L of Center Span.....	295
Figure C.41 Top Flange Vertical Displacement .....	296
Figure C.42 G2 Flange Lateral Displacement .....	296
Figure C.43 Outer-Edge Bottom Flange Tip Stresses at 0.5L of Center Span .....	298
Figure C.44 Inner-Edge Top Flange Tip Stresses at 0.5L of Center Span .....	298
Figure C.45 G2 Flange Tip Stresses at 0.4L of End Span .....	299
Figure C.46 Inner-Edge Bottom Flange Tip Stresses at 0.0L of Center Span.....	299
Figure C.47 Outer-Edge Top Flange Tip Stresses at 0.0L of Center Span.....	299
Figure C.48 Top Flange Vertical Displacement .....	300
Figure C.49 G2 Flange Lateral Displacement .....	300

Figure C.50 Outer-Edge Bottom Flange Tip Stresses at 0.5L of Center Span .....	301
Figure C.51 Inner-Edge Top Flange Tip Stresses at 0.5L of Center Span .....	301
Figure C.52 G2 Flange Tip Stresses at 0.4L of End Span .....	302
Figure C.53 Inner-Edge Bottom Flange Tip Stresses at 0.0L of Center Span.....	302
Figure C.54 Outer-Edge Top Flange Tip Stresses at 0.0L of Center Span.....	302
Figure C.55 Top Flange Vertical Displacement .....	303
Figure C.56 G2 Flange Lateral Displacement .....	303
Figure C.57 Outer-Edge Bottom Flange Tip Stresses at 0.5L of Center Span .....	304
Figure C.58 Inner-Edge Top Flange Tip Stresses at 0.5L of Center Span .....	304
Figure C.59 Top Flange Vertical Displacement .....	305
Figure C.60 G2 Flange Lateral Displacement .....	305
Figure C.61 Outer-Edge Bottom Flange Tip Stresses at 0.5L of Center Span .....	306
Figure C.62 Inner-Edge Top Flange Tip Stresses at 0.5L of Center Span .....	306
Figure C.63 Top Flange Vertical Displacement .....	307
Figure C.64 G2 Flange Lateral Displacement .....	307
Figure C.65 Outer-Edge Bottom Flange Tip Stresses at 0.5L of Center Span .....	309
Figure C.66 Inner-Edge Top Flange Tip Stresses at 0.5L of Center Span .....	309
Figure C.67 Top Flange Vertical Displacement .....	310
Figure C.68 G2 Flange Lateral Displacement .....	310
Figure C.69 Outer-Edge Bottom Flange Tip Stresses at 0.5L of Center Span .....	311
Figure C.70 Inner-Edge Top Flange Tip Stresses at 0.5L of Center Span .....	311
Figure C.71 Top Flange Vertical Displacement .....	312
Figure C.72 G2 Flange Lateral Displacement .....	312

Figure C.73 Outer-Edge Bottom Flange Tip Stresses at 0.5L of Center Span .....	313
Figure C.74 Inner-Edge Top Flange Tip Stresses at 0.5L of Center Span .....	313
Figure C.75 G2 Flange Tip Stresses at 0.4L of End Span .....	314
Figure C.76 Inner-Edge Bottom Flange Tip Stresses at 0.0L of Center Span.....	314
Figure C.77 Outer-Edge Top Flange Tip Stresses at 0.0L of Center Span.....	314
Figure C.78 Top Flange Vertical Displacement .....	315
Figure C.79 G2 Flange Lateral Displacement .....	315
Figure C.80 Outer-Edge Bottom Flange Tip Stresses at 0.5L of Center Span .....	317
Figure C.81 Inner-Edge Top Flange Tip Stresses at 0.5L of Center Span .....	317
Figure C.82 G2 Flange Tip Stresses at 0.4L of End Span .....	318
Figure C.83 Inner-Edge Bottom Flange Tip Stresses at 0.0L of Center Span.....	318
Figure C.84 Outer-Edge Top Flange Tip Stresses at 0.0L of Center Span.....	318
Figure C.85 Top Flange Vertical Displacement .....	319
Figure C.86 G2 Flange Lateral Displacement .....	319
Figure C.87 Outer-Edge Bottom Flange Tip Stresses at 0.5L of Center Span .....	320
Figure C.88 Inner-Edge Top Flange Tip Stresses at 0.5L of Center Span .....	320
Figure C.89 G2 Flange Tip Stresses at 0.4L of End Span .....	321
Figure C.90 Inner-Edge Bottom Flange Tip Stresses at 0.0L of Center Span.....	321
Figure C.91 Outer-Edge Top Flange Tip Stresses at 0.0L of Center Span.....	321
Figure C.92 Top Flange Vertical Displacement .....	322
Figure C.93 G2 Flange Lateral Displacement .....	322
Figure D.1 S4R Shell Element: 4-Nodes, Reduced Integration (ABAQUS 2003) .....	324
Figure D.2 General MITC-4 Shell Element (ADINA 2003) .....	325

## ACKNOWLEDGEMENTS

The author would like to thank his advisor, Dr. Kent Harries for his support and guidance during the completion of his graduate studies, and this dissertation. The author would also like to thank his previous advisor, Dr. Christopher Earls for his support during the early stages of this research, and throughout his graduate career. The author is also very appreciative of the support and assistance provided by his Ph.D. committee members, Dr. J.S. Lin, Dr. M.A.M. Torkamani, Dr. P. Rizzo, and Dr. P. Smolinski.

Most of all, the author would like to thank his wife, Lisa Chavel for all the love, support, and encouragement she has always given him; especially during the time when he was finishing this dissertation. Without her love and support, the author would not have completed this dissertation. The author would also like to thank his family members and friends for all the love and support they have provided him throughout his life, especially his parents, William and Debra Chavel. This dissertation is dedicated to the author's grandmother, Joan Brosius, who was very excited to see her grandson complete his doctoral studies, but left us too soon see him finish. She was, and always will be, an inspiration to her family.

## 1.0 INTRODUCTION

The construction of horizontally curved steel I-girder bridges is more complex than construction of corresponding straight steel I-girder bridges of similar span. This complication arises from the fact that, unlike a straight steel I-girder, a curved girder rotates out-of-plane due to torsional effects of eccentrically applied gravity loads acting on the curved geometry. Therefore, methods used in curved girder bridge construction must limit not only the vertical displacement of the I-girders, but also the out-of-plane displacements, such that structural components, including the cross frames, can be erected with limited difficulty and the eventual geometry of the completed structure be achieved. To prevent significant displacements during erection, temporary supports (falsework) and holding cranes can be utilized to provide stability to or relieve loads from individual or multiple curved girders prior to the final designed-for structural resistance being achieved.

In addition to problems related to the erection of the bridge, additional difficulties can result from the inconsistent detailing of cross frame members and girders (i.e. intentionally detailing each of these for different loading conditions). Based on prevailing detailing conventions, there are two anticipated final positions of horizontally curved steel I-girder bridge under load: girder webs vertically out-of-plumb or girder webs vertically plumb. Final position is referred to as the configuration of the completed bridge superstructure elements when all dead loads are placed on the structure.

The girder webs will be vertically out-of-plumb at the final position when the girders and cross frames are both detailed for the web-plumb position at the no-load condition (approximately achieved in a practical sense through the use of a discrete number of false-work supports located intermittently along the bridge longitudinal axis). Cross frame member lengths are determined assuming that the girders are to remain plumb in the no-load position (i.e. not subjected to any displacements or rotations due to self-weight or additional dead loads). Girder webs then rotate out-of-plumb upon the removal of the false work and transfer of the dead load to the structure. Currently, there are no code specifications (AASHTO 1993, 2003, 2006) which limit the amount of dead load out-of-plane rotation that can occur in a horizontally curved steel I-girder structure erected and detailed in this manner.

Conversely, the girder webs can be made to be vertically plumb at the final position when the girders and cross frames are both detailed to a condition in which the girders are out-of-plumb in the no-load (i.e. supported) condition and then subsequently allowed to rotate to a plumb position upon the application of dead loads. Cross frame member lengths are calculated based on the displacements of the structure due to applied dead loads, including steel self-weight. Because curved I-girders rotate out-of-plane by varying amounts along their longitudinal axis due to their curvature and support conditions, the girder web must be fabricated with a built-in twist about the longitudinal axis of the girder to accomplish this condition. Due to the complexity and costs associated with the fabrication of this twist, it is rarely done in practice. As an alternate approach, a common practice is to only detail the cross frames to fit between hypothetical girders whose webs are plumb in the loaded condition. Since the girders are actually fabricated to be web-plumb in a different loading condition, it is thought that this mismatch in members will force the girders into a web-plumb condition under the gravity

loading at issue. Such an approach requires the imposition of additional forces during construction to force the misaligned members into position. This method of forcing disparately detailed members together is referred to herein as inconsistent detailing.

Inconsistent detailing results in cross frame member lengths that are incompatible with girders in the theoretical no-load position at time of erection. Therefore, the cross frame members must be forced into place, twisting the girder webs out-of-plumb during erection. The direction of the out-of-plumb twist will be in the opposite direction of the natural out-of-plane rotation that will occur in the girders upon the application of dead load. Since the cross frames are being forced into position, locked-in girder and cross frame member stresses will develop, which are typically unaccounted for by the designer.

Curved girder bridge components are typically inconsistently detailed because the rotation of the girders, and the subsequent lateral displacement of the top flange due to applied or dead loads, are subjectively deemed to be excessive by the bridge engineer or owner. This determination is made without guidance from current design standards (AASHTO 1993, 2003, 2006). Furthermore, an additional analysis is almost never carried out showing that there will be no adverse effect on the structure with cross frames and girders detailed inconsistently; or, perhaps more importantly, to check if there will be an adverse effect on the bridge erection.

Consistent with the general lack of guidance concerning the detailing and fabrication of steel I-girder superstructure elements, there currently is no guidance given in the U.S. design standards (AASHTO 1993, 2003, 2006) pertaining to the complex erection problems associated with horizontally curved steel I-girder bridges. The objective of the National Cooperative Highway Research Program's (NCHRP) Project 12-38 was to develop a revised guide specification based on current practices and technologies. The final report for this project (Hall

et al. 1999) provided some guidance with regard to several of the construction issues at the heart of many horizontally curved I-girder bridge erection problems and was adopted as the AASHTO *Guide Specifications for Horizontally Curved Steel Girder Highway Bridges* (2003). Nonetheless, the authors of the report pointed out that the construction of curved steel I-girder bridges is an area where considerable further research is needed.

## 1.1 LITERATURE REVIEW

A significant amount of research has been accomplished in regard to the behavior of horizontally curved steel I-girder bridges, however little of this research has focused on the construction and detailing aspects of such bridges. Over the last half of the 20<sup>th</sup> century, horizontally curved I-girder bridge construction has steadily increased. It now comprises a significant amount of the steel bridge market in the United States. Zureick et al. (1994) published a report as part of the Federal Highway Administration's (FHWA) Curved Steel Bridge Research Project (CSBRP) which summarized the large amount of analytical, experimental, and theoretical research that had been accomplished to that time. Approximately 750 references were collected; 540 of these were considered significant and briefly discussed in the FHWA report. Of these, only one (Schelling et al. 1989) discussed construction aspects related to cross frame requirements during construction.

Prior to the initiation of the CSBRP in 1992, the development of the curved steel bridge design specifications in the United States stemmed from research work accomplished by the Consortium of University Research Teams (CURT) in the 1960's and 1970's. The CURT

project included researchers from Carnegie Mellon University, the University of Pennsylvania, the University of Rhode Island, and Syracuse University. Experimental and analytical research was conducted in regard to nominal bending strength, lateral stability, local buckling, and so forth (Brennan et al. 1970, McManus 1971, Mozer et al. 1970, 1971, 1973). An allowable stress design procedure (CURT 1975) was developed based mostly on the work carried out as part of the CURT project. During the late 1970's, a load factor design criteria for curved girder bridges was developed based on work done by Galambos (1978) and Stegmann et al. (1975) at Washington University in St. Louis. The developed allowable stress design criteria and the load factor design criteria ultimately became the AASHTO *Guide Specifications for Horizontally Curved Highway Bridges* in 1980 (revised 1993 (AASHTO 1993)), which contained design criteria for curved steel I-girder and box girder bridges, and hybrid I-girder and box bridges. However, at the time, little if any attention was given to the behavior of horizontally curved I-girder bridges during construction.

The more recent AASHTO *Guide Specification for Horizontally Curved Steel Girder Highway Bridges* (2003) and the current AASHTO-LRFD *Bridge Specifications*, 3<sup>rd</sup> Edition (2006) have addressed some aspects of construction and detailing methods typically used in curved steel I-girder bridge design. Both specifications are similar in that each presents methods and consequences of methods associated with detailing curved steel I-girder bridges, but neither specifies a definite method that should be used in a particular type of bridge. The provisions in the AASHTO-LRFD (2006) were essentially adapted from the AASHTO Curved Girder Guide Specification (2003), hence the similarity. Article 6.7.2 of the AASHTO-LRFD (2006) states that there are two intended erected portions of horizontally curved bridges: (1) girder webs theoretically vertical or plumb and, (2) girder webs out-of-plumb. The specifications address the

fact that girders and cross frames can be detailed to be in the web plumb position at the no load condition, or girders and cross frames can be detailed to be in the web plumb position at the steel, or full dead load condition. The latter condition may be achieved by introducing a necessary twist into the girders through fabrication, or by introducing the twist during the steel erection only (AASHTO 2006). The second method of introducing twist uses girders detailed to be web plumb at the no-load condition, and cross frames detailed for girders that are to be plumb at the specified dead load condition, thereby requiring the cross frames to be forced into place in the field. The AASHTO-LRFD (2006) does state that as the cross frames are forced into place twisting the girders out-of-plumb during erection, the curved girder flanges act to resist the induced change in radii, and the Engineer, based on engineering judgment alone, may or may not need to consider potential locked-in stresses and other effects resulting from this detailing method.

A recent synthesis of steel bridge erection practices was published by the Transportation Research Board, NCHRP Synthesis 345 (Beckman and Mertz 2005). The synthesis reports the results of and analyzes questionnaires, telephone conversations, specification reviews, and research reports solicited from bridge owners (individual states and Canadian provinces transportation/bridge departments), fabricators, erectors, and contractors. The report focuses on steel I-girder and box girder bridges, both curved and straight. Bridge owners and erectors point out that there are generally few problems with straight girder bridges; however several problems have been experienced with the erection of curved girder bridges. Erectors noted problems with regard to deflection and web verticality on highly skewed or curved bridges, and at what load condition the girder webs should be plumb and the tolerances to be applied to the girder plumbness. Some bridge owners also reported problems and concerns with maintaining girder

stability during various stages of construction. One owner reported that a girder fell because too few cross frames were installed before releasing the lifting crane. Several owners reported problems resulting from unanticipated differential deflections between adjacent girders in curved bridges, improper or inadequate use of temporary shoring, poor horizontal and vertical alignment control, or detailing inconsistencies. NCHRP Synthesis 345 shows that curved steel bridge erection, associated detailing practices, the issue of web plumbness, and the general lack of guidance in governing specifications are topics that require further investigation and study.

Despite the lack of guidance in design documents several significant contributions to the study of the behavior of horizontally curved steel I-girder bridges during construction have appeared in the literature. One such contribution emanated from a portion of the FHWA-CSBRP project in which a full-scale horizontally curved steel I-girder bridge structure was experimentally tested at the Turner-Fairbank Highway Research Center. A construction study was conducted as the 200 ft long structure was being erected: a series of elastic tests were performed that studied the behavior of portions of the experimental bridge as shoring was removed and replaced from beneath the girders. The experimental results, as well as comparisons with analytical results obtained using the finite element program ABAQUS, were presented by Linzell (1999). Linzell's study showed the applicability of shell element-based finite element modeling strategies in simulating curved steel I-girder superstructure erection. The construction studies also provided insight related to the load redistribution and subsequent deformations that occur during curved steel I-girder bridge construction. The studies showed that variations in temporary shoring conditions can lead to significant changes in the load distribution in curved I-girder bridges, and that there was no appreciable difference in the analytical results between models with nominal geometric properties and models using measured

geometric properties. Furthermore, additional elastic analyses carried out as part of the CSBRP project indicated that for the completed structure, the final deflected shape and load distribution would be different if a different erection sequence was followed (Duwadi et al. 2000)

Galambos et al. (1996) completed a substantial “in-field” experimental investigation on the behavior during erection of a two span continuous horizontally curved and skewed steel I-girder bridge with 4 concentric girders. The spans ranged from 139 to 155 feet with an inside radius of approximately 270 feet. The objective of this research was to investigate the strains in the steel superstructure during the erection of a curved steel I-girder bridge. These field measurements were then compared with results obtained using a finite element program developed at the University of Minnesota. Galambos et al. reports that careful attention to a well crafted erection sequence results in very low stresses being introduced into superstructure elements during erection.

A study at the University of Pittsburgh in 2001 investigated the problems encountered during the erection of the Ford City Veteran’s Bridge in Ford City Pennsylvania (Chavel 2001, and Chavel and Earls 2006a, 2006b). The three-span continuous steel I-girder Ford City Veteran’s Bridge has 322 ft end spans and a 417 ft center span, where the northern end span has a radius of curvature of approximately 510 ft measured at the bridge centerline. Figure 1.1 shows the completed Ford City Veteran’s Bridge steel superstructure with the North end span in the foreground. The investigation focused on the steel erection sequence employed to construct the bridge, as well as the detailing methods used to fabricate the bridge. Several construction difficulties developed due to the practice of inconsistent detailing of the girders and cross frames, in which the girders were detailed to be web-plumb at the no-load condition and the cross frames detailed for the web-plumb position at the steel dead load condition, an inconsistent combination.



**Figure 1.1** Ford City Veteran's Bridge Steel Superstructure (Chavel 2001)

Finite element models were developed using the finite element program ABAQUS to investigate the steel erection sequence and determine the effects of inconsistent detailing. Through the analytical study of the erection of the curved end-span, the inconsistent detailing was found to lead to cross frame connection misalignments of approximately 1.25 in. Interviews conducted with the contractor confirmed that during the erection of the curved span, cross frame connection misalignments of approximately 1.5 in were measured (Chavel 2001). These misalignments required the use of additional jacking methods and high-capacity cranes to correct these connection misalignments and install the cross frames. The study of the Ford City Veteran's Bridge served to validate the finite element techniques employed and showed that the pursuit of web-plumbness at steel dead load through inconsistent detailing can produce significant difficulties and expense in terms of construction (Chavel 2001).

Erection procedures of a large radius, horizontally curved steel I-girder bridge were investigated by Bell and Linzell (2007). A six-span steel I-girder bridge, with a centerline radius of 1939.5 ft, located in central Pennsylvania which experienced significant geometric

misalignments and fit-up complications during steel construction was studied to investigate curved girder bridge behavior during construction. The structure was monitored by the authors during corrective procedures to remedy misalignments, which included unintended lateral displacements in excess of 10 inches. The field data obtained as the girders were realigned to their design geometry was used to calibrate a three dimensional finite element model, using SAP2000. The model was then used to study various erection methods and sequences not employed in the field. From the analytical studies, the authors observed that erecting single girder lines beginning with the girder with the largest radius, and sequentially placing girders with smaller radii (outer girder to inner girder) resulted in smaller radial and vertical deformations in the final steel dead load condition than those obtained when erecting the girder with the smaller radius first (inner girder to outer girder). It was also observed that the implementation of a top flange lateral bracing system or the use of temporary support towers (falsework) are effective means to further reduce deformations during steel erection.

Although not explicitly discussed by Bell and Linzell (2007), the problems experienced during construction of the subject bridge were not only caused by the curvature, but additionally by the long spans coupled with insufficient temporary supports during steel erection. The bridge has a maximum span length of 333.2 ft, and employs girders having a web depth of 126 in., and minimum top flanges of 1 in. by 16 in. in the positive moment regions. The use of small flanges with a very deep girder can potentially lead to lateral torsional instabilities and significant deflections during erection due to large unbraced lengths of girders resulting from limited cross frame placement during steel erection. The types of problems experienced during the construction of the subject bridge tend to be a recurring theme in the erection of horizontally curved steel girder bridges.

Howell and Earls (2006, 2007) analytically studied the various effects that web out-of-plumbness in a curved steel I-girder bridge has on flange tip stresses, vertical and lateral deflections, cross-sectional distortion, and cross frame demands. A single idealized bridge was chosen for the investigation, based on a survey of 12 representative bridge designs. The model bridge is a three-span continuous structure with six concentric I-girders spaced at 10.21 ft on center. The bridge has a centerline radius of approximately 510 ft, and a center span length of 173.9 ft with dissimilar end spans of 129.9 ft and 139.1 ft. Nonlinear finite element models developed using the finite element program ADINA were used to investigate the effects of web out-of-plumbness in this particular idealized structure, for bridge girders having web out-of-plumbness magnitudes up to  $5^\circ$ . Results from this study indicate that web plumbness has an influence on flange tip stresses, vertical and lateral deflections, and cross frame member axial forces. Significantly, flange tip stress increases on the order of 20% were observed due to the web out-of-plumbness of the analyzed bridge girders. The authors point out that stress increases such as these can develop in the field during construction, and recommend that a more robust level of analysis be required in some cases of curved steel I-girder bridge construction. This study showed that there is a need to further explore the effects of girder web out-of-plumbness, and its influence on the behavior of horizontally curved steel I-girder bridges particularly during erection.

## 1.2 SCOPE OF RESEARCH

The current research is intended to be an analysis and assessment of construction and detailing issues associated with horizontally curved steel I-girder bridges. This includes a careful examination of the motivations for the dominant detailing practices as well as more practical issues associated with the applications of these techniques. Currently, only a limited number of the horizontally curved steel I-girder bridge erection sequencing studies have been reported in the literature. These include an analytical study of the erection and detailing methods of the Ford City Veterans Bridge (Chavel and Earls 2001), a continuous 3-span steel I-girder bridge with a 322 ft curved span with a radius of 510 ft; an experimental and analytical erection sequencing study single span curved I-girder bridge with a span length of 90 ft and a radius of 200 ft (Linzell 1999); a substantial “in-field” experimental investigation of the erection behavior of a 2-span horizontally curved steel I-girder with an average span length of 140 ft and a radius of 285 ft (Galambos et al. 1996); and an investigation of different erection procedures of a large radius, six span, horizontally curved steel I-girder bridge that experienced problems during steel erection (Bell and Linzell 2007).

At a very basic level, one aim of the present research work is to add to this current construction study database. An analytical investigation of the erection sequence and detailing methods of a single span horizontally curved and skewed steel I-girder bridge will be conducted to facilitate the contextualization of this work in terms of the earlier studies. The bridge chosen for this study is State Route 8002 Ramp A-1. This structure has an approximate curved length of 150 ft and a centerline radius of 279 ft. This structure will serve as a subject with which comparisons in regard to erection sequence and detailing methods will then be made with an earlier study carried out by the author for the Ford City Veteran’s Bridge.

Another aim of the current research is to understand and assess the motivations for various detailing and fabrication practices related to web-plumbness. The present research addresses this important issue of allowable web rotation through the use of experimentally verified nonlinear finite element modeling techniques. An evaluation of the structural capacity of a straight and a curved steel I-girder, rotated out-of-plane, will be carried-out and comparisons to similar I-girders, that are not rotated out-of-plane, will be performed. Additional analytical investigations will be carried out. These include a study of allowable girder web rotations for a two-girder curved steel superstructure. The curved steel I-girder bridge chosen for this portion of the study is based on I-girders used in the three-span approach unit of the Chelyan Bridge, which has a total length of 442 ft and a radius of 509 ft. A parametric study of this two girder structure will be performed, in which important parameters such as girder radius, girder spacing, cross frame spacing, and girder web depth will be varied.

Beyond the earlier aims of this work, the present study will also quantify the effects of the additional forces induced in the bridge superstructure components due to intentional misfits arising from inconsistent detailing. Because these misfit induced stresses are typically unaccounted for by bridge designers, the current study will investigate the resulting locked-in stresses required to force the girders and cross frames into place in the Chelyan two-girder system, in an inconsistently detailed state.

This study will contribute to the limited amount of research available in regard to girders in an out-of-plumb position, and determine whether or not a girder in an out-of-plumb position has a significantly reduced capacity. It is also hoped that this study promotes awareness of the issue of inconsistent cross frame and girder detailing, as well as the importance of a well-crafted

erection sequence. The concept of inconsistent detailing can be an extremely critical issue in relation to the successful erection of a horizontally curved steel I-girder bridge.

Research of the type described herein has not been reported on in the archival literature. In addition, to the best of the author's knowledge (and to that of the leading experts in the field), no similar study has ever been carried out. Beyond the novelty of this research effort, the importance of the findings have an enormous potential to improve the state of practice in the design and construction of horizontally curved steel I-girder bridges.

### **1.3 DISSERTATION ORGANIZATION**

Chapter 2 of this dissertation provides relevant theory with regard to the behavior of horizontally curved steel I-girder bridge systems. The concepts of the no-load, steel dead load, and final dead load conditions are presented. Additionally the three different detailing methods that can be employed in horizontally curved steel I-girder bridges are discussed. Chapter 3 describes a study of the erection sequence of the single span, curved and skewed S.R. 8002 Ramp A-1 bridge. A comprehensive nonlinear finite element analysis of each stage of the erection sequence is performed in which displacements, reactions, crane loads, and steel stresses are monitored. Chapter 4 presents a study of the structural behavior of web out-of-plumb curved steel I-girders, again employing nonlinear finite element modeling techniques. In this study, a single straight and a single curved beam are investigated for varying degrees of web out-of-plumbness. Additionally, a parametric study is carried out on a two-girder bridge subsystem, in which parameters such as radius of curvature, girder spacing, cross frame spacing, and web depth are

varied to investigate for the effects of web out-of-plumbness. A study investigating locked-in stresses due to inconsistent detailing of the girders and cross frames in a horizontally curved steel I-girder bridge is presented in Chapter 5. Conclusions and recommendations based on the results of these studies are provided in Chapter 6. Appendix A summarizes publications that have emanated from the author's research work. Results are presented in Appendix B for the as-built erection sequence and intended erection sequence (as-planned) of S.R. 8002 Ramp A-1. For each stage of construction, the girder vertical displacements, lateral (out-of-plane) displacements, and the girder out-of-plane rotation are shown. In Appendix C, results are presented for web out-of-plumbness parametric study carried out on the two-girder system. Details regarding the shell finite elements used throughout this research are provided in Appendix D.

## 2.0 CURVED I-GIRDER BRIDGE BEHAVIOR

The behavior of horizontally curved steel I-girder bridges is more complex than their straight girder counterparts. There are a number of behavior characteristics unique to curved bridges including, torsional effects, lateral flange bending effects, and global load shifting. Vertical loads applied to a curved girder will produce flexural moment and shear, as in a straight girder, but will also produce a torsional moment about the girders longitudinal axis. Additionally, due to their geometry, horizontally curved steel I-girders, supported only at their ends, will displace vertically and rotate out-of-plane upon application of vertical loads, thus causing an unequal lateral displacement (with respect to the section) of the top and bottom flanges. This deflection is manifest as an unequal radial displacement of the flanges with respect to the member geometry.

Similar to the different behavioral aspects of curved girder bridges from straight bridges, the terms no-load, steel dead load, and full dead load positions are more widely used in discussing curved steel I-girder bridges. Additionally, there are detailing methods used in curved I-girder bridges that are not typically used in straight, non-skewed, I-girder bridges. The load conditions and detailing methods employed in curved girder bridges are used with the intent of achieving some level of web verticality at some stage of erection (load condition). These behavioral aspects and the terminology of curved steel I-girder bridges will be described in greater detail in this section.

## 2.1 SINGLE CURVED I-GIRDER

The vertical bending moment for the single curved I-girder is obtained in a similar manner as for a straight girder, with the implementation of simple trigonometric relations to account for the geometry associated with the curvature. More importantly, for a curved I-girder, are the torsional effects which act in addition to the basic vertical bending effects. The torsion in curved girders results from the fact the center of loading of each span in a curved girder is offset from the chord line drawn between the supports for that span, as shown in Figure 2.1. This offset represents an eccentricity which, when multiplied by the vertical load, results in a torsional moment which varies longitudinally along the span of the girder.

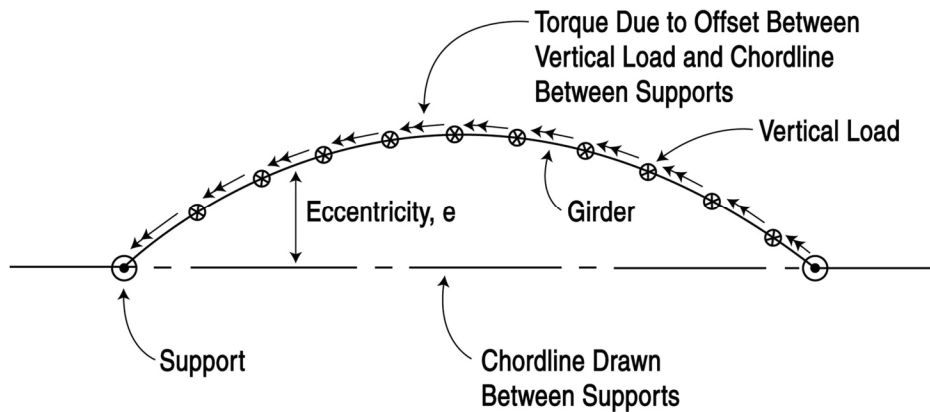


**Figure 2.1** Single Curved Girder (Coletti and Yadlosky 2005)

I-girders are an open cross-section, and therefore have a relatively small St. Venant torsional stiffness; they carry torsion primarily through warping. Assuming a general loading, the total state of shear stress in an I-girder is as shown in Figure 2.2, and is the combination of vertical shear stress, horizontal shear stress, a small amount of St. Venant torsional shear stress, and warping shear stress. The St. Venant torsional shear flow around the perimeter of the cross

section only develops force couples across the thickness of the flange and web plates and is therefore very low in the I-girder. Thus, the applied torsion is resisted almost entirely through warping of the cross-section, which manifests itself as an additional source of flange bending in an I-girder cross-section as indicated on the right-hand side of Figure 2.2.

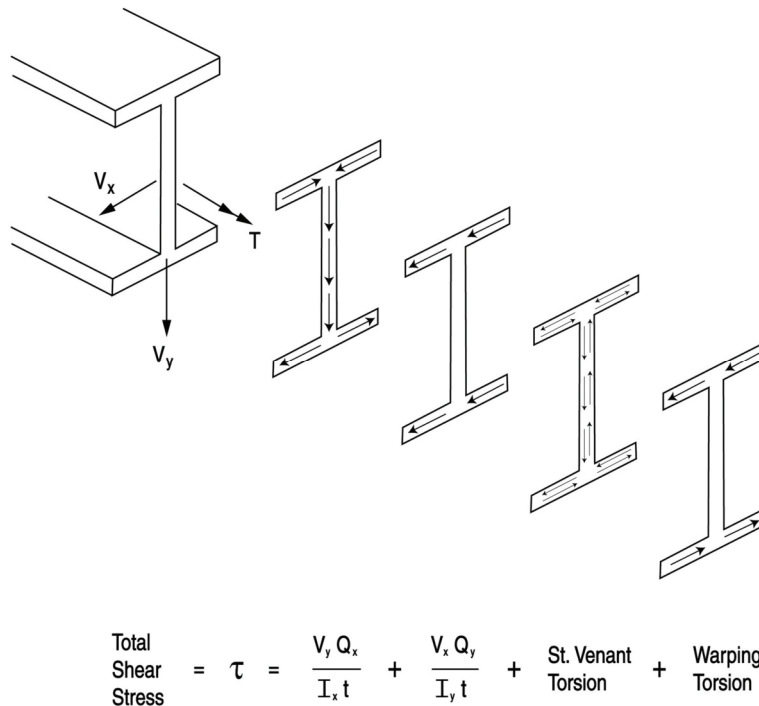


**Figure 2.2** Shear Stresses Which Can Occur in a Curved I-Girder (Coletti and Yadlosky 2005)

## 2.2 CURVED I-GIRDER BRIDGE SYSTEM

The interaction of steel I-girders in a horizontally curved bridge system varies significantly from that of a straight girder bridge. For example, in a straight I-girder bridge, the main functions of the cross frames are to stabilize the girders and provide support against lateral torsional buckling. However, cross frames in a curved I-girder bridge not only provide support against lateral

torsional buckling, they also serve as a primary load carrying member resisting the torsion that is inherent in a curved I-girder bridge. Additionally, girder flange stresses, deflections, reactions, and cross frame forces in a curved girder bridge are significantly different from those in a straight girder bridge.

### **2.2.1 Vertical Bending Effects**

The longitudinal flange stresses in a curved steel I-girder can be divided into four components, with three of these components resulting from vertical bending (Hall et al. 1999). The first component is due to vertical bending, with load applied directly through the shear center of the girder. The vertical bending moment and subsequent longitudinal flange stress can be computed by assuming that each girder is independent from the rest of the structure. This longitudinal flange stress is analogous to a straight girder bridge and is shown in Figure 2.3 as Component 1.

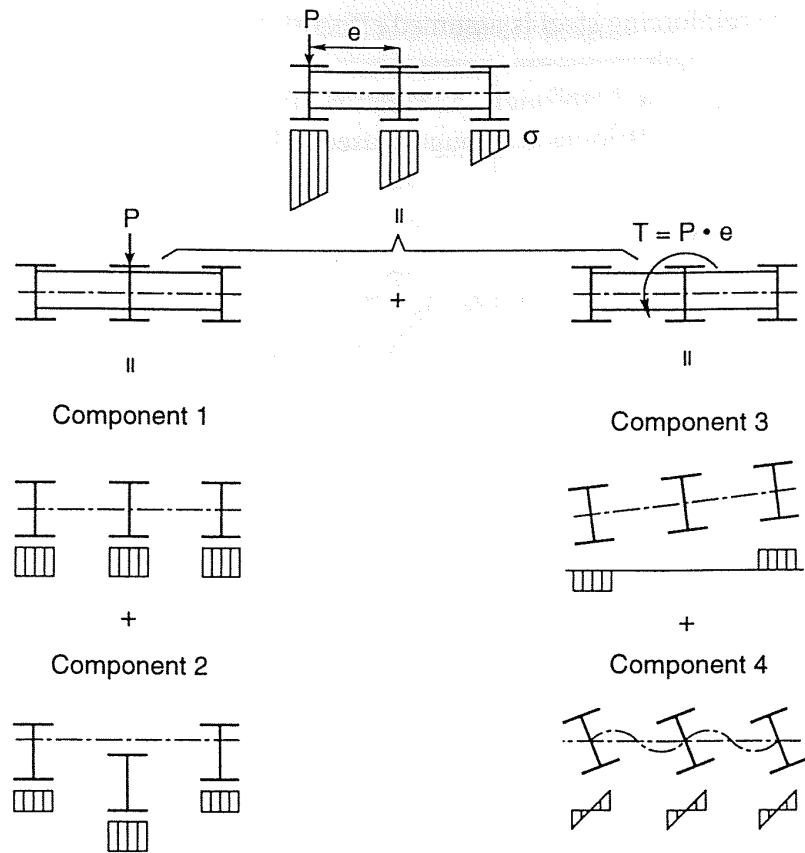


**Figure 2.3** Longitudinal Flange Stress Components (Hall et al. 1999)

The second component of longitudinal flange stress is due to the moment resulting from restoring forces in connecting members between the girders. This component, Component 2, shown in Figure 2.3, develops when adjacent girders have either a different stiffness or the girders are subjected to different loads, as in the case of a truck or lane live load. A nonuniform loading across the width of the bridge will cause the deflections in adjacent girders to be different, and the connecting members, such as cross frames, will impose a restoring force that tends to mitigate the difference in these deflections. This second component does not typically develop under uniform dead loads, unless the stiffness of adjacent girders varies significantly.

The portion of longitudinal flange stress caused by the horizontal curvature is the third component stress (Component 3 in Figure 2.3). This component results from the fact that the center of gravity of a curved bridge is eccentric with respect to a line drawn between the end supports. The eccentricity causes the entire structure to rotate about this chord line, and as the eccentricity increases, so does the rotation and the subsequent longitudinal flange stresses due to the torsional effects. For example, bridge B shown in Figure 2.4 has a larger eccentricity than bridge A, and will experience a larger rotation about the chord line due torsional effect. This global rotation, or overturning, is sometimes referred to as load shifting, whereby girders on the outside of the curve will carry larger forces than those on the inside of the curve. This load shifting phenomenon is significant for curved steel I-girder bridges, and so is the specific load path for this load shifting. Loads are transferred from one girder to the adjacent girder through the cross frames, which thus become primary load carrying members, and must be considered as such in design (Coletti and Yadlosky 2005). Loads are typically transferred from the girder with the smallest radius towards the girder with the largest radius, causing higher support reactions at the girder with the largest radius.

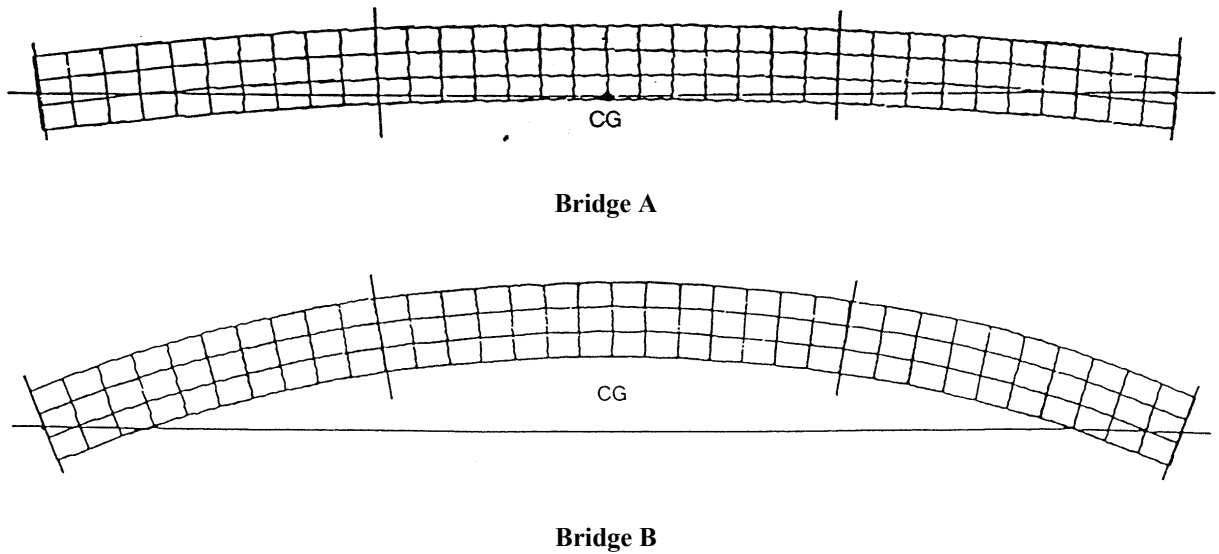


**Figure 2.4** Plan View of a Curved Girder Bridge

### 2.2.2 Lateral Flange Bending Effects

The fourth component of longitudinal flange stress is due to lateral flange bending, which results from the girders being subjected to non-uniform torsion. Lateral flange bending causes longitudinal stresses in the flanges which vary linearly from one flange tip to an equal and opposite value at the other flange tip, as shown in Figure 2.3 as Component 4. Lateral flange bending moment due to nonuniform torsion typically varies along the flange as shown in Figure 2.5 (Hall et al. 1999). In the Figure 2.5, radial forces shown are restoring forces provided by the cross frames and the axial force in the flange is due to vertical bending.

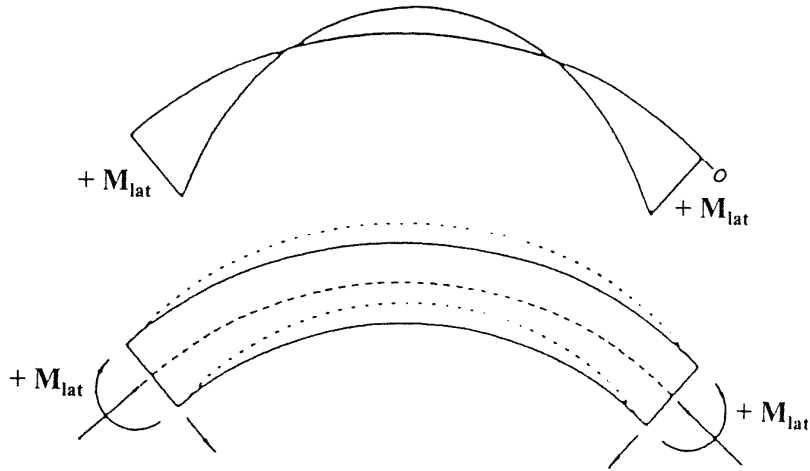


**Figure 2.5** Lateral Flange Bending Diagram (Hall et al. 1999)

The lateral flange bending in curved steel I-girders is mainly a result of the warping stresses that develop due to the restraint of nonuniform torsion. Equilibrium requires equal and opposite action in the top and bottom flanges, called the bimoment (Hall et al. 1999), shown schematically in Figure 2.2. In a curved steel I-girder bridge, the cross frames introduce restoring torques to the girders, restraining free warping and resulting in bimoments in the girders. The bimoments are manifest in equal but opposite lateral bending moments in the top and bottom flanges (Hall 1996).

Lateral flange bending moments at brace points can be estimated by the V-load equation (Poellot 1987):

$$M_{lat} = \frac{M_v L^2}{10DR} \quad (2-1)$$

where  $M_{lat}$  is the lateral flange bending moment at the brace point,  $M_v$  is the vertical bending moment,  $L$  is the distance between brace points,  $D$  is the girder depth, and  $R$  is the girder radius.

The V-load method is an approximate method for analyzing curved steel I-girder bridges, however the lateral flange bending moment given by equation (2-1) is widely used in design practice. Therefore, a brief description of the development of equation (2-1) is warranted. The theory of the V-load method is based upon the static behavior of a curved flange carrying axial stress or force. If a short segment of flange is considered, as in Figure 2.6, the axial force in the flange is not colinear due to curvature. This results in a radial component, which over the length of the flange, manifests itself as a radial distributed force as shown in Figure 2.7. The magnitude of the radial flange force is analogous to the classic case of hoop tension, shown in Figure 2.8. In the case of the hoop tension,

$$T = qR \tag{2-2}$$

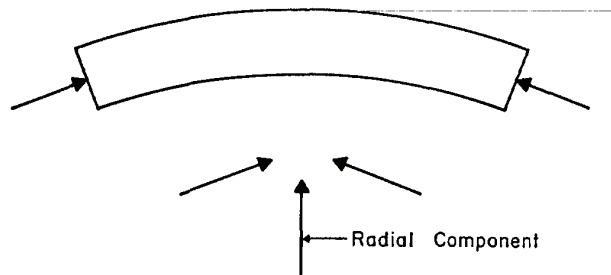


**Figure 2.6** Radial Flange Force Component (Poellet 1987)

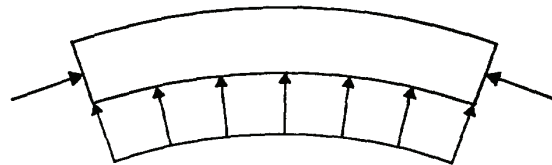


**Figure 2.7** Radial Distributed Flange Force (Poellet 1987)

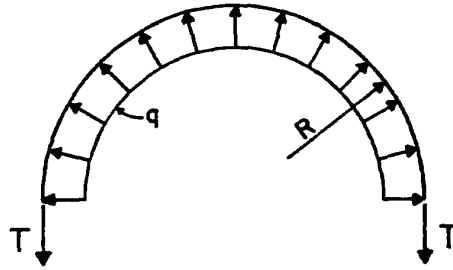


**Figure 2.8** Hoop Tension Analogy (Poellet 1987)

In a curved girder the hoop tension theory is the same, but the cause and effect is reversed. The curvature of the flange force (analogous to the hoop force,  $T$ ) produces the radial force,  $q$ , rather than  $q$  producing the hoop tension,  $T$ . In the curved girder case, the flange force,  $T$ , and can be represented by the girder vertical bending moment,  $M_v$ , divided by the girder depth,  $D$ ,

$$T = M_v / D \quad (2-3)$$

Setting equations (2-2) and (2-3) equal, and solving for  $q$  yields,

$$q = M_v / RD \quad (2-4)$$

The V-load equation for lateral flange moment (equation (2-1)) is then derived assuming the flange is a continuous beam on rigid intermediate supports, where,

$$M_{lat} = \frac{qL^2}{10} = \frac{M_v L^2}{10DR} \quad (2-5)$$

The lateral flange bending stresses, which are manifest as longitudinal stress in the flange, can be computed by dividing the lateral moment by the lateral section modulus of the flange,  $M_{lat}/S_{lat}$ . These lateral flange bending stresses are equivalent to the warping longitudinal stresses that result from nonuniform torsion.

### 2.2.3 Displacements

Due to their geometry, horizontally curved steel I-girders displace vertically in-plane ( $Y$ ) and rotate out-of-plane ( $\phi$ ) upon load application; thus resulting in unequal lateral displacement of the top ( $X_{TF}$ ) and bottom ( $X_{BF}$ ) flanges at any cross-section along the longitudinal axis of the girder, as shown in Figure 2.9. The out-of-plane rotation and subsequent lateral displacements are caused by the loading eccentricity as previously shown in Figure 2.1.

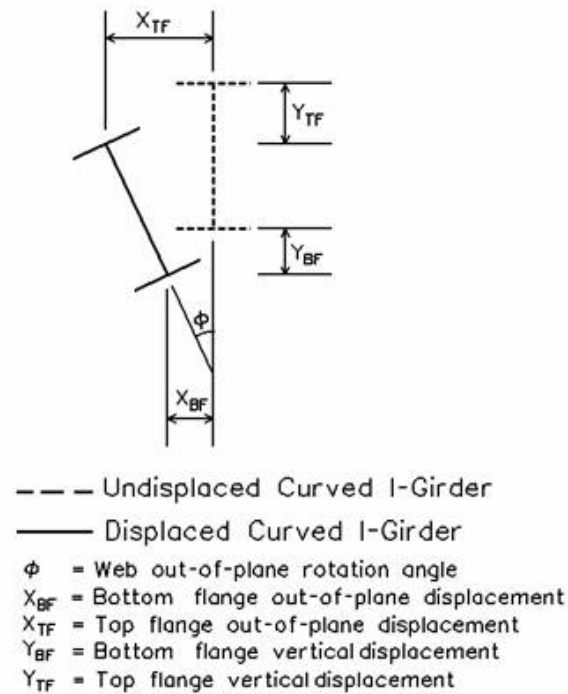


**Figure 2.9** Girder Rotation Due to a Given Loading

In a completed simple span curved steel superstructure resting on non-skewed (i.e. radially orientated) supports acted on by gravity, the girder with the larger radius (on the outside of the curve) displaces in the vertical direction more than the girder with the smaller radius (on the inside of curve). This behavior causes differential displacements to take place between all of

the girders in a given cross-section of the superstructure and is the case despite the fact that intermediate cross-framing members are present. In fact, the effect of the cross-framing members in the system is to induce a rotation of the overall bridge cross-section (i.e. the combined system consisting of all of the individual girder cross-sections, tied together with the cross-framing).

Since a horizontally curved steel I-girder rotates and displaces laterally immediately upon loading, a condition may arise wherein the owner or engineer becomes concerned about the effect of the resulting web out-of-plumbness. In these situations the engineer may resort to an inconsistent detailing practice; not realizing that it is impossible to have the girder webs vertically plumb at two different loading conditions (e.g. at no-load and then again at steel dead load). This condition might be ameliorated if guidance were to be provided to the designer by specification writing bodies. Unfortunately there currently are no guidelines that state at which load condition the girder webs ought to be vertically plumb, or conversely what degree of out-of-plumbness is acceptable and under what load condition.

### **2.3 NO-LOAD, STEEL AND FINAL DEAD LOAD CONDITIONS**

The no-load condition is defined as the theoretical condition in which the bridge is subjected to little or no deformations or stresses (i.e. the geometric configuration that the structure assumes once assembled, but not acted upon by any external forces – including gravity). For horizontally curved I-girders, the no-load condition typically occurs with the girders webs in a plumb position as a result of the dominant detailing convention currently used in practice. The theoretical no-load condition can be practically approached during construction with the proper use of

temporary supports (Chavel and Earls 2006a). Similarly, in the fabrication shop, girders are blocked to their desired camber to simulate the no-load condition during the shop assembly process.

The steel dead load condition is defined as the theoretical state of the assembled steel superstructure under the action of gravitational forces (i.e. deck self-weight is assumed to not be present). The placement of steel dead load on a curved I-girder, initially in a web-plumb state at the no-load condition, will cause the girder to immediately rotate to a girder web-out-of-plumb condition. Similarly, within a system context, the entire bridge cross-section will rotate and move out of plane in an analogous way. The steel dead load can be referred to as an intermediate loading condition, between no-load and final dead load.

The final dead load condition is defined as the theoretical state of the assembled steel structure under the action of steel and concrete deck self-weight (i.e. full noncomposite dead load). The application of these dead loads will cause an initially web-plumb I-girder to rotate to a web-out-plumb position, and the rotation will be greater than the rotation due to steel dead load only.

## **2.4     DETAILING METHODS**

Inconsistent detailing frequently arises when the rotation of the girders, and the subsequent lateral displacement of the top flange due to applied loads, or dead loads, are deemed to be of such a magnitude as to constitute an undesirable condition. In cases such as these, a strategy is sought to have the girder webs vertically plumb at a load condition other than no-load. To limit this out-of-plane rotation and displacement, it is often the case that the cross frames are detailed

to fit girders in the web-plumb position under the specified loading condition (in many cases steel dead load) while the girders remain conventionally detailed to be in the web-plumb position at the no-load condition; thus creating a detailing inconsistency. It is intended that detailing the cross frames in this manner will force the girder webs to be vertically plumb at the specified loading condition.

However, given that horizontally curved I-girders rotate out-of-plane immediately upon loading (including self-weight) the web of the girders cannot be in a vertically plumb position both before and after a given loading. Therefore, it is incorrect to assume that the combination of girders detailed to be web-plumb in the no-load condition, and cross frames detailed based on the web-plumb condition under a different specified load condition, will yield plumb girder webs in that load condition. In the case of an 'X' type cross frame, this detailing inconsistency will result in diagonal cross frame members that will either be too long or too short to connect with girders detailed and fabricated for the web-plumb position in the no-load condition.

There are three methods that could be used to detail girders and cross frames in horizontally curved I-girder bridges. The girders and cross frames can be detailed to be in the web-plumb position while under the no-load condition; the girders and cross frames can be detailed to be in the web-plumb position under a prescribed load condition (steel dead load or final dead load); or the girders and cross frames can be inconsistently detailed. Each of these is discussed in the following sections.

#### **2.4.1 Detail Method 1 – Girders and Cross Frames Detailed to be Web-Plumb at No-load**

In this method, the girders and cross frames are conventionally detailed such that the girder webs are vertically plumb in the no-load condition. Figure 2.10 shows a cross-sectional view of the

Ford City Veterans Bridge (Figure 1.1) at the mid-span of the curved section, with girders and cross frames detailed to be in the web-plumb position under the no-load condition. Superelevation effects are included in the bridge cross-sectional view shown in Figure 2.10. Girder G1 is the outside (larger radius) girder.

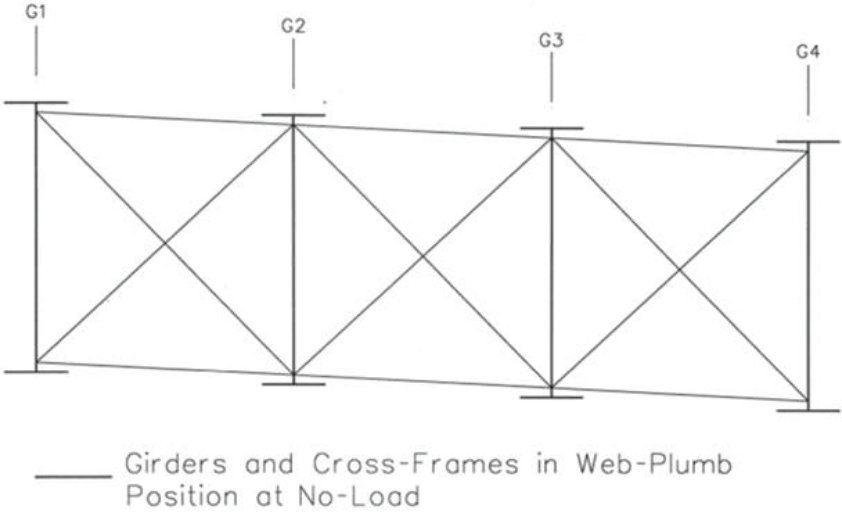


**Figure 2.10** Girders and Cross Frames Detailed for Method #1

The no-load condition can be practically approached during construction with the proper use of temporary supports. Upon the removal of these temporary supports, after the completion of steel erection, the structure will displace due to steel-self-weight, and the girder webs will no longer be vertically plumb since it is no longer in the no-load condition. A cross-sectional view of the same steel superstructure in the (exaggerated) displaced position due to the application of steel dead load is shown in Figure 2.11.

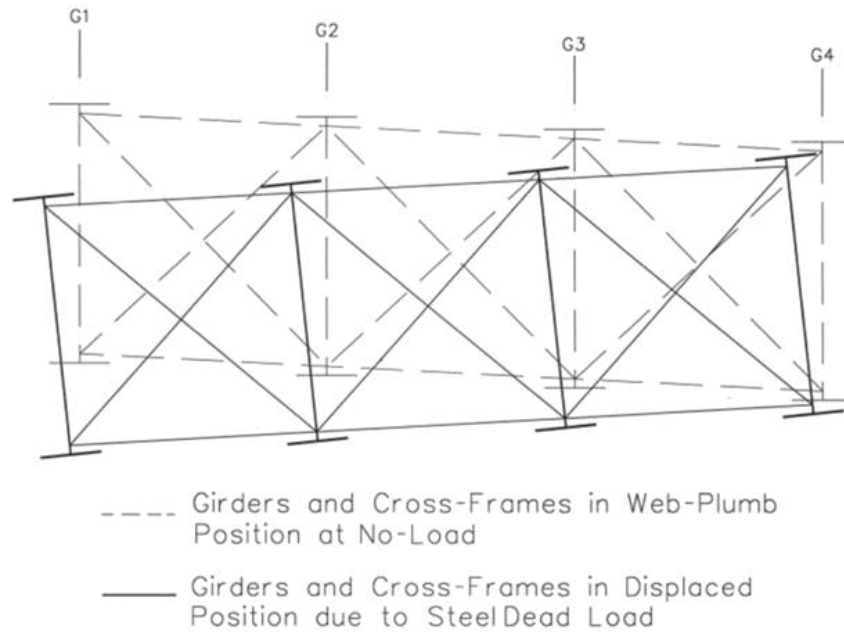


**Figure 2.11** Displaced Position (Steel Dead Load) of Cross-Section Detail Method #1

Theoretically, the structure will remain in an out-of-plumb position for the remainder of its service life and the girder rotations will subsequently increase with the placement of the concrete deck and live load application. Currently, no design guidelines exist as to what a maximum allowable girder out-of-plane girder rotation due to steel self-weight may be. Questions sometimes arise in the minds of owners and engineers as to whether or not the configuration so oriented after dead load application is compromised with respect to the undeformed configuration that is almost universally used as the basis for the design analysis.

#### **2.4.2 Detail Method 2 – Girders and Cross Frames Detailed to be Web-Plumb at Steel Dead Load (or Final Dead Load) Condition**

This detailing method is sometimes considered viable when the predicted out-of-plane rotation of the steel superstructure due to steel self-weight is deemed excessive. The girders and cross

frames can be detailed to a web-plumb position under steel dead load, thus causing the girder webs to be out-of-plumb in the no-load condition. Upon application of steel dead load, the girders will rotate to a plumb position. Detailing the cross frames and girders for web-plumbness in the final dead load is the same as detailing for the steel dead load condition, except that the displacements due to the final noncomposite dead loads are used. The current research focuses on the case where detailing for the steel dead load condition is employed since it represents the dominant practice in this condition.

The first step in Detail Method #2 is to determine the displaced position of the steel superstructure due to steel self-weight, with the girders and cross frames detailed to be web-plumb at the no-load condition (Detail Method #1), as shown in Figure 2.11.

The girders are then geometrically rotated back to a web-plumb position as independent rigid bodies pivoting about the bottom flange-web junction. This rotation is essentially equal for all girders at a section because the entire cross-section rotates by the same amount under the action of steel self-weight as a result of the presence of cross frames. With the girders in this new vertically plumb position, cross frame member lengths are determined by utilizing the same work-points on the girders as used for Detail Method #1. The new condition with cross frames detailed for the web-plumb position at steel dead load is shown in Figure 2.12.

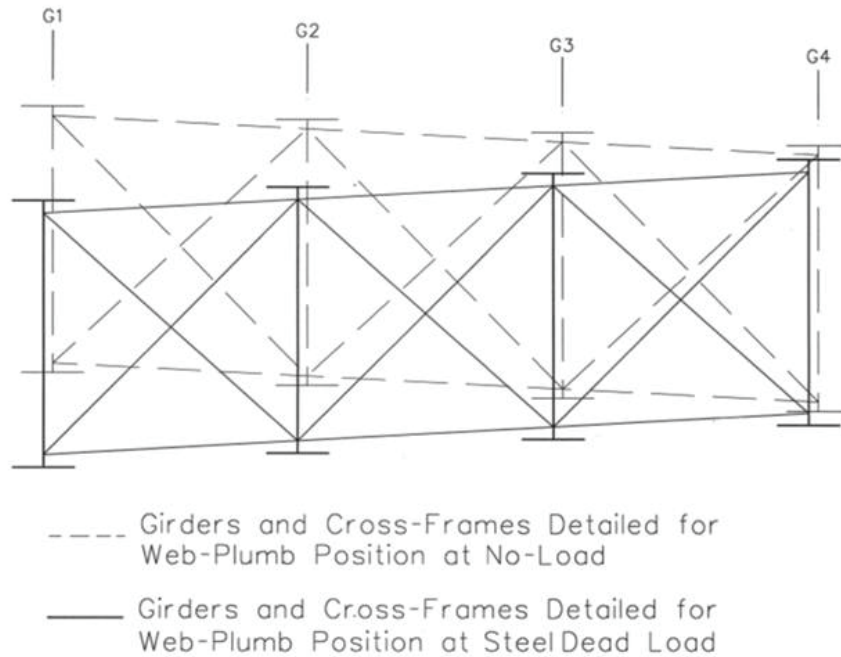


**Figure 2.12** Girders Rotated to Web-Plumb - New Cross Frame Member Lengths Determined

The next step in the process is then to rotate the entire bridge cross-section such that the work points at the bottom flange-web-junction move through the same angle they displaced through as a result of the application of steel dead load. The vertical and lateral displacements of these work points are basically reversed from those induced by the application of dead load. The net effect then is that the midpoint of each bottom flange is in the same location it was in for the no-load condition. As shown in Figure 2.13, this is the (no-load) starting position of erection for girders and cross frames detailed to be web-plumb at steel dead load application.

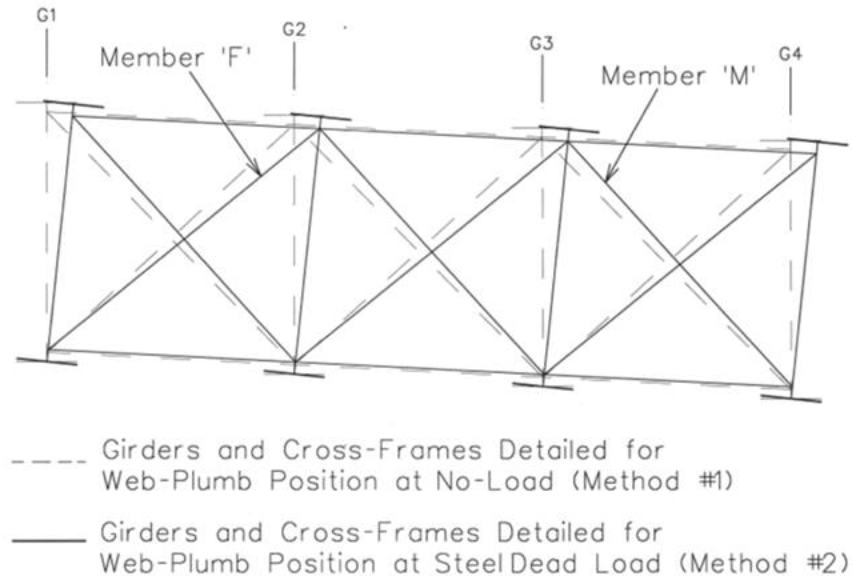


**Figure 2.13** Starting Points of Bridge Erection for Methods #1 and #2

Since the girder web out-of-plane rotation varies along the length of a horizontally curved steel I-girder (i.e. web rotation is a function of longitudinal position), each cross frame has to be specifically detailed for its location along longitudinal axis of the girder. In addition the girder web out-of-plane rotation due to steel self-weight must be built into the webs in order to have a consistent combination of detailed girders and cross frames. This out-of-plane rotation can be fabricated by pre-twisting the web, such that the girder web will be vertically plumb at the supports, where the web rotation must be zero due to the restraint of the end bearings. The pre-twisting will be the largest at the point of maximum web rotation due to steel dead load, typically at the mid-span location. Therefore, once steel dead load is applied, the girder web will rotate to a vertically plumb position at the mid-span location, and will remain vertically plumb at the support since the steel dead load rotation at the support is zero. This type of web pre-twisting technique is used in practice for the fabrication of a curved steel trapezoidal box girder webs.

Since these twists are difficult to accurately control in a quality assurance context, it is desirable to avoid them in most practical situations.

### **2.4.3 Detail Method 3 – Inconsistent Detailing of Girders and Cross Frames**

The typical detailing inconsistency occurs when the girders are detailed for the web-plumb position at the no-load condition (Detail Method #1), and the cross frames are detailed for the girder web-plumb position at a different prescribed load condition (Detail Method #2); typically steel dead load. It is then assumed that this combination will result in girder webs vertically plumb at the prescribed position; but this is incorrect as discussed previously. Instead, the detailing inconsistency results in cross frame members that are either too long, member ‘F’ in Figure 2.13, or too short, member ‘M’ in Figure 2.13. The difference in diagonal cross frame member length varies along the curved length of the bridge, since the girder out-of-plane rotation, vertical displacements, and subsequent girder differential displacements, vary in a similar fashion. Despite the fact that it may be possible to overcome the cross frame misfits through the introduction of external jacking and crane forces, the net effect is not what is desired. The girder webs will not be plumb as intended since inconsistent detailing results in the development of additional forces induced by the fact that the girders are resisting the tendency to be deformed into a configuration wherein the cross frame connections become possible. This may be a concern since the stresses induced by the misfit forces may grow to be large and are typically not specifically considered by the designer. It is therefore possible for problems to arise from a condition of overstress in the bridge, or lack of crane or jacking capacity on site during construction.

### 3.0 ERECTION STUDY S.R. 8002 RAMP A-1

The State Route 8002 (SR 8002) Ramp A-1 bridge is a single span composite horizontally curved steel I-girder bridge near King of Prussia, Pennsylvania. The northernmost abutment is radial, while the other abutment has a skew angle of 38.8 degrees measured from the longitudinal axis of the structure. Figure 3.1 shows the design drawing framing plan for the structure, and Figure 3.2 shows the naming convention utilized in the current research for the girders and cross frames of the structure.

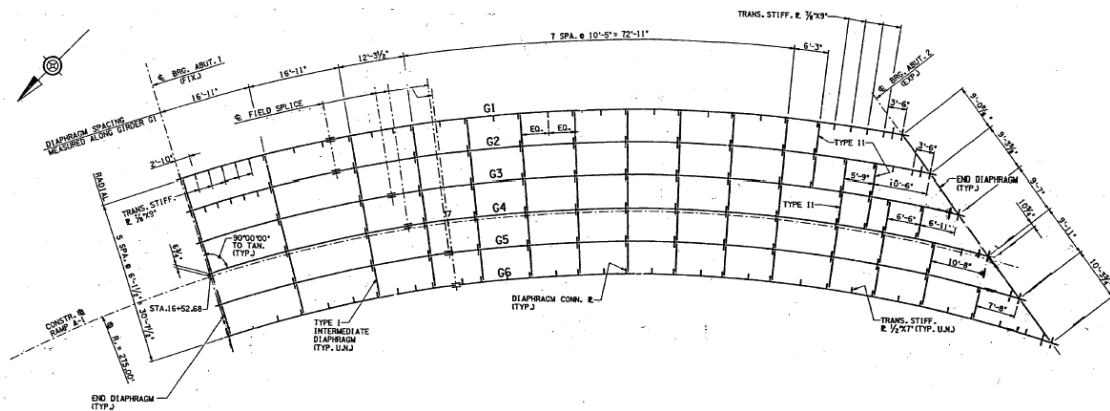


**Figure 3.1** SR 8002 Ramp A-1 Design Drawing Framing Plan

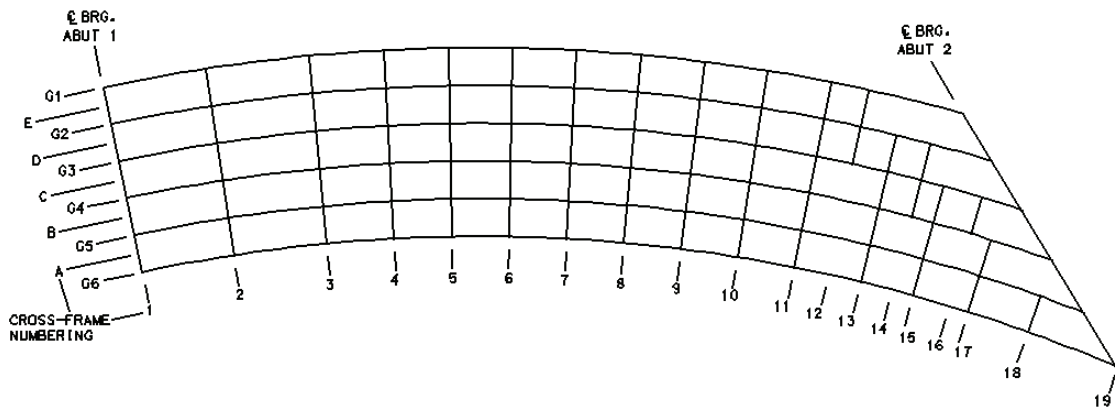


**Figure 3.2** SR 8002 Ramp A-1 Naming Convention

The centerline radius of the structure is approximately 279 ft, and the curved length of girder G1 is 162 ft while the curved length of girder G6 is 141 ft. The concrete deck out-to-out dimension is 35.625 ft and the deck thickness is 8 inches. The bridge consists of 6 girder lines equally spaced at 6.125 ft, with all girders having a constant web depth of 68 inches. Girders and cross frames are fabricated from A709 Grade 50 steel.

In general, the cross frame spacing varies throughout the structure as shown in Figure 3.1, but near the mid-span of the structure the radial spacing remains fairly constant at 10.417 ft. Intermediate cross frames have an “X” type geometry consisting of two diagonals and a top and bottom chord. Two types of “X” type cross frames are used in the structure, Type I and Type II, as shown in Figure 3.3 and Figure 3.4, respectively. The Type II cross frame is used only at three locations, cross frames 12D, 12E, and 13C. The end diaphragms at the northern abutment (abutment 1) are 43 in. deep built-up plate I-girders, while the end diaphragms at the skewed abutment (abutment 2) are a “K” type cross frame consisting of a top and bottom chord, and diagonals which intersect at the bottom chord.

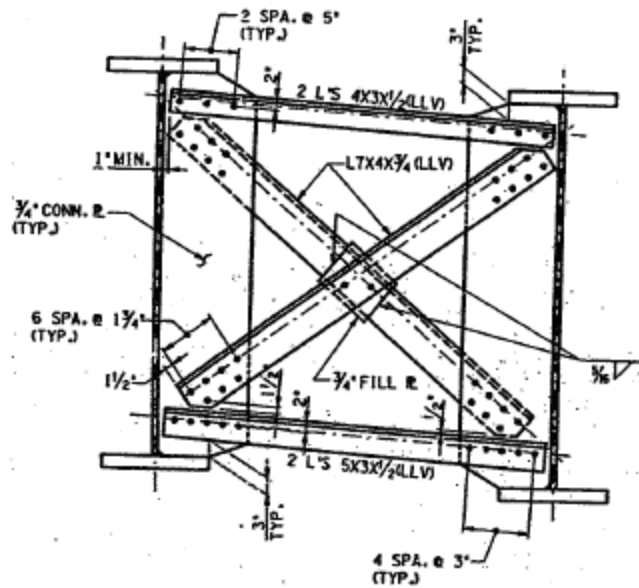


Figure 3.3 SR 8002 Ramp A-1 Type I Cross frame

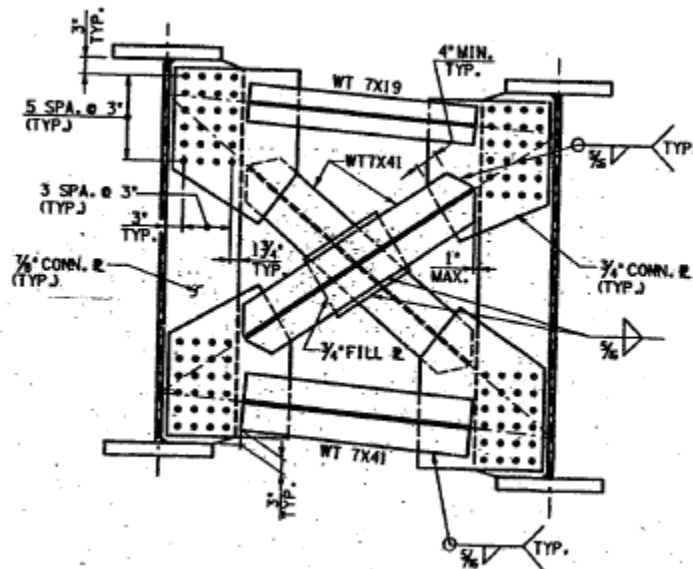


Figure 3.4 SR 8002 Ramp A-1 Type II Cross frame

For all of the girders, the web plate is a constant 9/16"x68" plate, while the top and bottom flange sizes vary throughout the span. The top and bottom flange sizes for all girders are as shown in Figure 3.5 and Table 3-1.

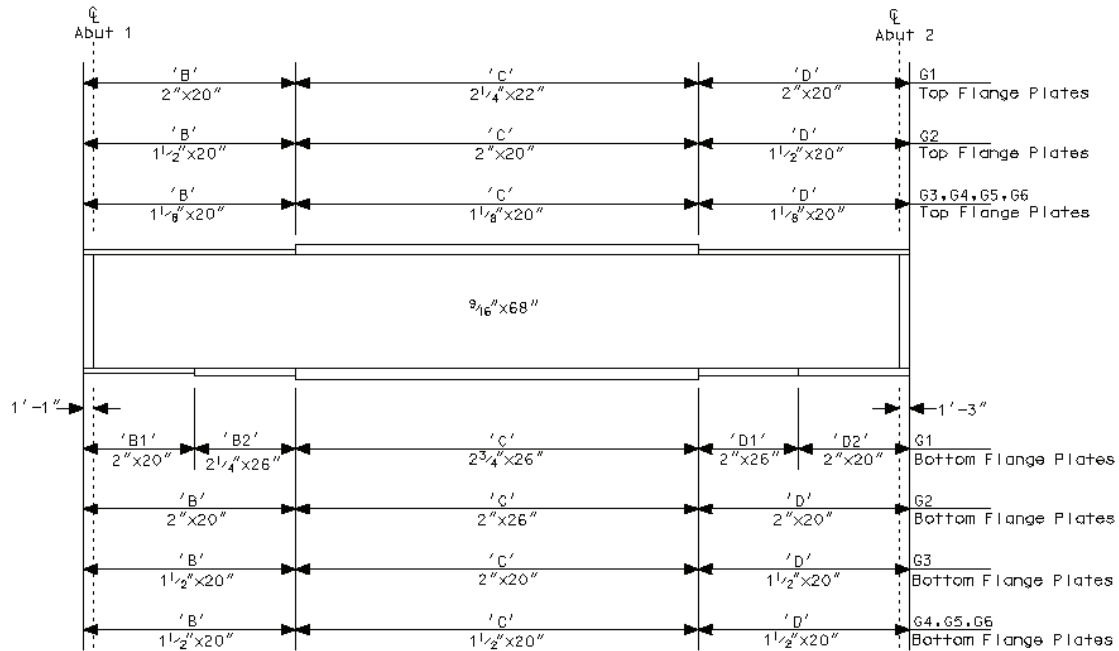


Figure 3.5 SR 8002 Ramp A-1 Girder Elevation

Table 3-1 SR 8002 Ramp A-1 Girder Dimensions for Figure 3.5

Girder	B	B1	B2	C	D	D1	D2
G1	30'-11"	11'-0"	19'-11"	84'-2"	28'-5 1/2"	18'-5 1/2"	10'-0"
G2	30'-3"	n/a	n/a	83'-5"	33'-6 3/8"	n/a	n/a
G3	39'-4"	n/a	n/a	73'-4"	38'-4 3/8"	n/a	n/a
G4	40'-10"	n/a	n/a	74'-4"	39'-11 1/8"	n/a	n/a
G5	46'-11"	n/a	n/a	68'-4"	44'-1 7/8"	n/a	n/a
G6	46'-5"	n/a	n/a	69'-3"	48'-4 1/2"	n/a	n/a

Furthermore, all full-depth transverse stiffeners in the SR 8002 Ramp A-1 structure are 1/2"x 7" plates, while bearing stiffeners at the abutments are 1"x10 1/2" plates for girder G1, and 3/4"x7 1/2" plates for girders G2 through G6. Pot bearings are used at all girder support locations; see Table 3-2 for the pot bearing layout.

**Table 3-2** SR 8002 Ramp A-1 Girder Dimensions for Figure 3.5

<b>Girder</b>	<b>Abutment 1</b>	<b>Abutment 2</b>
<b>G1</b>	Non-Guided Expansion Pot Bearing	Non-Guided Expansion Pot Bearing
<b>G2</b>	Fixed Pot Bearing	Longitudinally Guided Expansion Pot Bearing
<b>G3</b>	Fixed Pot Bearing	Longitudinally Guided Expansion Pot Bearing
<b>G4</b>	Fixed Pot Bearing	Longitudinally Guided Expansion Pot Bearing
<b>G5</b>	Non-Guided Expansion Pot Bearing	Non-Guided Expansion Pot Bearing
<b>G6</b>	Non-Guided Expansion Pot Bearing	Non-Guided Expansion Pot Bearing

### **3.1 SR 8002 RAMP A-1 FINITE ELEMENT MODEL**

A nonlinear finite element model of the SR 8002 Ramp A-1 structure is created to study the behavior of the bridge during steel erection. The commercial finite element program *ABAQUS* version 6.3 (*ABAQUS* 2001) is used for all modeling discussed herein. Since there was no field data obtained during the erection of the SR 8002 Ramp A-1 bridge, the finite element techniques used in this study had to be verified with results from a previous curved I-girder erection study. The verified finite element modeling techniques were subsequently applied to the SR 8002 Ramp A-1 bridge. Additionally, the results emanating from the SR 8002 Ramp A-1 finite element model for steel dead load application are compared to the actual design values for camber and reactions as a means of further model verification.

#### **3.1.1 Verification Study**

The experimental data from the Federal Highway Administration's (FHWA) Curved Steel Bridge Research Project (CSBRP) erection study ES1-4, as presented by Linzell (1999), is used as the basis for the verification of modeling techniques employed in the present study. The entire FHWA CSBRP experimental bridge is shown in Figure 3.6, however the CSBRP ES1-4

study only consisted of the two inner curved I-girders, G1 and G2. Both girders are 4 ft deep, with the outside girder, G2, having a radius of 200 ft and a curved length of 90 ft. The girders are spaced at approximately 8.75 ft, and connected by “K” type cross frames at each end (cross frames 1L and 1R), and at mid-span (cross frame 7).

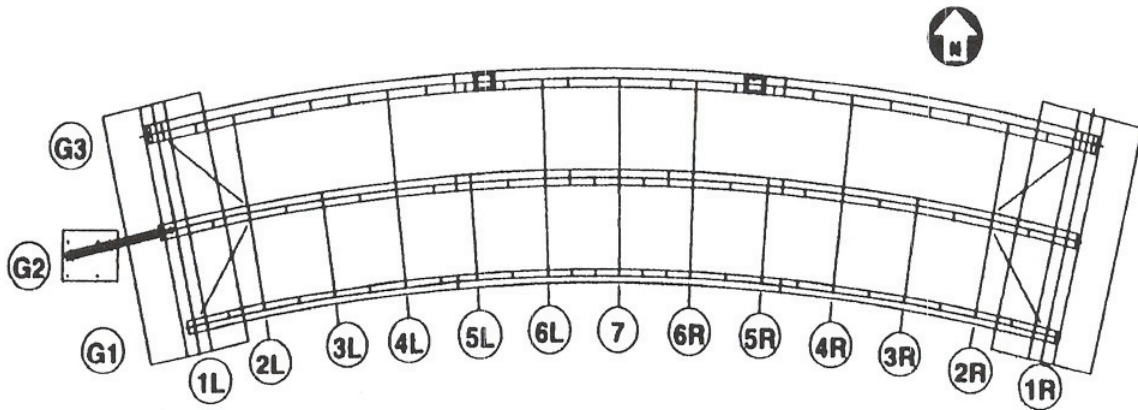


**Figure 3.6** CSBRP Experimental Bridge (Linzell 1999)

The CSBRP ES1-4 experimental study began with the structure in the no-load position. Shoring was placed below both girders at five locations along their lengths, not including the abutment supports. Shoring was then removed from below the inside girder, G1, except at mid-span. The mid-span shoring was then removed incrementally, as reactions and mid-span displacements were recorded.

A detailed nonlinear finite element model of the ES1-4 erection study is created as part of the current research, in order to validate modeling techniques to be used for simulating the construction of the SR 8002 Ramp A-1. The flanges, webs, and transverse stiffeners of both girders are modeled using ABAQUS S4R shell elements. A length to width aspect ratio of less than 2 to 1 is maintained for all shell elements. (Length for flanges is regarded as along the

tangential length of the flange; and length for the webs and stiffeners is considered to be the vertical length.)

The cross frames are modeled using ABAQUS B31 3-D beam elements. For simplicity, the cross frame connection plates (gusset plates) are not explicitly modeled. Instead, the cross frames are attached to the girders at their respective locations using ABAQUS multi-point constraint (MPC) TIE commands. The TIE constraint is used to enforce on a slave node all translations and rotations of a master node.

In addition to the prescribed boundary conditions, ABAQUS unidirectional GAP elements are used in the vertical directions at the abutments and shoring locations for both girders. The unidirectional GAP elements simulate a hard contact condition and thus permit the girders to lift-off the supports during the analysis, thus accommodating actual field response associated with the tendency of a curved I-girder to roll laterally.

The finite element model of the CSBRP ES1-4 experimental study considers nonlinear geometric effects, but does not consider material nonlinearity. Due to the geometric complexities of a curved I-girder, nonlinear geometric effects are considered germane to the proper analysis of this type of structure. Since this portion of the CSBRP structure was designed to remain elastic throughout all of the planned studies, nonlinear material effects are not considered in the verification analyses.

Self-weight of the girders and cross frames are the only loads considered in the verification study. A standard structural steel density of 490 lbs/ft<sup>3</sup> (7850 kg/m<sup>3</sup>) is applied to all girder shell elements. Cross frame weights are increased by 10% to account for gusset plate connections.

Favorable agreement is shown between the results of the experimental ES1-4 study presented by Linzell (1999) and the finite element results completed as part of the current study. The inside girder, G1, mid-span deflection / support reaction response, for both experimental and analytical studies is shown in Figure 3.7. Some of the disagreement in the plots may be due to discrepancies that occurred in the fabrication of the outside girder, G2. The outside girder was initially incorrectly cambered, and to correct the error and bring the girder back to the design camber, the girder was heated in a series of “V” heats along segments of the girder web. Correcting the camber resulted in transverse stiffeners that were slightly out-of-plumb, subsequently resulting in fit-up problems and minor forces that could not be measured (Linzell 1999).

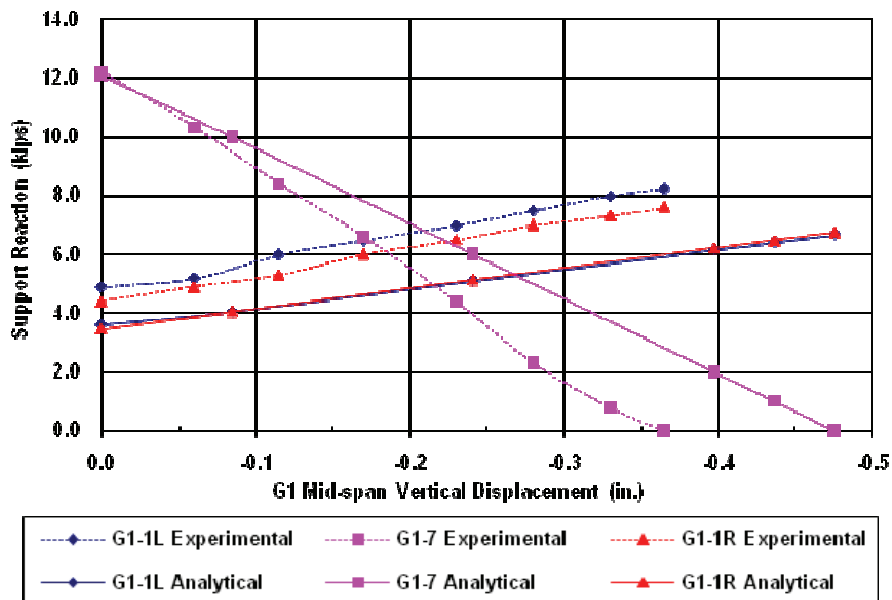


Figure 3.7 CSBRP ES1-4 Experimental Results (Linzell 1999) and Analytical Results

### 3.1.2 SR 8002 Ramp A-1 Finite Element Model

A detailed nonlinear finite element model is created to analyze the behavior of the SR 8002 Ramp A-1 steel superstructure during its construction as well as to illustrate the difference in cross frame dimensions resulting from inconsistent detailing methods. Most of the model preprocessing, such as node and element data, is carried out using Microsoft Excel spreadsheets, and then imported into ABAQUS input files. The model of the entire bridge uses approximately 148,000 elements with over 888,000 degrees of freedom. The modeling techniques used to create the SR 8002 Ramp A-1 finite element model are based on the same techniques utilized in the verification study.

Each of the six plate girders are discretized into meshes of shell elements placed along the middle surfaces of the plate components making up the plate girders. The *ABAQUS* S4R shell element (4-noded, reduced integration, shear deformable) is used for the flanges, webs, bearing and transverse stiffeners, and full-depth cross frame connection plates of each girder. The length to width aspect ratio for elements on any flange is approximately 1 to 1, while the length to width aspect ratio for web elements is 2 to 1. (Length for the flanges is regarded as along the tangential length of the flange; and length for the webs and stiffeners is considered to be the vertical length.) Shell element length to width ratios such as these have been validated by the verification study, as well as through additional research accomplished by the author in regard to the Ford City Veterans Bridge (Chavel and Earls 2001).

All of the cross frame members are modeled with *ABAQUS* B31 beam elements (2-noded, 3-D linearly interpolated isoparametric beams), irrespective of whether the member is part of an interior “X” type cross frame or a “K” type cross frame at abutment 2. Six B31 beam elements in all are used to model the “X” type cross frames, one each for the top and bottom

chords, and 2 each for both diagonals due to the bolted connection at the middle of the “X.” Five B31 beam elements in all are used to model the “K” type cross frames at abutment 2, one element for the top chord, one element for each diagonal, and two elements for the bottom chord due to the intersection with the diagonals. At abutment 1, a single B31 beam element in between each girder is used to model the 43 inch deep end diaphragm. Appropriate cross-sectional properties are input for each cross frame beam element section, such as moment of inertia and cross-sectional area.

Figure 3.8 shows the finite element model of SR 8002 Ramp A-1 in plan view and an elevation view of the finite element view looking in from the skew end of the structure. Figure 3.9 illustrates the mesh density employed for all of the girders in the structure.

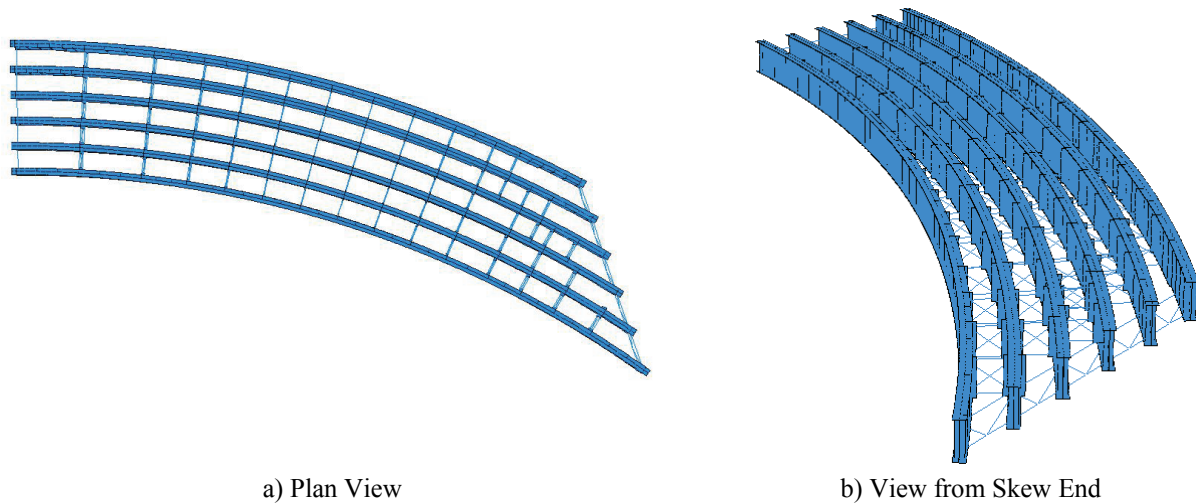


**Figure 3.8** SR 8002 Ramp A-1 FEM

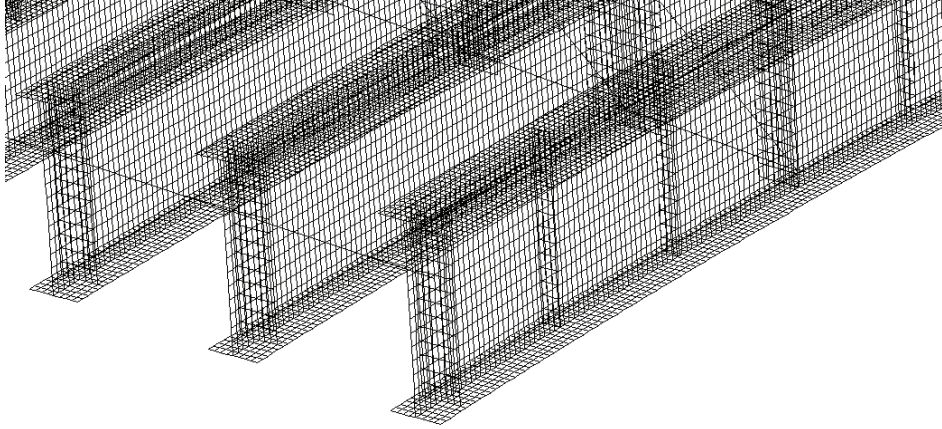


**Figure 3.9** SR 8002 Ramp A-1 FEM Mesh Density

The cross frame members are attached to the girders using the *ABAQUS* multi-point constraint (MPC) TIE and LINEAR commands. The TIE constraint is used to enforce on a given slave node all translations and rotations of a given master node, and the LINEAR constraint is used when a slave node (Figure 3.10 node ‘p’) must lie along a line defined by two master nodes (Figure 3.10 nodes ‘a’ and ‘b’). Furthermore, in the finite element model, the cross frames are attached to the girders at the work-points specified in the design and fabrication drawings and not at the flange-web junction. The cross frames and girders used in every model for the current research are proportioned for the web-plumb position at the no-load state of stress.

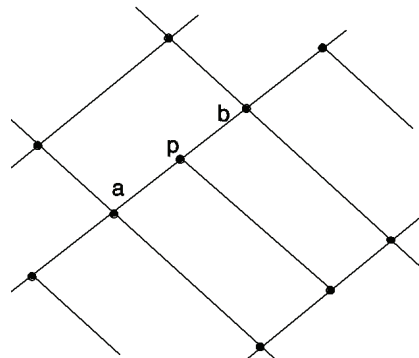


**Figure 3.10** MPC LINEAR constraint (*ABAQUS* 2001)

At the abutment support locations, *ABAQUS* unidirectional GAP elements are used, with the bottom end restrained in the vertical direction. The unidirectional GAP elements permit the consideration of classic Hertzian hard contact effects and thus allow the bridge girder to lift-off the supports during analysis; as they would be able to during the construction of the bridge in the field. Where applicable, additional boundary conditions in the longitudinal and lateral directions are applied to the girder nodes at the supports in order to simulate the fixed and longitudinally guided pot bearings used in the structure.

The loads implemented in this study consist of the self-weight of the steel superstructure components only. A standard steel density of 490 lbs/ft<sup>3</sup> (7850 kg/m<sup>3</sup>) is used for all of the girder components and cross frame members.

The finite element model of the SR 8002 Ramp A-1 considers nonlinear geometric effects, but does not consider material nonlinearity. Due to the geometric complexities of a curved I-girder, nonlinear geometric effects are deemed to be important and thus considered in the analysis. However, given that the steel superstructure is designed to remain elastic throughout the bridge erection, effects of nonlinear material properties are not considered in the erection staging analysis.

### **3.2 INCONSISTENT DETAILING AND SR 8002 RAMP A-1**

In most cases of inconsistent detailing, girders are detailed to have their webs vertically plumb at the beginning of construction, and cross frames are fabricated so that the webs of the girders are vertically plumb after steel erection (Detail Method 3, Section 2.4.3). This case of inconsistent

detailing occurred in the SR 8002 Ramp A-1 structure. For “X” type cross frames, like those used in SR 8002 Ramp A-1, inconsistent detailing leads to diagonal members that are either too long or too short to fit into girders detailed to be vertically plumb at the no-load state of stress. The amount that the cross frames and girders are misaligned due to inconsistent detailing is directly dependent on the displacement due to steel dead load. Therefore, the larger the structure and subsequent steel dead load deflection, the larger the misalignments due to inconsistent detailing.

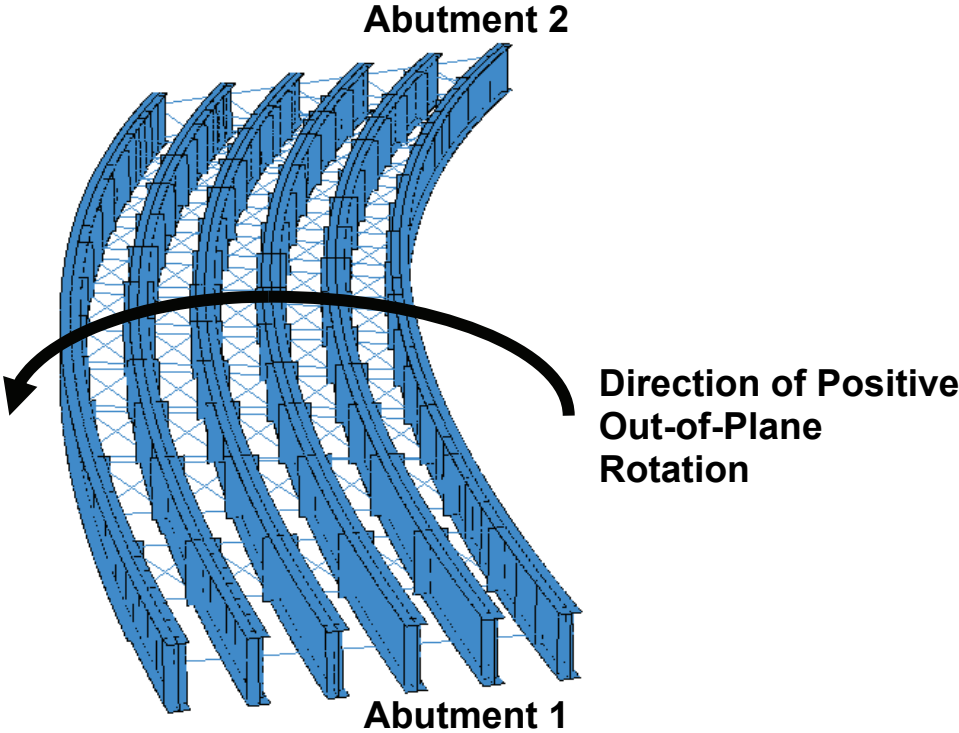
This section will discuss the steel dead load displacements of the SR 8002 Ramp A-1 finite element model with the girders and cross frames detailed for the web plumb position at the no-load condition. The steel dead load displacements are then used to determine cross frame member lengths for the web plumb position at the steel dead load condition. These cross frame member lengths are then compared to cross frame member lengths for girders and cross frames detailed for the girder web plumb position at the no-load state of stress.

### **3.2.1 Steel Dead Load Effects**

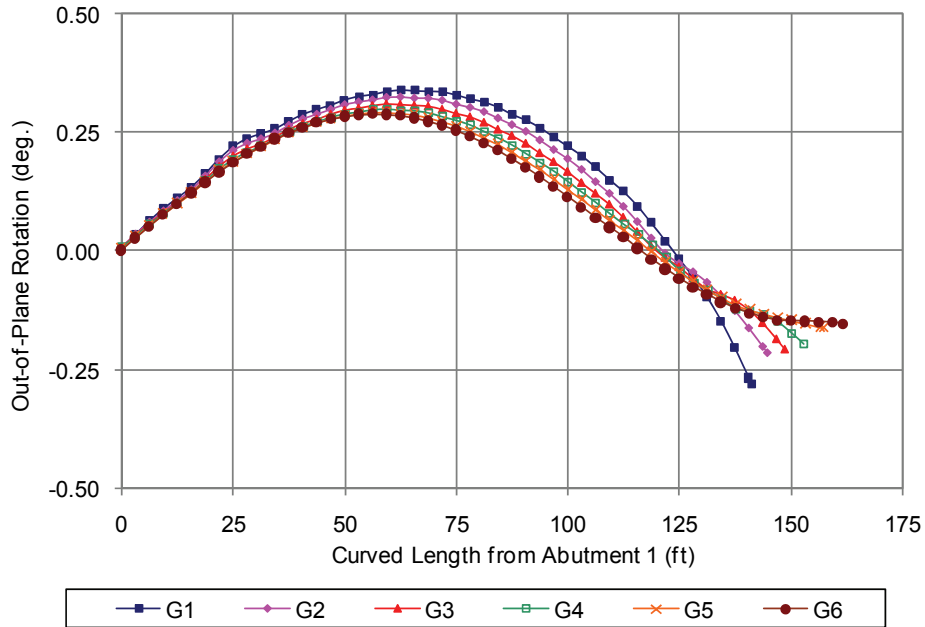
A complete horizontally curved steel I-girder superstructure will displace in the vertical direction and rotate in the out-of-plane direction upon load application. For the current discussion a positive out-of-plane rotation is defined as shown in Figure 3.11. Therefore, the expected out-of-plane rotation for a typical curved steel I-girder structure would be considered positive. Also, the out-of-plane displacement is to be considered positive when the displacement is towards the outer-most girder.

Figure 3.12 shows the out-of-plane rotation due to steel dead load for SR 8002 Ramp A-1. The structure undergoes and almost entirely positive out-of-plane rotation due to steel dead

load; however the skew at the abutment 2 end induces a negative out-of-plane rotation near the abutment 2 end, as shown in Figure 3.12. Furthermore, in the simple half nearer the skew end span, the skew also causes the positive out-of-plane rotation to vary slightly from girder to girder. In a non-skewed curved I-girder bridge, the out-of-plane rotation would be expected to be equal from girder to girder across the span.



**Figure 3.11** Direction of Positive Out-of-Plane Rotation



**Figure 3.12** Ramp A-1 FEM Out-of-Plane Rotation due to Steel Dead Load

Figure 3.13 shows that the out of-plane displacement for the SR 8002 Ramp A-1 structure due to steel dead load. It can be seen that the top flange for each girder displaces out-of-plane more than the bottom flange, leading to the out-of-plane rotation shown Figure 3.12. Again, in the case of SR 8002 Ramp A-1, the skew end causes an out-of-plane displacement in the opposite direction to the out-of-plane displacements caused by the horizontal curve. The vertical displacement caused by steel dead load is shown in Figure 3.14. As to be expected in a horizontally curved I-girder structure, the largest vertical displacement occurs at the outside girder, G1.

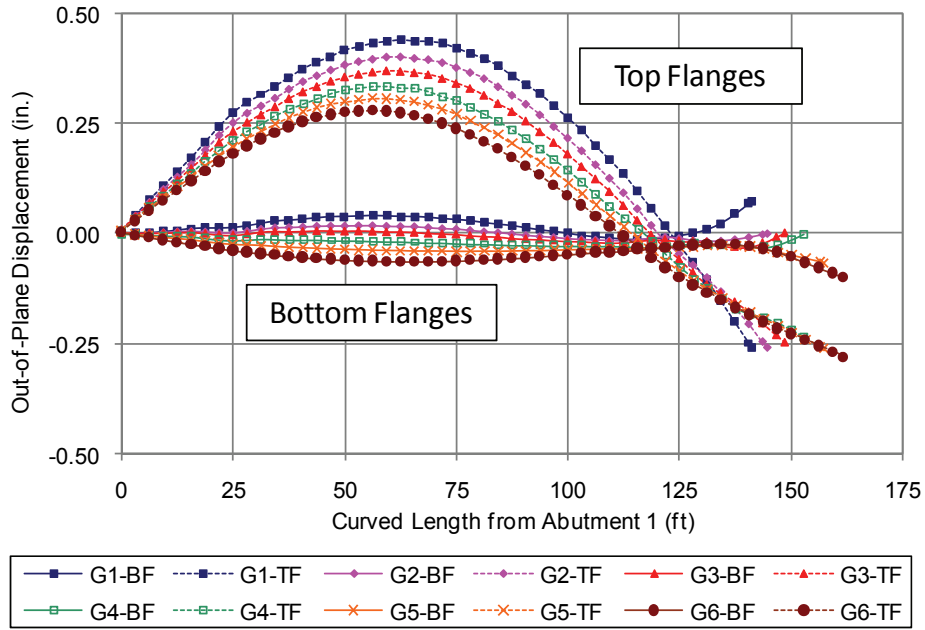


**Figure 3.13** Ramp A-1 FEM Out-of-Plane Displacement due to Steel Dead Load

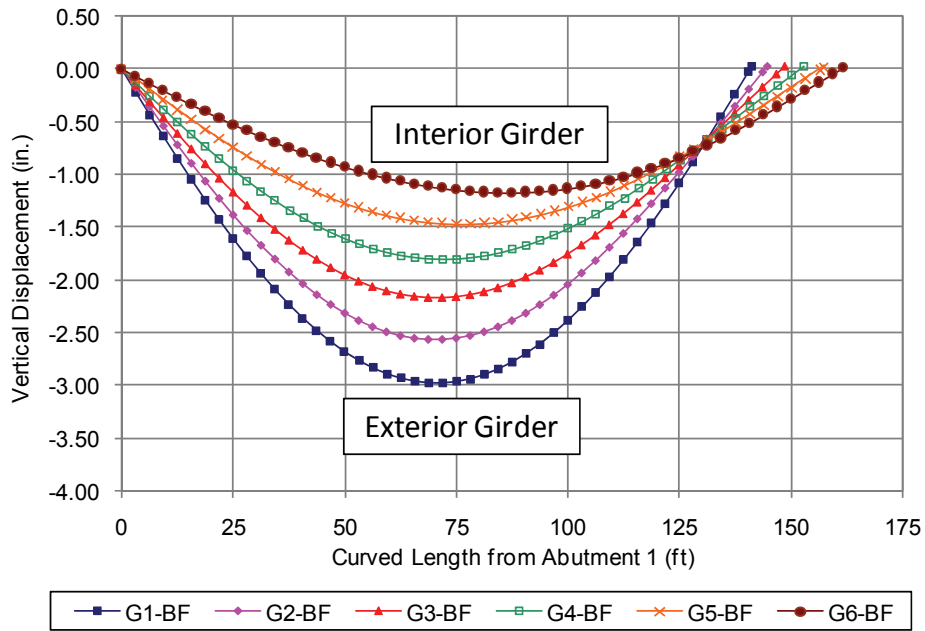


**Figure 3.14** Ramp A-1 FEM Vertical Displacement due to Steel Dead Load

### 3.2.2 Cross Frame Member Lengths

The cross frames in the SR 8002 Ramp A-1 bridge are fabricated for the web-plumb condition at steel dead load, while the girders are fabricated to be web-plumb at the no-load condition, otherwise known as inconsistent detailing (Detail Method 3, Section 2.4.3). Detailing in this manner results in diagonal members that are either too long or too short to fit-up with girders detailed for web-plumb at the no-load condition. These diagonal misalignments are shown in a general sense in Figure 3.15. Member 'F' detailed for web-plumb at steel dead load is too long to fit into the girders detailed for web-plumb at no-load. On the other hand, member 'M' detailed for web-plumb at steel dead load is too short to fit properly into girders detailed for web-plumb at no-load.

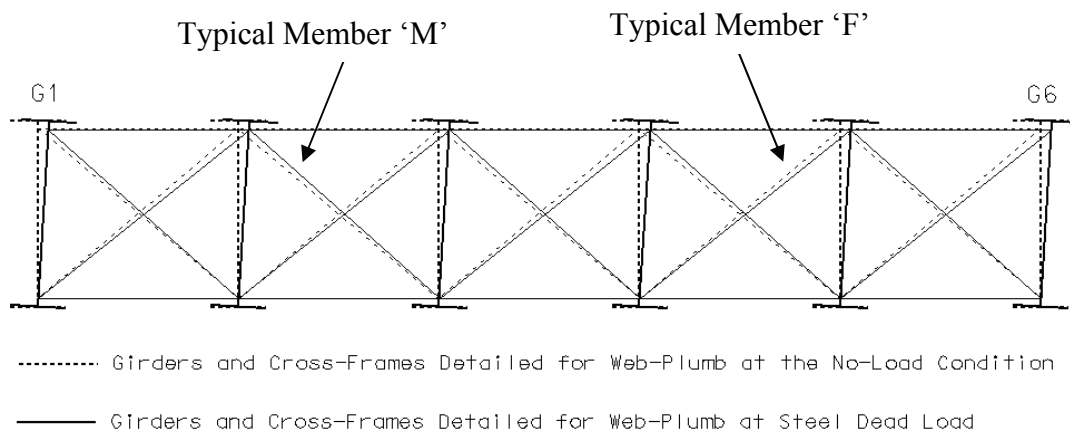


**Figure 3.15** Comparison of Diagonal Cross Frame Members for Different Detailing Methods

In the case of SR 8002 Ramp A-1, the misalignments due to inconsistent detailing are not extremely large. For example, considering the cross frame line 6 near the mid-span of the curve, the difference between diagonals detailed for web-plumb at no-load and diagonals detailed for web-plumb at steel dead load is 0.27 inches. See Table 3-3 for details. Results for all other cross

frame locations are similar although have smaller magnitudes; these can be found in the research report for the investigation of SR 8002 Ramp A-1 (Chavel and Earls 2004).

In the case of SR 8002 Ramp A-1, the girders are only 68 inches deep, and the average span length is 150 ft, therefore the steel dead load and hence the vertical deflections due to steel dead load are not very large. Furthermore, the differential vertical deflection between adjacent girders near the mid-span is only approximately 0.50 inches (see Figure 3.14). Since the driving issues behind cross frame misalignments due to inconsistent detailing are steel dead load vertical deflections and the differential deflection between adjacent girders, the maximum diagonal misalignment of approximately 0.27 inches is reasonable.

Since the differential deflection between adjacent girders varies throughout the span length, so too does the cross frame diagonal member misalignment when inconsistent detailing occurs. Figure 3.16 shows the cross frame diagonal member length difference for cross frame line 'A' in SR 8002 Ramp A-1 due to inconsistent detailing. From the North (non-skew) end to approximately 120 ft along the SR 8002 Ramp A-1 structure, horizontal curve effects control the differential deflections and hence the cross frame diagonal misalignments. However, from 120 ft to the South end of the structure, the skew effects control the differential deflection, "reversing" the effect of inconsistent detailing: diagonal member 'M' becomes too long and member 'F' becomes too short. While all cross frame lines show a similar behavior, cross frame line A has the most pronounced effect due to skew while cross frame line E has greater inconsistencies due to the horizontal curve.

**Table 3-3** Differences in Diagonal Member Lengths at Cross Frame Line 6

Cross frame	Detailed Condition	Diagonal Member Lengths (inches)	
		F	M
6A	Web-Plumb at No-Load	89.93	96.27
	Web-Plumb at Steel Dead Load	90.14	96.04
	Difference	0.21	-0.23
6B	Web-Plumb at No-Load	89.93	96.28
	Web-Plumb at Steel Dead Load	90.14	96.04
	Difference	0.21	-0.24
6C	Web-Plumb at No-Load	89.86	96.35
	Web-Plumb at Steel Dead Load	90.08	96.11
	Difference	0.22	-0.24
6D	Web-Plumb at No-Load	90.28	95.88
	Web-Plumb at Steel Dead Load	90.51	95.63
	Difference	0.23	-0.25
6E	Web-Plumb at No-Load	89.75	96.47
	Web-Plumb at Steel Dead Load	90.00	96.20
	Difference	0.25	-0.27

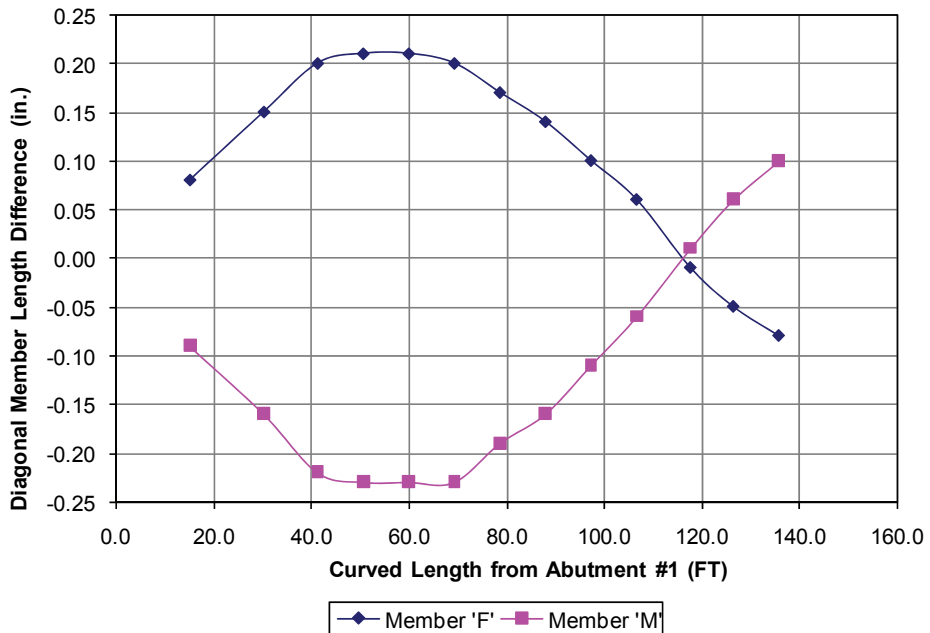


**Figure 3.16** Cross Frame Line A – Difference in Diagonal Member Lengths due to Detailing

### **3.2.3 Consequences of Inconsistent Detailing**

Due to the fact that inconsistent detailing results in cross frame diagonal members that are too long or too short to fit-up properly with the girders, significant construction difficulties can arise. The girders and cross frames in the bridge have to be forced into place during steel erection because of the misalignments that inconsistent detailing creates. The structure will become increasingly difficult to erect as the misalignments, due to inconsistent detailing, become larger.

In the case of SR 8002 Ramp A-1, the misalignments due to inconsistent detailing are generally small, with a maximum cross frame misalignment of 0.27 inches. It was noted that during steel erection of SR 8002 Ramp A-1, cross frame misalignments related to the inconsistent detailing did not produce significant difficulties during steel erection. This can be attributed to the fact that the misalignments were small, and the girders in the structure have a relatively small web depth and spacing, and therefore could be manipulated with relative ease in the field.

For comparison, in the case of the Ford City Veterans Bridge, it was determined that cross frame misalignments of approximately 1.25 inches occurred near the mid-span of the curved section (Chavel 2001). This misalignment, coupled with the fact the girders were approximately 14 ft deep and spaced at 13.5 ft, with a span length of 322 ft, led to significant steel erection problems. During steel construction, there were problems not only aligning girders and cross frames, but also in aligning the field splices. The problems during steel erection could be directly attributed to the inconsistent detailing and not the chosen erection sequence (Chavel 2001).

### 3.3 ANALYTICAL STUDY OF SR 8002 RAMP A-1 STEEL ERECTION

The nonlinear finite element model of SR 8002 Ramp A-1 is used to recreate the as-built and intended erection sequences. The as-built and intended erection sequences differ with regard to the sequencing of the releasing of cranes holding the girders during erection, as well as some slight differences in the sequence of components being placed towards the end of the steel erection plan. The steel erection of SR 8002 Ramp A-1 was completed without any field data being recorded, and therefore, quantitatively, no basis of comparison exists for the as-built and analytical erection sequences. However, discussions with personnel at the job site have provided details with regard to the as-built erection of the actual structure.

As is typically the case, erection began with the most outside girder, G1, and progressed inward to the innermost girder, G6. The field-splice for each girder was completed on the ground with the girder blocked to its correct no-load camber. Each complete girder was erected and placed on the abutments; temporary supports were not used for the erection of the structure. Temporary tie-downs in the form of a 6-ton come-along at each abutment for girder G1, were used during the steel erection of the structure. Additionally, two 130 ton lifting cranes, a 60 ton holding crane, and a boom truck were employed during the steel erection of SR 8002 Ramp A-1.

The steel erection began with girders G1 and G2 being placed, where G1 would be held with the 60 ton holding crane, while G2 is held in place with the two 130 ton lifting cranes. The boom truck is then used to erect cross frames at the abutments and at four intermediate locations. At this time, the intended erection sequence guidelines stated that all of the cranes could be released, however, in the field it was realized that the girders would become unstable. Therefore, the holding crane attached to girder G1 had to be kept in place. In fact, this holding crane was kept in place throughout the erection of the first four girders as a result of instability in the sub-

assemblage. This instability in the field will be shown in the results on the analytical study of the erection sequence discussed in this section.

For every stage of the analytical erection sequence, displacements, abutment reactions, crane loads, and steel stresses are monitored. The analytical erection sequence follows the erection sequence that was employed in the field during the actual construction of SR 8002 Ramp A-1. Practically every erection stage is analyzed in three different variations when reasonable, one where all cranes are assumed to be present, one where only a holding crane is assumed to be present, and one where no cranes are assumed to be present. Completing the analysis in this manner allowed for the investigation and comparison of the as-built and intended erection sequences. Several of the as-built construction stages are discussed in this section, however all of the results for each stage of erection can be found in Appendix B.

### **3.3.1 As-built Erection Sequence Study**

This section will describe selected stages from the as-built construction analytical results. Appendix B contains analytical results for those stages not discussed in this section. The placement of structural components in the finite element model follows exactly the order employed in the field during steel erection. A naming convention for each construction stage is adopted for the current report; where:

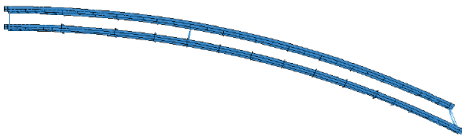
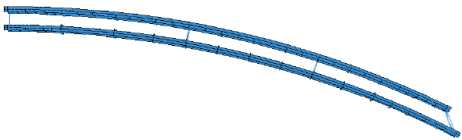
- The first numeric value indicates the most recent erected girder;
- The alphabetical descriptor indicates a particular set of cross frames placed;
- The second numeric value describes the set of boundary conditions employed in the finite element model to investigate various crane applications.

For example considering stage 4c1:

- The number '4' indicates that girder G4 is the most recent erected girder;
- The letter 'c' designates the particular group of cross frames that are erected, in this case cross frames 7C and 9C;
- The number '1' indicates the variation in boundary conditions simulating the cranes, in this case only the holding crane is assumed in the finite element model.

This naming convention is described in Table 3-4 for the as-built erection sequence. Note that in some cases a variation in the boundary conditions (holding and lifting cranes) is investigated for several of the construction stages. Furthermore, the letter 'F' prior to the stage description indicates that particular stage is part of the as-built sequence that deviates from the intended erection sequence (stages F6a through F6f1).

**Table 3-4** As-built Analytical Erection Sequence Naming Convention

Stage	Component Added <sup>1</sup>	Cranes		Plan
		Holding	Lifting	
1	G1	none	G1	 
<p style="text-align: right;">photo at right →</p> <p>erection of G1 using two lifting cranes each having a spreader beam resulting in 4 lift points as indicated on the plan finite element model image (above)</p>				
2	G2	G1	G2	 
<p style="text-align: right;">photo at right →</p> <p>Erection of G2 showing two lifting cranes (yellow, behind girders) and holding crane (white, in foreground) attached to G1</p>				
2a	1E & 19E	G1	G2	
2b	5E	G1	G2	
2c	9E	G1	G2	

<sup>1</sup>Gx = Girder x where x is numbered 1 through 6

<sup>1</sup>cross braces are numbered left to right (North to South) and lettered such that brace A is between G5 and G6; B between G4 and G5; C between G3 and G4; D between G2 and G3; and, E between G1 and G2.

\* noted stages are discussed more fully in subsequent sections. All stages are summarized in Appendix B.

Table 3-4 (continued)

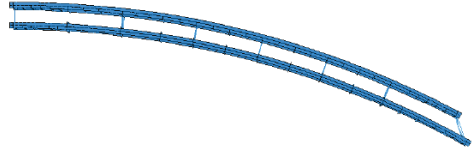
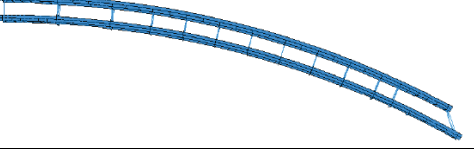
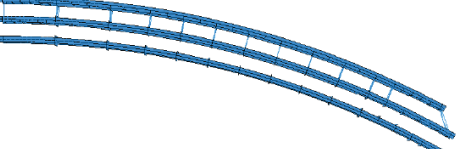
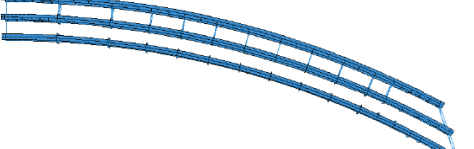
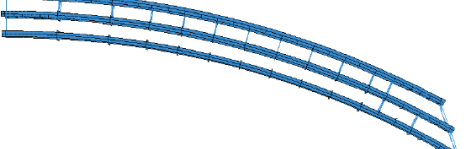
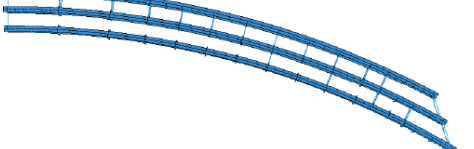
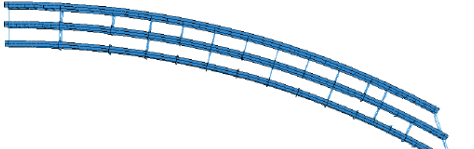
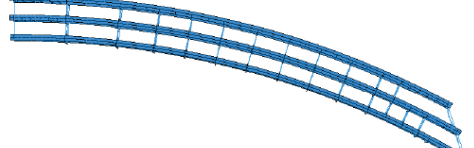
Stage	Component Added <sup>1</sup>	Cranes		Plan
2d	3E, 7E & 11E	G1	G2	
*2e	2E, 4E, 6E, 8E, 10E & 12E	G1	G2	
*2e1	none	G1	none	
3	G3	G1	G3	
3a	1D & 19D	G1	G3	
3b	12D & 14D	G1	G3	
*3c	8D & 10D	G1	G3	
*3c1	none	G1	none	
3d	2D, 4D & 6D	G1	G3	
3d1	none	G1	none	
3e	3D, 5D, 7D, 9D, 11D & 13D	G1	G3	
*3e1	none	G1	none	

Table 3-4 (continued)

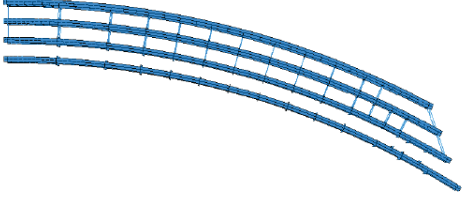
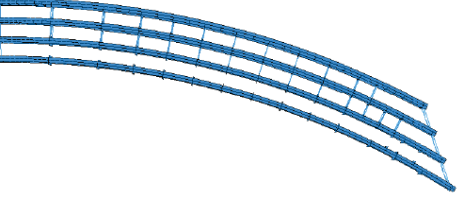
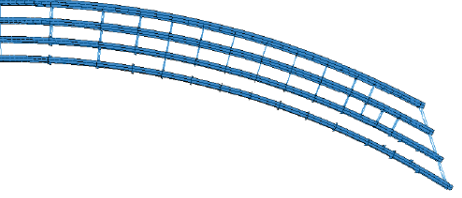
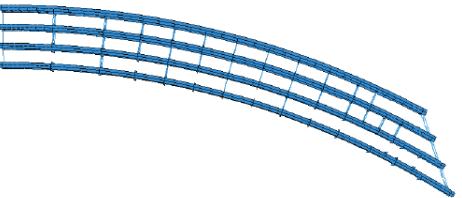
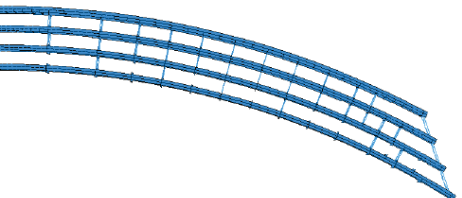
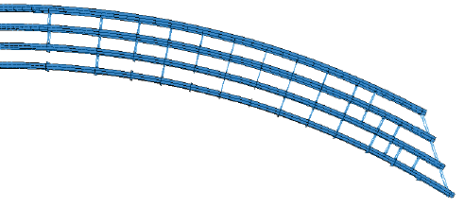
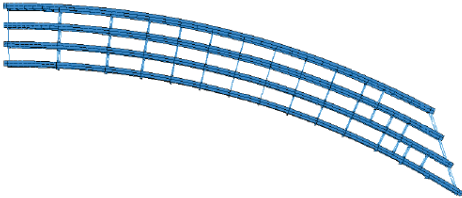
Stage	Component Added <sup>1</sup>	Cranes		Plan
4	G4	G1	G4	
4a	1C & 19C	G1	G4	
4b	3C & 5C	G1	G4	
4c	7C & 9C	G1	G4	
*4c1	none	G1	none	
4d	13C & 15C	G1	G4	
4d1	none	G1	none	
4e	10C, 11C, 14C & 16C	G1	G4	
4e1	none	G1	none	
4f	2C, 4C, 6C & 8C	G1	G4	
4f1	none	G1	none	

Table 3-4 (continued)

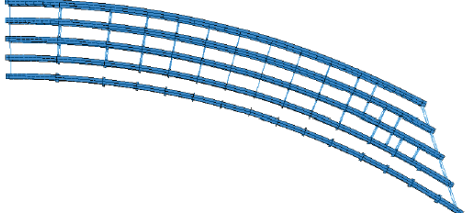
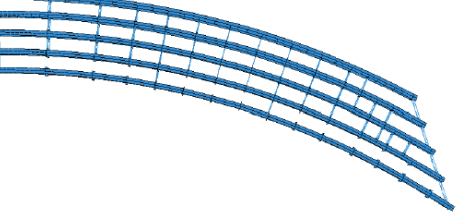
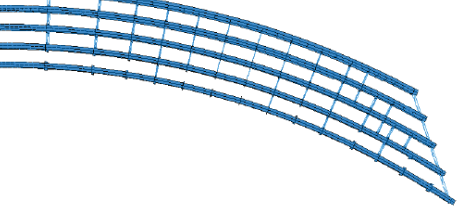
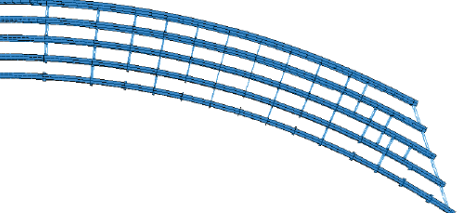
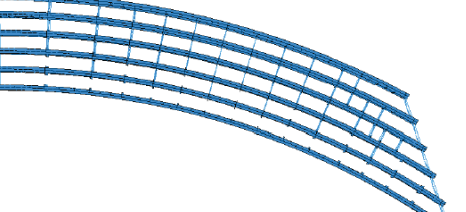
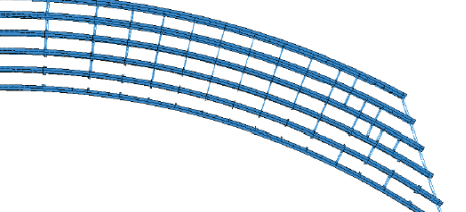
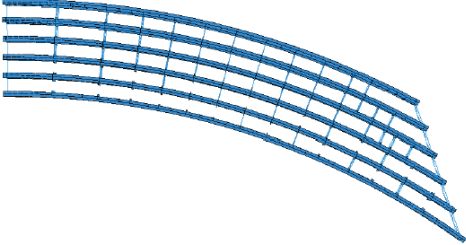
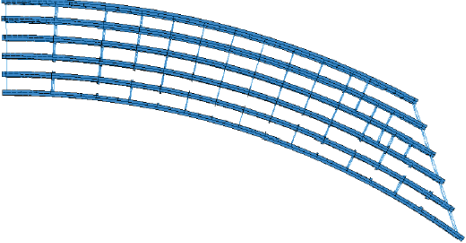
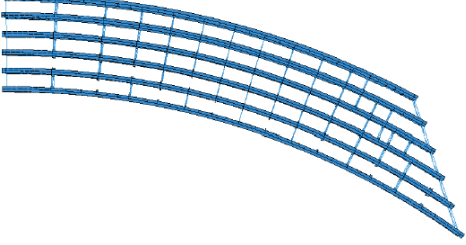
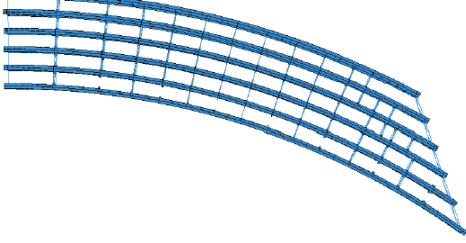
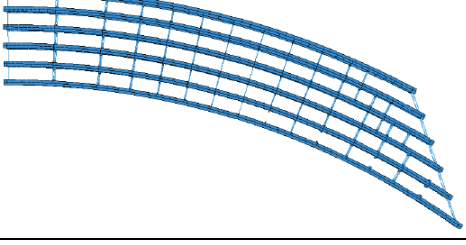
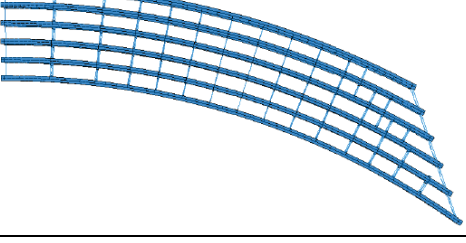
Stage	Component Added <sup>1</sup>	Cranes		Plan
5a	G5, 1B & 19B	G1	G5	
5b	5B & 9B	G1	G5	
5c	11B & 15B	G1	G5	
*5c1	none	G1	none	
*5c2	none	none	none	
5d	3B & 7B	G1	G5	
5d1	none	G1	none	
5d2	none	none	none	
F6a	G6	none	G6	
F6b	13A & 17A	none	G6	

Table 3-4 (continued)

Stage	Component Added <sup>1</sup>	Cranes		Plan
*F6c	8A & 10A	none	G6	
*F6c1	none	none	none	
F6d	2A, 4A & 6A	none	G6	
F6d1	none	none	none	
F6e	8B, 10B, 13B & 17B	none	G6	
F6e1	none	none	none	
F6f	2B, 4B & 6B	none	G6	
*F6f1	none	none	none	
*6d2	3A, 5A & 7A	none	none	
6e2	9A, 11A, 15A & 18A	none	none	

### 3.3.2 Construction Stage 2e and 2e1

The remaining cross frames between girders G1 and G2 are placed as construction stage 2e. Cross frames 2E, 4E, 6E, 8E, 10E, and 12E are placed in to the finite element model for this construction stage. All three cranes, the holding crane attached to G1, and the two lifting cranes attached to girder G2 are still in place for this stage of construction. The plan view of the finite element model at this stage of construction is shown in Table 3-4.

This construction stage is analyzed for three different sets of boundary conditions:

1. all three cranes are attached to the girders
2. the two lifting crane boundary conditions are removed from girder G2 and the holding crane boundary condition on girder G1 remains (construction stage 2e1)
3. all crane boundary conditions are removed

A modeling strategy such as this is followed in order to investigate what had occurred in the field, boundary condition sets 1 and 2, and then what had been intended in the erection guidelines, boundary condition set 3.

For the finite element model with all three cranes attached to the girders, it is found that the vertical and out-of-plane displacements are no greater than 0.05 in. There is little change in the structure's behavior from the previous construction stage, other than the fact the out-plane displacement for both girders are equal throughout the span. A maximum von Mises stress of 1.6 ksi occurs in the top flange of girder G1 at this stage of construction.

When the boundary conditions representing the two lifting cranes attached to girder G2 are released (construction stage 2e1), the vertical and out-of-plane displacements of girder G2 increase substantially. As shown in Figure 3.17a, girder G2 displaces vertically 0.25 in. while the vertical displacement of girder G1 is limited due to the holding crane. Furthermore, the

holding crane causes the girders to rotate towards the inward side of the curve, where the maximum top flange out-of-plane displacement for both girders is approximately 0.17 in. Figure 3.17b displays the girder out-of-plane displacement for construction stage 2e1.

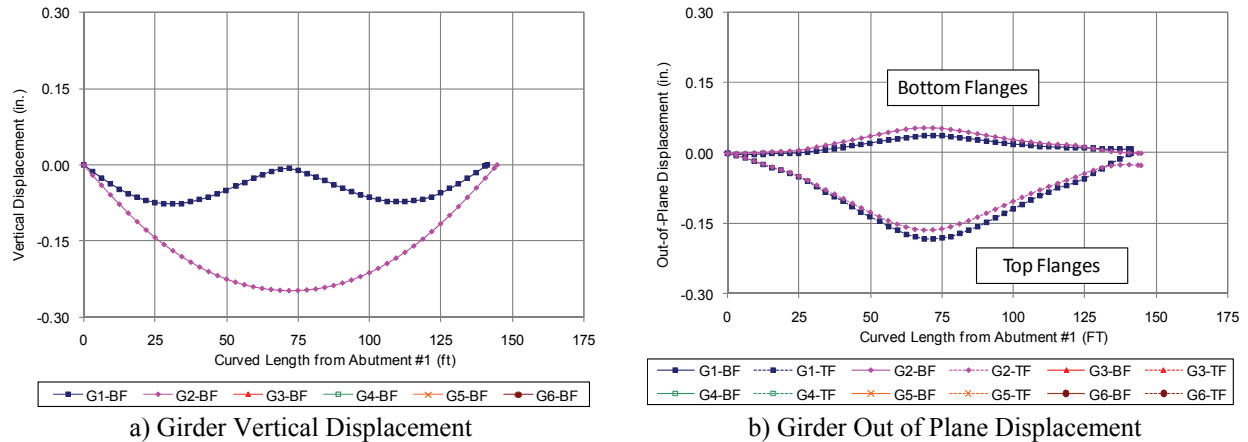


**Figure 3.17** Construction Stage 2e1

For construction stage 2e1, the maximum von Mises stress that manifests in the girders is approximately 2.0 ksi in the top flange of girder G2 at mid-span. The maximum von Mises stress induced in girder G1 is 1.8 ksi and occurs in the top flange near the one-quarter and three-quarter points of the span.

With the release of the two lifting cranes from girder G2, the girder reactions for both girders at both abutments increase. At the same time, the reaction provided by the holding crane attached to girder G1 increases to approximately 72 kips. Table 3-5 shows the reactions at both abutments and the loads assumed by the cranes for each stage of construction up to the current stage.

It is stated in the erection guidelines that the holding crane could have been released prior to this construction stage. However, when the holding crane boundary condition is removed from girder G1, the finite element model predicts that the structure would become unstable.

Similar to previous construction stages with all cranes released, girder G2 would completely uplift from the abutment supports, and all load is transferred to girder G1. The resulting tie down force is too large (27 kips) for the tie downs used in the actual erection (12 kips capacity), and the assembly would roll off of the abutments. It had been realized that the structure would become unstable in the field during construction if the holding crane was removed from girder G1. Therefore, the holding crane was left attached to G1 beyond the erection of girders G1 and G2.

**Table 3-5** Reactions – Construction Stage 1 to Stage 2e1

Location	Construction Stages							
	1	2	2a	2b	2c	2d	2e	2e1
	<b>Reactions (kips)</b>							
<b>G1 Abut 1</b>	4.80	13.69	13.75	12.65	12.58	13.98	14.66	24.94
<b>G1 Abut 2</b>	4.75	13.59	17.10	16.02	15.57	16.51	17.28	31.49
<b>G2 Abut 1</b>	-	4.29	4.35	4.24	4.27	2.38	1.92	13.66
<b>G2 Abut 2</b>	-	4.57	2.52	3.08	2.56	1.56	1.29	11.50
<b>G1 Holding Crane</b>	-	49.95	49.50	48.90	48.41	49.35	50.81	72.15
<b>Lifting Crane 1</b>	33.86	29.89	29.87	33.65	32.68	33.52	34.50	-
<b>Lifting Crane 2</b>	33.80	28.51	28.55	27.82	30.98	31.89	33.27	-

**3.3.3 Construction Stage 3c**

Cross frames 8D and 10D are placed between girders G2 and G3 as part of construction stage 3c. Cross frames 12D and 14D, as well as cross frames at the abutments, between girders G2 and G3 have already been placed in previous construction stages. Table 3-4 illustrates the finite element model of SR 8002 Ramp A-1 at construction stage 3c. At this point in the construction

sequence, boundary conditions are used to simulate the holding crane attached G1, and the lifting cranes attached to G3.

Due to the support provided by the cranes, the vertical and out-of-plane displacements are relatively small, not more than 0.1 in. It is interesting to note the out-of-plane displacement shown in Figure 3.18b. It is evident that the placement of cross frames on the abutment 2 side of the structure causes the out-of-plane displacements to be similar for all 3 girders. While on the abutment 1 side, where cross frames only connect girders G1 and G2, the out-of-plane displacement are not similar.

A maximum von Mises stress of 2.1 ksi occurs in the top flange and web of girder G1, near the location of the holding crane at mid-span. The von Mises stress that occurs in girders G2 and G3 is less than 1.0 ksi.

In regard to reactions, the cranes are subjected to a large share of the load, where as the lifting crane nearest abutment 1 would have a 27 kips load, the lifting crane nearest abutment 2 would have a 44 kips load, and the holding crane attached to G1 is predicted to have 73 kips load. Furthermore, girder G1 has the largest abutment reactions, where the reaction at abutment 1 is 18 kips and the reaction at abutment 2 is 26 kips.

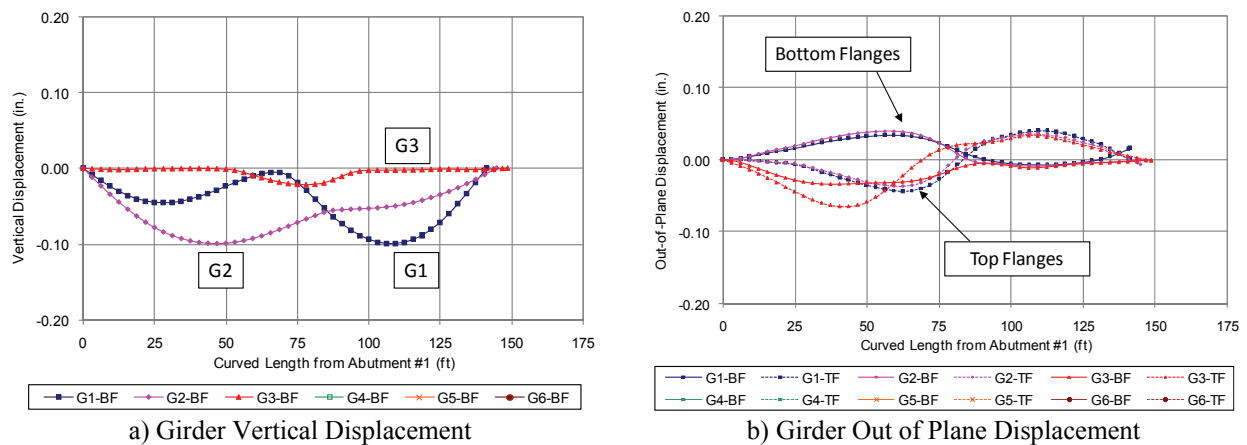
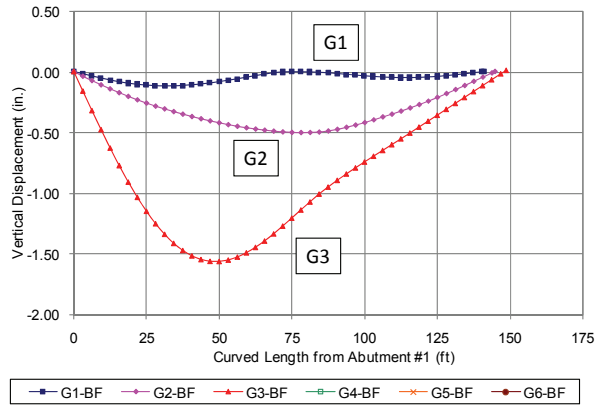


Figure 3.18 Construction Stage 3c

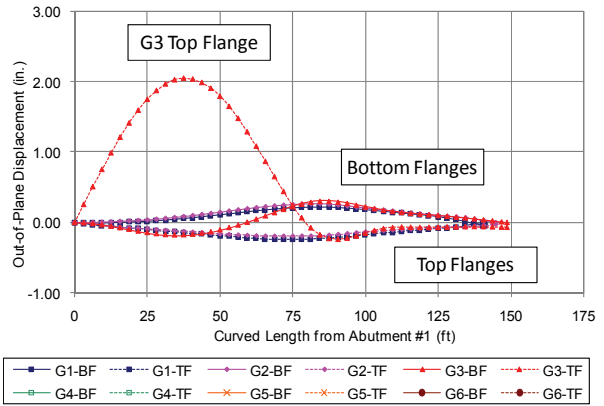
### 3.3.4 Construction Stage 3c1

Construction stage 3c1 consists of the same structure assembly as construction stage 3c, however the only differences is the release of the boundary conditions simulating the lifting cranes attached to G3. In the field, the releasing of the lifting cranes was attempted, however the structure was found to be somewhat unstable, therefore the lifting cranes were not removed. The results in this section will show that some significant displacements result from the release of the lifting cranes alone.

Based on the finite element model results, the vertical and out-of plane displacements of girder G3 increase significantly due to the removal of the lifting crane boundary conditions. This holds especially true for the abutment 1 side of girder G3, where there are no cross frames connecting it to the rest of the structure. Girder G3 experiences a 1.5 in. vertical displacement, as shown in Figure 3.19a, which is a significant increase from the 0.1 in. vertical displacement observed in construction stage 3c (Figure 3.18a). As shown in Figure 3.19b, an out-of-plane displacement of nearly 2.0 in. is observed at the top flange of girder G3 on the abutment 1 side of the structure. While on the abutment 2 side of G3, where cross frames attach G3 to girder G2, the top flange out-of-plane displacements are much smaller and more uniform between all of the girders. Figure 3.20 shows the displaced shape of the finite element model for construction stage 3c1. The large top flange out-of-plane displacement on the abutment 1 side of G3 is evident in Figure 3.20.



a) Girder Vertical Displacement



b) Girder Out of Plane Displacement

Figure 3.19 Construction Stage 3c1

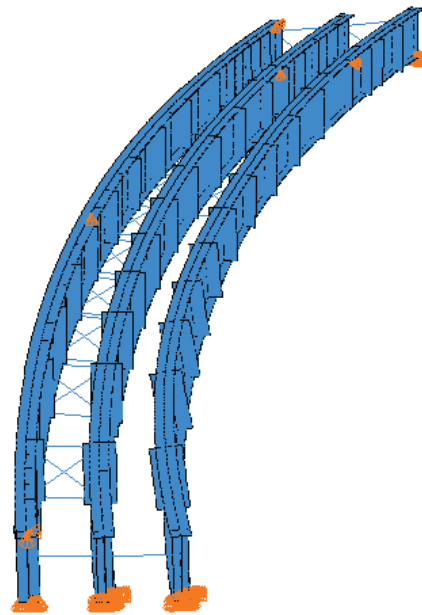


Figure 3.20 View of Construction Stage 3c1

### 3.3.5 Construction Stage 3e1

Construction stage 3e1 involves the placement of cross frames 3D, 5D, 7D, 9D, 11D, and 13D between girders G1 and G3, basically completing the structural framing of girders G1, G2, and

G3. Only the holding crane attached to G1 is assumed to be present at construction stage 3e1, while the two lifting cranes attached to girder G2 are removed. The plan view of the finite element model at this stage of construction is shown in Table 3-4.

The displacements at this point in the erection are slightly larger than at other construction stages, due to the fact that the lifting cranes attached to the innermost girder, G3, are not present in the analysis. However, since the holding crane at the mid-span of G1 is still in place, girder G3 experiences the largest vertical displacements, as shown in Figure 3.21a. As observed in previous erection stages, where the holding crane is the only crane present, the girders tend to rotate towards the inward side of the curve, due to the holding crane support effects. This behavior can be observed in Figure 3.21b, noting that all of the girder top flanges displace in the negative out-of-plane direction (towards the inward side of the curve).

In the field, the placement of cross frames between girders G3 and G4 in the following construction stages could be complicated by displacements of girder G3. The G3 mid-span vertical displacement of approximately 0.60 in., coupled with the top flange out-of-plane displacement of approximately 0.15 in. could create difficulties in erecting cross frames between G3 and G4. It may be the case that G4 would have to be slightly tilted and/or lowered to ease the connecting of cross frames to this girder.

The largest von Mises stresses occur in the near the mid-span of girder G3, in the top flange. The maximum von Mises stress at this location is approximately 4 ksi. Figure 3.22 displays the von Mises stresses in all of the girder top flanges at this stage of erection.

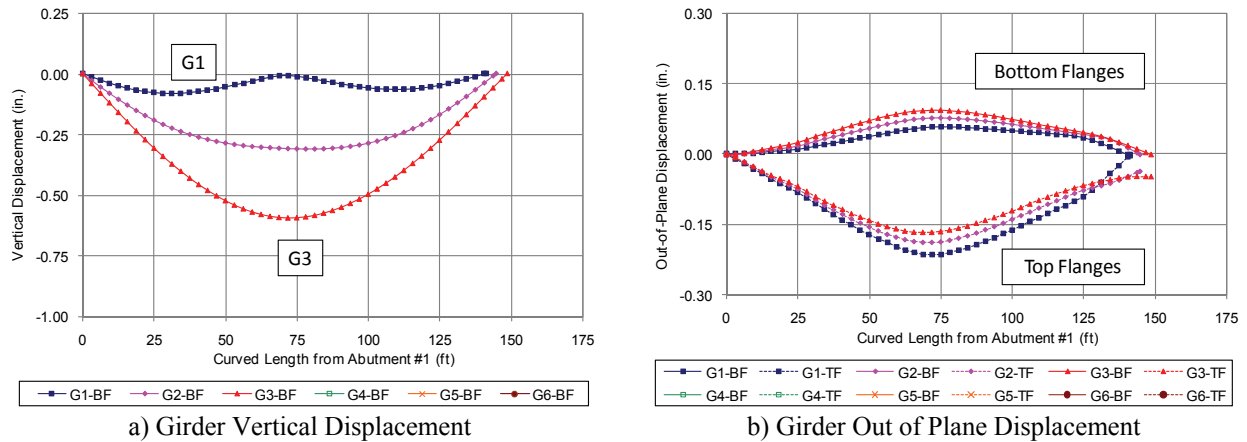


Figure 3.21 Construction Stage 3e1

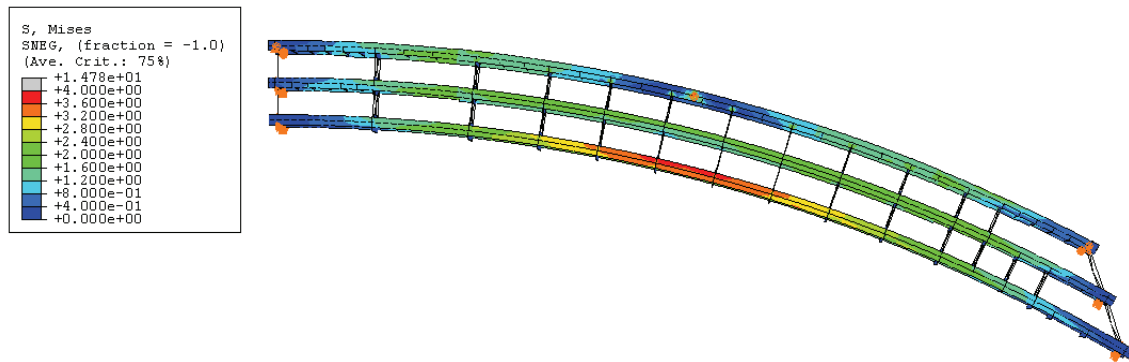


Figure 3.22 Construction Stage 3e1 – von Mises Stresses

With the release of the two lifting cranes from girder G3, the girder reactions for all three girders at both abutments increase, with the largest reactions occurring at girder G1. At the same time, the load assumed by the holding crane attached to girder G1 increases to approximately 85 kips. Table 3-6 shows the reactions at both abutments and the loads carried by the cranes for each stage of construction beginning with stage 3 up to the current stage.

When the holding crane boundary condition is removed from girder G1, the finite element model predicts that the structure would become unstable. Similar to previous construction stages with all cranes released, girders G2 and G3 would completely uplift from the

abutment supports, and all load would transfer to girder G1. It had been realized that the structure would become unstable in the field during construction if the holding crane was removed from girder G1. Therefore, the holding crane was left attached to G1 for the construction stages that follow stage 3e1.

**Table 3-6** Reactions – Construction Stage 3 to Stage 3e1

Location	Construction Stages								
	3	3a	3b	3c	3c1	3d	3d1	3e	3e1
	<b>Reactions (kips)</b>								
<b>G1 Abut 1</b>	24.9	24.9	22.6	18.2	35.4	17.1	27.7	17.0	28.2
<b>G1 Abut 2</b>	31.4	30.1	33.5	25.5	57.1	23.3	36.2	23.3	36.7
<b>G2 Abut 1</b>	13.6	13.6	13.8	12.4	12.1	8.5	16.2	8.7	15.6
<b>G2 Abut 2</b>	11.5	14.1	0.0	5.8	18.9	6.2	25.8	6.5	26.7
<b>G3 Abut 1</b>	3.6	3.6	3.3	3.9	16.6	2.0	17.1	2.1	18.3
<b>G3 Abut 2</b>	3.8	2.4	0.0	1.9	0.0	2.0	7.9	1.9	8.3
<b>G1 Holding Crane</b>	72.1	72.1	71.7	74.0	72.6	75.0	84.0	75.8	85.3
<b>Lifting Crane 1 (G3)</b>	23.8	23.7	23.4	26.6	-	41.1	-	42.6	-
<b>Lifting Crane 2 (G3)</b>	24.6	24.9	43.0	44.3	-	39.5	-	41.1	-

**3.3.6 Construction Stage 4c1**

Cross frames 7C and 9C are the structural components that are placed as part of construction stage 4c. Construction stage 4c1 consists of the identical structural assembly as construction stage 4c, except that the holding crane is released. The plan view of the finite element model at this stage of construction is shown in Table 3-4.

The vertical and out-of-plane girder displacements increase significantly from construction stage 4c, due to the release of the boundary conditions simulating the lifting cranes attached to girder G4. As shown in Figure 3.23a, girder G3 displaces vertically more than the other girders in the current structure. The vertical displacement of girder G3 is slightly irregular

on the abutment 2 side of the structure because there are no cross frames between girders G3 and G4 at this location. The absence of cross frame at the abutment 2 side of the structure is clearly evident in the plot of girder out-of-plane displacements. As shown in Figure 3.23b, the top flange of girder G3 at the 125 ft curved length, displaces in the out-of-plane direction by 1.1 in. Furthermore, because there are no cross frames between G3 and G4 on the abutment 2 side, girder G4 does not behave like the remainder of the structure at this location.

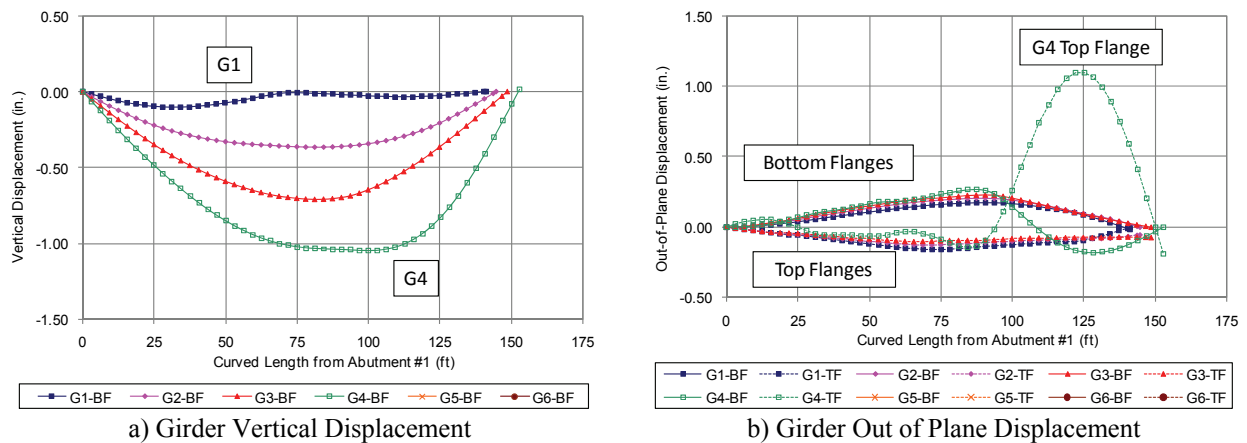


**Figure 3.23** Construction Stage 4c1

A maximum von Mises stress of approximately 6.5 ksi occurs in the top flange of girder G4, at the cross frame 9C location. This stress is due to the twisting that is occurring in girder G4 that results from the absence of cross frames between G3 and G4 on the abutment 2 side of the structure. Also at the cross frame 9c location, a von Mises stress of approximately 5.4 ksi develops in the top flange of girder G3.

All of the girder reactions increase from construction stage 4c, due to the release of the two lifting crane boundary conditions. The girder reactions for construction stage 4c1 are shown in Table 3-7. Additionally, the load carried by the holding crane attached to girder G1 is 93 kips.

**Table 3-7** Reactions – Construction Stage 4c1

	Abutment #1				Abutment #2				G1 Holding Crane
	G1	G2	G3	G4	G1	G2	G3	G4	
Reactions (kips)	31.41	15.89	17.69	20.57	35.08	35.23	23.56	7.12	93.00

### 3.3.7 Construction Stage 5c1

Construction stage 5c1 has the identical structural geometry as construction stage 5c, however the two lifting cranes attached to girder G5 are removed from the analysis. The holding crane attached to girder G1 is assumed to be present, and is considered in the finite element model for construction stage 5c1. The plan view of the finite element model at this stage of construction is shown in Table 3-4.

The release of the two lifting cranes allows the girders to displace much more so than the previous construction stage. As shown in Figure 3.24a, the maximum vertical displacement of approximately 1.30 in. occurs near the mid-span of girder G5. Furthermore, the holding crane causes the girders to rotate in the negative direction, such that the top-flanges of the girders displace towards the inward side of the horizontal curve. The girder out-of-plane displacement for construction stage 5c1 is shown in Figure 3.24b.

It is again noted that the presence or absence of cross frames has a significant effect on the out-of-plane behavior of the structure. Only one intermediate cross frame, cross frame 5B, is present in the 90 ft length from abutment 1 to the cross frame 9B location along girder G5. This allows girder G5 to rotate differently from the other girders, and in the opposite direction up to a curved length of approximately 55 ft, which is near the cross frame 5B location.

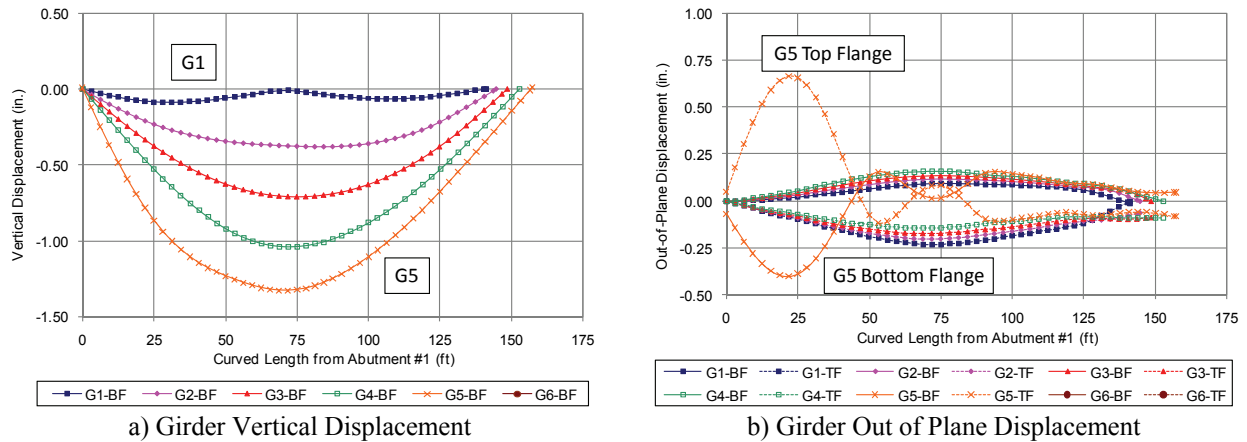


Figure 3.24 Construction Stage 5c1

### 3.3.8 Construction Stage 5c2

Construction stage 5c2 has the same structural geometry as construction stages 5c and 5c1, expect that the boundary condition representing the holding crane attached to girder G1 is released. At this point in the field erection of SR 8002 Ramp A-1, the holding crane was no longer attached to girder G1.

As would be expected, the girder displacements increase significantly with the removal of the holding crane. As shown in Figure 3.25a, girder G1 generally experiences the largest vertical displacement throughout the span of the steel structure. The girder G1 maximum vertical displacement of approximately 3.20 in. occurs at a curved length of 70 ft, which is near the mid-span of G1. However, the innermost girder of the current structure, girder G5, has the least vertical displacement, with no vertical displacement larger than 1.0 in. Furthermore, the differential vertical displacement between girders G4 and G5 has a maximum value of 0.5 in. This differential deflection is quite important in the erection of the remaining ‘B’ line cross frames of the structure. The smaller the differential, the easier it should be to fit cross frames between the subject girders.

The release of the holding crane causes the girders to rotate out-of-plane, in the positive sense, such that the top flange of each girder displaces towards the outside of the curve. It is observed that girder G1 has the largest top flange out-of-plane displacement of nearly 0.75 in. The girder out-of-plane displacements for this stage of construction are shown in Figure 3.25b. Again, it is important to point out the differential out-of-plane displacement between girders G4 and G5. The maximum differential out-of-plane displacement between G4 and G5 is only 0.20 in. In this case, the out-of-plane differential, coupled with the vertical differential, should not lead to significant difficulties in erecting the remaining ‘B’ line cross frames between girders G4 and G5.

For this stage of construction, due to the release of the holding crane, the maximum von Mises stress develops in the top flange of girder G1 near mid-span. The value of the von Mises stress at this location is approximately 10 ksi. Figure 3.26 illustrates the von Mises stress contours along the girder top flanges for the current stage of construction.

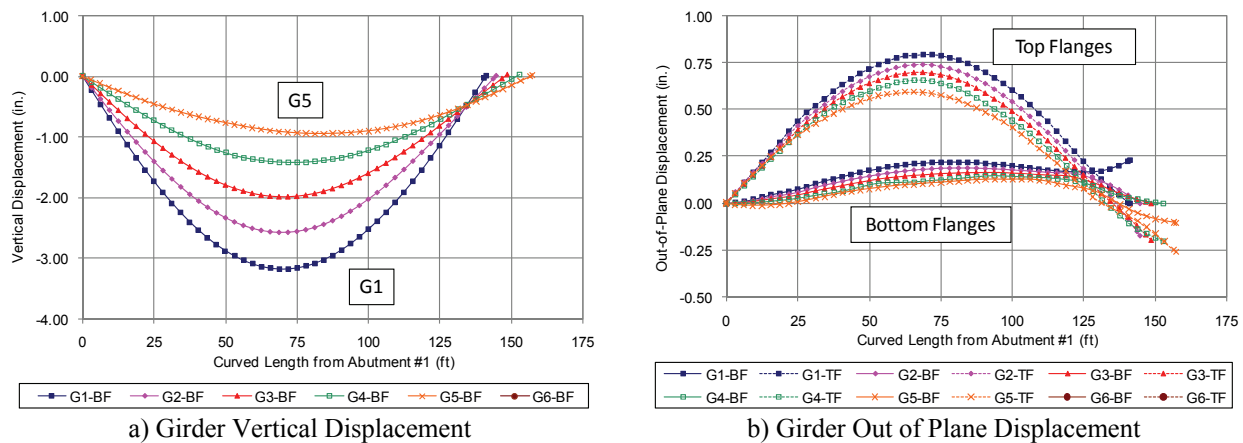
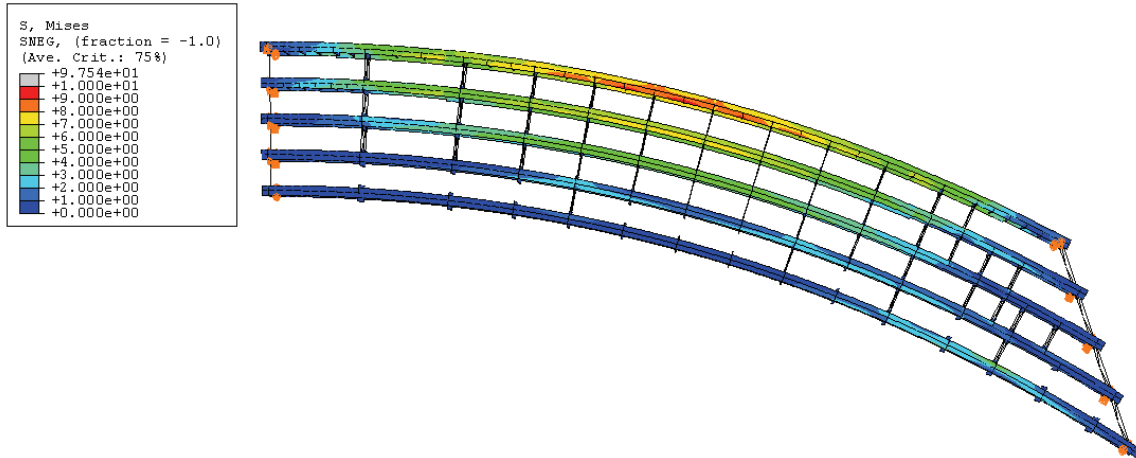


Figure 3.25 Construction Stage 5c2



**Figure 3.26** Construction Stage 5c2 – von Mises Stresses

With the release of the holding crane boundary conditions, the reactions at girder G1 increase significantly. The abutment 1 girder reactions increase from 31.0 kips at construction stage 5c1 to 76.9 kips at stage 5c2, and from 35.9 kips to 159.0 kips at abutment 2. The reactions for all of the girders at the current construction stage are shown in Table 3-8.

**Table 3-8** Reactions – Construction Stage 5c2

	Abutment #1					Abutment #2				
	G1	G2	G3	G4	G5	G1	G2	G3	G4	G5
<b>Reactions (kips)</b>	76.9	40.7	28.1	5.7	5.8	159.0	2.3	0.3	8.8	20.1

### 3.3.9 Construction Stage F6c1

Construction stage F6c1 consists of the same structural components as construction stage F6c, in which cross frames 8A and 10A are erected. However, stage F6c1 assumes that the lifting cranes attached to girder G6 are released.

The vertical and out-of-plane displacements of girder G6 increase significantly as the two lifting cranes are released, as shown in Figure 3.27. Due to the fact that there are no cross frames between girders G5 and G6 up to a curved length of approximately 80 ft, girder G6 displaces differently from the remainder of the structure. Girder G6 displaces vertically more than girder G3, G4, and G5 at the location of no cross frames. Furthermore, at this same location, the out-of-plane rotation of girder G6 is quite large, such that the top flange of G6 displaces outward by approximately 1.6 in. The relatively large displacements of girder G6 in this region could lead to some difficulties in erecting cross frames at this location.

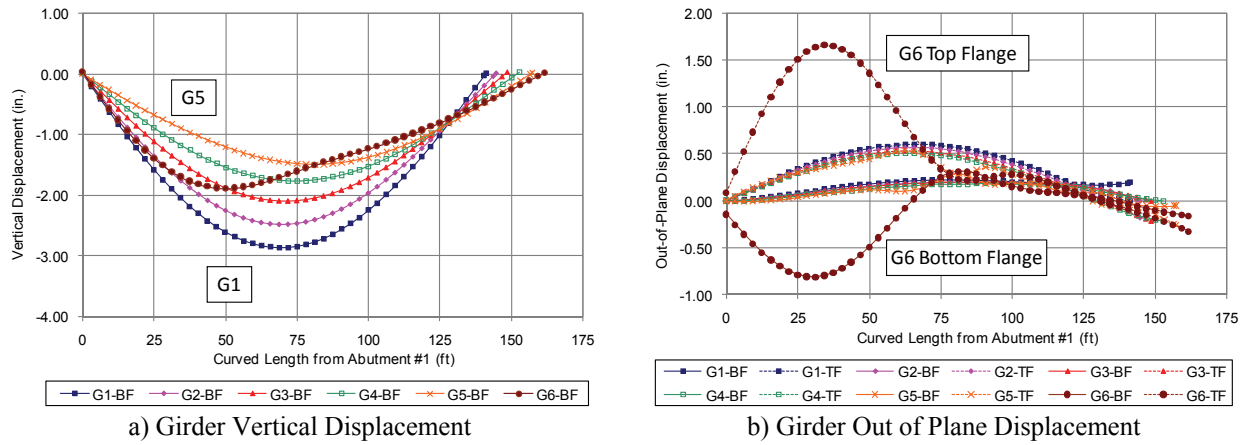


Figure 3.27 Construction Stage F6c1

### 3.3.10 Construction Stage F6f1

Intermediate cross frames 2B, 4B, and 6B are placed into the finite element model of SR 8002 Ramp A-1 as part of construction stage F6f1. The two lifting cranes are assumed to not be present at this stage of steel erection; therefore, the girders are only supported at the abutments. A plan view of the finite element model at this stage of steel erection is shown in Table 3-4.

The behavior of the structure at the current construction stage is much like the behavior of the completed structure under steel dead load effects. Generally, girder G1 experiences the

largest vertical displacements, while girder G6 vertically displaces the least. Furthermore, as illustrated in Figure 3.28a, the differential vertical displacement between girders G5 and G6 is relatively small, therefore the erection of the remaining cross frames in cross frame line ‘A’ could be accomplished with little difficulty.

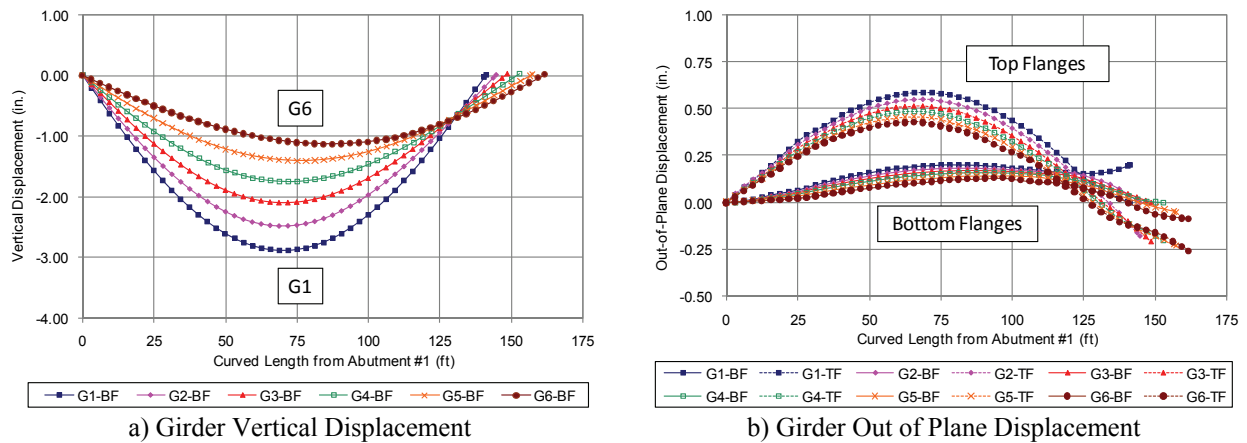


**Figure 3.28** Construction Stage F6f1

With the addition of cross frames between girders G5 and G6, as compared to construction stage F6c1, the girder out-of-plane displacement is generally identical for all of the girders in the structure. The out-of-plane displacement for the current construction stage is shown in Figure 3.28b. From observing the differences in girder displacements between stages F6c1 and F6f1, it can be seen that the cross frames play an important role in maintaining the geometry of the cross section. Furthermore, the horizontal curve controls the out-of-plane displacements up to a curved length of 120 ft such that the girders rotate in a positive sense, towards the outside of the curve. From 120 ft to the end of the structure, the skew effects control the girder out-of-plane displacement, such that the girders rotate in a negative sense, towards the inside of the curve. Additionally, the differential girder out-of-plane rotation is minimal between girders G5 and G6, thus aiding in the placement of the remaining line ‘A’ cross frames.

For the current construction stage, according to the finite element model, a maximum von Mises stress of approximately 10 ksi develops in the top flange of girder G1, near the mid-span. The largest girder reactions occur at the G1 abutment supports for the current construction stage, with the release of the two lifting cranes from girder G6. Table 3-9 shows all of the girder reactions for construction stage F6f1. The girder reactions do not change significantly for construction stage F6f1 from previous erection stages.

**Table 3-9** Reactions – Construction Stage 5c2

	Abutment #1						Abutment #2					
	G1	G2	G3	G4	G5	G6	G1	G2	G3	G4	G5	G6
<b>Reactions (kips)</b>	74	39	34	22	14	5	155	15	10	11	16	21

### 3.3.11 Summary of Analytical Study

The as-built and planned erection sequences are recreated using the finite element model of SR 8002 Ramp A-1, employing cross frames and girders detailed for the web-plumb position at the no-load condition. The as-built erection sequence follows exactly the erection sequence that had been performed in the field. For each stage of the as-built construction, girder displacements, stresses, and reactions are monitored. It was unexpectedly found in the field that the holding crane attached to girder G1, could not be released until much of the steel assembly was concluded, otherwise the structure would become unstable. This same behavior is noted in the current research via the results of the analytical study of the as-built erection sequence. The results of the analytical study show that the holding crane could not be released until after the construction stage 5c2, in which girder G5 and cross frames 5B, 9B, 11,B and 15B are the most

recent structural components placed in the finite element model. If the structure is released from the holding crane prior to the completion of stage 5c2, the structure has the possibility of becoming unstable due to large girder displacements and uplift at the abutment bearing locations.

The results of the analytical study show the importance of providing a temporary support to the structure to minimize girder displacements during steel erection. In this case, the holding crane limits girder displacements, and therefore differential displacements between the girders, as structural components are placed into the assembly. In many cases, the holding crane attached to the mid-span of girder G1 prevents the girder from rotating towards the outside of the curve, and instead the girder tends to rotate towards the inside of the curve. Furthermore, the use of a holding crane does not necessarily prevent out-of-plane displacements from occurring, whereas a temporary support tower near the mid-span probably could. The results also show the change in behavior of the bridge when certain cross frames are placed in the model. In horizontally curved I-girder bridges, the cross frames have a significant role in maintaining the geometry of the structure in service and during construction.

Generally throughout the analytical study of the as-built erection sequence, the differential girder displacements were relatively minimal. Therefore, the fit-up of cross frames between girders may be accomplished with only slight difficulties. This is the case that was noted in the field; in some cases cross frames were erected with relative ease, however the erection of some of the cross frames, especially near the skewed end, experienced moderate difficulties. Also through the analytical study, it is observed that the von Mises stresses are relatively low as well; showing that a condition nearing the no-load condition can be achieved in the field with the proper use of temporary supports, in this case, a holding crane. This study also illustrated significant increase and variability in the load carried by the G1 holding crane. In

some cases, this load may exceed that expected based on simple analyses and therefore affect the selection of crane size for this task. Additionally there is significant load transfer to the outermost girder supports upon the release of the holding crane which must be accounted for in the design of these bearings.

#### **4.0 STRUCTURAL BEHAVIOR OF OUT-OF-PLUMB CURVED I-GIRDERS**

Bridge components are typically inconsistently detailed because the rotation of the girders, and the subsequent lateral displacement of the top flange, due to applied or dead loads, are subjectively deemed excessive by the bridge engineer or owner. In many cases the bridge engineer or owner may believe that a girder with a web that is not plumb is not adequate for service conditions; in relation to required girder capacity and acceptable bending stresses. This assessment is made without any guidance from current design specifications (AASHTO 1993 and 2003). Even in a general sense, there is no guidance available in the literature concerning the limits of out-of-plane web rotation.

This section is aimed at addressing the issue of allowable web rotation through the use of experimentally verified nonlinear finite element modeling techniques. An evaluation of the structural capacity of a straight and a curved steel I-girder rotated out-of-plane is carried-out, and comparisons to similar I-girders, that are not rotated out-of-plane, are performed. Additional analytical investigations are carried out that include a study of allowable girder web rotations for a two-girder curved steel superstructure.

## 4.1 STRAIGHT I-GIRDER INVESTIGATION

This study analytically evaluates the structural capacity of a straight girder rotated out-of-plane, and compares the results to a girder that is not rotated out-of-plane. To provide finite element model verification it is necessary to choose an experimental study in which a steel girder is tested to ultimate capacity. Once the suitable study is identified, finite element analogs of the experimental tests can be constructed and tested to failure and the response compared with that of the experiments. An experimental test program conducted by Morcos (1988) at the University of Pittsburgh serves as the vehicle for this type of model validation. The verified model, which is not rotated out-of-plane, serves as the basis of comparison for analytical tests of the same girder, but rotated out-of-plane. Nonlinear finite element analysis is the vehicle by which all numerical models are analyzed. All nonlinear finite element models are created using the commercial software package *ABAQUS* (2003).

### 4.1.1 Verification Study

Morcos (1988) tested three full-scale bridge girders in the Watkins-Haggart Structural Engineering Laboratory at the University of Pittsburgh. For the current investigation, Morcos' specimen "S" is selected for the verification study. The specimen "S" plate girder was fabricated from ASTM A572 Grade 50 plate steel, all originating from the same heat. The girder cross-sectional dimensions are shown in Figure 4.1. The girder was 13 ft in length, with bearing stiffeners at the supports and at the midspan load point, as shown in Figure 4.2. The supports are located 0.5 ft from the end of the girder, resulting in a simple span length of 12 ft. A concentrated load was placed at midspan. Out-of-plane bracing, in the form of threaded bars

with eye-bar ends and turnbuckles was provided at the load point and at the supports. The eye-bars allowed for bracing to be attached at discrete points on the top and bottom of each bearing stiffener, on either side of the web. The turnbuckles at the center of the bracing provided some degree of bracing flexibility.

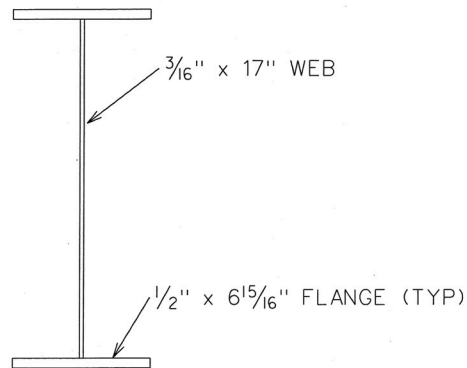


**Figure 4.1** "S" Specimen Cross-Section (Morcos 1988)

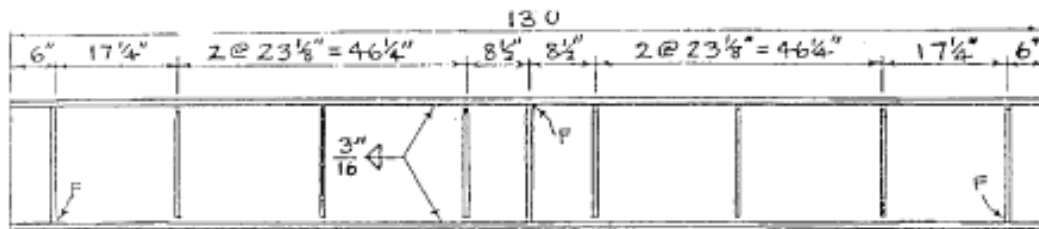


**Figure 4.2** "S" Specimen Elevation View (Morcos 1988)

The nonlinear finite element model of the Morcos girder employs the *ABAQUS* S4R shell elements to model the plate girder webs, flanges, and transverse and bearing stiffeners. The shell finite elements are specified at the middle surfaces of the constituent plate elements of the I-girder cross-section. Initial geometric imperfections associated with the first eigenmode, as well as variable bracing stiffness, are also considered.

Bracing flexibility is incorporated in the finite element with the use of *ABAQUS* SPRING1 elements whose stiffness is determined as a force of 3% of the flange yield capacity at a nodal displacement of  $L/1000$ , where  $L$  is the length of the span (this initial geometric imperfection is consistent with fabrication tolerances). The SPRING1 element is a linear element that can provide both tensile and compressive restraint just as actual cross-bracing would.

For models where inelastic buckling is investigated, it is important that the evolution of the modeling solution be carefully monitored so that any indication of bifurcation in the equilibrium path is carefully assessed so as to guarantee that the equilibrium branch being followed corresponds to the lowest energy state of the system. To ensure that the lowest energy equilibrium path in configuration space is taken, the strategy of seeding the finite element mesh with an initial displacement field is employed in this study (*ABAQUS* 2003). The finite element mesh is subjected to a linearized-eigenvalue buckling analysis; from which an approximation to the first buckling mode of the girder is obtained. A displacement field associated with this lowest mode, and scaled so that the maximum initial displacement anywhere in the mesh is equal to one-one-thousandth of the span length of the girder ( $L/1000$ ), is then superimposed onto the finite element model as a seed imperfection for use in the incremental nonlinear analysis.

Employing these modeling techniques, favorable agreement between the results of the experimental test and the finite element results are observed. The load-deflection responses for the experimental study and the analytical results are shown in Figure 4.3. The analytical results shown are for an initial imperfection seed of  $L/1000$ . It is also noted that there was very good agreement between the modal manifestations exhibited by the finite element model and those

observed and reported by Morcos in the failed experimental test girder, as shown in Figure 4.4 and Figure 4.5.

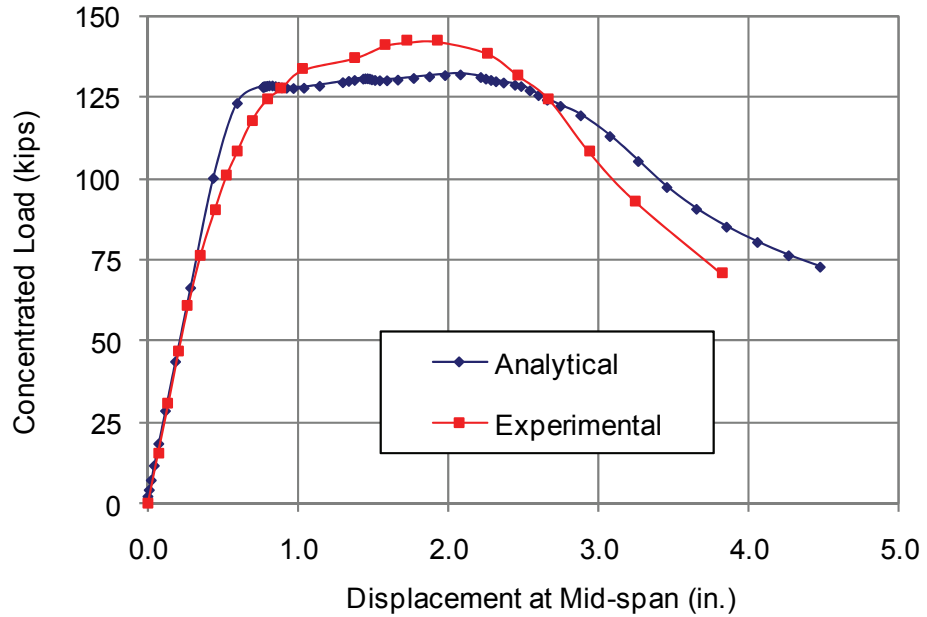


Figure 4.3 Straight Girder FEM Verification – Load-Deflection Response

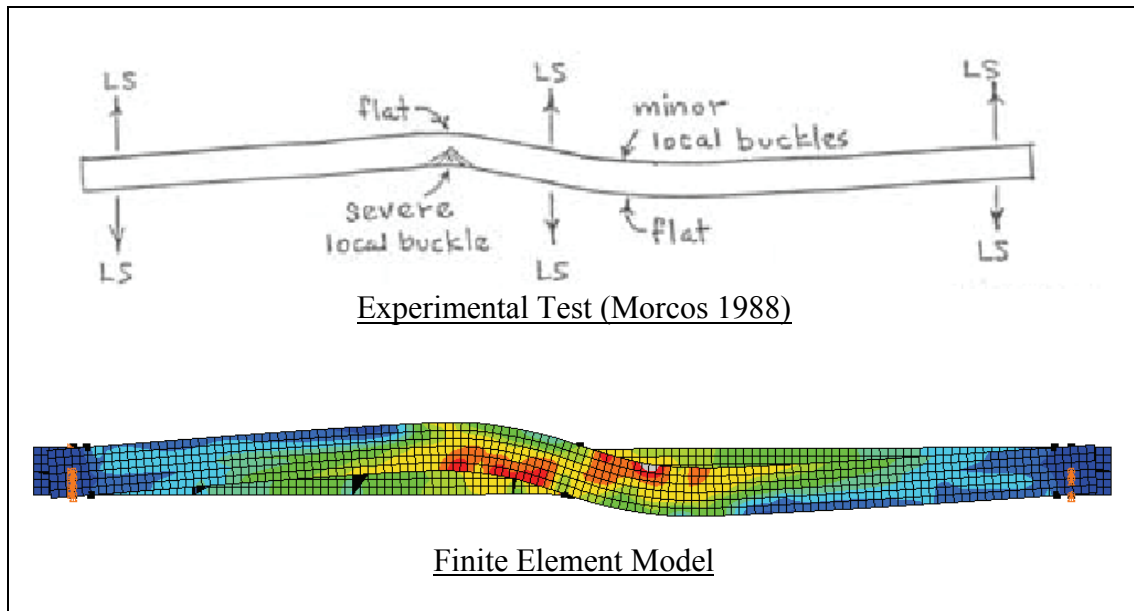
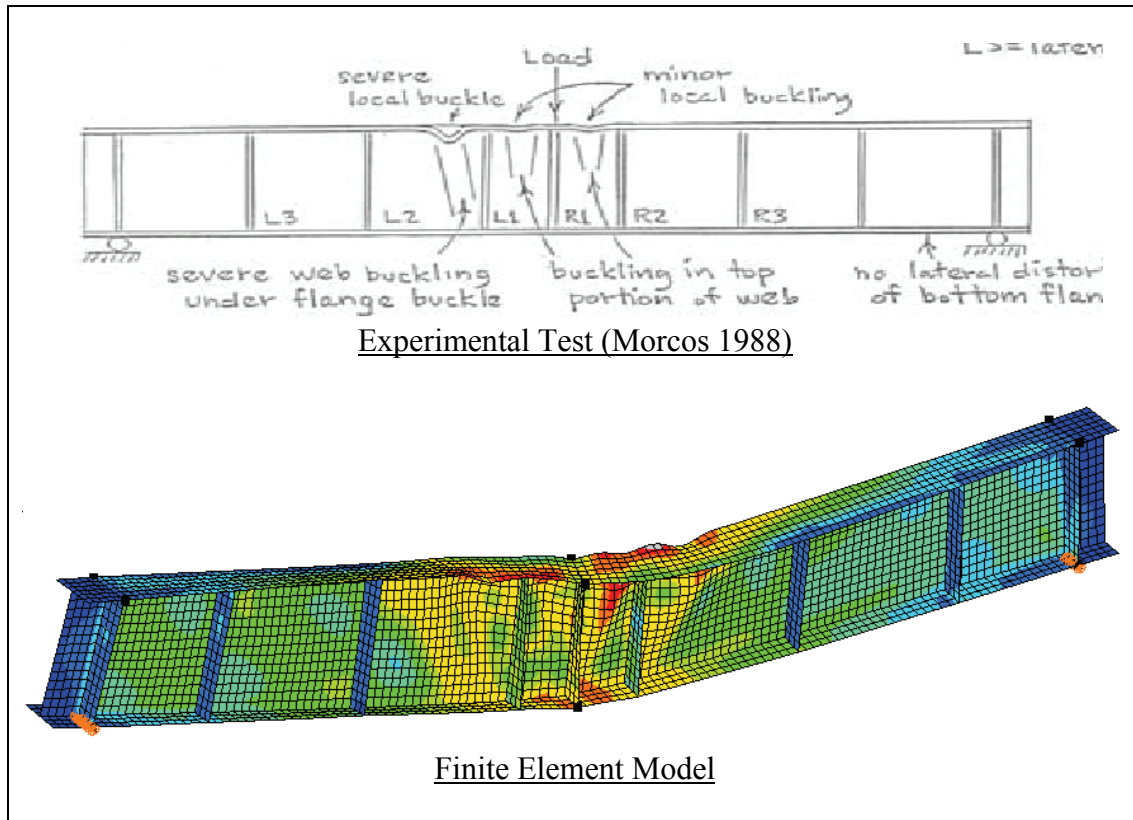


Figure 4.4 Straight Girder FEM Verification – Modal Manifestations in Plan View



**Figure 4.5** Straight Girder FEM Verification – Modal Manifestations in Elevation View

It is pointed out that the finite element models of the experimental beam were constructed using best modeling practices and only compared with the experimental results upon completion (i.e. no calibration or tweaking of the model was employed). Based on the results of this verification study, it appears that the modeling strategies employed are able to capture the complete behavior of the girder. Therefore, these same modeling strategies are employed for the same girder, but rotated out-of-plane.

#### **4.1.2 Behavior of Straight I-Girder Rotated Out-of-Plane**

Analytical studies are carried out on the same girder cross-section and span length as that of the Morcos girder, but with the girder rotated such that the girder web is no longer plumb. The

amount of out-of-plane rotation,  $\theta$ , is varied from 0 degrees to 5 degrees, in 1 degree increments; as shown in Figure 4.6. It has been seen in practice that the out-of-plane rotation due to dead loads of a curved girder bridge is on the order to 1 to 2 degrees (Chavel and Earls 2001, 2004), and thus the range of out-of-plumbness considered is thought to be sufficient for the purposes of the present study.

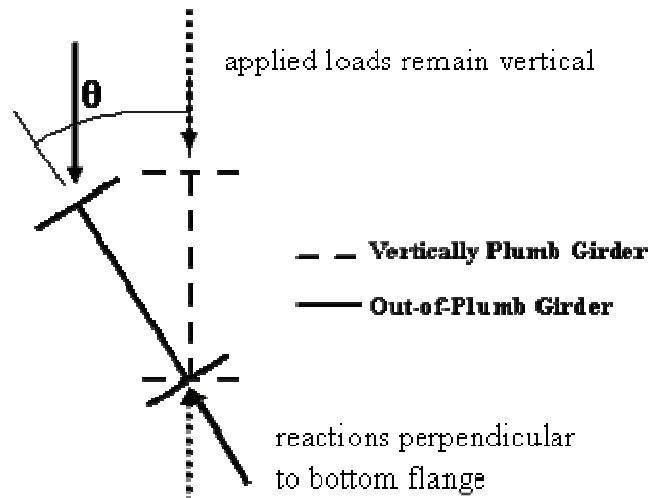


**Figure 4.6** Straight Girder Out-of-Plane Rotations

The analytical model for each angle of out-of-plane rotation is exactly the same from model to model except the orientation of the boundary conditions (i.e. the meshes are identical across web rotations). The boundary condition employed at the left end of the girder is assumed as pinned, and a roller is employed at the right end of the girder. The boundary conditions are rotated such that the vertical restraint remains perpendicular to the bottom flange (Figure 4.6). The lateral bracing, provided by the spring elements, remains in the horizontal plane (i.e. orthogonal to the applied loading) and the concentrated load at mid-span remains vertical (i.e. stays oriented at 0 - degrees), for each increment of out-of-plane rotation. This modeling strategy parallels the field conditions of a horizontally curved girder that has rotated due to self-

weight, as additional load, such as concrete self-weight is applied (i.e. gravity always acts vertically).

A comparison of the load-deflection results for each degree of web out-of-plane rotation is shown Figure 4.7. It is evident that the out-of-plane rotation, investigated in the current study, has only a small effect on the load-deflection response as compared to the 0-degree out-of-plane rotation case. As shown in Table 4-1, the ultimate load capacity of the beam does fall slightly as the angle of out-of-plane rotation increases.

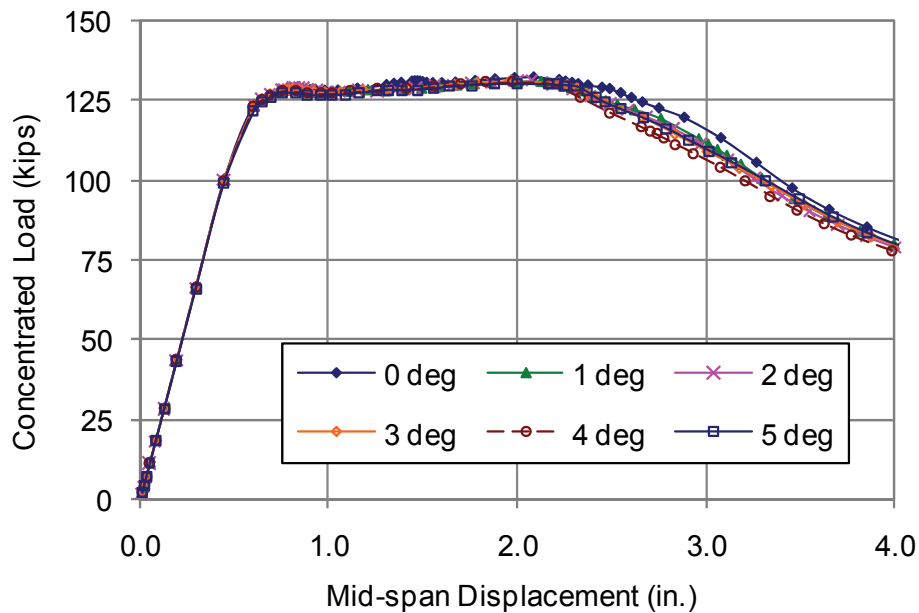


Figure 4.7 Straight Girder Load-Deflection Response

In addition to an investigation of the load-deflection behavior and the ultimate load capacity of the rotated girders, the stresses at the flange tips are monitored. An elastic finite element model, without any imperfections ( $L/1000$ ), is used to investigate the flange stresses for each angle of web out-of-plane rotation. The stresses are monitored at an applied load of 50 kips; a load at which the girder is still behaving elastically. Table 4-2 shows the maximum compressive stress that occurs in the top flange at the mid-span of the girder.

**Table 4-1** Straight I-Girder Ultimate Load Summary

<b>Web Out-of-Plane Rotation (deg)</b>	<b>Ultimate Load (kip)</b>	<b>% Reduction from 0-deg case</b>
0.0	132.0	n/a
1.0	131.0	0.76%
2.0	130.9	0.83%
3.0	130.6	1.06%
4.0	130.4	1.21%
5.0	130.0	1.51%

**Table 4-2** Maximum Top Flange Compressive Stress due to Concentrated Load of 50 kips

<b>Web Out-of-Plane Rotation (deg)</b>	<b>Compressive Top Flange Stress (ksi)</b>	<b>% Increase from 0-deg case</b>
0.0	23.71	n/a
1.0	24.78	4.5%
2.0	25.69	8.4%
3.0	26.58	12.1%
4.0	27.28	15.1%
5.0	28.82	17.3%

### 4.1.3 Theoretical Calculation of Flange Stresses

The top flange stresses shown in Table 4-2 can be replicated through simple analysis using the transformed moment of inertia calculated for the given web out-of-plane rotation. This will serve as a verification of the results predicted through the finite element models. The transformed moments of inertia are calculated from

$$I_x' = \frac{1}{2}(I_x + I_y) + \frac{1}{2}(I_x - I_y) \cos(2\theta) - I_{xy} \sin(2\theta) \quad (4-1)$$

$$I_y' = \frac{1}{2}(I_x + I_y) - \frac{1}{2}(I_x - I_y) \cos(2\theta) - I_{xy} \sin(2\theta) \quad (4-2)$$

$$I_{xy}' = \frac{1}{2}(I_x - I_y) \sin(2\theta) + I_{xy} \cos(2\theta) \quad (4-3)$$

Where:  $\theta$  = Web out-of-plane rotation angle

$I_x$  = Moment of inertia about x-axis for no rotation ( $\theta = 0$  deg.)

$I_y$  = Moment of inertia about y-axis for no rotation ( $\theta = 0$  deg.)

$I_{xy}$  = Centroidal product of inertia for no rotation ( $\theta = 0$  deg.)

$I_x$ ,  $I_y$ , and  $I_{xy}$  = Transformed moments of inertia for given  $\theta$ .

A summary of this fundamental approach is shown in Table 4-3. It should be noted that bending about the x-axis and y-axis is relevant in this case, since the applied load is at an angle to the top flange. However, since the girder is prevented from rotating out-of-plane due to restraint in the horizontal plane representing the lateral bracing at the girder supports and load point, torsional stresses are minimal for this case. As shown in Table 4-3, the theoretical results compare favorably with the analytical results, with only a 2% difference in the numerical values.

**Table 4-3** Top Flange Compressive Stress Comparison

$\theta$ (deg)	$I_x'$ (in <sup>4</sup> )	$I_y'$ (in <sup>4</sup> )	$S_x'$ (in <sup>3</sup> )	$S_y'$ (in <sup>3</sup> )	Theoretical			Analytical	% Difference
					$\sigma_{vert}$ (ksi)	$\sigma_{lat}$ (ksi)	$\sigma_{total}$ (ksi)	$\sigma_{total}$ (ksi)	
0	651.40	27.84	74.45	4.01	24.18	0.00	24.18	23.71	2.0%
1	651.21	28.03	73.92	4.23	24.35	0.94	25.29	24.78	2.1%
2	650.64	28.60	73.39	4.52	24.53	1.76	26.29	25.69	2.3%
3	649.69	29.55	72.84	4.91	24.71	2.44	27.15	26.58	2.1%
4	648.37	30.87	72.28	5.42	24.90	2.94	27.84	27.28	2.1%
5	646.66	32.58	71.70	6.00	25.10	3.32	28.42	27.82	2.2%

Note:  $I_y'$  is for the total section and  $S_y'$  is for a single flange.

Also, since the vertical load is applied directly to the top flange, most of the lateral bending resistance is assumed by the top flange. This is apparent when reviewing Table 4-4, which shows the bottom flange tensile stress comparison. For this loading case, the change in bottom flange stresses is attributed only to the change in  $I_x$ .

**Table 4-4** Bottom Flange Tensile Stress Comparison

$\theta$ (deg)	$I_x'$ (in <sup>4</sup> )	$S_x'$ (in <sup>3</sup> )	Theoretical	Analytical	% Difference
			$\sigma_{total}$ (ksi)	$\sigma_{total}$ (ksi)	
0	651.40	74.45	24.18	23.98	0.8%
1	651.21	73.92	24.35	24.19	0.7%
2	650.64	73.39	24.53	24.34	0.8%
3	649.69	72.84	24.71	24.57	0.6%
4	648.37	72.28	24.90	24.76	0.6%
5	646.66	71.70	25.10	24.94	0.6%

#### 4.1.4 Straight I-Girder Results Discussion

Based on the results of the analytical studies of the straight girders rotated out-of-plane, it is evident that there is little effect on the load-deflection behavior of the girder, as shown in Figure 4.7. Additionally, there is little effect on the ultimate load capacity of the girder, as shown in Table 4-1. In practice, curved steel I-girder bridges experience an out-of-plane rotation of approximately 1 to 2 degrees resulting in a decrease of ultimate load capacity of only 0.83% as compared to a vertically plumb girder.

However, as the girder is rotated out-of-plane, there is a more significant increase in the girder flange elastic-stresses, as shown in Table 4-2. For a web out-of-plane rotation of 2 degrees, the top flange longitudinal compressive stress at the flange tip increases by 8.4% for the girder section considered. This is a result of the fact that as the girder is rotated out-of-plane, the moment of inertia ( $I_x$ ) and section modulus ( $S_x$ ) of the cross-section about the horizontal axis decrease relative to the unrotated section, as shown in Table 4-3 and Table 4-4. This is in combination with an increase in top flange lateral bending stresses, due to the application of the vertical load on the top flange of the rotated cross-section. In the case of design, it may be

appropriate to consider the increased stress caused by the girder being in an out-of-plumb position.

It is important to note one of the limitations of this study. The girder investigated in this study is not nearly as large as a typical bridge girder. The flange stress results are affected by the ratio of  $I_x$  to  $I_y$ , which is generally much larger in a bridge girder than the section studied here. The girder studied here has an  $I_x / I_y$  ratio of 23, where values of  $I_x / I_y$  of 60 are common in design practice. Larger values of  $I_x / I_y$  will result in a marginal reduction in  $I_x'$ , and a more significant increase in  $I_y'$  and  $I_{xy}'$ . Therefore, a smaller increase in stress could be realized in bridge size girders as the reduction in  $I_x'$  is not as significant as that of girder analyzed here. Finally, the effects of out-of-plumbness on straight I-girders may be rapidly assessed using fundamental geometric properties of the rotated sections as shown in Section 4.1.3.

## 4.2 CURVED I-GIRDER INVESTIGATION

This study analytically evaluates, employing the nonlinear finite element method, the structural capacity of a single curved girder rotated out-of-plane, and compares the results to a girder that is not rotated out-of-plane. To provide finite element model verification it is necessary to choose an experimental study from the literature in which a curved steel I-girder is tested to ultimate capacity. An experimental test program conducted by Shanmugam et al. (1995) on a series of curved steel I-beams serves as the basis for the present validation study. The verified model, which is not rotated out-of-plane, serves as the basis of comparison for analytical tests of the same girder subject to out-of-plane web rotations.

#### 4.2.1 Verification Study

Shanmugam et al. (1995) performed experimental studies to investigate the ultimate load behavior of 10 different curved steel I-beams. The beam span lengths and radii of curvature were varied for the different tests. For the current research, the Shanmugam et al. “CB1” beam is selected as the basis of the verification study, as well as the basis for comparison for additional analytical tests of the same girder rotated out-of-plane so as to represent varying degrees of web-out-of-plumbness.

The CB1 beam is a hot-rolled section, having a total depth of 12.08 in., a web thickness of 0.31 in., a flange width of 4.89 in. and a flange thickness of 0.48 in. The beam has a radius of curvature of 65.6 ft and a clear span length of 16.4 ft. A concentrated load is placed on the beam 12.45 ft from the left support, as shown in Figure 4.8.

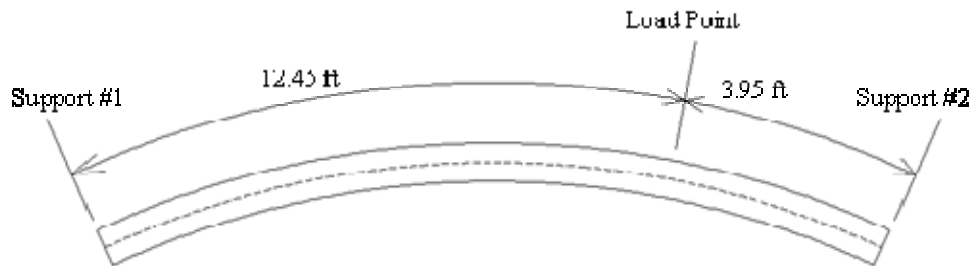


**Figure 4.8** CB1 Beam Plan View

The CB1 beam was cold bent to obtain the required curvature, and this slightly increased the material yield stress and elastic modulus (as a result of the cold working). It was determined by Shanmugam et al. (1995), via material tensile test coupons, that the flange material yield stress and elastic modulus were 57.3 ksi and 32,000 ksi, respectively. The web material yield stress and elastic modulus were determined to be 48.9 ksi and 29,800 ksi, respectively.

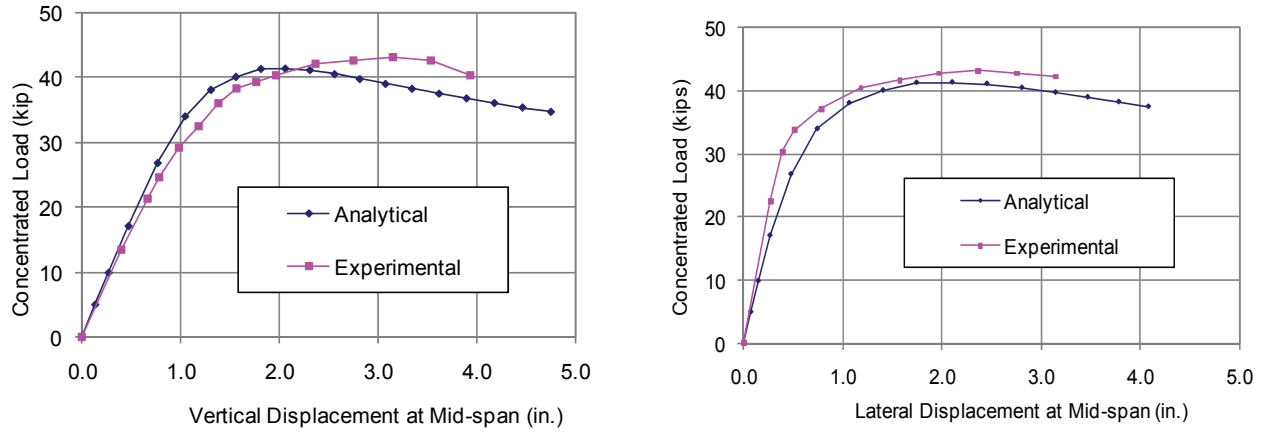
The CB1 beam had 0.79 in thick bearing stiffeners, on each side of the web, at the two supports. The beam was supported at the ends such that support 1 was essentially pinned, and support 2 only allowed movement in the tangential direction. Additionally, at the supports lateral movement was restrained at the top flange. The CB1 beam was also restrained in the lateral direction at the load point with a roller arrangement that only allowed vertical displacement at this location.

The nonlinear finite element model of the CB1 girder employs the *ABAQUS* S4R shell elements to model the plate girder webs, flanges, bearing stiffeners. The shell finite elements are specified at the middle surfaces of the constituent plate elements of the I-girder cross-section. A dense mesh of shell elements is employed in this portion of the validation study of the finite element techniques, and an aspect ratio of approximately 1 to 1 was maintained throughout the modeling. Nonlinear geometric effects, as well as nonlinear material properties were considered in this analysis.

Boundary conditions representing the pin-roller arrangement are applied to the supports at the bottom flanges. Lateral restraints are provided to the edges of the top flange at each support, as well as at the load point.

Employing these modeling techniques, favorable agreement between the results of the experimental test and the finite element analogs are observed. The load-vertical deflection response and top flange lateral deflection response at mid-span for the experimental study and the analytical results is shown in Figure 4.9. It is also noted that there was very good agreement between the modal manifestations exhibited by the finite element model and those observed and reported by Shanmugam et al. (1995) of the experimental test girder.

Based on the results of this verification study, it is concluded that the modeling strategies employed are able to capture the salient behavioral feature of the curved steel I-girder member. Therefore, these modeling strategies are employed for the same girder, but rotated out-of-plane.



a) Vertical Load-Deflection Response at Midspan

b) Top Flange Lateral-Deflection Response at Midspan

**Figure 4.9** Curved I-Girder FEM Verification

#### 4.2.2 Behavior of Curved I-Girder Rotated Out-of-Plane

Analytical studies to assess the effects of girder web out-of-plumbness are carried out on the same girder cross-section and span length as that of the CB1 girder. The amount of out-of-plane rotation,  $\theta$ , is varied from 0 degrees to 5 degrees, at 1 degree increments, as shown in Figure 4.6. It is pointed out that the out-of-plane rotation applied to the CB1 girder is constant along the span length of the girder (i.e. the end supports are inclined by the same angle and thus there is no twisting in the girder).

The analytical model considering each angle of out-of-plane rotation is exactly the same from case to case except for the boundary condition geometry itself. The boundary condition employed at the left end of the CB1 girder is assumed as pinned, and a roller is assumed at the right end of the girder. Additionally, the girder is supported at the loading point in the same

fashion as the experimental test. As alluded to previously, the boundary conditions are rotated such that the vertical restraint remains perpendicular to the bottom flange. The lateral restraint of the top flanges at the supports and at the load point remains horizontal, and the applied concentrated load remains vertical, for each increment of rotation. As in the case of the straight girder, this modeling strategy best represents the field conditions of a horizontally curved girder that has rotated due to dead loads such as concrete self-weight since support rotations can be accommodated at a typical pot bearing detail.

A comparison of the load versus vertical deflection response at mid-span, as well as the load-lateral deflection response at mid-span for each degree of web out-of-plane rotation is shown in Figure 4.10 and Figure 4.11, respectively. It is evident that the out-of-plane rotations investigated in the current study have only a small effect on the load-deflection response; as compared to the reference case involving 0-degree out-of-plane web rotation case. As shown in Table 4-5, the ultimate load capacity of the beam does fall slightly as the angle of out-of-plane rotation increases.

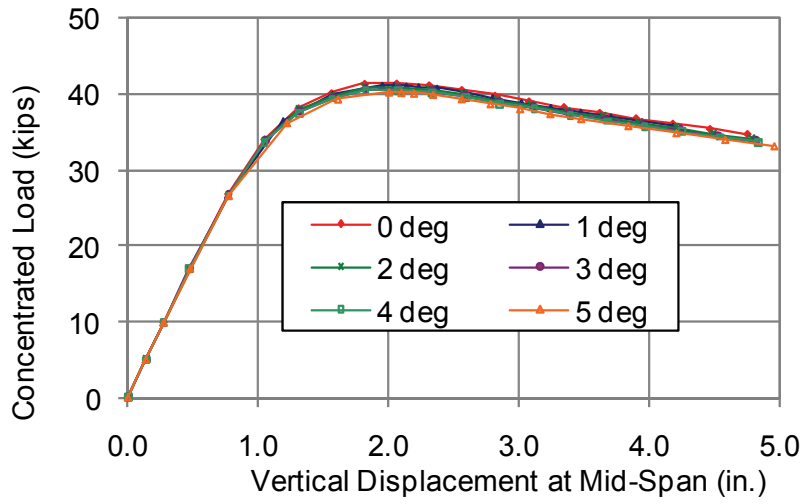


**Figure 4.10** Curved I-Girder Load-Vertical Deflection Response

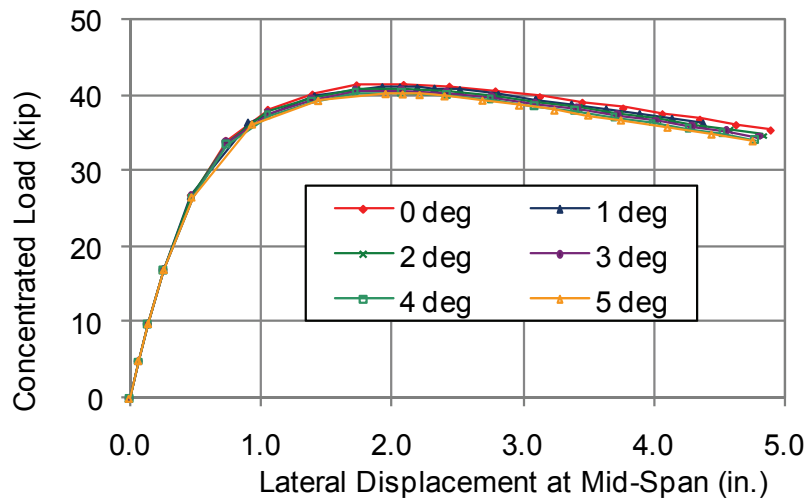


**Figure 4.11** Curved I-Girder Load-Lateral Deflection Response

**Table 4-5** Curved I-Girder Ultimate Load Summary

<b>Web Out-of-Plane Rotation (deg)</b>	<b>Ultimate Load (kip)</b>	<b>% Reduction from 0-deg case</b>
0.0	41.27	n/a
1.0	41.08	0.46%
2.0	40.84	1.05%
3.0	40.60	1.62%
4.0	40.33	2.28%
5.0	40.07	2.91%

In addition to an investigation of the load-deflection behavior and the ultimate load capacity of the rotated curved girders, the stresses at the flange tips are monitored. The stresses are monitored at an applied load of 20 kips, in which the girder is still behaving elastically. Table 4-6 shows the maximum tensile stress, in the longitudinal direction that occurs in the outside of the curved edge of the bottom flange at the mid-span of the girder.

**Table 4-6** Maximum Bottom Flange Stress due to Concentrated Load of 20 kips

<b>Web Out-of-Plane Rotation (deg)</b>	<b>Tensile Bottom Flange Longitudinal Stress (ksi)</b>	<b>% Increase from 0-deg case</b>
0.0	9.86	n/a
1.0	10.03	1.7%
2.0	10.16	3.0%
3.0	10.29	4.4%
4.0	10.44	5.9%
5.0	10.61	7.6%

### **4.2.3 Single Curved I-Girder Results Discussion**

Based on the results of the analytical studies of the particular curved girder rotated out-of-plane, it is evident that there is little effect on the load-deflection behavior of the girder (as shown in

Figure 4.10 and Figure 4.11). Additionally, there is little effect on the ultimate load capacity of the girder considered (as shown in Table 4-5). At a web out-of-plane rotation of 2 degrees, the ultimate load capacity is reduced by 1.05% as compared to a vertically plumb girder.

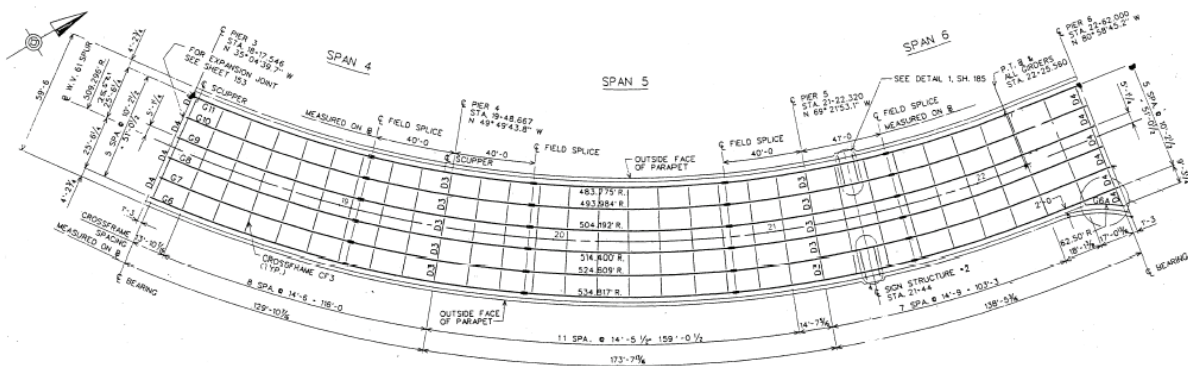
However, as the girder is rotated out-of-plane, there is also an increase in the girder flange elastic-stresses, as shown in Table 4-6. For a web out-of-plane rotation of 2 degrees, the bottom flange longitudinal tensile stress at the flange tip increases by 3.0%. This longitudinal stress is taken at the outside of the curved edge of the bottom flange. In the case of design, it may be appropriate to consider the increased stress caused by the girder being in an out-of-plumb position, for the case of additional loads applied to the girder when it is in an out-of-plumb state.

### **4.3 CURVED TWO I-GIRDER SYSTEM INVESTIGATION**

This study analytically evaluates, employing the nonlinear finite element method, the structural capacity of a curved two-girder system rotated out-of-plane, and compares the results to a curved two-girder system that is not rotated out-of-plane. Through a parametric study, the effects of changes to radius of curvature, girder spacing, web depth, and cross-frame spacing on the behavior of a curved two-girder system rotated out-of-plane are investigated. For each of these parameters, an out-of-plumb rotation angle of 0, 2, 3, and 5 degrees is investigated, similar to the studies presented in sections 4.1 and 4.2, with some modifications to the application of the out-of-plumbness that will be discussed later in this section. Again, it has been seen in practice that the out-of-plane rotation due to dead load of a curved girder bridge is on the order to 1 to 2

degrees (Chavel and Earls 2001, 2004), and thus the range of out-of-plumbness considered (0, 2, 3, and 5 degrees) is thought to be sufficient for the purposes of the present study.

The out-of-plumb studies presented in Sections 4.1 and 4.2 were carried out on beams that are not typical sized bridge beams. This study utilizes beams that are typical of a horizontally curved steel I-girder bridge. The two-girder system chosen for this parametric study is developed from the curved three-span Chelyan Bridge Approach Ramp, shown in Figure 4.12. Based on a review of several recent horizontally curved steel I-girder bridge designs, this structure was chosen because it is a more frequent application of a horizontally curved girder bridge: an access/approach ramp structure.



The Chelyan Bridge Approach Ramp is comprised of six concentric girder lines with a constant radius of 509.30 ft measured along the bridge centerline supporting a reinforced concrete deck. The span lengths measured along the centerline are: 129.87 ft – 174.65 ft – 138.43 ft. The girders in the structure are spaced at 10.21 ft, and all of the girders in the cross-section have a web depth of 72 inches. The cross frame spacing varies slightly in each span, with an average spacing of approximately 14.5 ft; as measured along the centerline of the

structure. All of the structure's supports are radial with the horizontal curve. The two girders adjacent to the centerline, G8 and G9, are utilized for the current two-girder system study.

### 4.3.1 Base Model

The curved two-girder system, shown in Figure 4.13, serves as the Base Model for the parametric studies, investigating the effects of web out-of-plumbness with changes in radius, girder spacing, web depth, and cross frame spacing. For simplicity, the naming convention for the two-girder system is different from that of the Chelyan Bridge Approach Ramp: the interior girder (G8) is named G1 and the exterior girder (G9) is named G2 in the two-girder system.

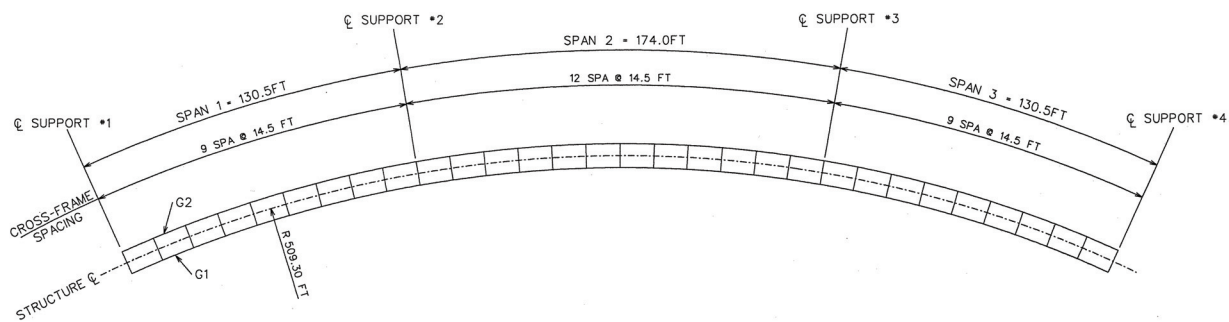


**Figure 4.13** Curved Two-Girder System in Plan View (Base Model)

Additional differences between the Base Model, and the actual Chelyan Ramp structure, facilitate creation of the finite element models for the parametric study, and mitigate the data reduction associated with study. First, the span lengths are adjusted slightly in order to have a symmetrical structure. The span lengths of the Base Model, as measured along the structure centerline are: 130.50 ft – 174.0 ft – 130.5 ft. A symmetrical structure is desired for this study so

that no anomalies in the results develop due to either an unsymmetrical structure or one with a non-ideal span balance (end to center span length ratio). Unlike the actual structure, a consistent cross-frame spacing of 14.5 ft is used throughout the Base Model. The centerline radius (509.30 ft) and girder spacing (10.21 ft) are maintained in the Base Model.

As is typical with bridge structures, there are variations in girder flange plate width and thickness, and web plate thickness, along the length of each girder. This is the case with the girders used in the Chelyan Approach Ramp Bridge. However, again to mitigate the considerable computational effort and results management, a single girder cross-section geometry is used along the entire length of each girder for the two-girder system Base Model. A weighted average of flange geometry is obtained based on plate width and thickness as a function of plate length, as measured along the girder’s longitudinal axis. The web depth and thickness are held constant throughout the Base Model. These resulting girder cross-section dimensions are shown in Table 4-7.

**Table 4-7** Girder Cross-Sections for Base Model

<b>Component</b>	<b>G1</b>	<b>G2</b>
Top Flange Width	18.0 in.	20.0 in.
Top Flange Thickness	1.103 in.	1.197 in.
Web Depth	72.0 in.	72.0 in.
Web Thickness	0.500 in.	0.500 in.
Bottom Flange Width	18.0 in.	20.0 in.
Bottom Flange Thickness	1.205 in.	1.591 in.
Section Weight	264 lbs/ft	312 lbs/ft

It should be noted that girder G2, the girder on the exterior of the curve, employs larger flange sizes than the interior girder G1, which is typical of horizontally curved steel I-girder

bridges. Typically, “outboard” girders have a proportionally larger role in resisting the internal bending moments in a horizontally curved steel I-girder bridge, therefore requiring larger cross-sections.

#### **4.3.2 Finite Element Modeling**

The nonlinear finite element program ADINA (2003) is utilized for all the models associated with this curved two-girder system investigation. The steel girders of the two-girder system are modeled using shell finite elements placed at the mid-plane of the cross-sectional plate components making up the plate girders. The shell elements used in these models are four node ADINA MITC-4 nonlinear shell finite elements. The MITC-4 shell element performs quite well in out-of-plane bending, such as plate bending (Bathe 1996). ADINA automatically assigns five degrees of freedom to each node of the MITC-4, unless loading or mesh compatibility requires six degrees of freedom (ADINA 2003). The elimination of the rotational degree of freedom about the axis normal to the shell surface helps to maintain efficiency with regard to computational time. However, at element intersections, such as web-flange junctions or cross frame connection locations, all six degrees of freedom are utilized.

The length to width aspect ratio for elements on any flange is approximately 1 to 1, while the length to height aspect ratio for web elements is 1 to 2. Shell element length to width ratios such as these were validated by verification study (section 3.1.1), as well as through additional research conducted by the author in regard to the Ford City Veterans Bridge (Chavel and Earls 2001). A modeling strategy such as this was successfully employed by Howell (2006), who investigated the web out-of-plumbness for the entire (idealized) Chelyan Approach Ramp Bridge, without performing a parametric study.

All of the cross frame members are modeled with linear beam elements. Six beam elements in all are used to model each “X” type cross frames, one each for the top and bottom chords, and 2 for each diagonal due to the bolted connection at the middle of the “X.” All cross frame members are WT 5x22.5 sections, and appropriate cross-sectional properties are input for each. The cross frame members are connected to the girders at the web-flange junction. Since the main objective of this study is to investigate flange stress and girder displacements, connection plates are not included in these models because they do not significantly contribute to the vertical, lateral, or torsional resistance of the girders. Figure 4.14 shows an oblique view of the finite element mesh near a cross frame.

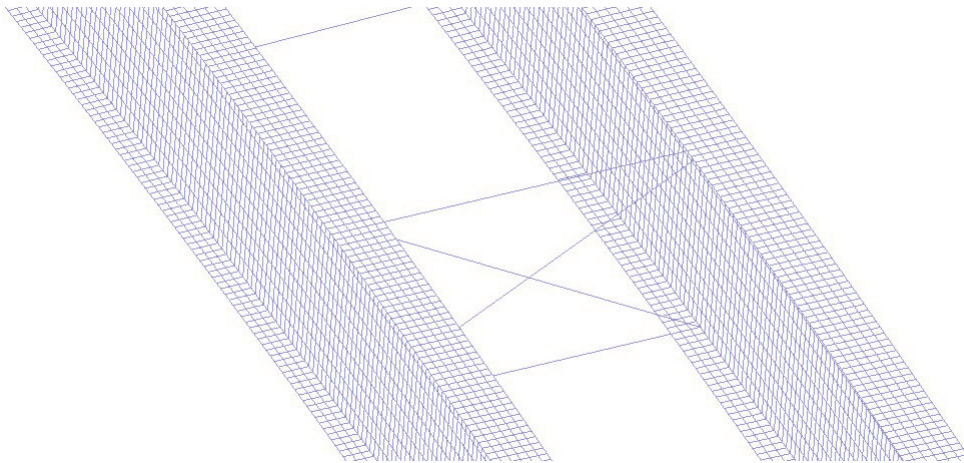


**Figure 4.14** Curved Two-Girder System Finite Element Model

The boundary conditions of the curved two-girder system models represent fixed bearings at Supports #2 and #3 (Figure 4.13), and longitudinally guided bearings and Supports #1 and #4. In order to accurately reproduce the effects of the fixed and guided bearings via the boundary conditions, local skewed (rotated) coordinate systems are applied to the nodes representing the supports. The use of local skewed coordinate systems forces the transverse

boundary condition to be radial to the girder, and the longitudinal boundary condition to be in the direction of the girder's longitudinal axis at the support location.

Rotation of the local coordinate axes is determined through trigonometric principles. The angle formed between the support radials is the same as the angle between the tangents of the same radial support lines, as shown in Figure 4.15. Support #1 is established to coincide with the global  $x$ - $y$  coordinate system, and successive transformed  $x'$ - $y'$  coordinate systems are established for the other support locations.

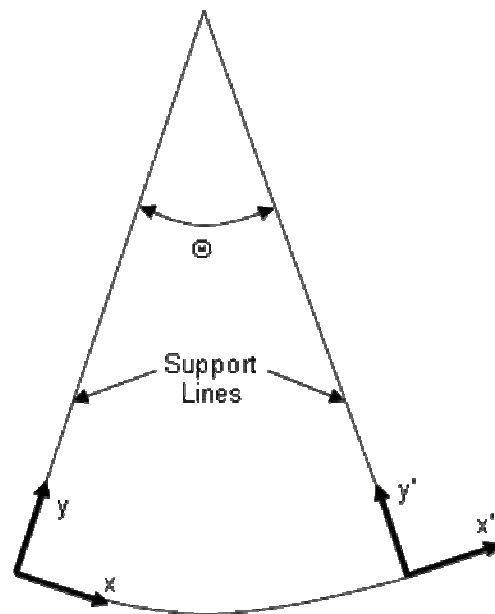


**Figure 4.15** Local Coordinate System for Support Locations

All models are investigated for girder displacement and flanges stresses due to various angles of web-plumbness associated with the two-girder system's steel self-weight. By specifying the material density of steel as  $490 \text{ lb/ft}^3$ , a mass-proportional body force is applied to the structure in order to model the influence of gravity induced self-weight. This load case reproduces the steel dead load case which would exist after the girders and cross frames are erected, assuming no temporary support structures are used. Since dead load behavior is

expected to be linear, the inclusion of a superimposed slab dead load would result in greater stresses and displacements although trends evident in the results would not be expected to change. Since the objective of this study is to investigate the trends, the slab dead load may be neglected without affecting conclusions. Furthermore, the application of the slab load will necessarily vary based on the parametric variations chosen; this by neglecting this load, this additional dependent parameters is also neglected.

#### **4.3.2.1 Artificially induced out-of-plumbness**

In order to study effects of web out-of-plumbness in the curved two-girder system under steel dead load, an artificially induced web out-of-plumbness is applied to the respective models. Four variations of web out-of-plumbness are investigated in this study: 0, 2, 3, and 5 degrees. It has been seen in practice that the out-of-plane rotation due to dead load of a curved girder bridge is on the order to 1 to 2 degrees (Chavel and Earls 2001, 2004), and thus the range of out-of-plumbness considered is thought to be sufficient for the purposes of the present study. The implementation of 5 degrees of web out-of-plumbness serves as an absolute maximum that could be experienced.

In a typical field condition, each girder in the cross section deflects vertically and rotates about the web-bottom flange junction. This rotational behavior is similarly applied to the models developed in this study. Additionally, in a typical curved girder bridge, the out-of-plumbness angle will be largest at the center of a span and approximately zero at the supports where rotation is assumed to be restrained (i.e. no out-of-plane rotation at the supports). In the case of a three-span curved two-girder system, with an ideal span arrangement, the center span will have a larger vertical displacement and top flange lateral displacement (out-of-plane rotation) than the end spans. This behavior is seen in the steel dead load analysis of the Base Model, as shown in

Figure 4.16. Therefore, the artificially induced web out-of-plumbness is developed so that the maximum angle of rotation occurs at the mid-span of the center span, and an out-of-plumbness proportional to the dead load rotation (for example Figure 4.16b) is applied to the end-spans. The proportion (end span to center span out-of-plane rotation) ratio is based on the analysis of the web-plumb model for each set of models created for the parametric studies.

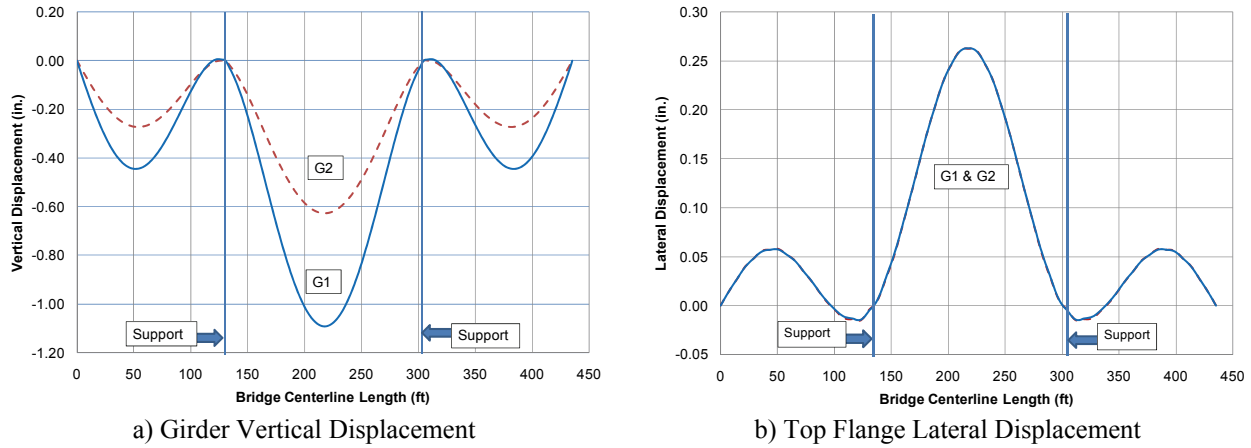


**Figure 4.16** Base Model Steel Dead Load Analysis

Considering the out-of-plane rotation behavior of curved girder bridges, a sine function is fit to the web-top flange junction such that the function has a period of twice the span length measured along the girder's centerline.

$$y(x, \delta) = \delta \sin\left(\frac{\pi x}{L}\right); \delta = A f(h) \quad (4-4)$$

Where:  $\delta$  = Maximum lateral displacement; occurring at mid-span

$L$  = Span length

$x$  = Longitudinal position from support, measured along girder centerline

$y(x)$  = incremental lateral displacement imperfection imposed at position 'x'

$A$  = proportion of out-of-plane rotation based on analysis of non-rotated girders,

$A = 1$  for center span,

$$A = (\text{end span} \div \text{center span out-of-plane rotation for 0 deg. model})$$

h = vertical distance from web-bottom flange junction

This function's values represent lateral displacement, measured from the girder's centerline, imposed to achieve the desired degree of web out-of-plumbness at the mid-span of each span. Superposition of the lateral displacement determined via equation (4-4) and the original position for the plumb model (0 degree case), yields the new web-top flange junction for the girder, for a given out-of-plumb rotation angle. Figure 4.17 depicts the position of the web-top flange junction for 5 degrees of web out-of-plumbness, as measured from the plumb location of the web-top flange junction for the Base Model. Note that the artificially applied top flange displacement (Figure 4.17) for the five-degree case is qualitatively similar to the measured top flange displacement for the zero-degree case (Figure 4.16b).

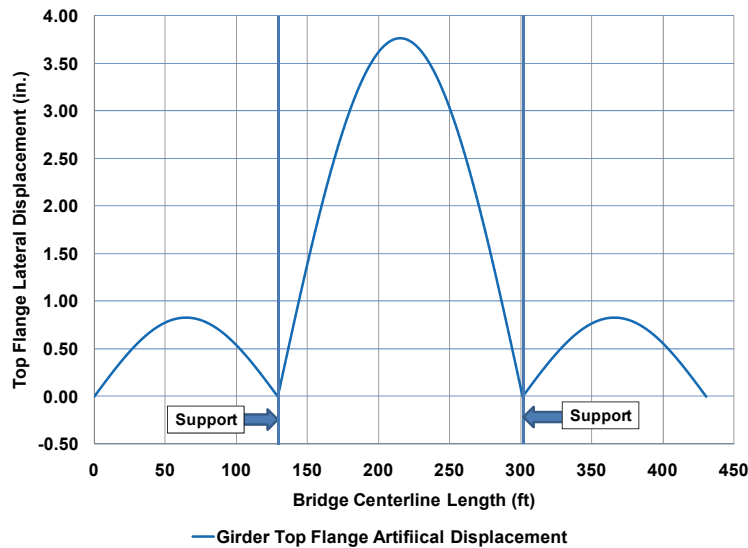


**Figure 4.17** Base Model – 5 Deg. Web Out-of-Plumb – Artificial Top Flange Displacement

From this new web-top flange junction, certain assumptions about each girder cross section are preserved. First, the cross section is assumed to retain its original shape, such that throughout the span the flanges are perpendicular to the web. Second, the boundary conditions

representing the bearings are not changed since the angle of web-plumbness is always zero at the support. Third, the cross frames are still assumed to intersect the girders at the web-flange junctions, as previously discussed.

The following sections discuss the individual parameters varied in this study. It is important to note that the variation of these parameters in practice will, in many cases, require the girder to be redesigned to carry loads distributed to them. This has not been done here so as to affect a direct comparison between models and assess the effects of each varied parameter without introducing other dependent parameters or properties.

### **4.3.3 Radius Variation**

The first parametric study carried out examines web out-of-plumbness effects as the structure's centerline radius is varied. Five different structure centerline radii are investigated: 309.3 ft, 509.3 ft (Base Model), 709.3 ft, 909.3 ft, and 1109.3 ft. The centerline span lengths are held constant for all five structures: 130.50 ft – 174.0 ft – 130.5 ft, resulting in R/L (radius/center span length) ratios of 1.8, 2.9, 4.1, 5.2, and 6.4, respectively. For each of these radii, the flange von Mises stresses and girder displacements predicted by the nonlinear finite element models are monitored and compared to determine the effects of the applied web out-of-plumb angle for the steel dead load case. Total dead load, steel and concrete deck, is not investigated in these studies. The behavior would be similar to that shown herein, with only a different magnitude of stresses and displacements. Appendix C contains results for all analyses conducted regarding the radius parameter.

### 4.3.3.1 Flange Stresses

The girder flange von Mises stresses are monitored at three specific location in each model to quantify the effects of web out-of-plumbness on the vertical and lateral bending moments and torsional behavior. As shown in Figure 4.18, the chosen locations are at points centered about the maximum vertical bending locations:  $0.4L$  of the End Span,  $0.0L$  of the Center Span (i.e. Support #2), and  $0.5L$  of the Center Span (where  $L$  is the span length). At each location, flange tip stresses are observed at the quarter points between cross frames, in order to obtain an accurate representation of the lateral flange bending effects.

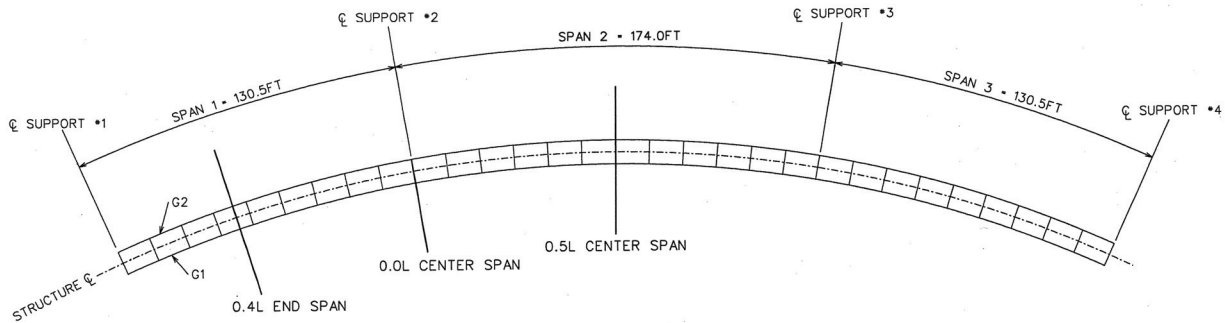


**Figure 4.18** Monitored Flange Stress Locations (Plan View)

For both girders G1 and G2, the flange stresses are investigated at the top and bottom flange tips, as shown in Figure 4.19, where the stresses are most affected by web out-of-plane rotation. By investigating the flange tip stresses, conclusions can be made about the effects of the varying distance of the flange tips from the neutral axis, as well as the interaction effects between the vertical bending moment and bi-moment (lateral bending).

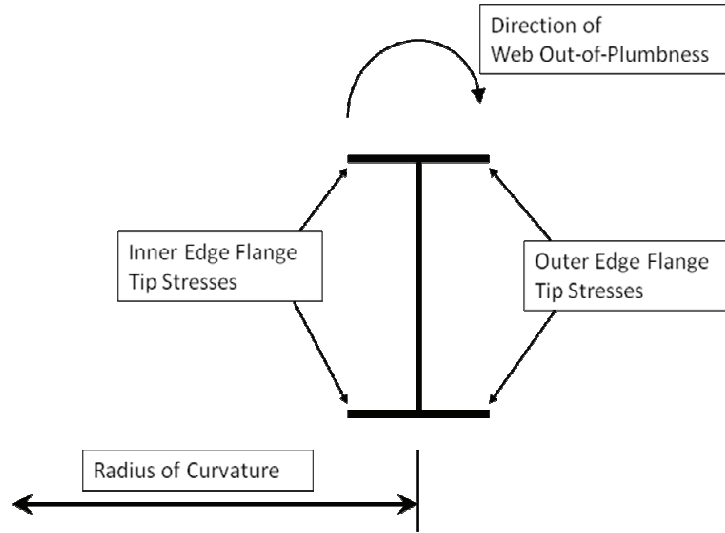
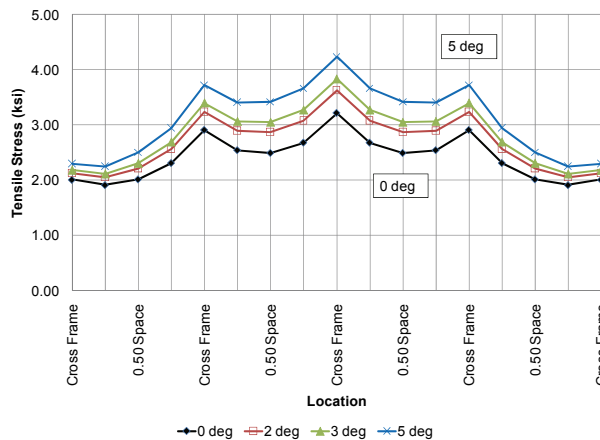


Figure 4.19 Flange Tip Stress Locations

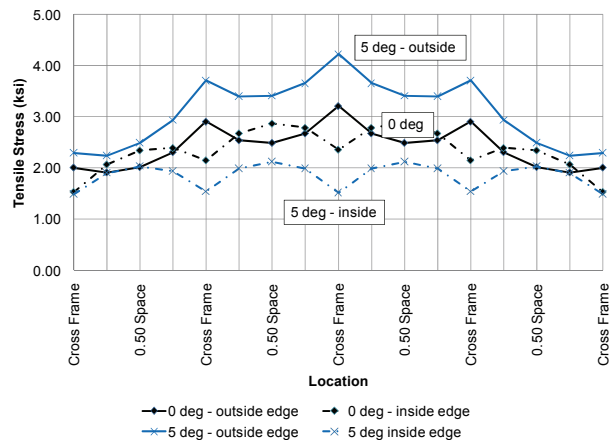
**Flange Stresses at Maximum Positive Vertical Bending Moment**

The outer-edge bottom flange tip stress at 0.5L of the center span increases for increasing angles of web out-of-plumbness, yielding the maximum tensile stress in the section. For the web-plumb two-girder system with a centerline radius of 509.3 ft (Base Model), the girder G2 outer-edge bottom flange stress at 0.5L of the center span is 3.22 ksi. At the same location, the tensile stresses for 2 and 5 degrees web out-of-plumbness are 3.63 ksi and 4.23 ksi, respectively.

Figure 4.20a shows the results for girder G2 at the 0.5L center span location.



a) Outside Flange Tip – All Web Out-of-Plumb Angles



b) Inside and Outside Flange Tip Stresses

Figure 4.20 G2 Bottom Flange Tip Stresses at 0.5L Center Span (R=509.3 ft)

Also of note is the difference in bottom flange tip stresses between the outside and inside edges of the flange, as shown in Figure 4.20b. The bi-moment and subsequent lateral flange bending cause the stresses to be different on each side of the flange. On the outer-edge of the flange, at the cross-frame locations, the lateral bending causes an additional tensile stress. While on the inner-edge of the flange, the lateral bending causes a compression stress, which reduces the total flange edge tensile stress at the cross frame location. The inner-edge flange tip tensile stress is 2.36 ksi while the outer-edge stress is 3.22 ksi for the web plumb model (0 degrees) resulting in a stress gradient across the 20 inch wide flange of 0.043 ksi/in. Likewise, the inner and outer-edge flange tip tensile stresses are 1.52 ksi and 4.23 ksi, respectively for the web out-of-plumbness angle of 5 degrees; a gradient of 0.136 ksi/in. From this observation, it is evident that as the web out-of-plumbness angle increases, the stress gradient across the flange due to lateral flange bending increases substantially.

As expected, lateral flange bending of the flanges is less significant as the girders become straighter (i.e.: the radius increases). Thus the flange tip stresses become more uniform across the flange width and the maximum value falls as the radius increases (Table 4-8). These stresses will trend toward the uniaxial (and thus uniformly distributed) bending stress as the radius tends to infinity (straight girder). Nonetheless, investigation of the girder G2 maximum bottom flange tip stresses at 0.5L of the center span for all radii shows that as the structure centerline radius becomes larger, there is a relative increase in the maximum flange tip stress as the applied web out-of-plumbness increases. As shown in Table 4-8, for a centerline radius of 309.3 ft, the bottom flange tip stresses increase by 0.38 ksi for the web out-of-plumbness angle of 2 degrees, while the structure with a centerline radius of 1109.3 ft experiences 0.51 ksi increase (although

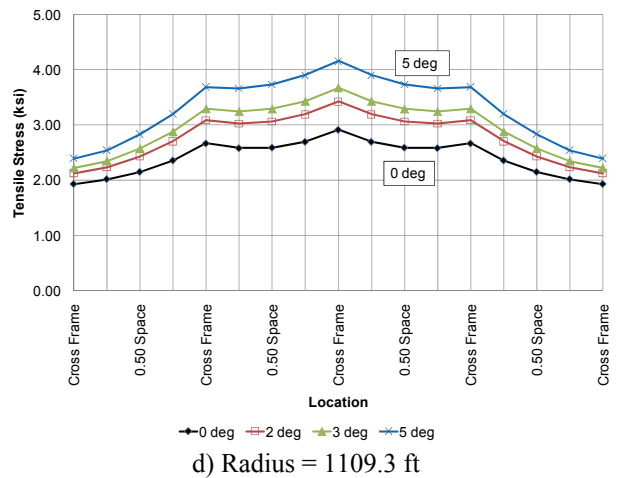
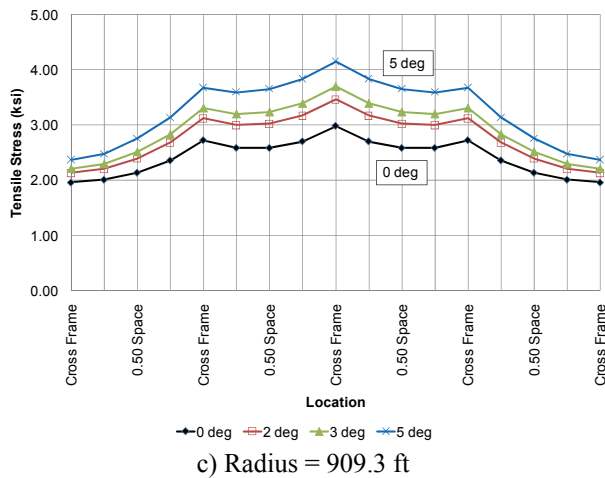
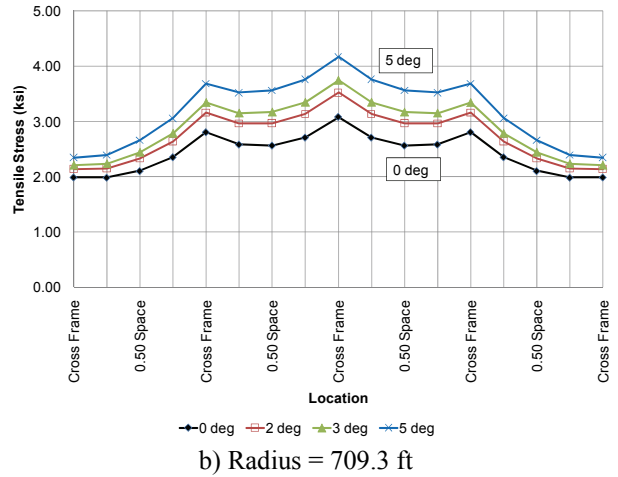
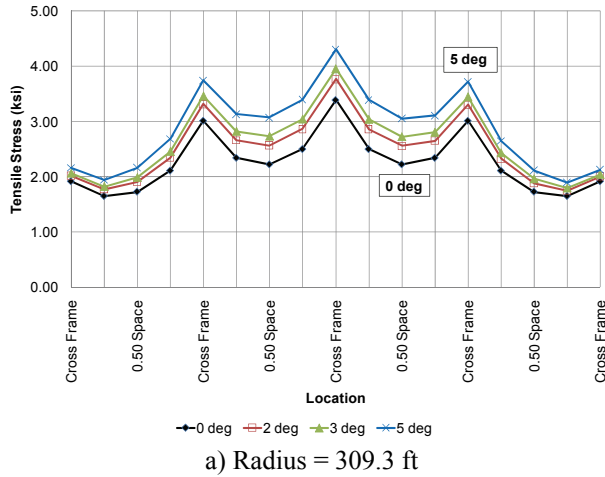
the magnitude of stresses is reduced with increasing radii). This observation is a manifestation of the behavior of the girder shifting from being dominated by the effects of curvature (at small radii) to being dominated by the effects of web out-of-plumbness (at greater radii).

Figure 4.21 provides a graphical representation of the girder G2 maximum bottom flange tensile stresses for radii of a) 309.3 ft, b) 709.3 ft, c) 909.3 ft, and d) 1109.3 ft. From this figure it is observed that as the radius of curvature increases, the peaks in the flange stress at the cross frames become less prominent. This illustrates that as the structure becomes straighter (larger radius) the effects of lateral flange bending have a less significant effect on the flange stress.

**Table 4-8** G2 Maximum Bottom Flange Tip Stress at 0.5L Center Span

Centerline Radius (ft)	$\theta = 0$ deg	$\theta = 2$ deg		$\theta = 3$ deg		$\theta = 5$ deg	
	$\sigma$ (ksi)	$\sigma$ (ksi)	% inc.*	$\sigma$ (ksi)	% inc.*	$\sigma$ (ksi)	% inc.*
309.3	3.39	3.77	11%	3.95	17%	4.31	27%
509.3	3.22	3.63	13%	3.83	19%	4.23	31%
709.3	3.08	3.53	15%	3.75	22%	4.18	36%
909.3	2.98	3.47	16%	3.70	24%	4.16	40%
1109.3	2.92	3.43	18%	3.68	26%	4.16	44%

\* % inc. is the percentage increase in flange stress from the web-plumb case (0 deg)



**Figure 4.21** G2 Maximum Bottom Flange Tip Stresses at 0.5L Center Span

The inner-edge top flange tip stress near 0.5L of the center span increases for increasing angles of web out-of-plumbness, yielding the maximum compressive stress in the section. These compressive stresses do not occur exactly at the cross frame locations, but at a location midway between cross frame points (0.5 cross frame space). This behavior is illustrated in Figure 4.22a for the Base Model. For the web-plumb two-girder system with a centerline radius of 509.3 ft (Base Model), the girder G2 inner-edge top flange stress near 0.5L of the center span is 3.75 ksi. At the same location, the compressive stresses for 2 and 5 degrees web out-of-plumbness are 4.10 ksi and 4.62 ksi, respectively.

Also of note is the difference in top flange tip stresses between the outside and inside edges of the flange, at the mid-span of the cross frame spacing, as shown in Figure 4.22b. The effects of lateral flange bending result in an additive compressive stress on the inner-edge of the flange. While on the outer-edge of the flange, the lateral bending causes a tensile stress, which reduces the total flange outer-edge compressive stress at the mid-span between cross frames. The inner-edge flange tip compressive stress is 3.75 ksi, while the outer-edge flange tip stress is 2.65 ksi for the web-plumb model (0 degrees) (0.055 ksi/in. gradient). Likewise, the inner and outer-edge flange tip compressive stresses are 4.61 ksi and 1.75 ksi, respectively for web out-of-plumbness angle of 5 degrees (0.132 ksi/in.). As expected, the stress gradients across the top and bottom flanges due to lateral flexural are similar. Due to the boundary conditions (rotation about the web-bottom flange interface), the top flange should experience greater lateral bending effects. The difference in stress gradients reported between the top and bottom flanges here reflect the fact that the peak stresses are obtained at different locations for each flange: at the cross frame on the bottom flange and between cross frames for the top flange.

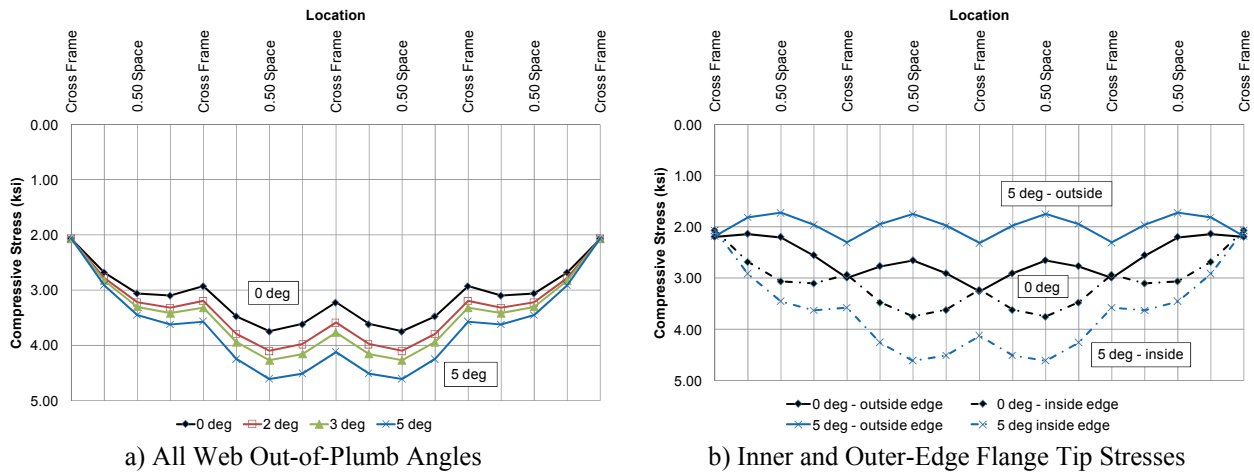


**Figure 4.22** G2 Inner-Edge Top Flange Stresses at 0.5L Center Span (R=509.3 ft)

Investigation of the girder G2 inner-edge top flange tip stresses at 0.5L of the center span for all radii shows that as the centerline radius becomes larger, there is a relative increase in the maximum flange tip stress as the applied web out-of-plumbness increases. As the web out-of-plumbness angle increases, the inner-edge tip of the top flange moves further away from the neutral axis resulting in a smaller section modulus for this flange tip and an increase in stress. As shown in Table 4-9, for a centerline radius of 309.3 ft, the top flange tip stress increases by 0.33 ksi for the web out-of-plumbness angle of 2 degrees, while the structure with a centerline radius of 1109.3 ft experiences an 0.40 ksi increase (although the magnitude of stresses is reduced with increasing radii). Again, this observation is a manifestation of the behavior of the girder shifting from being dominated by the curvature effects (at small radii) to being dominated by the web out-of-plumbness effects (at greater radii).

**Table 4-9** G2 Maximum Inner-Edge Top Flange Tip Stress near 0.5L Center Span

Centerline Radius (ft)	$\theta = 0$ deg	$\theta = 2$ deg		$\theta = 3$ deg		$\theta = 5$ deg	
	$\sigma$ (ksi)	$\sigma$ (ksi)	% inc.*	$\sigma$ (ksi)	% inc.*	$\sigma$ (ksi)	% inc.*
309.3	3.86	4.19	9%	4.35	13%	4.67	21%
509.3	3.75	4.10	9%	4.27	14%	4.61	23%
709.3	3.59	3.95	10%	4.13	15%	4.48	25%
909.3	3.47	3.85	11%	4.03	16%	4.39	27%
1109.3	3.38	3.78	12%	3.97	18%	4.33	28%

\* % inc. is the percentage increase in flange stress from the web-plumb case (0 deg)

Note: Flange stresses are taken at midpoint between cross frames near 0.5L.

Figure 4.23 provides a graphical representation of the girder G2 maximum top flange compressive stresses for radii of a) 309.3 ft, b) 709.3 ft, c) 909.3 ft, and d) 1109.3 ft. From this figure it is observed that as the radius increases, the peaks in the flange stress at the cross frames become less prominent. This illustrates that as the structure becomes straighter (larger radius) the effects of lateral flange bending have a less significant effect on the flange stress.

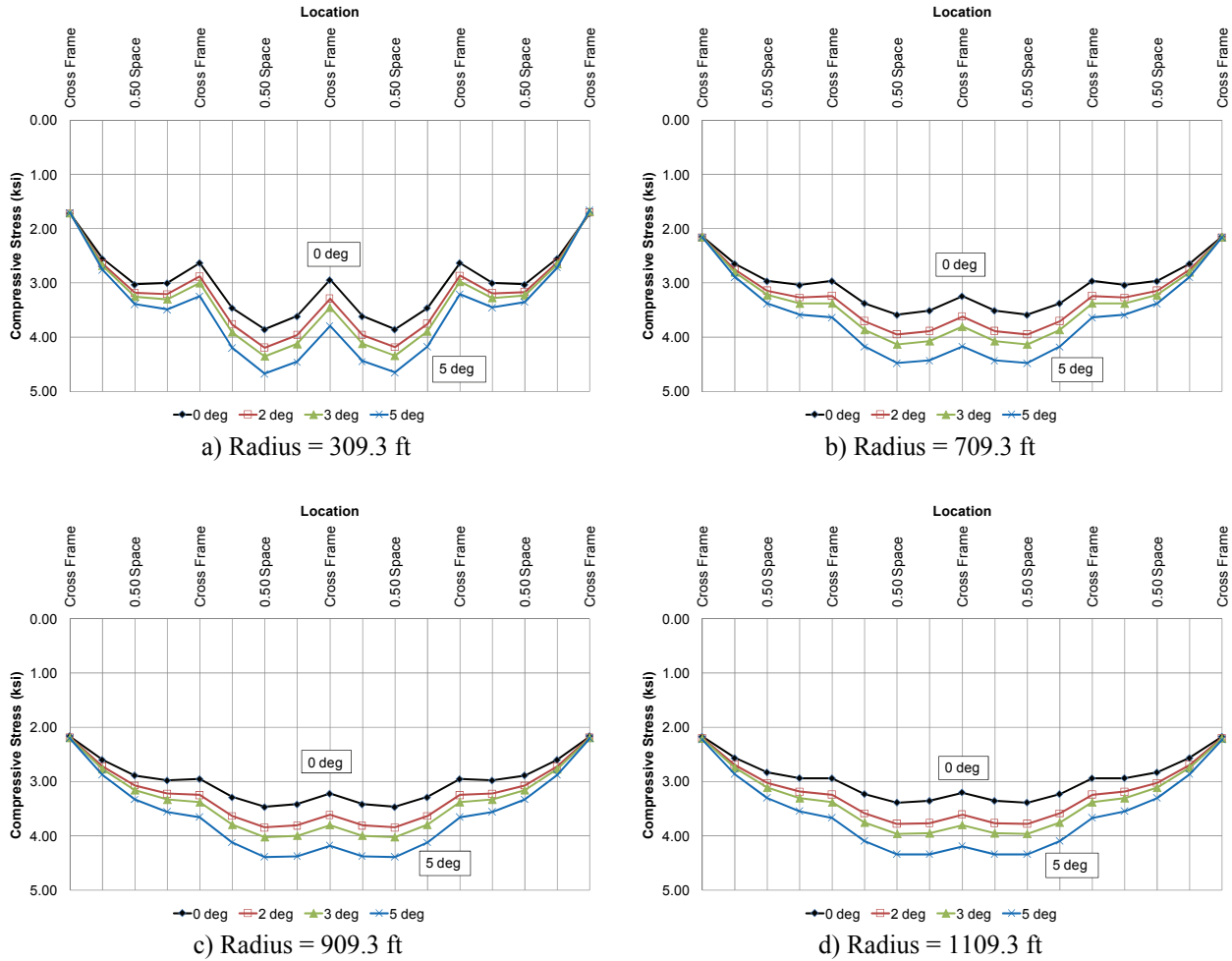
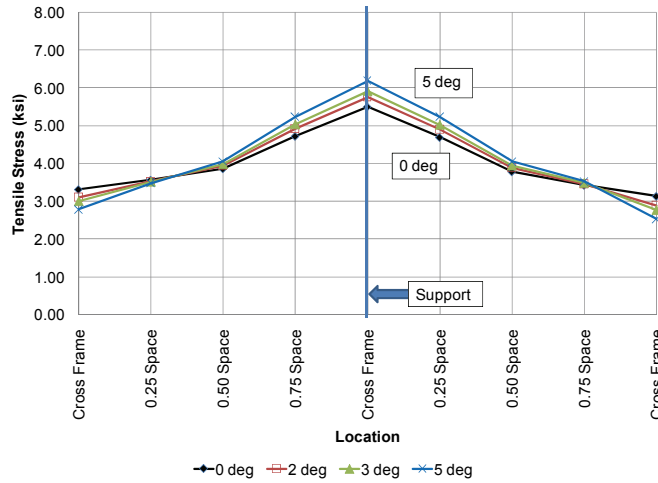


Figure 4.23 G2 Maximum Top Flange Tip Stresses at 0.5L Center Span

**Flange Stresses at Maximum Negative Vertical Bending Moment**

The top flange tip stress at 0.0L of the center span increases for increasing angles of web out-of-plumbness. At this location, at the interior support, the top flange experiences maximum tensile stress. For the web-plumb two-girder system with a centerline radius of 509.3 ft (Base Model), the girder G2 outer-edge top flange stress at 0.0L of the center span is 5.51 ksi. At the same location, the top flange tip tensile stress for 2 and 5 degrees web out-of-plumbness are 5.77 ksi and 6.20 ksi, respectively. This results in a flange tip stress increase of 5% for a web out-of-

plumbness of 2 degrees, and a 13% increase for a web out-of-plumbness angle of 5 degrees. Figure 4.24 shows the results for girder G2 at the 0.0L center span location, for the Base Model.



**Figure 4.24** G2 Top Flange Outer-Edge Stresses at 0.0L Center Span (R=509.3 ft)

The outer-edge top flange tip stress at the 0.0L center span location increases for increasing angles of web out-of-plumbness, yielding the maximum tensile stress in the section. As shown in Table 4-10, for a centerline radius of 309.3 ft, the top flange tip stress increases by 0.44 ksi for the web out-of-plumbness angle of 2 degrees, while the structure with a centerline radius of 1109.3 ft experiences a 0.25 ksi increase. It should be noted that as the structure becomes straighter, the outer-edge top flange tip stress decreases. This behavior illustrates that the top flange lateral bending moments decrease with an increase in radius of curvature. However, since the stress increases as the web out-of-plumbness increases are similar for each radius, the stress increase is attributed to web out-of-plumbness and not lateral flange bending associated with the radius of curvature.

**Table 4-10** G2 Maximum Outer-Edge Top Flange Tip Stress at 0.0L Center Span

Centerline Radius (ft)	$\theta = 0$ deg	$\theta = 2$ deg		$\theta = 3$ deg		$\theta = 5$ deg	
	$\sigma$ (ksi)	$\sigma$ (ksi)	% inc.*	$\sigma$ (ksi)	% inc.*	$\sigma$ (ksi)	% inc.*
309.3	6.40	6.84	7%	7.08	11%	7.60	19%
509.3	5.51	5.77	5%	5.91	7%	6.20	13%
709.3	5.07	5.34	5%	5.48	8%	5.77	14%
909.3	4.82	5.09	6%	5.22	8%	5.51	14%
1109.3	4.66	4.91	5%	5.05	8%	5.33	14%

\* % inc. is the percentage increase in flange stress from the web-plumb case (0 deg)

Figure 4.25 provides a graphical representation of the girder G2 maximum inner-edge top flange tensile stresses for radii of a) 309.3 ft, b) 709.3 ft, c) 909.3 ft, and d) 1109.3 ft. From this figure it is observed that as the radius of curvature increases, the maximum top flange stresses at the support become smaller.

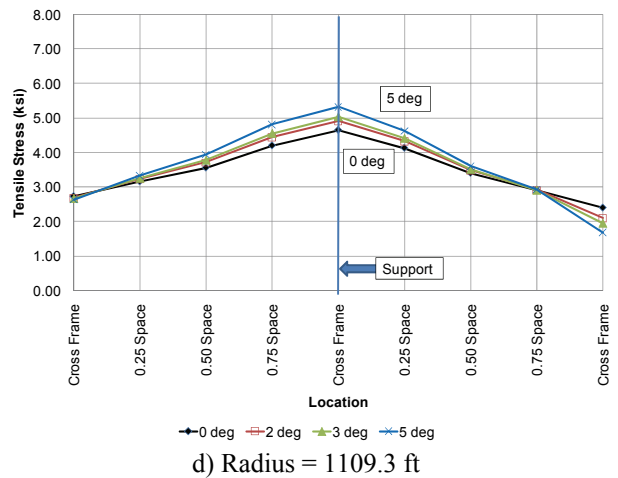
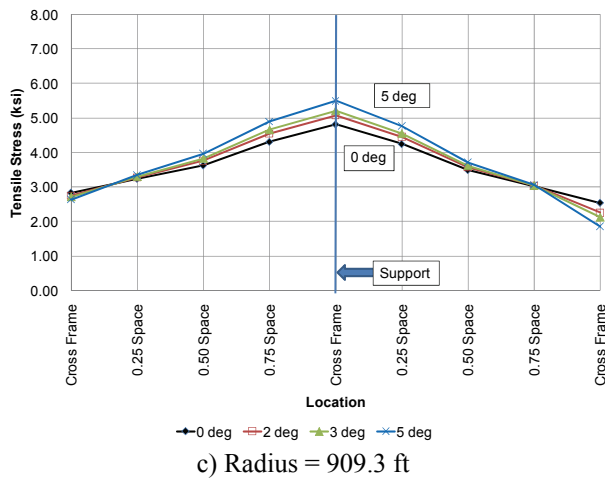
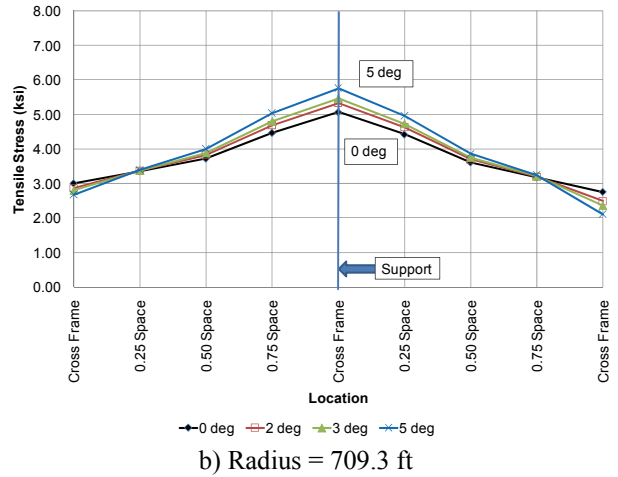
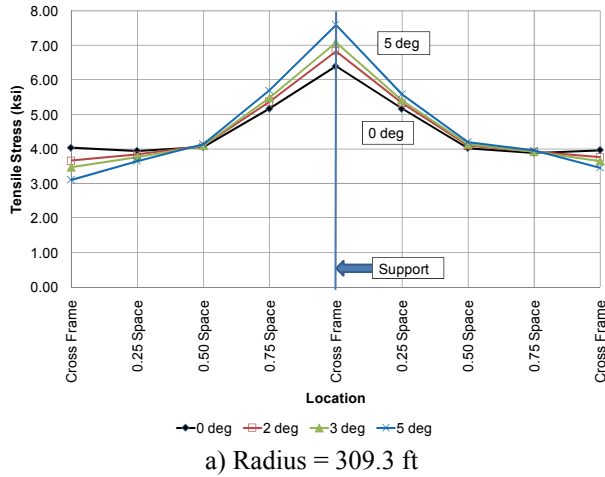


**Figure 4.25** G2 Maximum Outer-Edge Top Flange Tip Stresses at 0.0L Center Span

The inner-edge bottom flange tip stress at 0.0L of the center span increases for increasing angles of web out-of-plumbness. At this location, which is at the interior support, the bottom flange experiences its maximum tensile stress. For the web-plumb two-girder system with a centerline radius of 509.3 ft (Base Model), the girder G2 outer-edge top flange stress at 0.0L of the center span is 6.28 ksi. At the same location, the bottom flange tip compressive stress for 2 and 5 degrees web out-of-plumbness are 6.68 ksi and 7.29 ksi, respectively. Figure 4.26 shows the results for girder G2 at the 0.0L center span location, for the Base Model. It should be noted that the localized affect of the boundary condition creates the large peak seen in Figure 4.26 at

the support. In the case of the models, the boundary condition representing the support is applied across the bottom flange at a line of nodes. However, in an actual structure the bearing providing the support has a definitive length, and is not a single point. If an actual bearing was modeled, this modeling anomaly would not exist in the figure, however the trend of increasing stress due to web out-of-plumbness would remain the same.

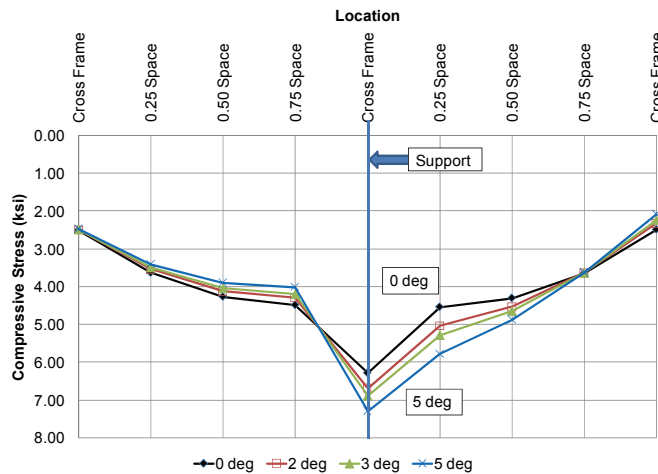


**Figure 4.26** G2 Bottom Flange Inner-Edge Stresses at 0.0L Center Span (R=509.3 ft)

The G2 inner-edge bottom flange tip stress at 0.0L of the center span increases for increasing angles of web out-of-plumbness, yielding the maximum compressive stress in the section. As shown in Table 4-11, for a centerline radius of 309.3 ft, the top flange tip stress increases by 0.43 ksi for the web out-of-plumbness angle of 2 degrees, while the structure with a centerline radius of 1109.3 ft experiences a 0.36 ksi increase, although again, absolute stress falls with increasing radii.

**Table 4-11 G2 Maximum Inner-Edge Bottom Flange Tip Stress at 0.0L Center Span**

Centerline Radius (ft)	$\theta = 0$ deg	$\theta = 2$ deg		$\theta = 3$ deg		$\theta = 5$ deg	
	$\sigma$ (ksi)	$\sigma$ (ksi)	% inc.*	$\sigma$ (ksi)	% inc.*	$\sigma$ (ksi)	% inc.*
309.3	6.38	6.81	7%	7.08	11%	7.60	19%
509.3	6.28	6.68	6%	6.89	10%	7.29	16%
709.3	6.20	6.59	6%	6.79	10%	7.19	16%
909.3	6.11	6.48	6%	6.67	10%	7.06	16%
1109.3	6.03	6.39	6%	6.57	10%	6.94	15%

\* % inc. is the percentage increase in flange stress from the web-plumb case (0 deg)

Figure 4.27 provides a graphical representation of the girder G2 maximum inner-edge top flange tensile stresses for radii of a) 309.3 ft, b) 709.3 ft, c) 909.3 ft, and d) 1109.3 ft.

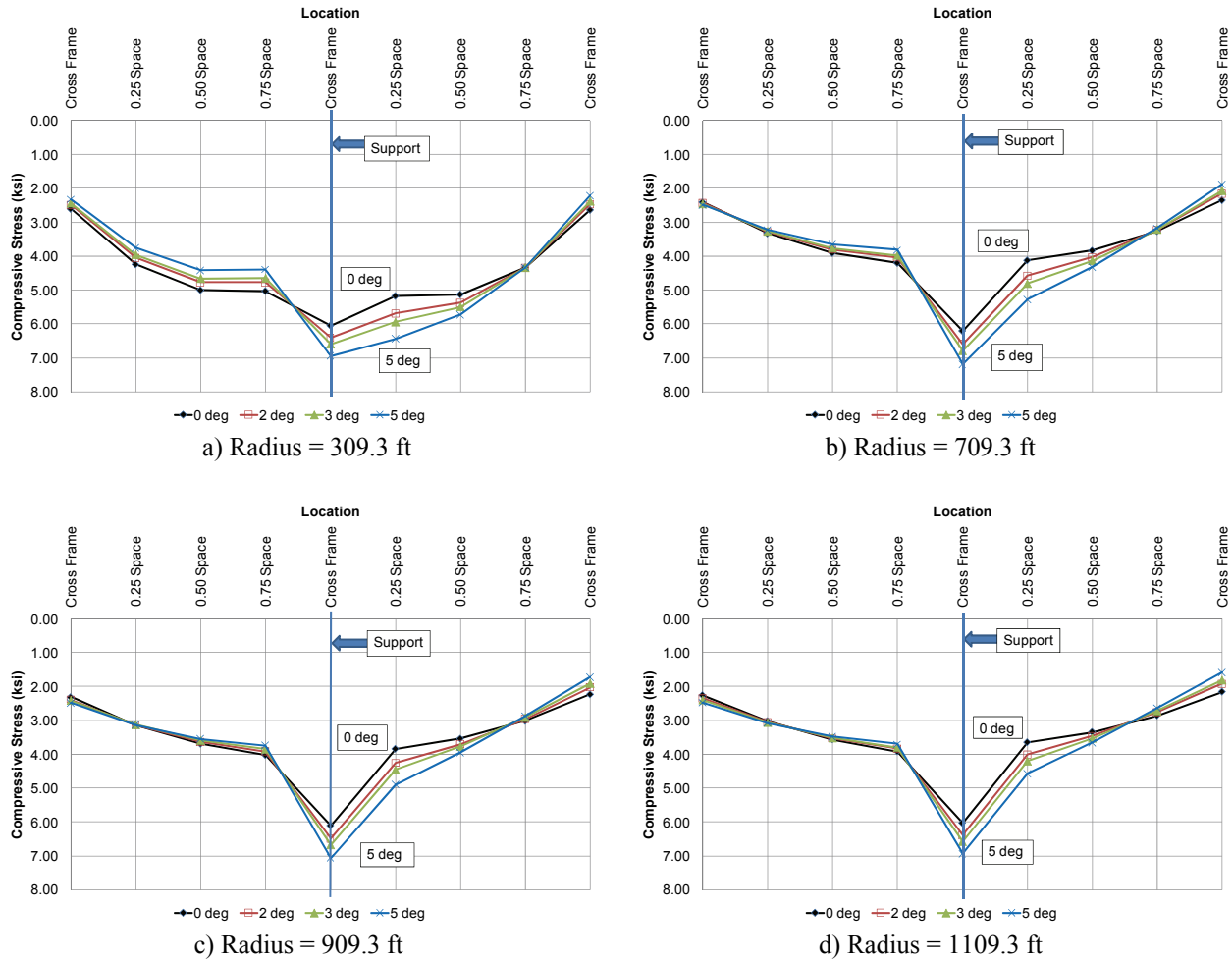


**Figure 4.27 G2 Maximum Inner-Edge Bottom Flange Tip Stresses at 0.0L Center Span**

#### 4.3.3.2 Girder Displacements

Vertical and lateral displacements are monitored for the top and bottom flange-web junctions along the length of the structure, and in particular at the midpoint of the center span, for each radius investigated.

The vertical displacements for the top flange (and bottom flange) are different for girders G1 and G2, such that the outer girder G2 has larger vertical displacements than girder G1, which is typical of curved I-girder bridges. These vertical displacements increase slightly as a result of increasing initial web out-of-plumbness. Figures 4.28a) and b) show the girder top flange vertical displacements along the length of the structure for the model with a centerline radius of 509.3 ft (Base Model), for each angle of web out-of-plumbness. For closer inspection of the boxed section in Figures 4.28a) and b), Figure 4.28c) and d) show the girder vertical displacements at the 0.5L of the center span location. Girder G2 has a vertical displacement of 1.09 in. at the mid-span for the web-plumb condition (0 degrees), and increases to 1.18 in. for a web out-of-plumbness of 5 degrees; an increase of 8% for the extreme out-of-plumb case.

Investigation of the girder G2 top flange vertical displacements at 0.5L of the center span for all radii analyzed shows that as the structure centerline radius becomes larger, there is a decrease in absolute vertical displacement although the incremental effect of web out-of-plumbness becomes more pronounced. As shown in Table 4-12, for a centerline radius of 309.3 ft, the vertical displacement increases by 0.02 in. for the web out-of-plumbness angle of 2 degrees, while the structure with a centerline radius of 1109.3 ft experiences a 0.04 in. increase. Given that these vertical displacements increases are quite small, web out-of-plumbness has relatively little effect on the on the vertical displacements due to steel dead load. This observation reinforces the sectional analysis presented in Section 4.1.3 where the moment of

inertia about the axis of flexure ( $I_x'$ ) is not significantly affected by the angles of web out-of-plumbness considered.

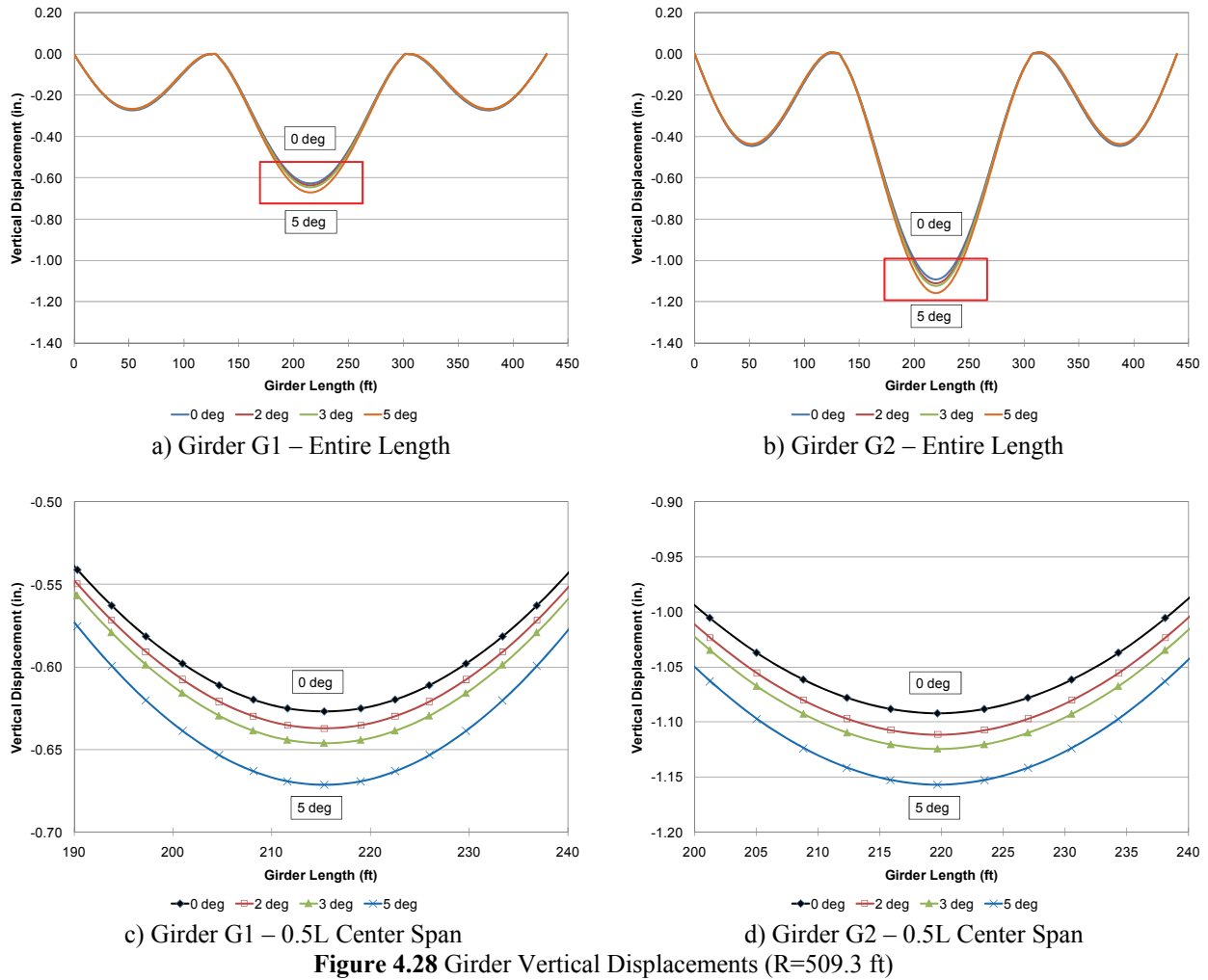


**Table 4-12** G2 Top Flange Vertical Displacement at 0.5L Center Span

Centerline Radius (ft)	$\theta = 0$ deg	$\theta = 2$ deg		$\theta = 3$ deg		$\theta = 5$ deg	
	$\Delta_V$ (in.)	$\Delta_V$ (in.)	% inc.*	$\Delta_V$ (in.)	% inc.*	$\Delta_V$ (in.)	% inc.*
309.3	1.25	1.27	2%	1.28	2%	1.31	5%
509.3	1.09	1.12	3%	1.14	5%	1.18	8%
709.3	0.99	1.03	4%	1.05	6%	1.10	11%
909.3	0.94	0.97	3%	0.99	5%	1.04	11%
1109.3	0.90	0.94	4%	0.96	7%	1.01	12%

\* % inc. is the percentage increase in vertical displacement from the web-plumb case (0 deg)

The top and bottom flange lateral displacements are generally the same for girders G1 and G2, since both girders rotate out-of-plane the same amount due to the applied loading. However, for any particular girder, the lateral displacements of the top and bottom flange are different, causing an out-of-plane rotation of the cross section, as shown in Figure 2.9. Table 4-13 shows the top and bottom flange lateral displacements and subsequent out-of-plane rotation ( $\phi$ ) for each radii and web out-of-plumbness angle investigated at the mid-span of the center span (0.5L location). In this data rotations should be interpreted as additional rotation beyond the original web out-of-plumbness. As expected, this maximum out-of-plane rotation is larger for the structures with a smaller centerline radius. The maximum out-of-plane rotation for a centerline radius of 309.3 ft is  $0.276^\circ$ , while the structure with a centerline radius of 1109.3 ft has a maximum out-of-plane rotation of  $0.110^\circ$  (no web out-of-plumbness).

Closer investigation of the girder G2 out-of-plane rotation at 0.5L of the center span for all radii shows that as structure centerline radius becomes larger, there is a relative increase in maximum out-of-plane rotation, as the applied web out-of-plumbness increases. As shown in Table 4-14, for a centerline radius of 309.3 ft, the out-of-plane rotation increases by  $0.002^\circ$  for the web out-of-plumbness angle of 2 degrees, while the structure with a centerline radius of 1109.3 ft experiences  $0.008^\circ$  increase. However, it is realized that the maximum top flange lateral displacements increase by no more than 0.139 in. for a web out-of-plumbness of 2 degrees, which is quite small as compared to the size of the structure investigated. These results further illustrate the dominate effect of curvature radius on relative rotation of the girder sections. The greatest contribution to relative rotation attributable to out-of-plumbness is 14.5% of the total rotation (Radius = 1109.3 ft,  $\theta = 5$  deg.). Indeed the effect of out-of-plumbness is virtually negligible for a small curvature radius (309.3 ft).

**Table 4-13** G2 Flange Lateral Displacements at 0.5L Center Span

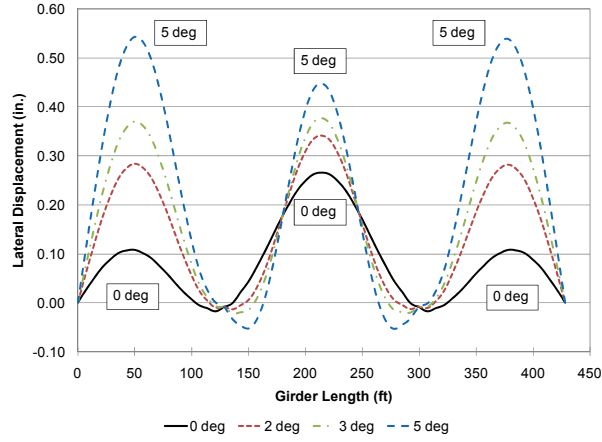
Radius (ft)	$\theta = 0$ deg			$\theta = 2$ deg			$\theta = 3$ deg			$\theta = 5$ deg		
	$\Delta_L$ (in.)		$\phi$ (deg)	$\Delta_L$ (in.)		$\phi$ (deg)	$\Delta_L$ (in.)		$\phi$ (deg)	$\Delta_L$ (in.)		$\phi$ (deg)
	Top	Bot.		Top	Bot.		Top	Bot.		Top	Bot.	
309.3	0.266	-0.081	0.276	0.341	-0.008	0.278	0.378	0.028	0.279	0.449	0.098	0.279
509.3	0.263	-0.013	0.220	0.350	0.069	0.224	0.393	0.109	0.226	0.475	0.188	0.228
709.3	0.256	0.043	0.169	0.358	0.137	0.176	0.407	0.184	0.177	0.502	0.273	0.182
909.3	0.256	0.087	0.134	0.376	0.198	0.142	0.433	0.252	0.144	0.542	0.354	0.150
1109.3	0.262	0.124	0.110	0.401	0.253	0.118	0.466	0.315	0.120	0.590	0.432	0.126

**Table 4-14** G2 Out-of-Plane Rotation at 0.5L Center Span

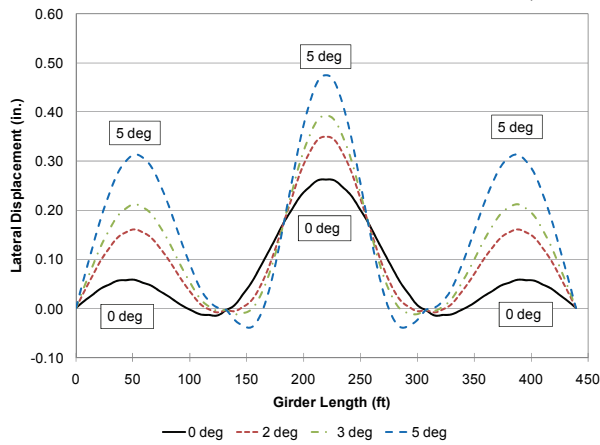
Centerline Radius (ft)	$\theta = 0$ deg	$\theta = 2$ deg		$\theta = 3$ deg		$\theta = 5$ deg	
	$\phi$ (deg.)	$\phi$ (deg.)	% inc.*	$\phi$ (deg.)	% inc.*	$\phi$ (deg.)	% inc.*
309.3	0.276	0.278	0.7%	0.279	1.1%	0.279	1.1%
509.3	0.220	0.224	1.8%	0.226	2.7%	0.228	3.6%
709.3	0.169	0.176	4.1%	0.177	4.7%	0.182	7.7%
909.3	0.134	0.142	6.0%	0.144	7.5%	0.150	11.9%
1109.3	0.110	0.118	7.3%	0.120	9.1%	0.126	14.5%

\* % inc. is the percentage increase in vertical displacement from the web-plumb case (0 deg)

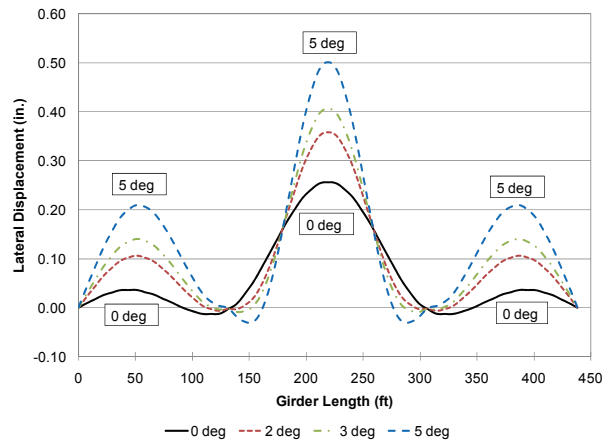
Figure 4.29 provides a graphical representation of the girder G2 top flange lateral displacements for radii of a) 309.3 ft, b) 509.3 ft, c) 709.3 ft, d) 909.3 ft, and e) 1109.3 ft. From this figure it is observed that as the radius increases, the top flange lateral displacements in the center span moderately increase and decrease more significantly in the end spans, with increasing web out-of-plumbness.



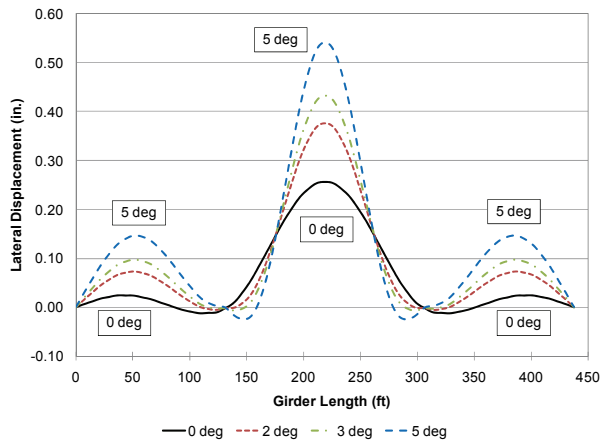
a) Radius = 309.3 ft



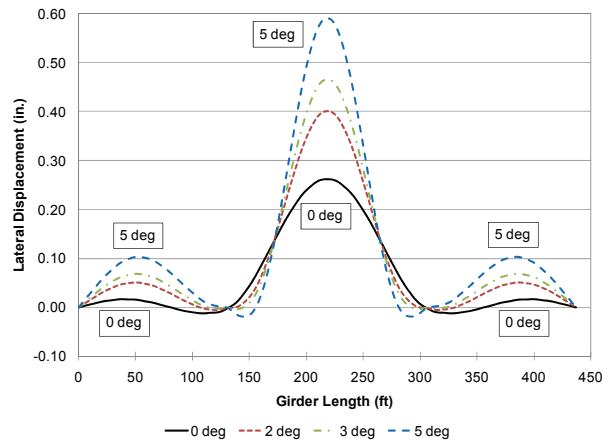
b) Radius = 509.3 ft



c) Radius = 709.3 ft



d) Radius = 909.3 ft



e) Radius = 1109.3 ft

**Figure 4.29 G2 Top Flange Lateral Displacement**

#### 4.3.3.3 Results Discussion

In general, for all radii investigated, the flange tip stresses are more significantly affected in the maximum positive moment location than in the maximum negative moment location as the web out-of-plumbness angle increases. The increase in flange tip stresses varies from 9% to 18% at the positive moment location for a web out-of-plumbness of 2 degrees. However, the increase in flange tip stresses is no more than 7% at the maximum negative moment location, for web out-of-plumbness of 2 degrees. For a web out-of-plumbness of 2 degrees, the largest magnitude stress increase attributable to the out-of-plumb condition is 0.51 ksi occurring at the outer-edge of the bottom flange at 0.5L (tension stress) for a radius of 1109.3 ft.

The greatest increases in flange tip stresses are to be expected in the positive moment location due to the fact that this location has the maximum initial web out-of-plumbness (i.e. 2 deg, 3 deg, or 5 deg). The out-of-plane rotation at this location, results in an increased distance from the neutral axis to the bottom flange outside tip, reducing the section modulus, thus resulting in a larger flange tip stress. Additional flange tip stresses result from the lateral flange bending associated with the restoring forces provided by cross frames. As the torsion on the section increases due to curvature (smaller radius), these cross frame restoring forces increase. It is shown in Figure 4.21 that for structures with smaller radii, the effects of lateral flange bending increase. At the support, the initial web out-of-plumbness for each model is zero, and there is little or no out-of-plane rotation caused by the steel dead load at a radial support. Hence, the change in flange tip stresses due to web out-of-plumbness will be less at the maximum negative moment location (0.0L of center span) than at the maximum positive moment location (0.5L of center span).

Investigation of the girder G2 top flange vertical displacements at 0.5L of the center span for all radii shows that as the centerline radius becomes larger, there is a decrease in absolute vertical displacement although the incremental effect of web out-of-plumbness becomes more pronounced. The girder out-of-plane rotation follows a similar behavior; there is a decrease in the out-of-plane rotation as the structure become straighter resulting in the effect of web out-of-plumbness becoming more pronounced. However, it should be noted that the increases in vertical displacement and out-of-plane rotation are quite small, relative to the size of the structure studied.

Girder G1 exhibited a similar behavior to girder G2, with regard to flange stresses and girder displacements. Analytical results for girder G1 can be found in Appendix C.

#### **4.3.4 Girder Spacing Variation**

The second parametric study carried out examines web out-of-plumbness effects as the girder spacing is varied. Four different girder spacings are investigated as part of this study: 8.21 ft, 10.21ft (Base Model), 12.21 ft, and 14.21 ft. The two-girder system centerline radius is held constant at 509.3 ft, and the centerline span lengths are held constant for four structures: 130.50 ft – 174.0 ft – 130.5 ft. Cross frame member sizes are also unchanged. In practice, a change in girder spacing would require a significant redesign of the girders themselves (as they carry proportionally greater loads). However, the girders are not redesigned as part of this parametric study, allowing a direct comparison between the models to be made.

For each girder spacing, the flange von Mises stresses and girder displacements predicted by the nonlinear finite element models are monitored and compared to determine the effects of

the applied web out-of-plumb angle for the steel dead load case. Appendix C contains results for all analyses conducted regarding the girder spacing parameter.

#### **4.3.4.1 Flange Stresses**

Similar to the radius variation models, the girder flange von Mises stresses are monitored at three locations in each model to quantify the effects of web out-of-plumbness on the vertical and lateral bending moments and torsional behavior. As shown in Figure 4.18, the chosen locations are centered about points of maximum vertical bending: 0.4L of the End Span, 0.0L of the Center Span (i.e. Support #2), and 0.5L of the Center Span (where L is the span length). At each location, flange tip stresses are observed at the quarter points between cross frames, in order to obtain an accurate representation of the lateral flange bending effects. For both girders G1 and G2, the flange stresses are investigated at the top and bottom flange tips, as shown in Figure 4.19, where the stresses are most affected by web out-of-plane rotation.

#### **Girder G2 Flange Stresses**

The girder G2 outer-edge bottom flange tip stress at 0.5L of the center span increases for increasing angles of web out-of-plumbness, yielding a maximum tensile stress in the section. As previously reported for the web-plumb two-girder system with a girder spacing of 10.21 ft (Base Model), the girder G2 outer-edge bottom flange stress at 0.5L of the center span is 3.22 ksi. At the same location, the tensile stress for 2 and 5 degrees web out-of-plumbness are 3.63 ksi and 4.23 ksi, respectively.

As the girder spacing is varied, however, there is little significant net affect on flange stress as is shown in Table 4-15. There is an interaction of effects that affects this result however: As the girder spacing becomes larger, there is less load redistribution from girder G1 to girder G2 via the cross frames, therefore reducing the stresses in the G2 flanges. At the same time, as

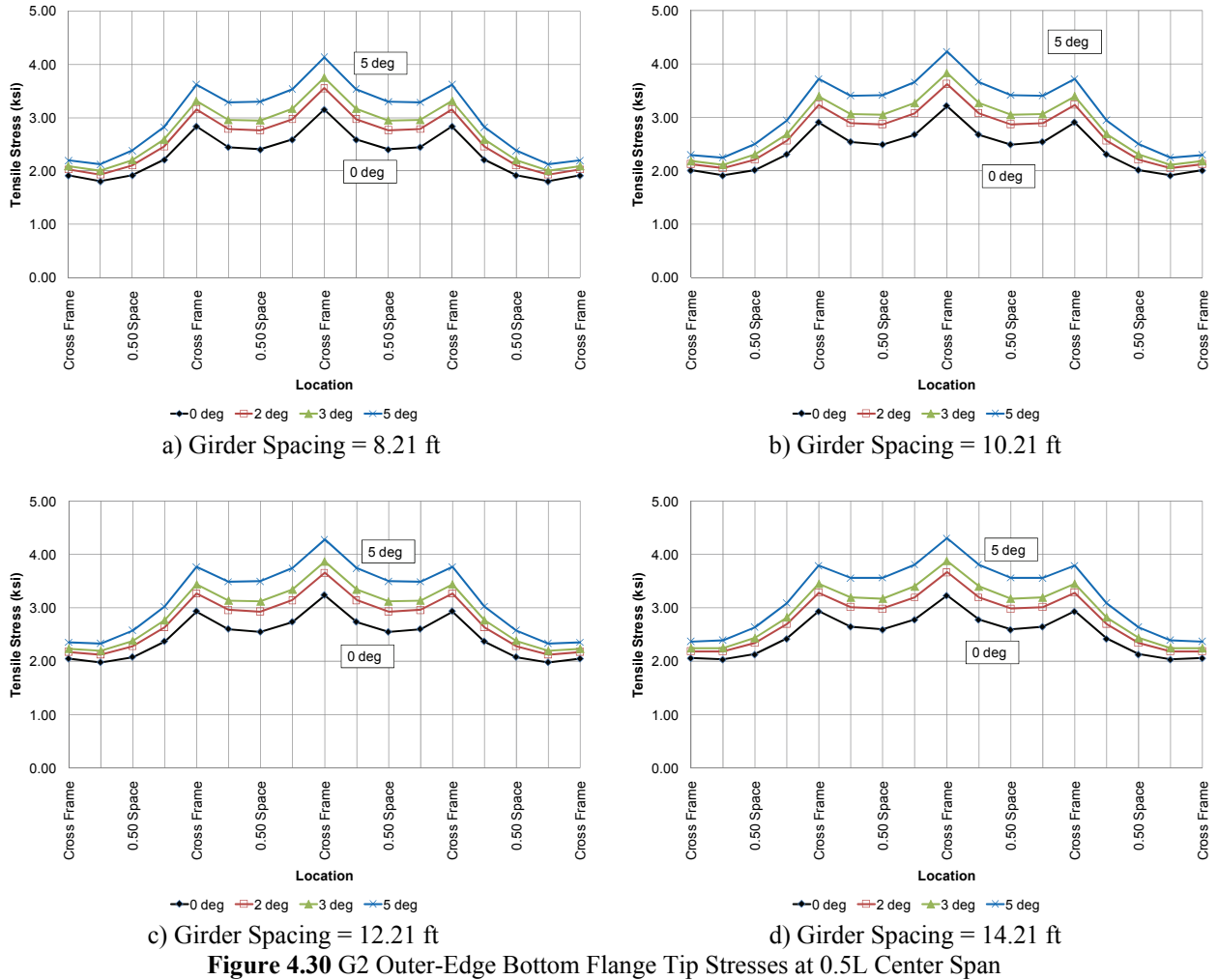
the girder spacing become larger, the individual radius and span length of girder G2 become slightly larger, since the centerline of the structure remains at a radius of 509.3 ft. The slightly larger radius (1 ft) has little effect with regard to lateral flange bending, however the larger span length results in an increase in bending moment and flange stress. These two phenomena offset each other, resulting in a similar outer-edge bottom flange stress for all girder spacings investigated.

**Table 4-15** G2 Maximum Outer-Edge Bottom Flange Tip Stress at 0.5L Center Span

Girder Spacing (ft)	$\theta = 0$ deg	$\theta = 2$ deg		$\theta = 3$ deg		$\theta = 5$ deg	
	$\sigma$ (ksi)	$\sigma$ (ksi)	% inc.*	$\sigma$ (ksi)	% inc.*	$\sigma$ (ksi)	% inc.*
8.21	3.16	3.56	13%	3.75	19%	4.14	31%
10.21	3.22	3.63	13%	3.83	19%	4.23	31%
12.21	3.24	3.66	13%	3.87	19%	4.28	32%
14.21	3.24	3.67	13%	3.89	20%	4.30	32%

\* % inc. is the percentage increase in flange stress from the web-plumb case (0 deg)

Figure 4.30 provides a graphical representation of the girder G2 maximum bottom flange tensile stresses for girder spacings of a) 8.21 ft, b) 10.21 ft, c) 12.21 ft, and d) 14.21 ft. From this figure it is observed that as the girder spacing changes, there is little or no change in the outer-edge bottom flange tip stresses.



Similarly, a review of the girder G2 inner-edge top flange tip compressive stresses at 0.5L of the center span for all girder spacing variations shows that there is an increase in stress as the applied web out-of-plumbness increases. However, as the girder spacing is varied, there is no significant difference in the relative increase in bottom flange tip stresses caused by the web out-of-plumbness. As shown in Table 4-16, for a girder spacing of 8.21 ft and 14.21 ft, the top flange tip stress increases by 0.35 ksi for the web out-of-plumbness angle of 2 degrees. In fact, there is no appreciable difference for a web out-of-plumbness of 5 degrees, in which these girder spacings see an increased tip stress of 0.84 ksi and 0.89 ksi, respectively.

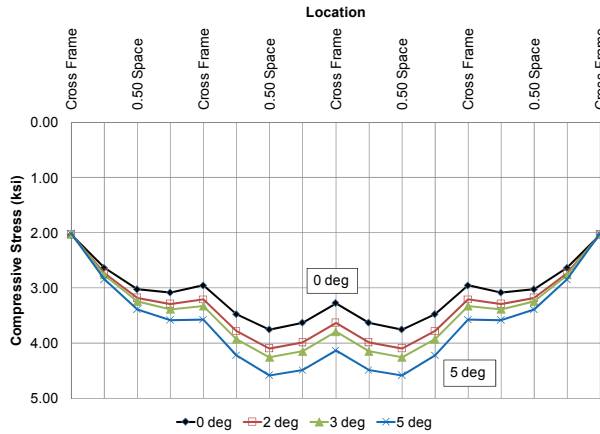
**Table 4-16** G2 Maximum Inner-Edge Top Flange Tip Stress near 0.5L Center Span

Girder Spacing (ft)	$\theta = 0$ deg	$\theta = 2$ deg		$\theta = 3$ deg		$\theta = 5$ deg	
	$\sigma$ (ksi)	$\sigma$ (ksi)	% inc.*	$\sigma$ (ksi)	% inc.*	$\sigma$ (ksi)	% inc.*
8.21	3.75	4.10	9%	4.26	14%	4.59	22%
10.21	3.75	4.10	9%	4.27	14%	4.61	23%
12.21	3.74	4.10	9%	4.28	14%	4.62	23%
14.21	3.74	4.10	9%	4.29	14%	4.64	24%

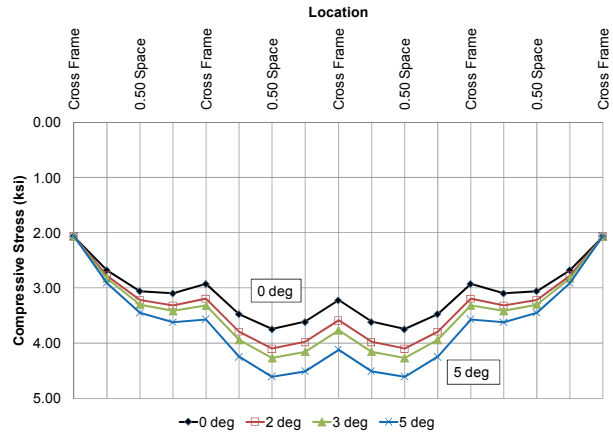
\* % inc. is the percentage increase in flange stress from the web-plumb case (0 deg)  
Note: Flange stresses are taken at midpoint between cross frames near 0.5L.

Figure 4.31 provides a graphical representation of the girder G2 maximum inner-edge top flange compressive stresses for girder spacings of a) 8.21 ft, b) 10.21 ft, c) 12.21 ft, and d) 14.21 ft. From this figure it is observed that as the girder spacing changes, there is little or no change in the inner-edge top flange tip stresses. This behavior supports the fact that the amount of load transferred from girder G1 to girder G2 via the cross frames is reduced as the girder spacing is increased.

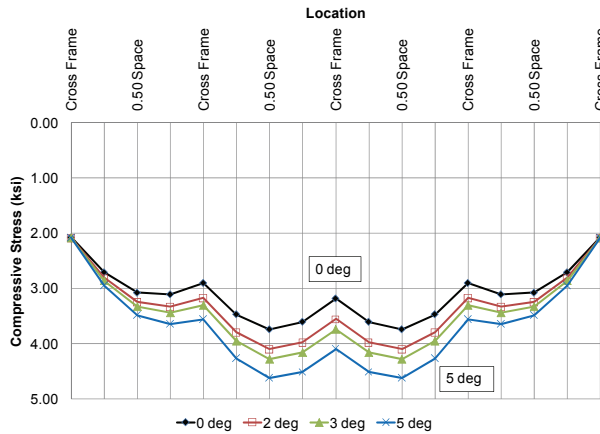
The same general behavior is observed for the location of maximum negative vertical bending moment, at 0.0L of the center span, for girder G2. The variation in girder spacing has no significant effect on change in the bottom or top flange tip stresses caused by the web out-of-plumbness. Analytical results regarding girder the maximum negative moment location can be found in Appendix C.



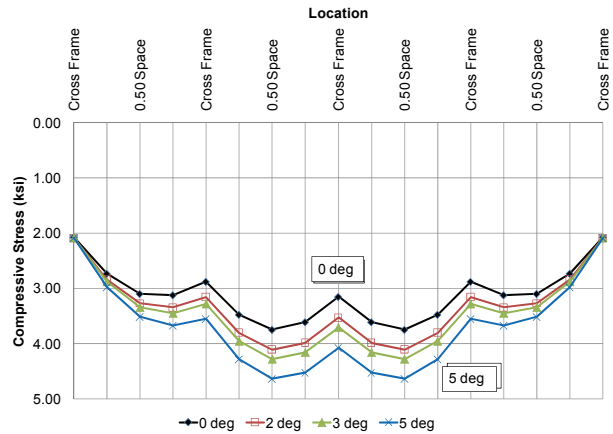
a) Girder Spacing = 8.21 ft



b) Girder Spacing = 10.21 ft



c) Girder Spacing = 12.21 ft



d) Girder Spacing = 14.21 ft

Figure 4.31 G2 Inner-Edge Top Flange Tip Stresses Near 0.5L Center Span

### Girder G1 Flange Stresses

Unlike girder G2, an investigation of the girder G1 flange stresses shows that the variation in girder spacing does have an effect on the flange tip stresses of this interior girder. As shown in Table 4-17, for a girder spacing of 8.21 ft, the outer-edge bottom flange tip stress is 1.55 ksi for the web-plumb model, while the structure with a girder spacing of 14.21 ft experiences a stress of 2.49 ksi. This increase in the flange stress is directly related to the increase of the girder spacing. The increase in girder spacing causes less load to be transferred from girder G1 to girder G2 via the cross frames. Therefore, G1 is required to resist a greater

portion of its own self weight, redistributing less load to the outside girder G2; hence the general increase in flange stresses.

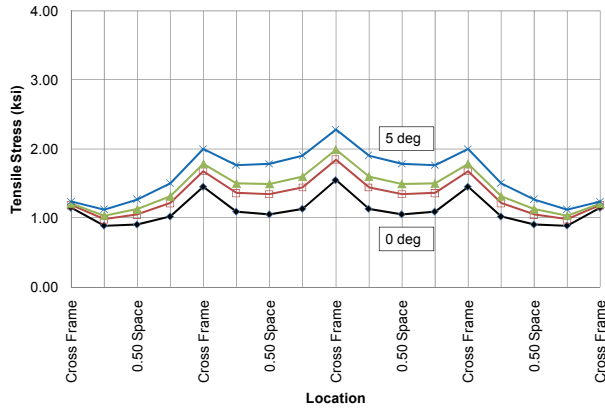
Furthermore, increasing web out-of-plumbness causes the outer-edge bottom flange tip stresses to increase. However, this stress increase is inversely related to the girder spacing: as the girder spacing is increased, the incremental increase in flange stress caused by web out-of-plumbness decreases. Considering the girder G1 and G2 results together, suggests that increasing web out-of-plumbness actually facilitates the redistribution of loads from G1 to G2, although this effect is relatively negligible even at  $\theta = 5$  degrees.

**Table 4-17** G1 Maximum Outer-Edge Bottom Flange Tip Stress at 0.5L Center Span

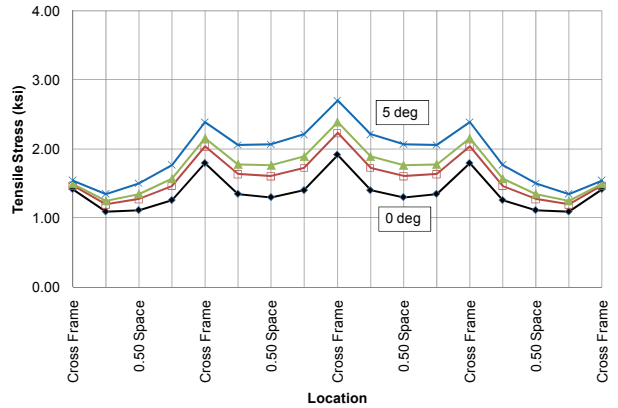
Girder Spacing (ft)	$\theta = 0$ deg	$\theta = 2$ deg		$\theta = 3$ deg		$\theta = 5$ deg	
	$\sigma$ (ksi)	$\sigma$ (ksi)	% inc.*	$\sigma$ (ksi)	% inc.*	$\sigma$ (ksi)	% inc.*
8.21	1.55	1.85	19.4%	2.00	29.0%	2.28	47.1%
10.21	1.92	2.24	16.7%	2.40	25.0%	2.70	40.6%
12.21	2.22	2.56	15.3%	2.73	23.0%	3.06	37.8%
14.21	2.49	2.85	14.5%	3.03	21.7%	3.37	35.3%

\* % inc. is the percentage increase in flange stress from the web-plumb case (0 deg)

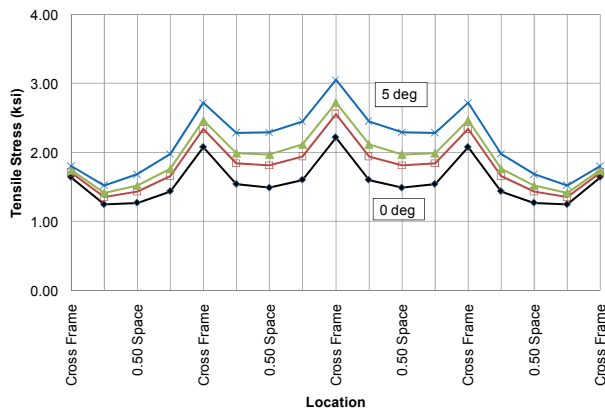
Figure 4.32 provides a graphical representation of the girder G1 maximum outer-edge bottom flange tensile stresses for girder spacings of a) 8.21 ft, b) 10.21 ft, c) 12.21 ft, and d) 14.21 ft. From this figure it is observed that as the girder spacing increases, there is an increase in the girder G1 outer-edge bottom flange tip stresses.



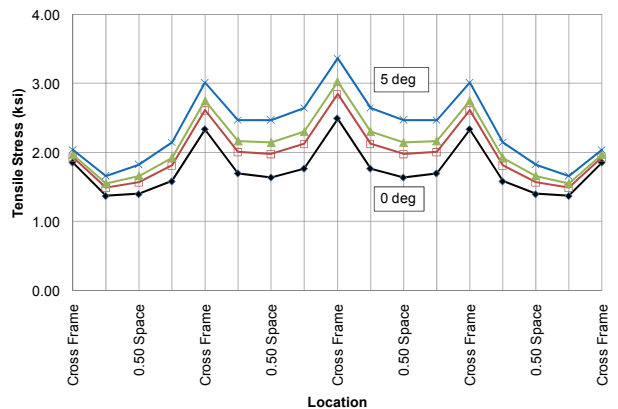
a) Girder Spacing = 8.21 ft



b) Girder Spacing = 10.21 ft



c) Girder Spacing = 12.21 ft



d) Girder Spacing = 14.21 ft

**Figure 4.32** G1 Outer-Edge Bottom Flange Tip Stresses at 0.5L Center Span

The same general behavior is also noted for the girder G1 inner-edge flange tip, at 0.5L of the center span. An increase in the girder spacing causes an increase in the girder G1 inner-edge flange tip compressive stress. Additionally, increasing web out-of-plumbness causes the inner-edge bottom flange tip stresses to increase for the girder spacings studied. These analytical results regarding girder G1 can be found in Appendix C.

#### 4.3.4.2 Girder Displacements

Vertical and lateral displacements are monitored for the top and bottom flange-web junctions along the length of the structure, and in particular at the midpoint of the center span, for each girder spacing investigated.

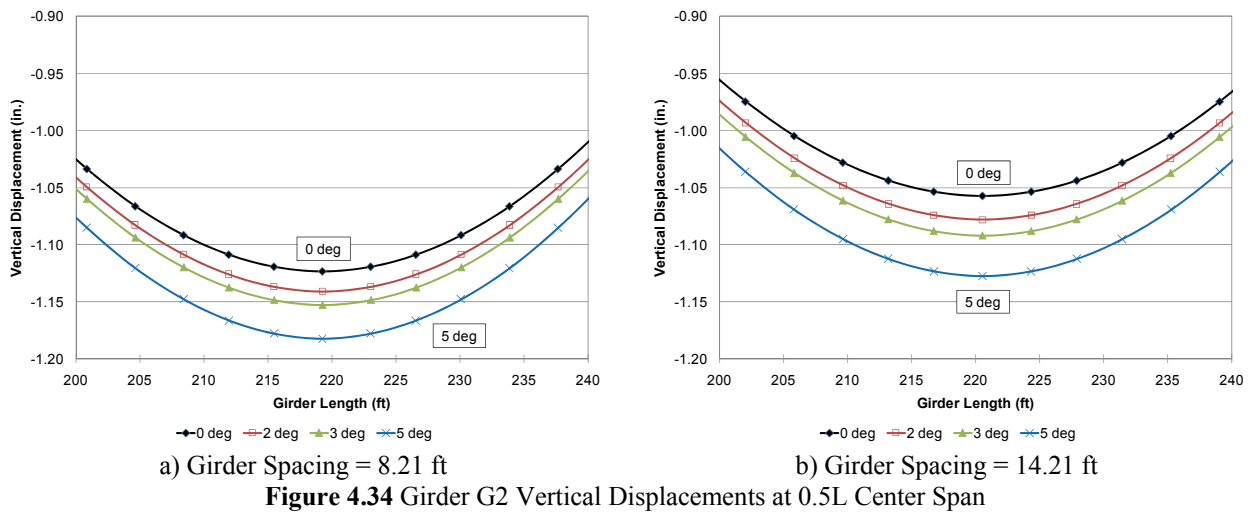
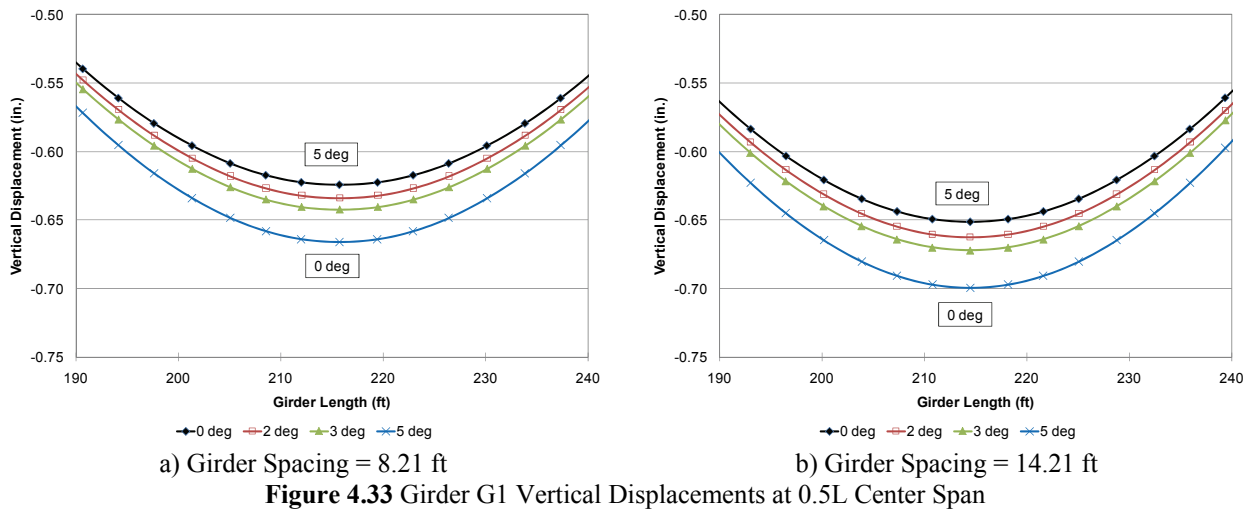
The vertical displacements increase slightly as a result of increasing web out-of-plumbness. Figure 4.33a) and b) show the girder G1 top flange vertical displacements at the 0.5L of the center span location for girder spacing of 8.21 ft and 14.21 ft. Figure 4.34a) and b) show the girder G2 top flange vertical displacements at the 0.5L of the center span location for girder spacing of 8.21 ft and 14.21 ft.

For a girder spacing of 8.21 ft, girder G1 has a vertical displacement of 0.63 in. at the mid-span for the web-plumb condition (0 degrees), and increases to 0.67 in. for a web out-of-plumbness of 5 degrees. Girder G2 has vertical displacement of 1.12 in. for the web-plumb condition, and increases to 1.18 in. for a web out-of-plumbness of 5 degrees.

Likewise, for a girder spacing of 14.21 ft, girder G1 has a vertical displacement of 0.65 in. at the mid-span for the web-plumb condition (0 degrees), and increases to 0.70 in. for a web out-of-plumbness of 5 degrees. Girder G2 has vertical displacement of 1.06 in. for the web-plumb condition, and increases to 1.13 in. for a web out-of-plumbness of 5 degrees.

The increase in vertical displacements caused by the initial web out-of-plumbness is generally small, and is relatively unaffected by the changes in girder spacing studied herein. However, it is noted that girder G1 exhibits a slightly larger vertical displacement as the girder spacing increases. Girder G2 experiences a smaller vertical displacement as the girder spacing increases. This behavior implies that as the girder spacing becomes narrower, the rigid body rotation of the cross section increases, causing the exterior girder G2 to displace more vertically.

As the structure becomes wider, there is less rigid body rotation of the cross section, thus less vertical displacement at the exterior girder. Additionally, as discussed previously, since girder G2 is receiving less load from girder G1 via the cross-frames, its vertical displacement of G2 should indeed reduce with increase in girder spacing.



The top and bottom flange lateral displacements are generally the same for girders G1 and G2, since both girders rotate out-of-plane the same amount due to the applied loading. However, for any particular girder, the lateral displacement of the top and bottom flange are

different, causing an out-of-plane rotation of the cross section as shown in Figure 2.9. This out-of-plane rotation can be calculated from the flange lateral displacements, as shown previously in section 4.3.3.2. Table 4-18 shows the maximum relative out-of-plane rotation at 0.5L of the center span for each girder spacing investigated. As expected, this maximum out-of-plane rotation is larger for the structures with a smaller girder spacing since the torsional resistance of this assembled cross section is less than the structures with a larger girder spacing.

**Table 4-18** G2 Out-of-Plane Rotation at 0.5L Center Span

Girder Spacing (ft)	$\theta = 0$ deg	$\theta = 2$ deg		$\theta = 3$ deg		$\theta = 5$ deg	
	$\phi$ (deg.)	$\phi$ (deg.)	% inc.*	$\phi$ (deg.)	% inc.*	$\phi$ (deg.)	% inc.*
8.21	0.293	0.297	1.4%	0.299	2.0%	0.302	3.1%
10.21	0.220	0.224	1.8%	0.226	2.7%	0.228	3.6%
12.21	0.171	0.175	2.3%	0.177	3.5%	0.180	5.3%
14.21	0.139	0.142	2.2%	0.143	2.9%	0.146	5.0%

\* % inc. is the percentage increase in vertical displacement from the web-plumb case (0 deg)

Closer examination of the girder G2 out-of-plane rotation at 0.5L of the center span shows that as the girder spacing is increased, there is a relatively little in the maximum out-of-plane rotation, as the web out-of-plumbness increases. As shown in Table 4-18, for a girder spacing of 8.21 ft, the out-of-plane rotation increases by 0.004° for the web out-of-plumbness of 2 degrees, while the structure with the girder spacing of 14.21 ft undergoes a 0.003° increase.

Figure 4.35 provides a graphical representation of the girder G2 top flange lateral displacements for girder spacings of a) 8.21 ft, b) 10.21 ft, c) 12.21 ft, and d) 14.21 ft. From this figure it is observed that as the girder spacing increases, the top flange lateral displacements in the center and end spans decrease. Also, the top flange lateral displacements increase as the web out-of-plumbness increases, for all girder spacing studied.

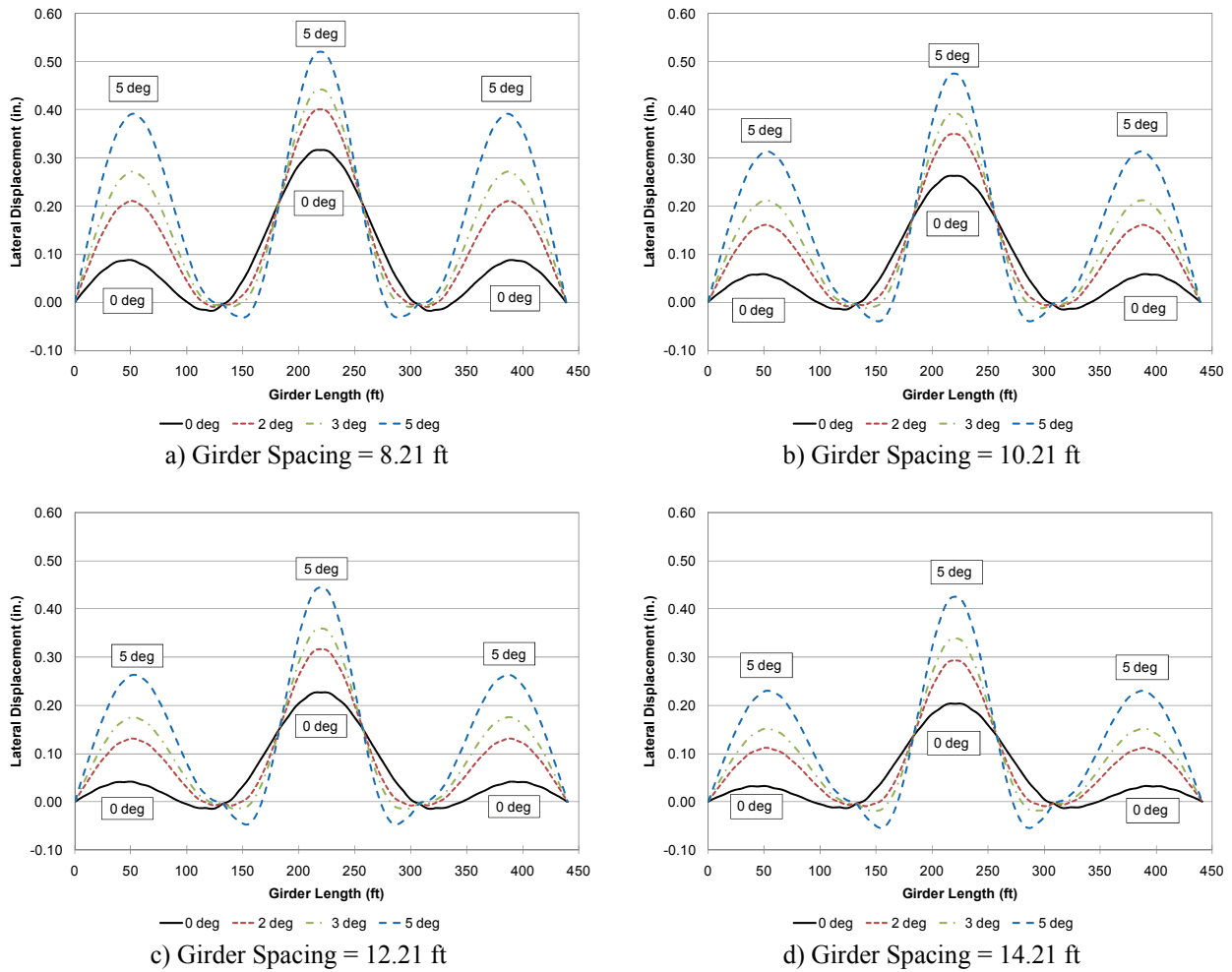


**Figure 4.35** G2 Top Flange Lateral Displacement

#### 4.3.4.3 Results Discussion

The effects of variation of girder spacing are relatively minor and reflect the changes in girder geometry and girder-pair geometry. Larger girder spacing results in less load being distributed from the interior (G1) to exterior girder (G2) of the two-girder system. This increases stresses in G1 and decreases those in G2. This effect is tempered by the global geometry change required by changing the girder spacing. The exterior girder span and radius of horizontal curvature is increased resulting in marginal increase in stresses, offsetting the previously described decreases.

Similarly, vertical and lateral deflections are affected by the redistribution of forces, increased span and radius of the external girder. In addition, however, deflections are affected by the change in torsional properties of the two-girder system resulting from the change in girder spacing. Significantly, the relative out-of-plane rotations (measured relative to the initial out-of-plumb condition) are reduced with increasing girder spacing and its associated increase in girder pair torsional resistance.

#### **4.3.5 Cross Frame Spacing Variation**

The third parametric study carried out examines web out-of-plumbness effects as the cross frame spacing is varied. Five different cross frame spacing arrangements are investigated as part of this study, as shown in Table 4-19. The two-girder system centerline radius is held constant at 509.3 ft, and the centerline span lengths are held constant for the five structures: 130.50 ft – 174.0 ft – 130.5 ft. Cross frame members cross-sectional properties also remain constant and are those described in Section 4.3.2. The model that employs the 14.5 ft cross frame spacing is the Base Model. As a result of maintaining the same span lengths, a non-uniform spacing throughout the structure is used some cases. The cross frame spacing was held uniform in the positive moment locations since this is the area of concern for this study. The cross frame spacing near the center and end supports will vary slightly from the spacing in the in the positive moment locations. Figure 4.36 shows the cross frame arrangement for the entire structure for each cross frame spacing investigated.

**Table 4-19** Cross Frame Spacing Variation

<b>Spacing ID</b>	<b>Center Span Main Spacing (ft)</b>	<b>End Span Main Spacing (ft)</b>
1	10.25	10.00
2	11.50	10.50
3	14.50	14.50
4	19.50	18.75
5	21.75	21.75

For each of these different cross frame spacings, the flange von Mises stresses and girder displacements predicted by the nonlinear finite element models are monitored and compared to determine the effects of the applied web out-of-plumb angle. Appendix C contains results for all analyses conducted regarding the cross frame spacing parameter.

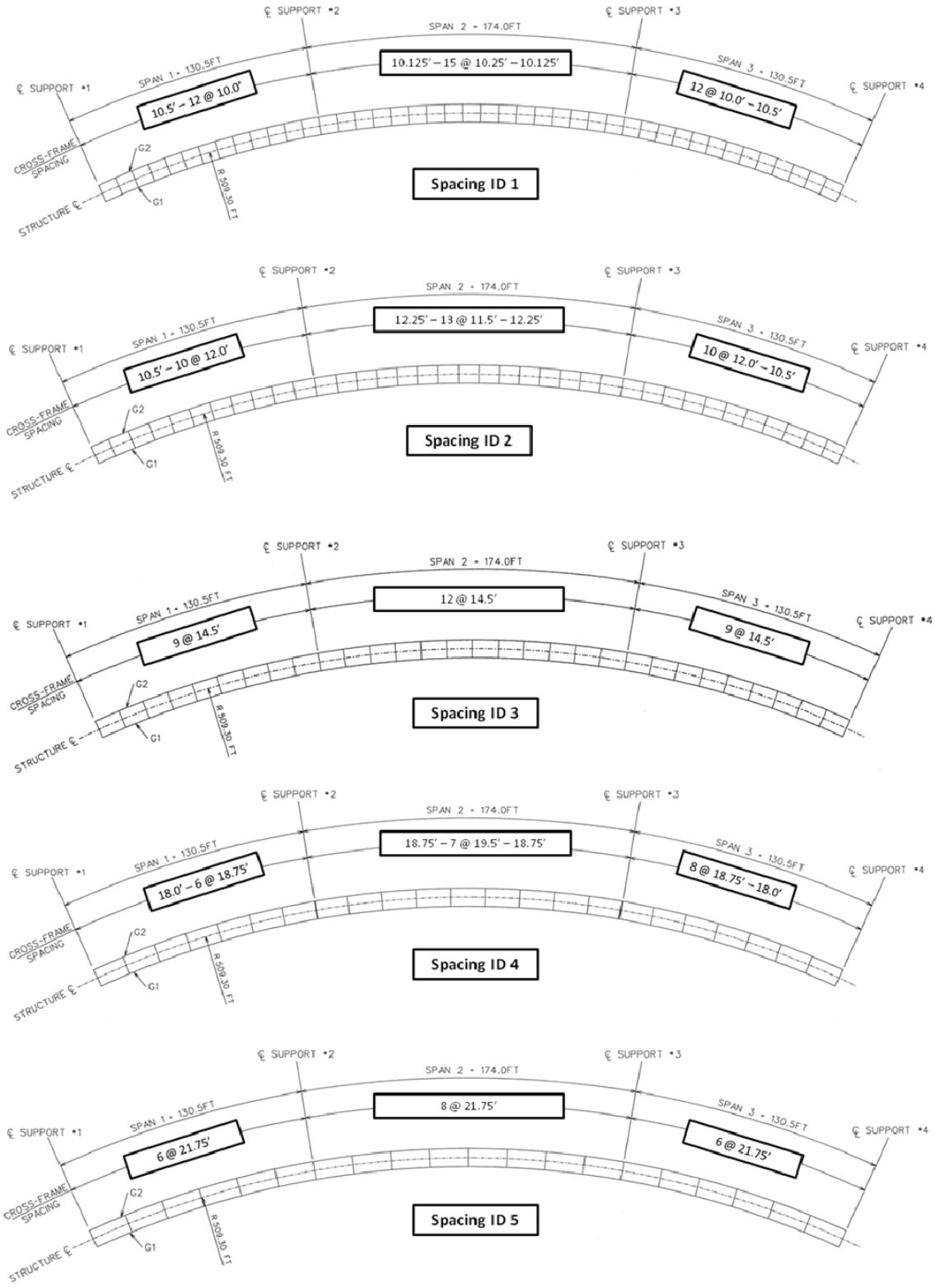


**Figure 4.36** Cross Frame Spacing Arrangements

#### 4.3.5.1 Flange Stresses

Similar to the previous parametric studies, the girder flange von Mises stresses are monitored at three locations in each model to quantify the effects of web out-of-plumbness on the vertical and lateral bending moments and torsional behavior. As shown in Figure 4.18, the chosen locations are centered about points of maximum vertical bending:  $0.4L$  of the End Span,  $0.0L$  of the Center Span (i.e. Support #2), and  $0.5L$  of the Center Span (where  $L$  is the span length). At each location, flange tip stresses are observed at the quarter points between cross frames, in order to obtain an accurate representation of the lateral flange bending effects. For both girders G1 and G2, the flange stresses are investigated at the top and bottom flange tips, as shown in Figure 4.19, where the stresses are most affected by web out-of-plane rotation.

The girder G2 outer-edge bottom flange tip stress at  $0.5L$  of the center span increases for increasing angles of web out-of-plumbness, yielding the maximum tensile stress in the section. For the web-plumb two-girder system with a cross frame spacing of 10.25 ft, the girder G2 outer-edge bottom flange stress at  $0.5L$  of the center span is 3.05 ksi. At the same location, the tensile stress for 2 and 5 degrees web out-of-plumbness are 3.44 ksi and 4.01 ksi. Furthermore, as shown in Table 4-20, as the girder spacing increases, the outer-edge bottom flange tensile stress also increases. This latter observation results from the greater distance between cross frames permitting greater girder rotations between brace points. The cross frames do provide some restraint from rotation where they intersect the girders as is clearly evident throughout this study.

Figure 4.37 provides a graphical representation of the girder G2 maximum outer-edge bottom flange tensile stresses for cross frame spacings of a) 10.25 ft, b) 11.50 ft, c) 14.50 ft, d) 19.50 ft, and e) 21.75 ft. From this figure it is observed that as the cross frame spacing increases, there is an increase in the girder G2 outer-edge bottom flange tip stresses. Furthermore, it is

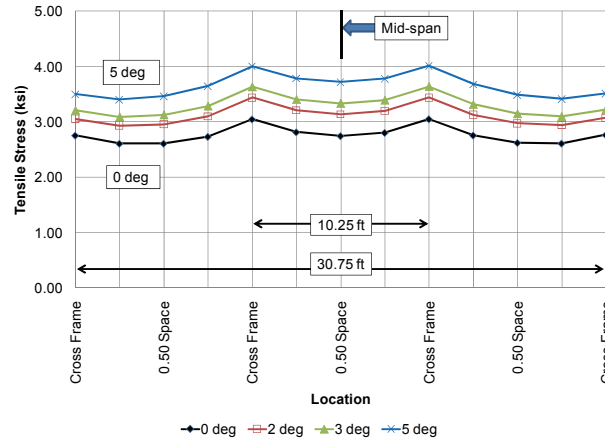
shown that as the cross frame spacing increases, the peaks in the flange stress at the cross frames become more prominent. This illustrates that as the cross frame spacing becomes larger, the effects of lateral flange bending have a more significant effect on the maximum flange stress. However, a change in cross frame spacing does not appreciably affect the increase in flange tip stresses caused by increasing the angle of web out-of-plumbness.

**Table 4-20** G2 Maximum Outer-Edge Bottom Flange Tip Stress near 0.5L Center Span

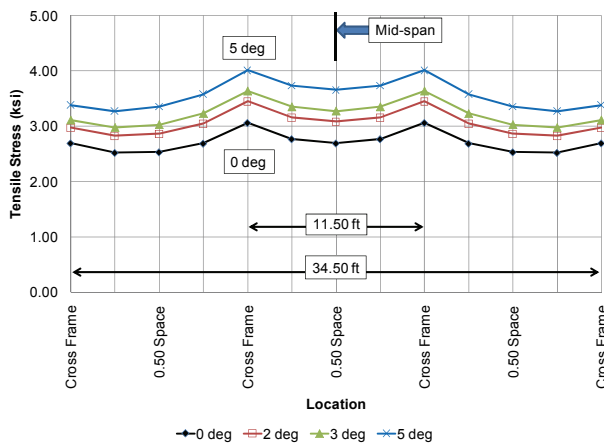
Cross Frame Spacing (ft)	$\theta = 0$ deg	$\theta = 2$ deg		$\theta = 3$ deg		$\theta = 5$ deg	
	$\sigma$ (ksi)	$\sigma$ (ksi)	% inc.*	$\sigma$ (ksi)	% inc.*	$\sigma$ (ksi)	% inc.*
10.25	3.05	3.44	13%	3.63	19%	4.01	32%
11.50	3.06	3.45	13%	3.64	19%	4.02	32%
14.50	3.22	3.63	13%	3.83	19%	4.23	31%
19.50	3.24	3.60	11%	3.78	17%	4.14	28%
21.75	3.53	3.94	12%	4.14	17%	4.54	28%

\* % inc. is the percentage increase in flange stress from the web-plumb case (0 deg)

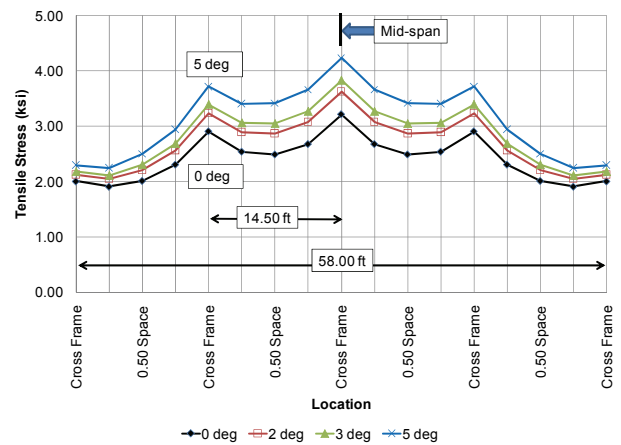
Note: Maximum flange stresses are taken at point nearest 0.5L.



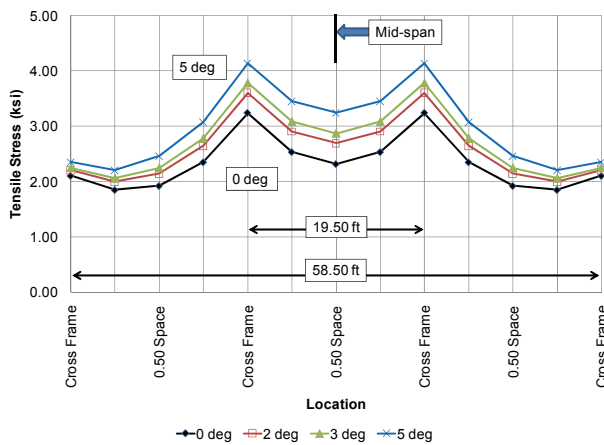
a) Cross Frame Spacing = 10.25 ft



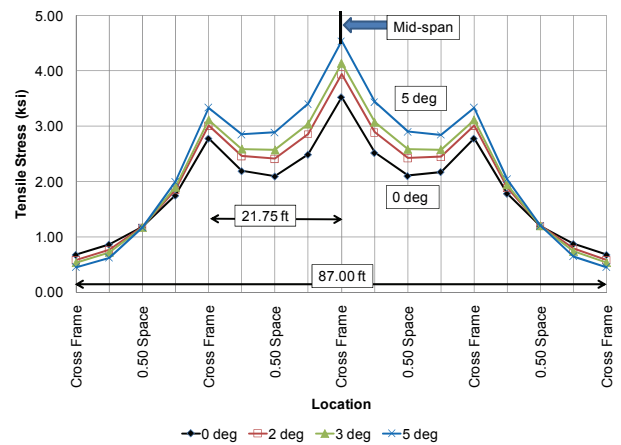
b) Cross Frame Spacing = 11.50 ft



c) Cross Frame Spacing = 14.50 ft



d) Cross Frame Spacing = 19.50 ft



e) Cross Frame Spacing = 21.75 ft

**Figure 4.37** G2 Outer-Edge Bottom Flange Tip Stresses at 0.5L Center Span

Also of note is the difference in bottom flange tip stresses between the outside and inside edges of the flange, as shown in Figure 4.38. The bi-moment and subsequent lateral flange

bending cause the stresses to be different on each side of the flange. On the outer-edge of the flange, at the cross-frame locations, the lateral bending causes an additional tensile stress. While on the inner-edge of the flange, the lateral bending causes a compression stress, which reduces the total flange inner-edge tensile stress at cross frame location. The increase in lateral flange bending is caused by the larger spacing between the cross frames. The cross frames transfer load from girder G1 to girder G2. Therefore, as the cross frame spacing increases the forces in the cross frame members increase, resulting in larger discrete lateral loads applied to the top and bottom flanges of the girder.

As shown in Figure 4.38, for a cross frame spacing of 10.25 ft, the inner-edge flange tip tensile stress is 2.64 ksi, and 3.05 ksi (0.020 ksi/in. gradient) at the outer flange tip for the web plumb model (0 degrees), at the cross frame location nearest 0.5L of the center span. Likewise, the inner-edge flange tip tensile stress is 1.88 ksi and 4.01 ksi (0.106 ksi/in. gradient) at the outer flange tip for the web out-of-plumbness angle of 5 degrees. As shown previously, it is evident that as the web out-of-plumbness angle increases, the change in stress across the flange increases. This effect is significantly more pronounced as locations between cross frames where the cross frame spacing is increased.

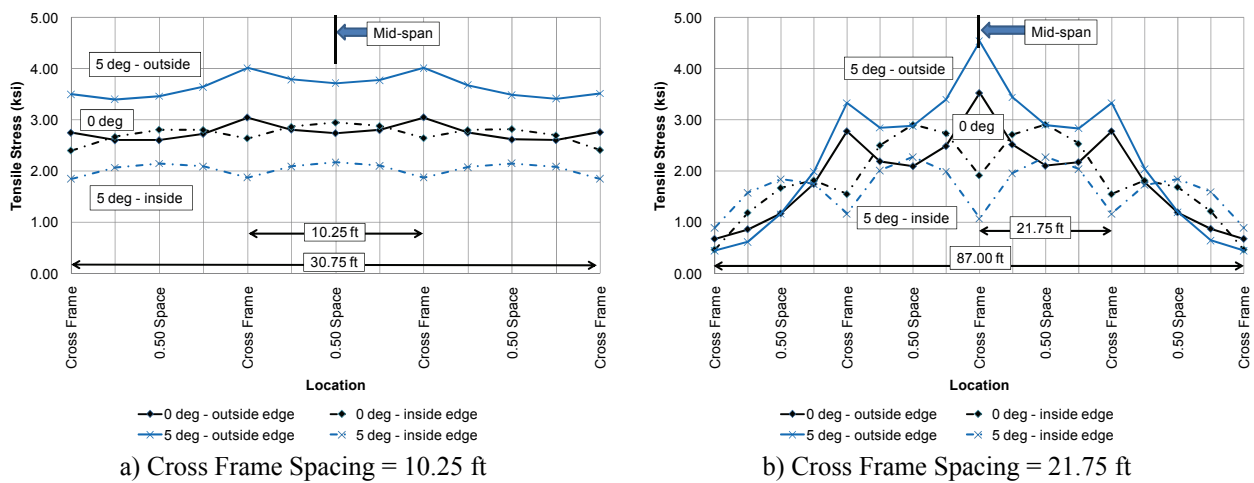
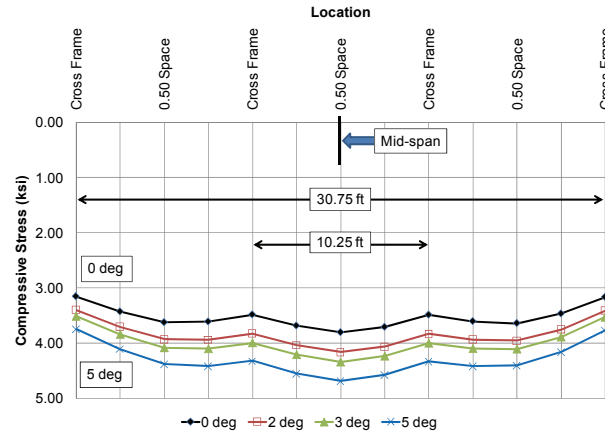


Figure 4.38 G2 Bottom Flange Tip Stresses at 0.5L Center Span

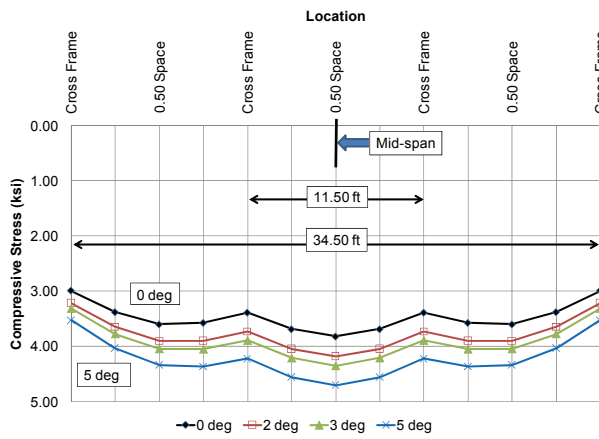
The girder G2 inner-edge top flange stress near 0.5L of the center span increases for increasing angles of web out-of-plumbness, yielding the maximum compressive stress in the section. These compressive stresses do not occur at the cross frame locations, but midway between cross frame points (0.5 cross frame space). This behavior is illustrated in Figure 4.39a for cross frame spacing of 10.25 ft.

Closer investigation of the girder G2 inner-edge top flange tip stresses near 0.5L of the center span for all cross frame spacing shows that as the cross frame spacing increases, there is a relative increase in the top flange maximum tip stress as the applied web out-of-plumbness increases. For the web-plumb two-girder system with a cross frame spacing of 10.25 ft, the girder G2 inner-edge top flange stress near 0.5L of the center span is 3.80 ksi. At the same location, the compressive stress for 2 and 5 degrees web out-of-plumbness are 4.16 ksi and 4.69 ksi, respectively.

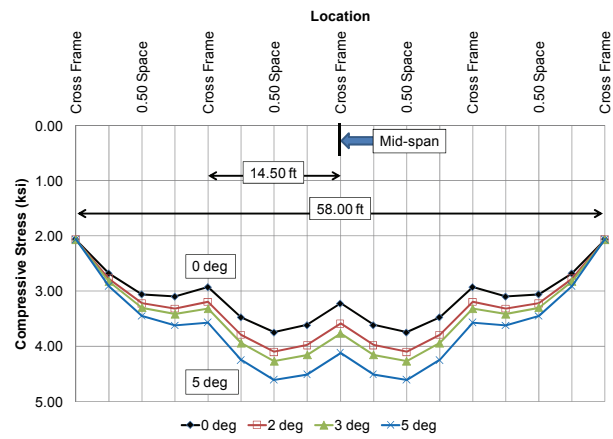
Also of note is the difference in top flange tip stresses between the inside and outside edges of the flange, at the mid-span of the cross frame spacing, as shown in Figure 4.40. The effects of lateral flange bending result in an additive compressive stress on the inner-edge of the flange. While on the outer-edge of the flange, the lateral bending causes a tensile stress, which reduces the total flange outer-edge compressive stress at the mid-span between cross frames. For a cross frame spacing of 21.75 ft, the inner-edge flange tip compressive stress is 3.84 ksi, while the outer-edge flange tip stress is 2.14 ksi (0.085 ksi/in. gradient) for the web-plumb model (0 degrees). Likewise, the inner and outer-edge flange tip compressive stresses are 4.62 ksi and 1.32 ksi, respectively, (0.165 ksi/in. gradient) for web out-of-plumbness angle of 5 degrees.



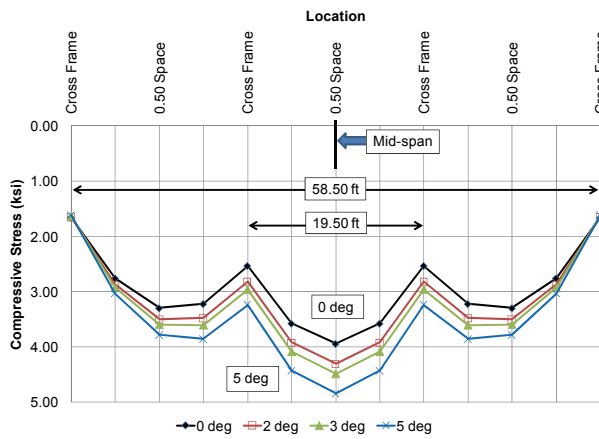
a) Cross Frame Spacing = 10.25 ft



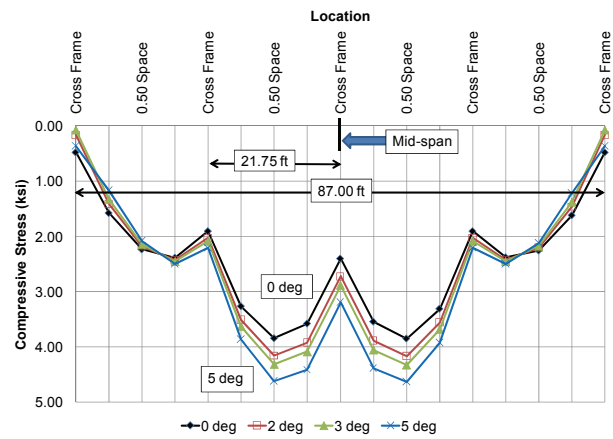
b) Cross Frame Spacing = 11.50 ft



c) Cross Frame Spacing = 14.50 ft

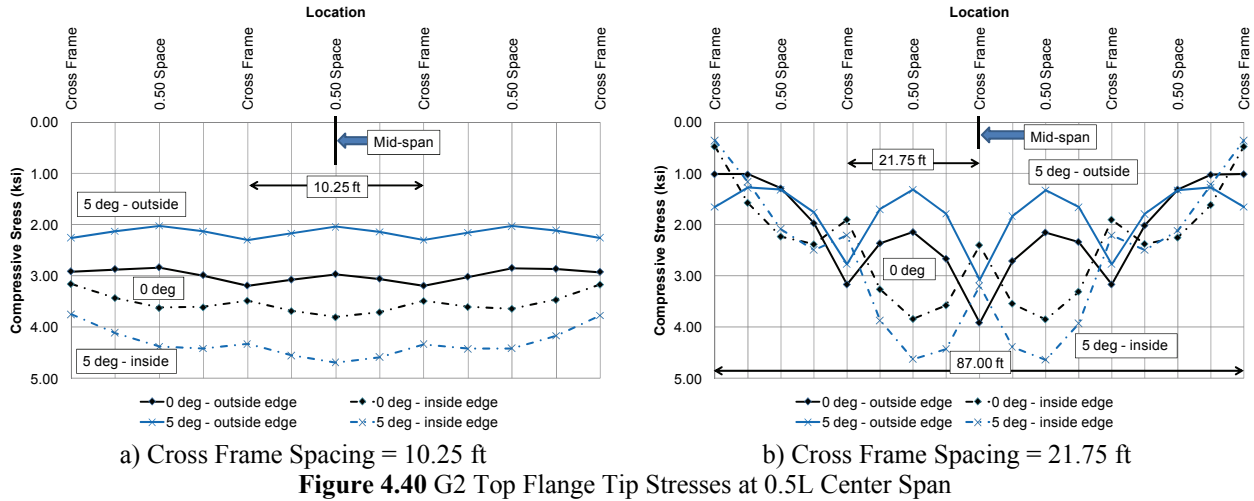


d) Cross Frame Spacing = 19.50 ft



e) Cross Frame Spacing = 21.75 ft

**Figure 4.39** G2 Inner-Edge Top Flange Tip Stresses at 0.5L Center Span

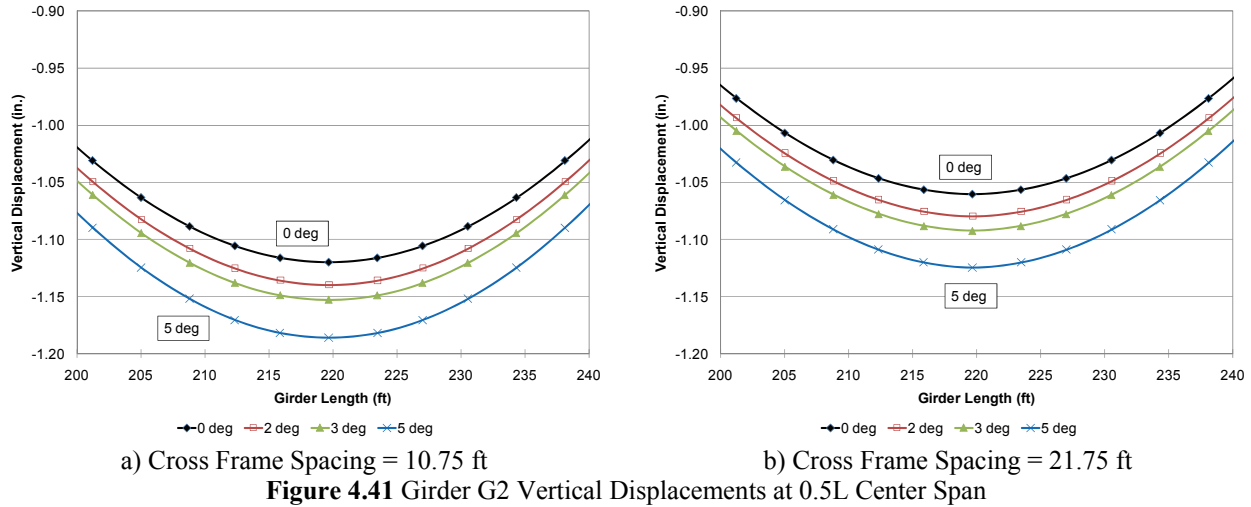


It is noted that girder G1 exhibits a similar behavior to girder G2, with regard to flange stresses discussed previously. Analytical results regarding girder G1 can be found in Appendix C.

#### 4.3.5.2 Girder Displacements

Vertical and lateral displacements are monitored for the top and bottom flange-web junctions along the length of the structure, and in particular at the midpoint of the center span, for each cross frame spacing arrangement investigated.

The vertical displacements increase slightly as a result of increasing initial web out-of-plumbness for all cross frame spacing arrangements analyzed. Figure 4.41a) and b) show the girder G2 vertical displacements at the 0.5L of the center span location for cross frame spacing arrangements of 10.75 ft and 21.75 ft.



For a cross frame spacing of 10.75 ft, girder G2 has a vertical displacement of 1.12 in. at 0.5L of the center span for the web-plumb condition (0 degrees), and increases to 1.19 in. for a web out-of-plumbness of 5 degrees. Likewise, for a cross frame spacing of 21.75ft, girder G2 has a vertical displacement of 1.06 in. at the mid-span for the web-plumb condition (0 degrees), and increases to 1.13 in. for a web out-of-plumbness of 5 degrees. The decrease in vertical displacement associated with larger cross frame spacing reflects the reduced redistribution of force from G1 to G2 resulting from the use of fewer cross frames. Although not shown here, girder G1 exhibits a similar behavior due to web out-of-plumbness, although an increase in vertical displacement with increasing cross frame spacing is evident.

The top and bottom flange lateral displacements are generally the same for girders G1 and G2, since both girders rotate out-of-plane the same amount due to the applied loading. However, for any particular girder, the lateral displacements of the top and bottom flanges are different, causing an out-of-plane rotation of the cross section as shown in Figure 2.9. This out-of-plane rotation can be calculated from the flange lateral displacements, as shown previously in section 4.3.3.2. Table 4-21 shows the maximum out-of-plane rotation at 0.5L of the center span

for each cross frame spacing arrangement investigated. Note that depending on the cross frame arrangement, results are reported at a cross frame location, or midway between cross frames. The incremental increase of out-of-plane rotation at the 0.5L center span location due to initial web out-of-plumbness is not significantly affected by a change in the cross frame arrangement. It is noted however, that the individual girder out-of-plane rotation between cross frames increases as the cross frame spacing increases. This is a direct result of increasing the spacing of the girder lateral supports provided by the cross frames.

**Table 4-21** G2 Out-of-Plane Rotation at 0.5L Center Span

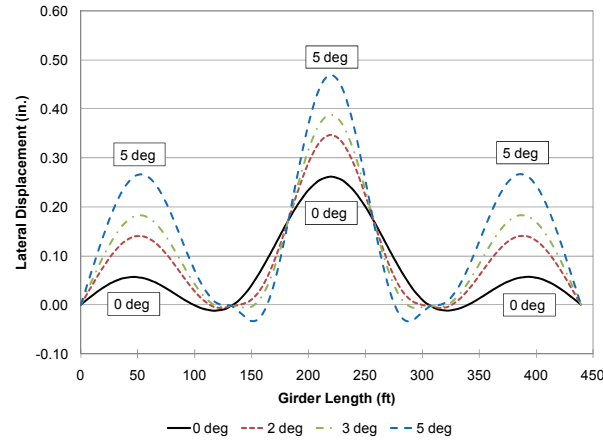
Cross Frame Spacing (ft)	$\theta = 0$ deg	$\theta = 2$ deg		$\theta = 3$ deg		$\theta = 5$ deg	
	$\phi$ (deg.)	$\phi$ (deg.)	% inc.*	$\phi$ (deg.)	% inc.*	$\phi$ (deg.)	% inc.*
10.25 <sup>(1)</sup>	0.221	0.225	1.8%	0.227	2.7%	0.231	4.5%
11.50 <sup>(1)</sup>	0.223	0.227	1.8%	0.229	2.7%	0.233	4.5%
14.50 <sup>(2)</sup>	0.220	0.224	1.8%	0.226	2.7%	0.229	4.1%
19.75 <sup>(1)</sup>	0.225	0.229	1.8%	0.231	2.7%	0.234	4.0%
21.75 <sup>(2)</sup>	0.213	0.217	1.9%	0.219	2.8%	0.222	4.2%

\* % inc. is the percentage increase in vertical displacement from the web-plumb case (0 deg)

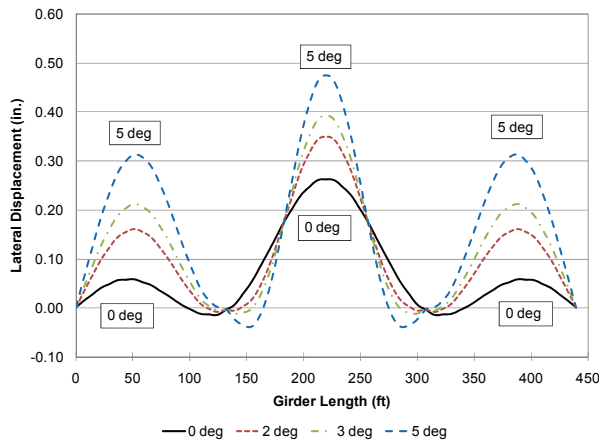
(1) Results are reported midway between cross frames

(2) Results are reported at a cross frame

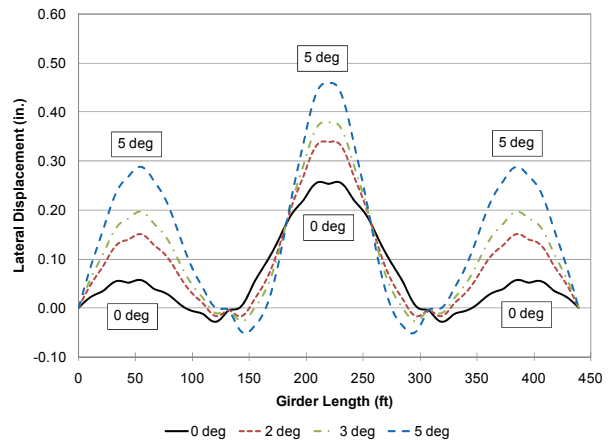
Figure 4.42 provides a graphical representation of the girder G2 top flange lateral displacements for cross frame spacing arrangements of a) 10.25 ft, b) 14.50 ft, and c) 21.75 ft. The lateral displacement for girders G1 and G2 are relatively similar along the length of the structure, therefore only the lateral displacements for G2 are shown herein. From this figure it is observed that as the girder out-of-plumbness increases, the lateral displacements also increase. However, as the cross frame spacing is varied, the top flange lateral displacements in the center and end spans are not significantly affected.



a) Cross Frame Spacing = 10.25 ft



b) Cross Frame Spacing = 14.50 ft



c) Cross Frame Spacing = 21.75 ft

**Figure 4.42** Girder G2 Top Flange Lateral Displacements

### 4.3.5.3 Results Discussion

Variation of cross frame spacing has little effect in the global girder-pair behavior but affects local stresses significantly. Cross frames introduce discrete lateral forces to the girders resulting in increased local stresses. Fewer cross frames results in greater forces being carried by each individual cross frame. Cross frames also provide some degree of lateral restraint to the girders at their connections. Effects of lateral flange bending between cross frame locations are therefore more significant as the cross frame spacing increases. Finally, cross frames affect the

redistribution of force from interior to exterior girders: fewer cross frame will necessarily reduce this redistribution, although in the present study, this effect as minimal.

#### **4.3.6 Web Depth Variation**

The final parametric study carried out examines web out-of-plumbness effects as the girder web depth is varied. Four different girder web depths are investigated as part of this study: 60 in., 72 in. (Base Model), 84 in., and 96 in. The same web depth is applied to both girders G1 and G2. The four web depth variations are chosen because they represent typical web dimensions of designed bridges. The two-girder system centerline radius is held constant at 509.3 ft, and the centerline span lengths are held constant for four structures: 130.50 ft – 174.0 ft – 130.5 ft. Additionally the flange dimensions are held constant for this study. Therefore there is no significant change in the weak axis moment of inertia; only a change in the strong axis moment of inertia. This study allows the investigation of different  $I_x$  to  $I_y$  ratios, as shown in Table 4-22.

It is noted that as the web depth increases, the applied steel dead load also increases; therefore this study investigates the effects of web-plumbness as related to the variation in web depth only. Table 4-22 shows the steel dead load applied to each structure.

Once again, it is noted that changing web depth affects other aspects of the section design. These are not considered in this parametric study whose objective is to assess the effects of varying  $I_x/I_y$ . Nonetheless, it is recognized that the 84 in. and 96 in. deep by 0.5 in. thick webs violate AASHTO web slenderness limits for webs without longitudinal stiffeners. Providing a thicker web will have only a marginal effect on the calculation of  $I_x$  and  $I_y$  in any event.

**Table 4-22** Girder Section Properties

Web Depth (in.)	$I_x$ (in <sup>4</sup> )	$I_y$ (in <sup>4</sup> )	$I_x / I_y$	% inc. $I_x$	weight (lb/ft)	% inc. weight
<b>Girder G1</b>						
60	47,803	1,122	42.6	-33%	244	-8%
72 (Base Model)	71,081	1,122	63.3	n/a	264	n/a
84	99,941	1,123	89.0	41%	284	8%
96	134,815	1,123	120.1	90%	305	16%
<b>Girder G2</b>						
60	60,887	1,859	32.7	-32%	292	-6%
72 (Base Model)	89,763	1,859	48.3	n/a	312	n/a
84	125,229	1,860	67.3	40%	332	6%
96	167,719	1,860	90.2	87%	353	13%

For each of these different girder web depths, the flange von Mises stresses and girder displacements predicted by the nonlinear finite element models are monitored and compared to determine the effects of the applied web out-of-plumb angle. Appendix C contains results for analyses conducted regarding the web depth parameter.

#### 4.3.6.1 Flange Stresses

Similar to the previous parametric studies, the girder flange von Mises stresses are monitored at three specific location in each model to quantify the effects of web out-of-plumbness on the vertical and lateral bending moments and torsional behavior. As shown in Figure 4.18, the chosen locations are centered about points of maximum vertical bending: 0.4L of the End Span, 0.0L of the Center Span (i.e. Support #2), and 0.5L of the Center Span (where L is the span length). At each location, flange tip stresses are observed at the quarter points between cross frames, in order to obtain an accurate representation of the lateral flange bending effects. For both girders G1 and G2, the flange stresses are investigated at the top and bottom flange tips, as shown in Figure 4.19, where the stresses are most affected by web out-of-plane rotation.

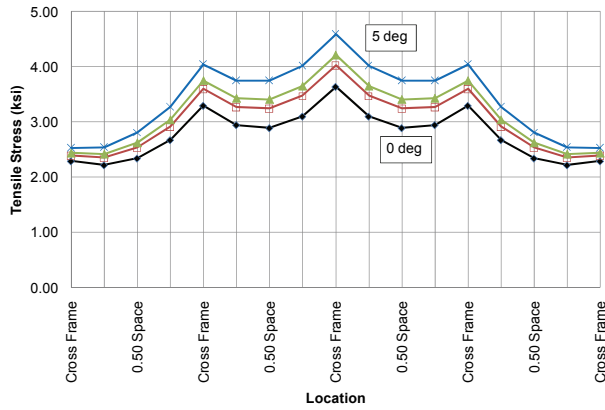
Clearly, stresses in the section having a deeper web will be reduced as compared to shallower girders. This effect is not considered in the following discussion where only relative stresses attributed to web out-of-plumbness are considered. The girder G2 outer-edge bottom flange tip stress at 0.5L of the center span increases for increasing angles of web out-of-plumbness, yielding the maximum tensile stress in the section. For the web-plumb two-girder system with a web depth of 60 in., the girder G2 outer-edge bottom flange stress at 0.5L of the center span is 3.64 ksi. At the same location, the tensile stress for 2 and 5 degrees web out-of-plumbness are 4.03 ksi and 4.22 ksi, respectively. Furthermore, as shown in Table 4-23, the web out-of-plumbness causes the flange tip stresses to increase more significantly for the two-girder systems with a larger web depth, although this effect is minimal.

Figure 4.43 provides a graphical representation of the girder G2 maximum bottom flange tensile stresses for web depths of a) 60 in., b) 72 in., c) 84 in., and d) 96 in. From this figure the effect of increasing girder stiffness,  $I_x$ , is seen as a reduction in flange stress with increasing girder depth as described above. It is apparent that a change in web depth does not significantly affect the lateral bending effects, since the peaks in the flange tip stresses do not necessarily vary with web depths. This observation reflects the fact that an increasing web depth has only a marginal effect on lateral flange bending stiffness,  $I_y$ .

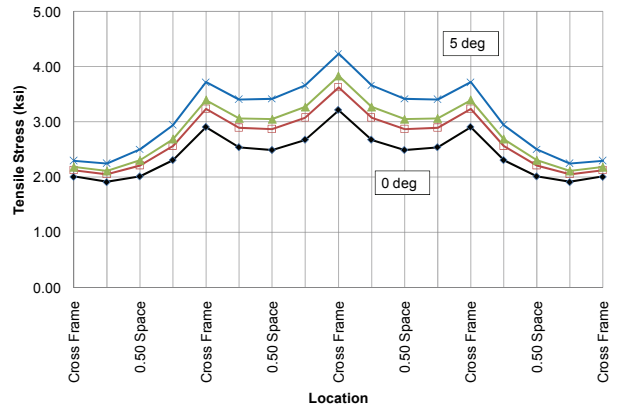
**Table 4-23** G2 Maximum Outer-Edge Bottom Flange Tip Stress at 0.5L Center Span

Web Depth (in.)	$\theta = 0$ deg	$\theta = 2$ deg		$\theta = 3$ deg		$\theta = 5$ deg	
	$\sigma$ (ksi)	$\sigma$ (ksi)	% inc.*	$\sigma$ (ksi)	% inc.*	$\sigma$ (ksi)	% inc.*
60	3.64	4.03	11%	4.22	16%	4.56	25%
72	3.22	3.63	13%	3.83	19%	4.23	31%
84	2.84	3.25	14%	3.45	22%	3.85	36%
96	2.59	3.02	17%	3.23	25%	3.64	41%

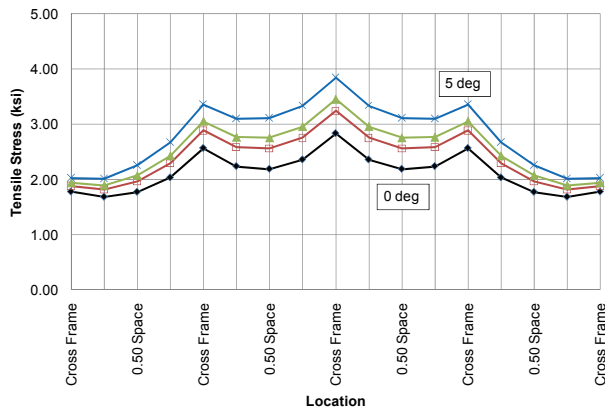
\* % inc. is the percentage increase in flange stress from the web-plumb case (0 deg)



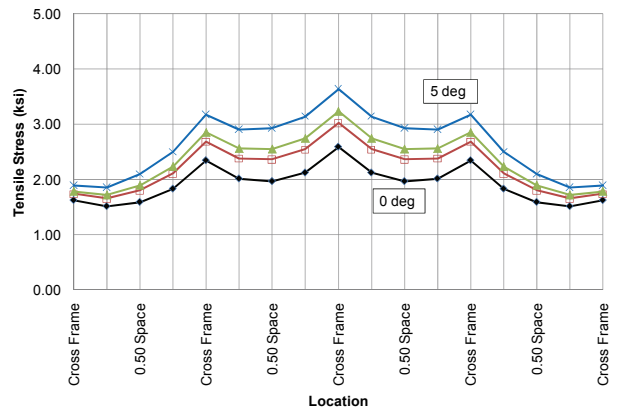
a) Web Depth = 60 in.



b) Web Depth = 72 in.



c) Web Depth = 84 in.



d) Web Depth = 96 in.

**Figure 4.43** G2 Bottom Flange Maximum Tip Stresses at 0.5L Center Span

The girder G2 inner-edge top flange tip stress at 0.5L of the center span increases for increasing angles of web out-of-plumbness, yielding the maximum compressive stress in the section. As shown in Table 4-24, for a web depth of 60 in., the top flange tip stress increases by 0.33 ksi for the web out-of-plumbness angle of 2 degrees, while the structure with a web depth of 96 in. experiences a 0.41 ksi increase. The web out-of-plumbness causes the inner-edge top flange tip stresses to increase more significantly for the two-girder systems with a larger web depth.

**Table 4-24** G2 Inner-Edge Top Flange Tip Stress at 0.5L Center Span

Web Depth (in.)	$\theta = 0$ deg	$\theta = 2$ deg		$\theta = 3$ deg		$\theta = 5$ deg	
	$\sigma$ (ksi)	$\sigma$ (ksi)	% inc.*	$\sigma$ (ksi)	% inc.*	$\sigma$ (ksi)	% inc.*
60	3.61	3.94	9%	4.10	14%	4.41	22%
72	3.23	3.59	11%	3.77	17%	4.12	28%
84	2.84	3.21	13%	3.39	19%	3.75	32%
96	2.61	3.02	16%	3.21	23%	3.59	38%

\* % inc. is the percentage increase in flange stress from the web-plumb case (0 deg)

It is noted that girder G1 exhibits a similar behavior to girder G2, with regard to flange stresses discussed previously. Analytical results regarding girder G1 can be found in Appendix C.

#### 4.3.6.2 Girder Displacements

Vertical and lateral displacements are monitored for the top and bottom flange-web junctions along the length of the structure, and in particular at the midpoint of the center span, for each web depth investigated.

For the web depths investigated, the girder G2 vertical displacement at 0.5L of the center span increases as the web out-of-plumbness increases. As shown in Table 4-25, for a web depth of 60 in., the vertical displacement increases by 0.04 in. for the web out-of-plumbness angle of 2 degrees, while the structure with a web depth of 96 in. experiences a 0.03 in. increase. Given that these vertical displacements increases are quite small, web out-of-plumbness has relatively little effect on the on the vertical displacements due to steel dead load. This observation has been seen in all previous aspects of this study.

**Table 4-25** G2 Vertical Displacement at 0.5L Center Span

Web Depth (in.)	$\theta = 0$ deg	$\theta = 2$ deg		$\theta = 3$ deg		$\theta = 5$ deg	
	$\Delta_V$ (in.)	$\Delta_V$ (in.)	% inc.*	$\Delta_V$ (in.)	% inc.*	$\Delta_V$ (in.)	% inc.*
60	1.49	1.53	3%	1.55	4%	1.56	5%
72	1.09	1.12	3%	1.14	5%	1.18	8%
84	0.84	0.86	2%	0.88	5%	0.92	10%
96	0.67	0.69	3%	0.71	6%	0.75	12%

\* % inc. is the percentage increase in vertical displacement from the web-plumb case (0 deg)

The top and bottom flange lateral displacements are generally the same for girders G1 and G2, since both girders rotate out-of-plane the same amount due to the applied loading. However, for any particular girder, the lateral displacements of the top and bottom flanges are different, causing an out-of-plane rotation of the cross section as shown in Figure 2.9. This out-of-plane rotation can be calculated from the flange lateral displacements, as shown previously in section 4.3.3.2. Table 4-27 shows the maximum out-of-plane rotation at 0.5L of the center span for each web depth investigated. As expected, this maximum out-of-plane rotation is smaller for the structures with a larger web depth since the torsional resistance of this cross section is increased with deeper webs.

Closer examination of the girder G2 out-of-plane rotation at 0.5L of the center span shows that as the web depth is increased, there is a relatively no change in the maximum out-of-plane rotation, as the web out-of-plumbness increases. As shown in Table 4-26, for a web depth of 60 in., the out-of-plane rotation increases by  $0.004^\circ$  for the web out-of-plumbness of 2 degrees, while the structure with the girder spacing of 96 in. undergoes a  $0.005^\circ$  increase.

**Table 4-26** G2 Out-of-Plane Rotation at 0.5L Center Span

Web Depth (in.)	$\theta = 0$ deg	$\theta = 2$ deg		$\theta = 3$ deg		$\theta = 5$ deg	
	$\phi$ (deg.)	$\phi$ (deg.)	% inc.*	$\phi$ (deg.)	% inc.*	$\phi$ (deg.)	% inc.*
60	0.249	0.253	2%	0.255	3%	0.258	4%
72	0.220	0.224	2%	0.226	3%	0.229	4%
84	0.193	0.197	2%	0.199	3%	0.202	5%
96	0.175	0.180	3%	0.182	4%	0.185	6%

\* % inc. is the percentage increase in vertical displacement from the web-plumb case (0 deg)

#### 4.3.6.3 Results Discussion

Variation in web depth has little effect on girder behavior beyond that resulting from marked increase in the  $I_x/I_y$  ratio. That is, deeper girders are stiffer in strong axis flexure and torsion.

The effects of web out-of-plumbness are marginally more pronounce in deeper girders.

## 5.0 LOCKED-IN STRESSES DUE TO INCONSISTENT DETAILING

Inconsistent detailing of girders and cross frames was introduced in Section 2.4.3. This chapter addresses the effects of such detailing practices on the stresses in a horizontally curved steel I-girder bridge.

Inconsistent detailing frequently arises when the out-of-plane rotation of the girders, and the subsequent lateral displacement of the top flange due to dead loads are deemed to be of such a magnitude as to constitute an undesirable condition. The strategy of inconsistent detailing forces the girder webs to be plumb under dead load. With this strategy, the cross frames are detailed to fit girders in the web-plumb position under a specified load (usually dead load) while the girders remain conventionally detailed to be in the web-plumb position at the no-load condition; thus creating a detailing inconsistency. It is intended that detailing the cross frames in this manner will force the girders to be vertically plumb at the specified loading condition. This method of inconsistent detailing is also sometimes referred to as Steel Dead Load Fit, or Total Dead Load Fit, depending on the load at which web-plumbness is enforced.

Inconsistent detailing results in cross frame member lengths that are incompatible with girders in the theoretical no-load position at time of erection. Therefore, the cross frame members will have to be forced into place, twisting the girder webs out-of-plumb during erection and generating stresses in the girder and cross frames. The direction of the erection-induced out-of-plumb twist is in the direction opposite of the natural out-of-plane rotation that occurs due to

application of dead load. This, when loaded, the web rotate to a plumb position. Since the cross frames must be forced into position, locked-in girder and cross frame stresses will develop. These locked-in stresses are typically unaccounted for in design, when it is specified that the girder webs be plumb at either steel or total dead load. Motivated by the application of inconsistent detailing, the final portion of this research study will investigate the locked-in stresses resulting from the use of inconsistent detailing. The previously created nonlinear finite element model of the Chelyan Approach Ramp Bridge two-girder system will serve as the prototype structure for this study. The prototype used is the Base Model employed for the web out-of-plumb studies, and is described in detail in Section 4.3.1.

## **5.1 TOTAL DEAD LOAD BEHAVIOR**

When out-of-plane rotation, and/or top flange lateral displacement, of a curved girder bridge is deemed a problem, it is desired by the design engineer or bridge owner to have the girder webs plumb at the steel dead load or total dead load condition. For the analysis presented herein, it is assumed that it is desired to have the Base Model girder webs plumb under total dead load; that is the weight of the steel girders and the concrete deck.

The concrete deck thickness is taken as 8.5 inches, which is the thickness of the concrete deck of the as-designed Chelyan Approach Ramp Bridge. The weight of the concrete haunches is not taken into account in this study. Thus, based on the 10.21 ft girder spacing, a uniformly distributed load of 1085 lbs/ft is placed on each of the girders G1 and G2. A deck placement sequence is not employed, rather the weight of the concrete deck is applied as a uniform load to

the steel girders at one time. The steel self-weights of G1 and G2 are 264 lbs/ft and 312 lbs/ft, respectively, as described in Section 4.3.1.

An initial analysis is performed to determine the behavior of the Base Model due to the total dead load. Shown in Figure 5.1 are the vertical dead load displacements of girders G1 and G2. The maximum top flange vertical displacement occurs at mid-span of the center span, where girders G1 and G2 have displacements of 2.75 in. and 4.51 in., respectively ( $\delta_1$  and  $\delta_2$  in Figure 5.2). The differential vertical displacement between girders G1 and G2 of 1.76 in. is a result of the natural behavior of curved girder bridges, in which the entire cross section rotates out-of-plane due to a given loading. This out-of-plane rotation results in a greater vertical displacement of exterior girders.

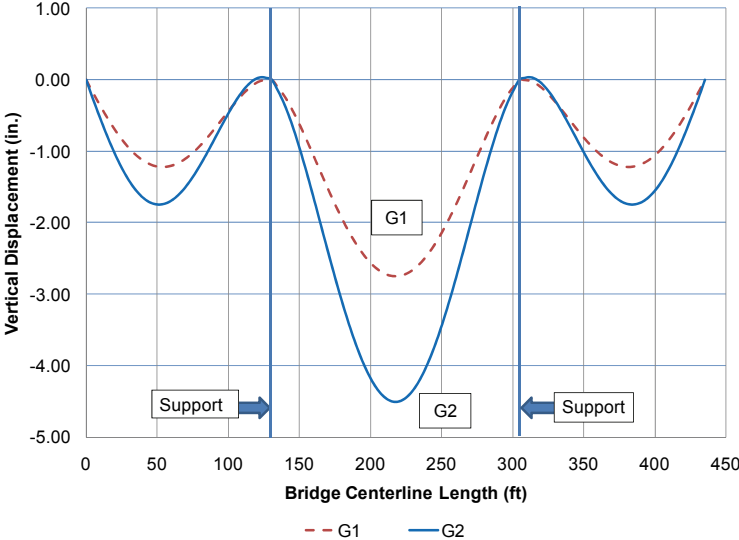


**Figure 5.1** Base Model Total Dead Load Vertical Displacement

The web out-of-plumbness due to the total dead load is caused by the natural behavior of curved girder bridges to rotate due to a given loading, as illustrated in Figure 5.2. (Note: In the analysis model, cross frames attach to girders at the flange-web junctions. However, for illustrative purposes and clarity, cross frame members are shown offset from flange-web junction

in Figure 5.2.) The top and bottom flanges displace laterally due to the total dead load, however the magnitude of this lateral displacement is different. As shown in Figure 5.3a, the lateral displacement of the top flange is significantly greater than the bottom flange, resulting in the out of plane rotation shown in Figure 5.3b. The lateral displacements of the flanges of adjacent girders are essentially similar.

The differential lateral displacement of the top and bottom flanges results in the web out-of-plumbness for the total dead load condition. As shown in Figure 5.3b, the maximum web out-of-plumbness occurs at the mid-span of the center span, and is found to be  $0.832^\circ$  for the Base Model. The maximum lateral displacement of the top flange, 1.09 in. ( $\Delta_{LAT}$  in Figure 5.2), also occurs at the mid-span of the center span.

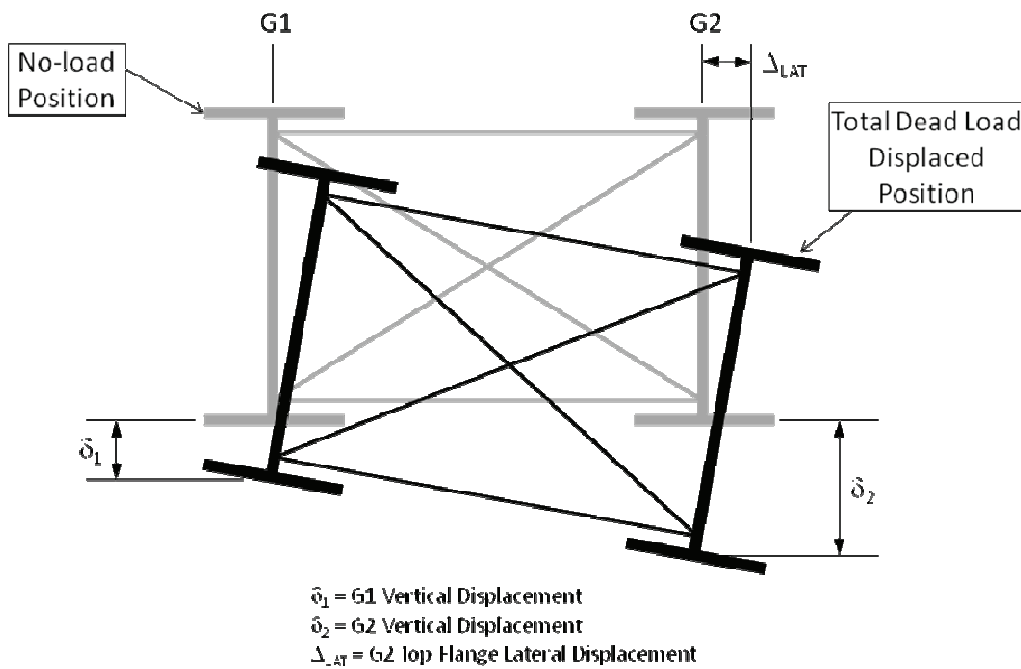


**Figure 5.2** Total Dead Load Displaced Position

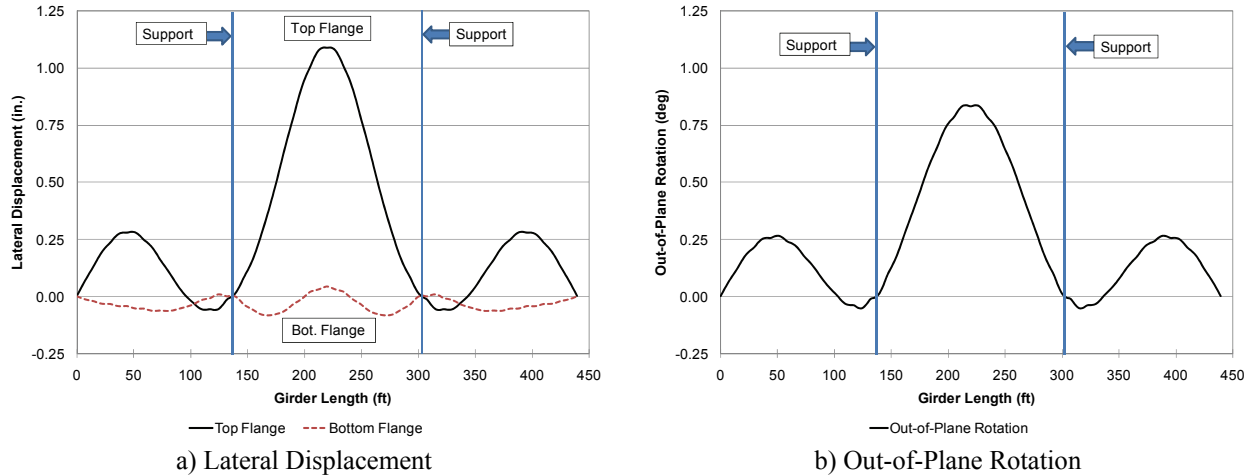


**Figure 5.3** G2 Lateral Displacement and Rotation due to Total Dead Load

## 5.2 CROSS FRAME MEMBER LENGTHS

The out-of-plane rotation shown in Figure 5.3b, also known as the web out-of-plumbness, is the behavior that is to be mitigated through inconsistent detailing. When the web out-of-plumbness is deemed to be excessive, such that it will have a detrimental effect on the structure, inconsistent detailing is employed to reduce the web out-of-plumbness once total dead load is applied. The inconsistent detailing method, however will result in diagonal cross frame members that do not fit with the girders detailed to be web-plumb at the no-load condition. This lack of fit will induce stresses into the girders that are not typically accounted for during the design.

The cross frame member lengths for the web-plumb position at the no-load condition are simply calculated, assuming the cross frame members intersect the girders at the flange-web junction. For the Base Model, the diagonal cross frame member length (measured from working points at the web-flange interstices) for the girders in the web-plumb position at no-load is 142.09 in., and the horizontal top and bottom member lengths are 122.50 in.

In order to achieve girder webs plumb at total dead load, different cross frame member lengths must be calculated. The following steps are used to make this calculation:

1. The total dead load displacement must be calculated, as shown in Figure 5.2.
2. The out-of-plane rotation is removed from the girders, and they are placed in a vertically plumb position. This is the web-plumb position at total dead load illustrated by the darker lines in Figure 5.4.
3. New cross frame member lengths are determined, such that they fit the girders in the web-plumb position at total dead load (Diagonal Members F and M in Figure 5.4). The cross frame members still intersect the same work points (flange-web junctions) on the girder as they did for the web-plumb position at the no-load condition.

In practice, the web-plumb vertical displacements are calculated from the dead load vertical camber provided in the design drawings, since the dead load vertical camber is the reverse of the dead load displacement.

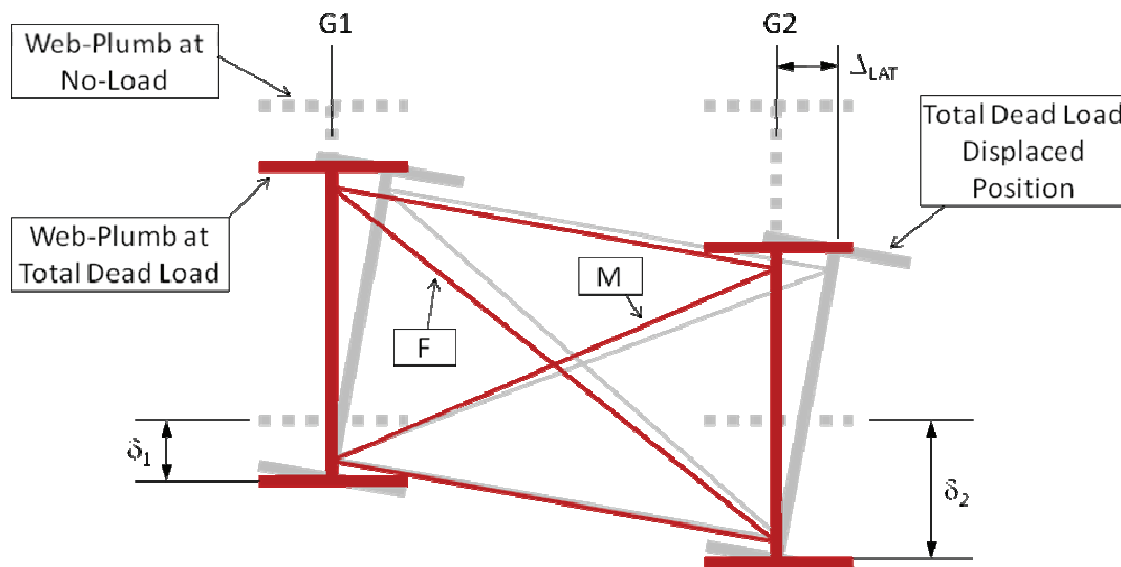


**Figure 5.4** Cross Frames Detailed for Web-Plumb at Total Dead Load

Figure 5.5 shows these new (inconsistently detailed) cross frame members, detailed for the web-plumb position at total dead load, inserted into the girders detailed for the web-plumb position at the no-load condition. It is seen from this figure that cross frame member F is too long to fit into the girder detailed for web plumb at no-load, while cross frame member M is too short. The resulting diagonal cross frame member lengths for this inconsistent detailing method are summarized in Table 5-1, and graphically in Figure 5.6. It should be noted that the top and bottom horizontal members of the cross frames are not appreciably affected by the inconsistent detailing method ( $\pm 1/64$  in. maximum difference in length).

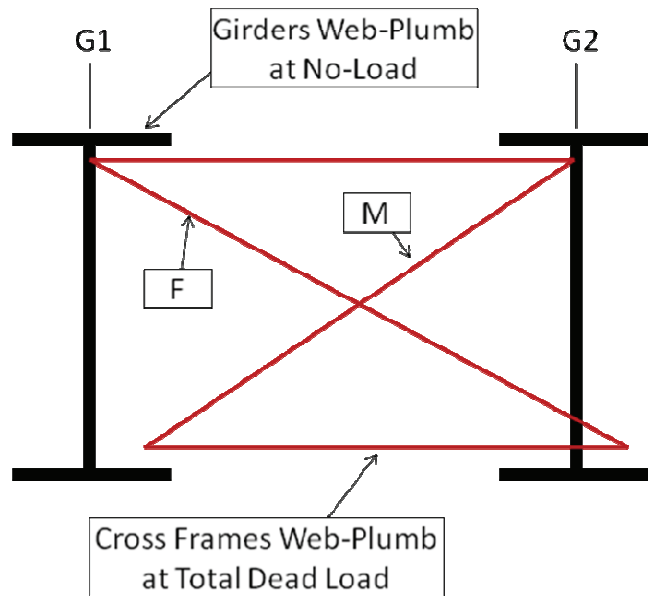


**Figure 5.5** Cross Frames Detailed for Web-Plumb at Total Dead Load

As expected, the largest cross frame diagonal member length difference caused by inconsistent detailing is at the mid-span of the center span, cross frame 16. (Cross frames are numbered sequentially from the left end of Span 1 (see Figure 4.13). This is due to the fact that this location undergoes the maximum out-of-plane rotation under total dead load. Therefore, the diagonal member length differences required to bring the girder back to web-plumb at total dead

load are the largest at this location. During steel erection, the difference in the diagonal member length at cross frame 16 would result in a connection misalignment of 0.88 in. Cross frames 1, 10, 22, and 31 are those located at the bridge supports where rotation is restrained, thus these cross frames have no misfit.

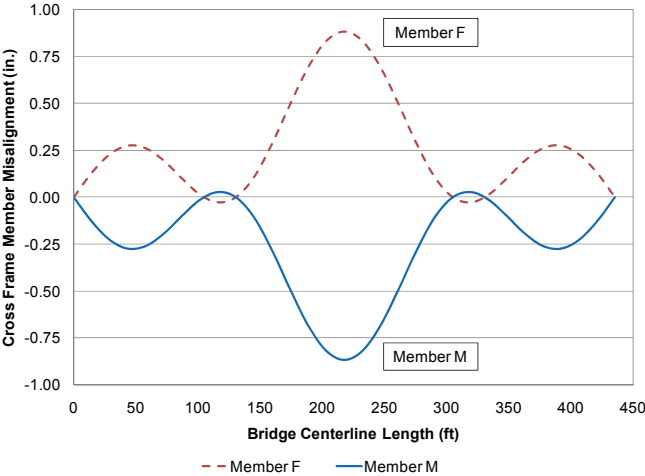


Figure 5.6 Cross Frame Diagonal Member Misalignment

**Table 5-1** Cross Frame Diagonal Member Lengths for Web-Plumb at Total Dead Load

Cross Frame ID	Length at Centerline (ft)	Member Length		Member Difference	
		F (in.)	M (in.)	$\Delta F$ (in.)	$\Delta M$ (in.)
1	0.0	142.09	142.09	0.00	0.00
2	14.5	142.22	141.96	0.13	-0.13
3	29.0	142.32	141.86	0.23	-0.23
4	43.5	142.36	141.82	0.28	-0.27
5	58.0	142.35	141.83	0.26	-0.26
6	72.5	142.28	141.90	0.19	-0.19
7	87.0	142.19	141.99	0.10	-0.10
8	101.5	142.10	142.08	0.01	-0.01
9	116.0	142.06	142.12	-0.03	0.03
10	130.5	142.09	142.09	0.00	0.00
11	145.0	142.20	141.98	0.11	-0.11
12	159.5	142.38	141.80	0.29	-0.28
13	174.0	142.59	141.60	0.50	-0.49
14	188.5	142.78	141.40	0.69	-0.69
15	203.0	142.92	141.27	0.84	-0.82
16	217.5	142.97	141.22	0.88	-0.87
17	232.0	142.92	141.27	0.84	-0.82
18	246.5	142.78	141.40	0.69	-0.69
19	261.0	142.59	141.60	0.50	-0.49
20	275.5	142.38	141.80	0.29	-0.28
21	290.0	142.20	141.98	0.11	-0.11
22	304.5	142.09	142.09	0.00	0.00
23	319.0	142.06	142.12	-0.03	0.03
24	333.5	142.10	142.08	0.01	-0.01
25	348.0	142.19	141.99	0.10	-0.10
26	362.5	142.28	141.90	0.19	-0.19
27	377.0	142.35	141.83	0.26	-0.26
28	391.5	142.36	141.82	0.28	-0.27
29	406.0	142.32	141.86	0.23	-0.23
30	420.5	142.22	141.96	0.13	-0.13
31	435.0	142.09	142.09	0.00	0.00

### **5.2.1 Inconsistently Detailed FEM**

The inconsistently detailed cross frames are placed in the Base Model finite element model in order to study the effects that inconsistent detailing has on the structure. An axial strain is applied to the WT5x22.5 diagonal members of the cross frames, to either lengthen (Member F) or shorten (Member M) the particular diagonal member. This strain is calculated based on the member length determined for the inconsistently detailed cross frame. This modeling approach is similar to a lack-of-fit analysis. From the application of these initial strains, the behavior of the structure due to inconsistent detailing is investigated.

## **5.3 ANALYSIS RESULTS**

### **5.3.1 Girder Displacements**

As expected, the inconsistently detailed cross frames cause an out-of-plane rotation in the opposite direction of the out-of-plane rotation caused by the application of the total dead load, as shown in Figure 5.7a. This is the intended result of inconsistent detailing: initially start with the girders in a web out-of-plumb position, rotated opposite of the natural behavior so that the girders will rotate to a plumb position after total dead load is applied. However, as shown in Figure 5.7a, after total dead load is applied to the inconsistently detailed structure, the cross section still undergoes some out-of-plane rotation in the center span, although not nearly as much as the total dead load condition for the consistently detailed structure. At the mid-span of the

center span, the out-of-plane rotation due to total dead load is reduced from  $0.832^\circ$  for the consistently detailed structure, to  $0.152^\circ$  for the inconsistently detailed structure.

Also, as shown in Figure 5.7b, the inconsistent detailing causes the top flange to displace laterally towards the inside of the curve. However, after the total dead load is applied to the inconsistently detailed structure, the top flange still displaces laterally outward of the curve. Although, the top flange lateral displacement is reduced from the total dead load condition. At the mid-span of the center span, the lateral displacement due to total dead load is reduced from 1.09 in. for the consistently detailed structure, to 0.45 in. for the inconsistently detailed structure.

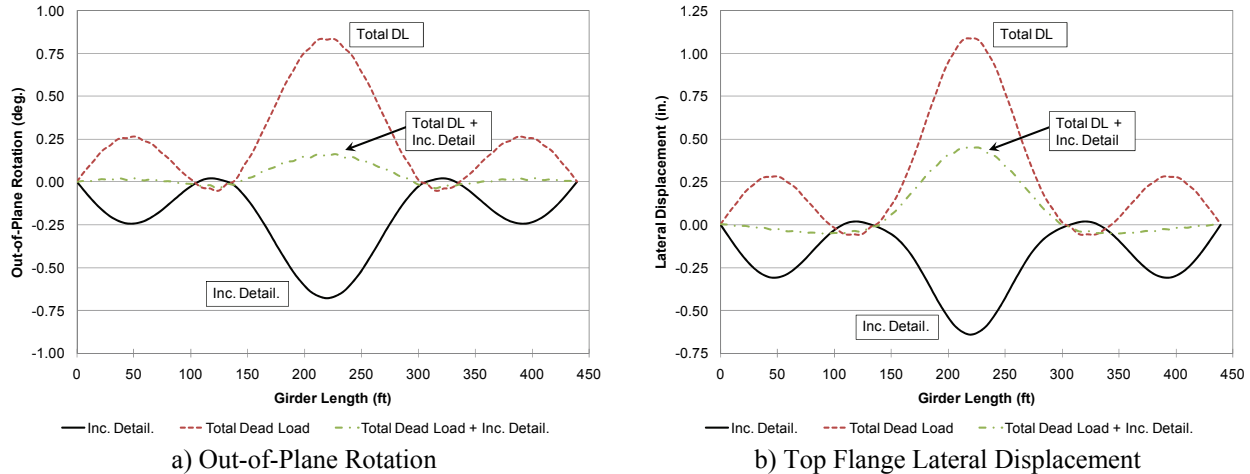


**Figure 5.7 G2 Lateral Displacement and Rotation Comparison**

The center span out-of-plane rotation and top flange lateral displacement due to the total dead load applied to the inconsistently detailed structure is a result of the natural behavior of the curved structure to rotate as a rigid body out-of-plane. This can be realized from reviewing Figure 5.8. As shown in Figure 5.8, girders G1 and G2 have different vertical displacement due the application of the total dead load on the inconsistently detailed structure, resulting in a differential displacement between girder G1 and G2.

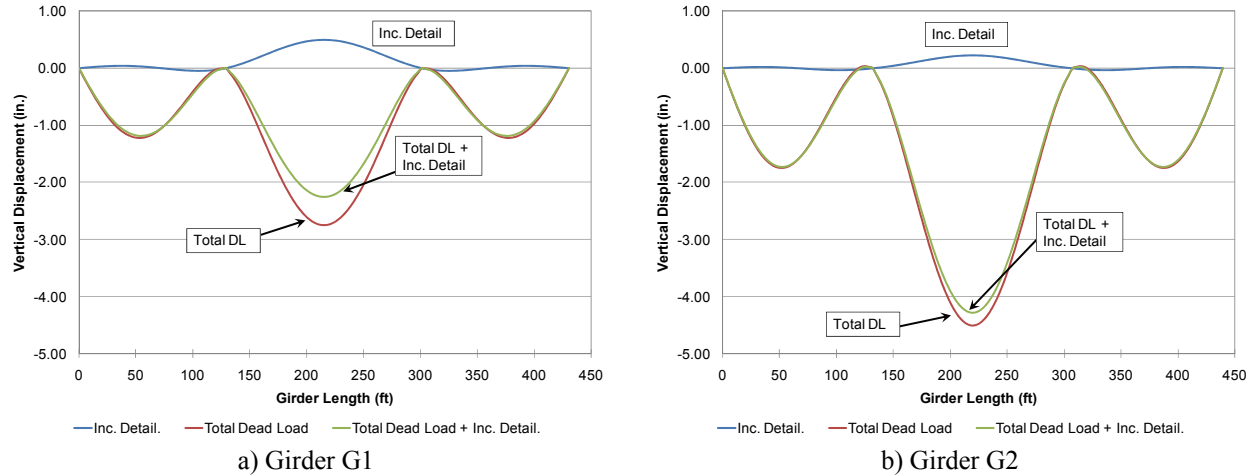


**Figure 5.8** Vertical Displacement Comparison

This differential displacement shows that the cross section still undergoes a rigid body rotation. This rigid body rotation results from the fact that the center of gravity of a curved girder bridge is eccentric with respect to a line drawn between spans end supports. The eccentricity causes the entire structure to rotate about this chord line, and as the eccentricity increases so does the out-of-plane rotation. In the case of the Base Model, the eccentricity for the center span is much greater than the end spans, resulting in the larger out-of-plane rotation for the center span. Given this natural behavior of curved girder bridges to also rotate as rigid bodies, it is evident that inconsistent detailing can mitigate the out-of-plane rotation and top flange lateral displacement, but not completely eliminate them.

Additionally, it is noted that the inconsistent detailing slightly reduces the maximum vertical displacement due to total dead load at the mid-span of the center span. At this location for the consistently detailed structure, girders G1 and G2 have vertical displacements of 2.75 in. and 4.51 in., respectively. For the inconsistently detailed structure, girders G1 and G2 experience vertical displacements of 2.25 in. and 4.28 in., respectively. Although the overall vertical displacements are reduced the differential displacement between G1 and G2 is increased

for the case of inconsistent detailing. This differential effects the concrete slab and haunch details.

### 5.3.2 Flange Stresses

The outer-edge bottom flange tip stress at the mid-span of the center span increases due to the inconsistently detailed cross frames, yielding the maximum tensile stress in the section. (See Figure 4.19 for outer and inner-edge flange locations.) As shown in Figure 5.9, the inconsistently detailed cross frame causes the total dead load outer-edge bottom flange stress to increase to 11.59 ksi for girder G1, and 16.79 ksi for girder G2. As compared to the consistently detailed structure, the inconsistent detailing results in a flange tip tensile stress increase of 36% and 21%, for girders G1 and G2, respectively.

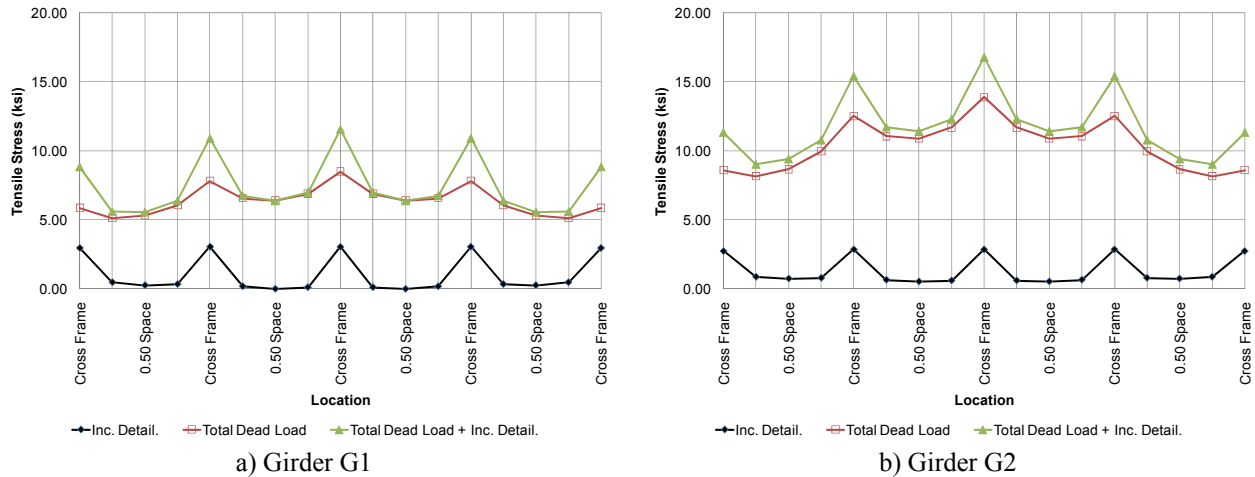
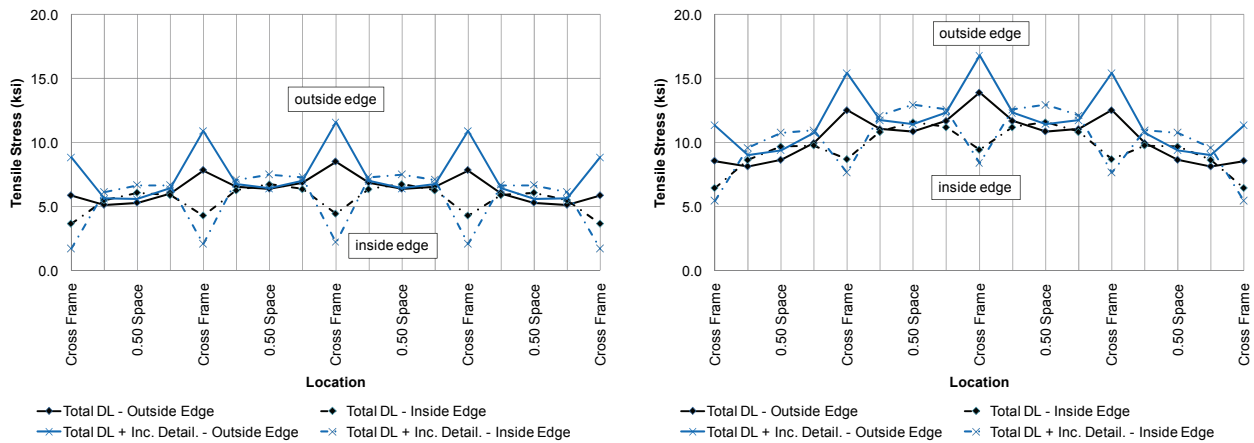


**Figure 5.9** Outer-Edge Bottom Flange Tip Stresses at Mid-span of Center Span

Also of note is the difference in the bottom flange tip stresses between the outer and inner-edges of the flange, for girders G1 and G2, as shown in Figure 5.10. The lateral flange bending causes the stresses to be different on each side of the flange. On the outer-edge of the

flange, at the cross frame locations, the lateral bending causes an additional tensile stress. While on the inner-edge of the flange, the lateral bending causes a compression stress, which reduces the total flange edge tensile stress at the cross frame location. This difference in outer and inner-edge flange stress is more significant at the cross frame locations. For girder G2 at the mid-span cross frame location, the inner-edge flange tip tensile stress is 9.44 ksi while the outer-edge stress is 13.92 ksi, resulting in a gradient across the 20 in. flange of 0.224 ksi/in., for the consistently detailed model. Likewise, the inner and outer-edge flange tip stresses are 8.41 ksi and 16.79 ksi, respectively for the inconsistently detailed structure, resulting in a larger gradient of 0.419 ksi/in. From this observation, it is evident that inconsistent detailing will cause the stress across the flange due to lateral flange bending to increase substantially. This effect is much less significant between cross frame locations as shown in Figure 5.10.



a) Girder G1  
b) Girder G2  
**Figure 5.10** Bottom Flange Tip Stresses at Mid-span of Center Span

Similarly, the inner-edge top flange tip stress at the mid-span of the center span increases due to the inconsistently detailed cross frames, yielding the maximum compressive stress in the section. (See Figure 4.19 for outer and inner-edge flange locations.) As shown in Figure 5.11, the inconsistently detailed cross frame causes the total dead load inner-edge top flange stress to

increase to 9.02 ksi for girder G1, and 16.38 ksi for girder G2. As compared to the consistently detailed structure, the inconsistent detailing results in a flange tip compression stress increase of 31% and 20%, for girders G1 and G2, respectively, for the total dead load case.

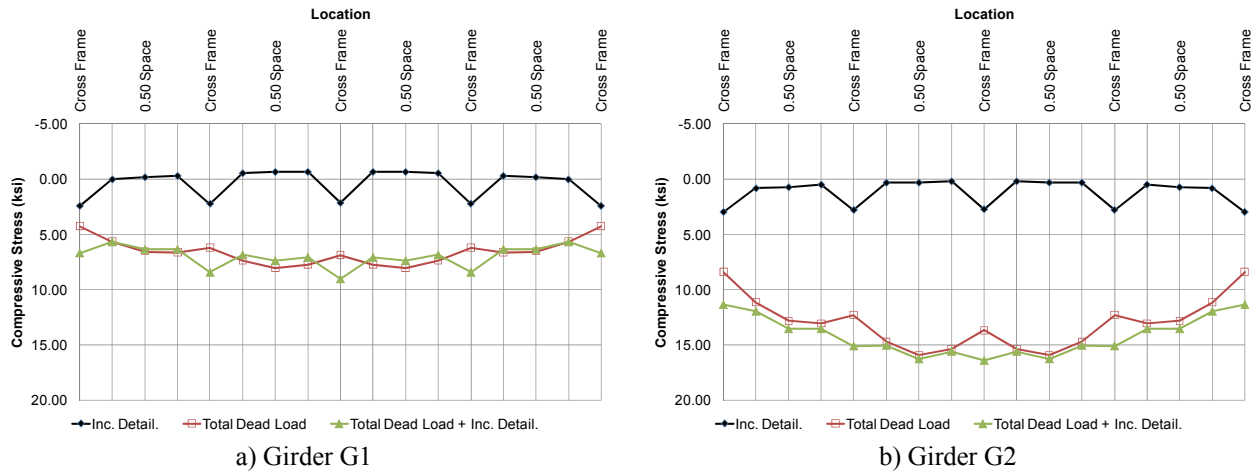


Figure 5.11 Inner-Edge Top Flange Tip Stresses at Mid-span of Center Span

### 5.3.3 Results Discussion

In general, inconsistent detailing causes the Base Model structure to behave differently than the consistently detailed structure. The use of inconsistent detailing does indeed mitigate the web out-of-plumbness that results from the total dead load case. For this structure, inconsistent detailing reduces the maximum out-of-plane rotation at the mid-span of the center span by  $0.680^\circ$ , or 81% compared to the consistent detailing case. However, the out-of-plane rotation is not completely eliminated, and the girder webs are still out-of-plumb. The residual out-of-plane rotation is caused by the plan eccentricity of the structure. Even though it is inconsistently detailed, the two-girder cross section still rotates as a rigid body, resulting in an out-of-plane rotation not affected by the cross frame detailing method.

A reduction in vertical displacements due to inconsistent detailing is observed. This reduction is more pronounced on the interior girder G1, resulting in a greater differential vertical displacement between G1 and G2. This difference in total dead load elevation has a significant effect on the concrete haunch sizes and shear stud lengths if inconsistent detailing is not accounted for during design.

Investigation of flange stress at the mid-span of the curved span demonstrates that there is an increased stress caused by inconsistent detailing. This increase is more pronounced at the locations of the cross frames where the forces associated with inconsistent detailing are transmitted into the girders. For the structure considered, the maximum flange stresses due to total dead load increased significantly at the cross frame locations, as a result of inconsistent detailing. For girder G1, a maximum stress increase of 36% is observed. Likewise, for girder G2, the maximum flange stress at the mid-span of the center span increased by 21%. From this observation it is evident that the increase in flange stresses due to inconsistent detailing may need to be considered by the designer.

From a constructability standpoint, the inconsistent detailing of the cross frames results in diagonal member lengths that are either too short or too long to fit the consistently detailed girders. At the mid-span of the center span, the diagonal member length difference is 0.88 in. During steel erection, the erector will have to close this misalignment in order to make the connection. In many cases, this will require external loads to be applied to the structure by cranes or jacking devices. These externally applied loads can cause additional stresses in the girders and cross frames, in addition to the increase in stresses caused by the inconsistent detailing methods. More likely, the additional effort required to close these connection

misalignments will increase the time it takes to erect the structure, and potentially delay the bridge construction project.

Finally it is noted that the discussion of inconsistent detailing and its effects applies only to steel and concrete slab dead loads. Additional dead loads (wearing surface, appurtenances) and live loads are applied to a composite structure having significantly different behavior to that described in this work.

## 6.0 CONCLUSIONS

The current research shows that considerable attention must be given to the construction and detailing methods employed in horizontally curved steel I-girder bridges. The eccentric application of gravity load resulting from horizontal curvature results in torsional forces being applied to the girder section of a horizontally curved bridge. Due to the relative torsional flexibility of steel I-girders, these forces can result in a marked girder rotation, quantifies in this work as web out-of-plumbness. Nonlinear finite element modeling techniques were employed to investigate the erection sequence and behavior of a constructed curved and skewed I-girder bridge; investigate the effects of web out-of-plumbness on a single beam and a two-girder bridge system; and examine the effects that inconsistent detailing has on a two-girder bridge system.

The practice of inconsistent detailing horizontally curved girder bridges arises when the out-of-plane rotation of the girders, and the subsequent lateral displacement of the top flange due to applied loads are considered excessive. In such cases, inconsistent detailing is used to have the girder webs vertically plumb at a load condition other than no-load. To limit out-of-plane rotation and displacement, cross frames are detailed to fit girders in the web-plumb position under the specified loading condition (usually steel-only load or full dead load) while girders remain conventionally detailed to be in the web-plumb position at the no-load condition: thus creating a detailing inconsistency. It is intended that detailing the cross frames and girders in this manner will force the girder webs to be vertically plumb at the specified loading condition.

However, given that horizontally curved I-girders rotate out-of-plane immediately upon loading (including self-weight), the web of the girders cannot be in a vertically plumb position both before and after a given loading. Therefore, it is incorrect to assume that the combination of girders detailed to be web-plumb in the no-load condition, and cross frames detailed based on the web-plumb position under a different specified load condition, will yield plumb girder webs in that load condition. In the case of an 'X' type cross frame considered in this work, this detailing inconsistency will result in diagonal cross frame members that will either be too long or too short to connect with the girders detailed and fabricated for the web-plumb position in the no-load condition.

The as-built and planned erection sequences of the S.R. 8002 Ramp A-1 curved and skewed steel I-girder bridge were recreated using a finite element model. This study showed the importance of investigating a detailed steel erection sequence for a horizontally curved steel I-girder bridge. If not predicted correctly prior to bridge construction, the vertical and out-of-plane girder displacements may result in cross frame misalignments with bridge girders and/or girder misalignments at field-splice locations that may produce substantial construction related problems. Furthermore, the erection sequence must be examined to ensure proper temporary supports are utilized, and that the girders remain stable during all stages of steel erection.

The inconsistent detailing of the cross frames in the S.R. 8002 Ramp A-1 bridge resulted in small connection misalignments, less than 0.25 in. in most cases. It was noted in the field that during steel erection of the subject bridge, cross frame misalignments related to the inconsistent detailing did not produce significant steel erection difficulties. This was attributed to that fact that the cross frame misalignments were indeed small, and the girders had a relatively small web depth and spacing, and therefore could be manipulated with some ease in the field. It was

observed from this investigation that under certain circumstances, detailing inconsistencies can be tolerated, however this may not be the case for structures that are proportionally larger than S.R. 8002 Ramp A-1.

The main goal of inconsistent detailing in horizontally curved steel I-girder bridges is to limit the web-out-of-plumbness caused by the natural behavior of a horizontally curved structure. Finite element analyses were carried out to investigate the effect that web out-of-plumbness has on a single straight beam, a single curved beam, and a two-girder bridge system. Artificially induced initial web out-of-plumbness was applied to these models, and flange stresses and girder vertical and lateral displacements are monitored. In all cases it was observed that the initial web out-of-plumbness increased the maximum flange tip stresses due to the applied loadings.

For the single straight and curved beams studied, the load-displacement behavior was relatively unchanged as the beams' initial geometry was rotated out-of-plane from zero to five degrees at one degree increments. In practice, out-of-plane rotations due to dead load are typically observed to be less than 2 degrees. The results of the current research showed that for the curved I-girders studied, the ultimate load capacity of the girder will be reduced by only about 1% due to the effects of web out-of-plumbness. However, provided the girder responds elastically, it was seen that the flange tip stresses increase due to the reduced cross-sectional properties resulting from the beam being rotated out-of-plane. The increase in flange tip stress results from the fact that the section modulus at the flange tip decreases as the initial out-of-plane rotation increases.

For the two-girder bridge system it was observed that the flange stresses and girder displacements were also affected by the initial web out-of-plumbness. Through a parametric study it was shown that variation in radius of horizontal curvature and cross frame spacing have

a more significant effect on the behavior of the structure than variation in web depth or girder spacing. In general, the web-out-plumbness caused an increase in the maximum flange tip stresses, most notably at the location of maximum positive moment. Lateral flange bending resulting from girder rotation results in a transverse stress gradient across the flange width which becomes more significant as the web out-of-plumbness is increased for all the parameters studied herein.

If the web out-of-plumbness is mitigated through the use of inconsistent detailing, cross frames diagonal members will be intentionally fabricated too short or too long to fit into girders that are vertically plumb at the no-load condition. As shown through the investigation of the two-girder bridge system, this method of detailing will result in an increase in the maximum flange stresses due to total dead load. This increase results primarily from the locally-induced forces associated with the cross frame misfits. Additionally, inconsistent detailing is shown to affect the vertical and lateral displacement of the girders. In practice, it is typically the case that the effects of inconsistent detailing are not analyzed and ignored. This study indicates that the effects of inconsistent detailing can be significant enough to affect design values and should be accounted for in design.

Based on the analytical studies conducted, it is proposed that the effects of web out-of-plumbness need to be specifically considered for the effects on flange stresses in design, as an alternative to the practice of inconsistent detailing. Consideration of these effects during design and conventionally detailing girders and cross frames for the web-plumb position at no-load, in lieu of specifying inconsistent detailing to control web out-of-plumbness, will reduce construction problems that typically result from the practice of inconsistent detailing. It should be noted, that although not considered in the present work, secondary effects associated with

deck slab placement, final deck elevations, haunch size, and shear stud effectiveness will be affected by the degree of web out-of-plumbness

However, if inconsistent detailing is employed to mitigate web out-of-plumbness, it must be recognized by bridge designers that this approach has complex effects on “locked-in” stresses and constructability of curved I-girder bridges. These “locked-in” stresses and constructability issues need to be considered by bridge designers and steel erectors, respectively. While a simple method for inconsistent detailing is demonstrated, further study of the objective of such detailing (presently: web-plumb at dead load) is warranted to optimize both behavior and constructability.

## **6.1 RECOMMENDATIONS**

The importance of a carefully planned and analyzed erection sequence is shown through the analytical investigation of the S.R. 8002 Ramp A-1 bridge. Therefore, it is recommended that bridge engineers investigate each stage of steel erection for horizontally curved steel I-girder bridges in order to limit the problems that may develop in the field during construction. The steel erection analysis can be utilized to determine the optimal erection sequence, as well as highlight more difficult portions of the procedure for the erector.

Inconsistent detailing has been shown to increase girder flange stresses and have an effect on girder displacements. These additional stresses and effects need to be investigated by the bridge engineer during the design process. Failure to do so may result in an overstress condition, especially when the cross frame misalignments are large. Girder displacement may be changed such that interior girders are at a higher elevation than predicted for a consistently detailed structure, thus affecting haunch design. Additionally, when significant cross frame connection

misalignments result from inconsistent detailing, problems during the construction can develop. The steel erector must consider these intentional misalignments during steel erection analysis; otherwise additional problems may develop as the bridge is assembled.

However, if the effects of web out-of-plumbness are considered during the design of the bridge, there may not be a need to control web out-of-plumbness. For example, an estimate of the additional flange tip stresses caused by an out-of-plumb cross section can be calculated by considering the reduced section modulus of the cross section. Alternatively, additional models can be analyzed to determine the effects that an out-of-plumb girder will have on the behavior of the structure. If the web out-of-plumbness effects are considered during design, there may not be a need for inconsistent detailing, in turn, reducing the potential for problems during construction related to cross frame connections misalignments.

## **6.2 FUTURE RESEARCH NEEDS**

Further studies of erection sequences and methods for bridges of different radii, span length, girder spacing, girder depth, cross frame spacing, and skew would be useful to practicing engineers in quantifying the magnitude of effect discussed in this work over a braider design space. Ultimately, these studies should evolve into a set of guidelines for the erection of horizontally curved I-girder bridges. Also, in-field or experimental construction studies of curved I-girder bridges could serve to eliminate typical construction problems. Monitoring of girder displacements and stresses, crane loads, and bearing forces during an in-field steel erection procedure would provide useful data to steel erectors and bridge engineers and provide verification for the type of erection study conducted herein.

While a simple method for inconsistent detailing is demonstrated, further study of the objective of such detailing (presently: web-plumb at dead load) is warranted to optimize both behavior and constructability. Additional research should be conducted to determine at what stage of construction it is most advantageous to have the girder webs vertically plumb (no-load, steel dead load, total dead load, or another combination altogether). This should include a survey of bridge engineers, fabricators, steel erectors, and bridge owners, focusing solely on curved I-girder bridge erection and detailing methods. Investigations should be carried out to determine if the web out-of-plumbness has a significant effect on the deck placement and bearing rotations during construction. The present work also suggest possible alternative means of affecting control of curved girder bridge out-of-plumbness by affecting other design parameters. Provision of additional cross-braces, for example, may affect results similar to inconsistent detailing.

Furthermore, it is necessary to determine the magnitude of girder rotation due to dead loads that is tolerable, such that the rotation does not have a detrimental effect on the live load rating of the final structure. If such a magnitude is determined, the idea that a curved I-girder needs to be inconsistently detailed might be eliminated altogether.

## APPENDIX A

### REPRESENTATIVE PUBLICATIONS

#### ***Masters Thesis:***

Chavel, B.W., “Evaluation of Erection Procedures of the Curved Span of the Ford City Steel I-Girder Bridge,” Department of Civil Engineering, University of Pittsburgh, Pittsburgh, Pennsylvania

#### ***Reports:***

Chavel B.W., Earls, C.J., (2001), “Evaluation of Erection Procedures of the Curved Span of the Ford City Steel I-Girder Bridge,” Report No. CE/ST 18, Department of Civil Engineering, University of Pittsburgh, Pittsburgh, Pennsylvania.

Chavel B.W., Earls, C.J., (2004), “Deflection of Horizontally Curved I-Girder Bridge Members Under Construction,” Report No. CE/ST 28, Department of Civil Engineering, University of Pittsburgh, Pittsburgh, Pennsylvania.

#### ***Refereed Journal Papers:***

Chavel, B.W., and Earls, C.J., (2006a). “Construction of a Horizontally Curved Steel I-Girder Bridge. Part I: Erection Sequence.” *Journal of Bridge Engineering*, Vol. 11, No. 1, January, pp. 81-90.

Chavel, B.W., and Earls, C.J., (2006b). “Construction of a Horizontally Curved Steel I-Girder Bridge. Part 2: Inconsistent Detailing.” *Journal of Bridge Engineering*, Vol. 11, No. 1, January, pp. 91-98.

#### ***Conference Proceedings:***

Chavel, B.W., Howell, T.D., and Earls, C.J., “The Influence of Web-Plumbness in Horizontally Curved Steel I-Girder Bridges,” Structural Stability Research Council Conference, San Antonio, Texas, 2006.

- Chavel, B.W. and Earls, C.J., “Structural Capacity of Curved Steel I-Girders in a Web-Out-of-Plumb Position,” Structural Stability Research Council Conference, Montreal, Quebec, Canada, 2005.
- Chavel, B.W. and Earls, C.J., “Inconsistent Detailing of Cross frame Members in Horizontally Curved Steel I-Girder Bridges,” American Society of Civil Engineers Structures Congress, New York City, New York, 2005.
- Chavel, B.W. and Earls, C.J., “Nonlinear Finite Element Modeling of Horizontally Curved I-Girder Bridges,” Federal Highway Administration Workshop – Innovative Applications of Finite Element Modeling in Highway Structures, New York City, New York, 2003.
- Chavel, B.W. and Earls, C.J., “Investigation of Construction Issues and Inconsistent Detailing in Horizontally Curved Steel I-Girder Bridges,” 82<sup>nd</sup> Annual Meeting of the Transportation Research Board, Washington, D.C., 2003.
- Chavel, B.W. and Earls, C.J., “Evaluation of Construction Issues and Inconsistent Detailing of Girders and Cross frame Members in Horizontally Curved Steel I-Girder Bridges,” 19th Annual International Bridge Conference, Pittsburgh, Pennsylvania, 2002.
- Chavel, B.W. and Earls, C.J., “Stability of Curved Steel I-Girder Bridge Components During Erection,” Structural Stability Research Council Conference, Seattle, Washington, 2002.
- Chavel, B.W. and Earls, C.J., “Evaluation of Erection and Construction Procedures for a Curved Steel I-Girder Bridge,” American Society of Civil Engineers Structures Congress, Denver, Colorado, 2002.

## **APPENDIX B**

### **S.R. 8002 RAMP A-1 STEEL ERECTION STUDY RESULTS**

Results are presented for the as-built erection sequence and intended erection sequence (as-planned). For each stage of construction, the girder vertical displacements, lateral (out-of-plane) displacements, and the girder out-of-plane rotation are shown.

#### **B.1 AS-BUILT ERECTION SEQUENCE ANALYTICAL RESULTS**

Results are presented for the as-built erection sequence analytical studies. For each construction stage the following three figures are included:

- A. Figure 'A' – Girder Vertical Displacement
- B. Figure 'B' – Girder Lateral (out-of-plane) Displacement
- C. Figure 'C' – Girder Out-of-Plane Rotation

Table B-1 shows the naming convention for each stage and structural configuration analyzed. Note that in some cases a variation in boundary conditions (holding and lifting cranes) is investigated for several construction stages.

**Table B-1** As-Built Erection Sequence Naming Convention

<b>Construction Stage Name</b>	<b>Component(s) Placed in Finite Element Model</b>	<b>Holding Crane</b>	<b>Lifting Crane</b>
Stage 1	G1	None	G1
Stage 2	G2	G1	G2
Stage 2a	Cross-frames 1E & 19E	G1	G2
Stage 2b	Cross-frame 5E	G1	G2
Stage 2c	Cross-frame 9E	G1	G2
Stage 2d	Cross-frames 3E, 7E, 11E	G1	G2
Stage 2e	Cross-frames 2E, 4E, 6E, 8E, 10E, 12E	G1	G2
Stage 2e1	None	G1	None
Stage 3	G3	G1	G3
Stage 3a	Cross-frames 1D and 19D	G1	G3
Stage 3b	Cross-frames 12D and 14D	G1	G3
Stage 3c	Cross-frames 8D and 10D	G1	G3
Stage 3c1	None	G1	None
Stage 3d	Cross-frames 2D, 4D, 6D	G1	G3
Stage 3d1	None	G1	None
Stage 3e	Cross-frames 3D, 5D, 7D, 9D, 11D, 13D	G1	G3
Stage 3e1	None	G1	None
Stage 4	G4	G1	G4
Stage 4a	Cross-frames 1C and 19C	G1	G4
Stage 4b	Cross-frames 3C and 5C	G1	G4
Stage 4c	Cross-frames 7C and 9C	G1	G4
Stage 4c1	None	G1	None
Stage 4d	Cross-frames 13C and 15C	G1	G4
Stage 4d1	None	G1	None
Stage 4e	Cross-frames 10C, 11C, 14C, 16C	G1	G4
Stage 4e1	None	G1	None
Stage 4f	Cross-frames 2C, 4C, 6C, 8C	G1	G4
Stage 4f1	None	G1	None
Stage 5a	G5 and Cross-frames 1B and 19B	G1	G5
Stage 5b	Cross-frames 5B and 9B	G1	G5
Stage 5c	Cross-frames 11B and 15B	G1	G5
Stage 5c1	None	G1	None
Stage 5c2	None	None	None
Stage 5d	Cross-frames 3B and 7B	G1	G5
Stage 5d1	None	G1	None
Stage 5d2	None	None	None
Stage F6a	G6	None	G6
Stage F6b	Cross-frames 13A and 17A	None	G6
Stage F6c	Cross-frames 8A, 10A	None	G6
Stage F6c1	None	None	None
Stage F6d	Cross-frames 2A, 4A, 6A	None	G6
Stage F6d1	None	None	None
Stage F6e	Cross-frames 8B, 10B, 13B, 17B	None	G6
Stage F6e1	None	None	None
Stage F6f	Cross-frames 2B, 4B, 6B	None	G6
Stage F6f1	None	None	None
Stage 6d2	Cross-frames 3A, 5A, 7A	None	None
Stage 6e2 (Final)	Cross-frames 9A, 11A, 15A, 18A	None	None

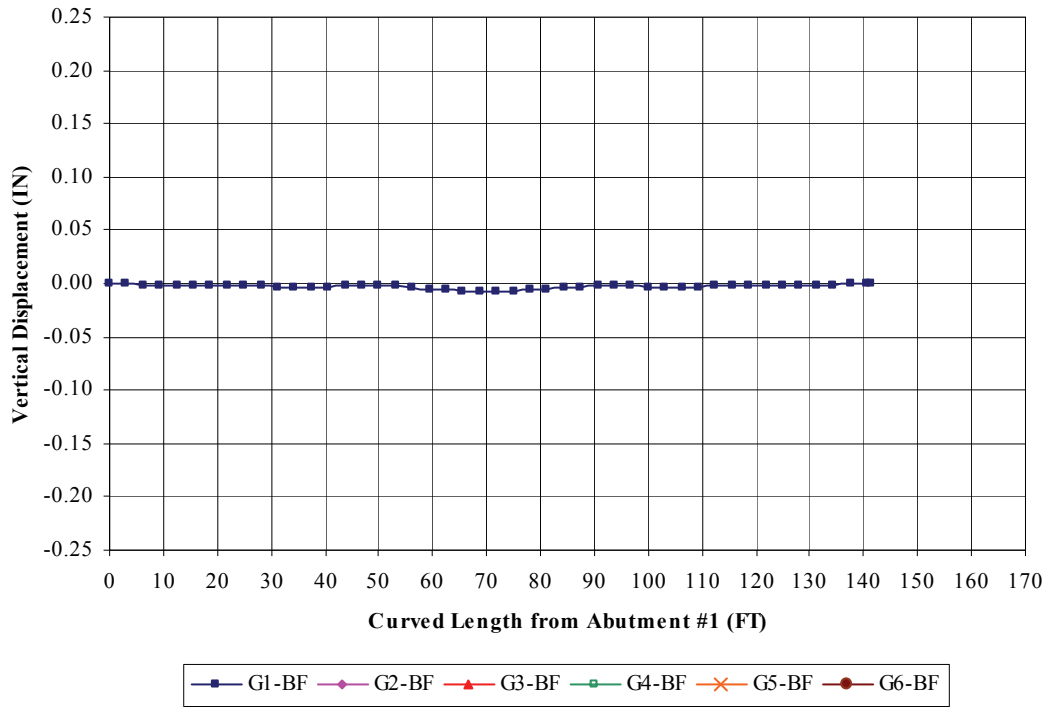


**Figure B.1** Construction Stage 1 – Girder Vertical Displacement

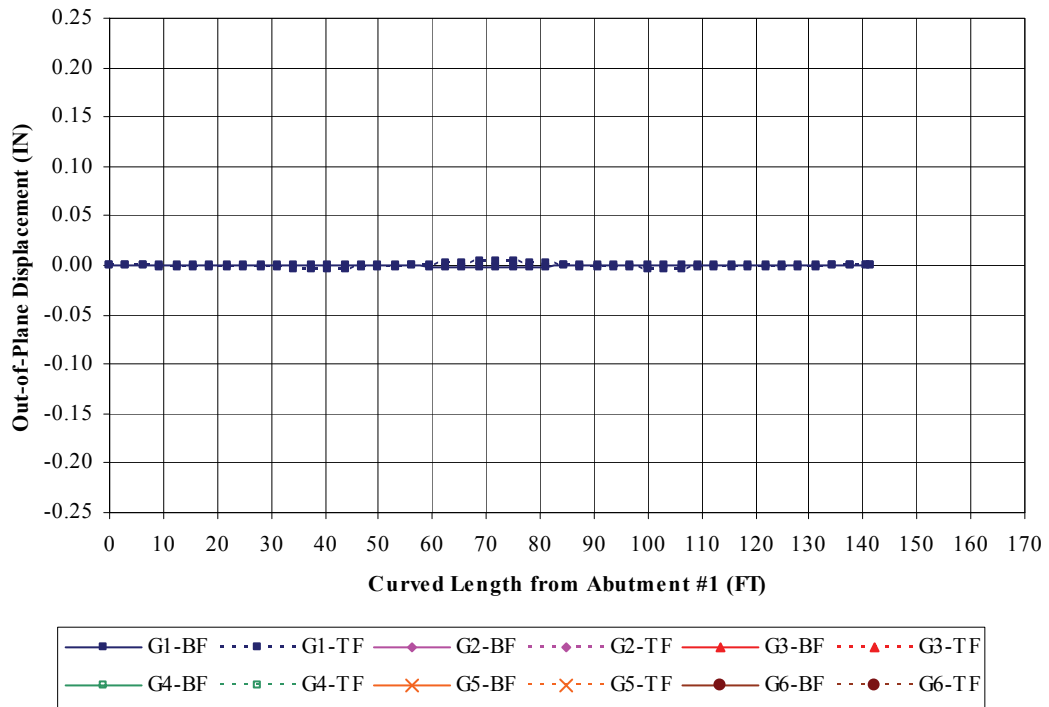


**Figure B.2** Construction Stage 1 – Girder Lateral Displacement

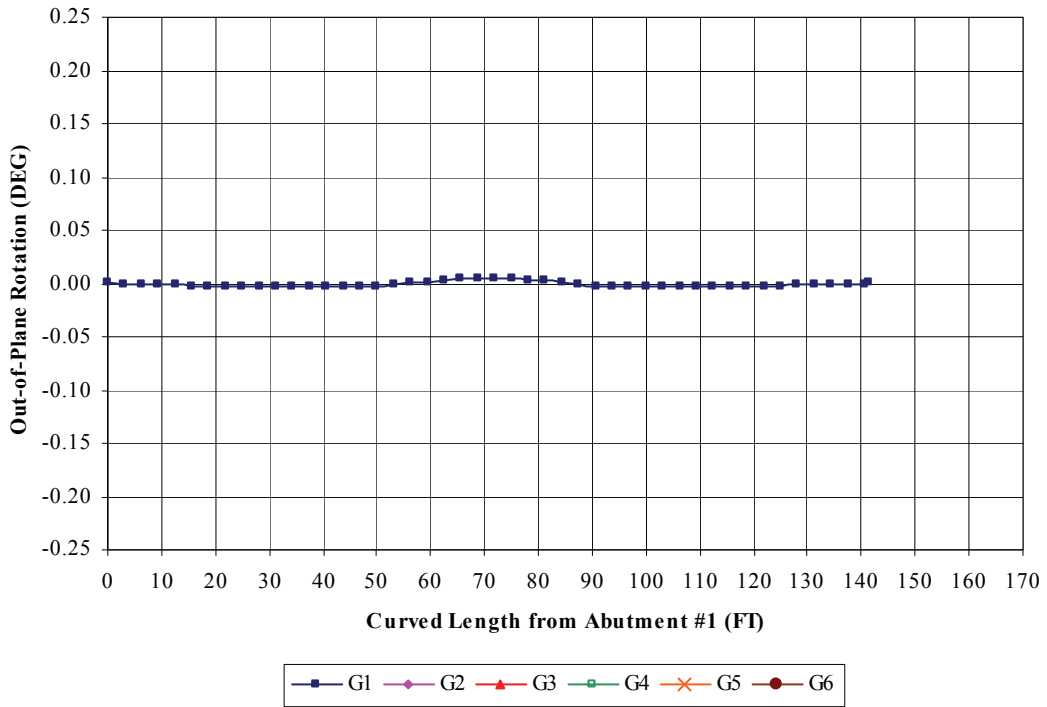


**Figure B.3** Construction Stage 1 – Girder Out-of-Plane Rotation

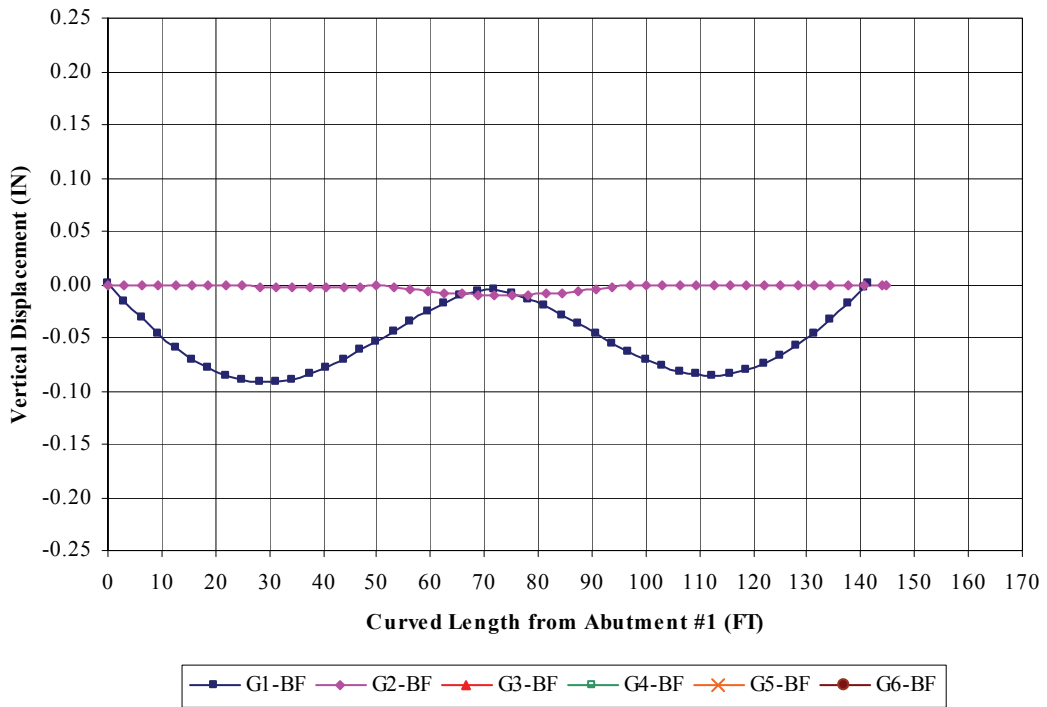


**Figure B.4** Construction Stage 2 – Girder Vertical Displacement

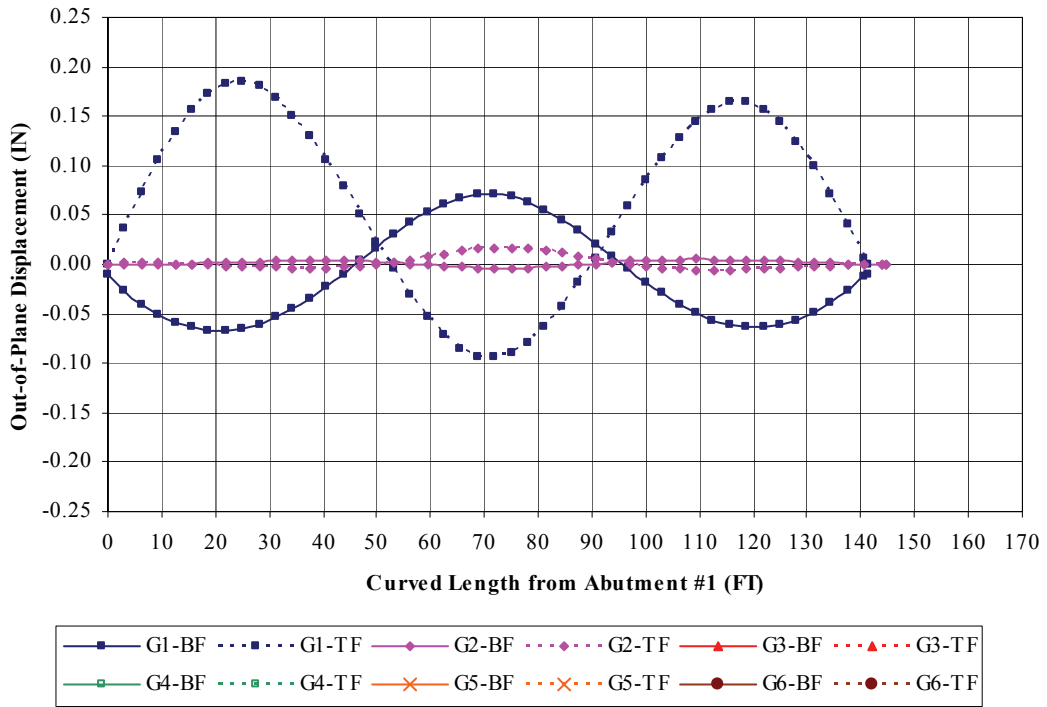


**Figure B.5** Construction Stage 2 – Girder Lateral Displacement

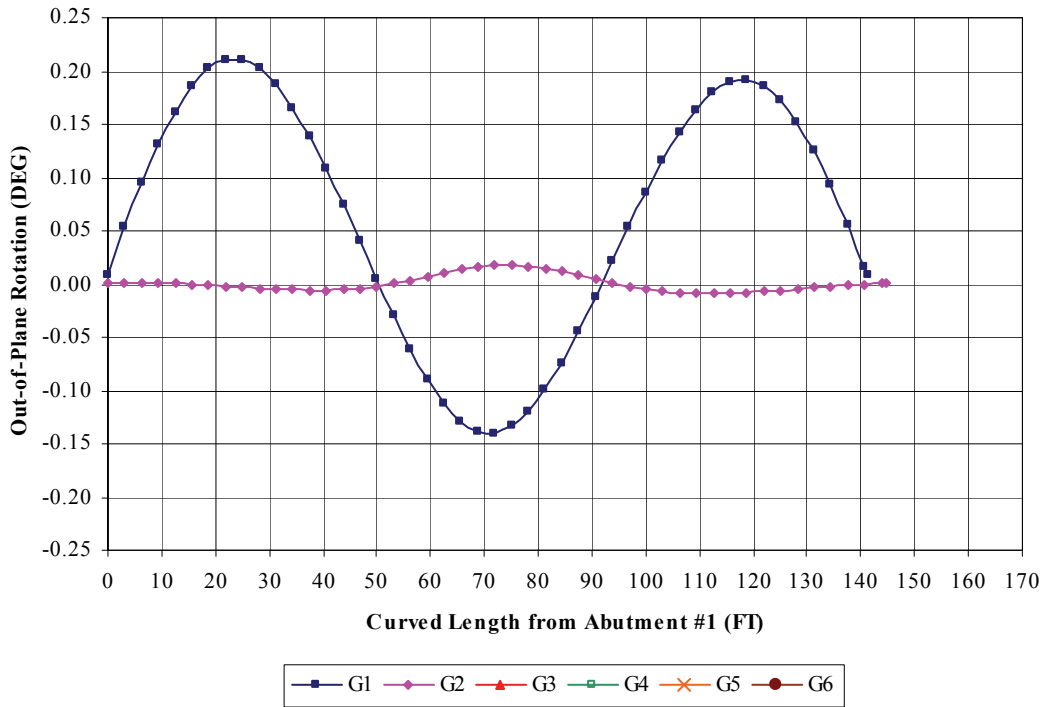


**Figure B.6** Construction Stage 2 – Girder Out-of-Plane Rotation

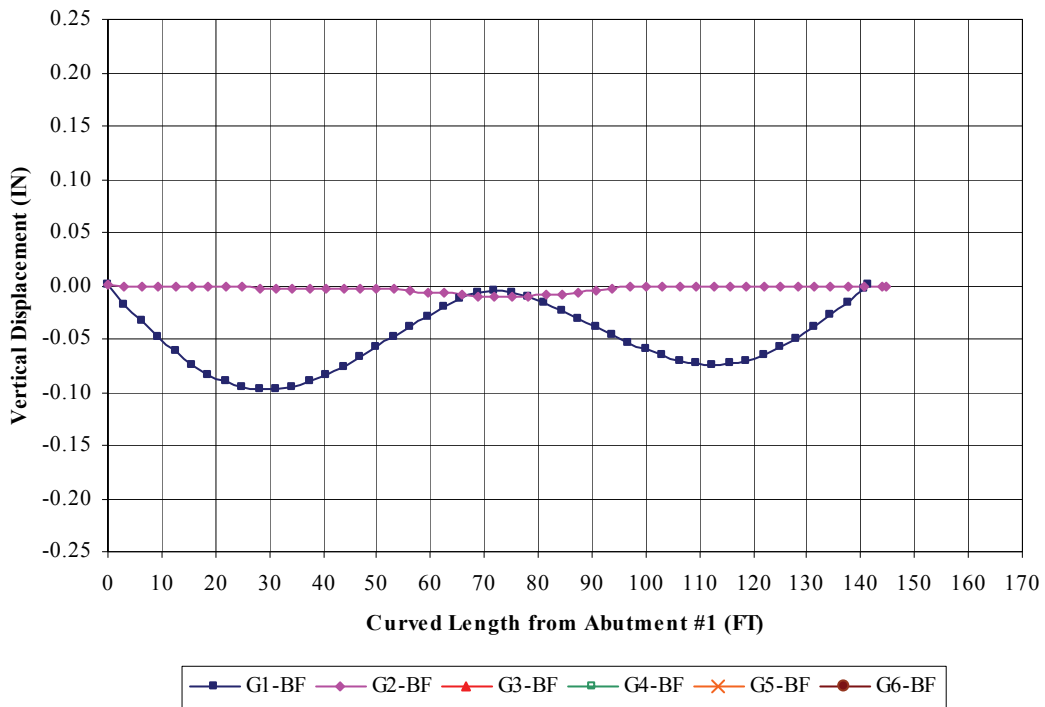


Figure B.7 Construction Stage 2a – Girder Vertical Displacement

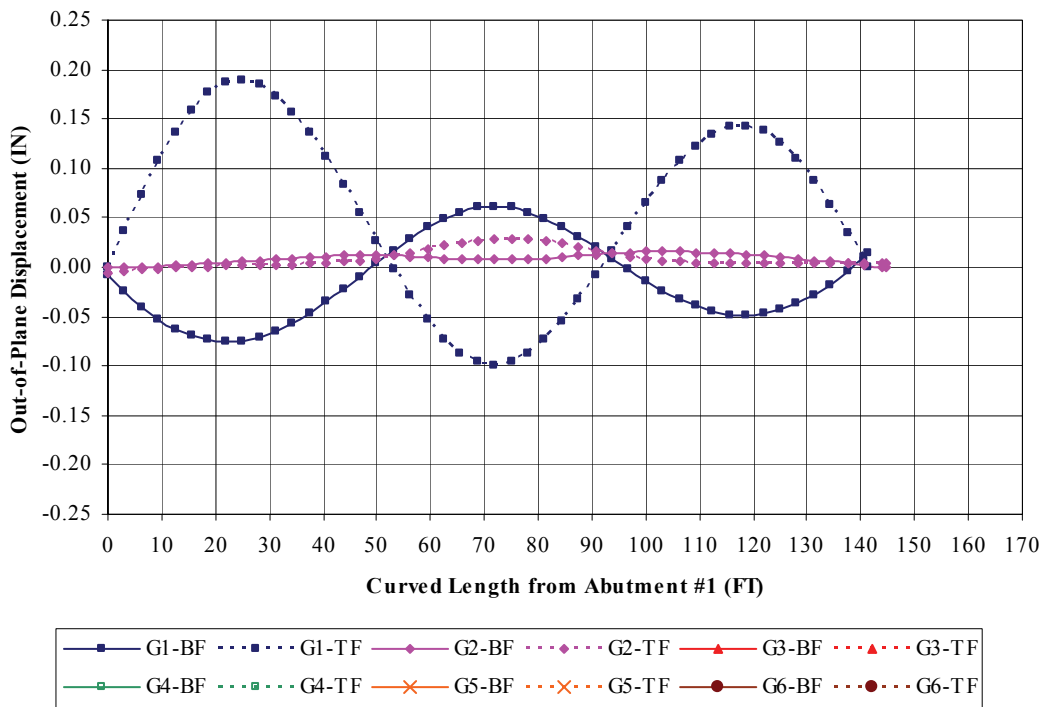
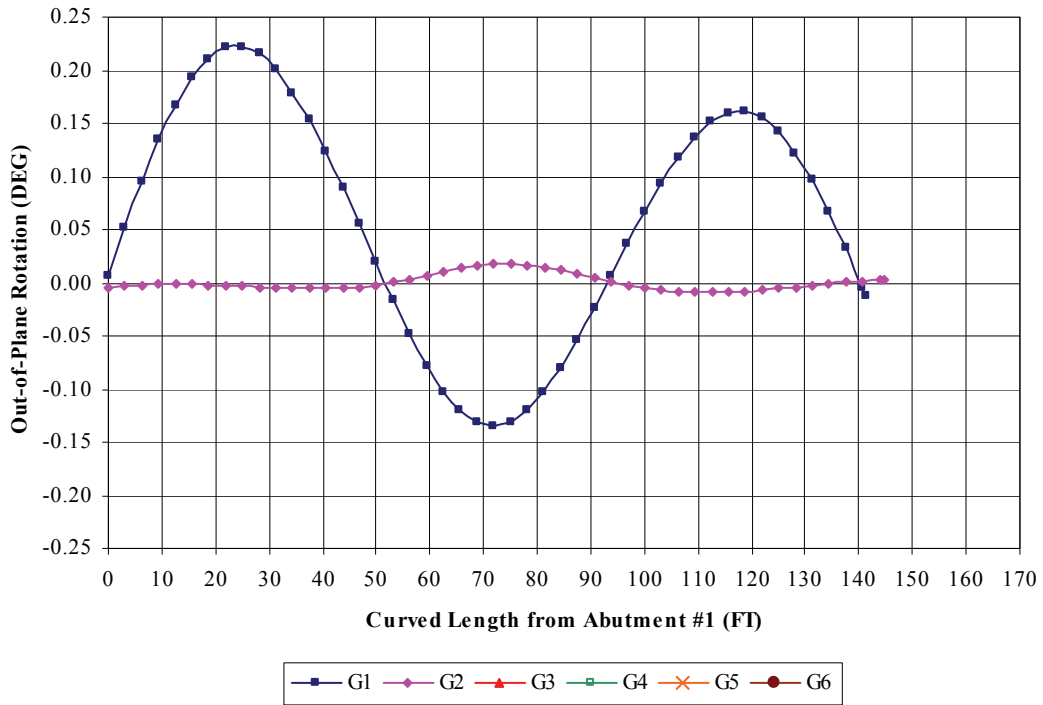
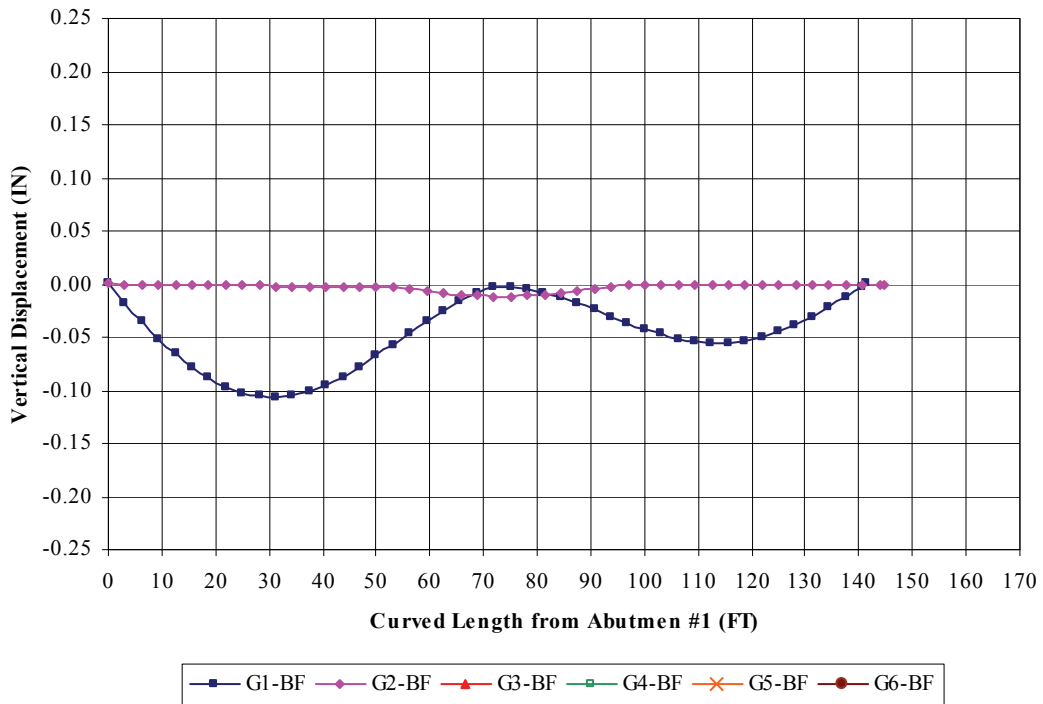


Figure B.8 Construction Stage 2a – Girder Lateral Displacement



**Figure B.9** Construction Stage 2a – Girder Out-of-Plane Rotation



**Figure B.10** Construction Stage 2b – Girder Vertical Displacement

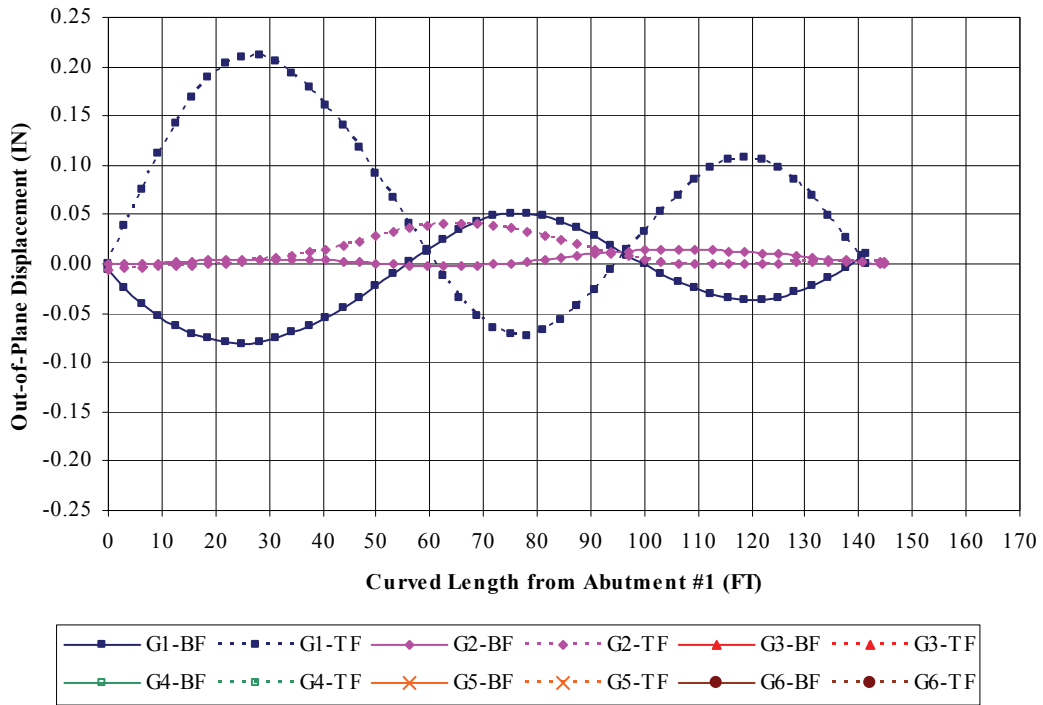


**Figure B.11** Construction Stage 2b – Girder Lateral Displacement

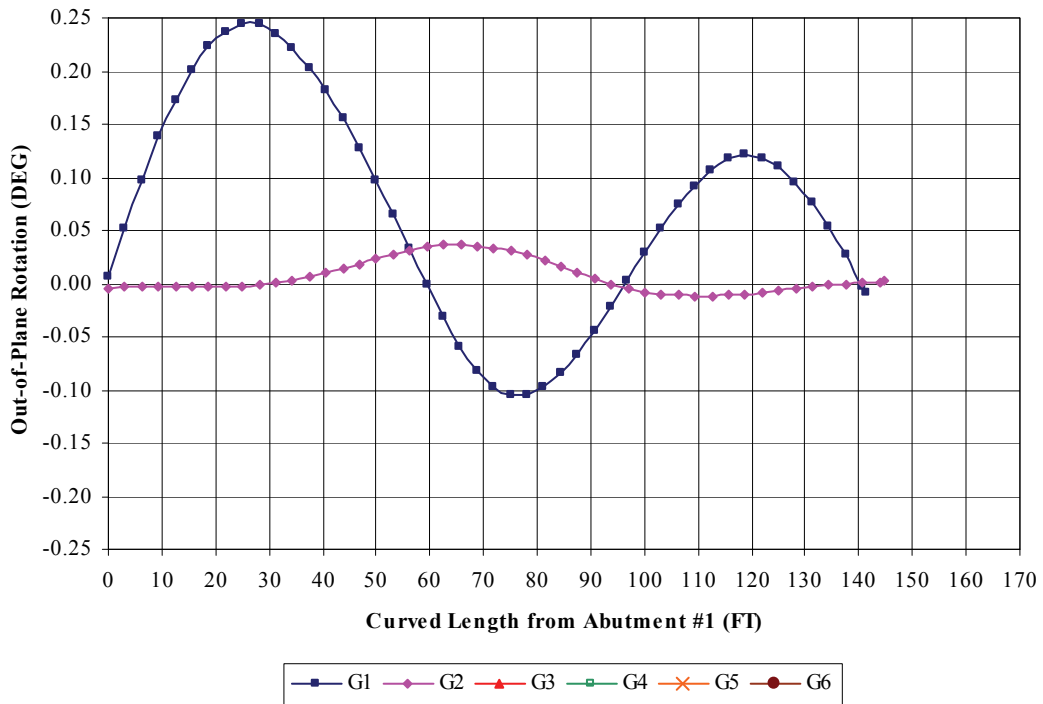


**Figure B.12** Construction Stage 2b – Girder Out-of-Plane Rotation

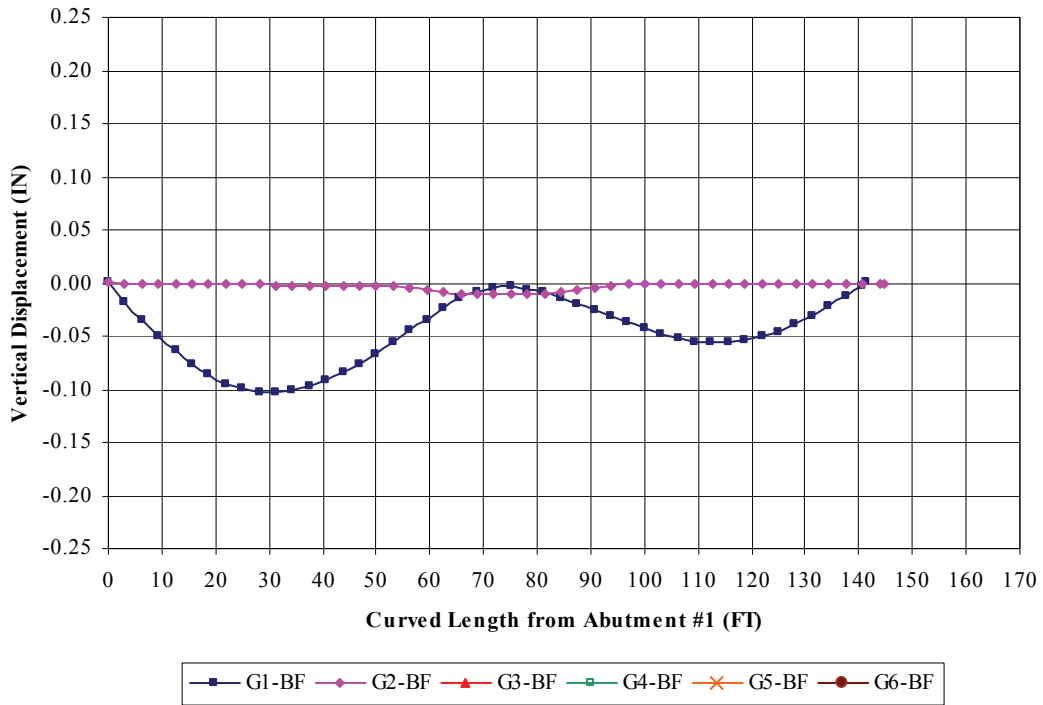


**Figure B.13** Construction Stage 2c – Girder Vertical Displacement

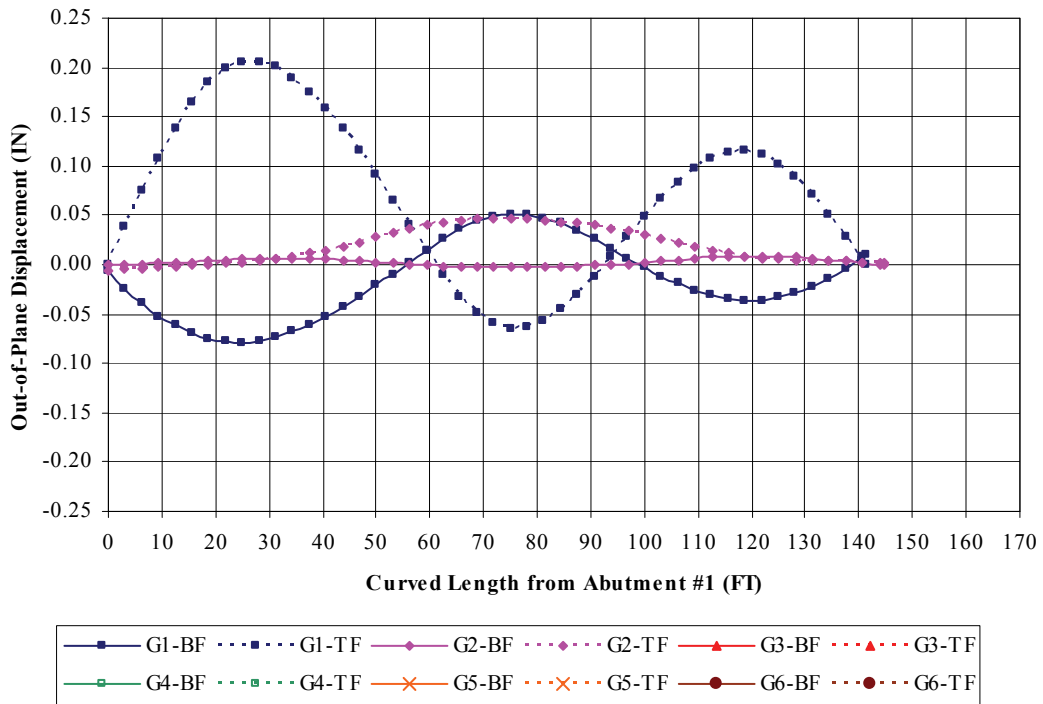


**Figure B.14** Construction Stage 2c – Girder Lateral Displacement

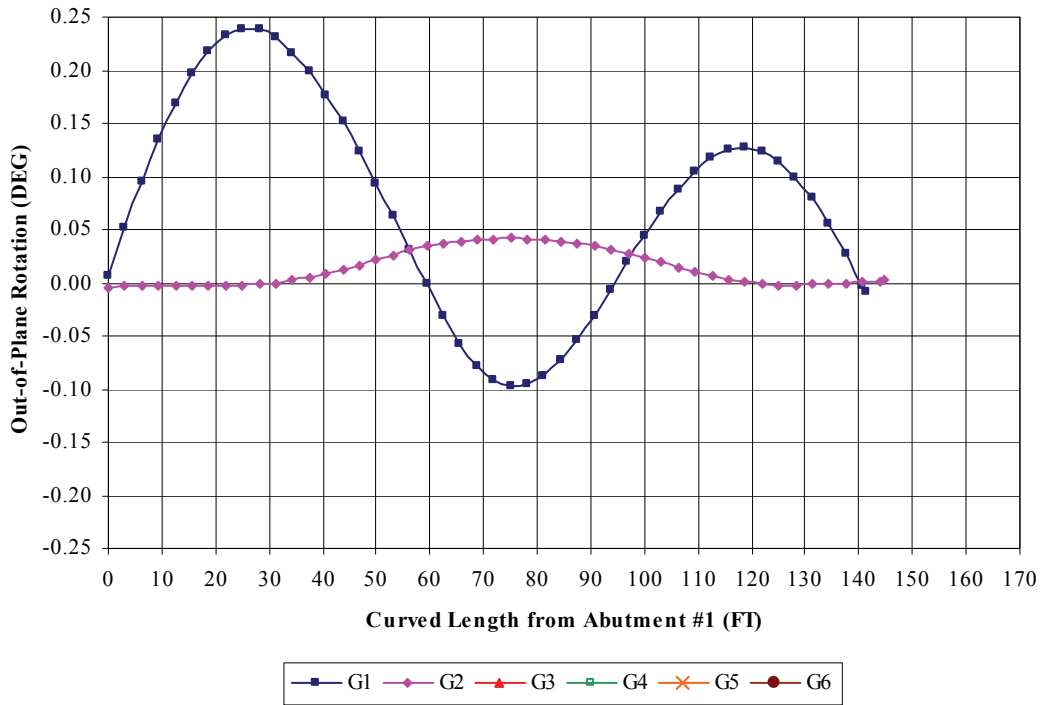


**Figure B.15** Construction Stage 2c – Girder Out-of-Plane Rotation

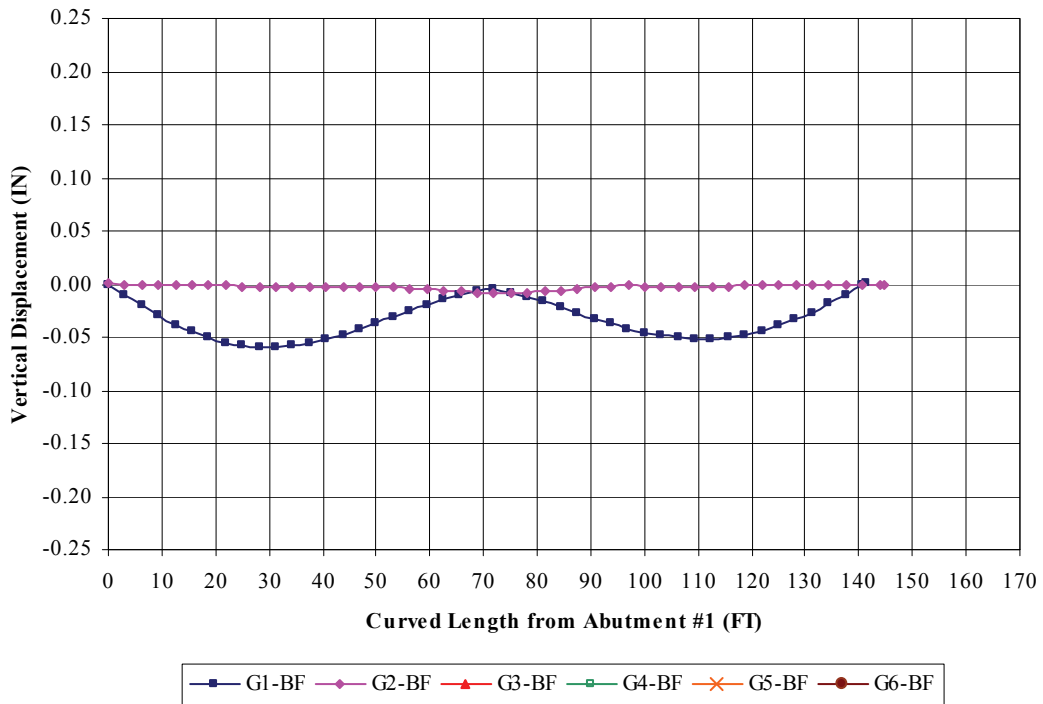


**Figure B.16** Construction Stage 2d – Girder Vertical Displacement

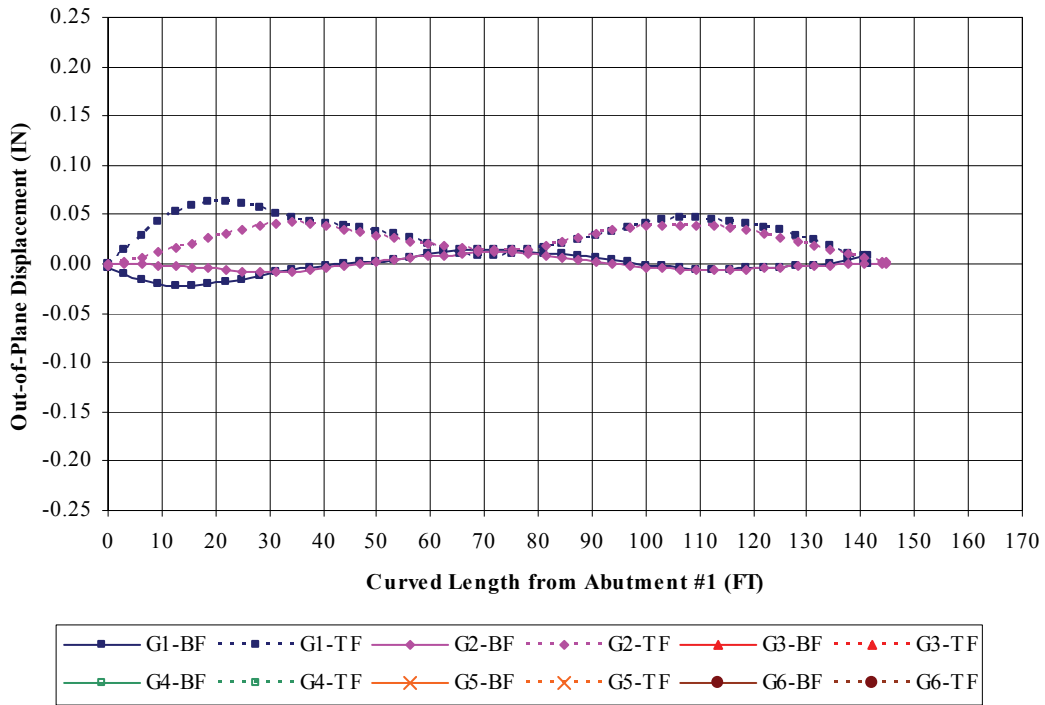


**Figure B.17** Construction Stage 2d – Girder Lateral Displacement

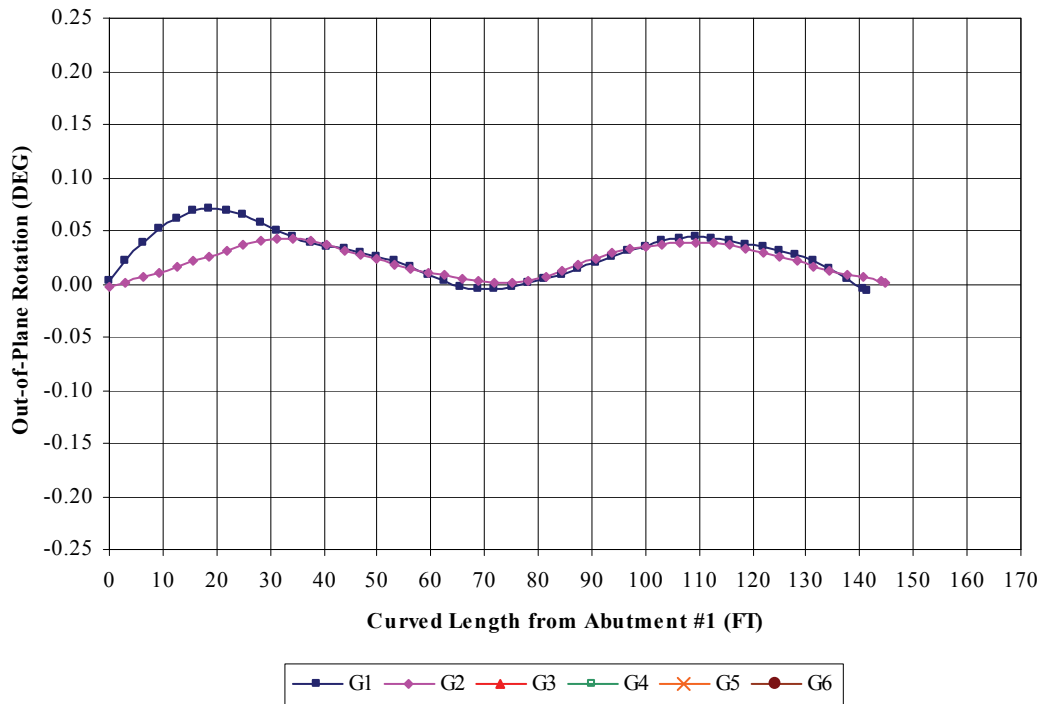


**Figure B.18** Construction Stage 2d – Girder Out-of-Plane Rotation

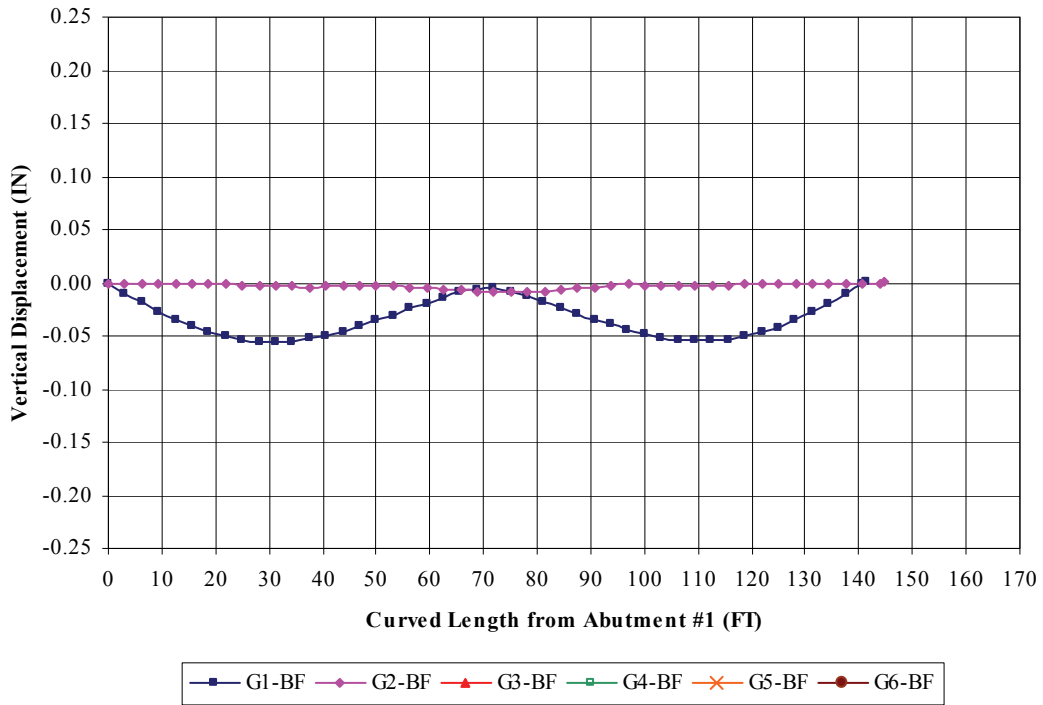


Figure B.19 Construction Stage 2e – Girder Vertical Displacement

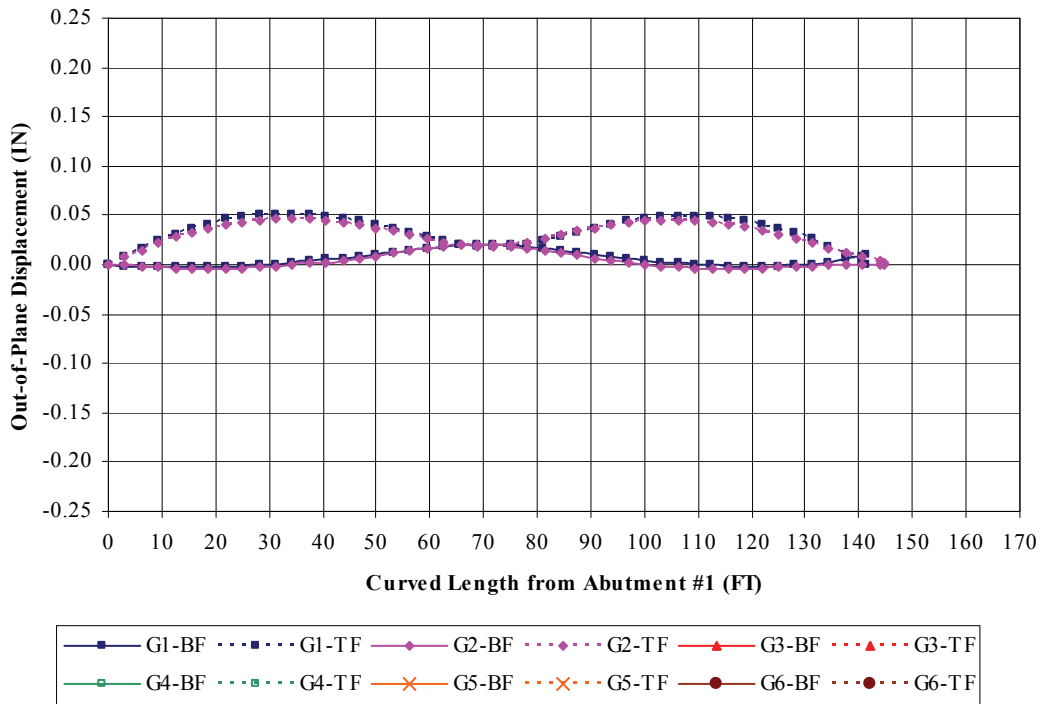
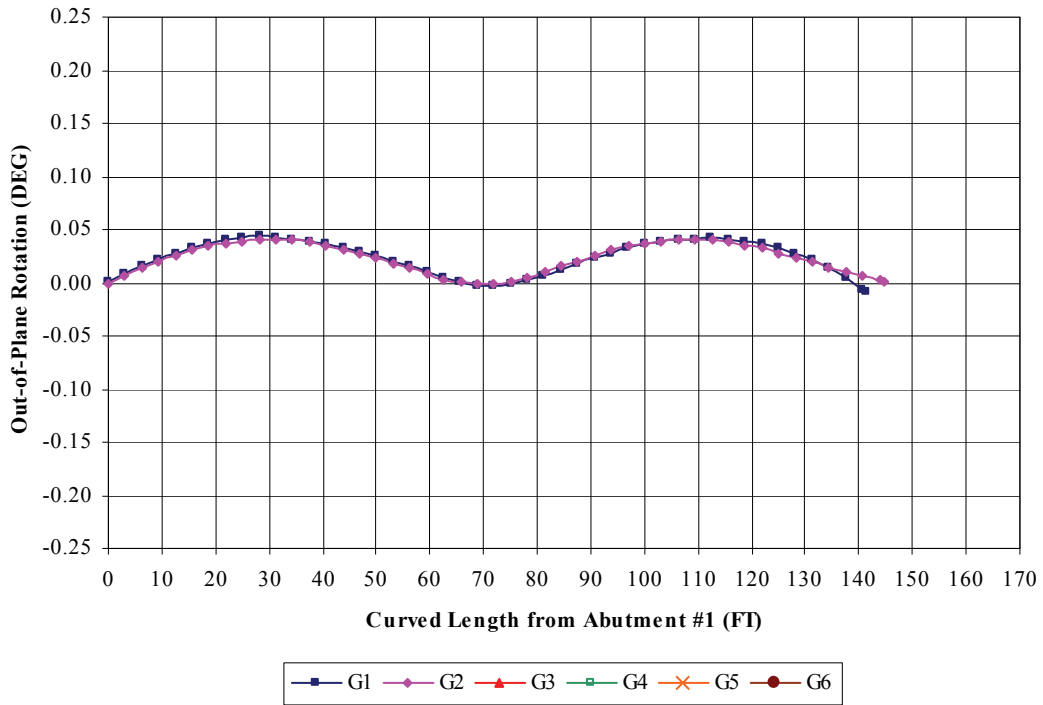
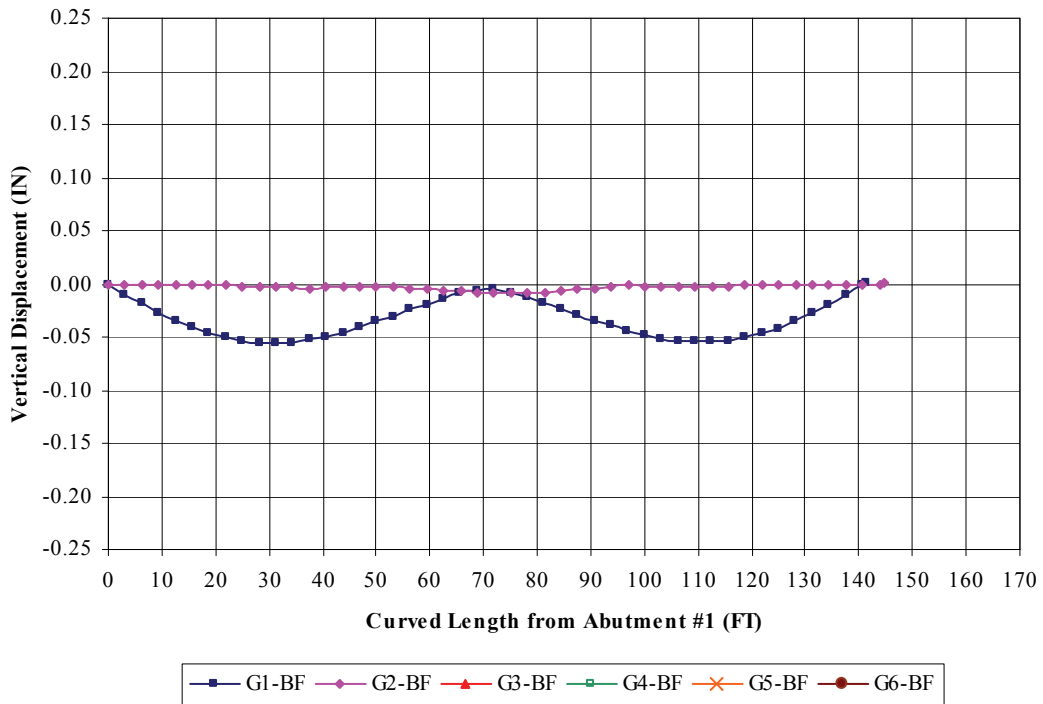


Figure B.20 Construction Stage 2e – Girder Lateral Displacement



**Figure B.21** Construction Stage 2e – Girder Out-of-Plane Rotation



**Figure B.22** Construction Stage 2e1 – Girder Vertical Displacement

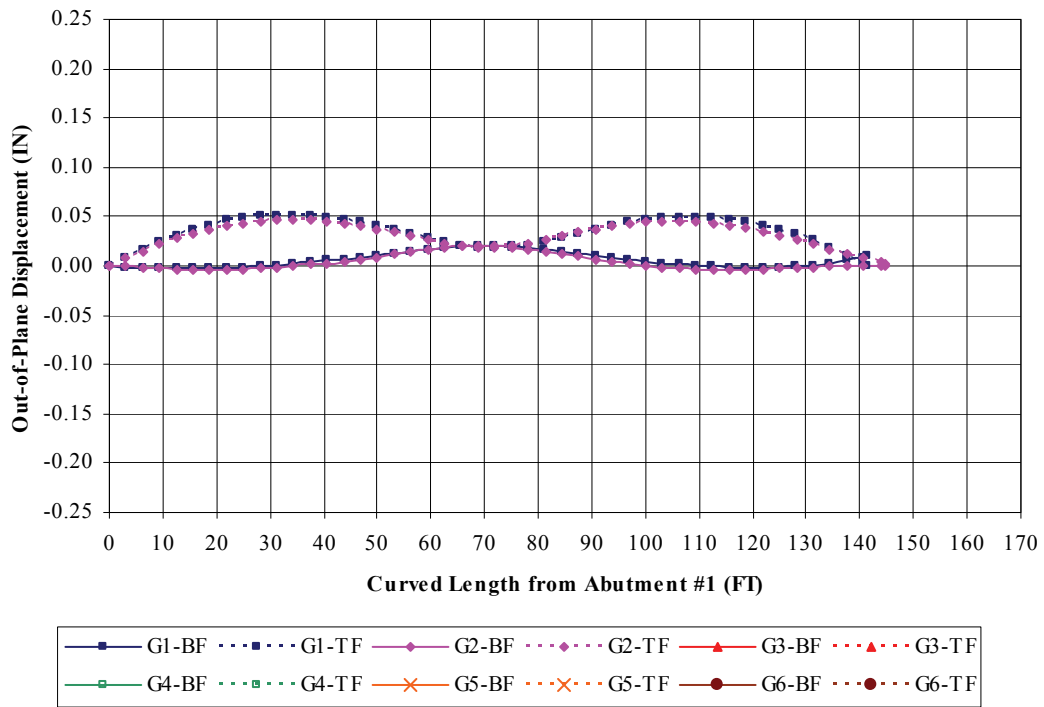


**Figure B.23** Construction Stage 2e1 – Girder Lateral Displacement

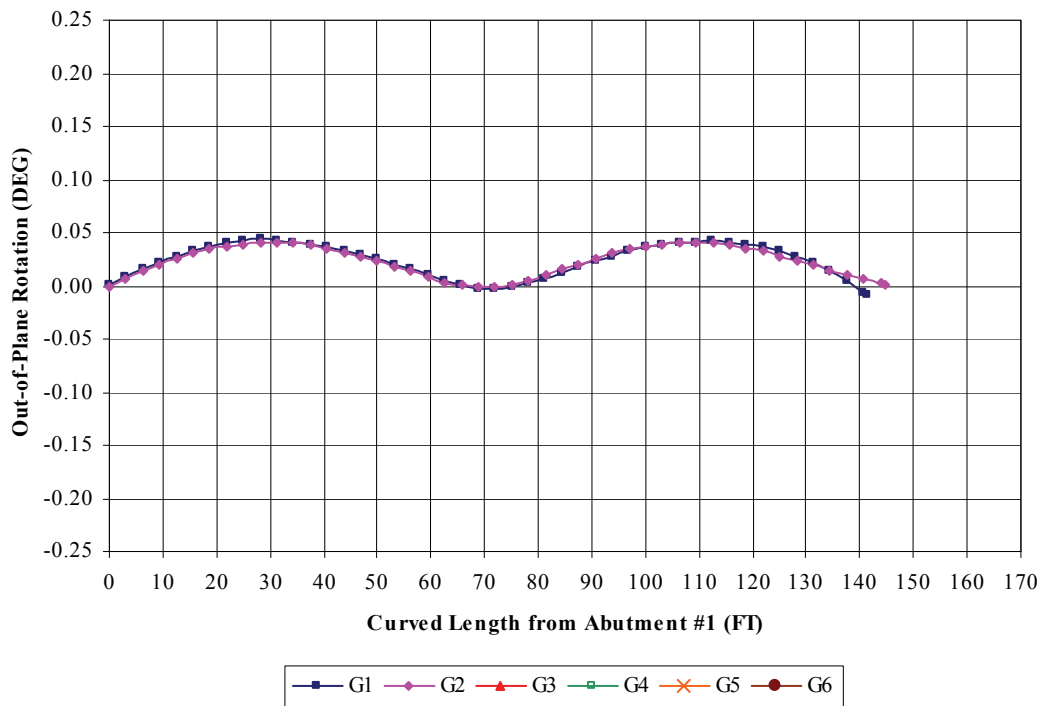


**Figure B.24** Construction Stage 2e1 – Girder Out-of-Plane Rotation

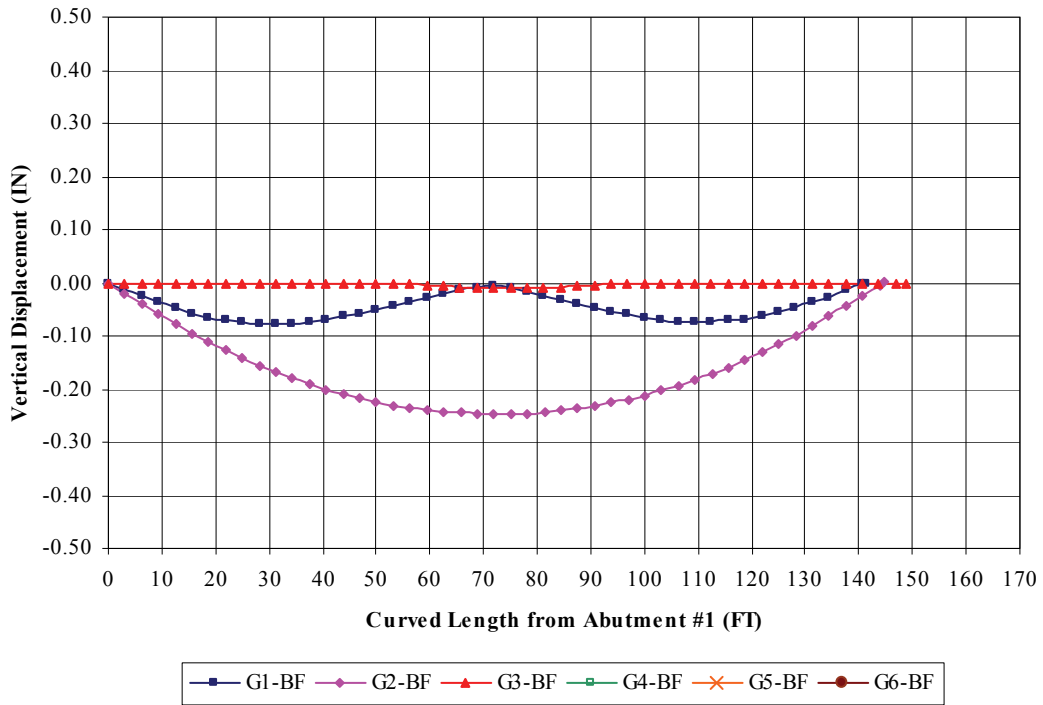


Figure B.25 Construction Stage 3 – Girder Vertical Displacement

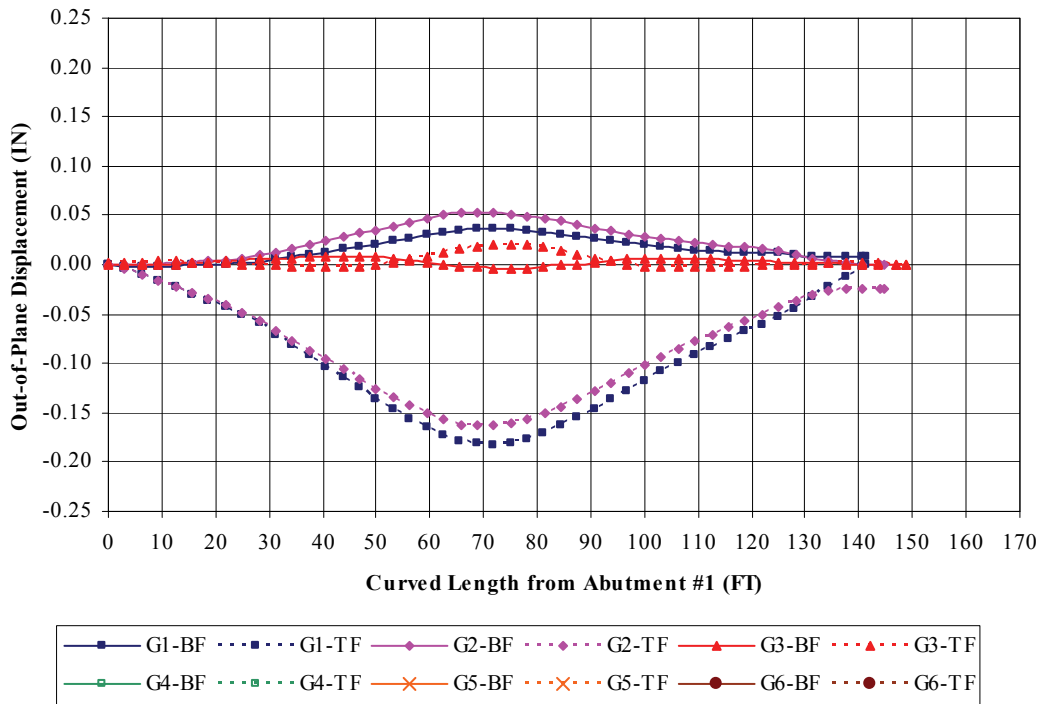


Figure B.26 Construction Stage 3 – Girder Lateral Displacement

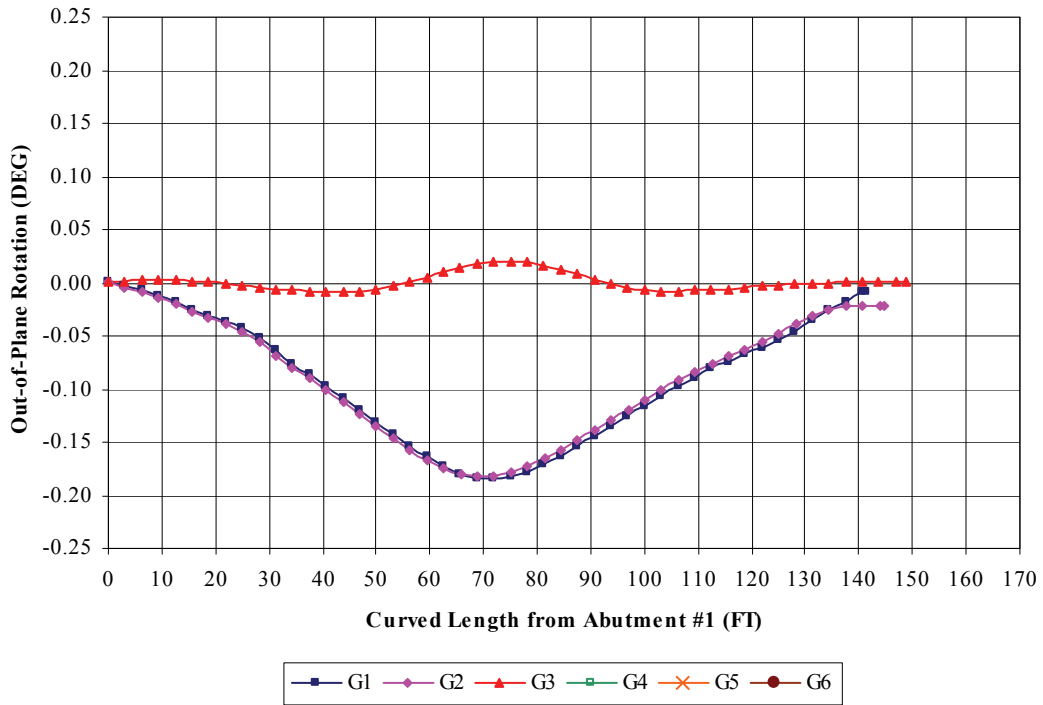


Figure B.27 Construction Stage 3 – Girder Out-of-Plane Rotation

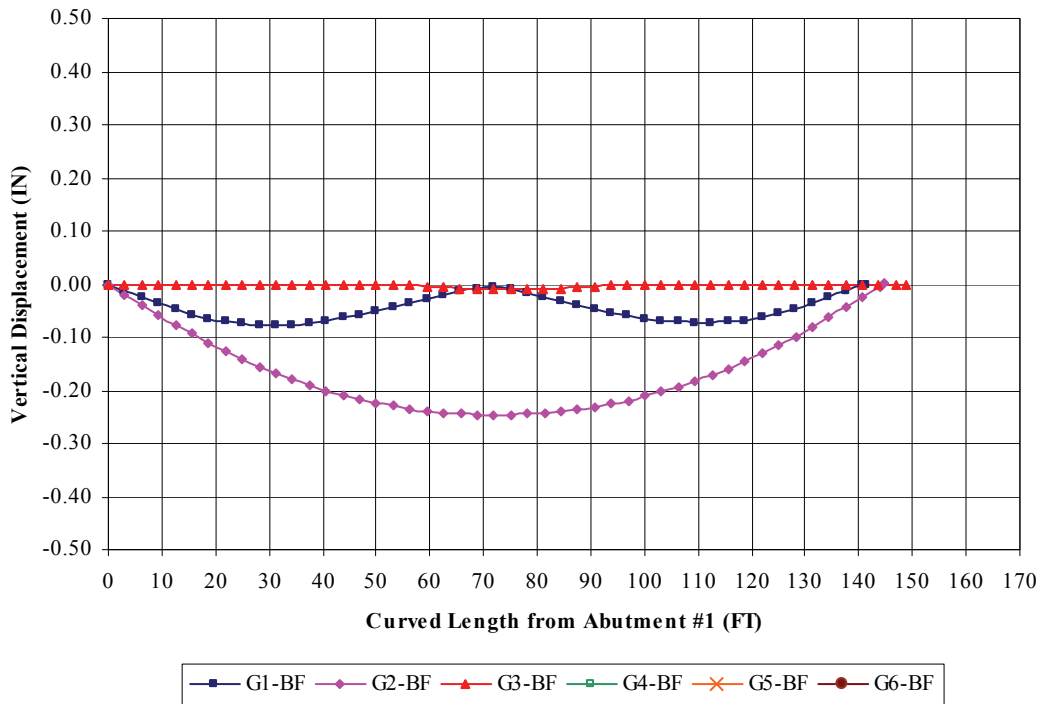


Figure B.28 Construction Stage 3a – Girder Vertical Displacement

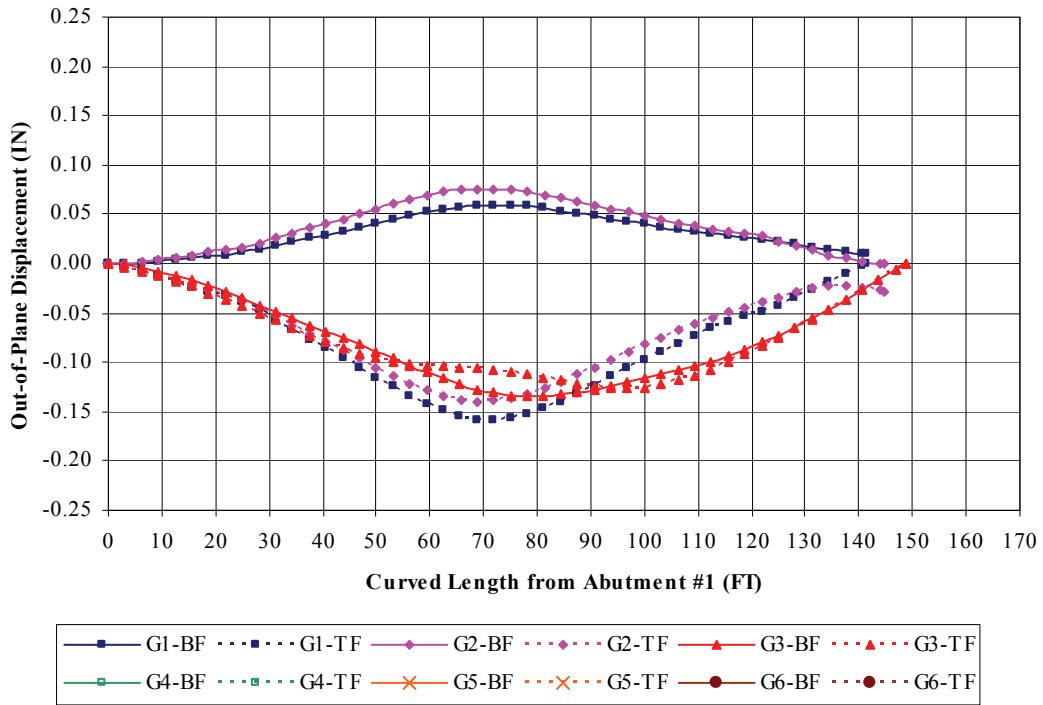


Figure B.29 Construction Stage 3a – Girder Lateral Displacement

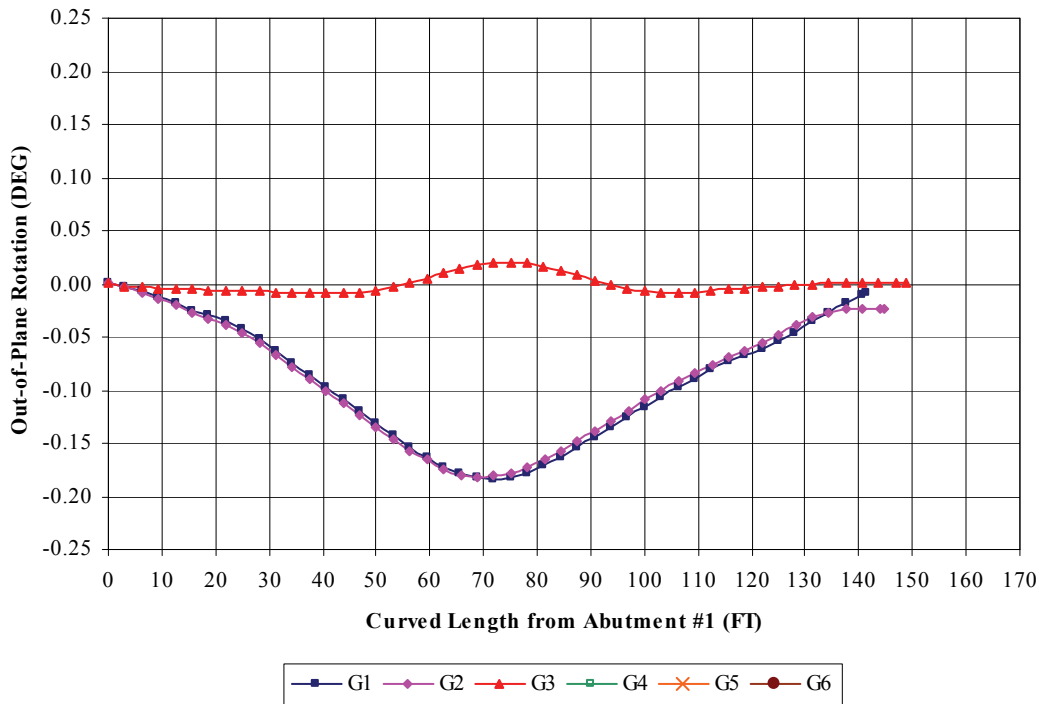
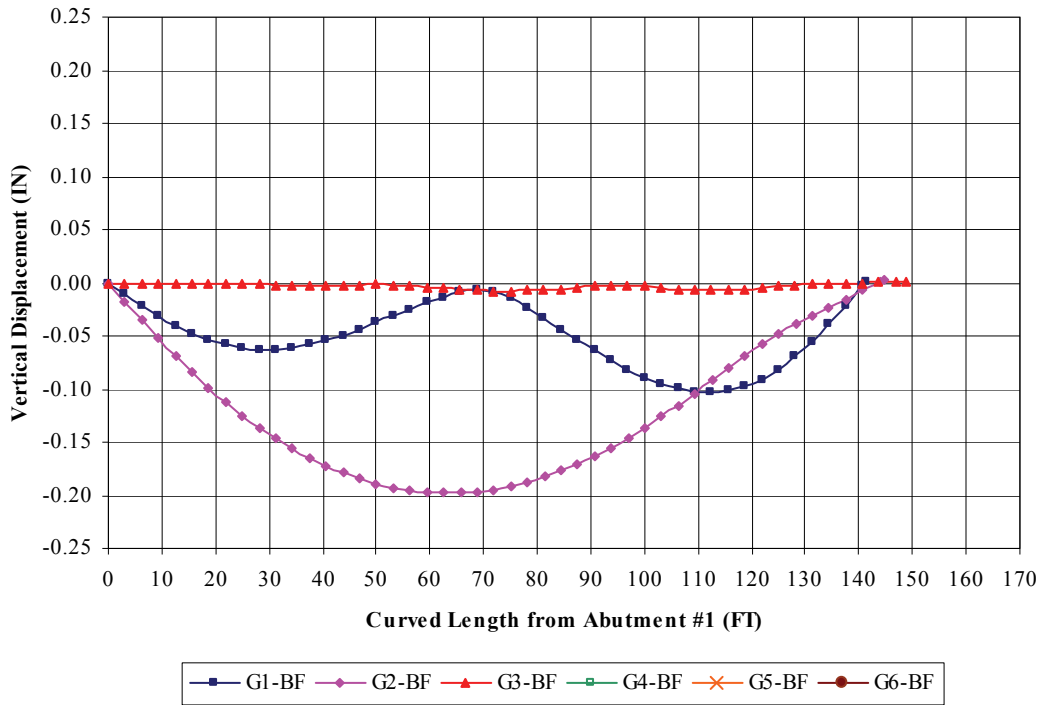
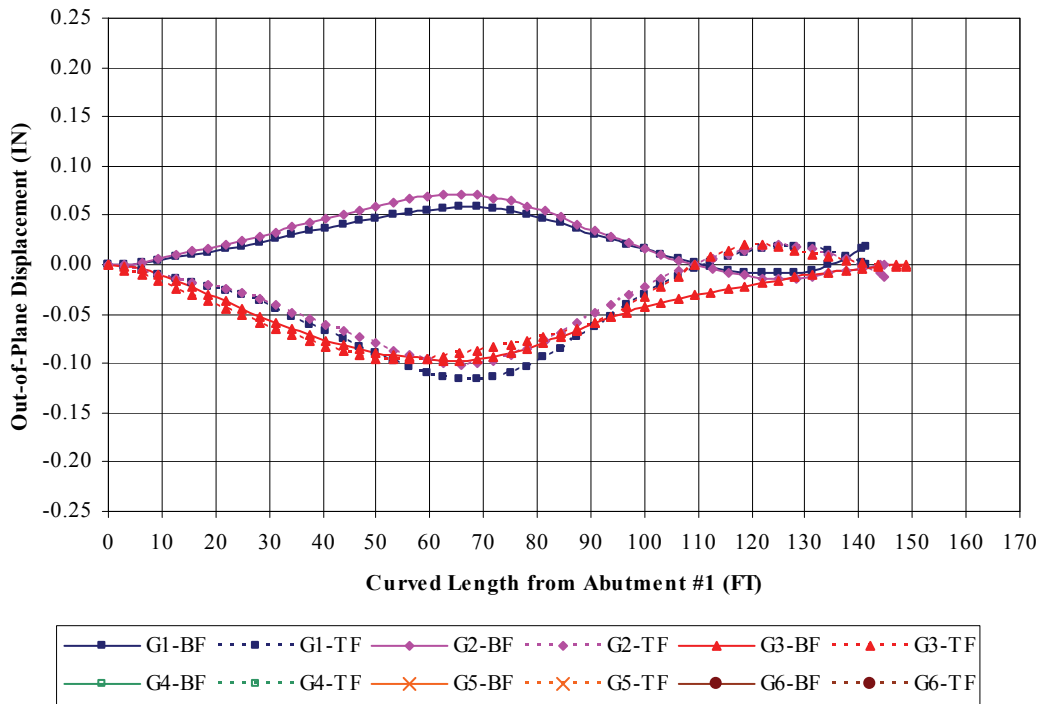


Figure B.30 Construction Stage 3a – Girder Out-of-Plane Rotation



**Figure B.31** Construction Stage 3b – Girder Vertical Displacement



**Figure B.32** Construction Stage 3b – Girder Lateral Displacement

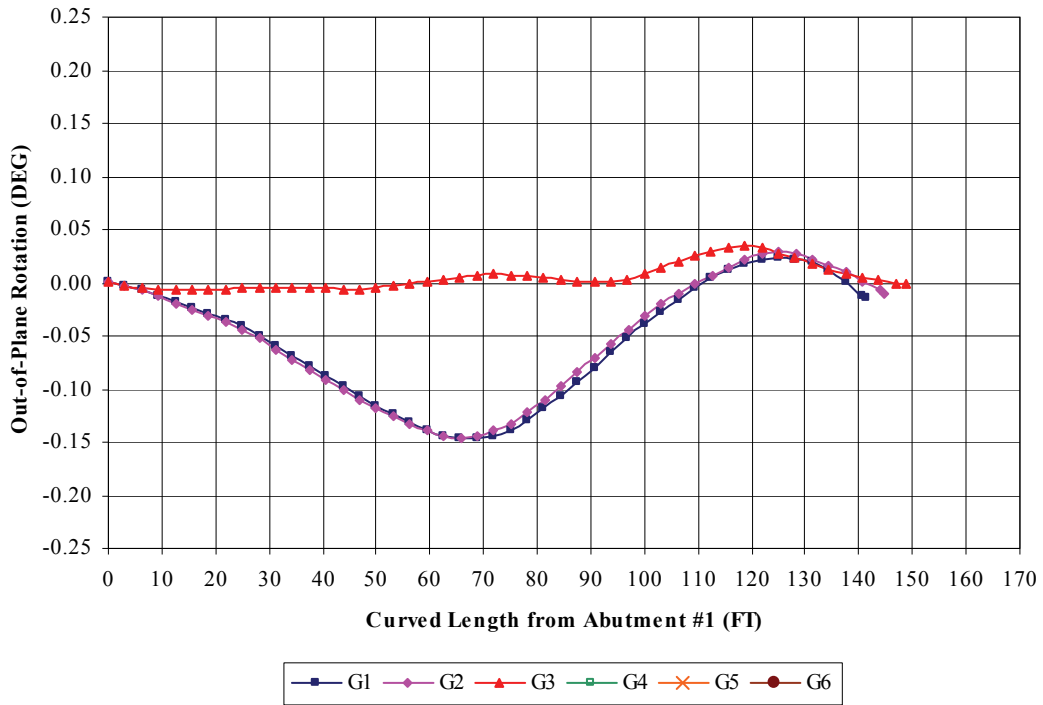


**Figure B.33** Construction Stage 3b – Girder Out-of-Plane Rotation

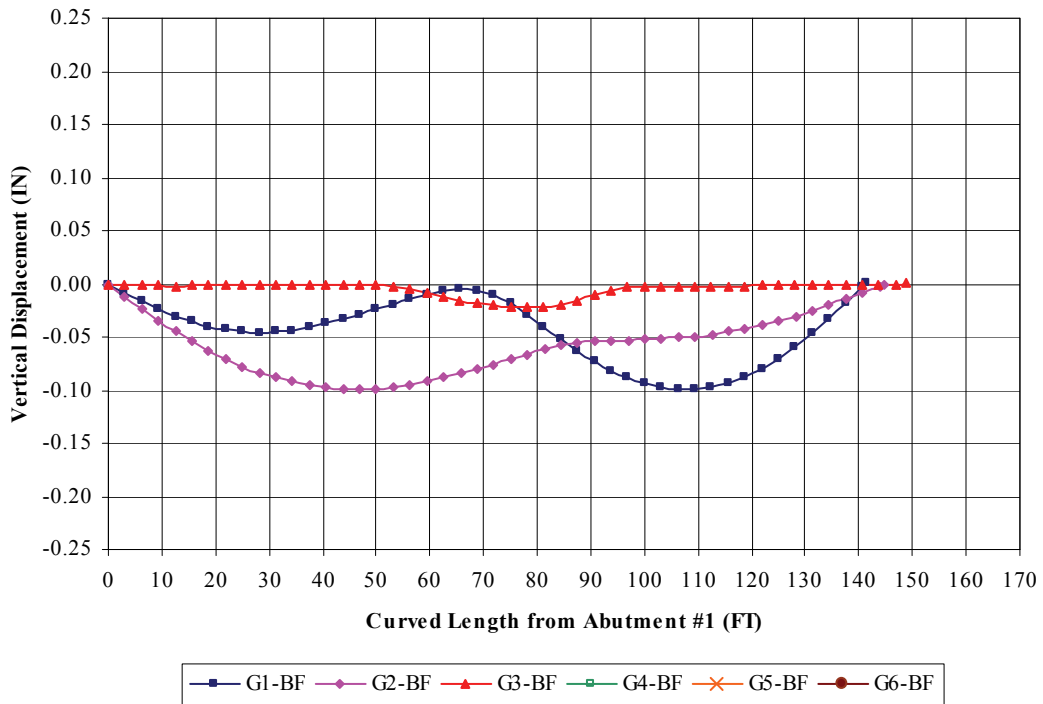


**Figure B.34** Construction Stage 3c – Girder Vertical Displacement

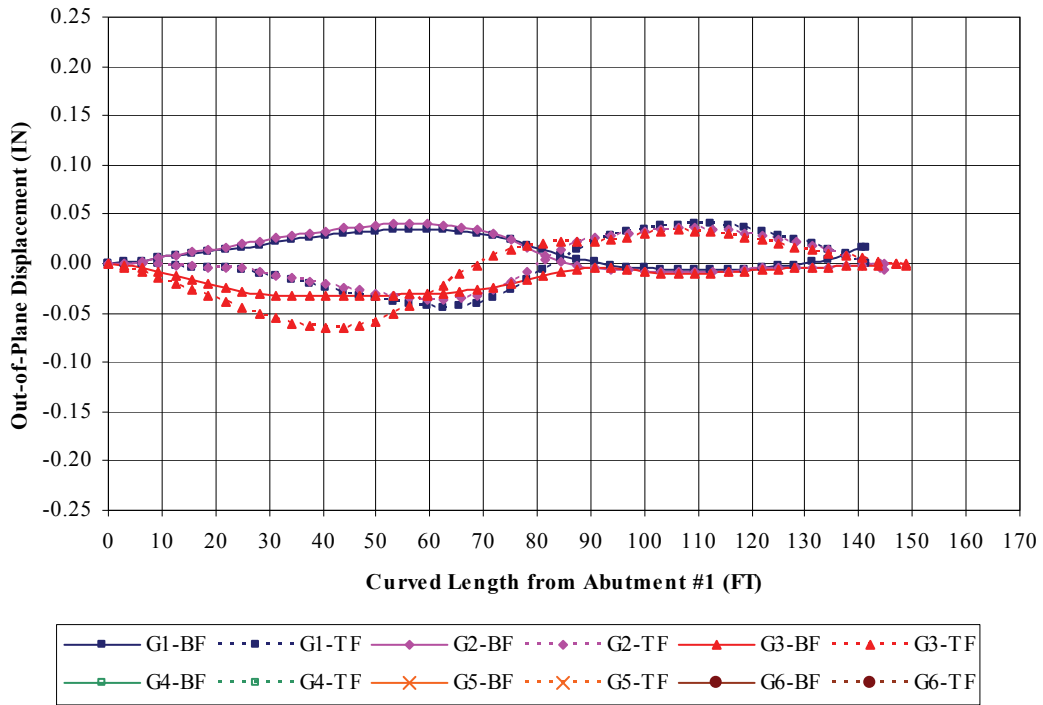


**Figure B.35** Construction Stage 3c – Girder Lateral Displacement

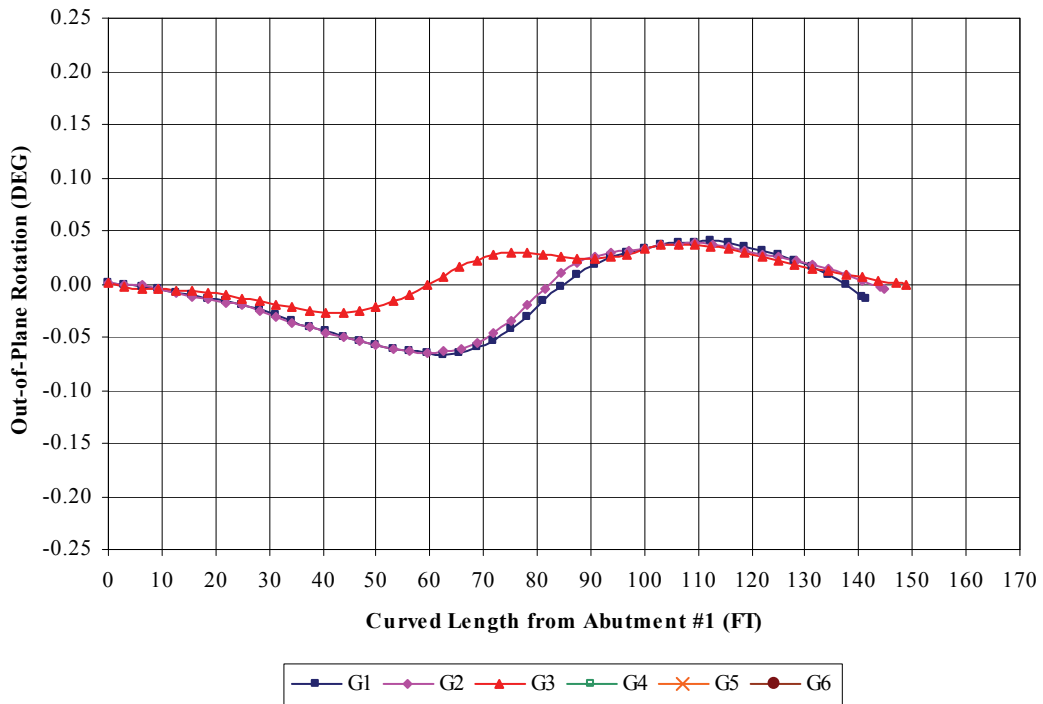


**Figure B.36** Construction Stage 3c – Girder Out-of-Plane Rotation

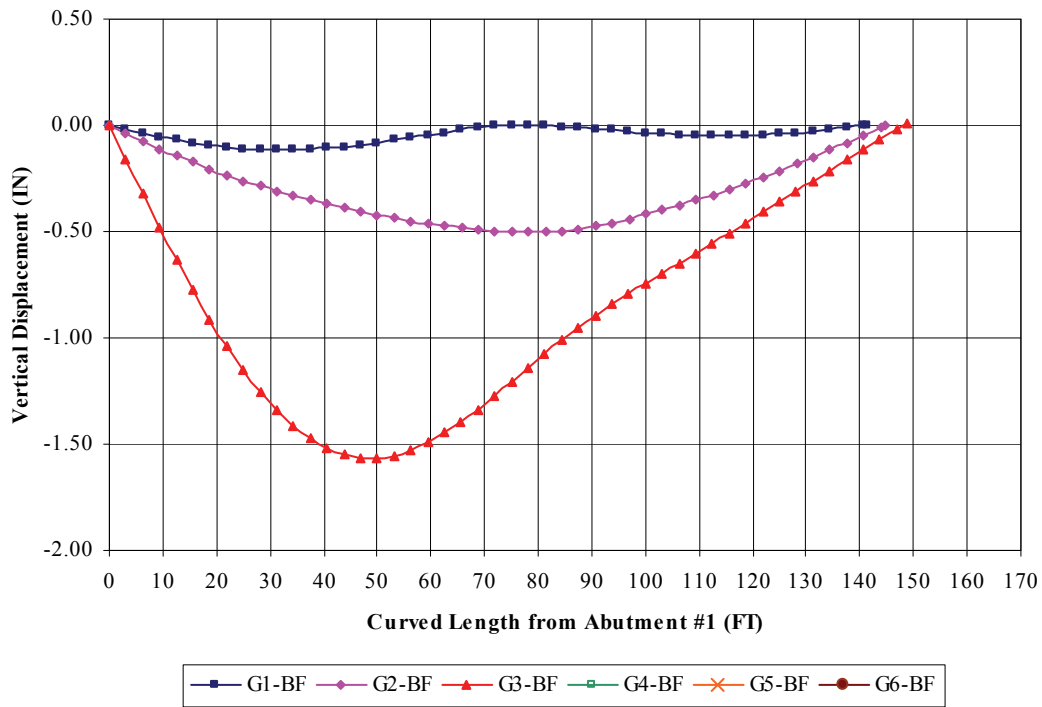


**Figure B.37** Construction Stage 3c1 – Girder Vertical Displacement

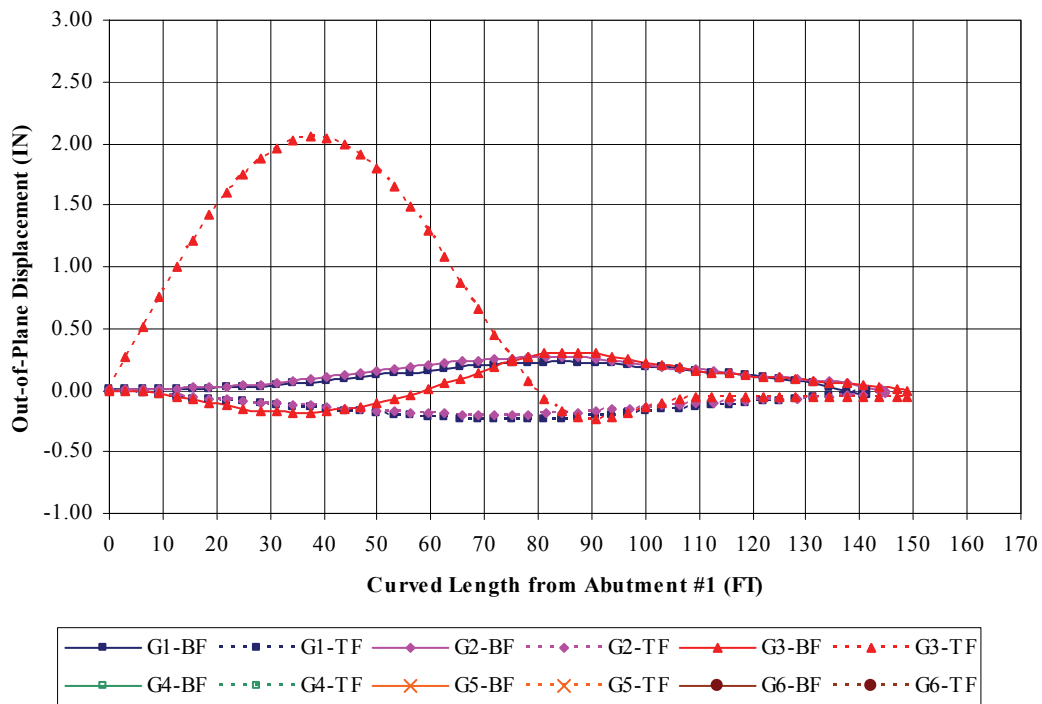


**Figure B.38** Construction Stage 3c1 – Girder Lateral Displacement

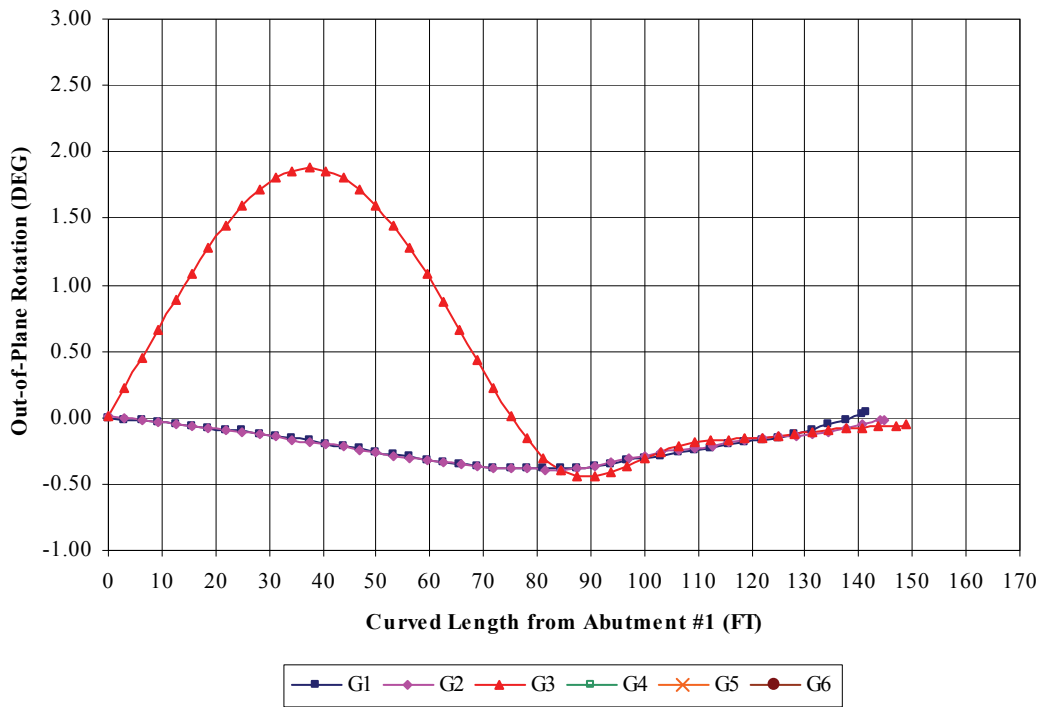


Figure B.39 Construction Stage 3c1 – Girder Out-of-Plane Rotation

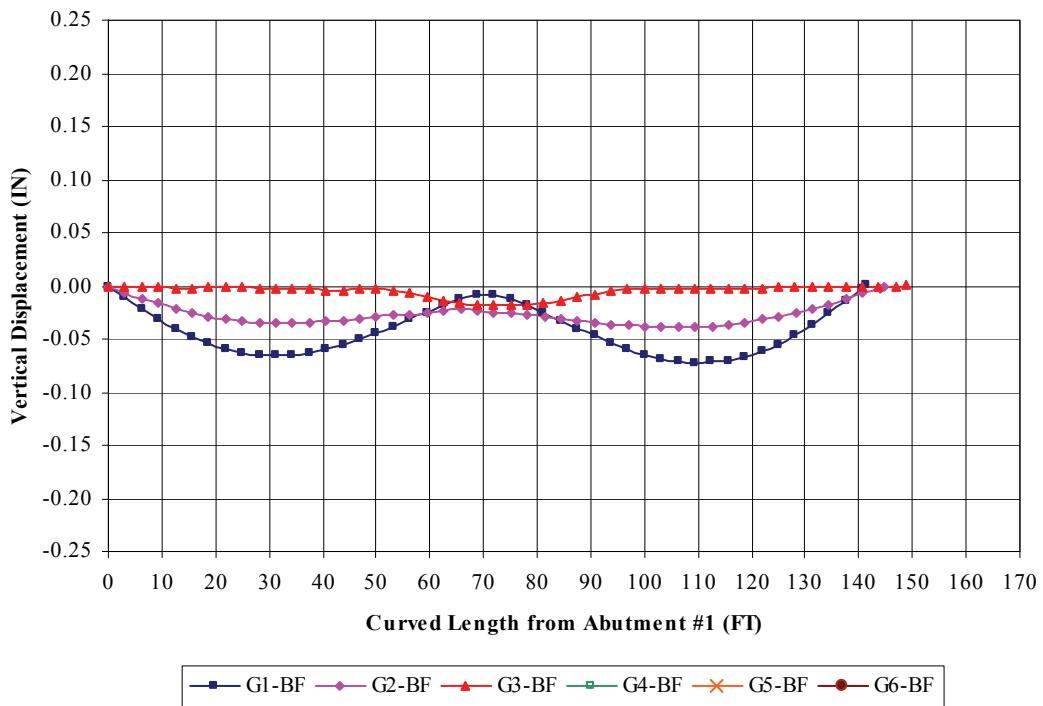


Figure B.40 Construction Stage 3d – Girder Vertical Displacement

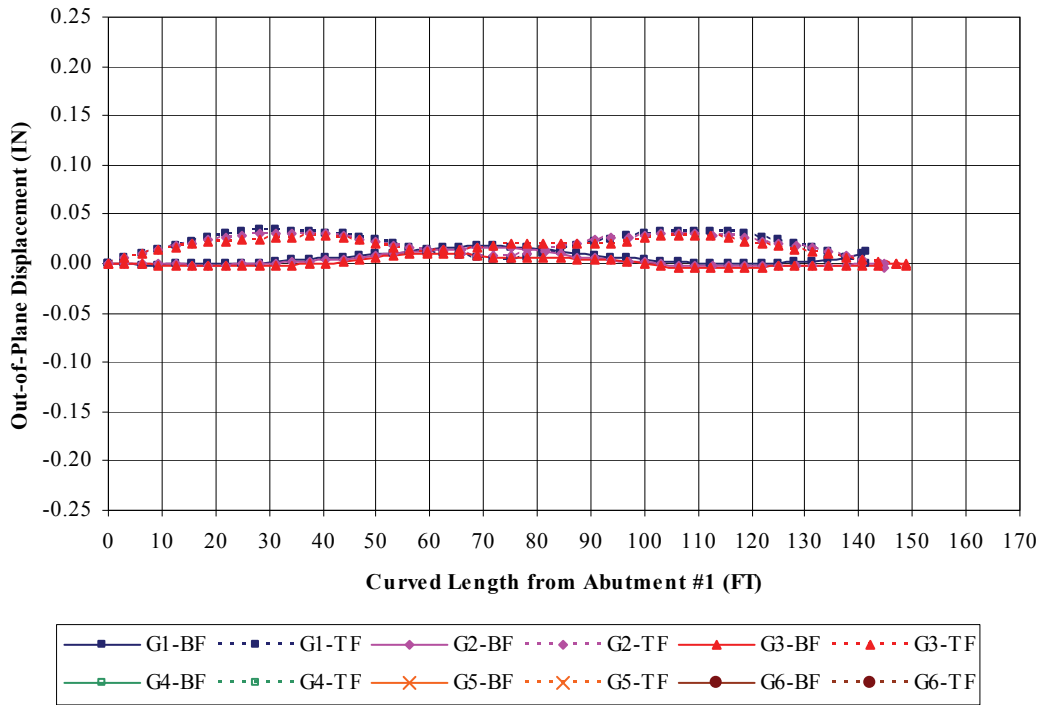


Figure B.41 Construction Stage 3d – Girder Lateral Displacement

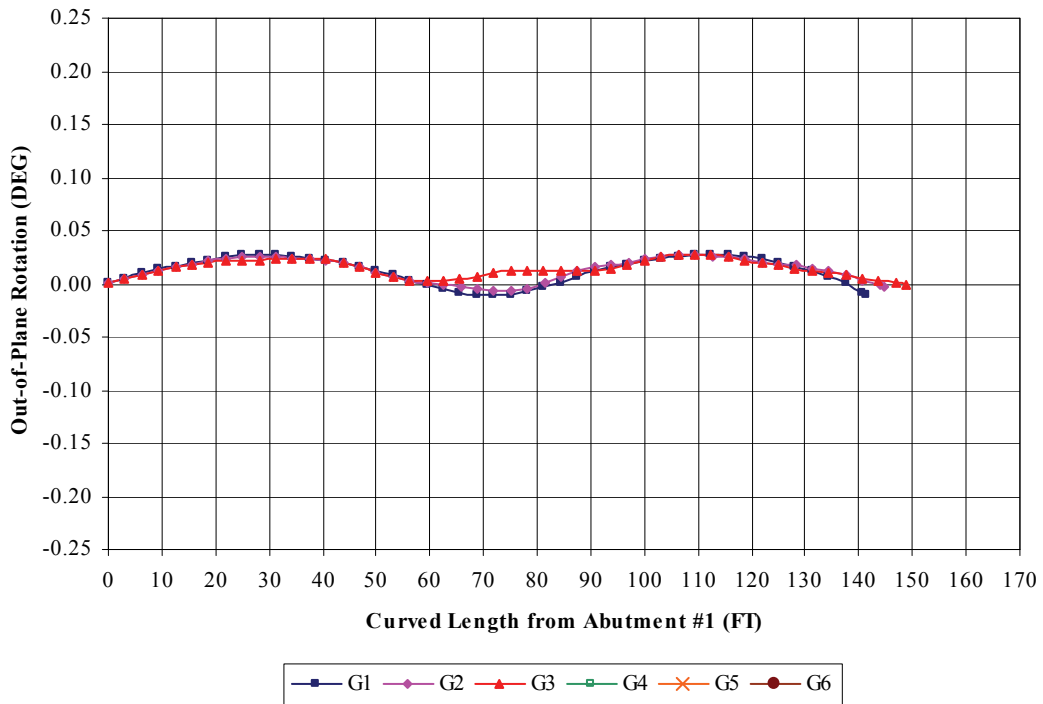


Figure B.42 Construction Stage 3d – Girder Out-of-Plane Rotation

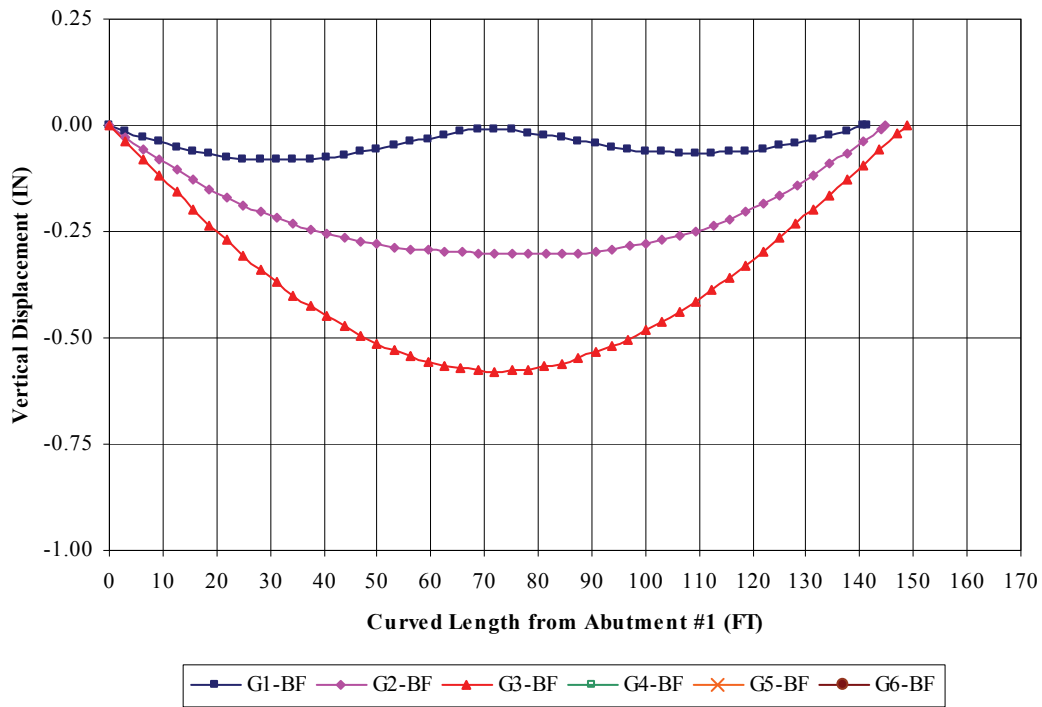


Figure B.43 Construction Stage 3d1 – Girder Vertical Displacement

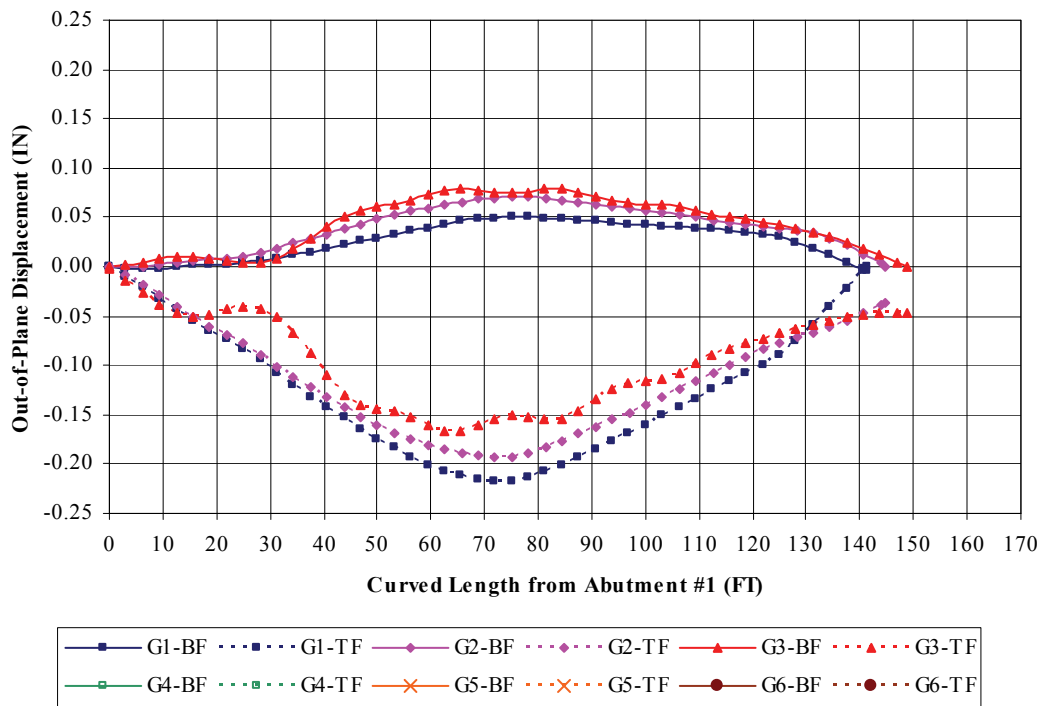


Figure B.44 Construction Stage 3d1 – Girder Lateral Displacement

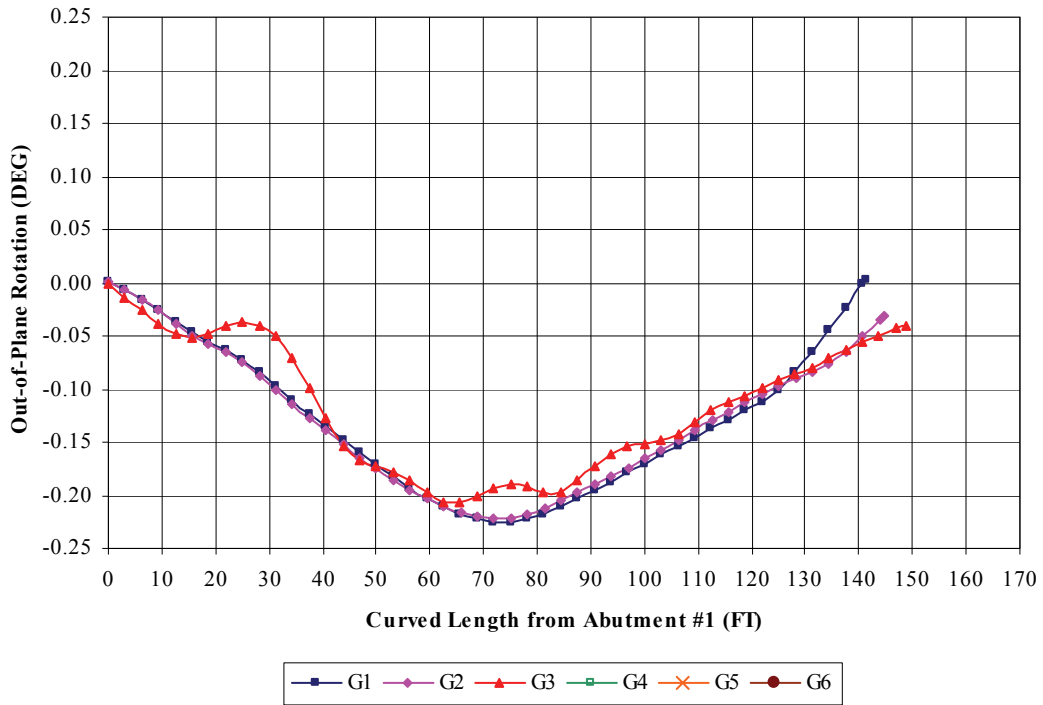


Figure B.45 Construction Stage 3d1 – Girder Out-of-Plane Rotation

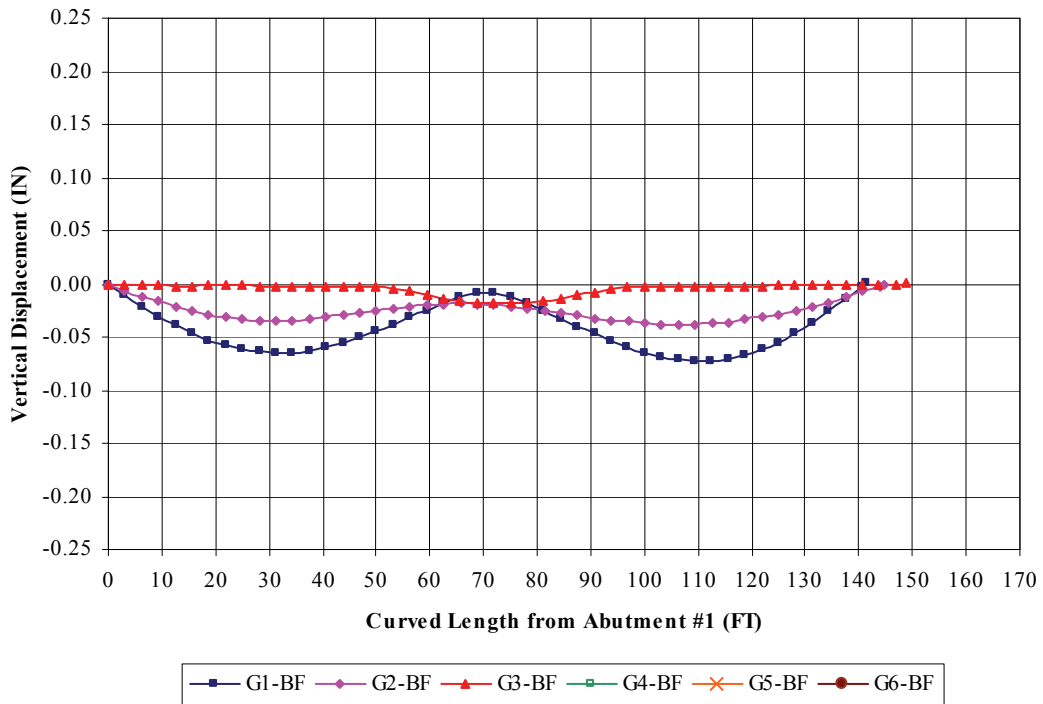
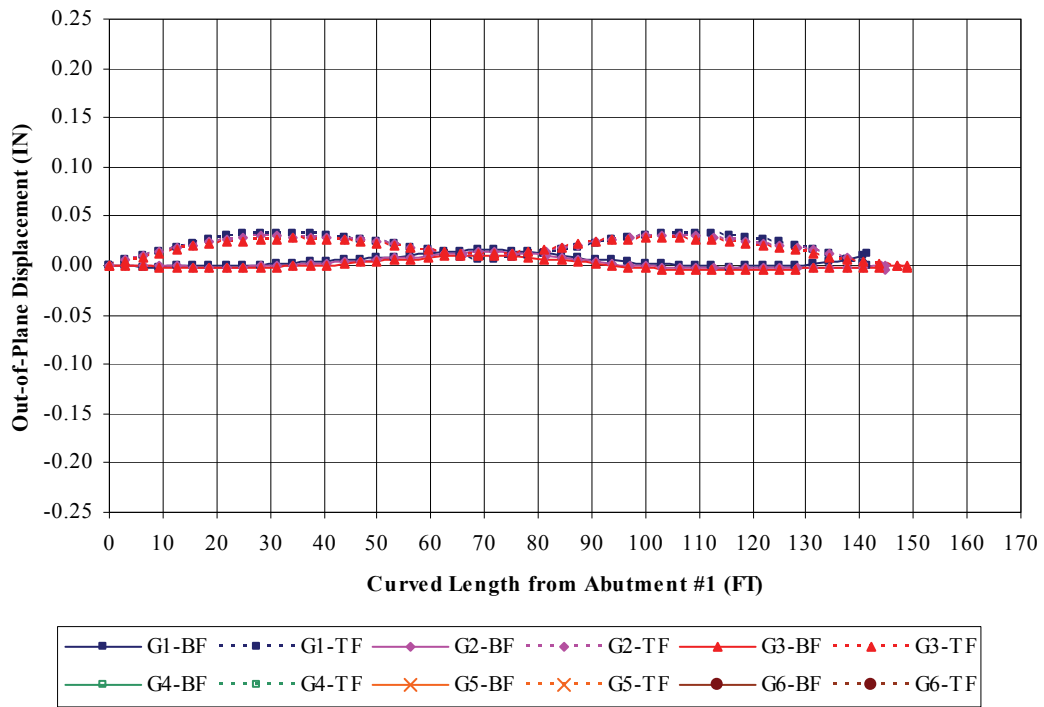
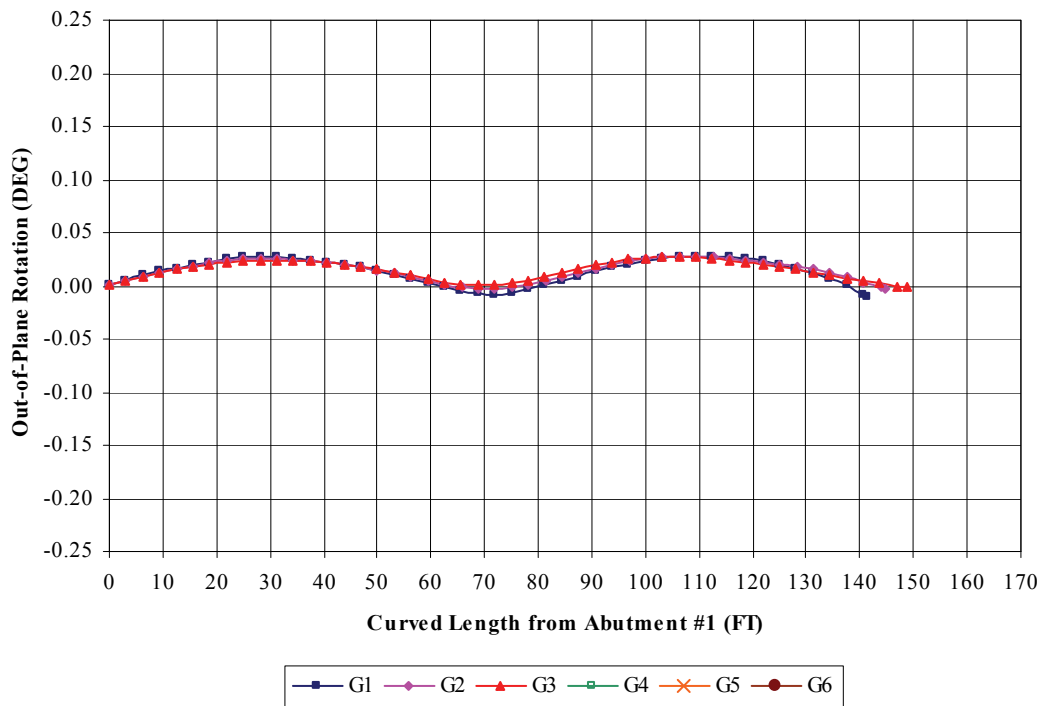


Figure B.46 Construction Stage 3e – Girder Vertical Displacement



**Figure B.47** Construction Stage 3e – Girder Lateral Displacement



**Figure B.48** Construction Stage 3e – Girder Out-of-Plane Rotation

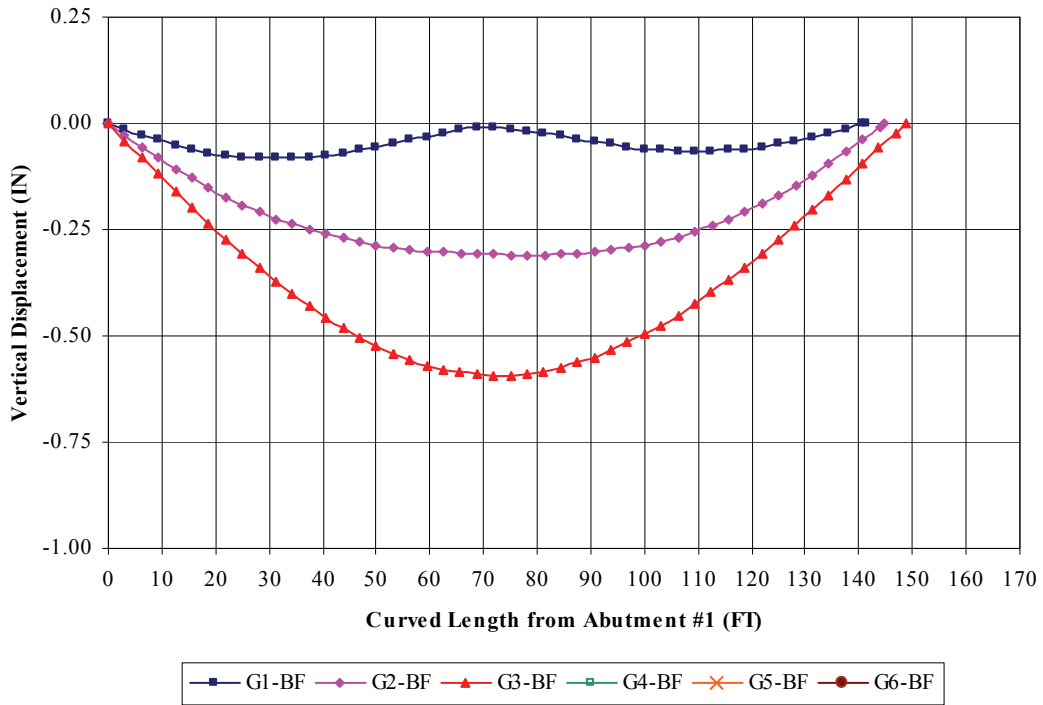


Figure B.49 Construction Stage 3e1 – Girder Vertical Displacement

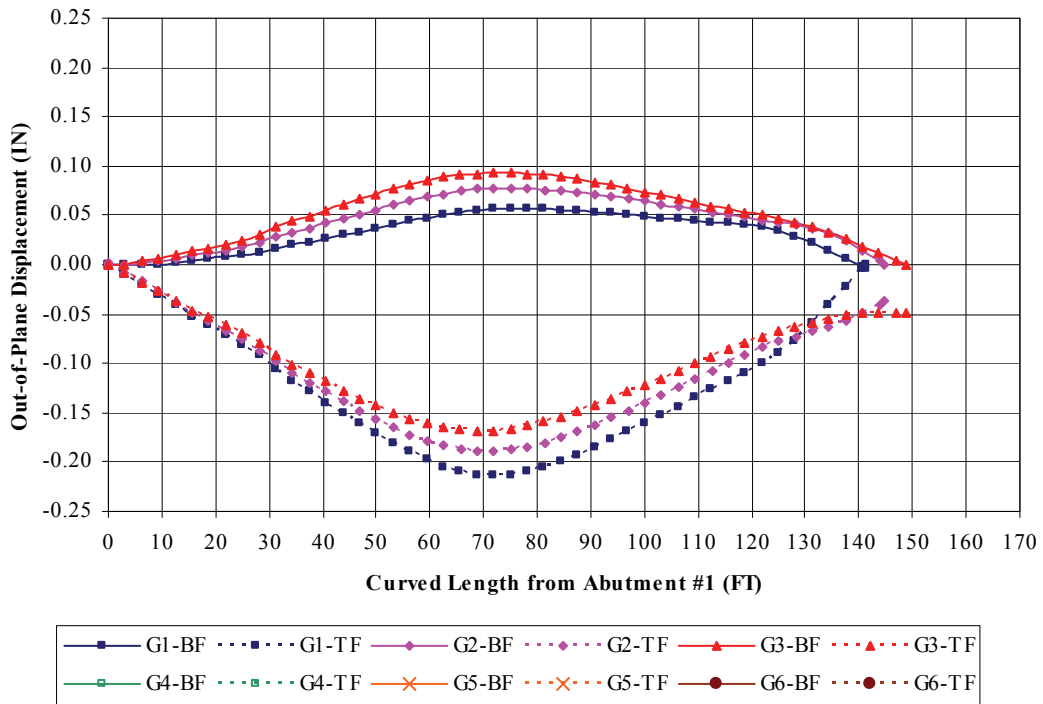


Figure B.50 Construction Stage 3e1 – Girder Lateral Displacement

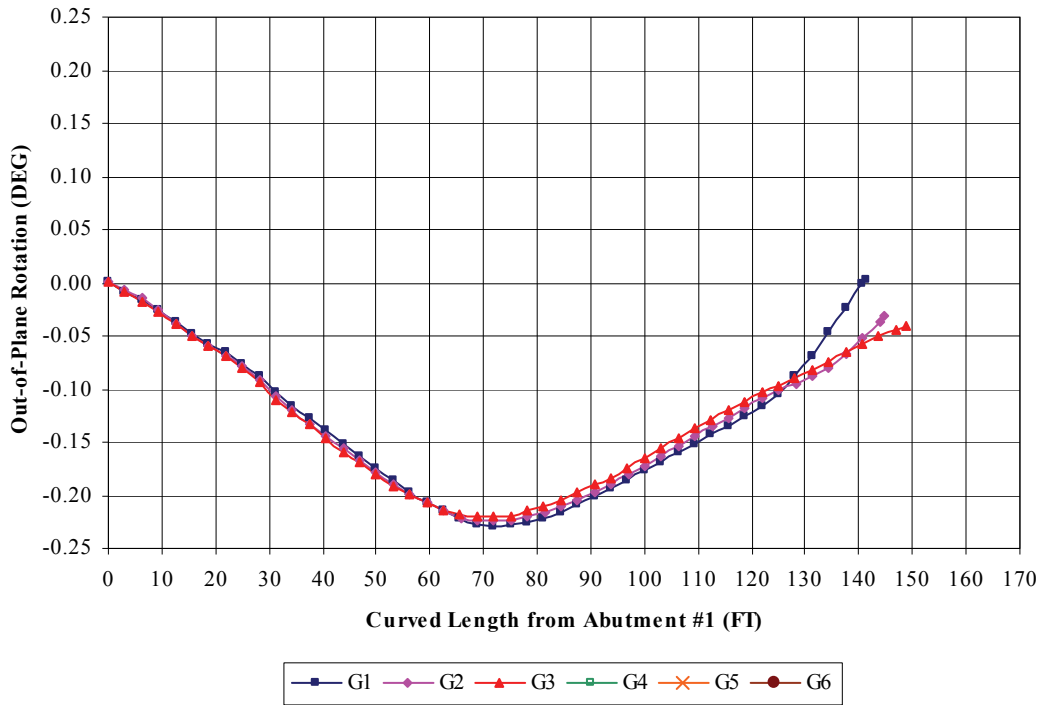


Figure B.51 Construction Stage 3e1 – Girder Out-of-Plane Rotation

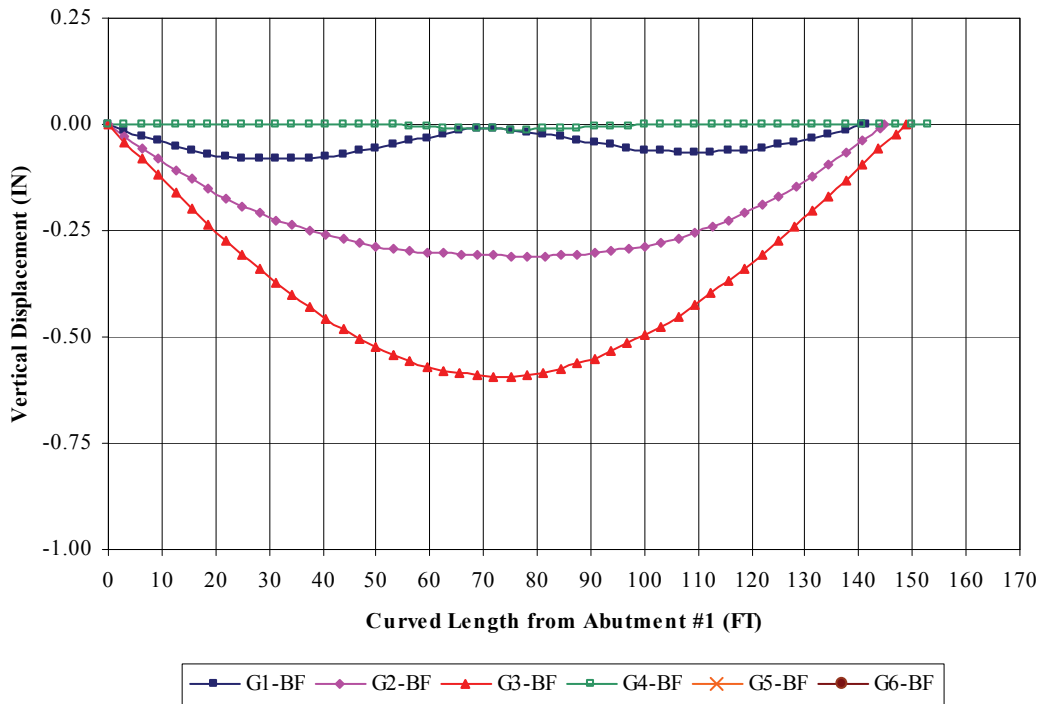


Figure B.52 Construction Stage 4 – Girder Vertical Displacement

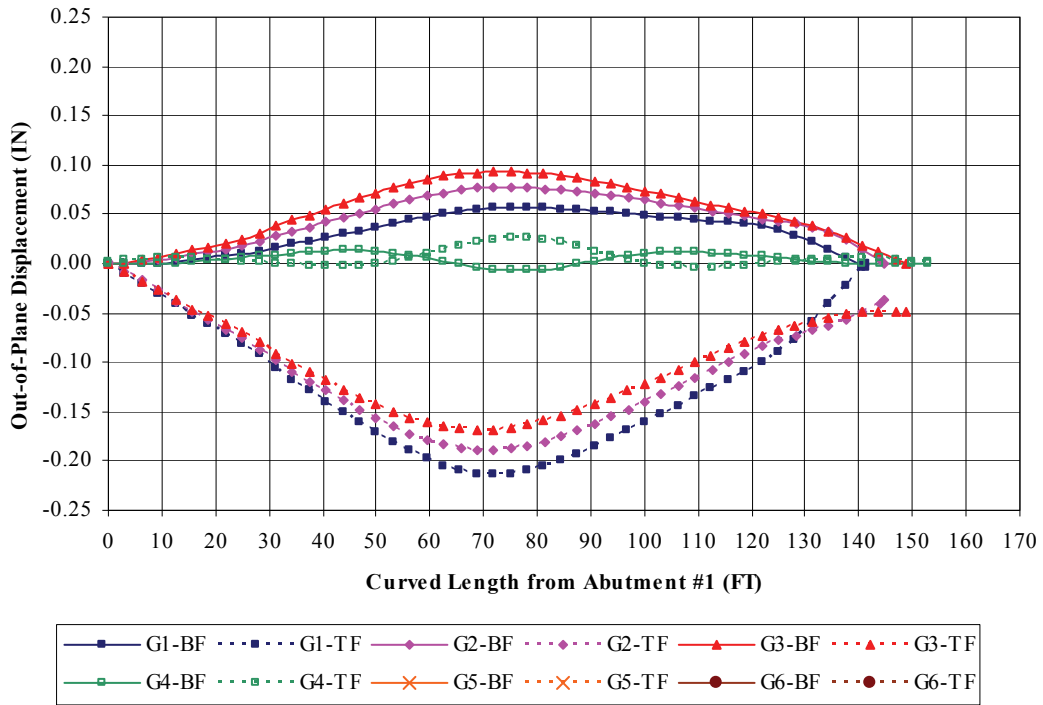


Figure B.53 Construction Stage 4 – Girder Lateral Displacement

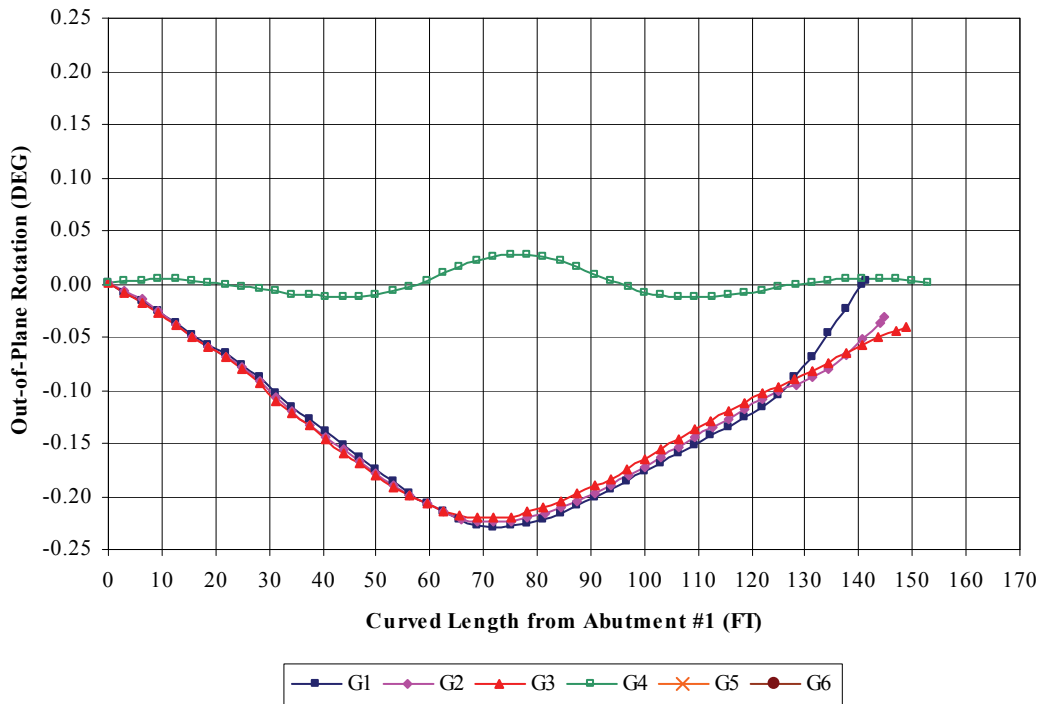


Figure B.54 Construction Stage 4 – Girder Out-of-Plane Rotation

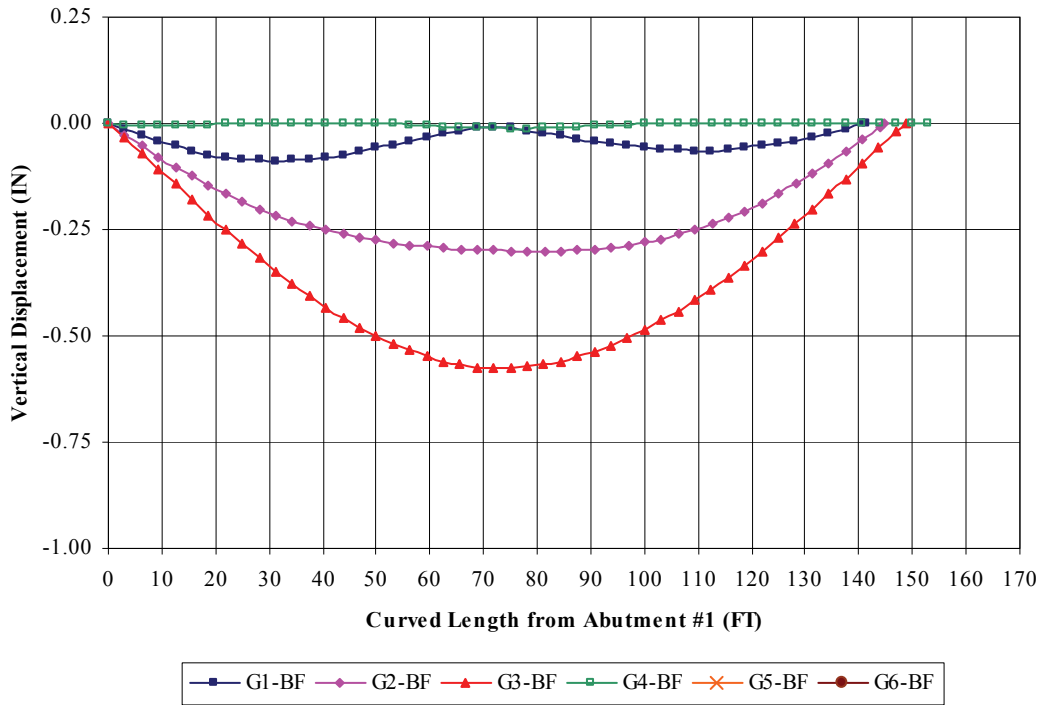


Figure B.55 Construction Stage 4a – Girder Vertical Displacement

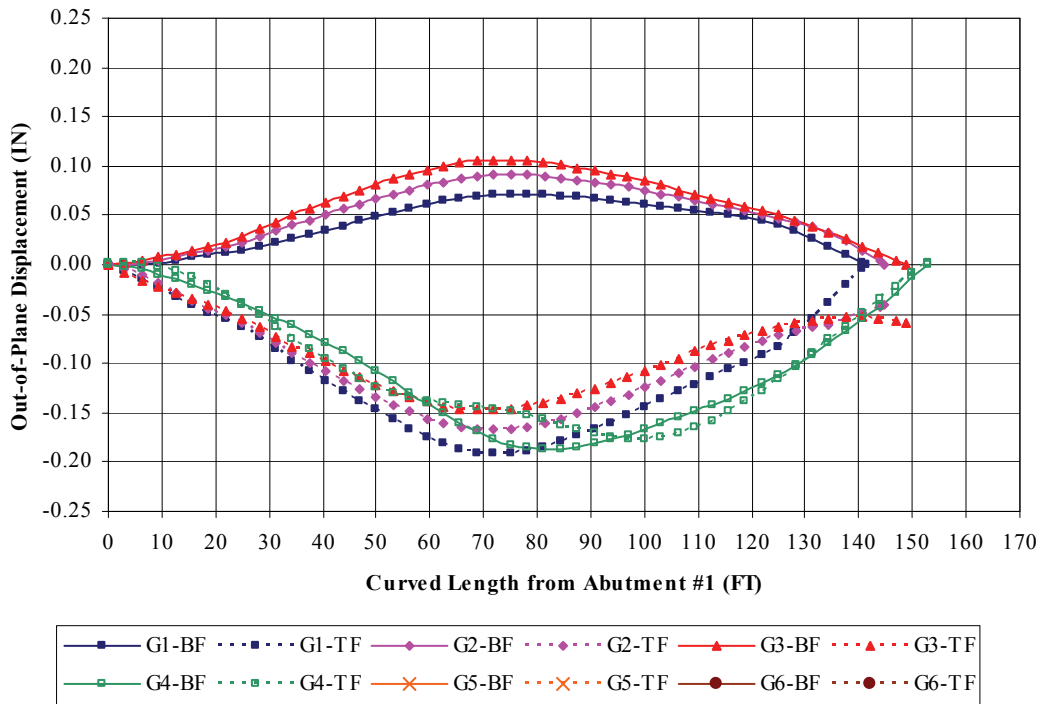
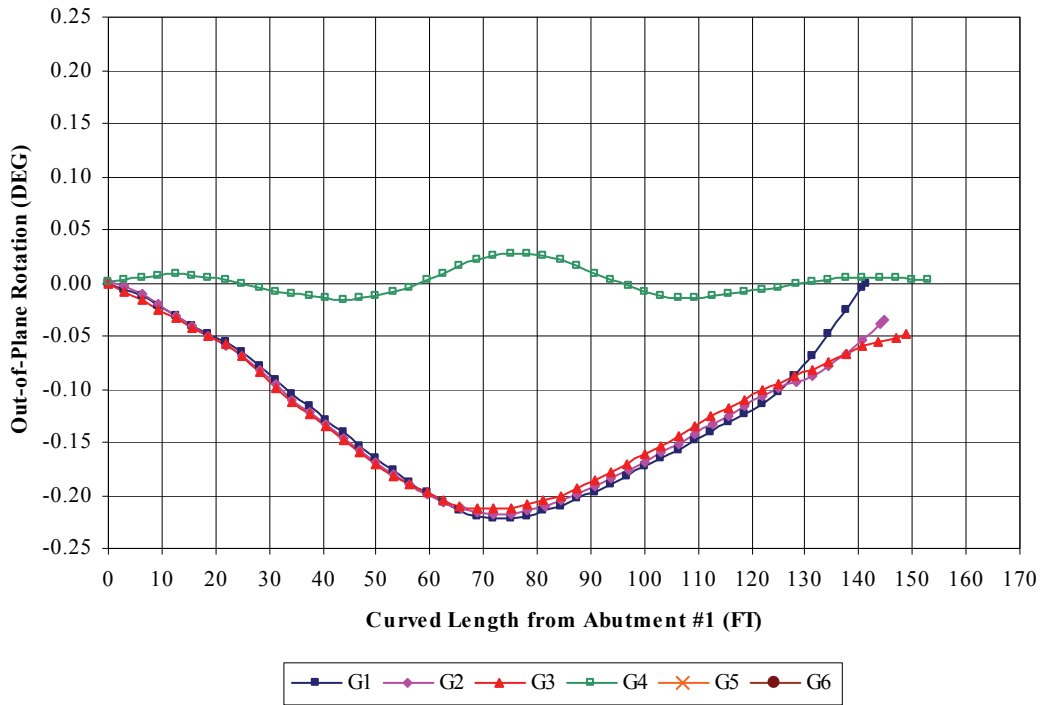
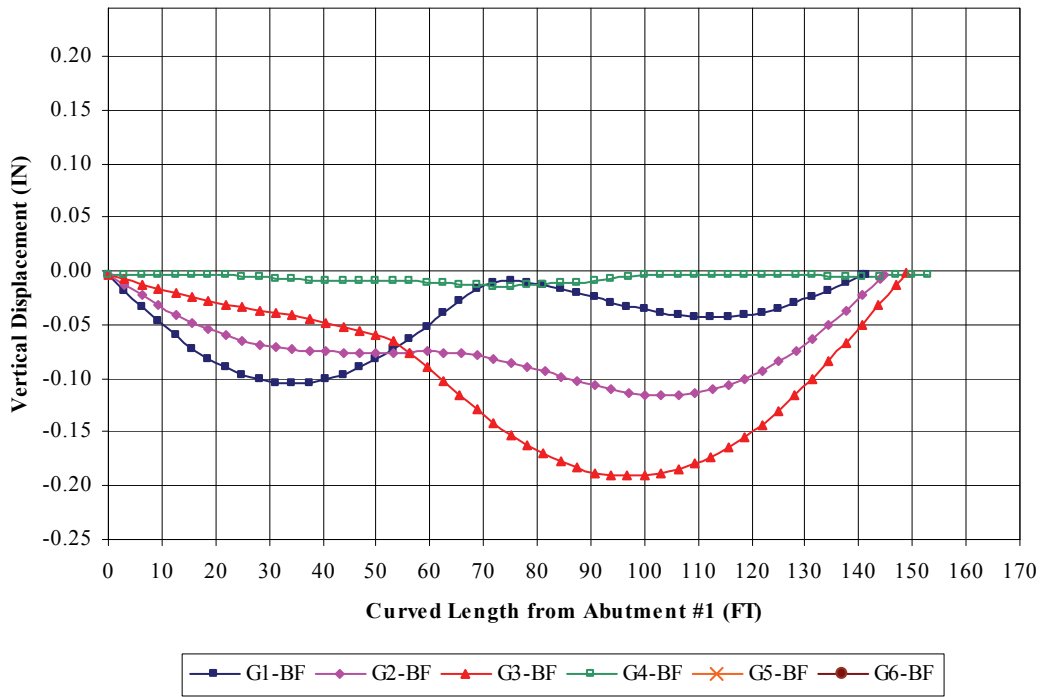


Figure B.56 Construction Stage 4a – Girder Lateral Displacement



**Figure B.57** Construction Stage 4a – Girder Out-of-Plane Rotation



**Figure B.58** Construction Stage 4b – Girder Vertical Displacement

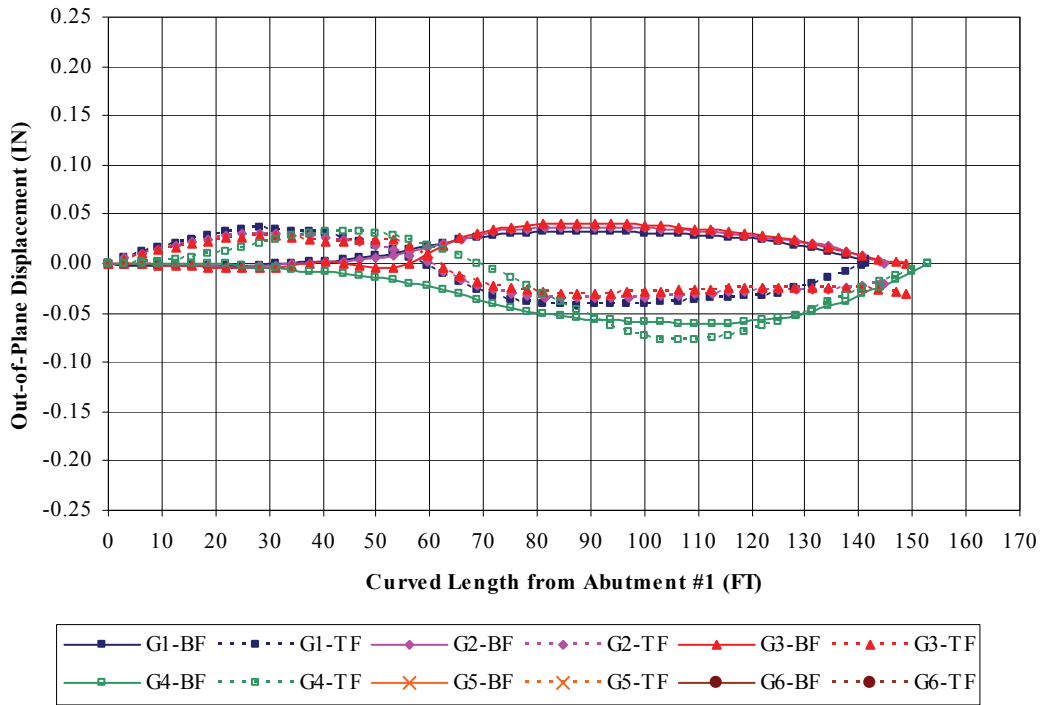


Figure B.59 Construction Stage 4b – Girder Lateral Displacement

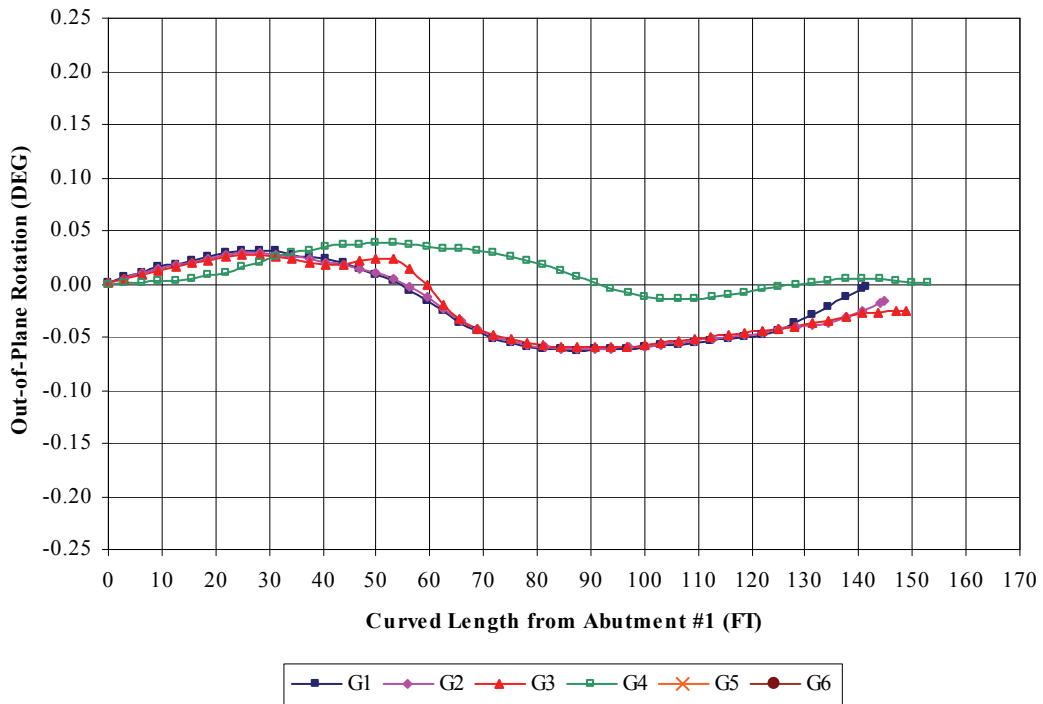


Figure B.60 Construction Stage 4b – Girder Out-of-Plane Rotation

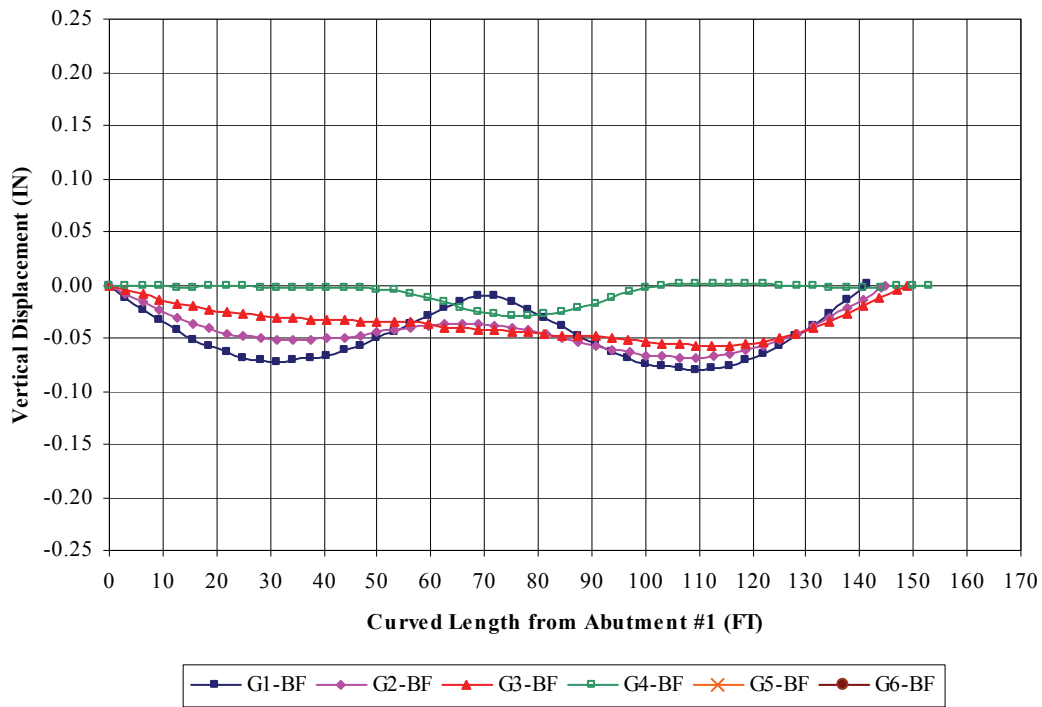


Figure B.61 Construction Stage 4c – Girder Vertical Displacement

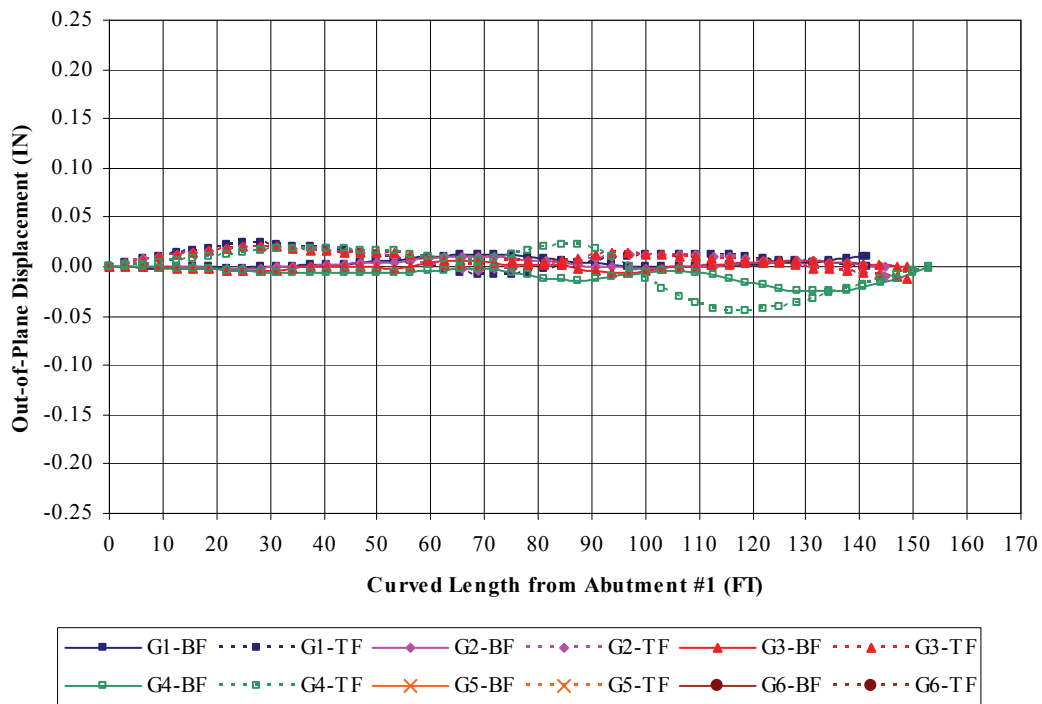
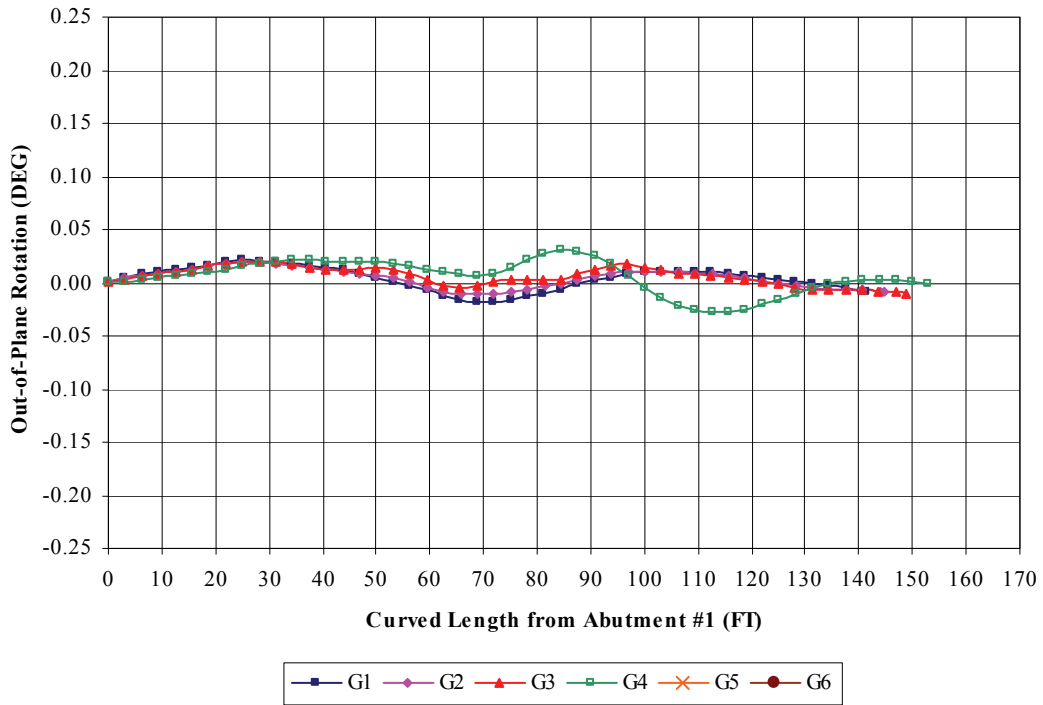
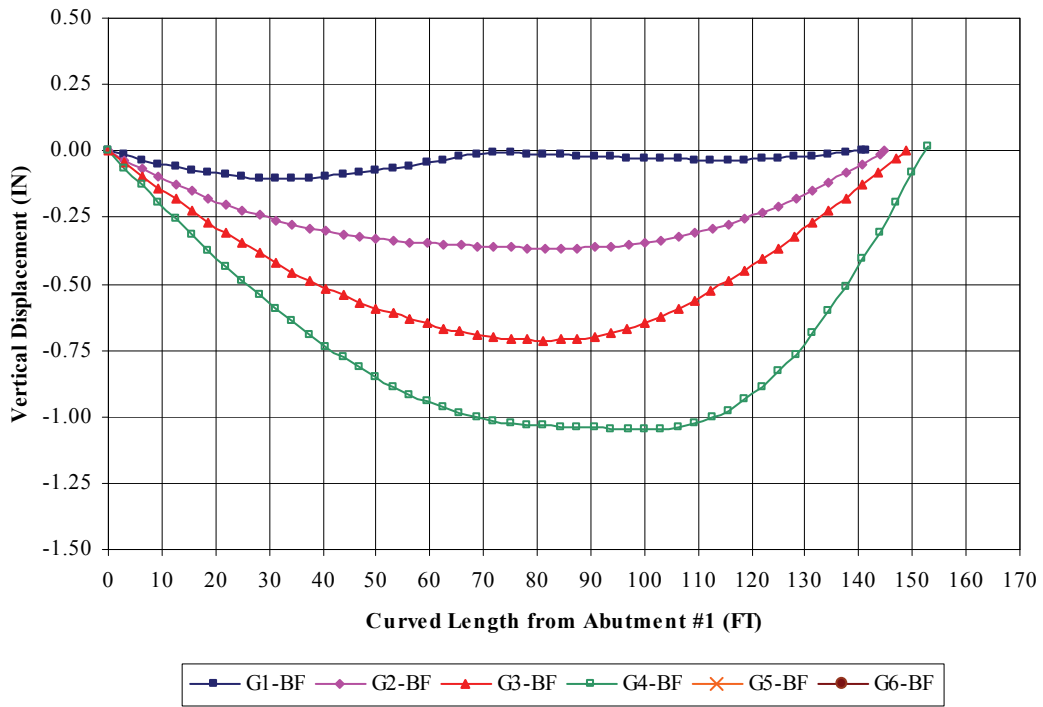


Figure B.62 Construction Stage 4c – Girder Lateral Displacement



**Figure B.63** Construction Stage 4c – Girder Out-of-Plane Rotation



**Figure B.64** Construction Stage 4c1 – Girder Vertical Displacement

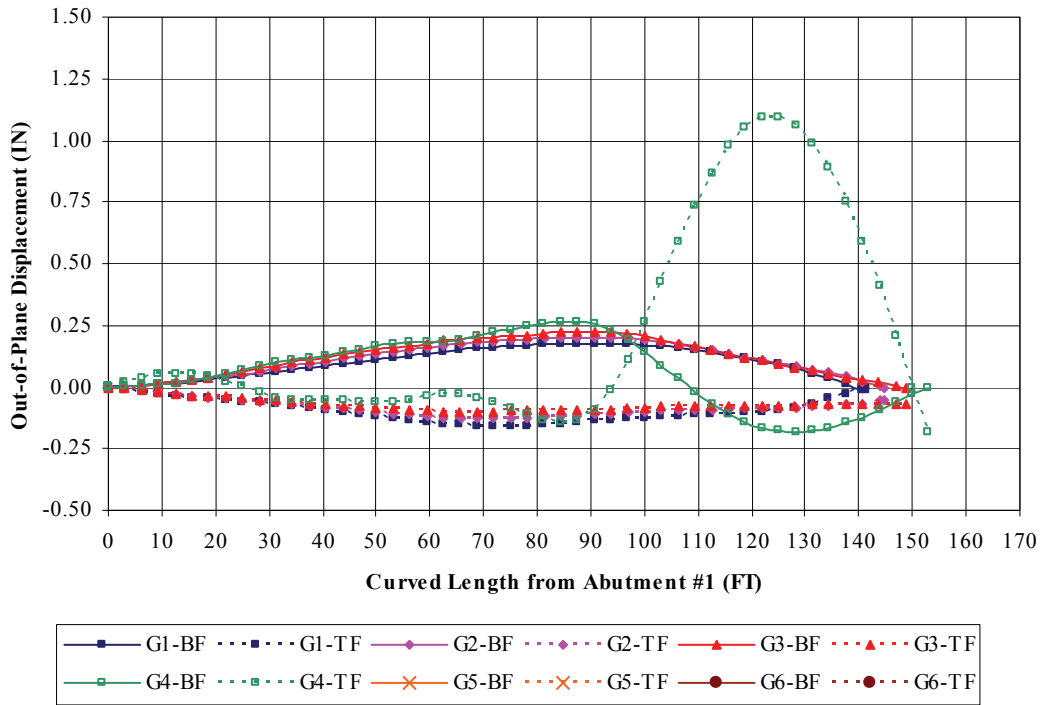


**Figure B.65** Construction Stage 4c1 – Girder Lateral Displacement

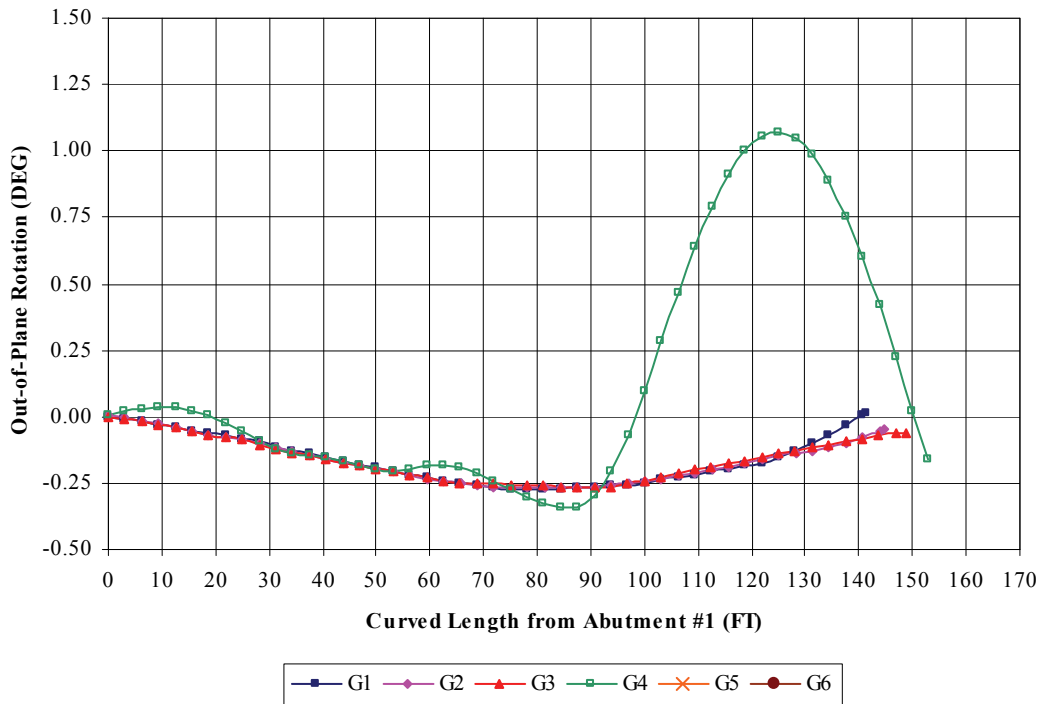


**Figure B.66** Construction Stage 4c1 – Girder Out-of-Plane Rotation

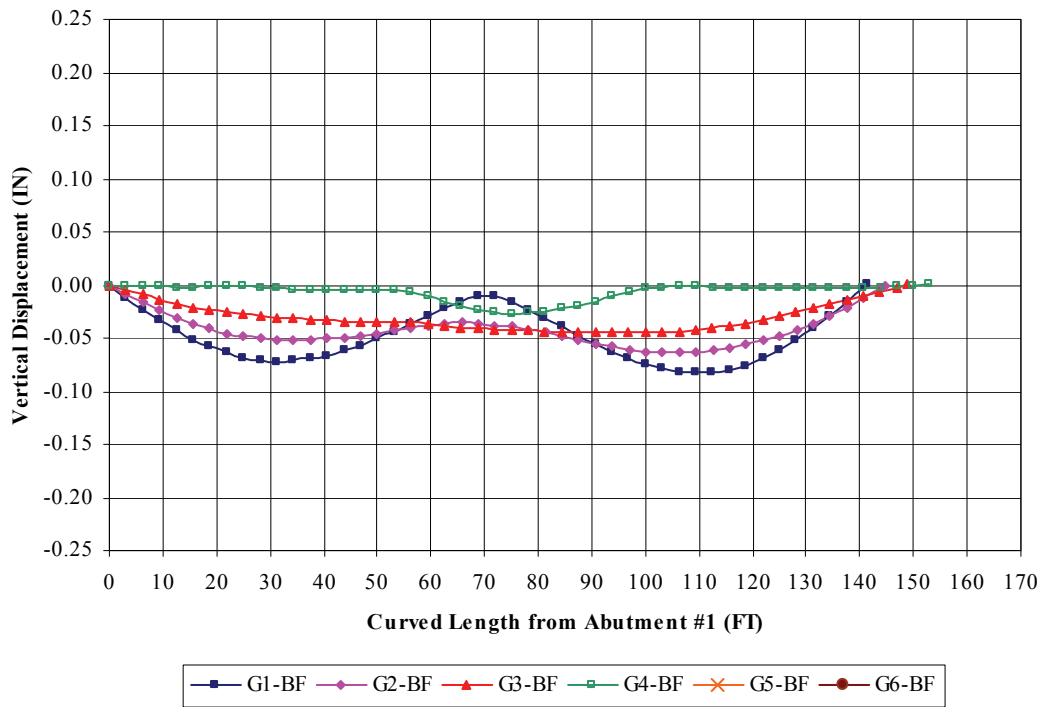


Figure B.67 Construction Stage 4d – Girder Vertical Displacement

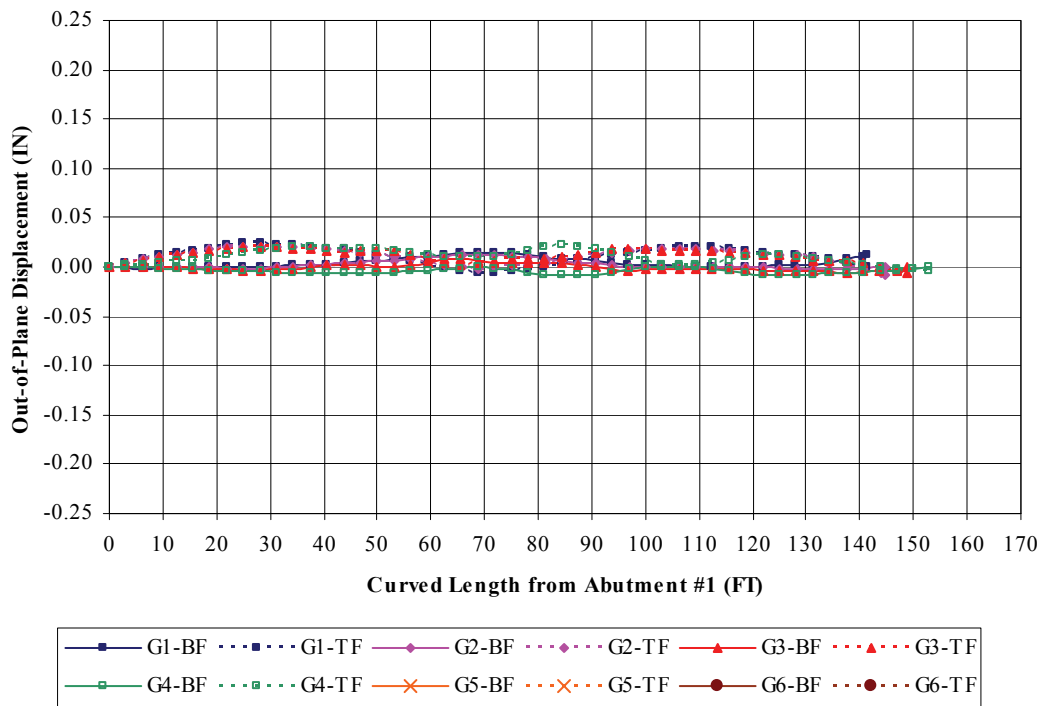
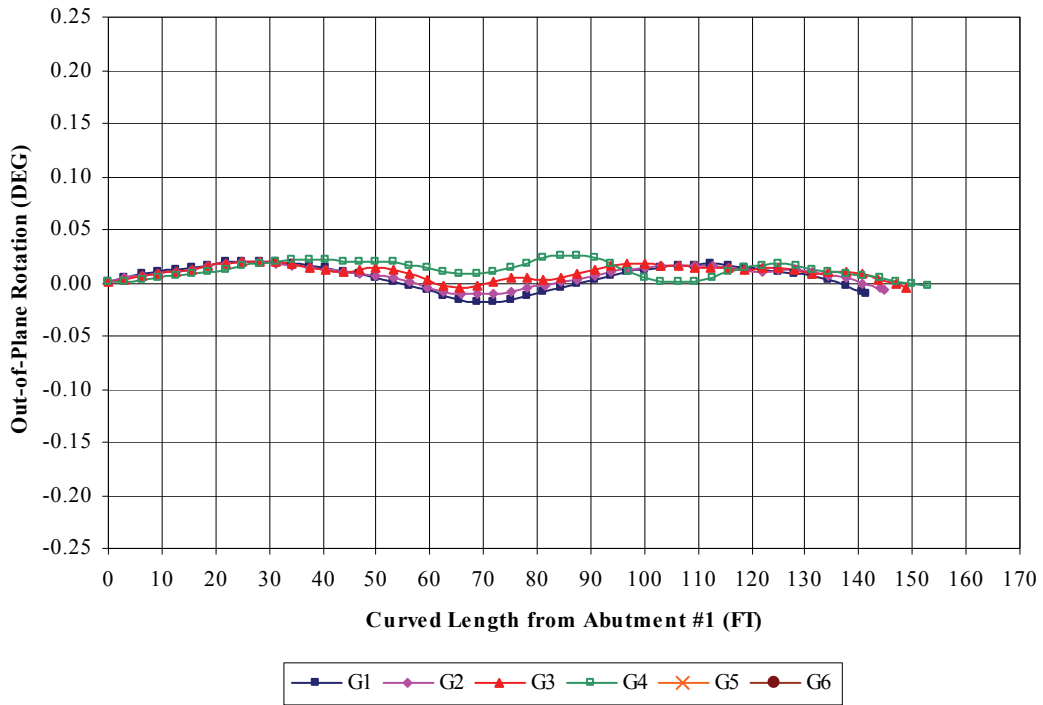
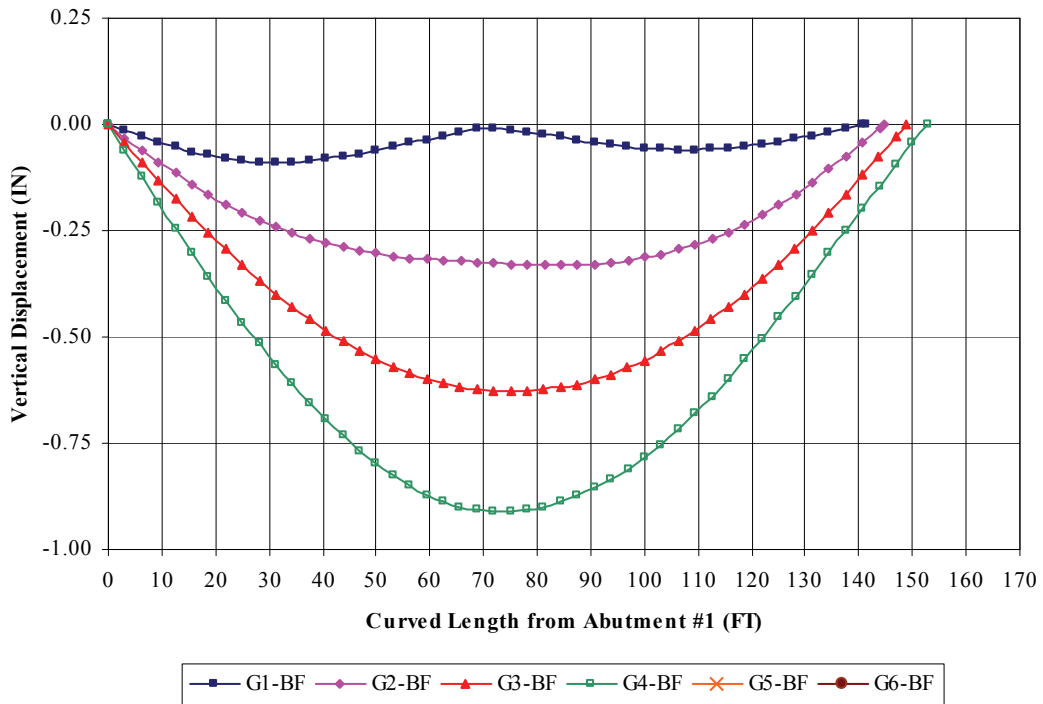


Figure B.68 Construction Stage 4d – Girder Lateral Displacement



**Figure B.69** Construction Stage 4d – Girder Out-of-Plane Rotation



**Figure B.70** Construction Stage 4d1 – Girder Vertical Displacement

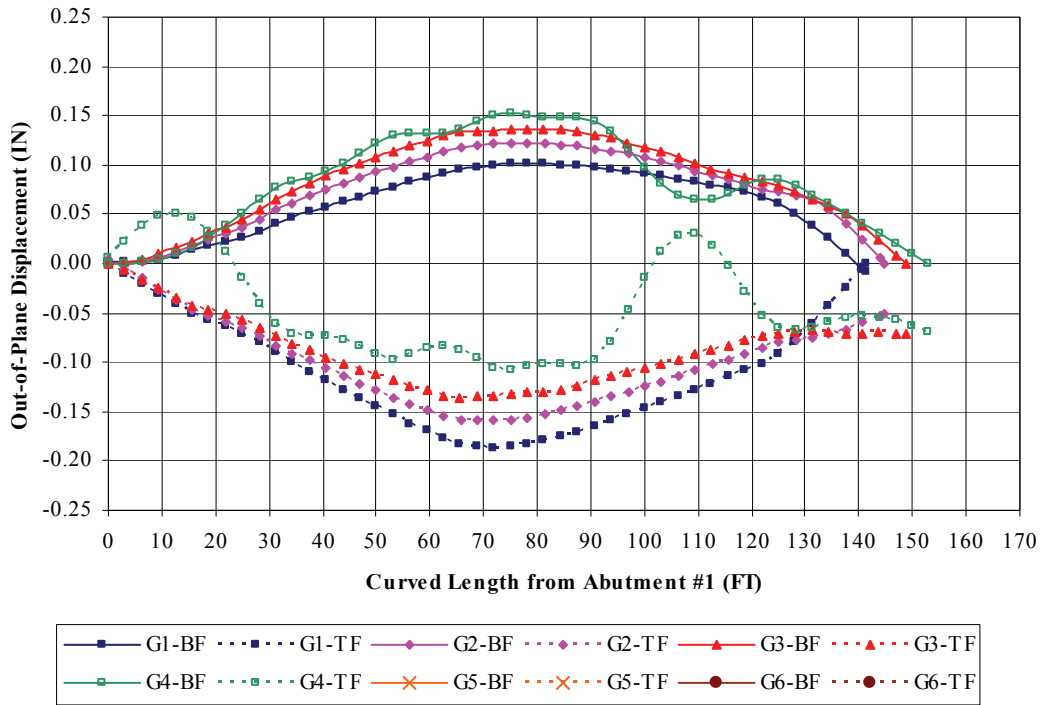


Figure B.71 Construction Stage 4d1 – Girder Lateral Displacement

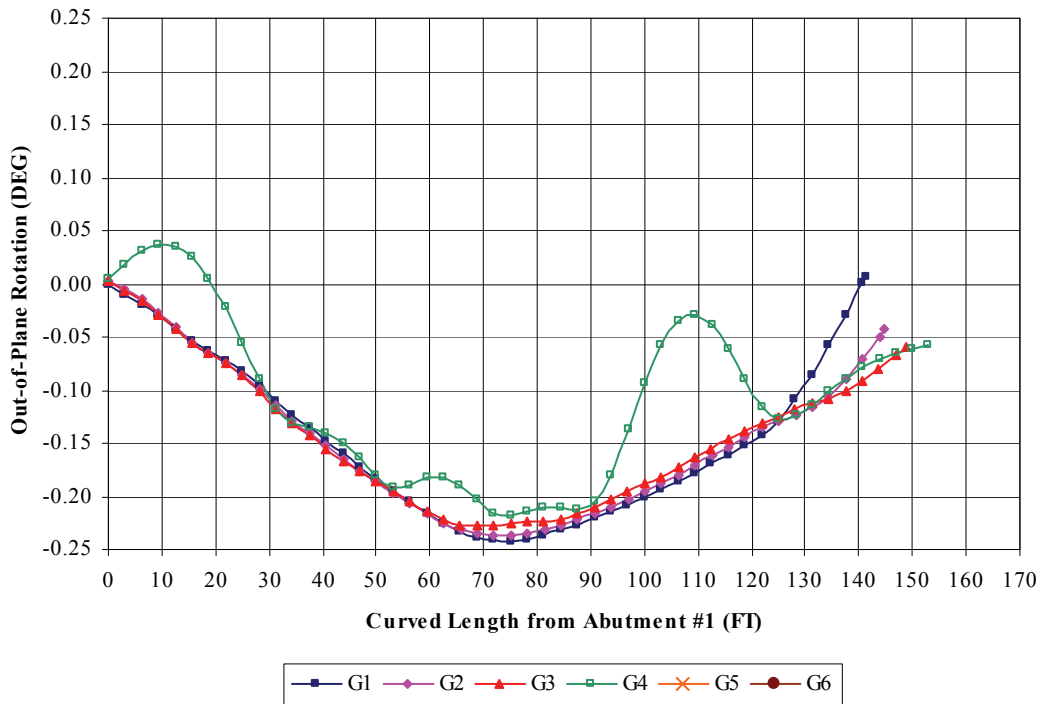


Figure B.72 Construction Stage 4d1 – Girder Out-of-Plane Rotation

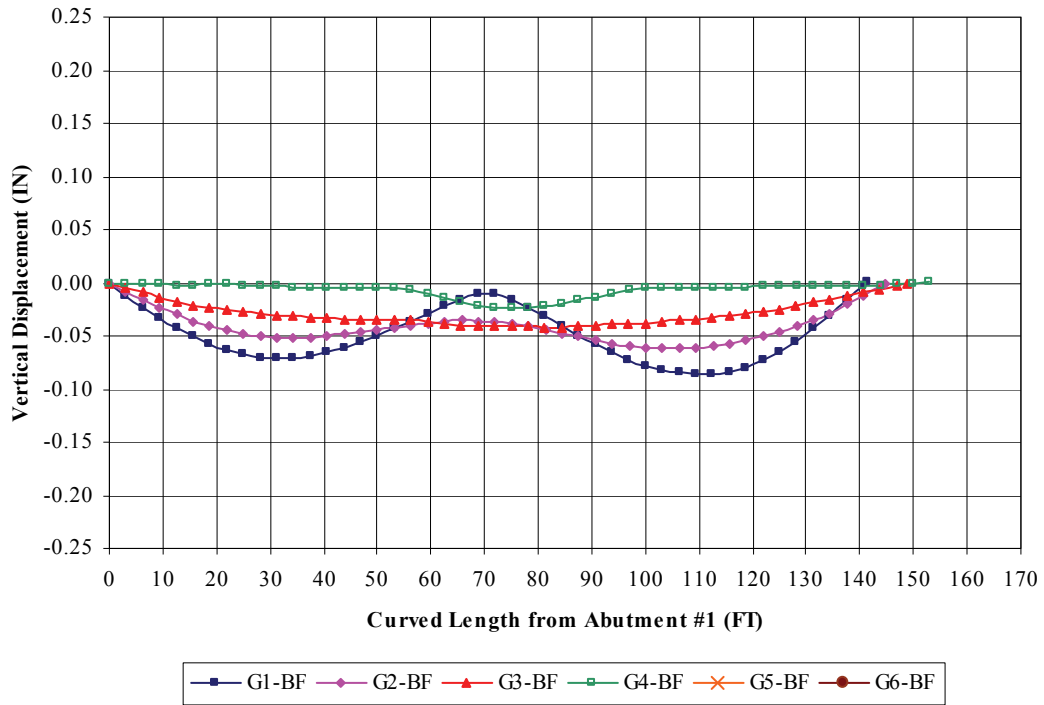


Figure B.73 Construction Stage 4e – Girder Vertical Displacement

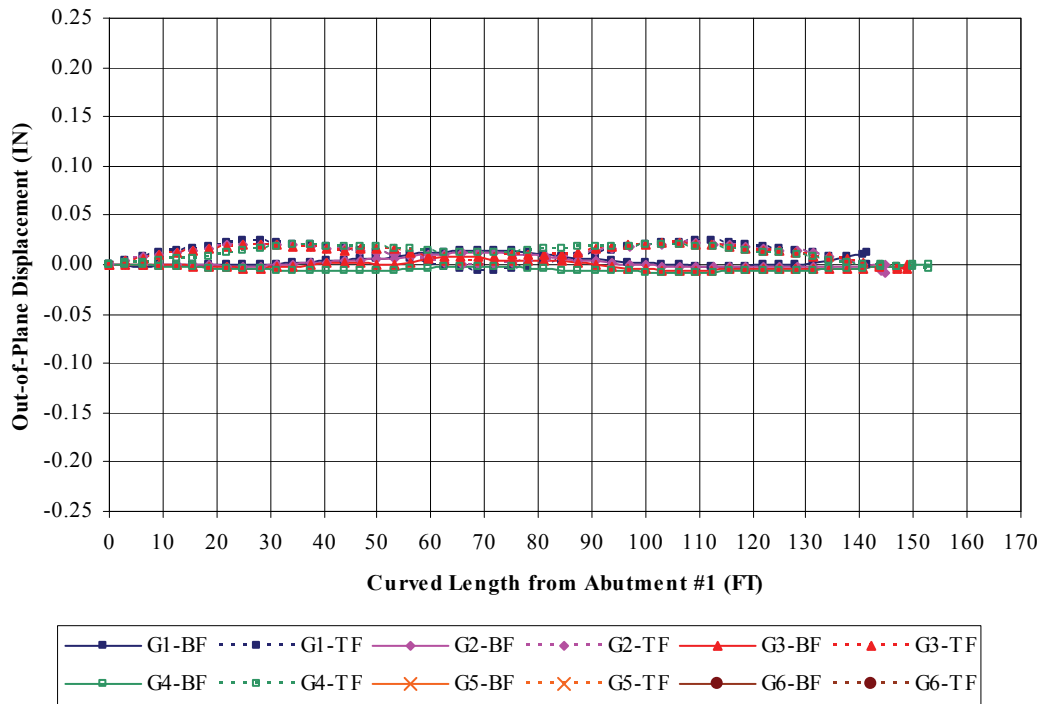
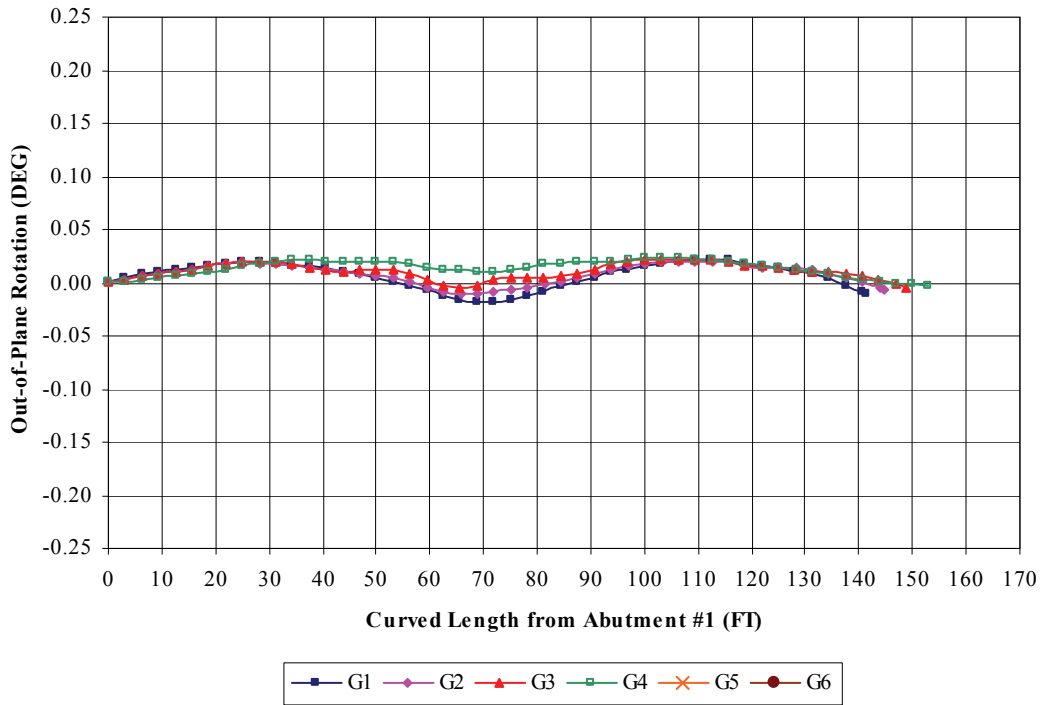
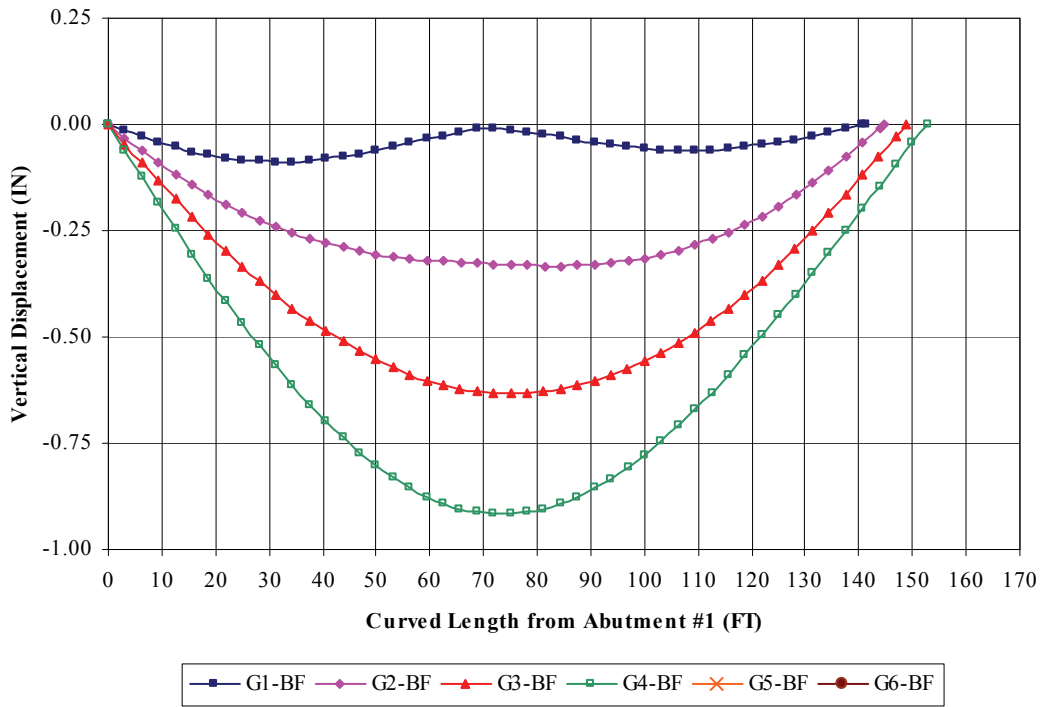


Figure B.74 Construction Stage 4e – Girder Lateral Displacement



**Figure B.75** Construction Stage 4e – Girder Out-of-Plane Rotation



**Figure B.76** Construction Stage 4e1 – Girder Vertical Displacement

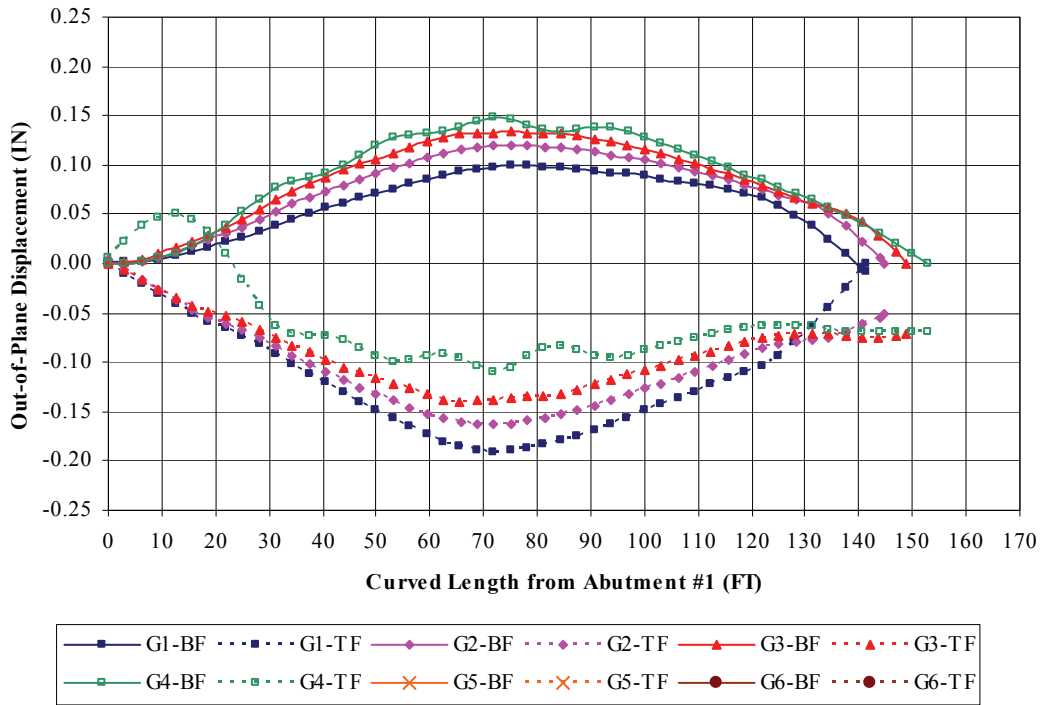


**Figure B.77** Construction Stage 4e1 – Girder Lateral Displacement

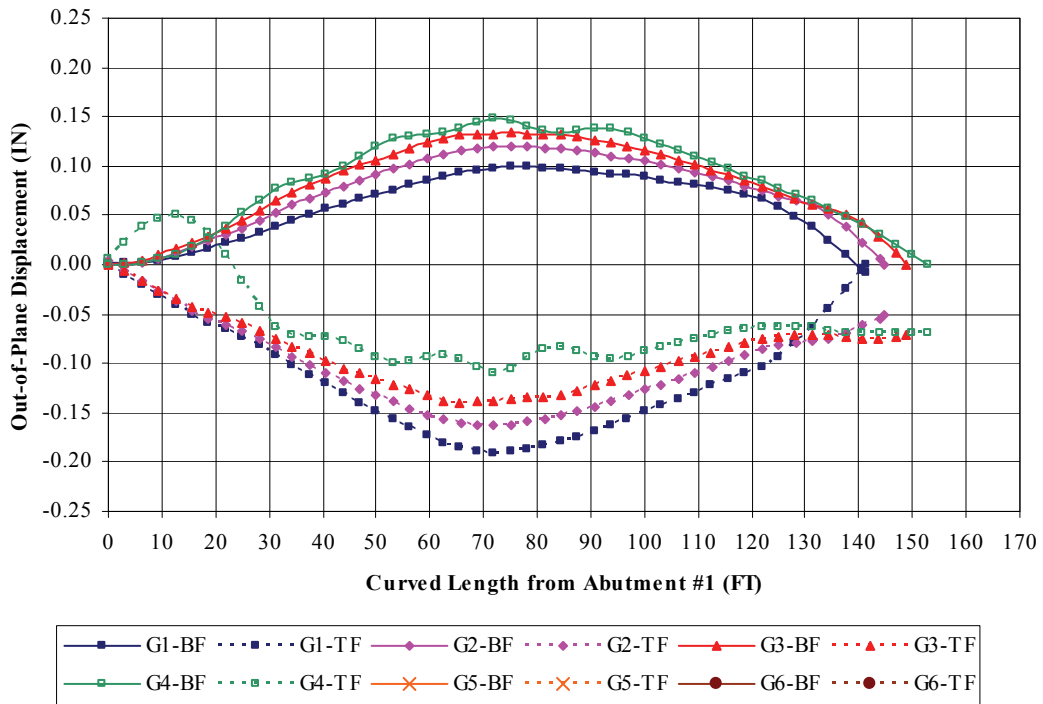


**Figure B.78** Construction Stage 4e1 – Girder Out-of-Plane Rotation

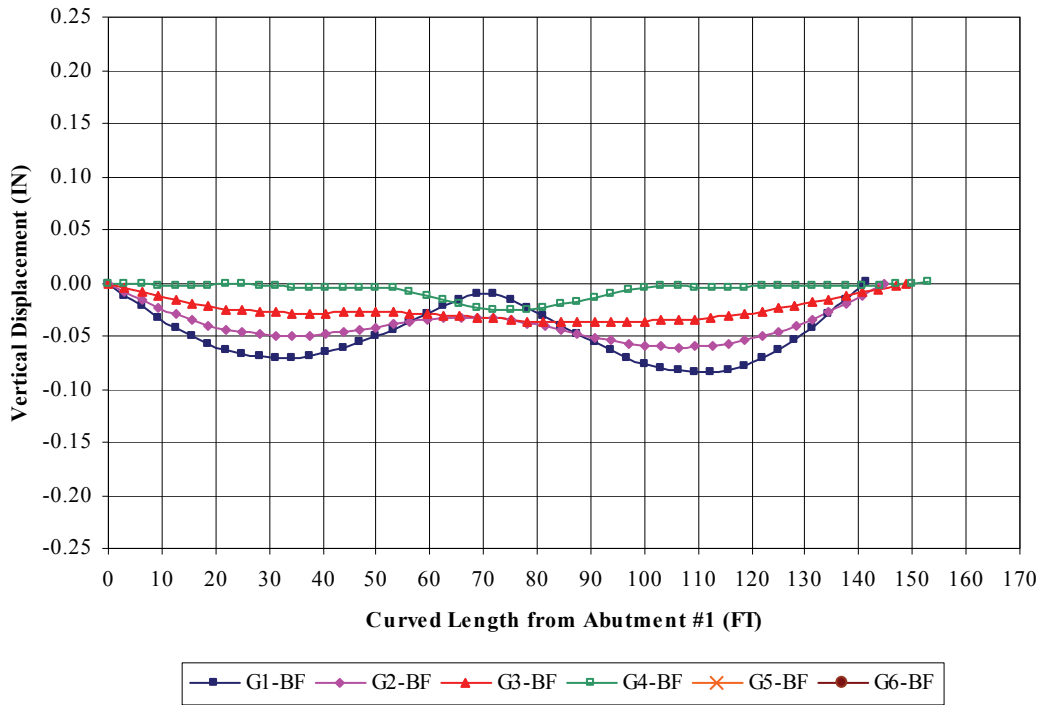


Figure B.79 Construction Stage 4f – Girder Vertical Displacement

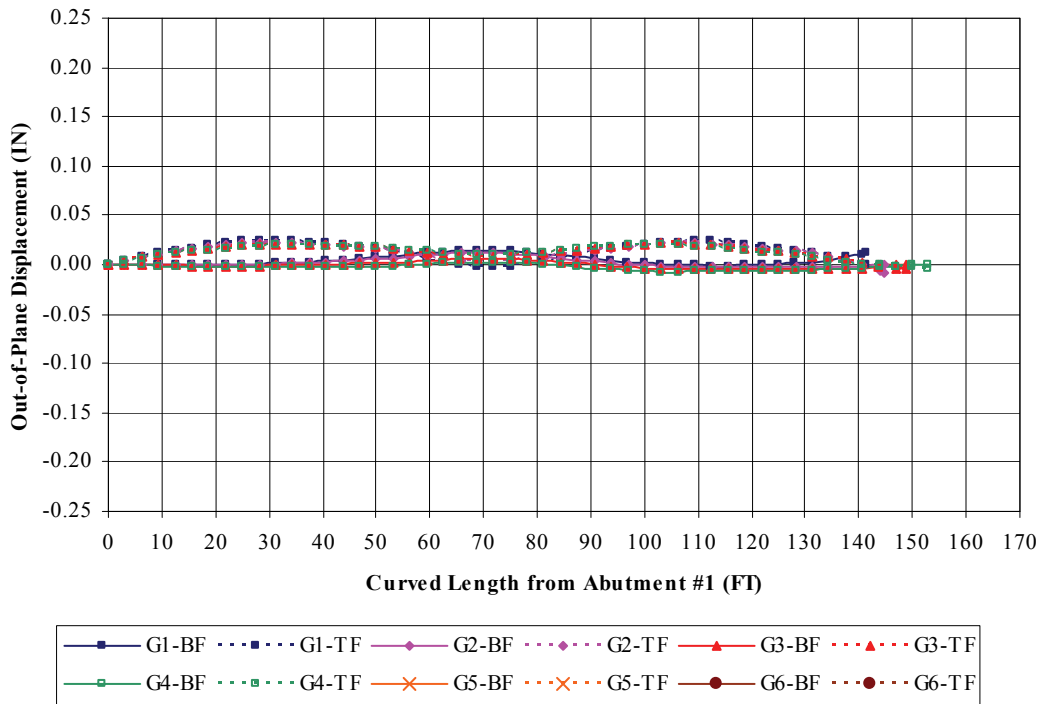


Figure B.80 Construction Stage 4f – Girder Lateral Displacement

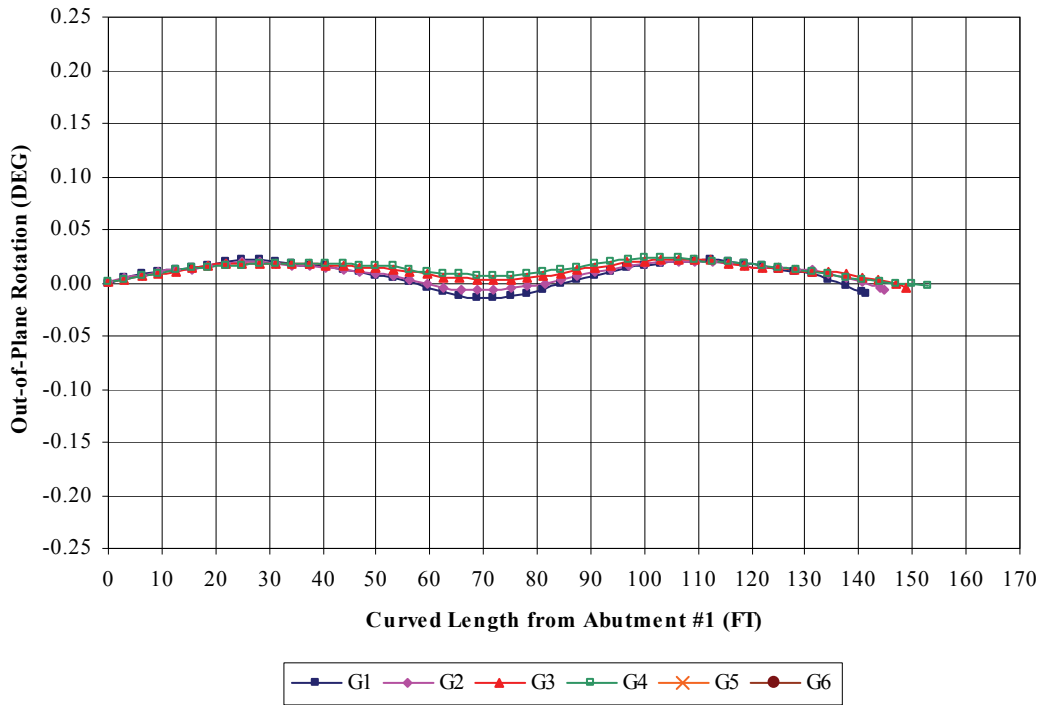


Figure B.81 Construction Stage 4e1 – Girder Out-of-Plane Rotation

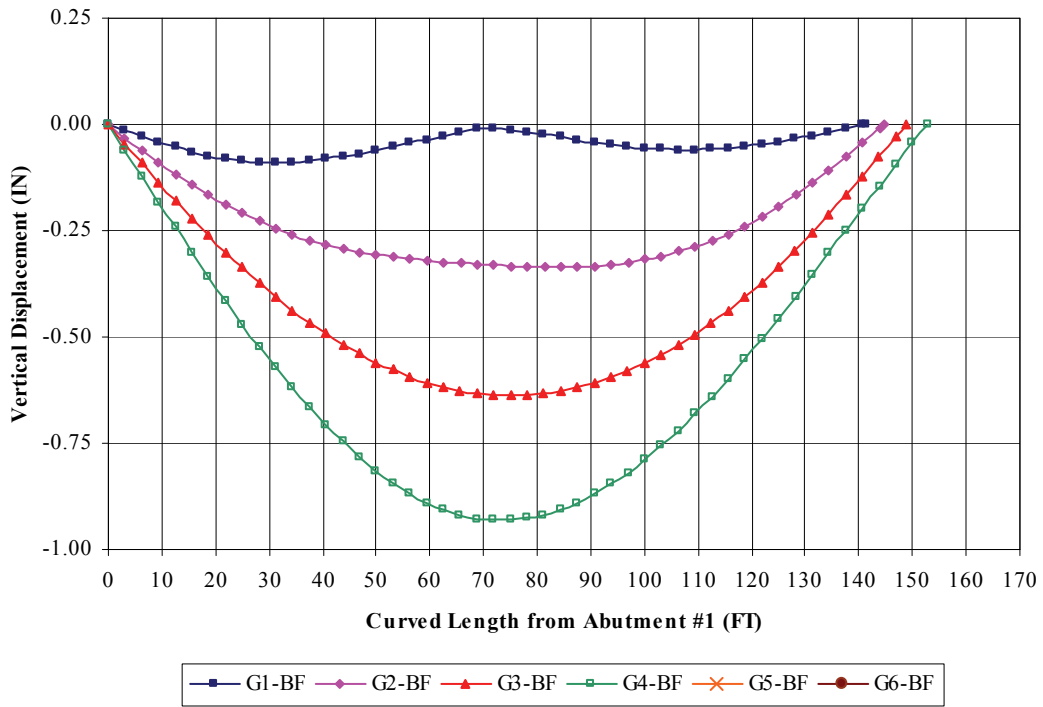
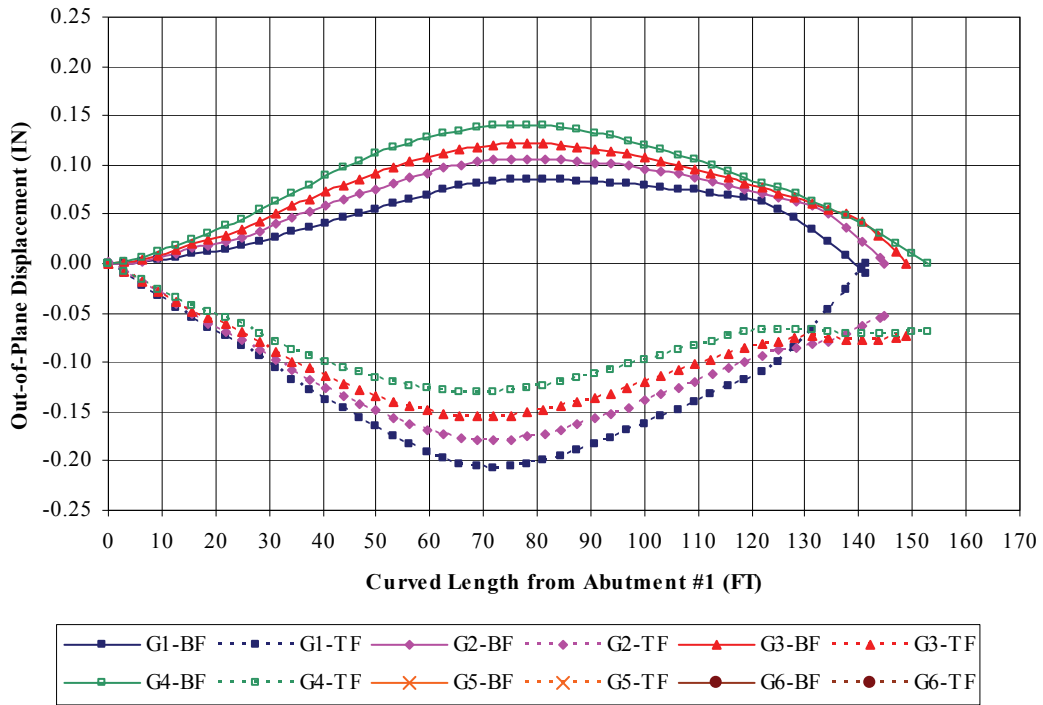
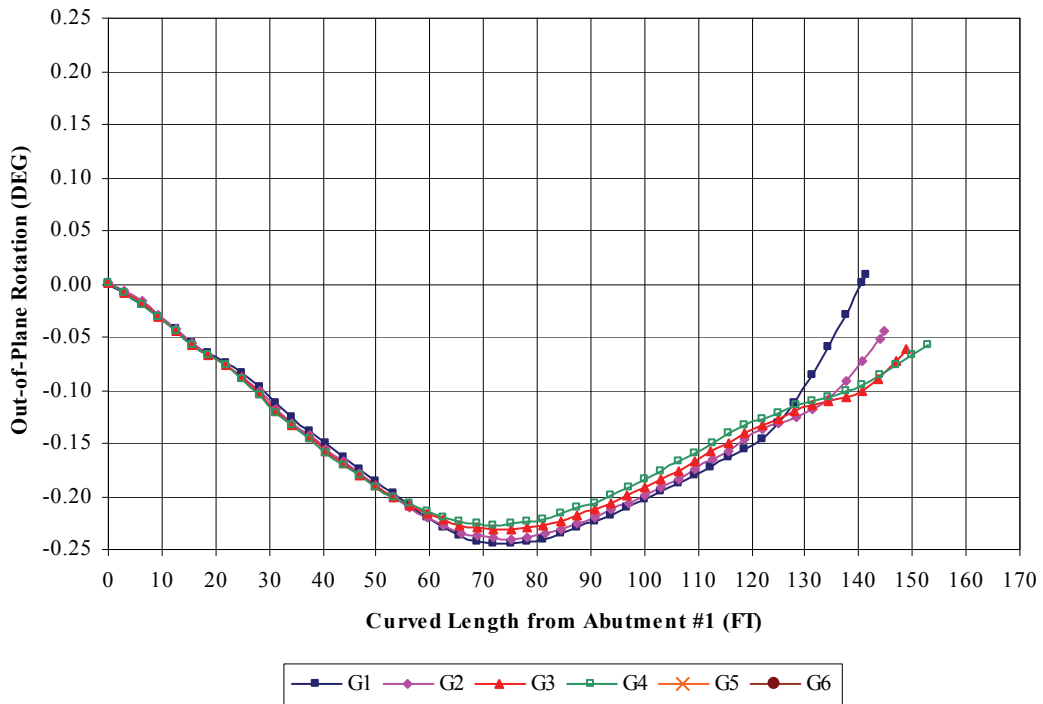


Figure B.82 Construction Stage 4f1 – Girder Vertical Displacement



**Figure B.83** Construction Stage 4f1 – Girder Lateral Displacement



**Figure B.84** Construction Stage 4f1 – Girder Out-of-Plane Rotation

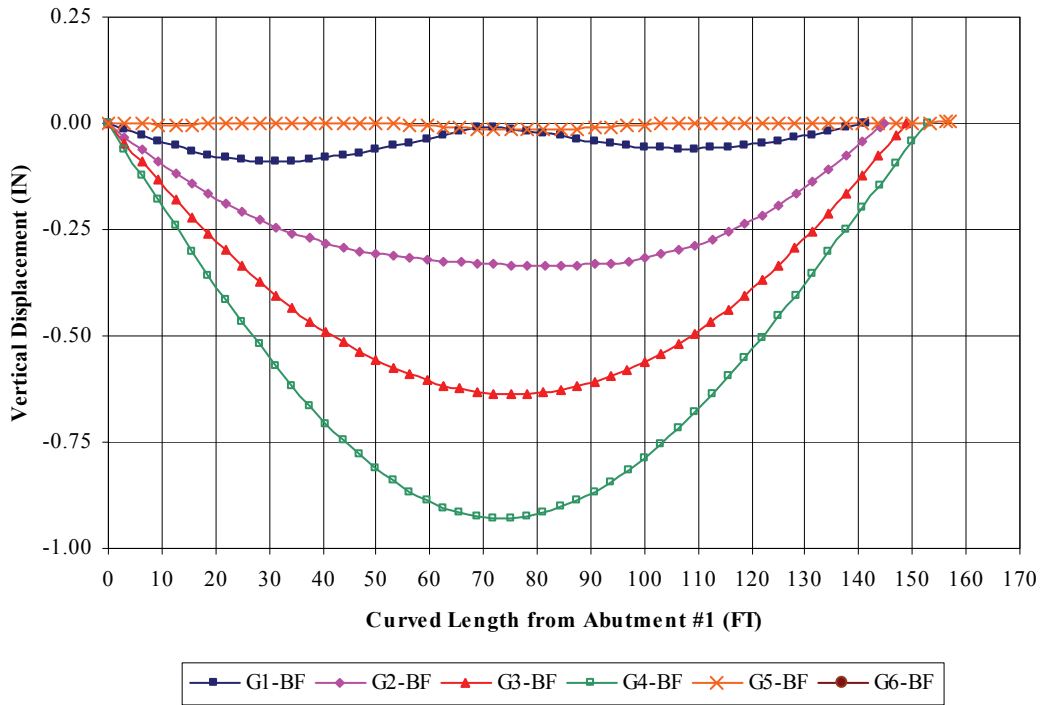


Figure B.85 Construction Stage 5a – Girder Vertical Displacement

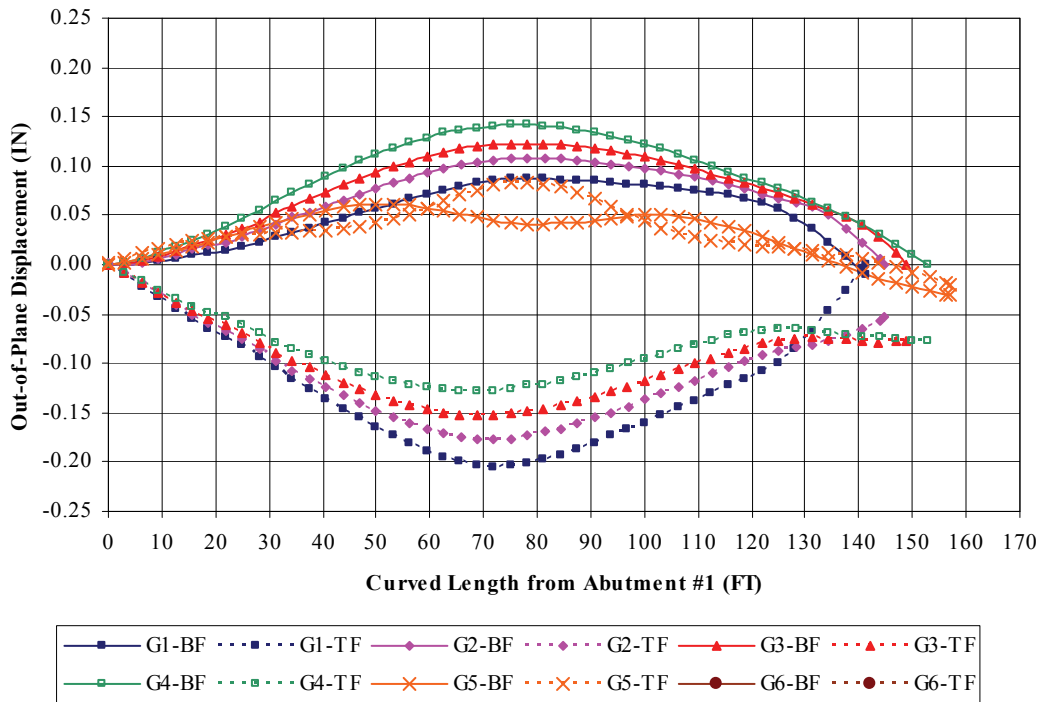
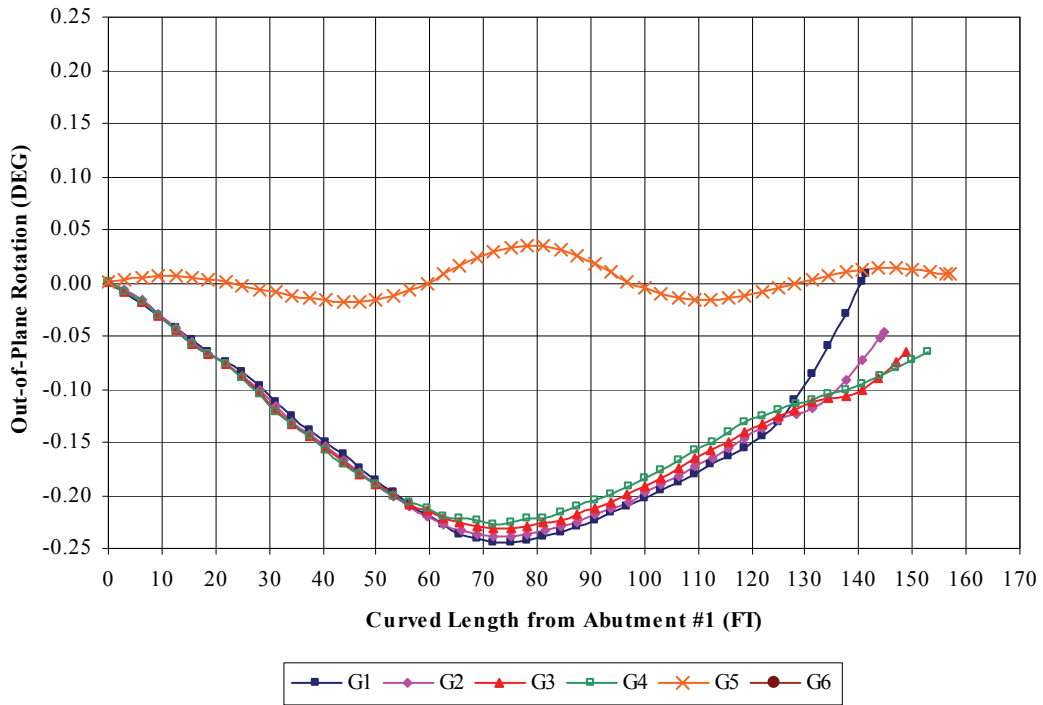
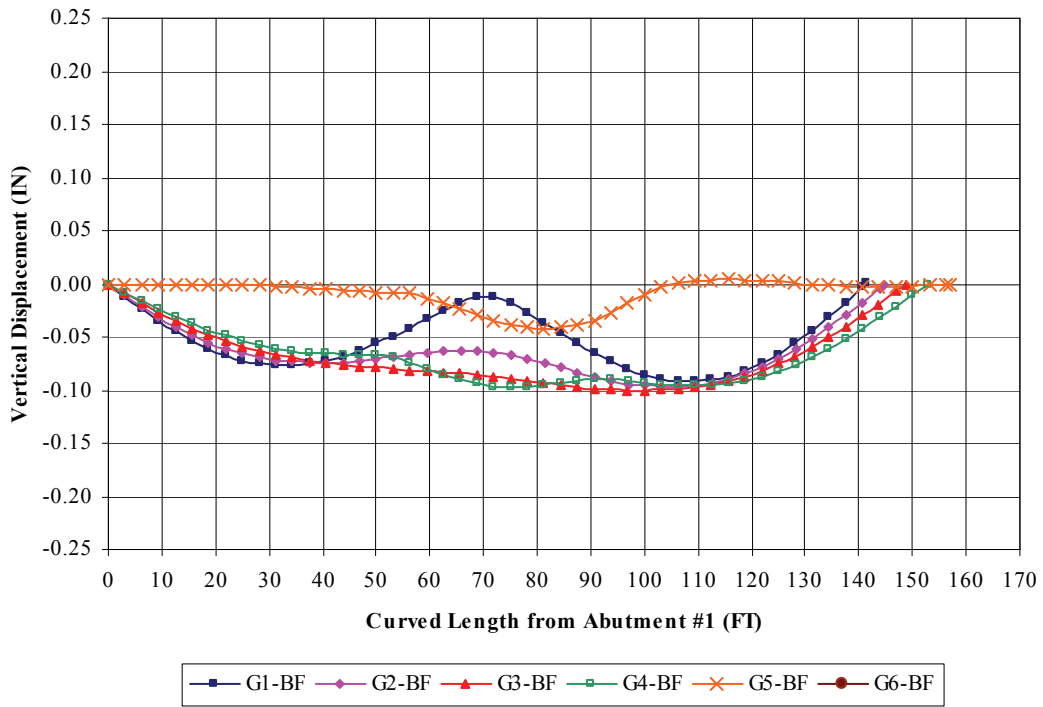


Figure B.86 Construction Stage 5a – Girder Lateral Displacement



**Figure B.87** Construction Stage 5a – Girder Out-of-Plane Rotation



**Figure B.88** Construction Stage 5b – Girder Vertical Displacement

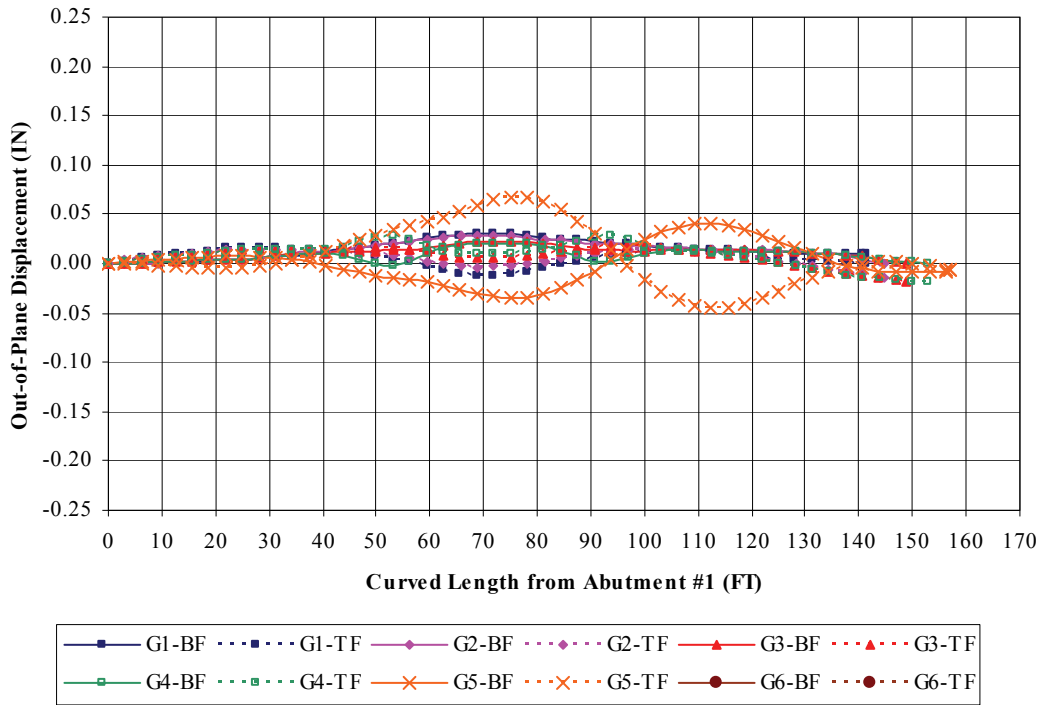


Figure B.89 Construction Stage 5b – Girder Lateral Displacement

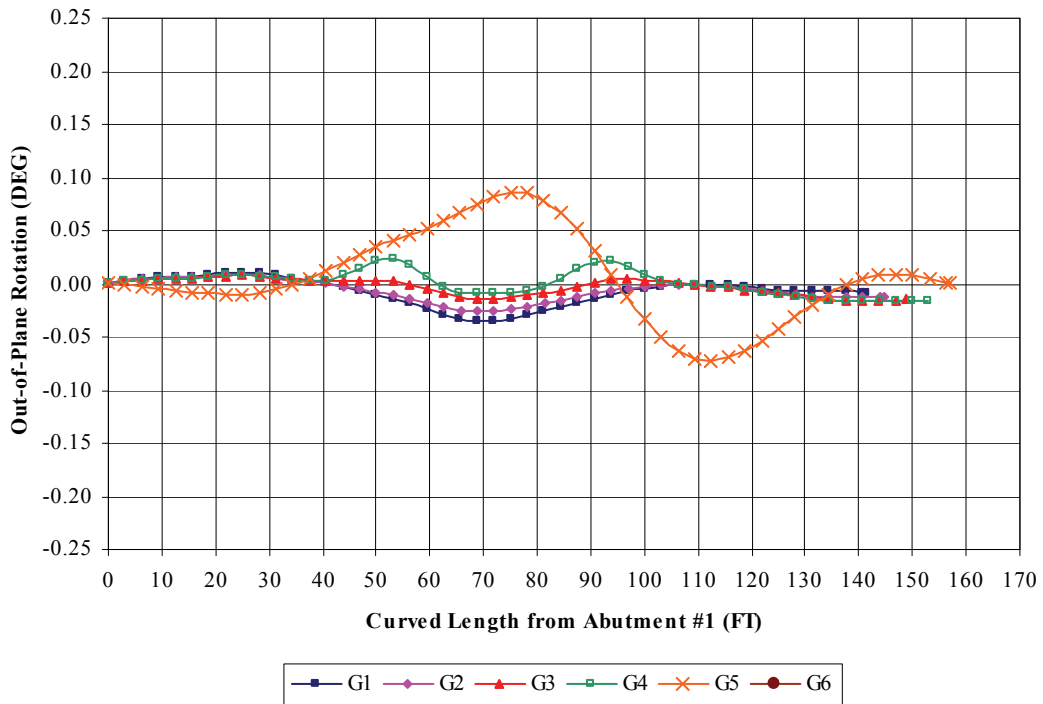


Figure B.90 Construction Stage 5b – Girder Out-of-Plane Rotation

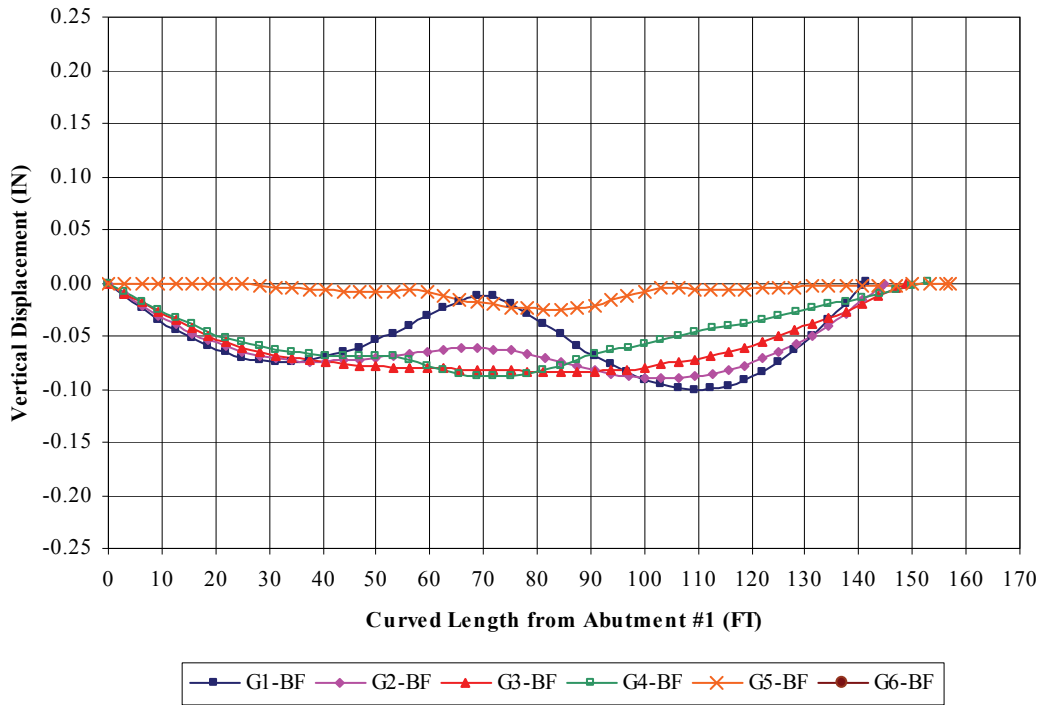


Figure B.91 Construction Stage 5c – Girder Vertical Displacement

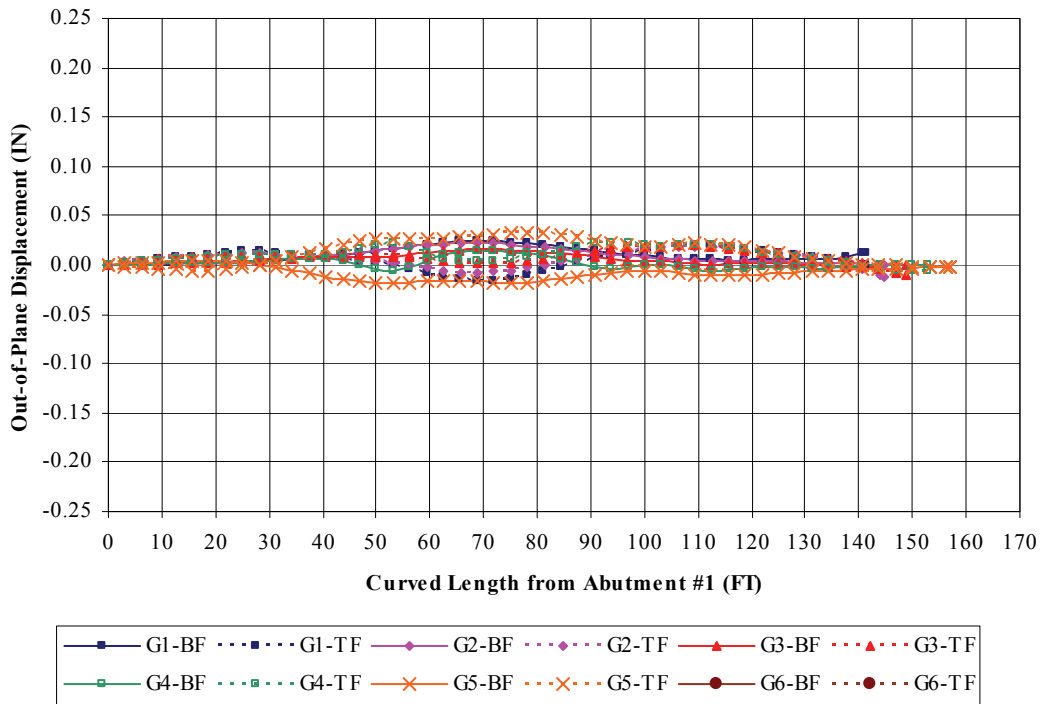
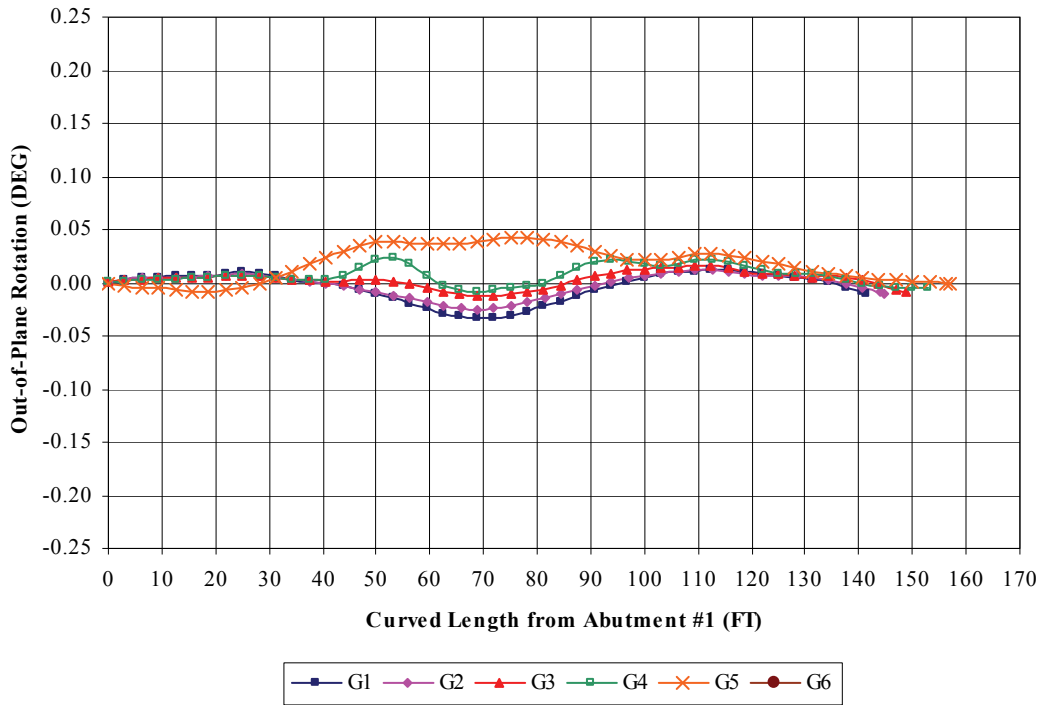
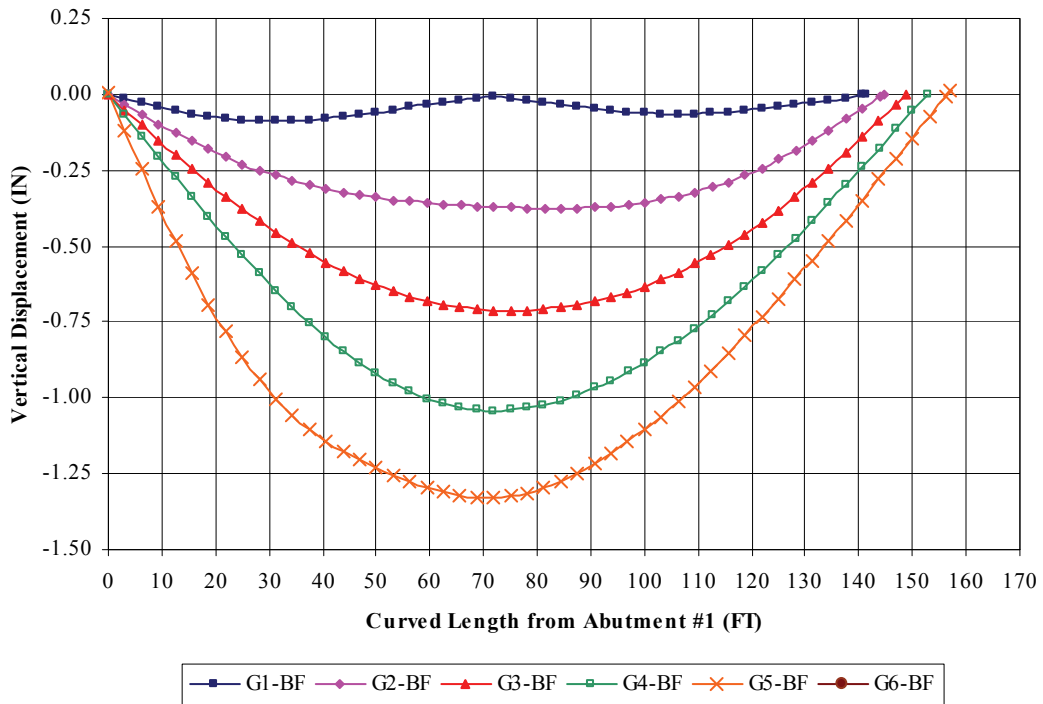


Figure B.92 Construction Stage 5c – Girder Lateral Displacement



**Figure B.93** Construction Stage 5c – Girder Out-of-Plane Rotation



**Figure B.94** Construction Stage 5c1 – Girder Vertical Displacement

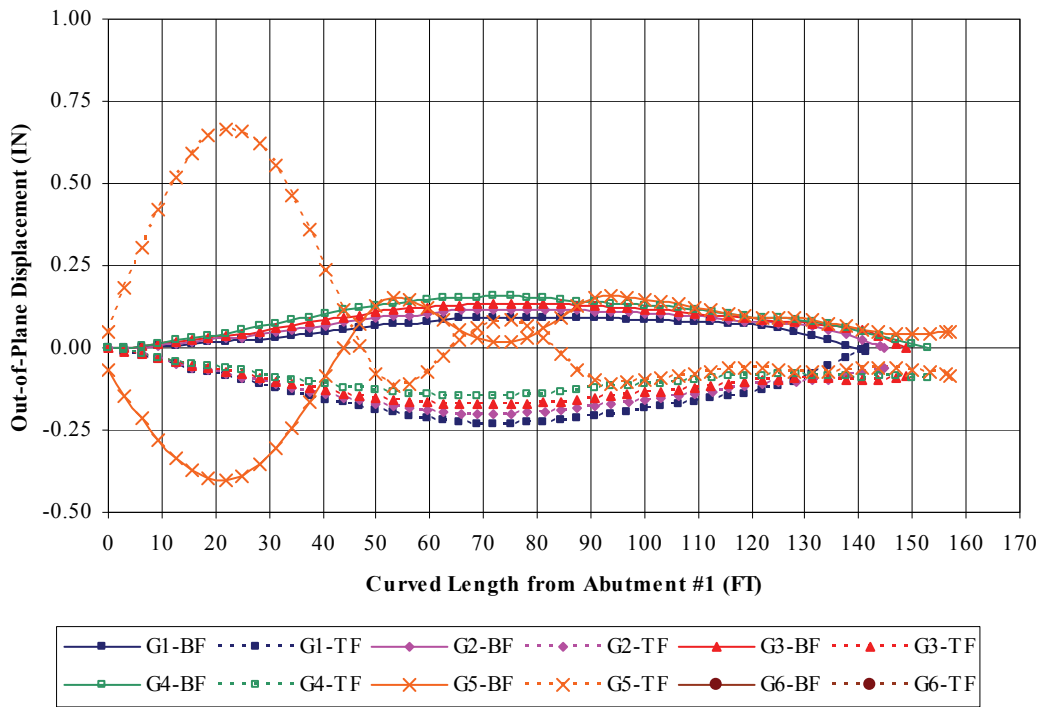


Figure B.95 Construction Stage 5c1 – Girder Lateral Displacement

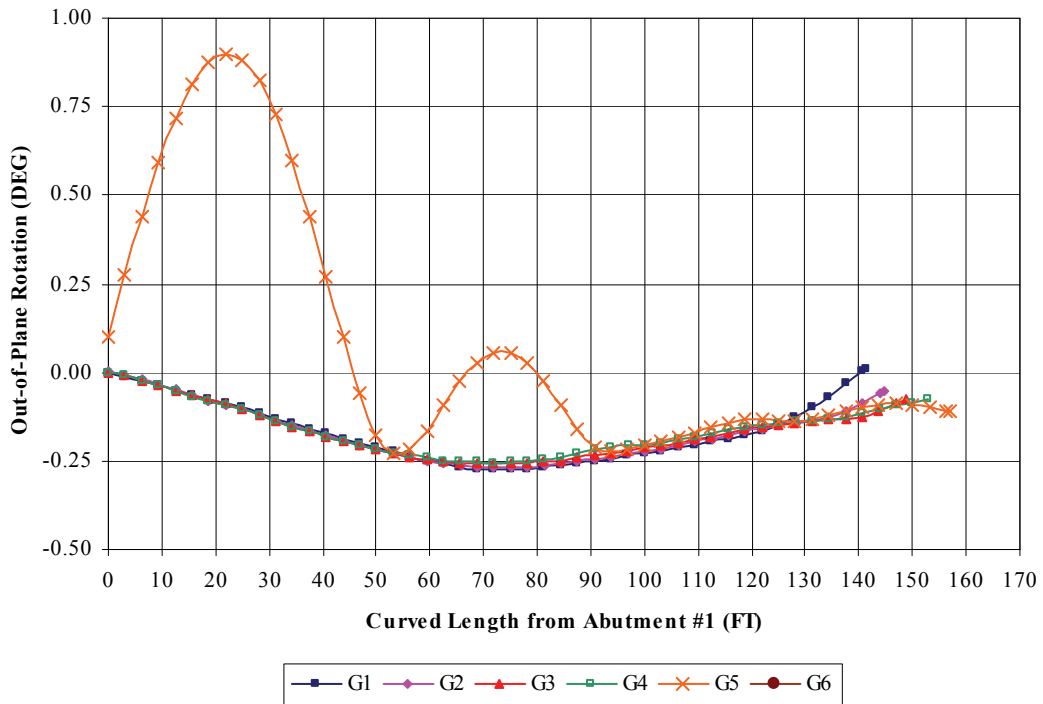
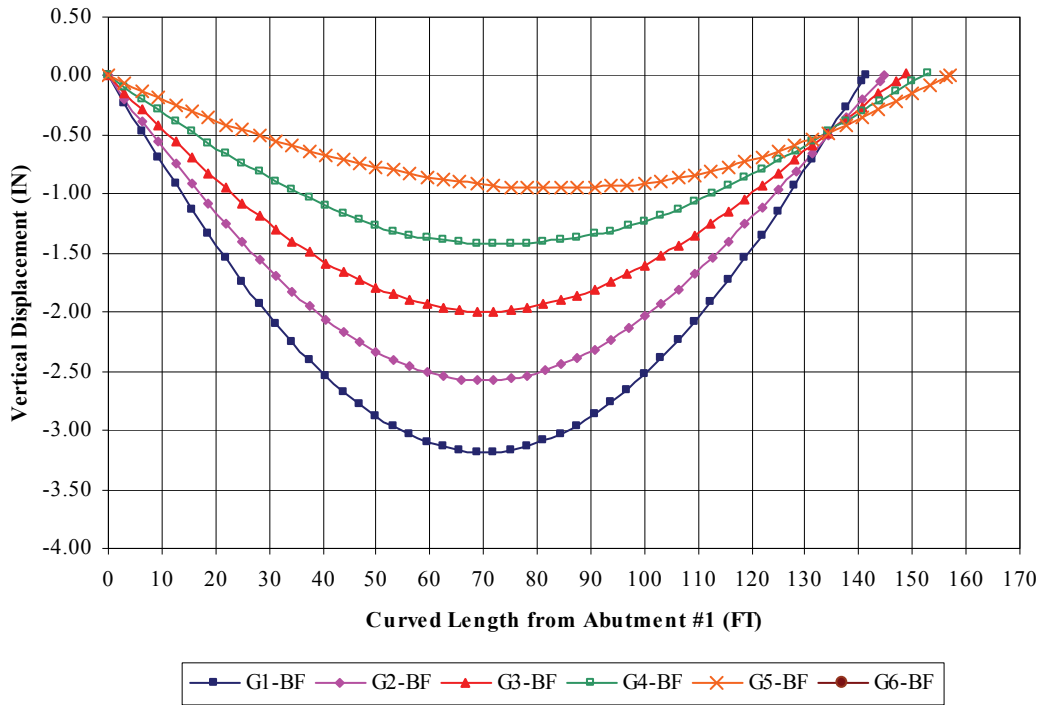
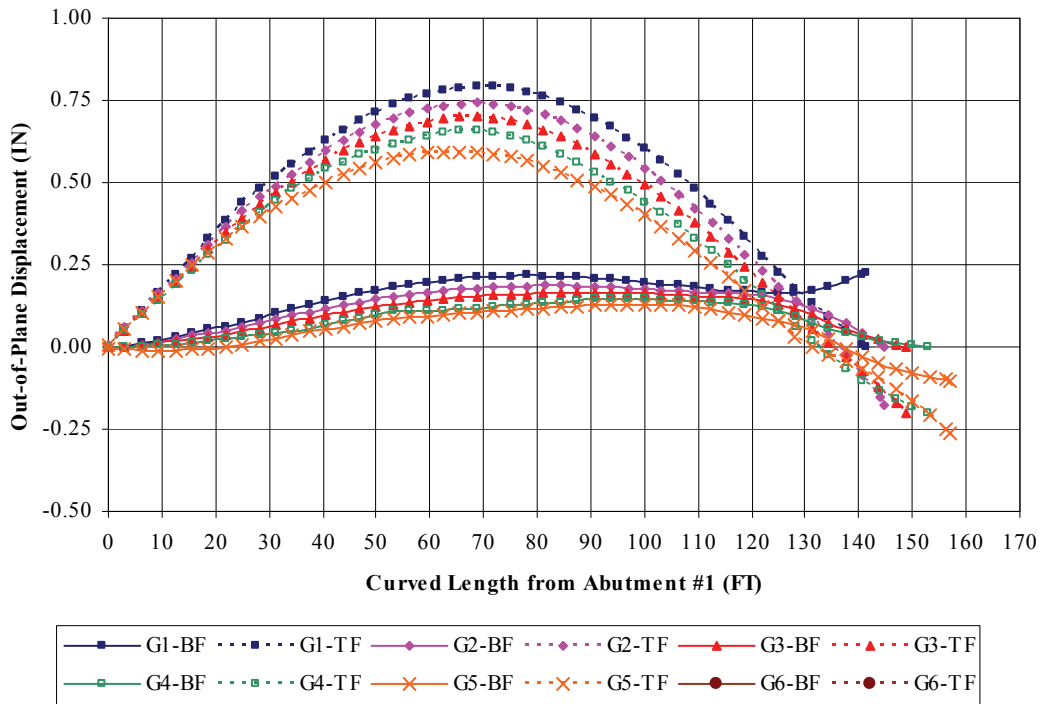


Figure B.96 Construction Stage 5c1 – Girder Out-of-Plane Rotation



**Figure B.97** Construction Stage 5c2 – Girder Vertical Displacement



**Figure B.98** Construction Stage 5c2 – Girder Lateral Displacement

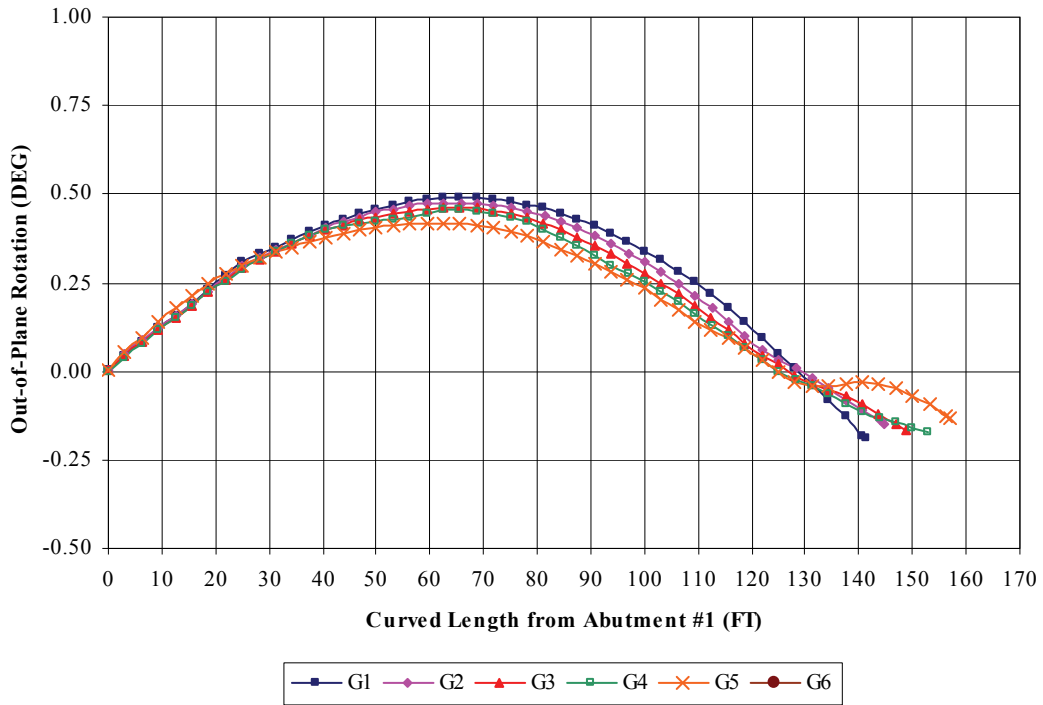


Figure B.99 Construction Stage 5c2 – Girder Out-of-Plane Rotation

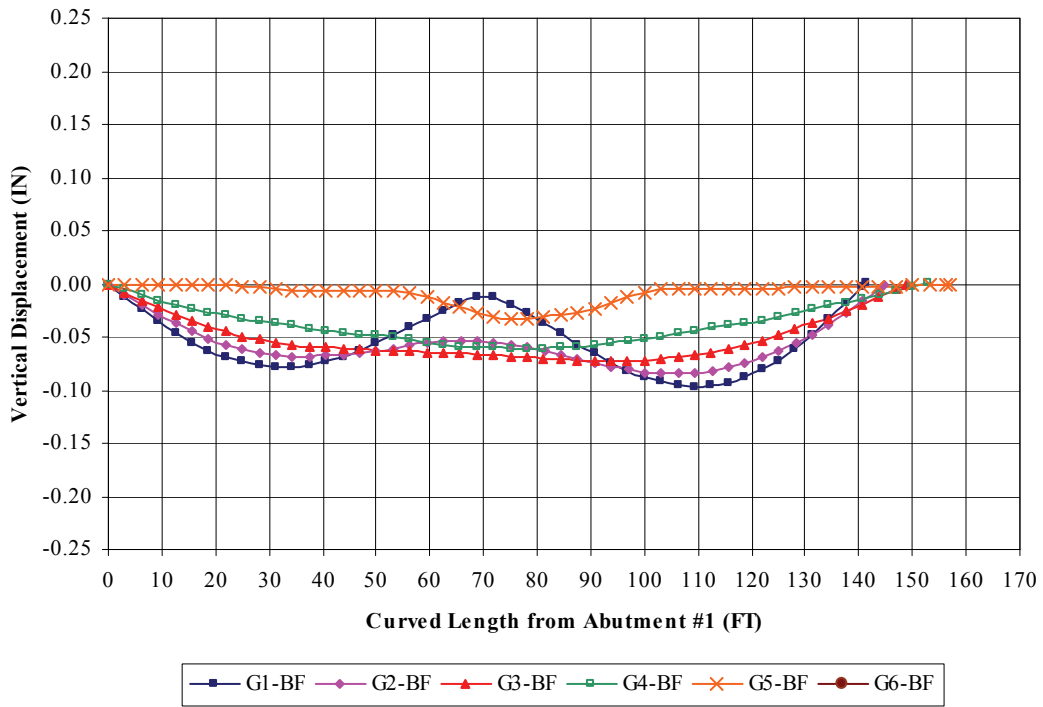


Figure B.100 Construction Stage 5d – Girder Vertical Displacement

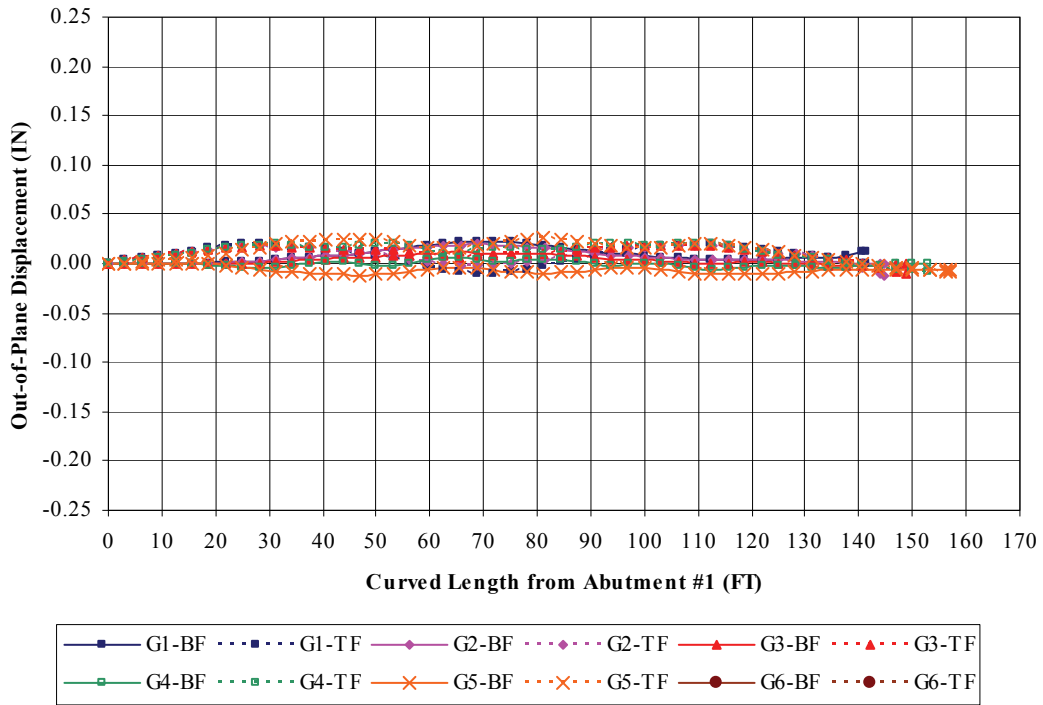


Figure B.101 Construction Stage 5d – Girder Lateral Displacement

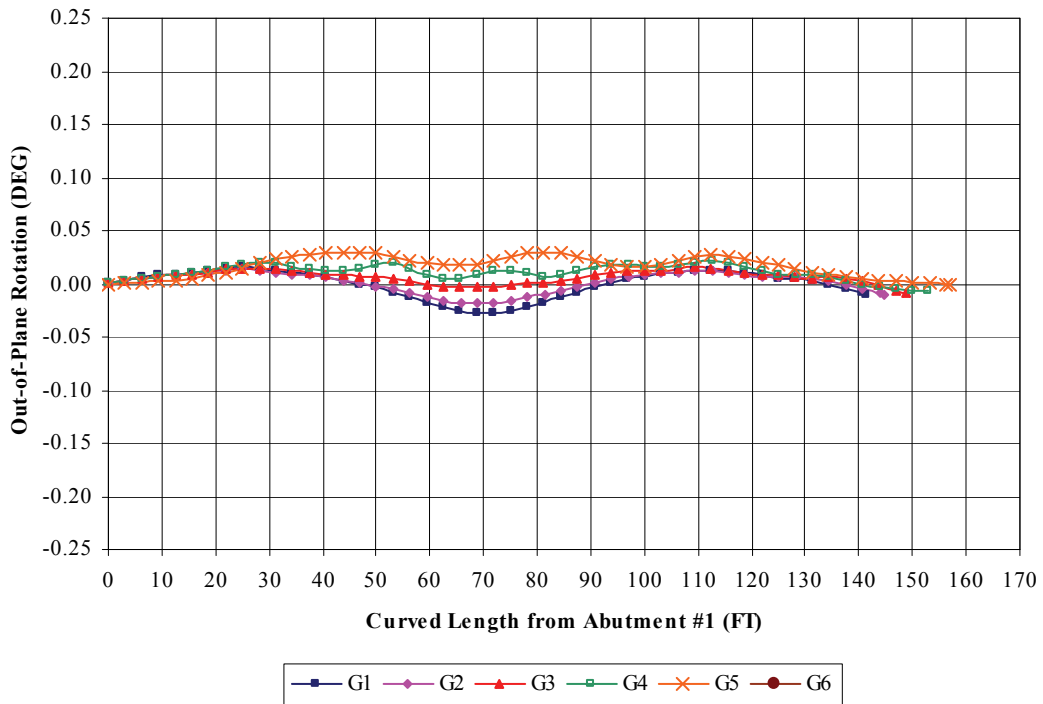


Figure B.102 Construction Stage 5d – Girder Out-of-Plane Rotation

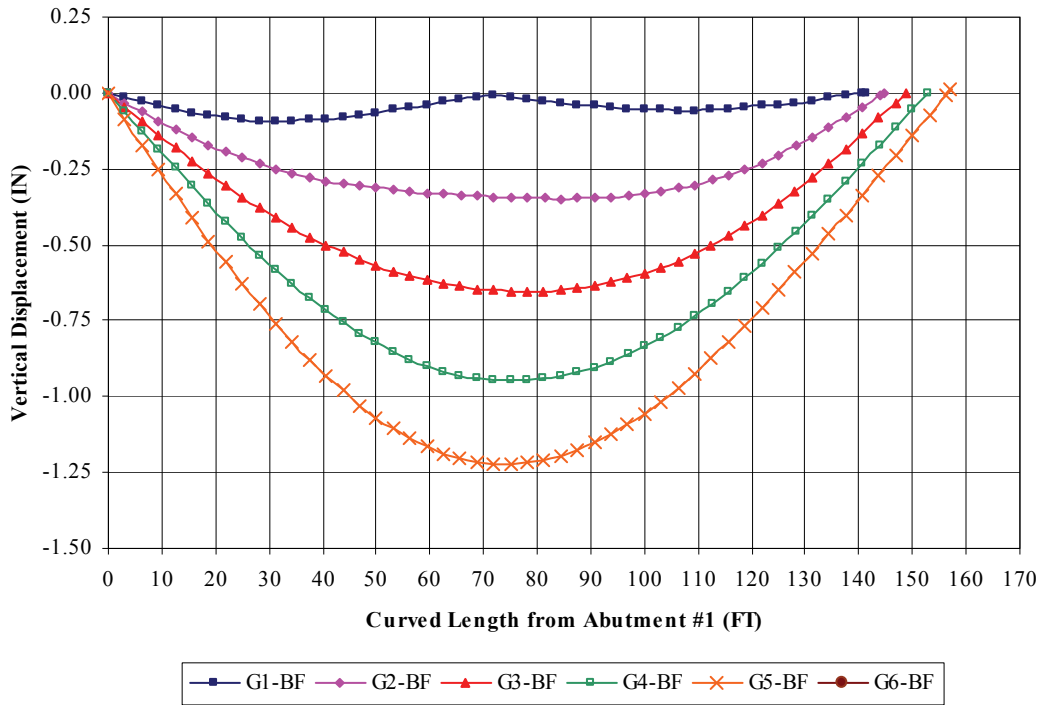


Figure B.103 Construction Stage 5d1 – Girder Vertical Displacement

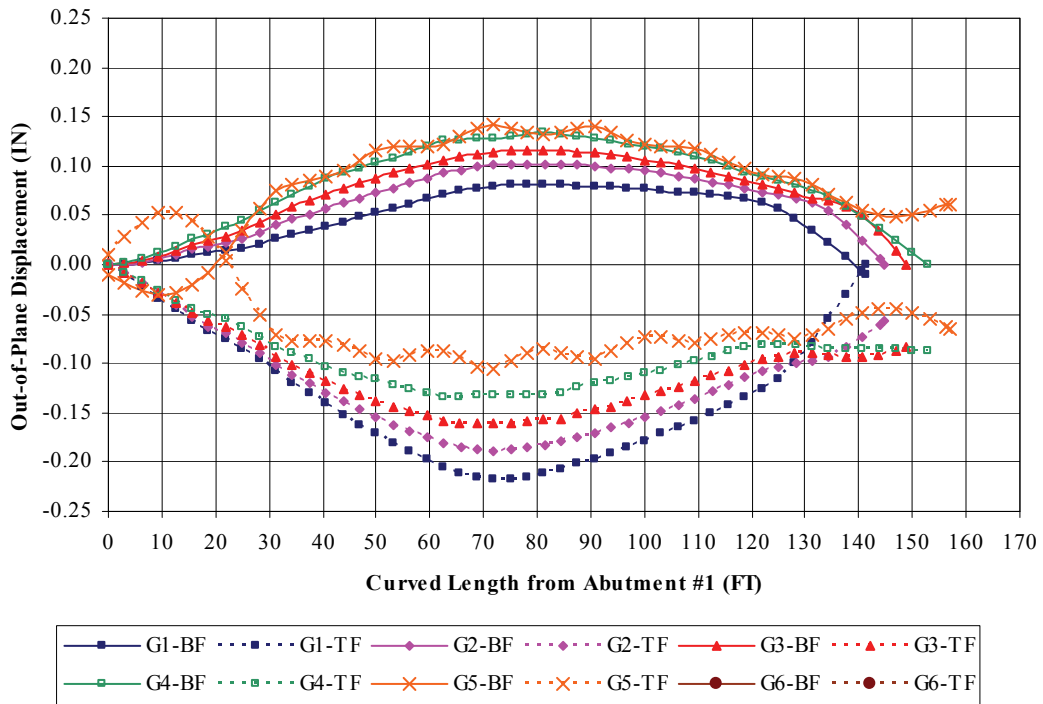


Figure B.104 Construction Stage 5d1 – Girder Lateral Displacement

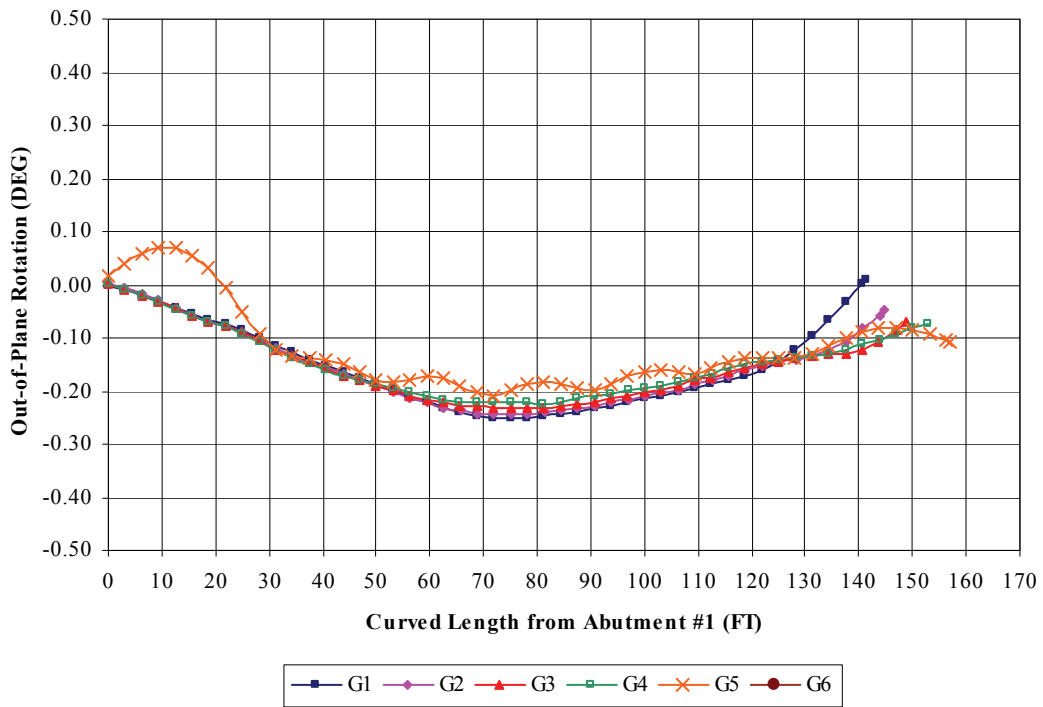


Figure B.105 Construction Stage 5d1 – Girder Out-of-Plane Rotation

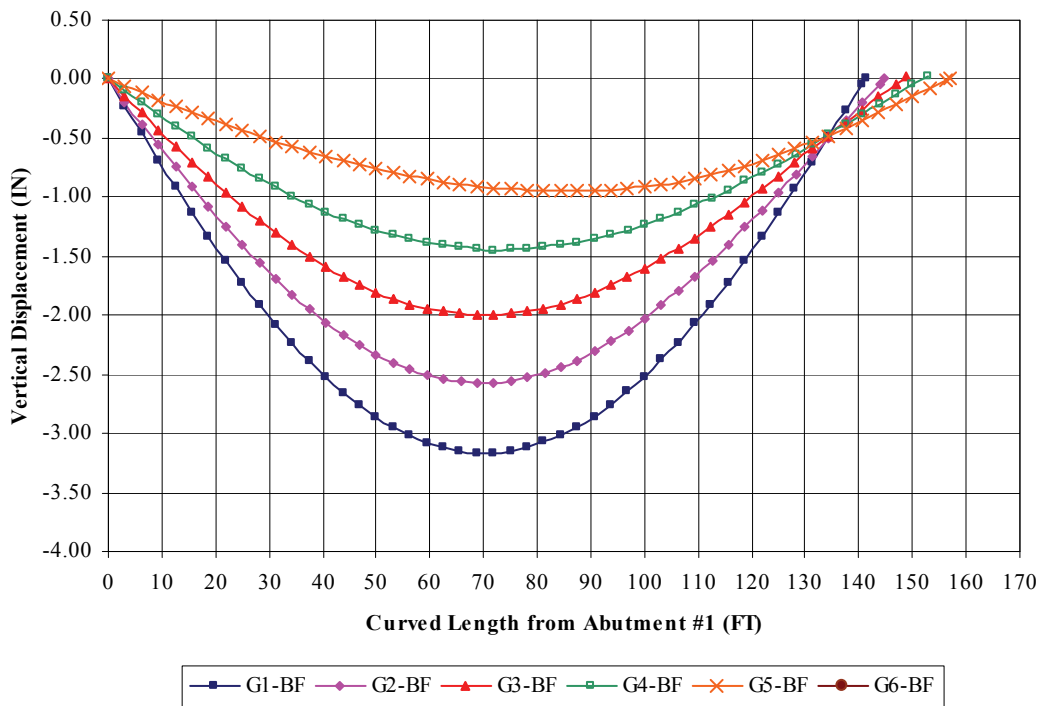


Figure B.106 Construction Stage 5d2 – Girder Vertical Displacement

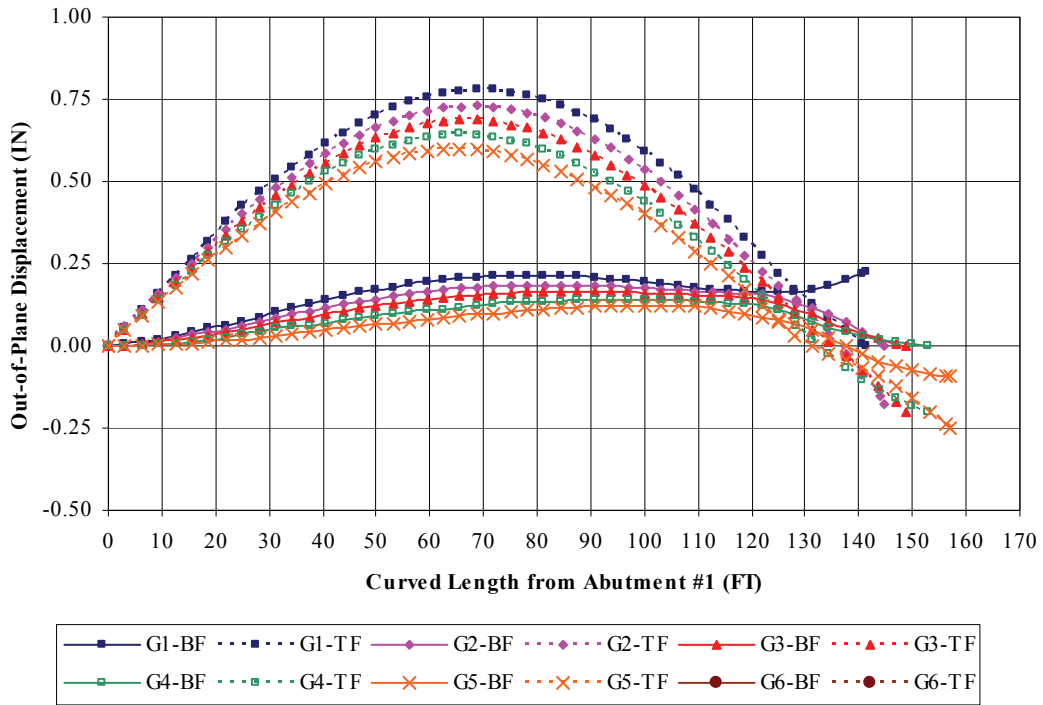


Figure B.107 Construction Stage 5d2 – Girder Lateral Displacement

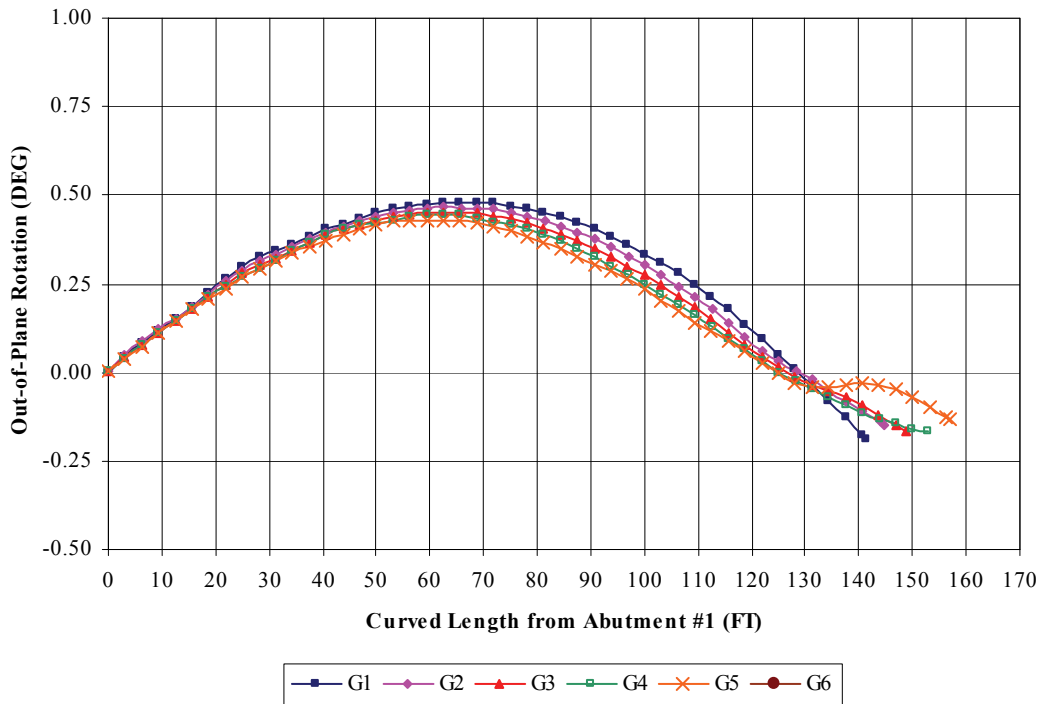


Figure B.108 Construction Stage 5d2 – Girder Out-of-Plane Rotation

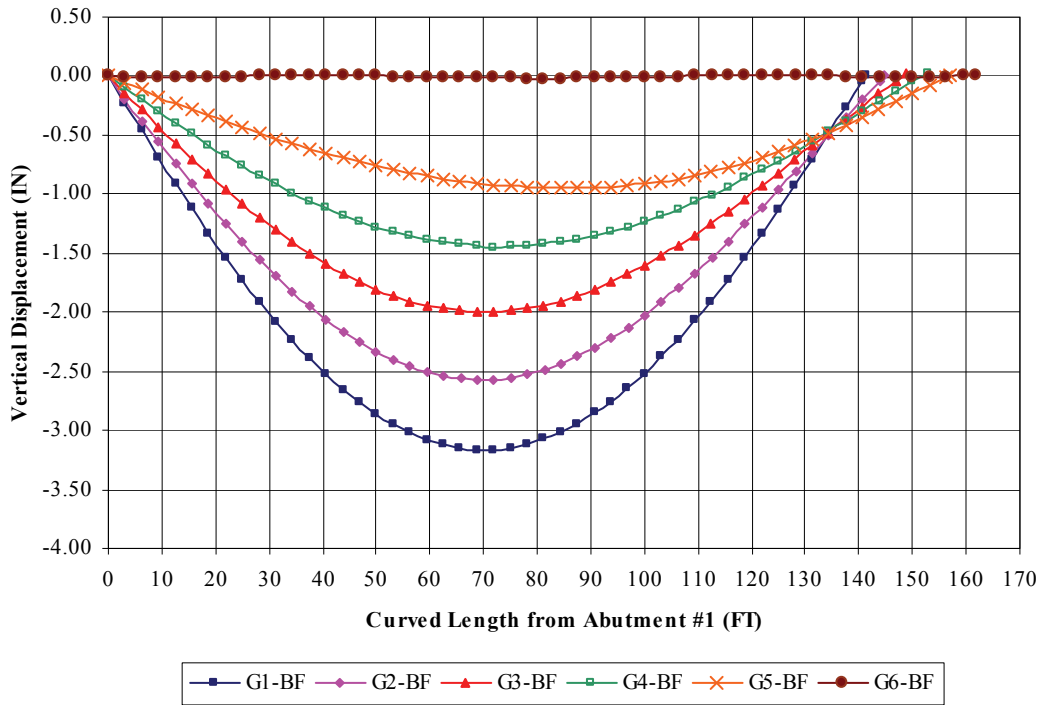


Figure B.109 Construction Stage F6a – Girder Vertical Displacement

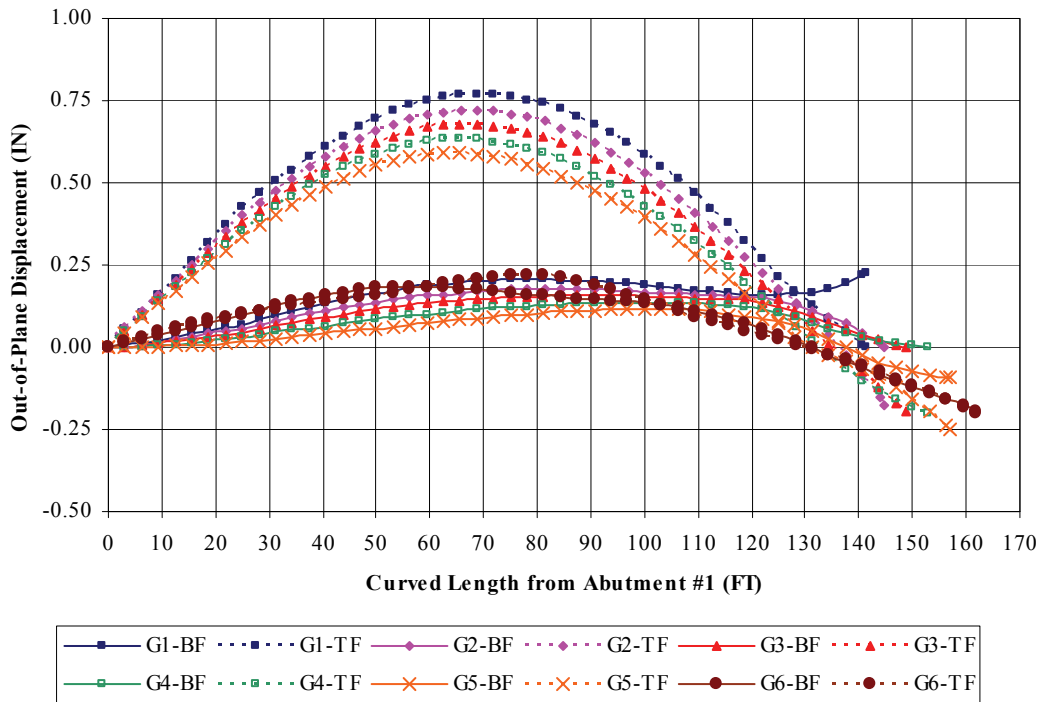
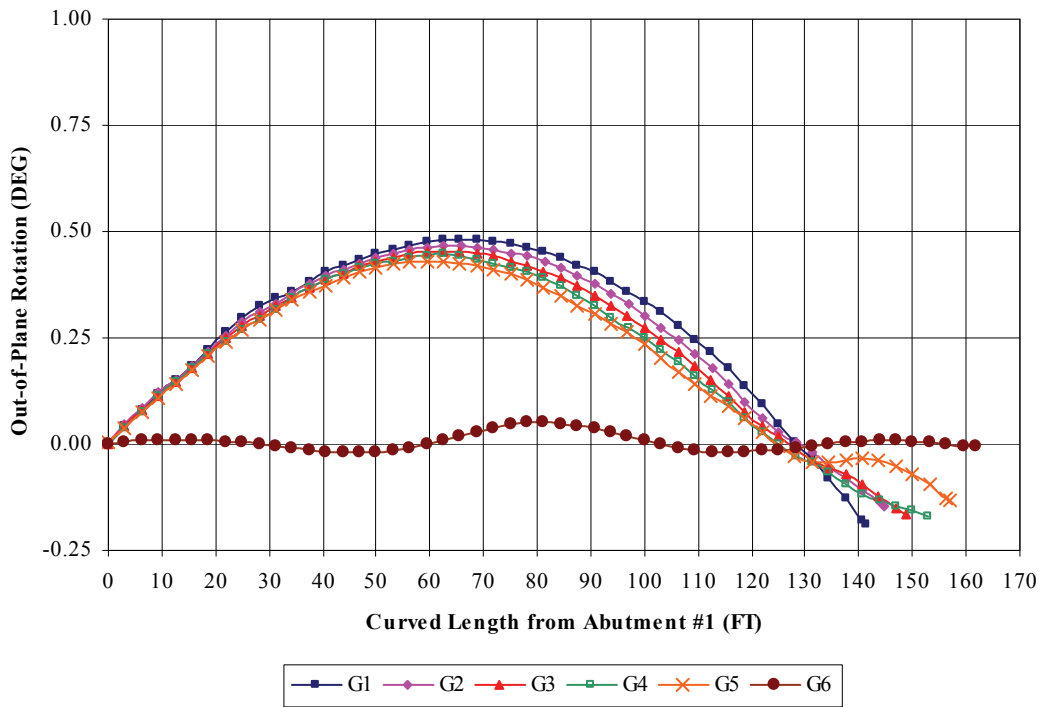
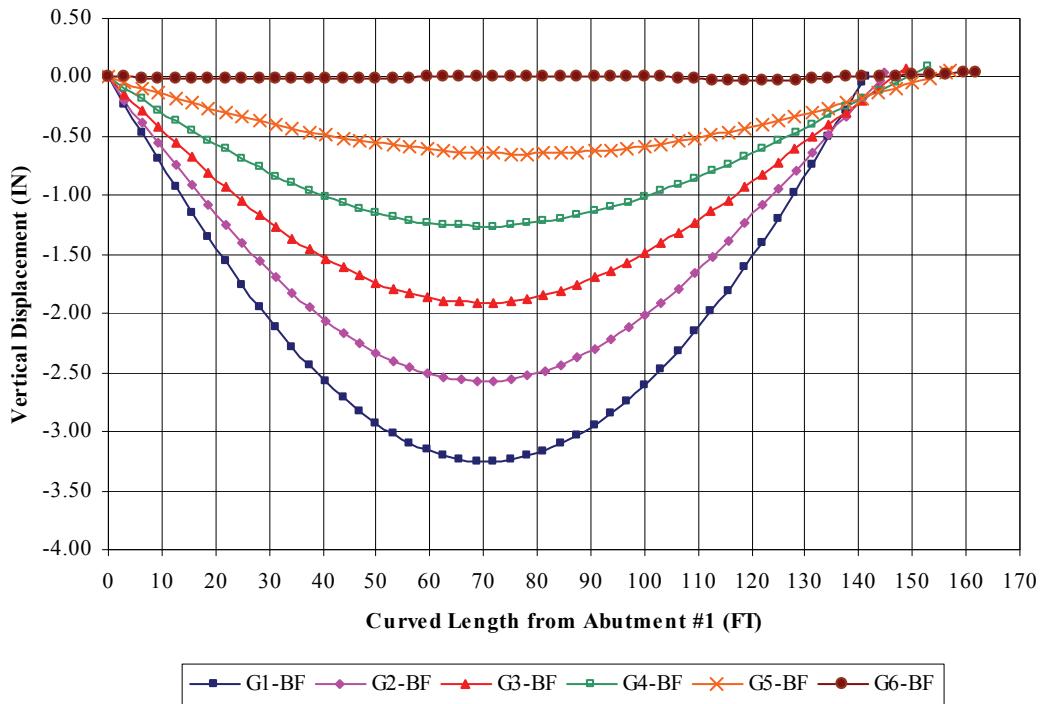


Figure B.110 Construction Stage F6a – Girder Lateral Displacement



**Figure B.111** Construction Stage F6a – Girder Out-of-Plane Rotation



**Figure B.112** Construction Stage F6b – Girder Vertical Displacement

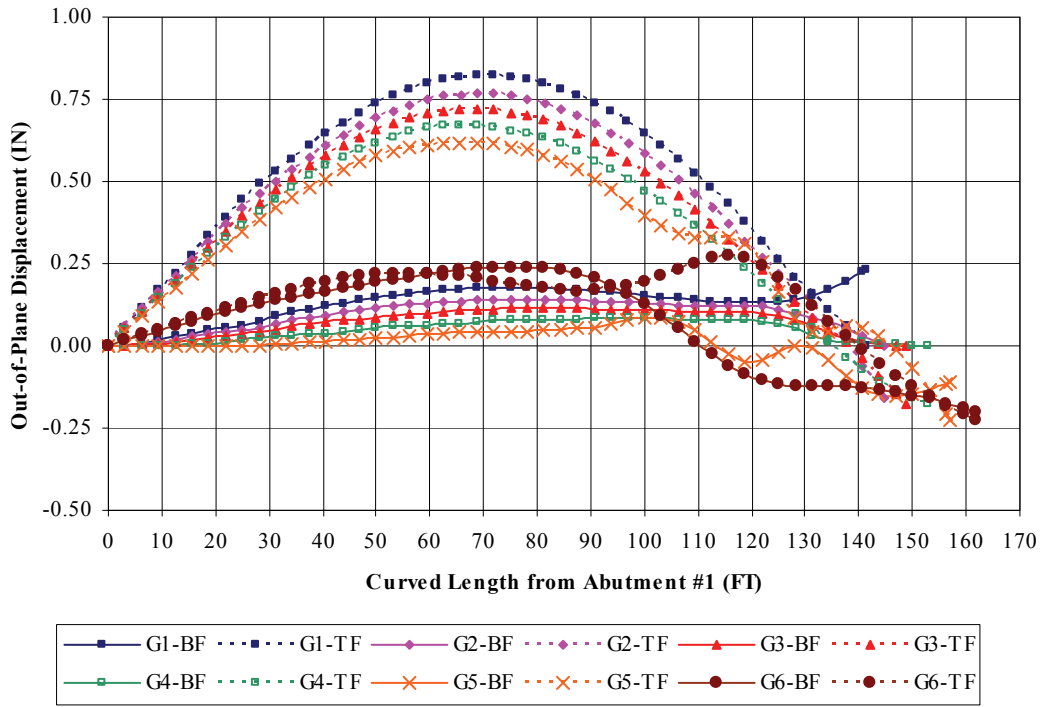


Figure B.113 Construction Stage F6b – Girder Lateral Displacement

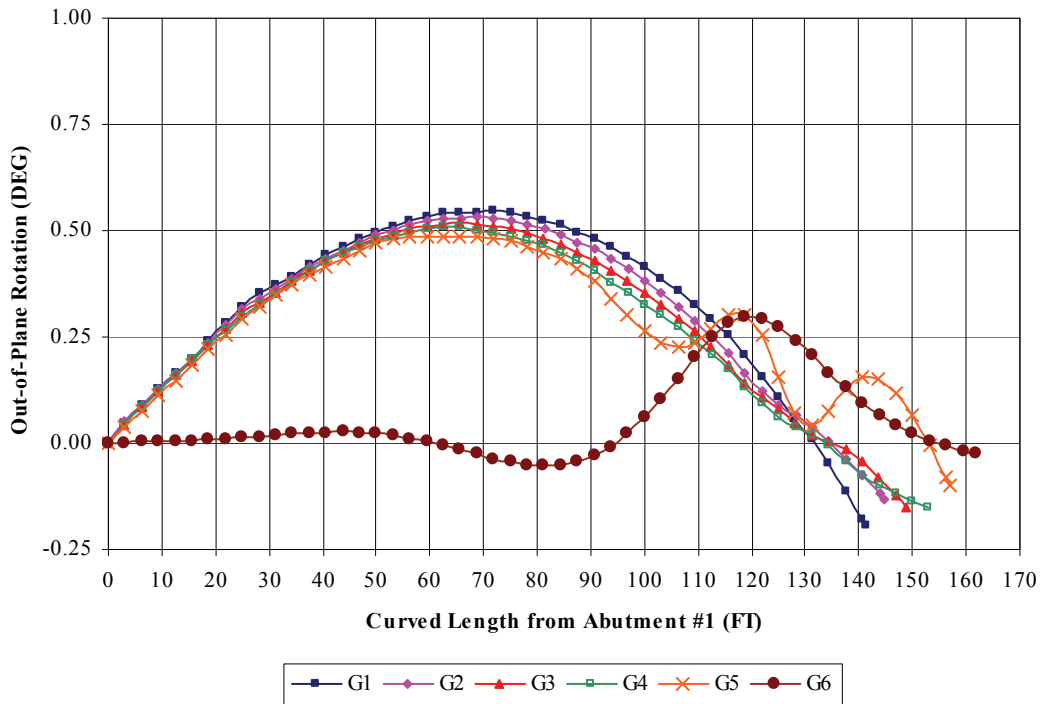


Figure B.114 Construction Stage F6b – Girder Out-of-Plane Rotation

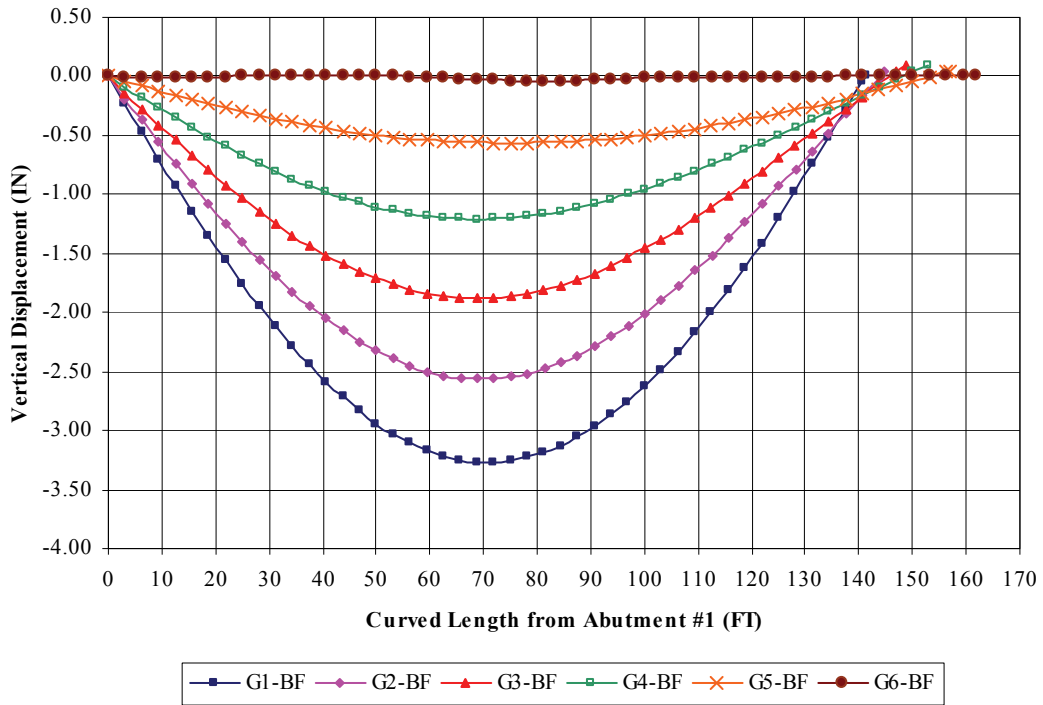


Figure B.115 Construction Stage F6c – Girder Vertical Displacement

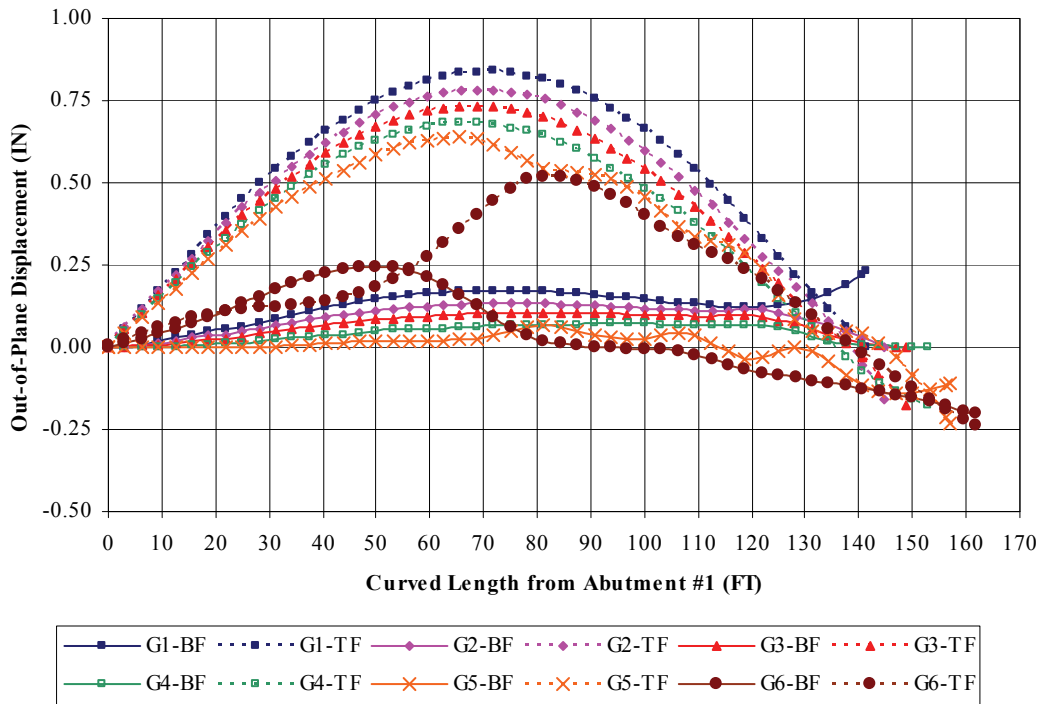
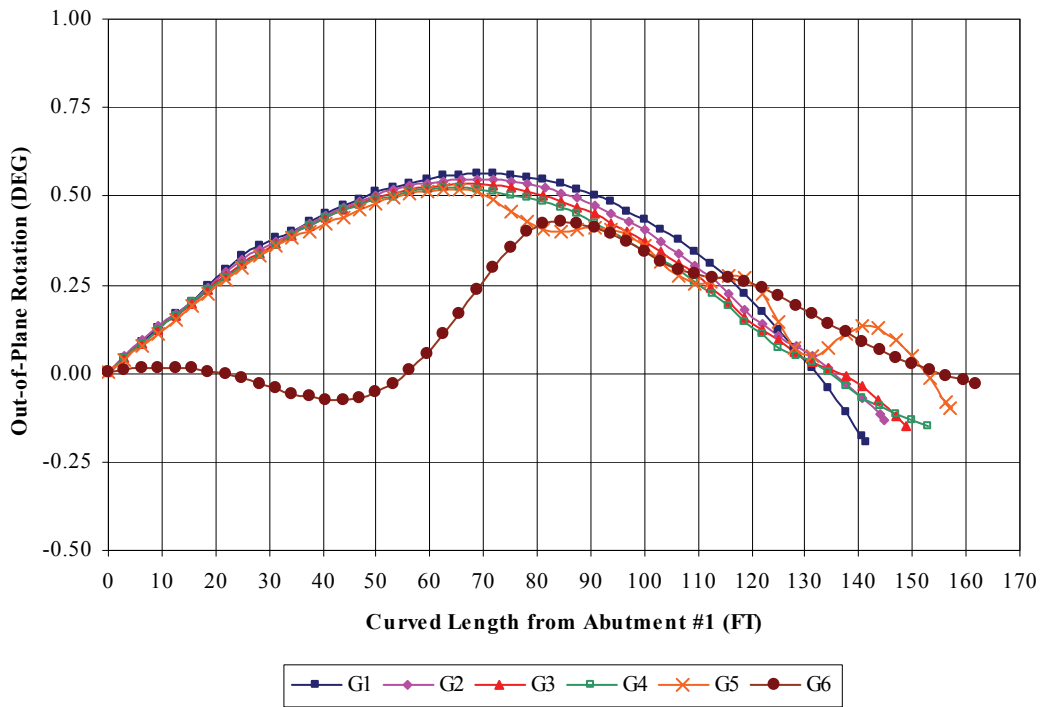
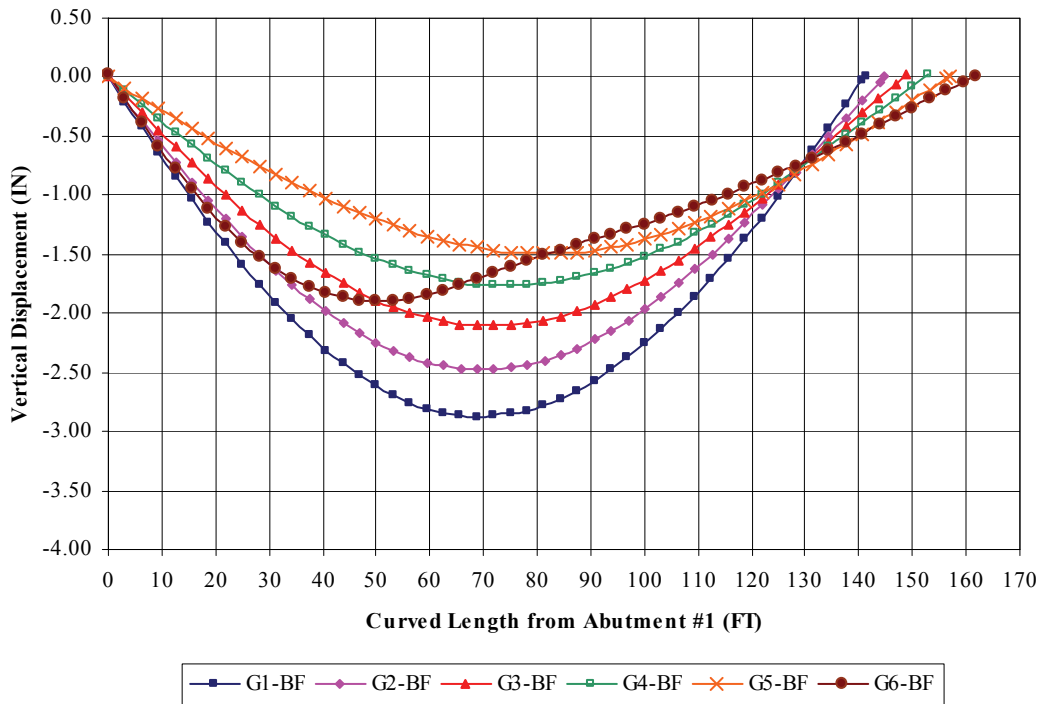


Figure B.116 Construction Stage F6c – Girder Lateral Displacement



**Figure B.117** Construction Stage F6c – Girder Out-of-Plane Rotation



**Figure B.118** Construction Stage F6c1 – Girder Vertical Displacement

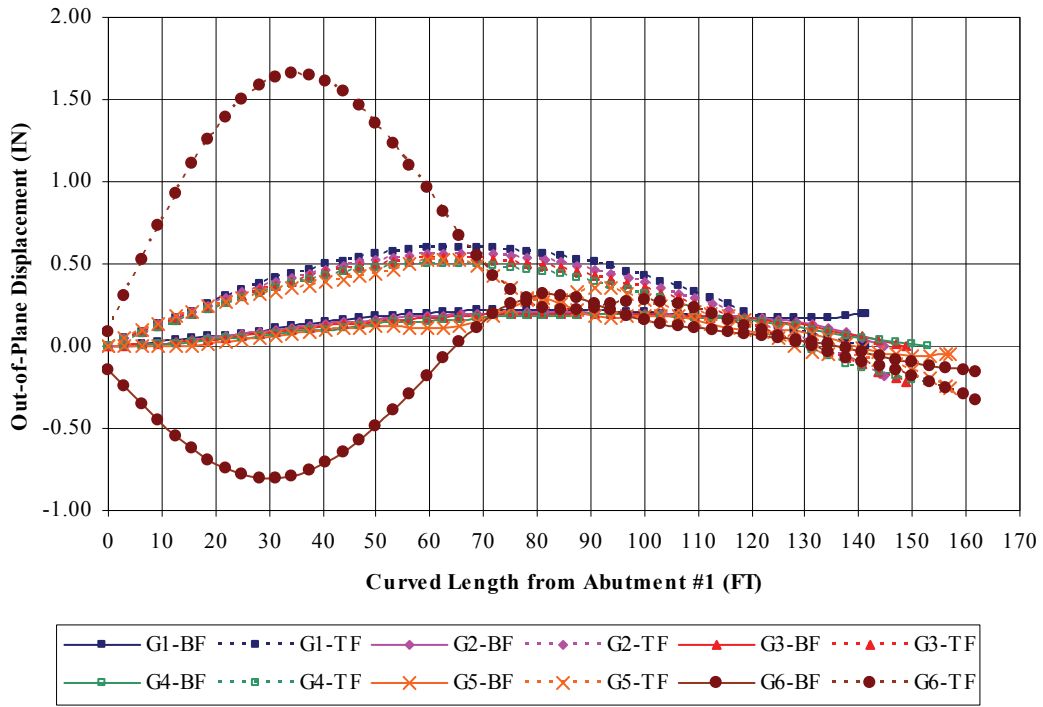


Figure B.119 Construction Stage F6c1 – Girder Lateral Displacement

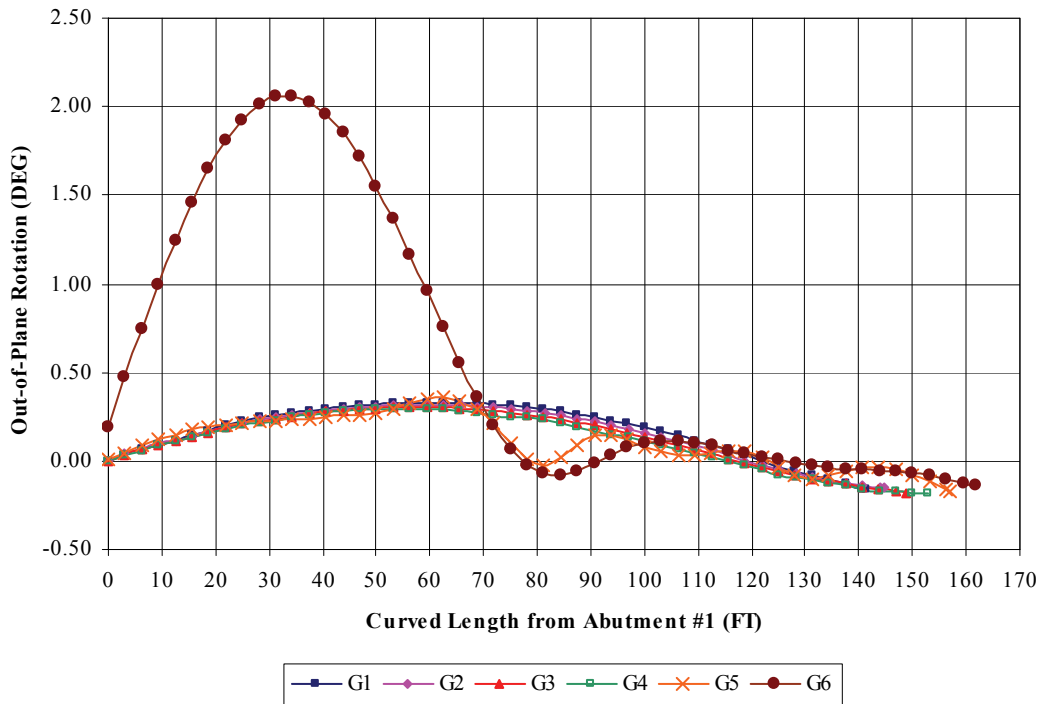


Figure B.120 Construction Stage F6c1 – Girder Out-of-Plane Rotation

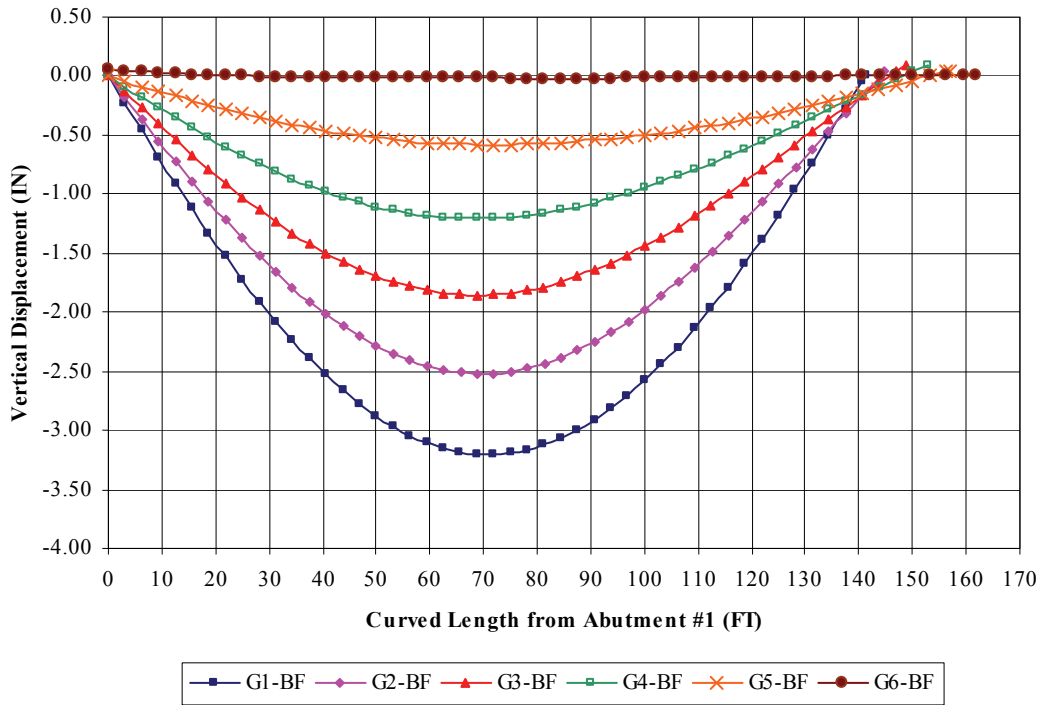


Figure B.121 Construction Stage F6d – Girder Vertical Displacement

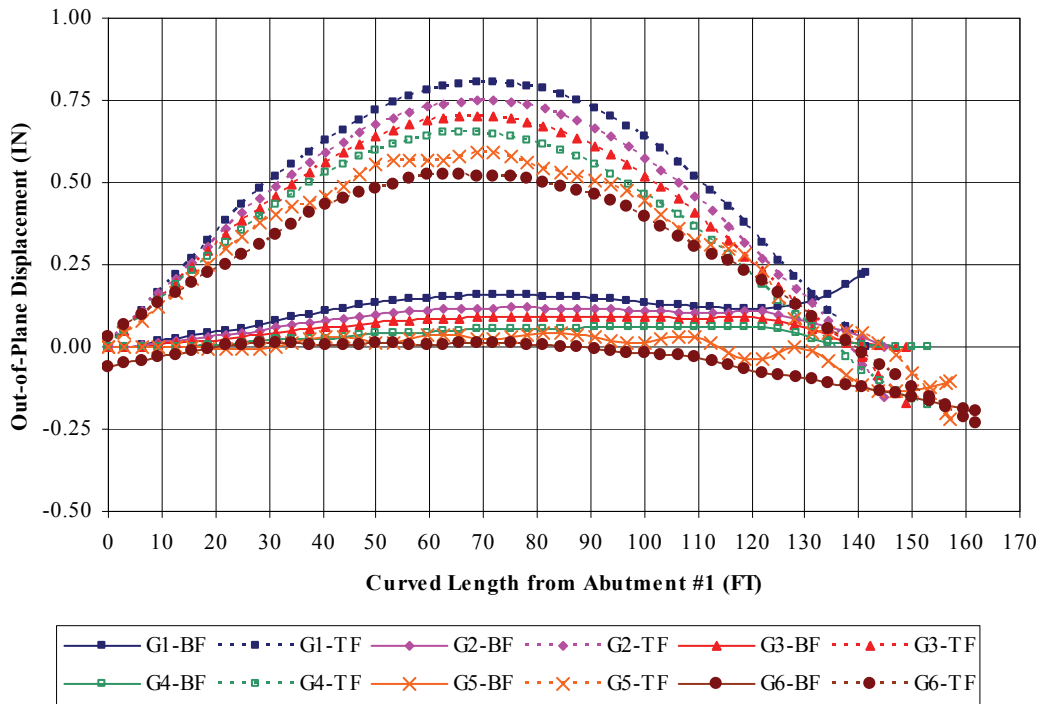
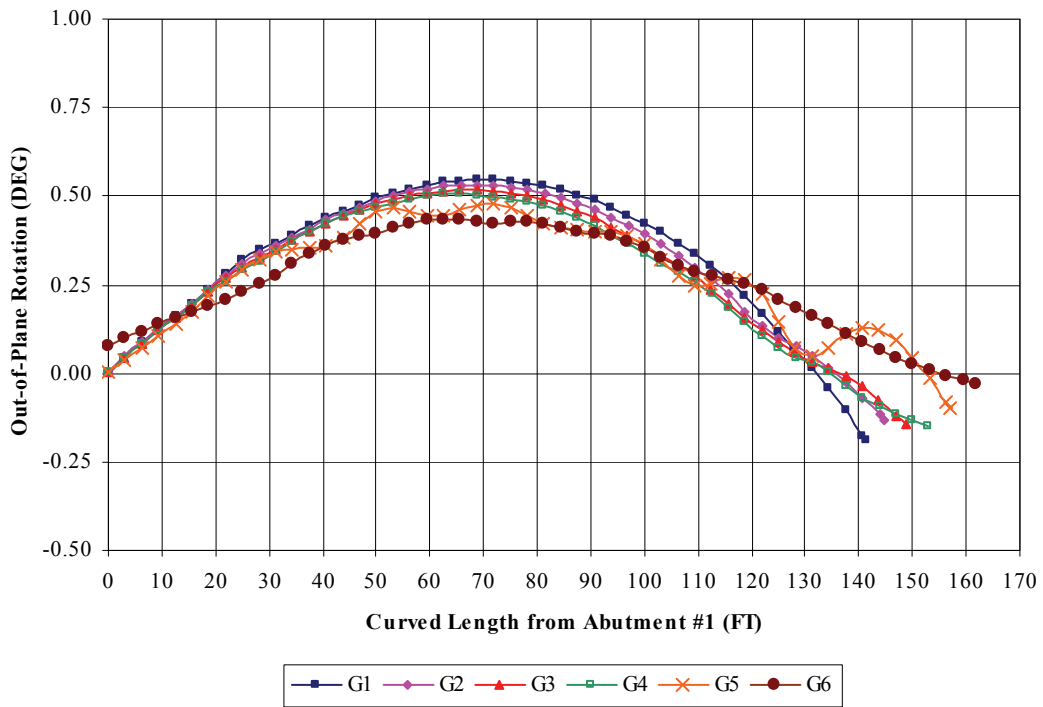
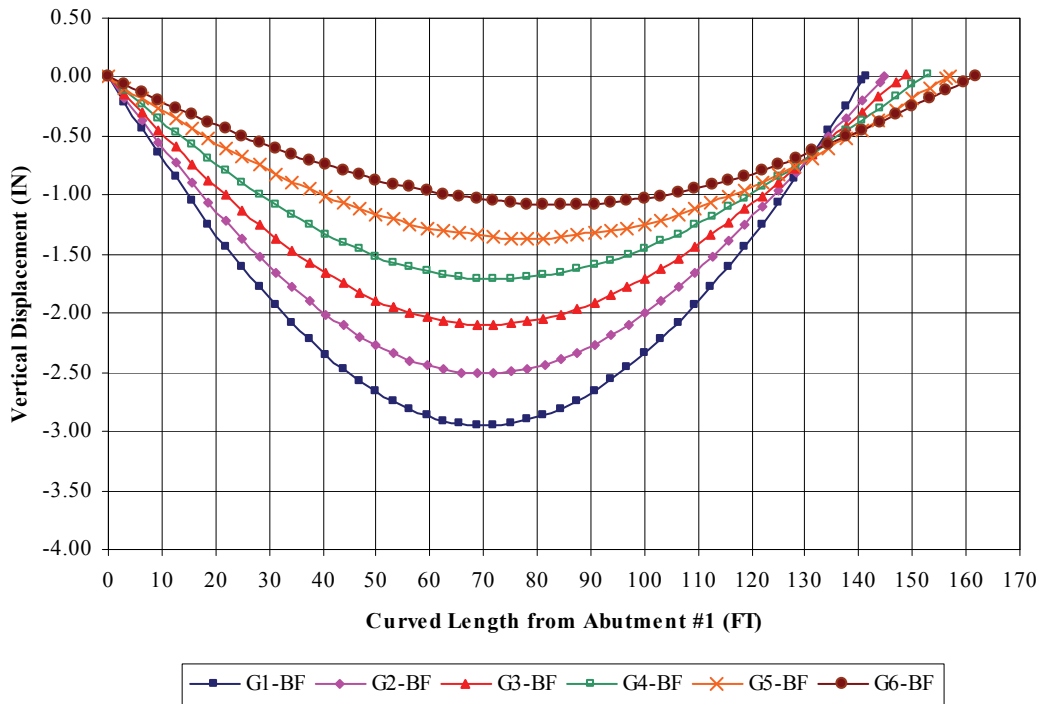


Figure B.122 Construction Stage F6d – Girder Lateral Displacement



**Figure B.123** Construction Stage F6d – Girder Out-of-Plane Rotation



**Figure B.124** Construction Stage F6d1 – Girder Vertical Displacement

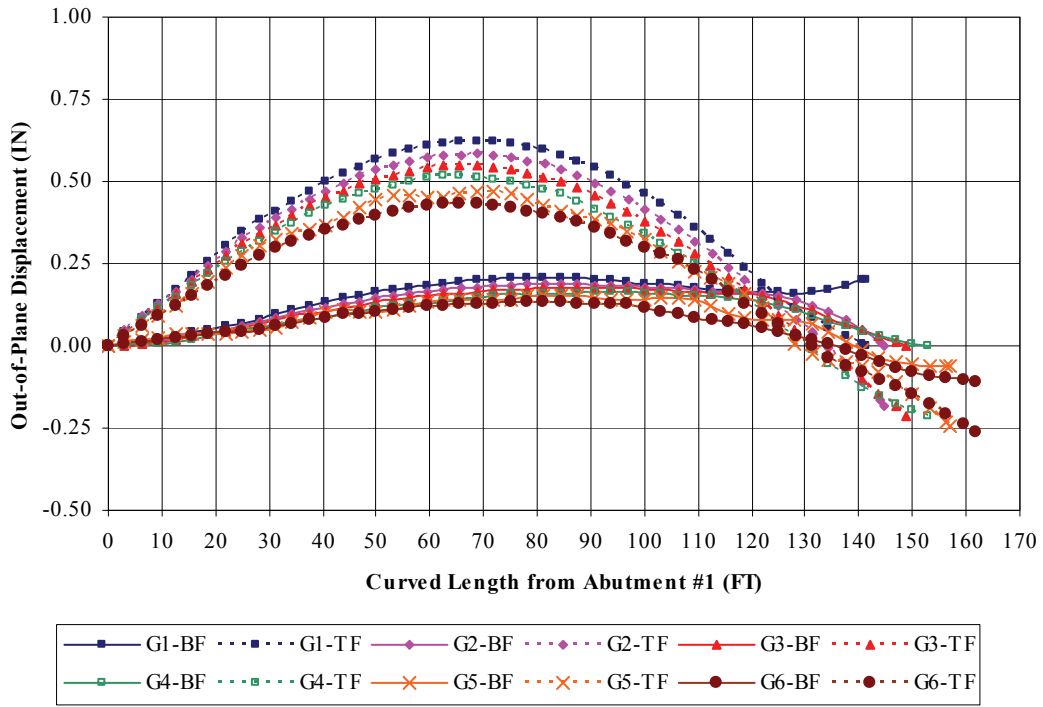


Figure B.125 Construction Stage F6d1 – Girder Lateral Displacement

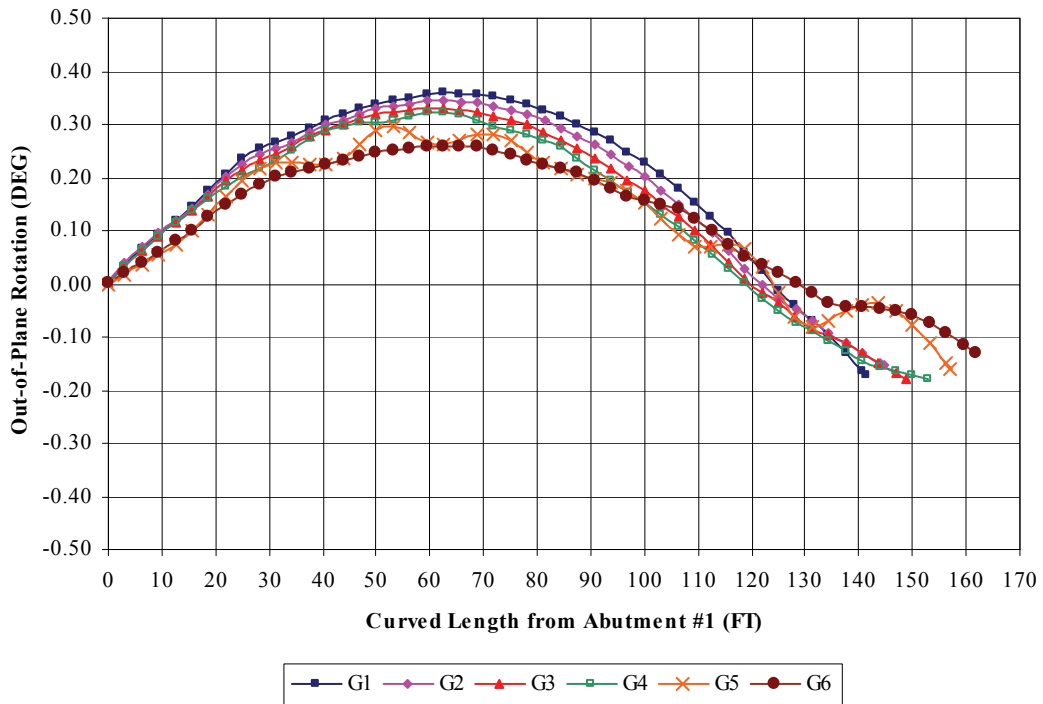


Figure B.126 Construction Stage F6d1 – Girder Out-of-Plane Rotation

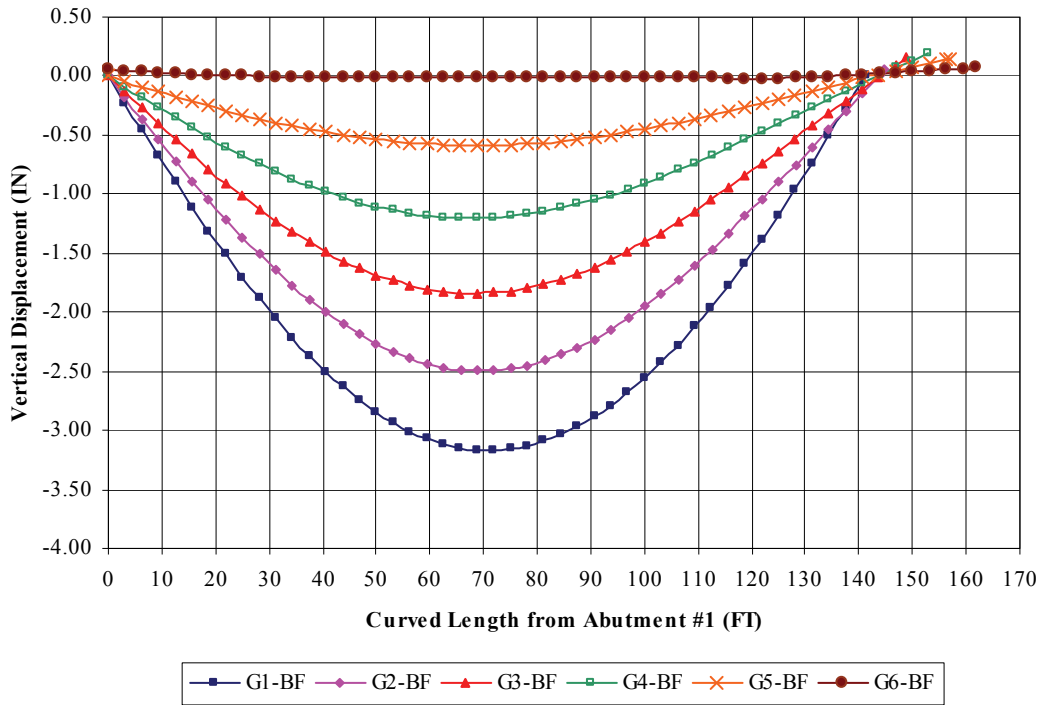


Figure B.127 Construction Stage F6e – Girder Vertical Displacement

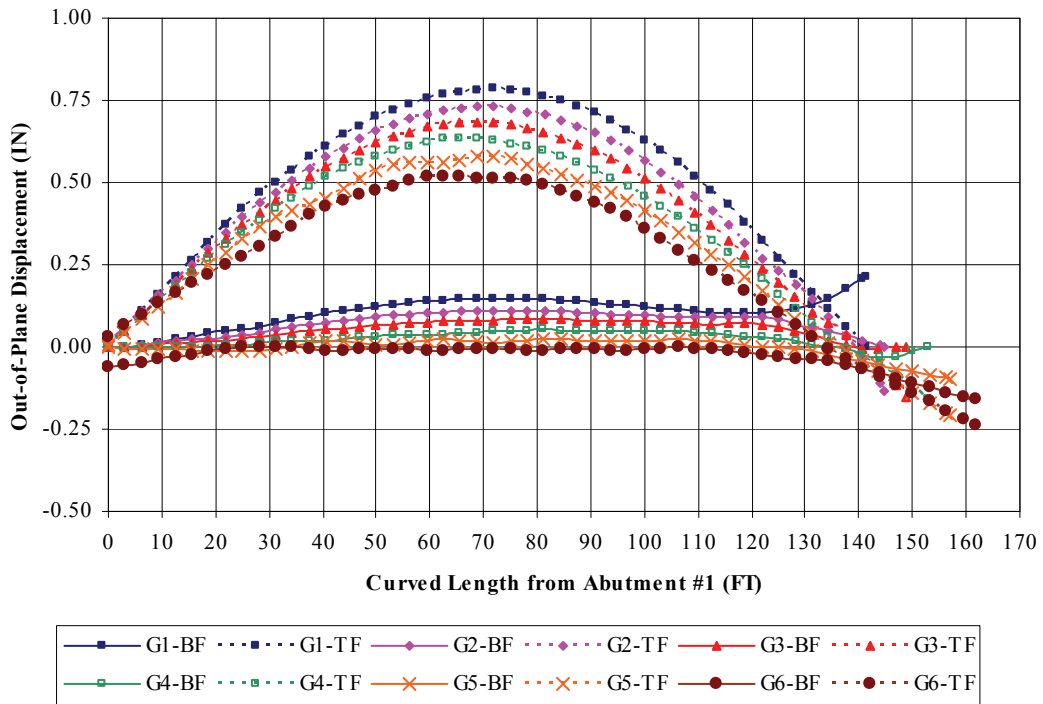
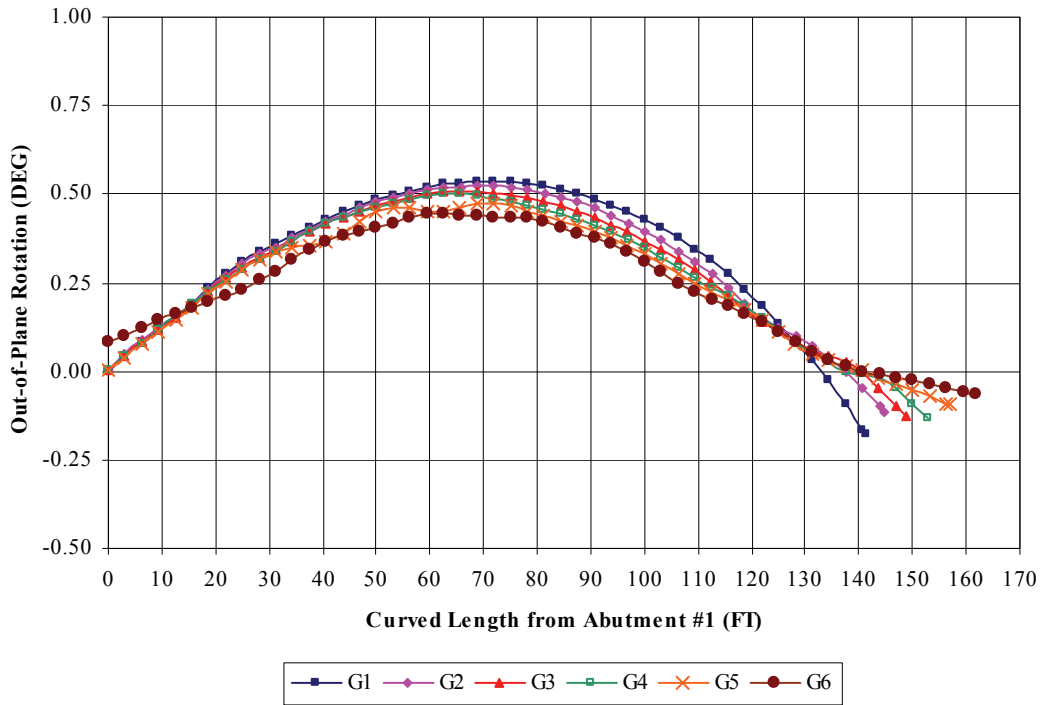
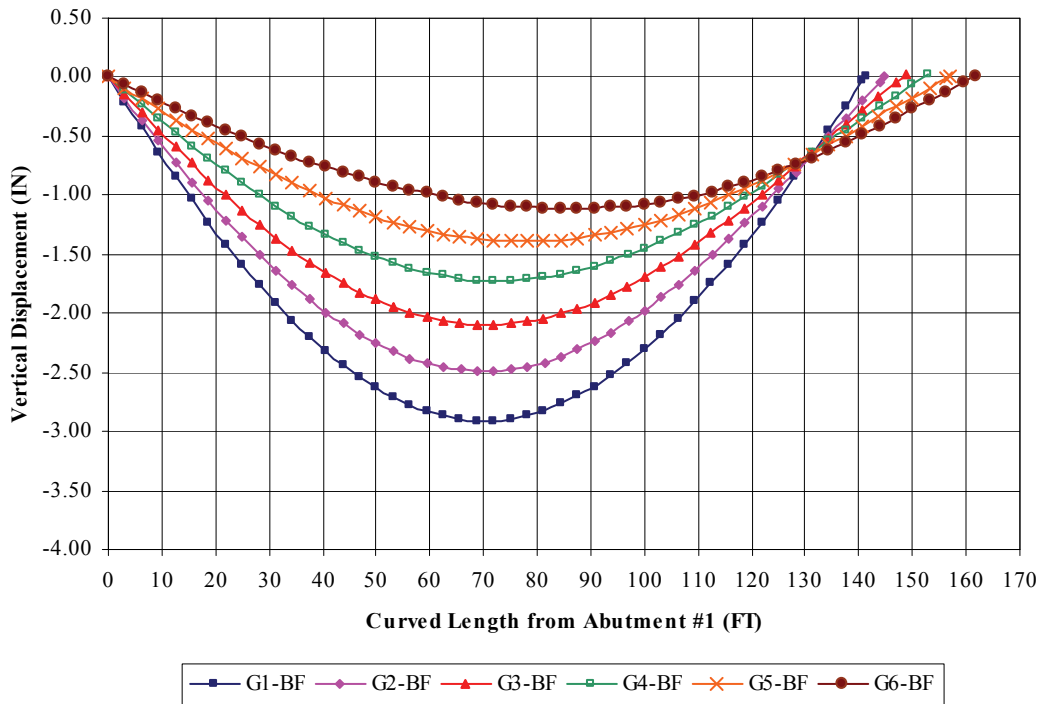


Figure B.128 Construction Stage F6e – Girder Lateral Displacement



**Figure B.129** Construction Stage F6e – Girder Out-of-Plane Rotation



**Figure B.130** Construction Stage F6e1 – Girder Vertical Displacement

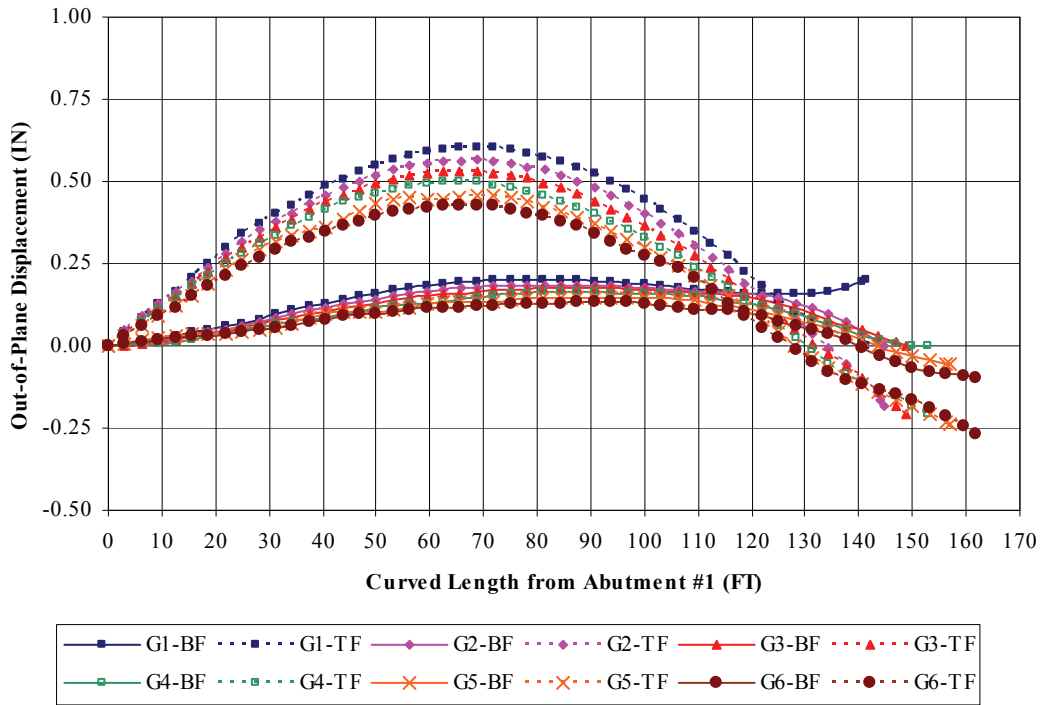


Figure B.131 Construction Stage F6e1 – Girder Lateral Displacement

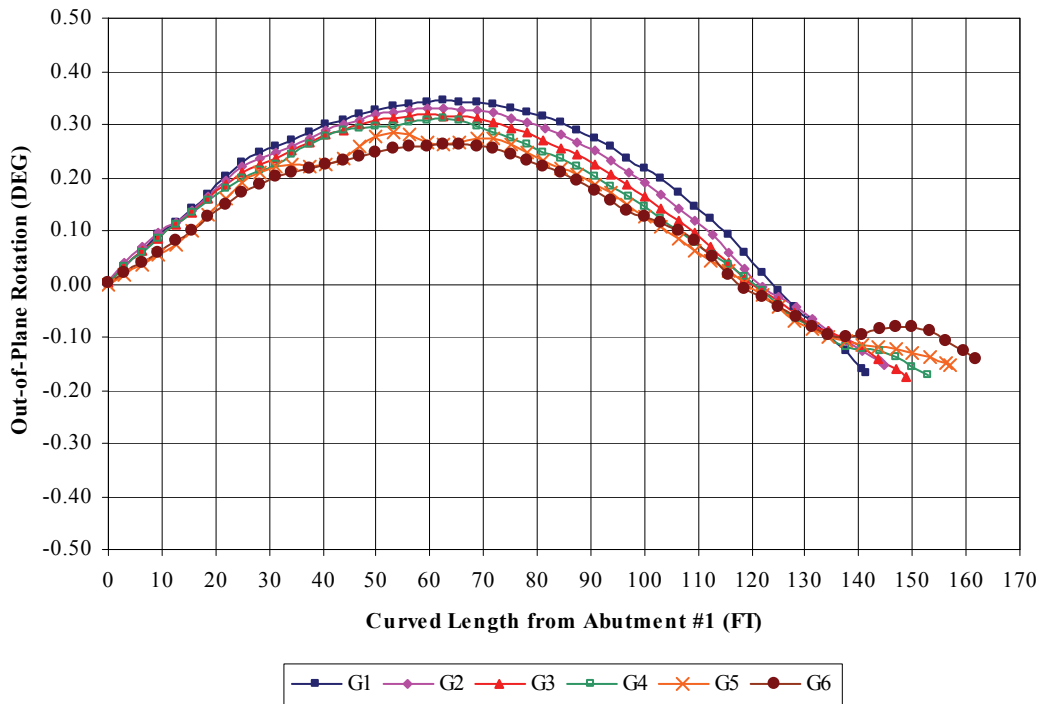


Figure B.132 Construction Stage F6e1 – Girder Out-of-Plane Rotation

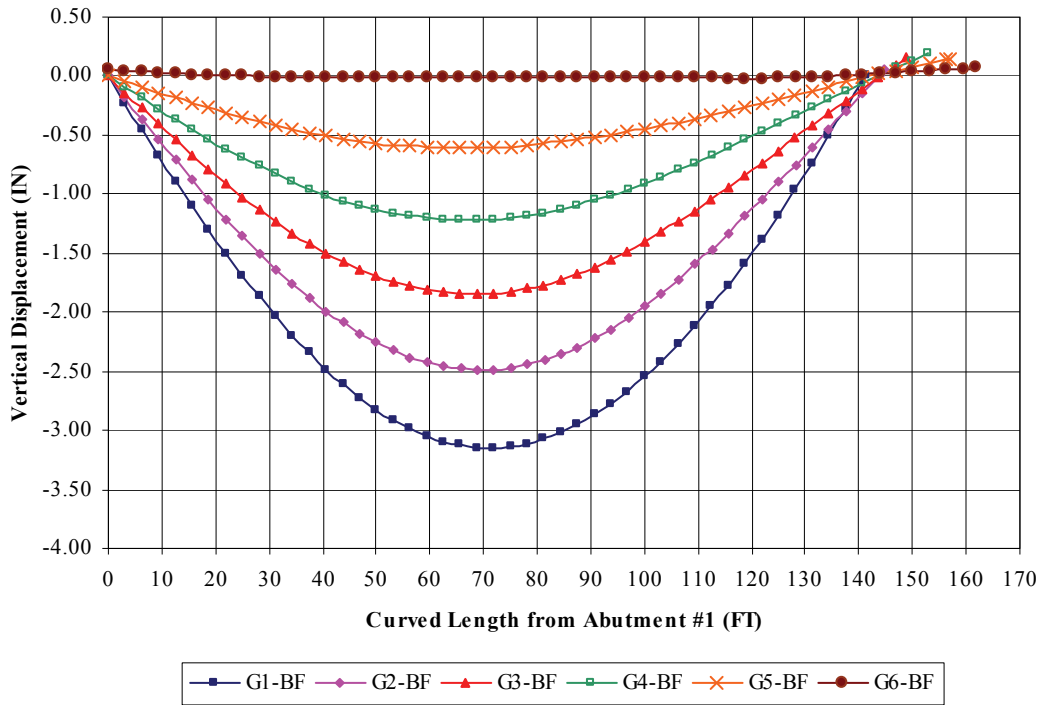


Figure B.133 Construction Stage F6f – Girder Vertical Displacement

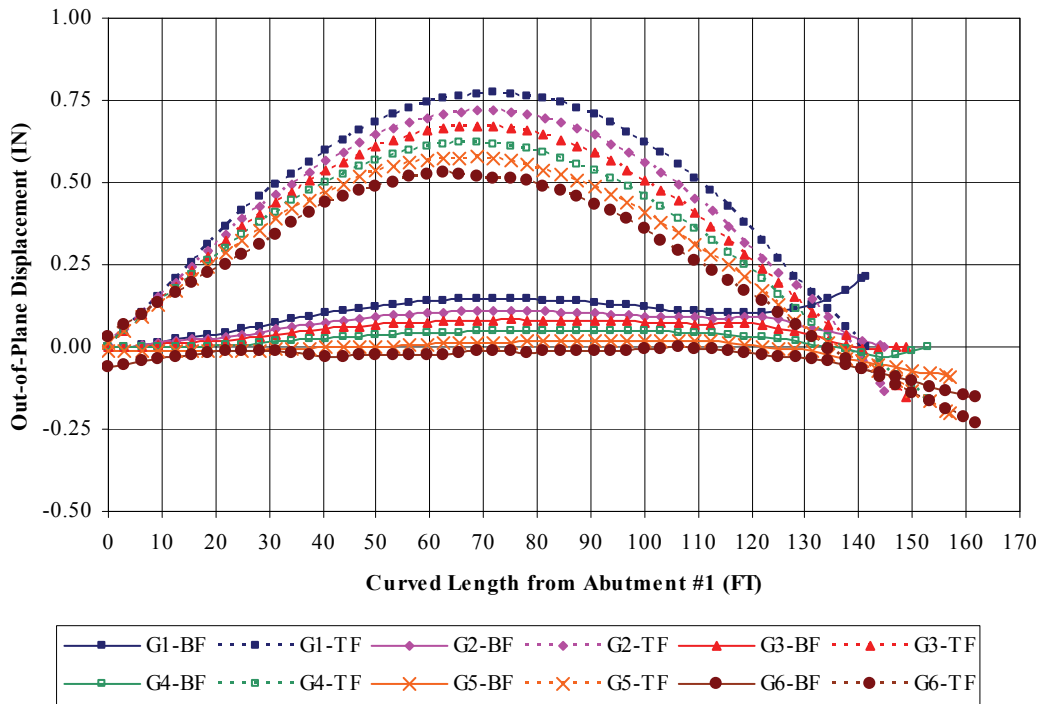


Figure B.134 Construction Stage F6f – Girder Lateral Displacement

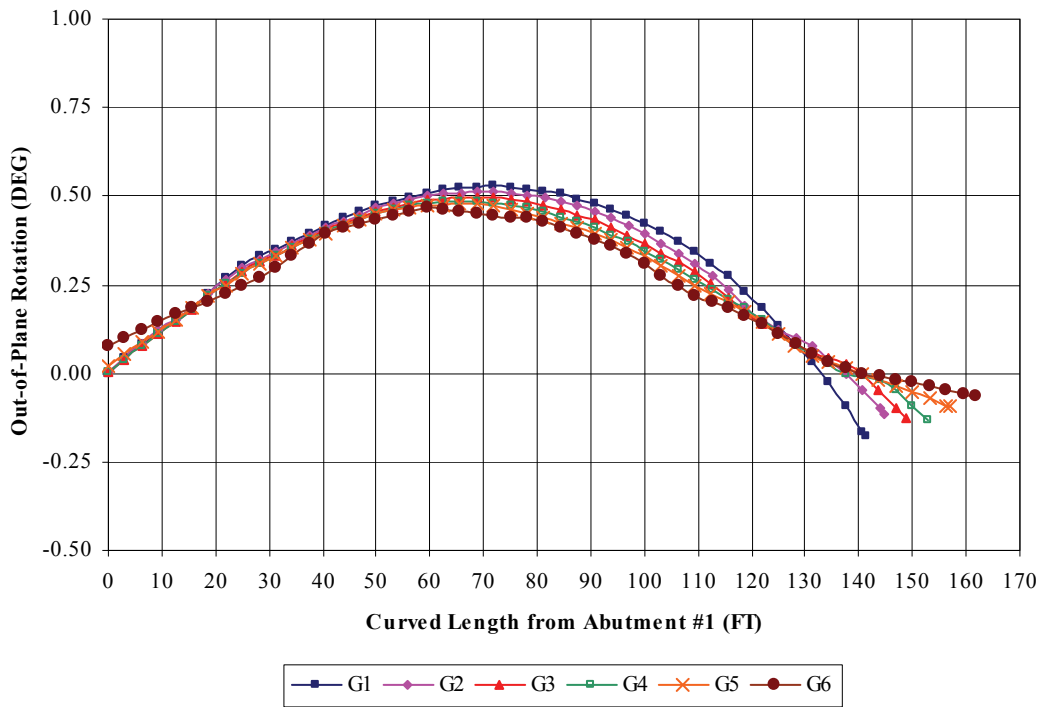


Figure B.135 Construction Stage F6f – Girder Out-of-Plane Rotation

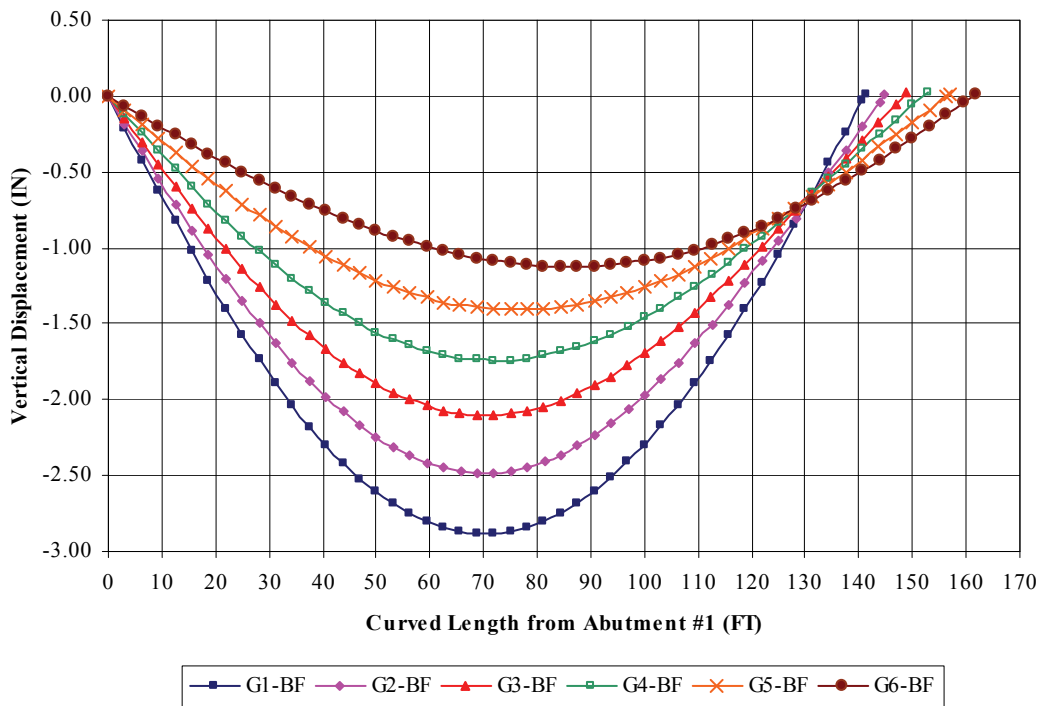


Figure B.136 Construction Stage F6f1 – Girder Vertical Displacement

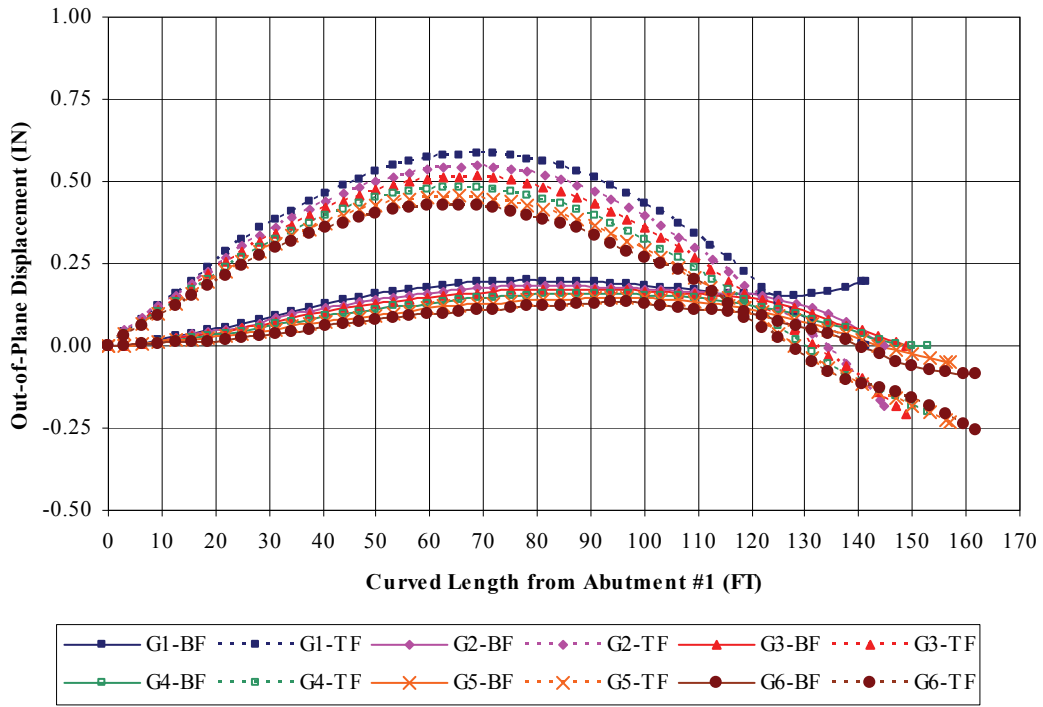


Figure B.137 Construction Stage F6f1 – Girder Lateral Displacement

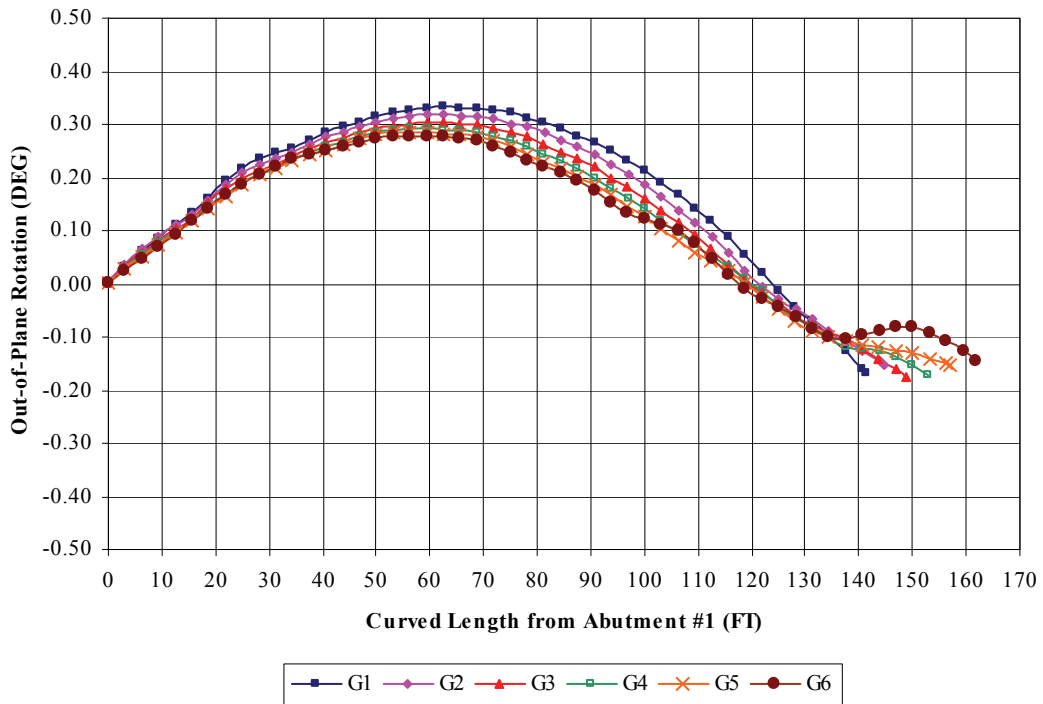


Figure B.138 Construction Stage F6f1 – Girder Out-of-Plane Rotation

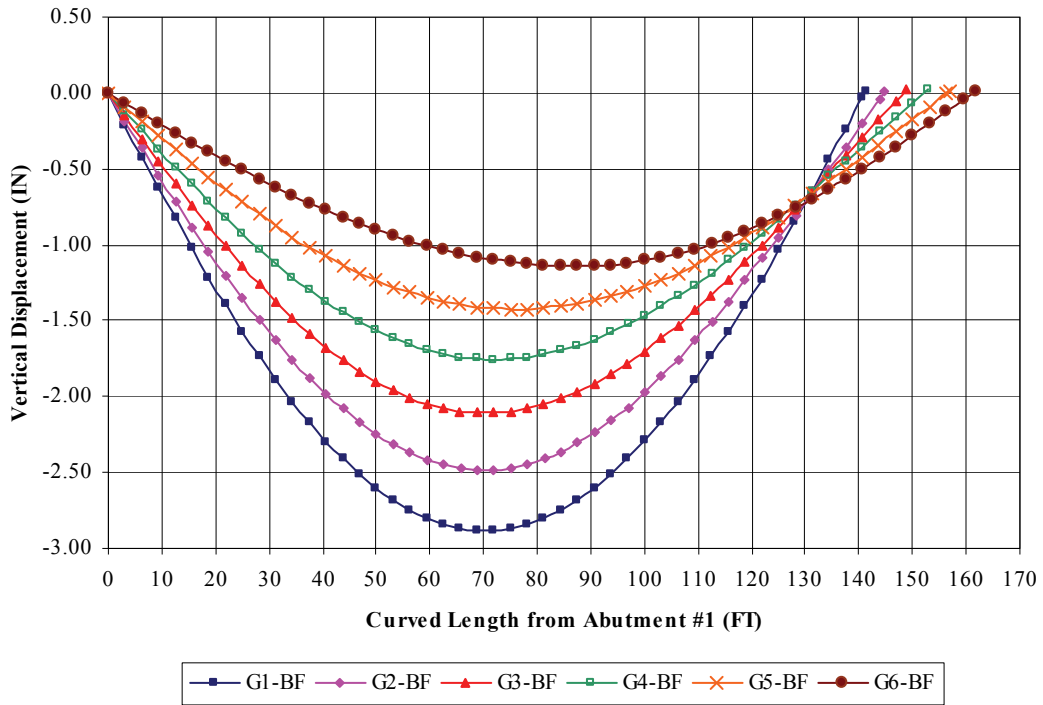


Figure B.139 Construction Stage 6d2 – Girder Vertical Displacement

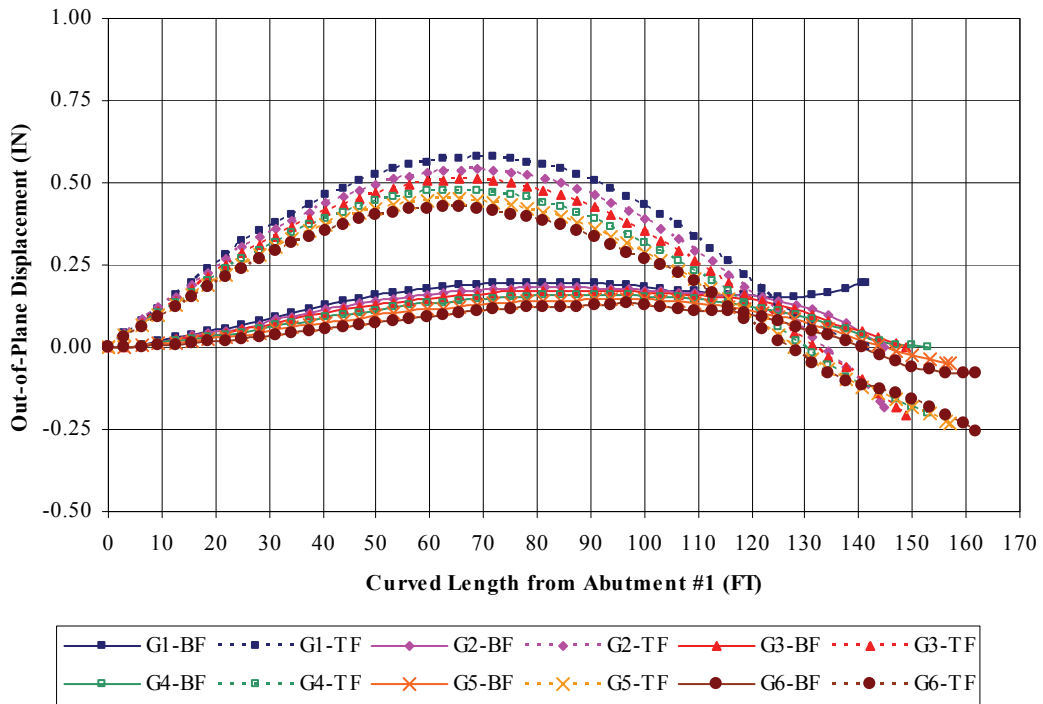
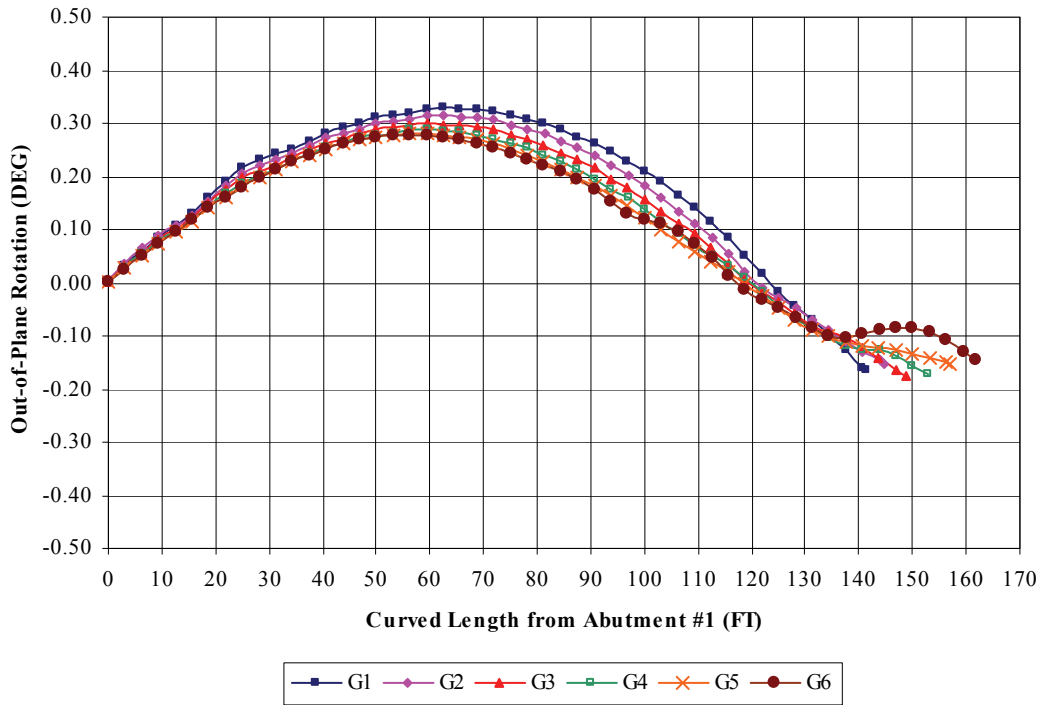
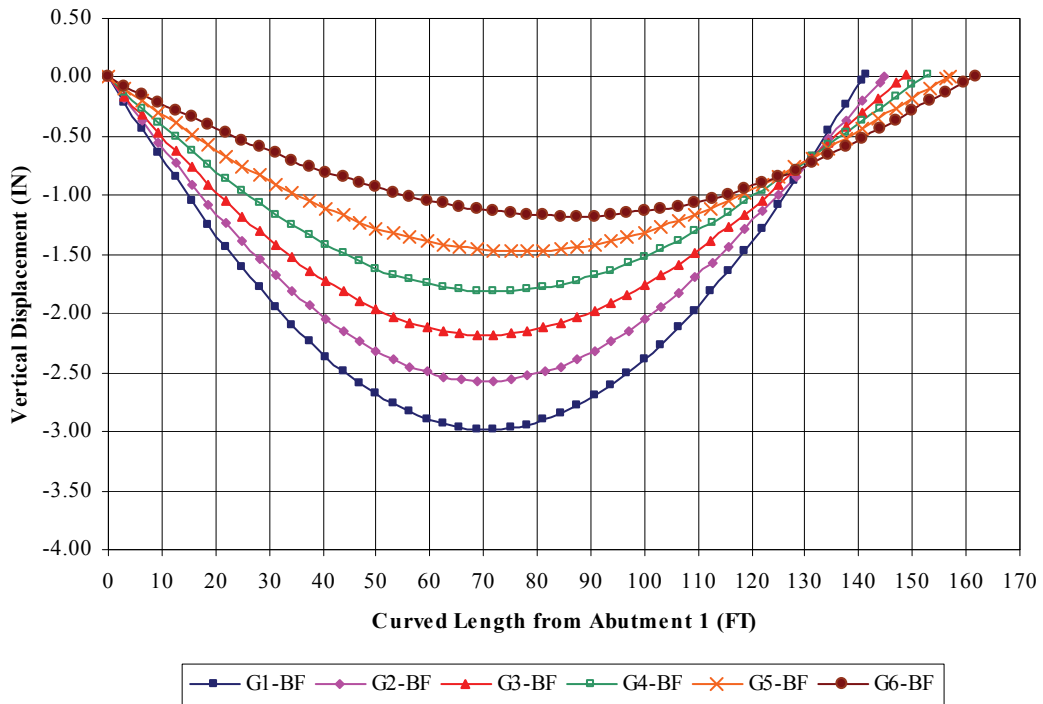


Figure B.140 Construction Stage 6d2 – Girder Lateral Displacement



**Figure B.141** Construction Stage 6d2 – Girder Out-of-Plane Rotation



**Figure B.142** Construction Stage 6e2 (Final) – Girder Vertical Displacement

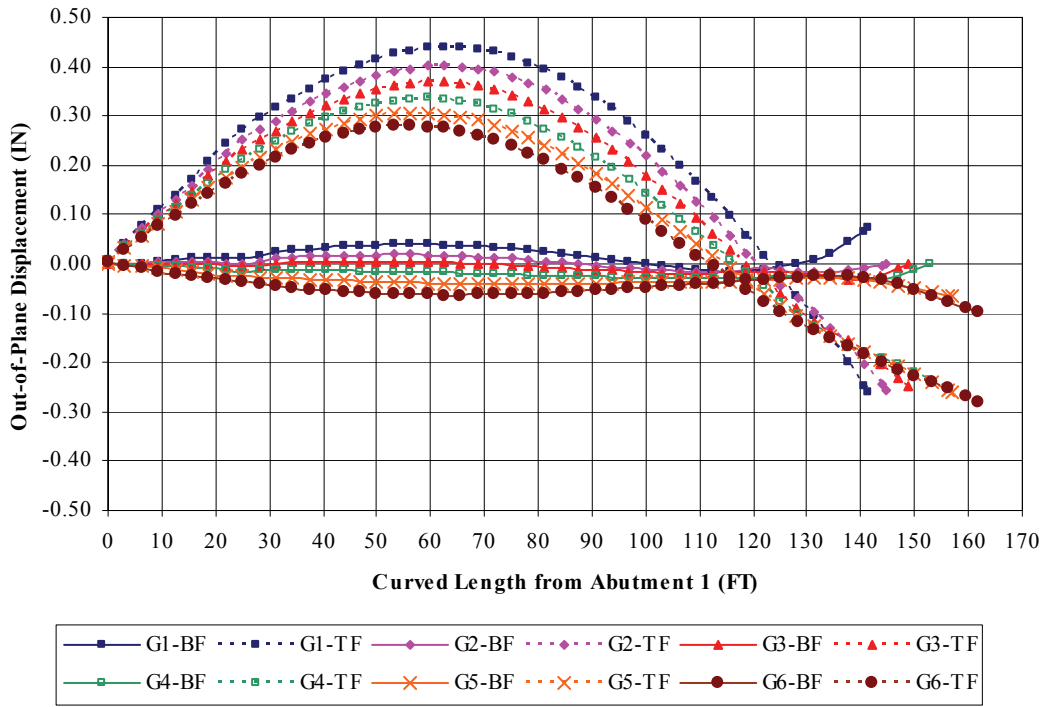


**Figure B.143** Construction Stage 6e2 (Final) – Girder Lateral Displacement

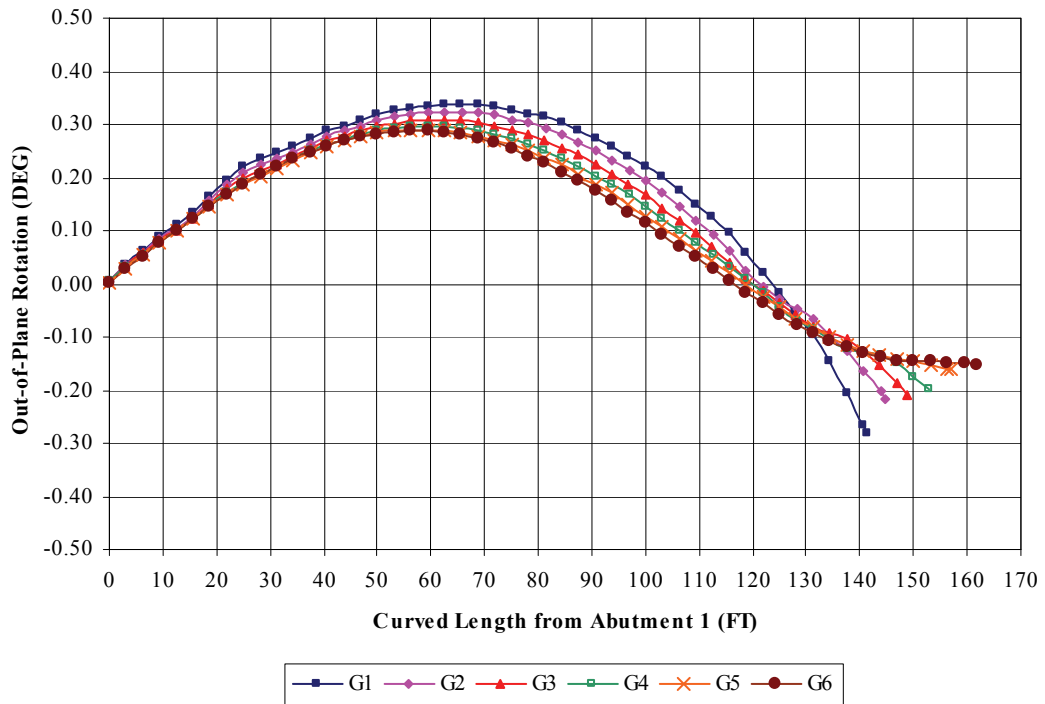


**Figure B.144** Construction Stage 6e2 (Final) – Girder Out-of-Plane Rotation

## B.2 INTENDED ERECTION SEQUENCE ANALYTICAL RESULTS

Results are presented for the intended (as-planned) erection sequence analytical studies. For each construction stage the following three figures are included:

- A. Figure ‘A’ – Girder Vertical Displacement
- B. Figure ‘B’ – Girder Lateral (out-of-plane) Displacement
- C. Figure ‘C’ – Girder Out-of-Plane Rotation

Table B-2 shows the naming convention for each stage and structural configuration analyzed. Note that in some cases a variation in boundary conditions (holding and lifting cranes) is investigated for several construction stages.

**Table B-2** Intended Erection Sequence Naming Convention

<b>Construction Stage Name</b>	<b>Additional Component(s) Placed in Finite Element Model</b>	<b>Holding Crane</b>	<b>Lifting Crane</b>
Stage 5e2	Cross-frames 8B, 10B, 13B, 17B	None	None
Stage 5f2	Cross-frames 2B, 4B, 6B	None	None
Stage 6a2	G6 and Cross-frames 1A and 19A	None	G6
Stage 6b2	Cross-frames 13A and 17A	None	G6
Stage 6c2	Cross-frames 2A, 4A, 6A, 8A, 10A	None	G6
Stage 6c3	None	None	None
Stage 6d2	Cross-frames 3A, 5A, 7A	None	G6
Stage 6d3	None	None	None
Stage 6e3 (Final)	None	None	None

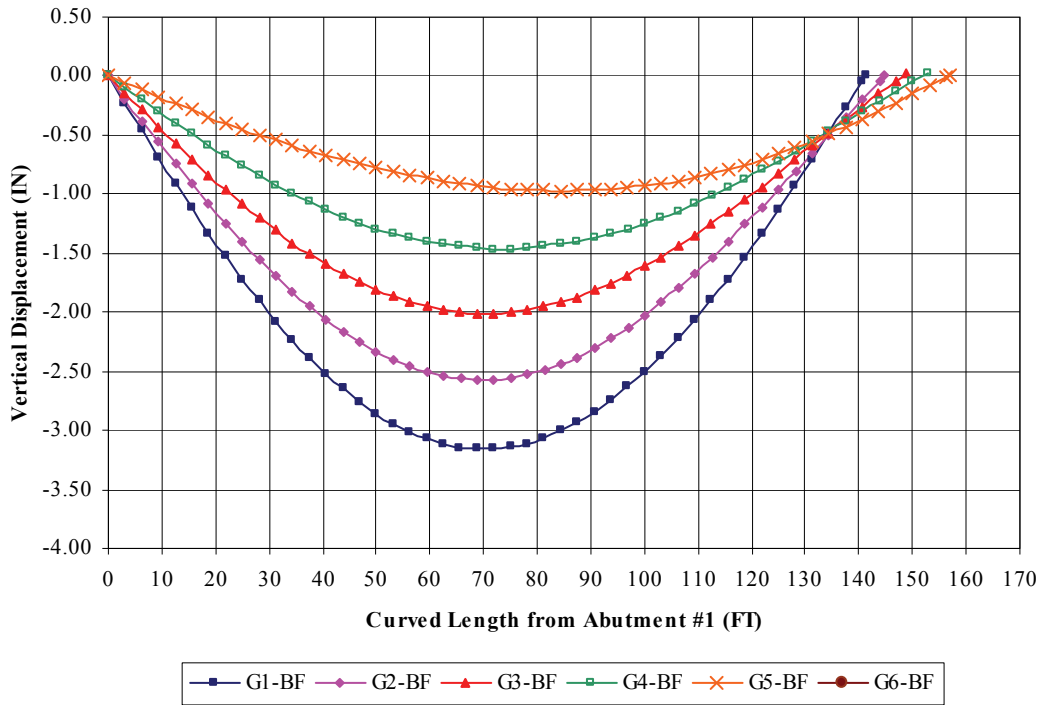


Figure B.145 Construction Stage 5e2 – Girder Vertical Displacement

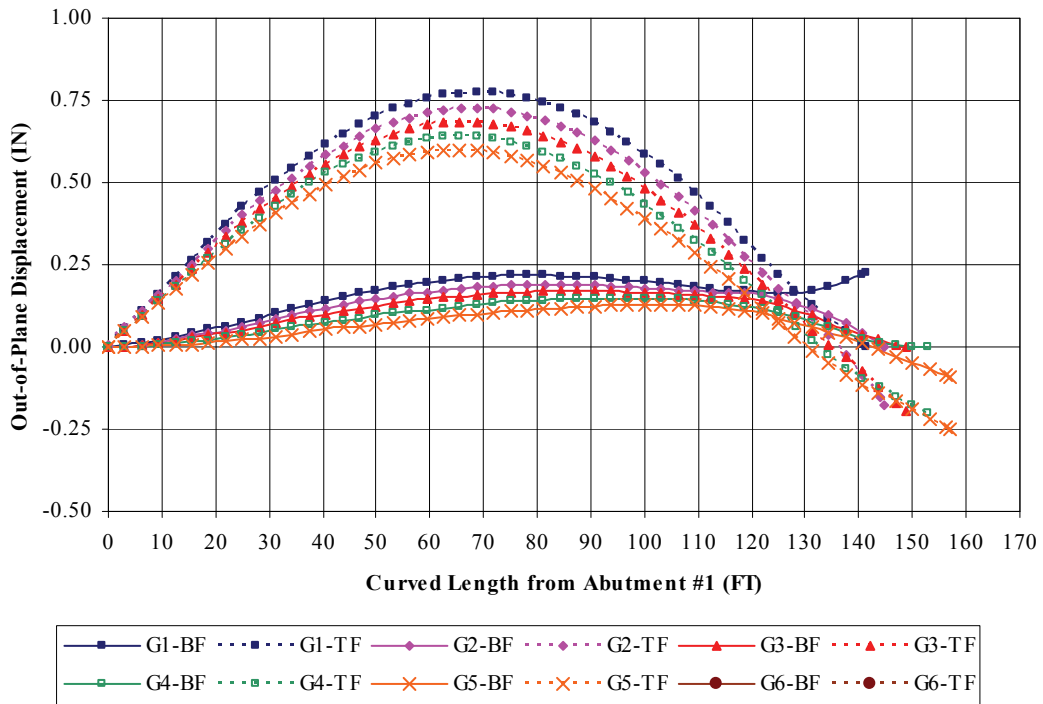
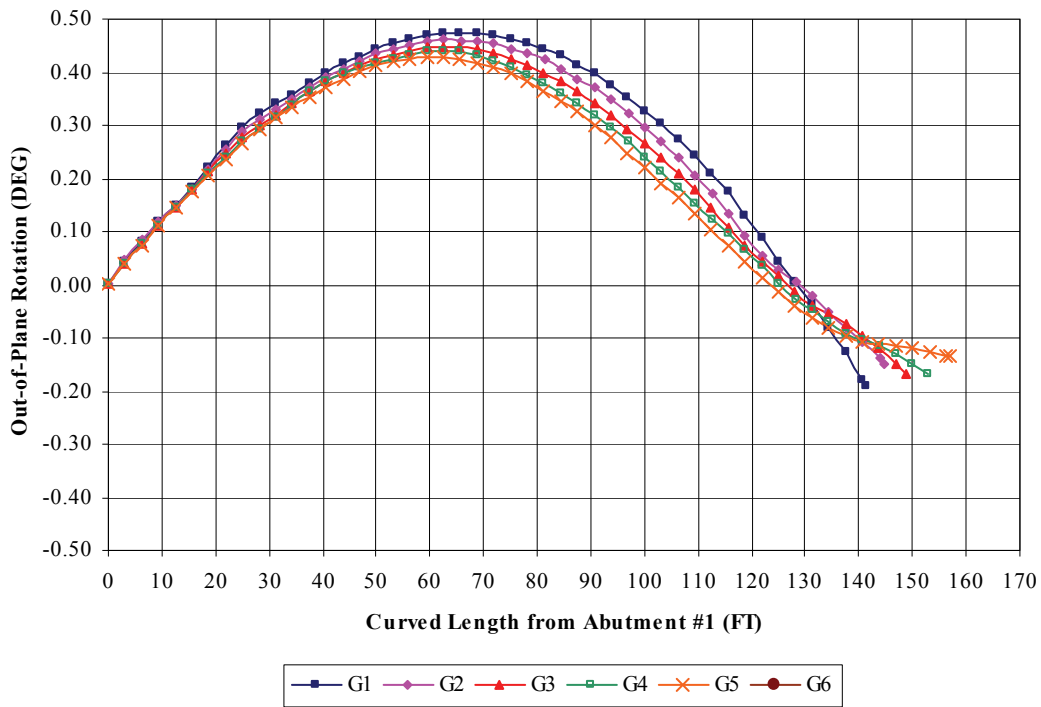
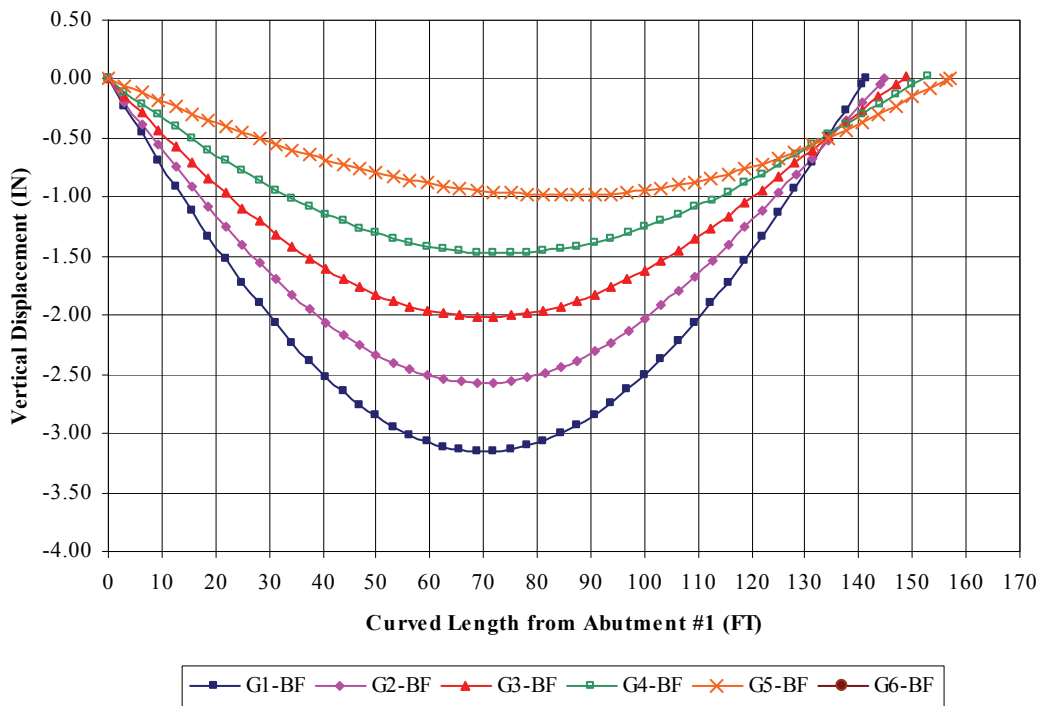


Figure B.146 Construction Stage 5e2 – Girder Lateral Displacement



**Figure B.147** Construction Stage 5e2 – Girder Out-of-Plane Rotation



**Figure B.148** Construction Stage 5f2 – Girder Vertical Displacement

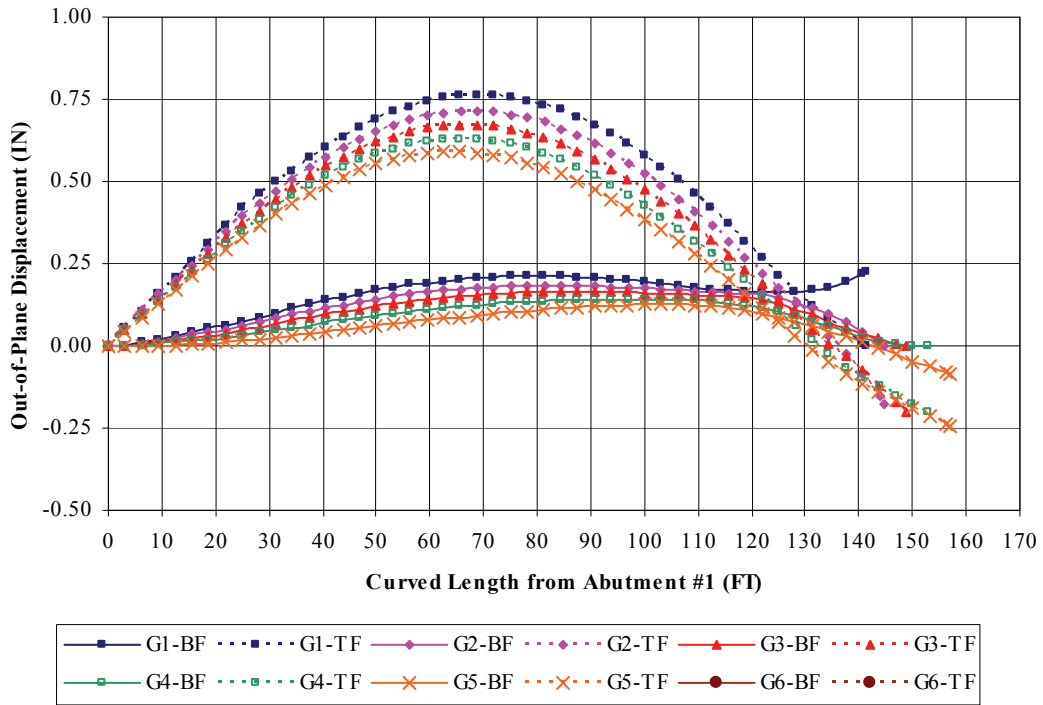


Figure B.149 Construction Stage 5f2 – Girder Lateral Displacement

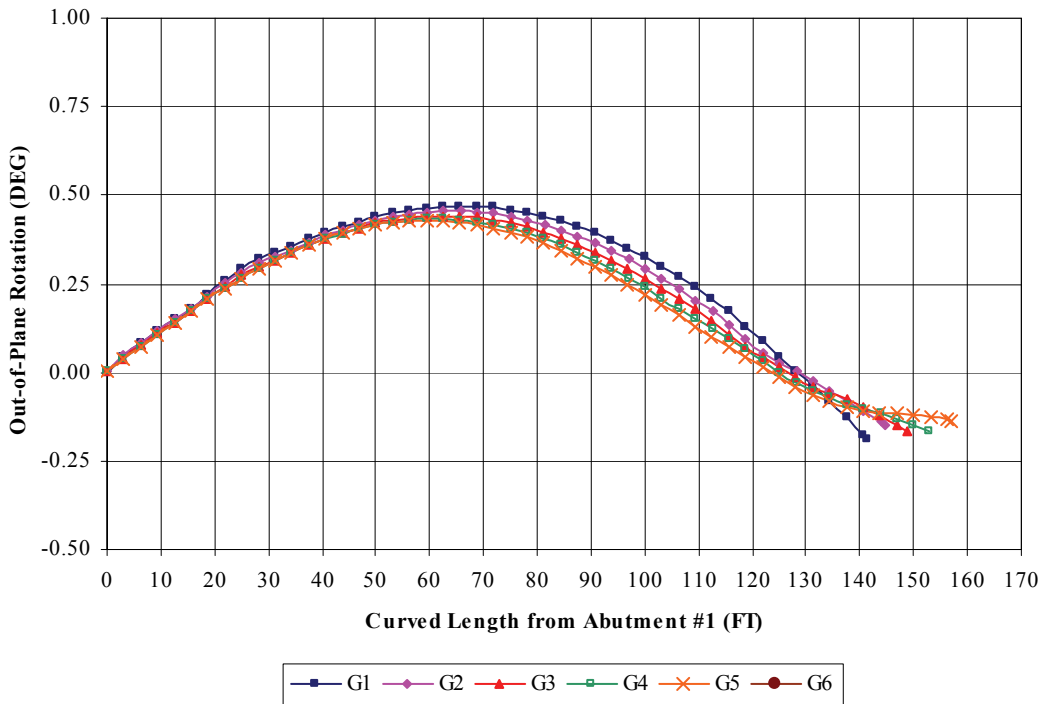


Figure B.150 Construction Stage 5f2 – Girder Out-of-Plane Rotation

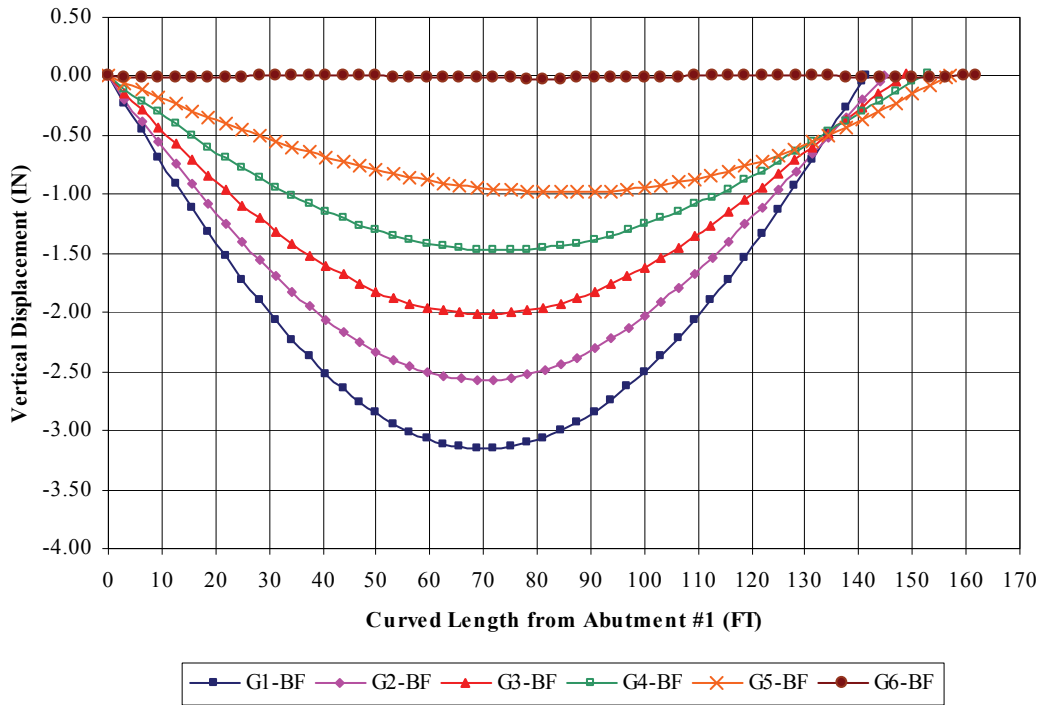


Figure B.151 Construction Stage 6a2 – Girder Vertical Displacement

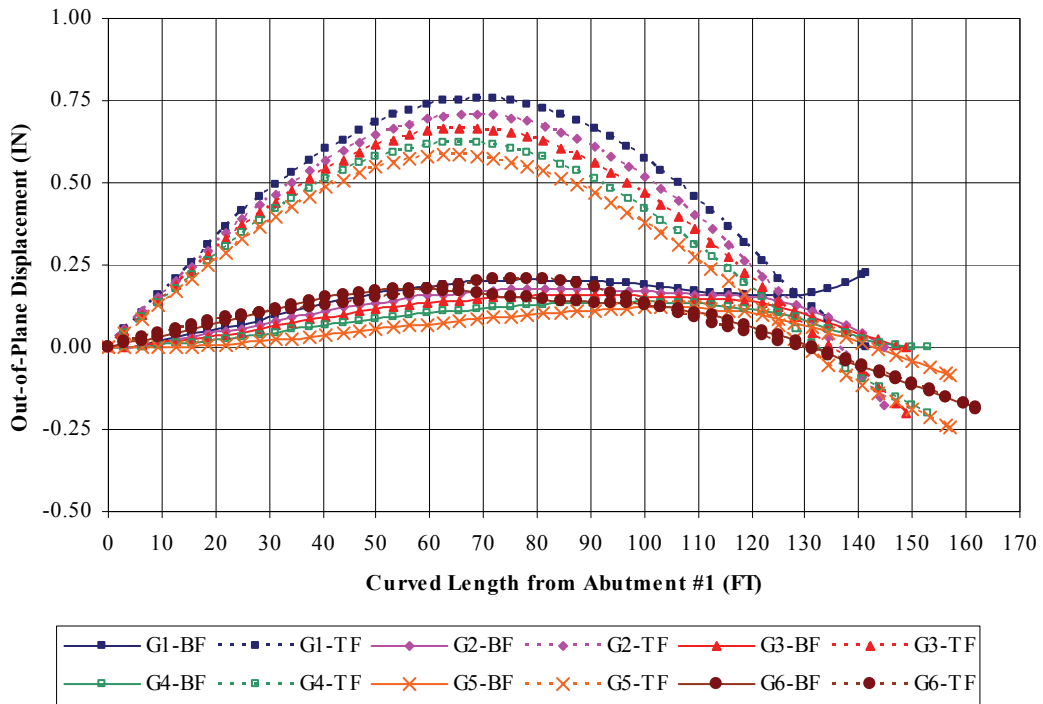


Figure B.152 Construction Stage 6a2 – Girder Lateral Displacement

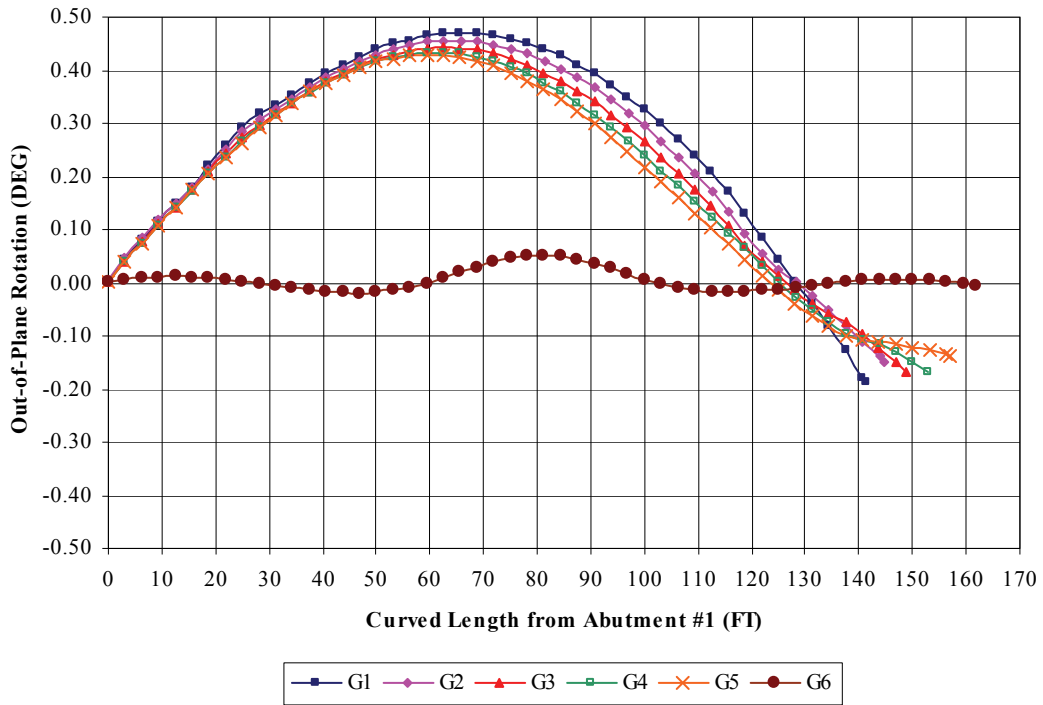


Figure B.153 Construction Stage 6a2 – Girder Out-of-Plane Rotation

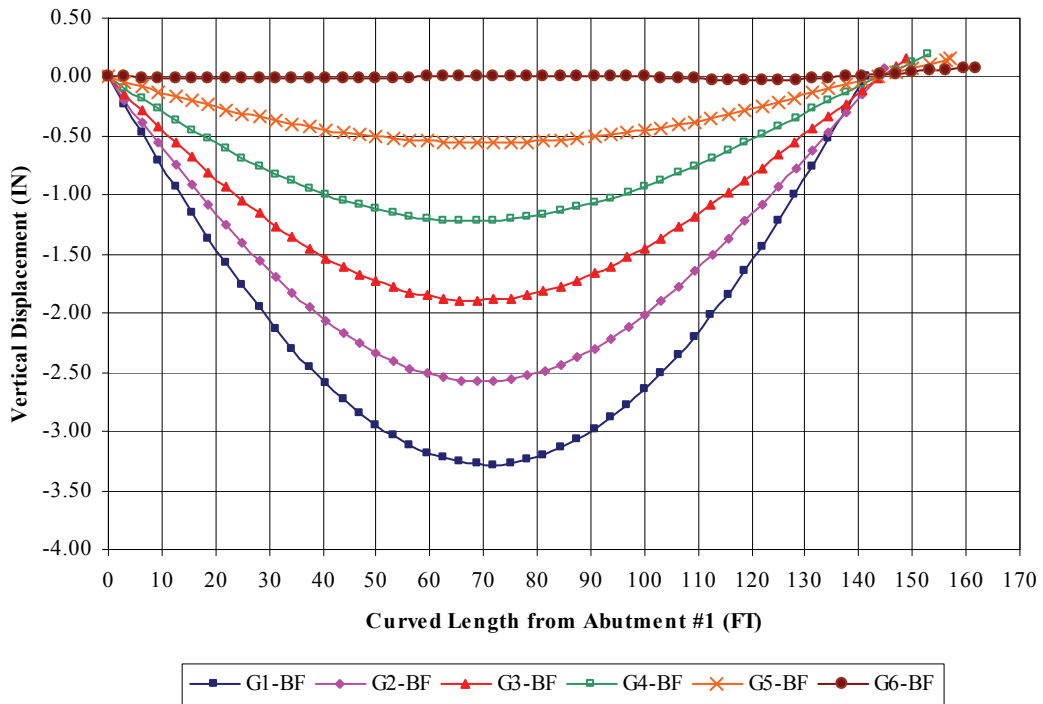


Figure B.154 Construction Stage 6b2 – Girder Vertical Displacement

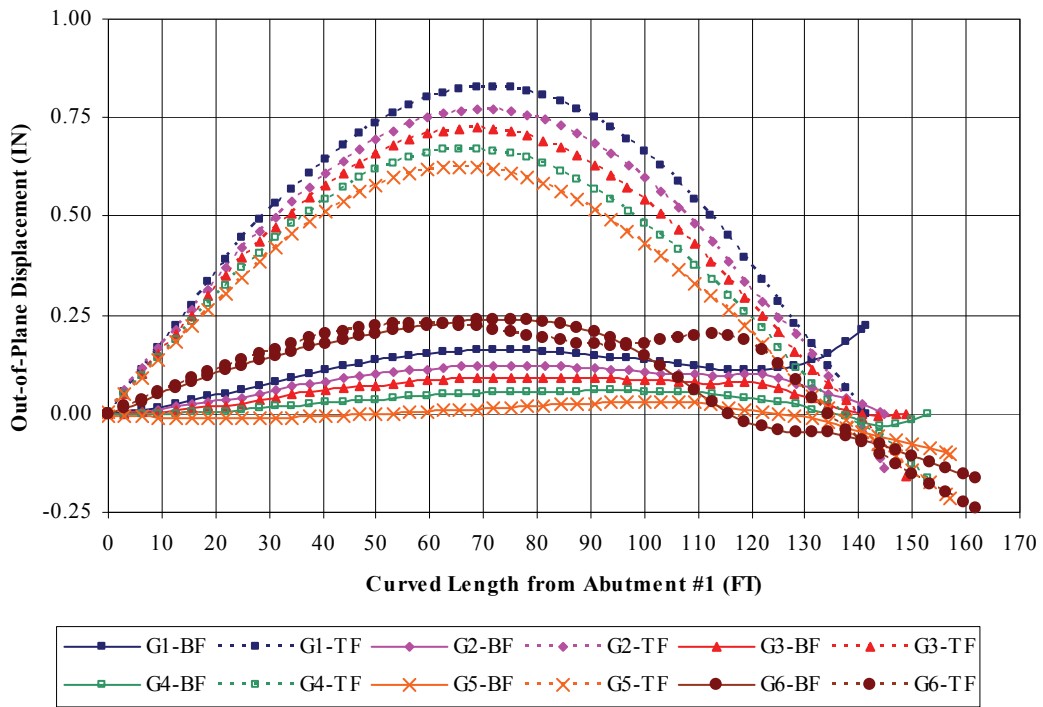


Figure B.155 Construction Stage 6b2 – Girder Lateral Displacement

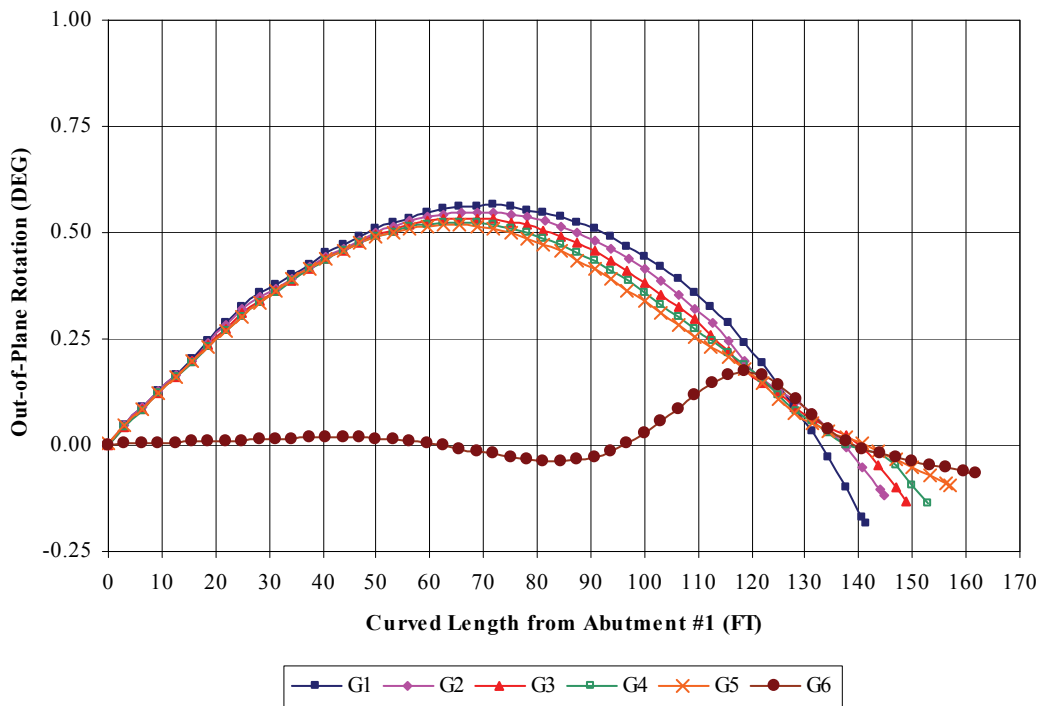
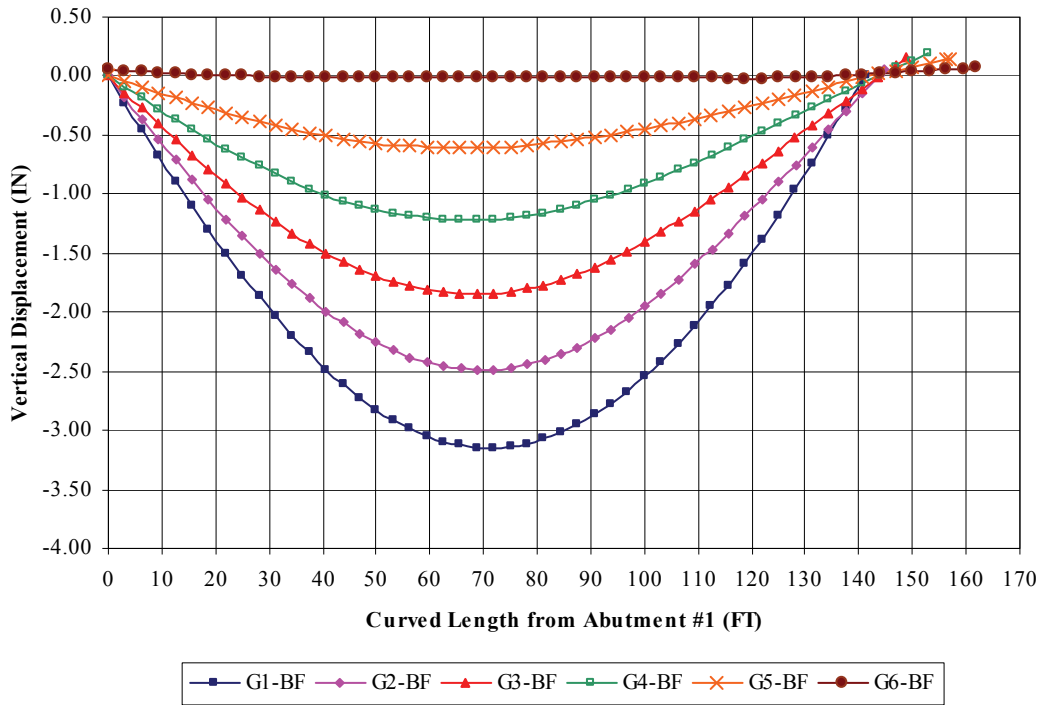
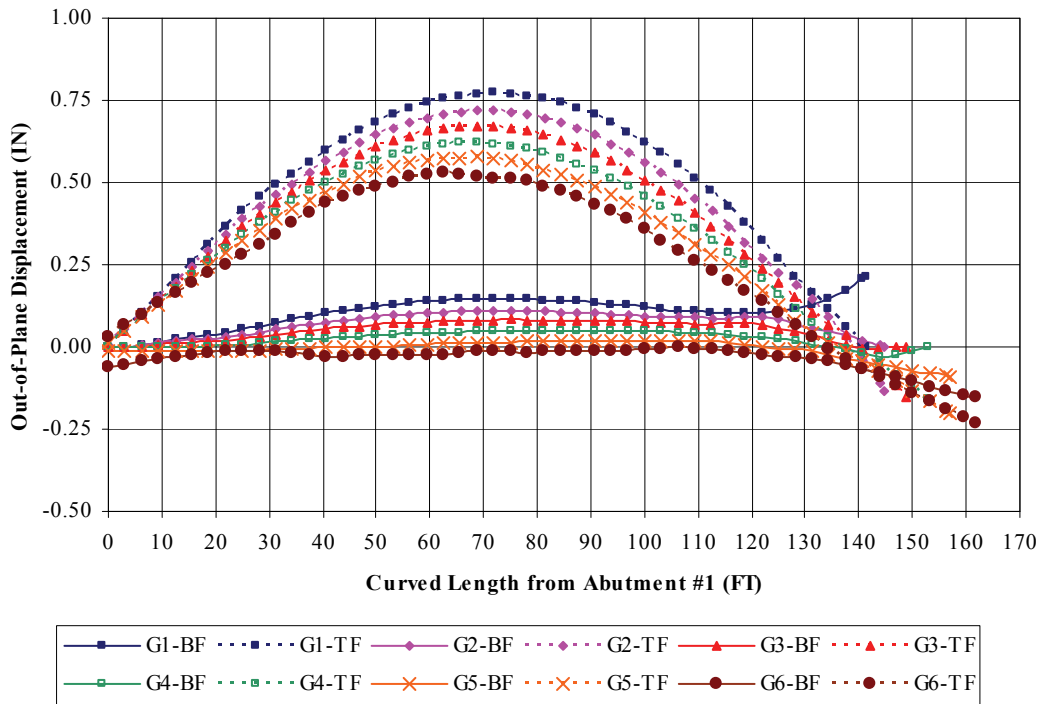


Figure B.156 Construction Stage 6b2 – Girder Out-of-Plane Rotation



**Figure B.157** Construction Stage 6c2 – Girder Vertical Displacement



**Figure B.158** Construction Stage 6c2 – Girder Lateral Displacement

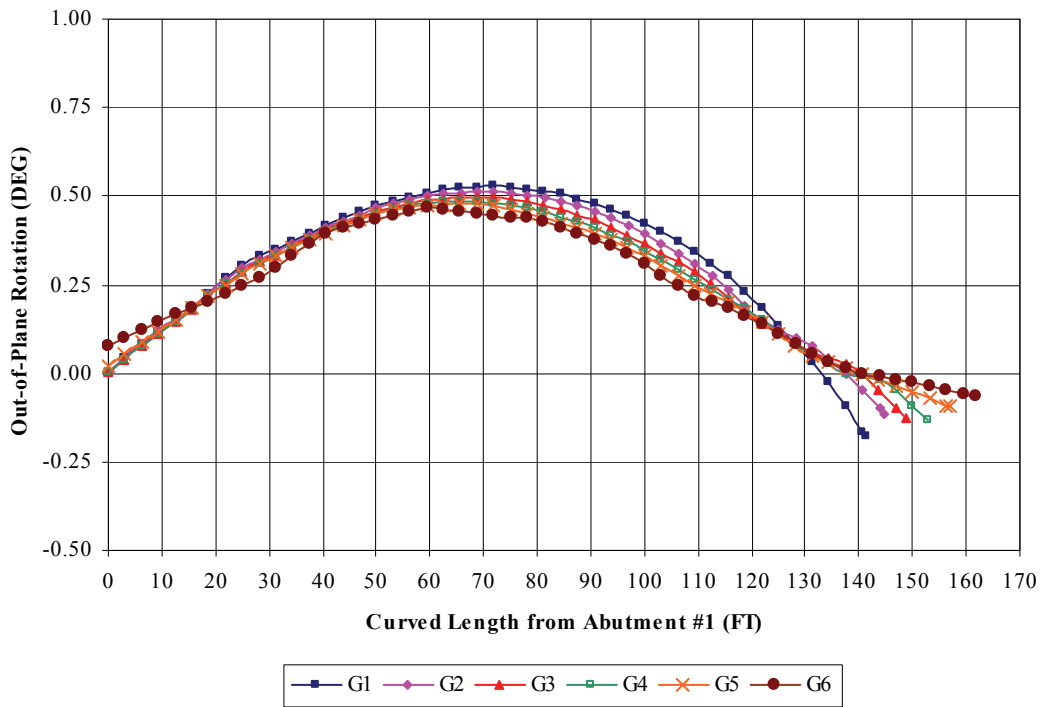


**Figure B.159** Construction Stage 6c2 – Girder Out-of-Plane Rotation

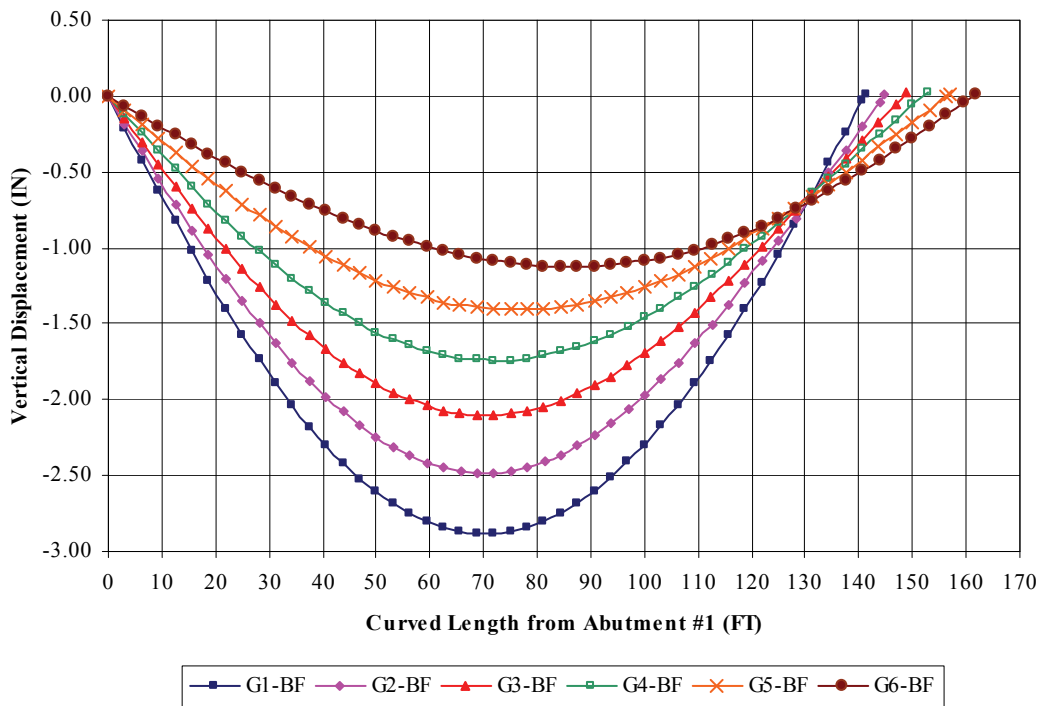


**Figure B.160** Construction Stage 6c3 – Girder Vertical Displacement

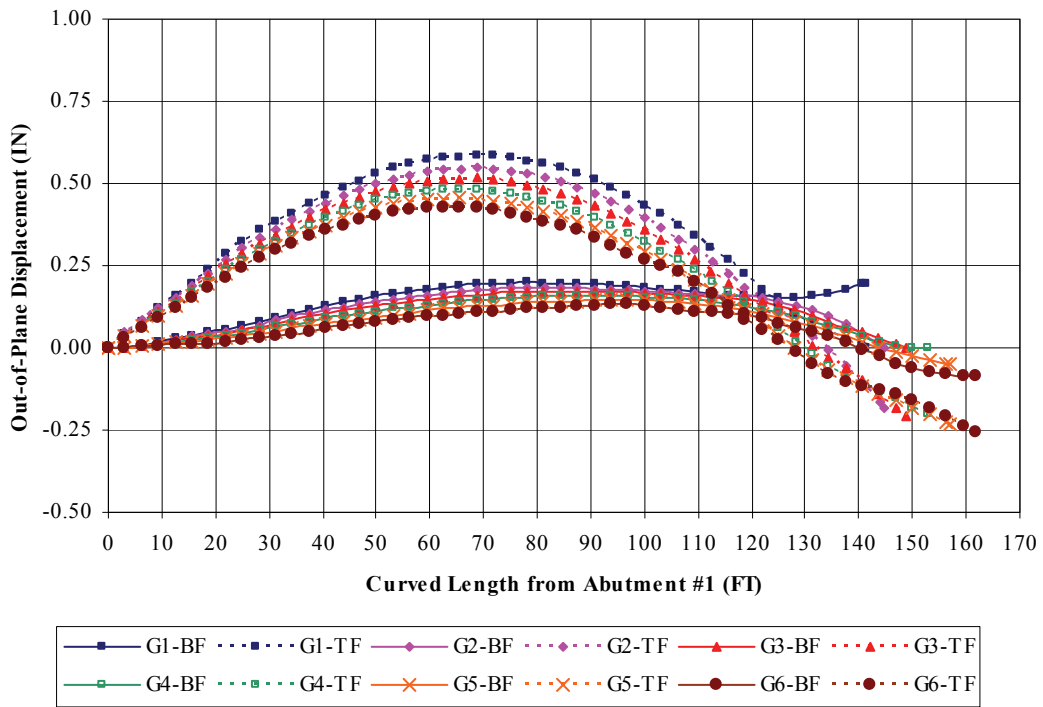


Figure B.161 Construction Stage 6c3 – Girder Lateral Displacement

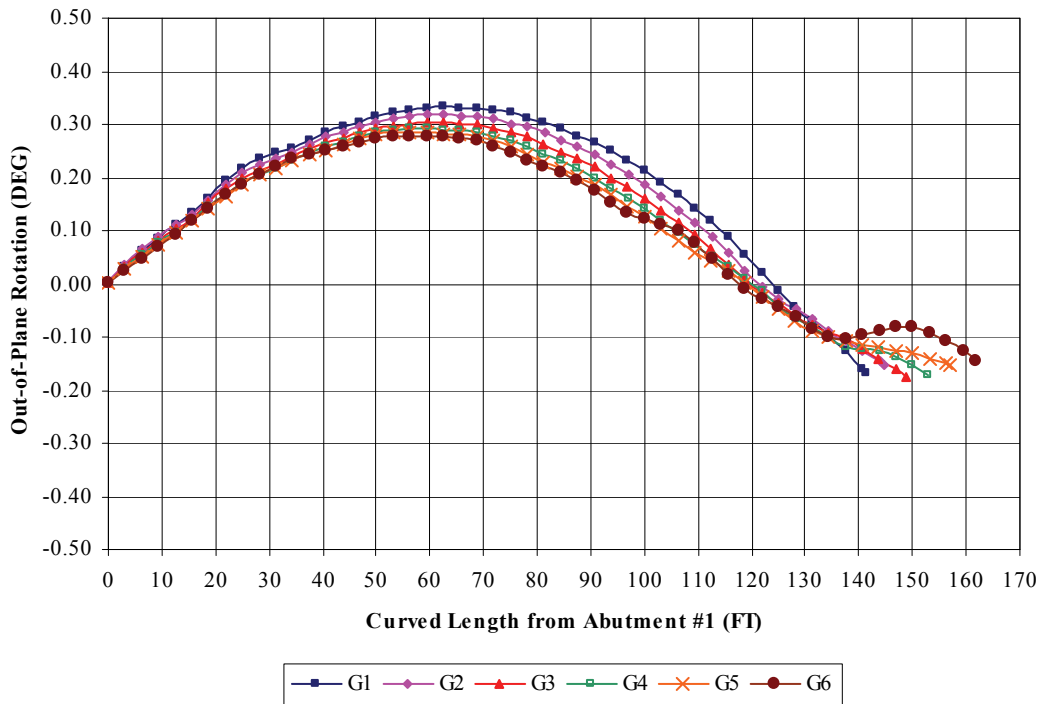


Figure B.162 Construction Stage 6c3 – Girder Out-of-Plane Rotation

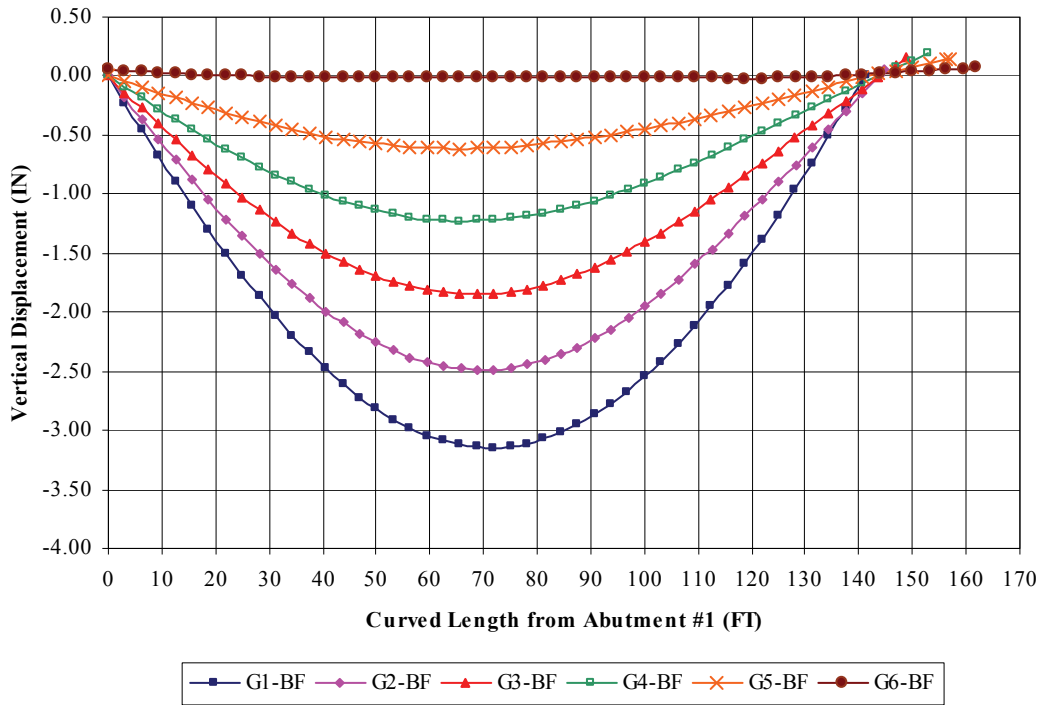


Figure B.163 Construction Stage 6d2 – Girder Vertical Displacement

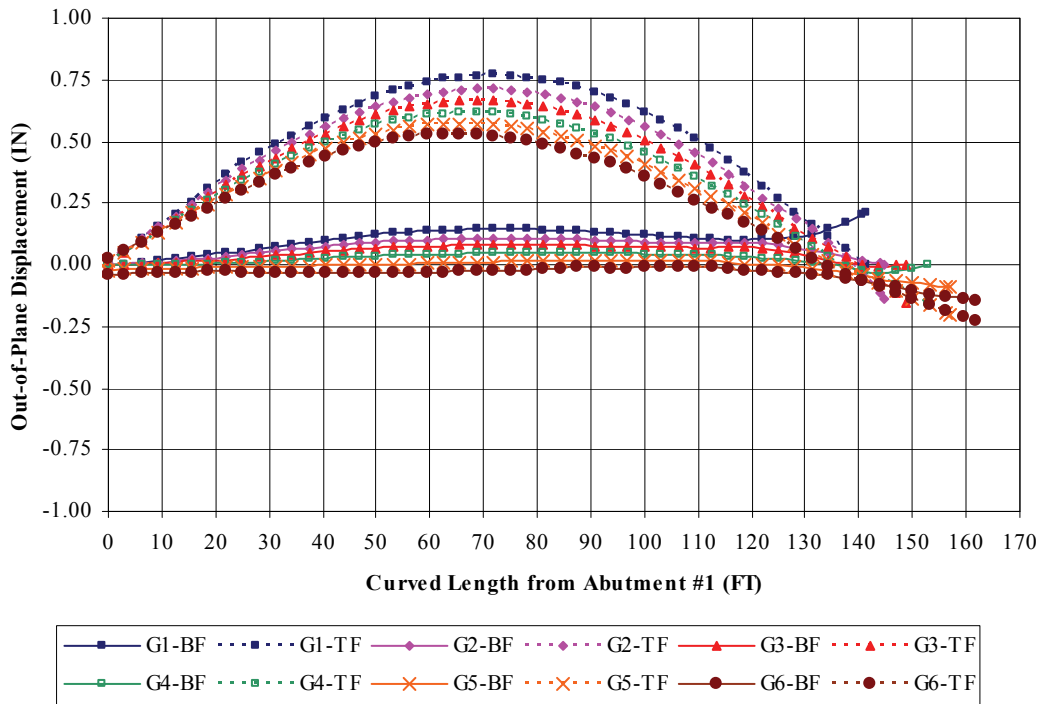
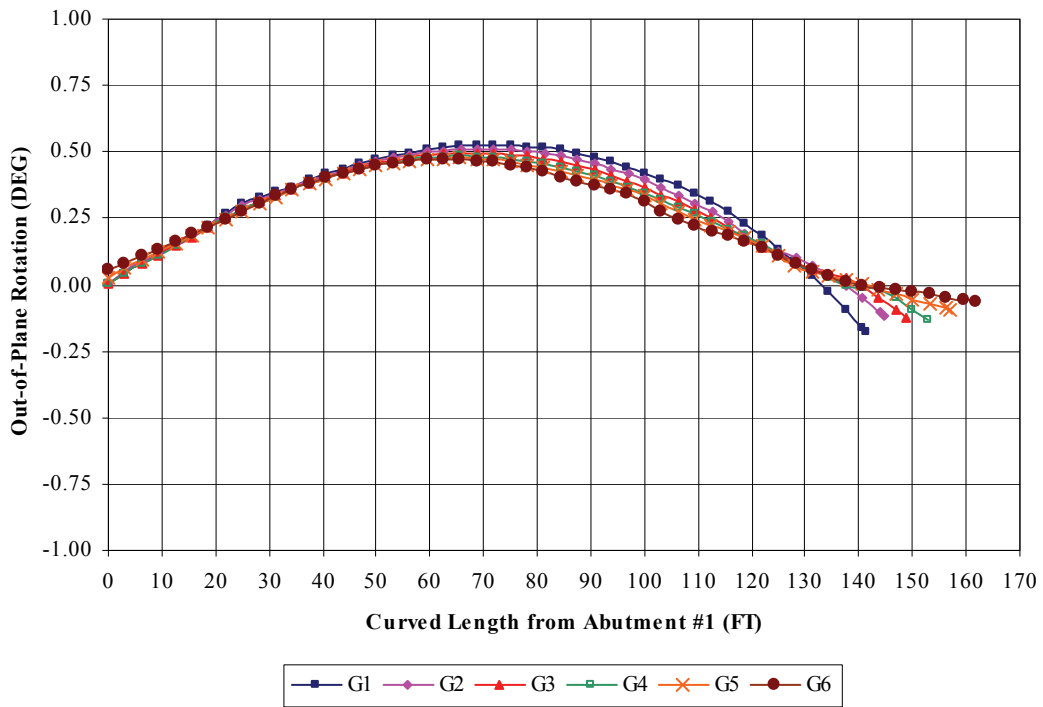
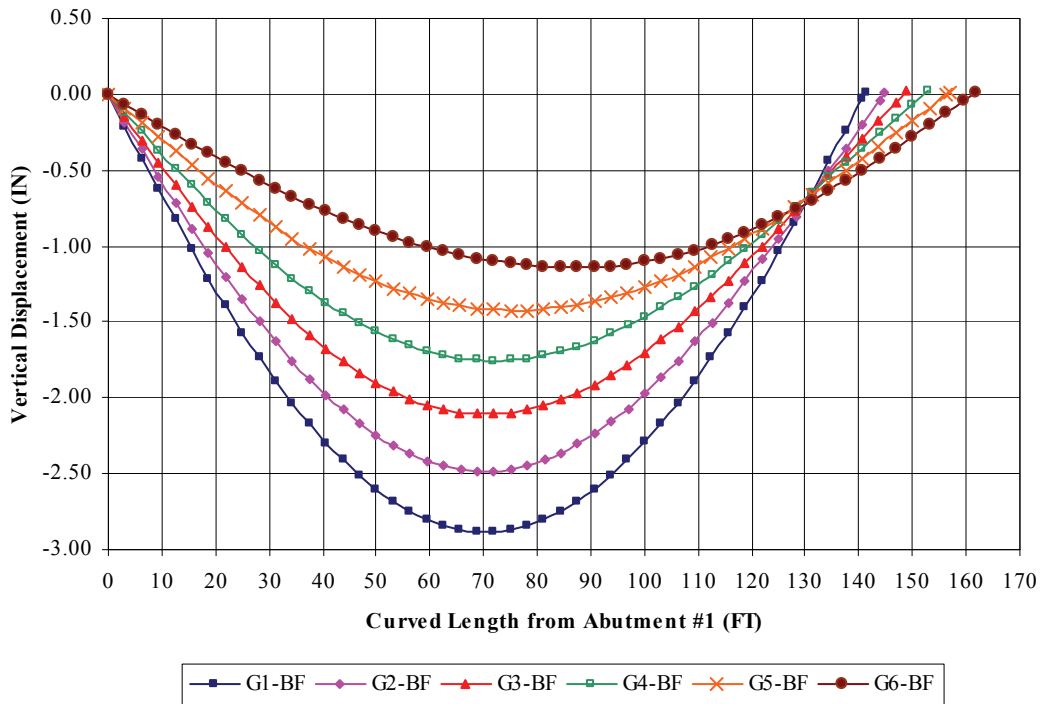


Figure B.164 Construction Stage 6d2 – Girder Lateral Displacement



**Figure B.165** Construction Stage 6d2 – Girder Out-of-Plane Rotation



**Figure B.166** Construction Stage 6d3 – Girder Vertical Displacement

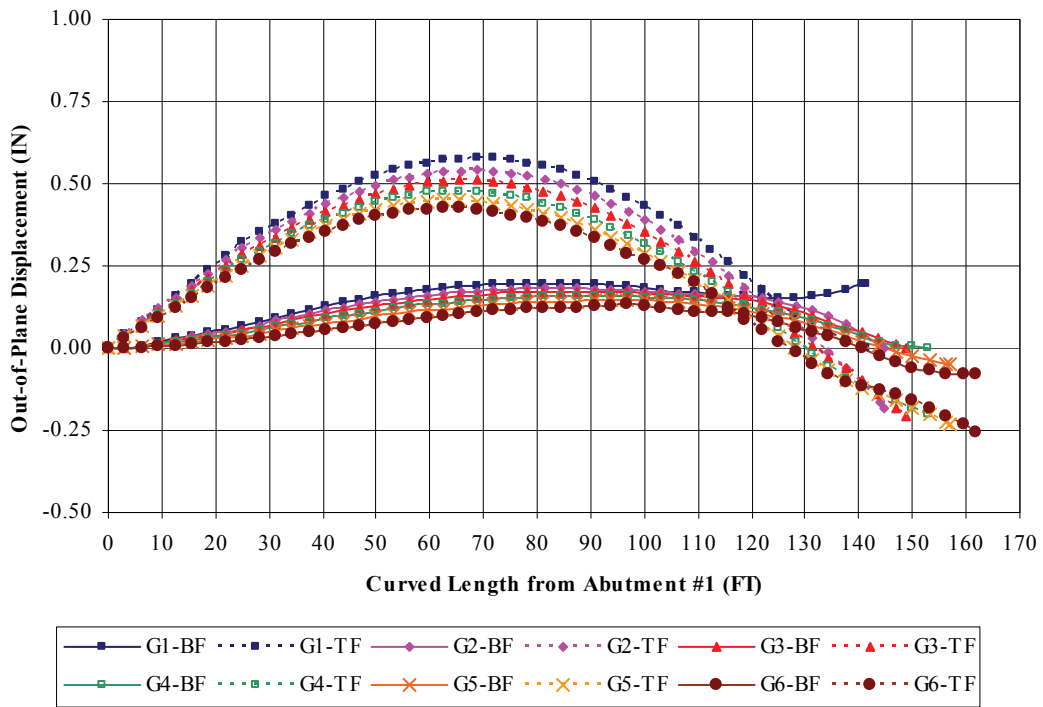


**Figure B.167** Construction Stage 6d3 – Girder Lateral Displacement

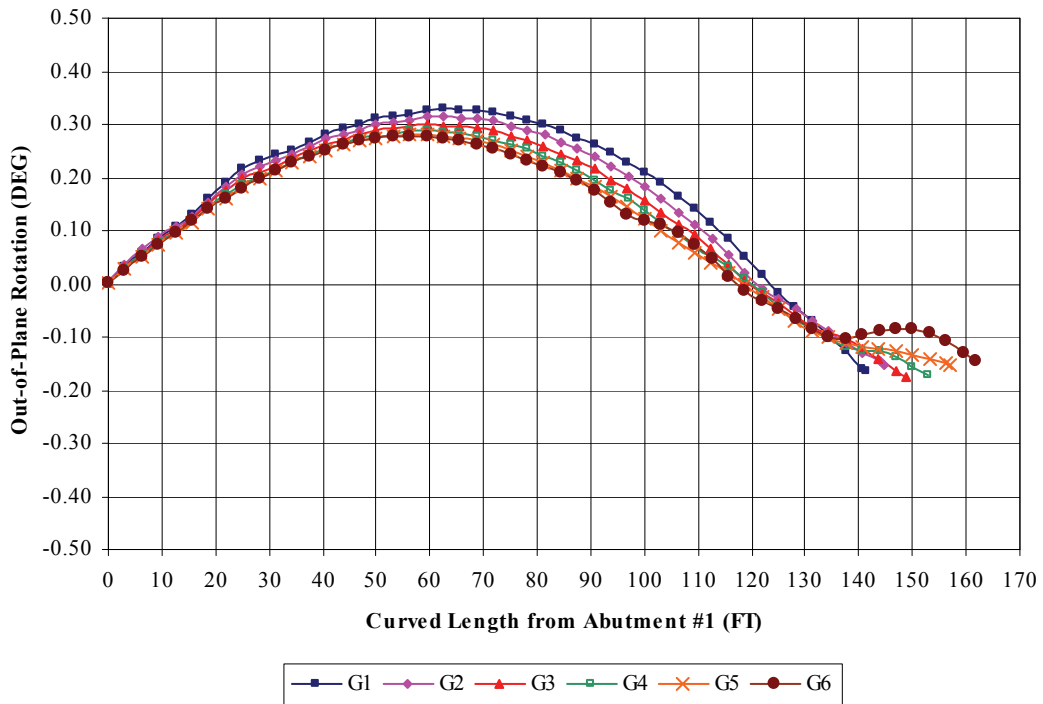


**Figure B.168** Construction Stage 6d3 – Girder Out-of-Plane Rotation

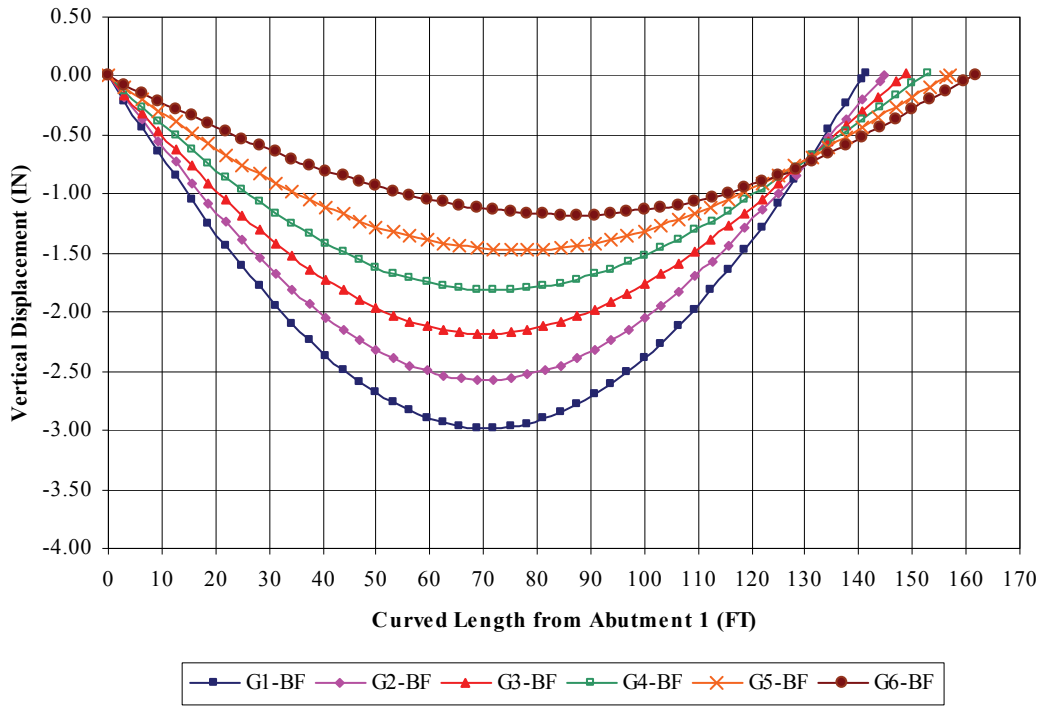


Figure B.169 Construction Stage 6e3 (Final) – Girder Vertical Displacement

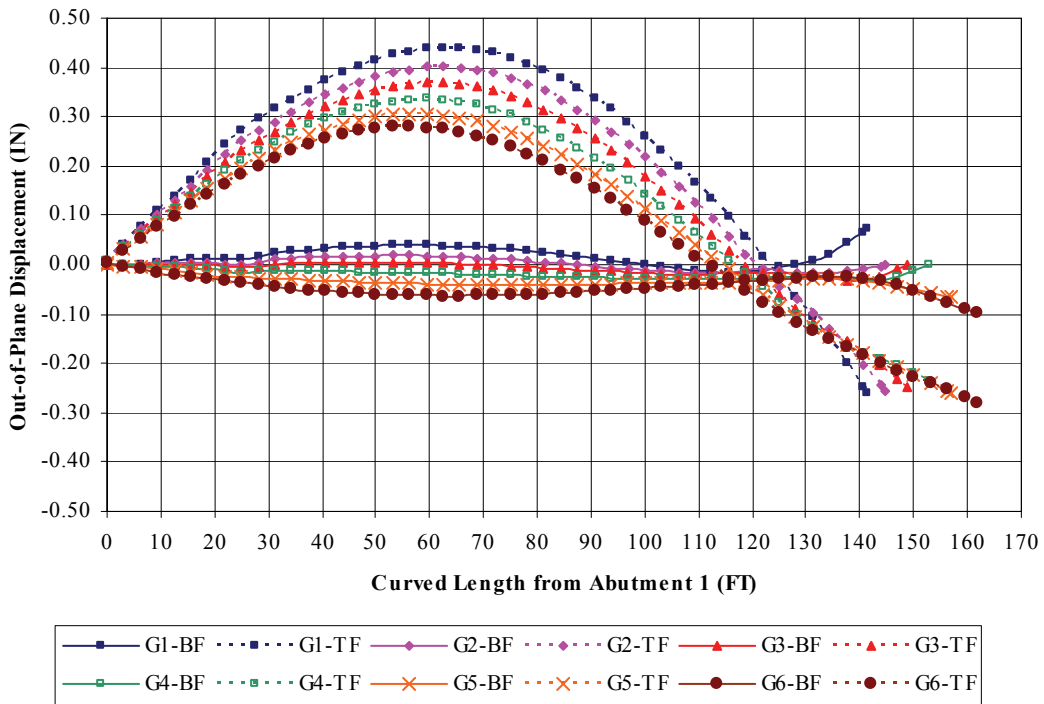
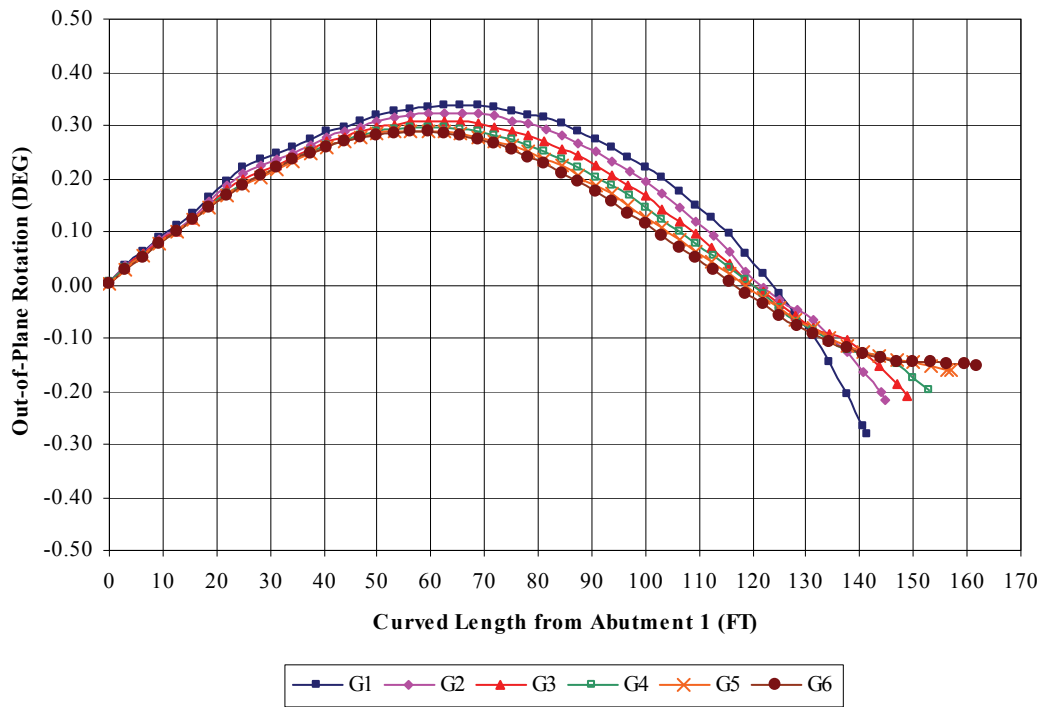


Figure B.170 Construction Stage 6e3 (Final) – Girder Lateral Displacement



**Figure B.171** Construction Stage 6e3 (Final) – Girder Out-of-Plane Rotation

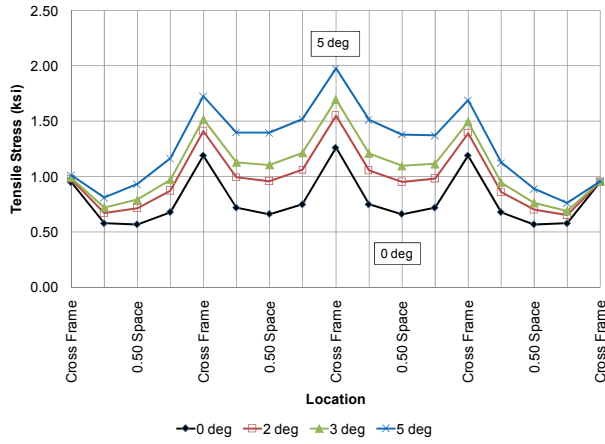
## **APPENDIX C**

### **WEB OUT-OF-PLUMBNESS PARAMETRIC STUDY RESULTS**

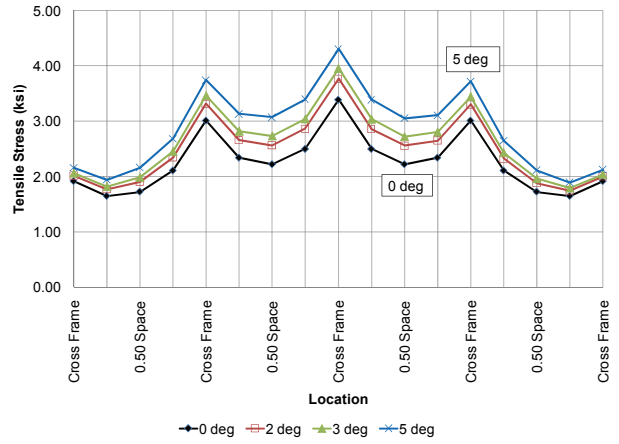
Results are presented for web out-of-plumbness parametric study carried out on the two-girder system. Included in the results are flanges stresses at  $0.5L$  of the center span,  $0.4L$  of the end span, and  $0.0L$  of the center span (Support #2). Also included are the girder vertical and lateral displacements for each parameter studied.

#### **C.1 RADIUS PARAMETER**

### C.1.1 Flange Stresses (R=309.3 ft)

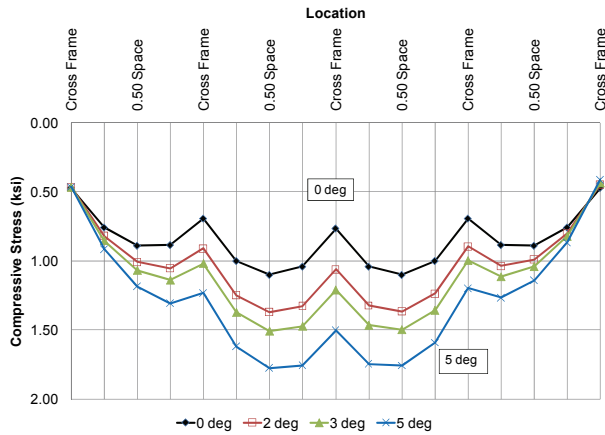


a) Girder G1

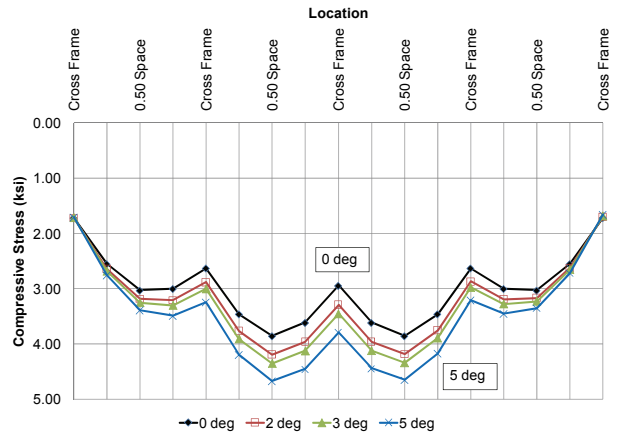


b) Girder G2

**Figure C.1 Outer-Edge Bottom Flange Tip Stresses at 0.5L of Center Span**

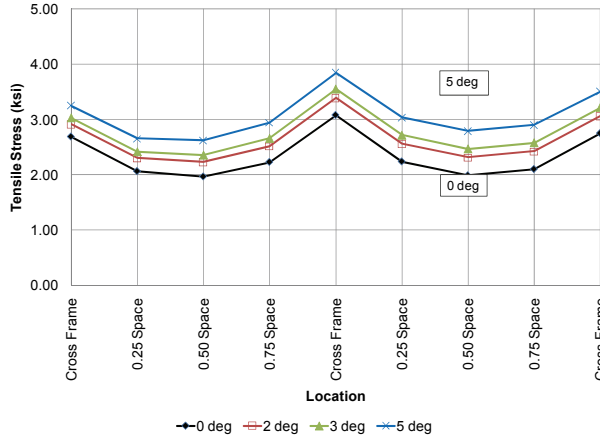


a) Girder G1

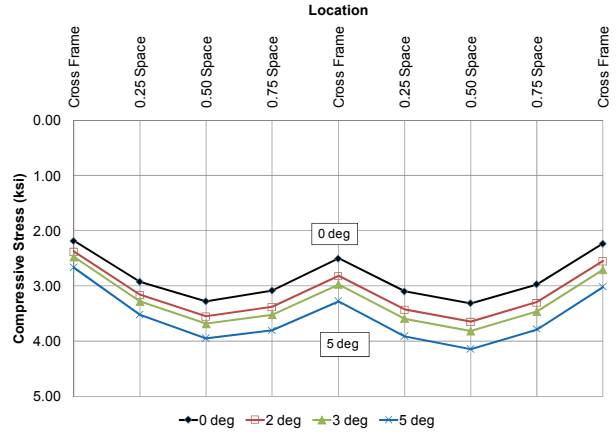


b) Girder G2

**Figure C.2 Inner-Edge Top Flange Tip Stresses at 0.5L of Center Span**

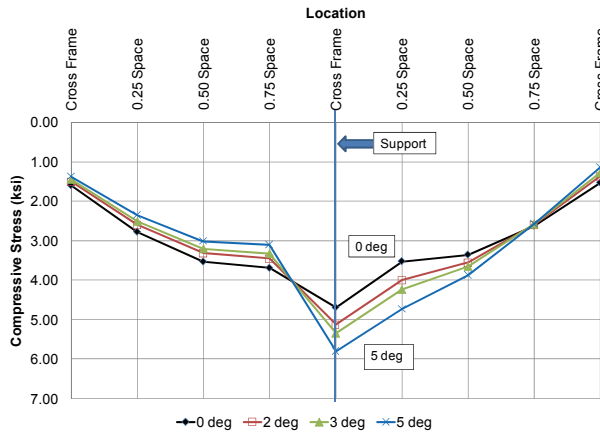


a) Outer-Edge Bottom Flange

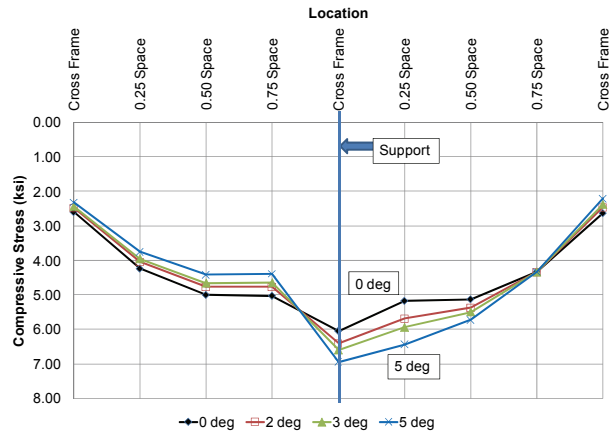


b) Inner-Edge Top Flange

Figure C.3 G2 Flange Tip Stresses at 0.4L of End Span

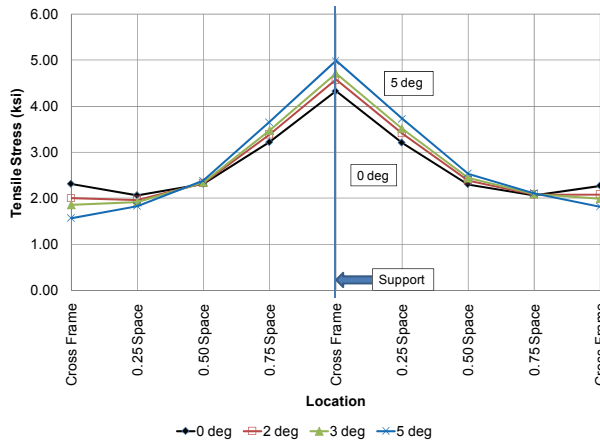


a) Girder G1

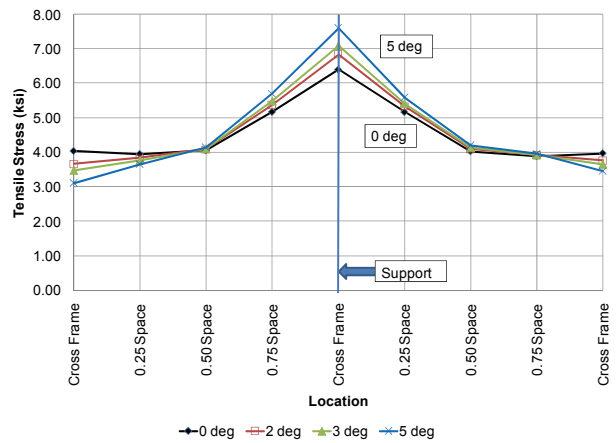


b) Girder G2

Figure C.4 Inner-Edge Bottom Flange Tip Stresses at 0.0L of Center Span



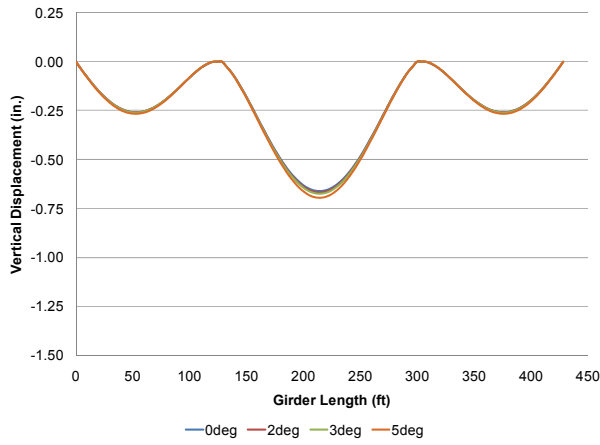
a) Girder G1



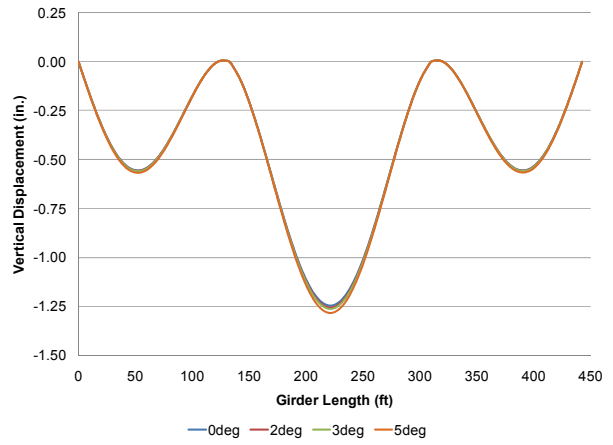
b) Girder G2

Figure C.5 Outer-Edge Top Flange Tip Stresses at 0.0L of Center Span

### C.1.2 Girder Displacements (R=309.3 ft)

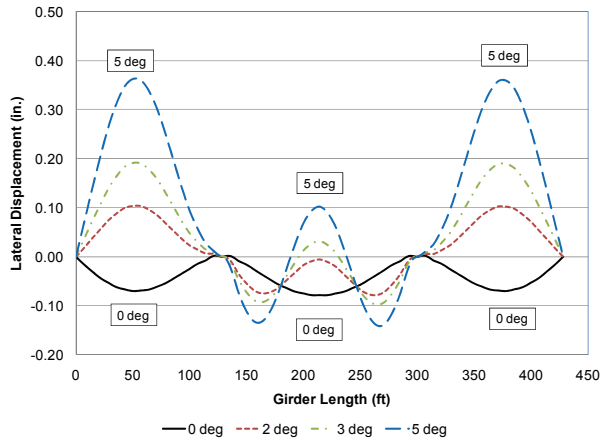


a) Girder G1

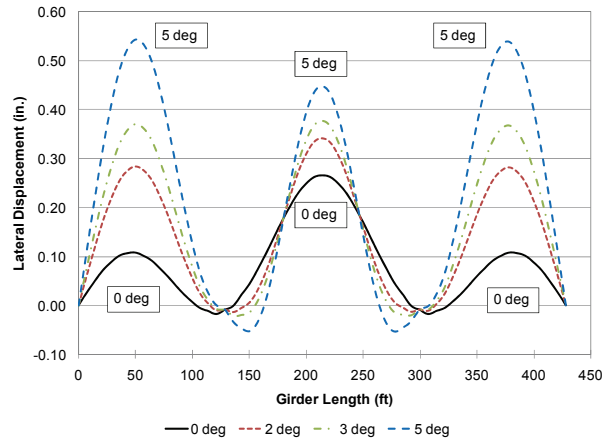


b) Girder G2

Figure C.6 Top Flange Vertical Displacement



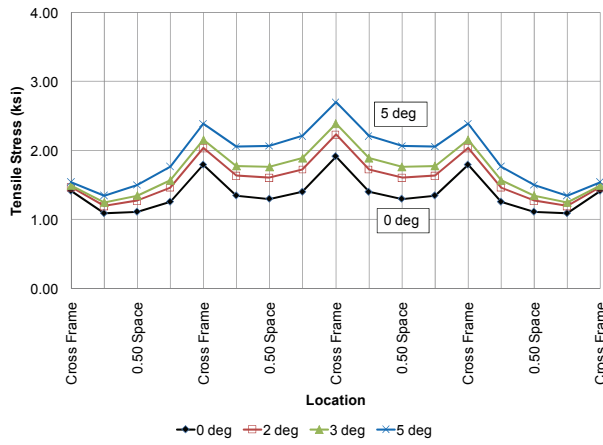
a) Bottom Flange



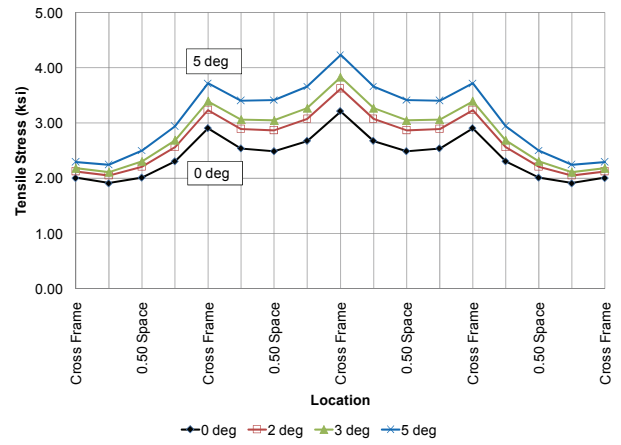
b) Top Flange

Figure C.7 G2 Flange Lateral Displacement

### C.1.3 Flange Stresses – Base Model (R=509.3 ft)

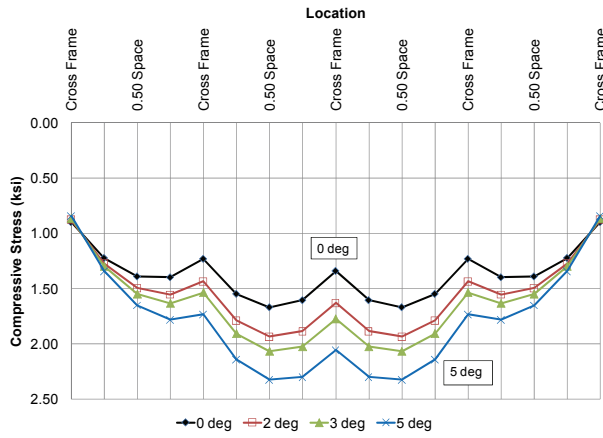


a) Girder G1

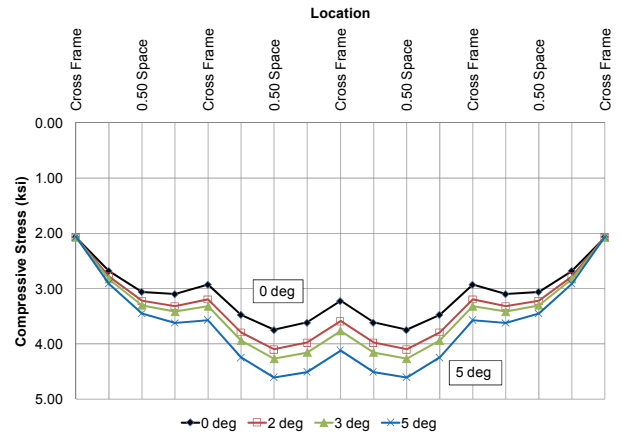


b) Girder G2

**Figure C.8** Outer-Edge Bottom Flange Tip Stresses at 0.5L of Center Span

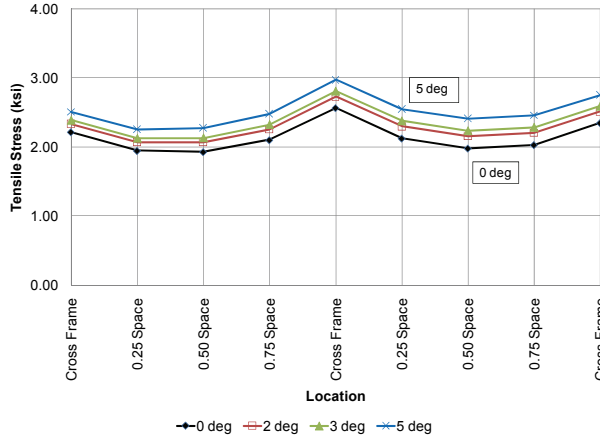


a) Girder G1

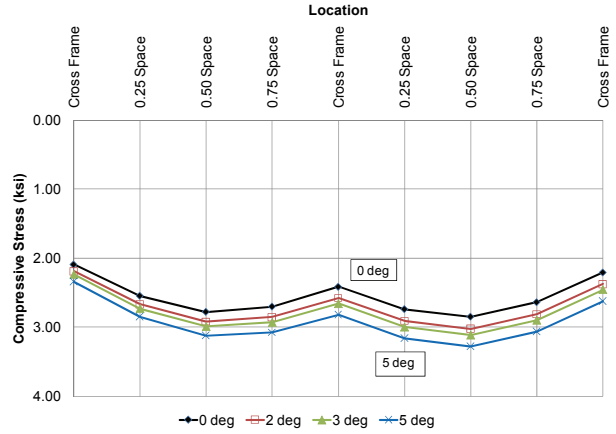


b) Girder G2

**Figure C.9** Inner-Edge Top Flange Tip Stresses at 0.5L of Center Span

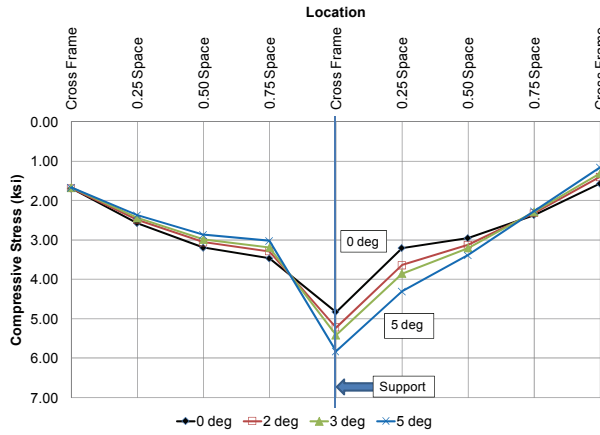


a) Outer-Edge Bottom Flange

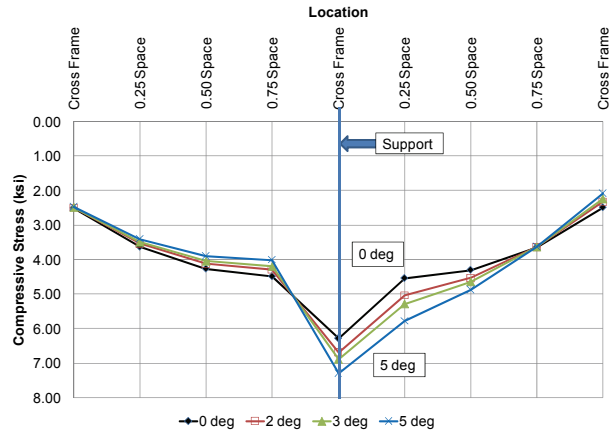


b) Inner-Edge Top Flange

Figure C.10 G2 Flange Tip Stresses at 0.4L of End Span

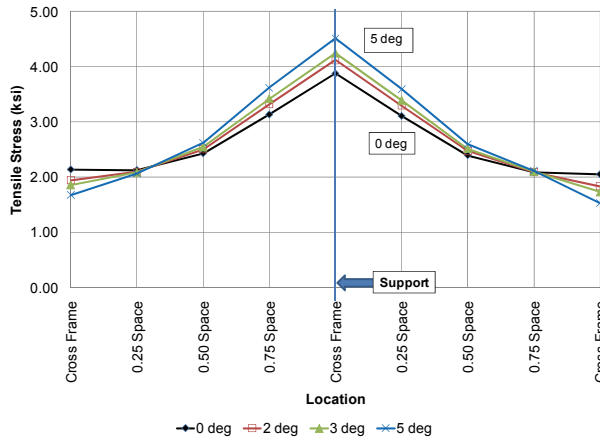


a) Girder G1

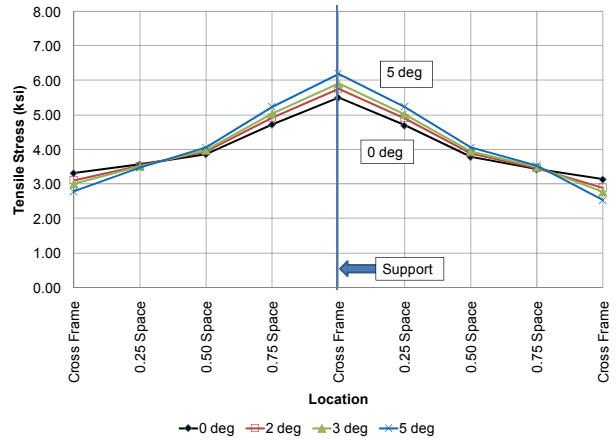


b) Girder G2

Figure C.11 Inner-Edge Bottom Flange Tip Stresses at 0.0L of Center Span



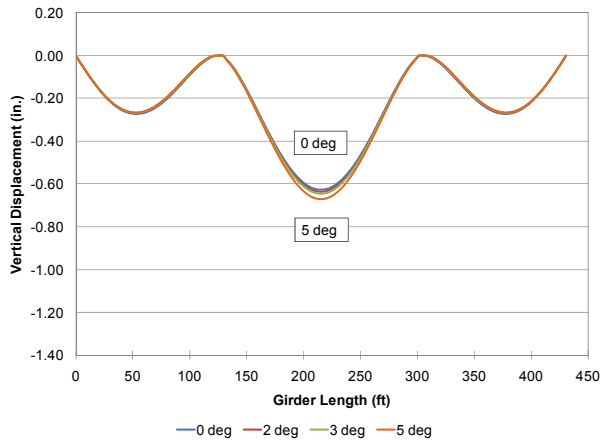
a) Girder G1



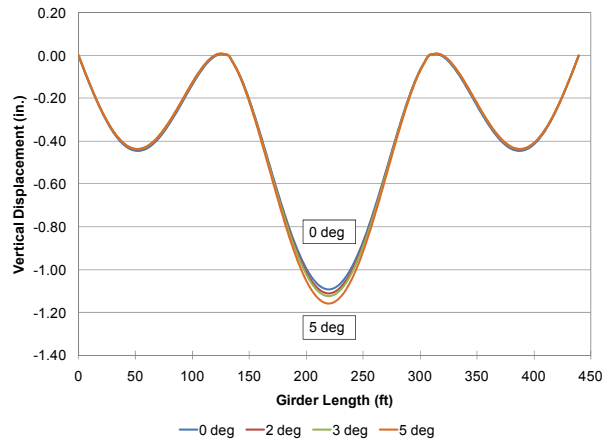
b) Girder G2

Figure C.12 Outer-Edge Top Flange Tip Stresses at 0.0L of Center Span

### C.1.4 Girder Displacements – Base Model (R=509.3 ft)

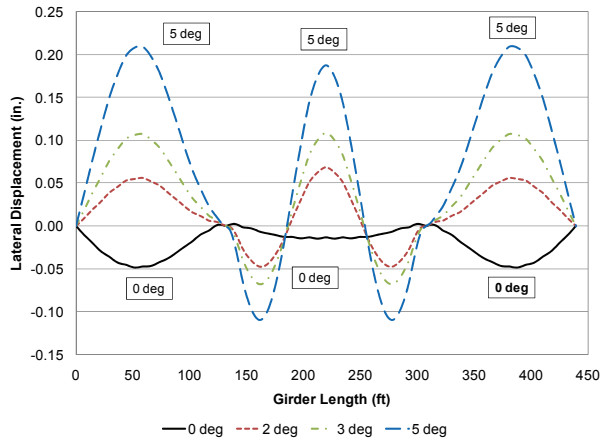


a) Girder G1

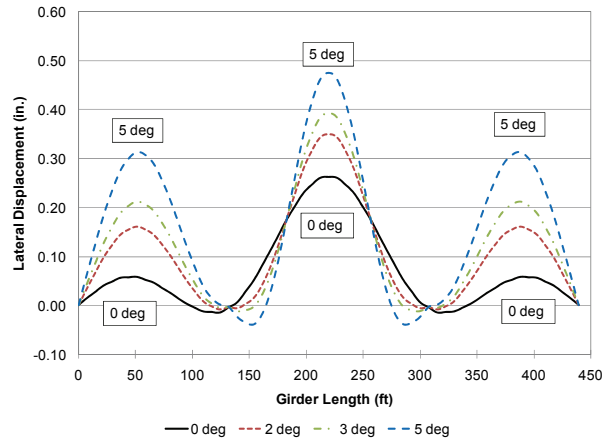


b) Girder G2

Figure C.13 Top Flange Vertical Displacement



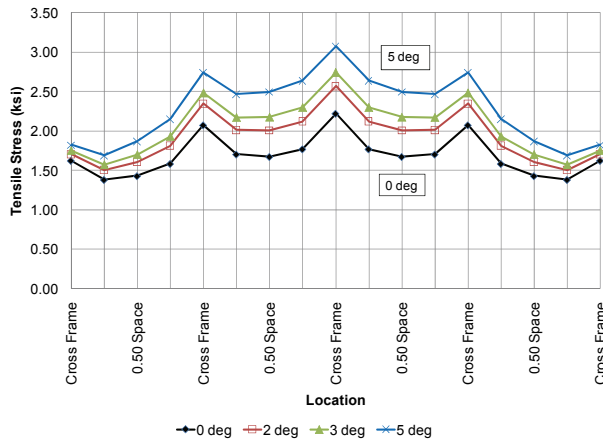
a) Bottom Flange



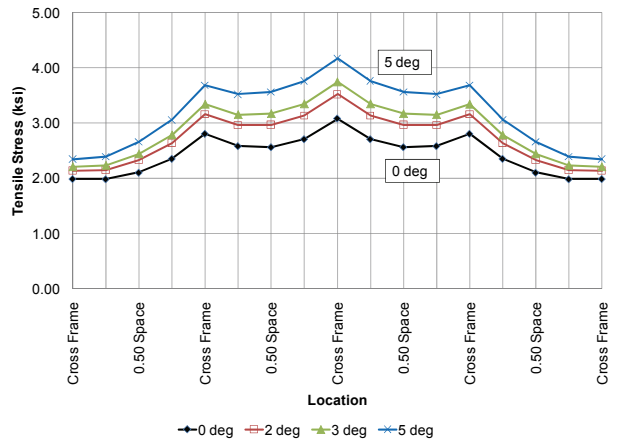
b) Top Flange

Figure C.14 G2 Flange Lateral Displacement

### C.1.5 Flange Stresses (R=709.3 ft)

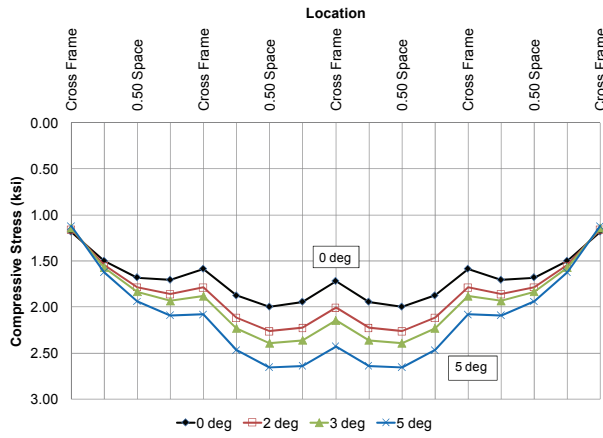


a) Girder G1

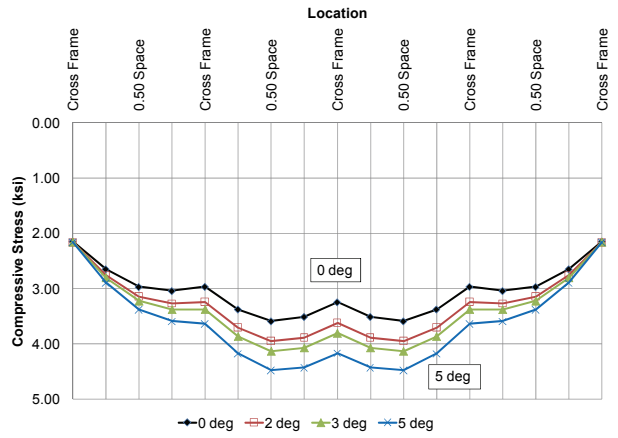


b) Girder G2

**Figure C.15** Outer-Edge Bottom Flange Tip Stresses at 0.5L of Center Span

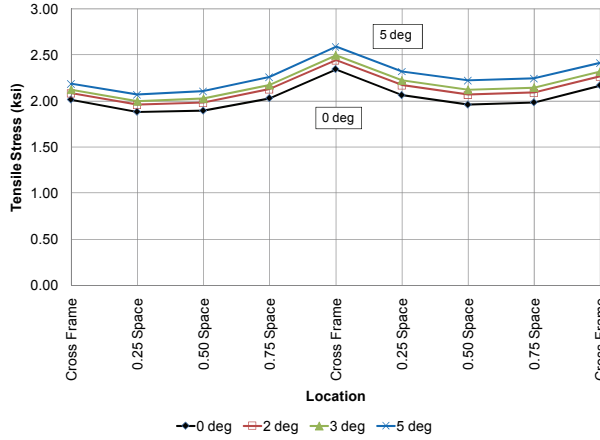


a) Girder G1

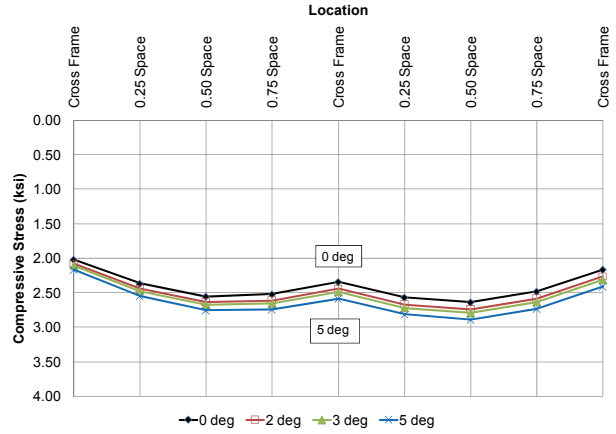


b) Girder G2

**Figure C.16** Inner-Edge Top Flange Tip Stresses at 0.5L of Center Span

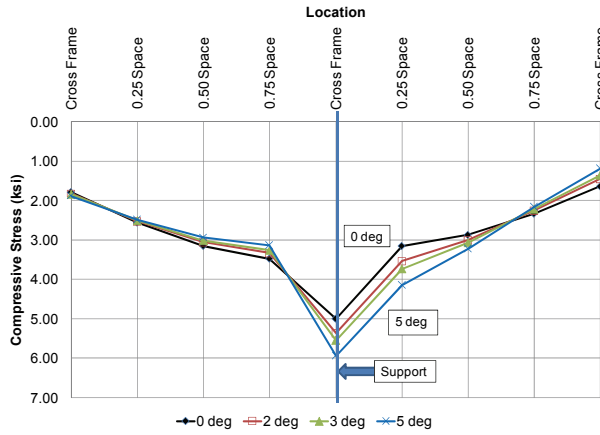


a) Outer-Edge Bottom Flange

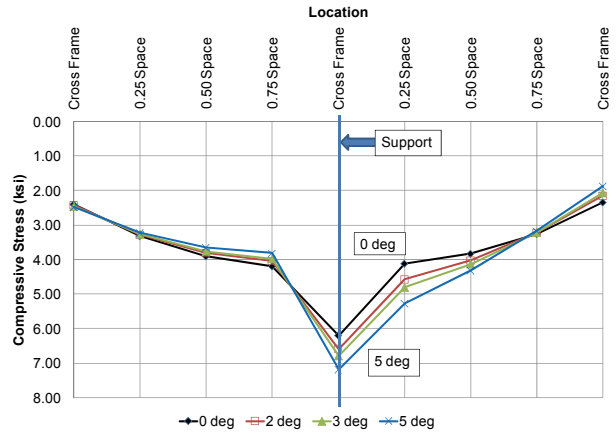


b) Inner-Edge Top Flange

**Figure C.17 G2 Flange Tip Stresses at 0.4L of End Span**

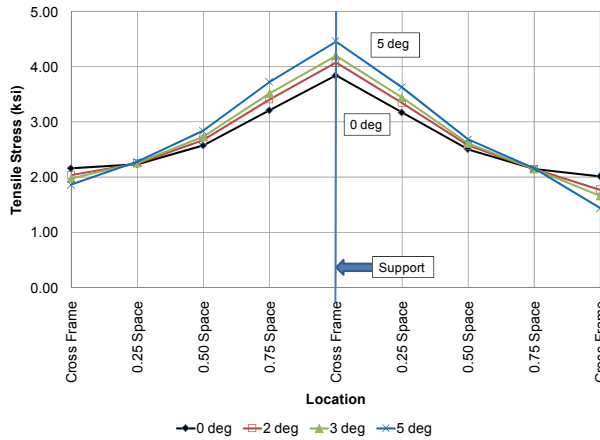


a) Girder G1

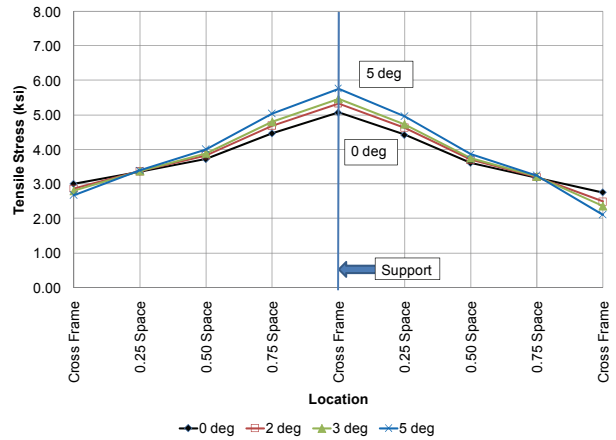


b) Girder G2

**Figure C.18 Inner-Edge Bottom Flange Tip Stresses at 0.0L of Center Span**



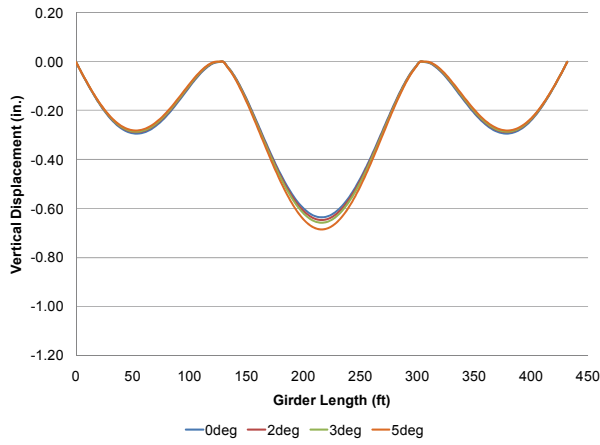
a) Girder G1



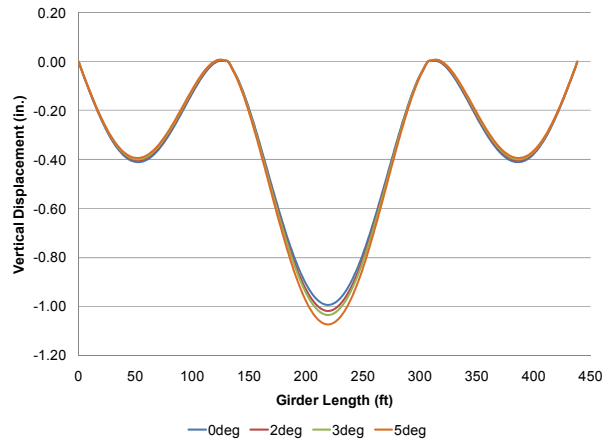
b) Girder G2

**Figure C.19 Outer-Edge Top Flange Tip Stresses at 0.0L of Center Span**

### C.1.6 Girder Displacements (R=709.3 ft)

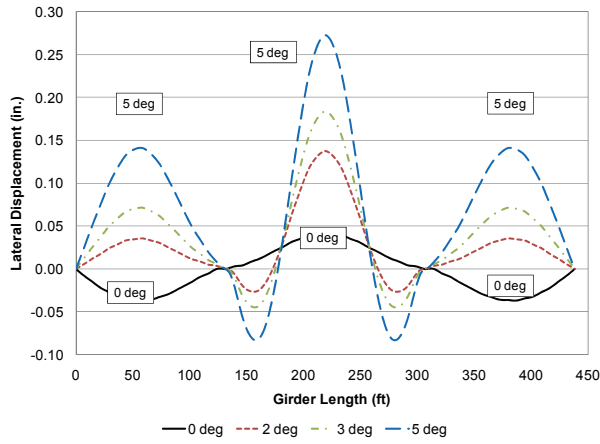


a) Girder G1

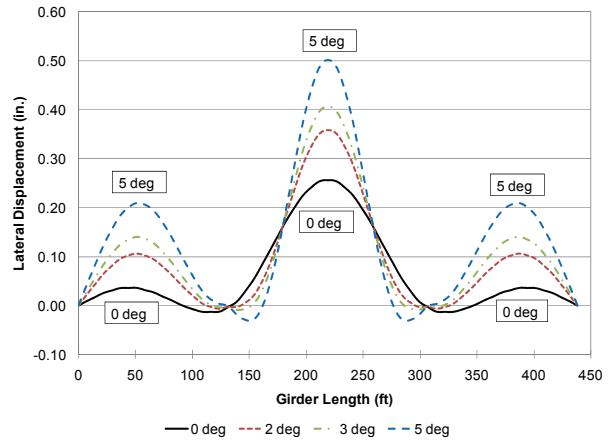


b) Girder G2

Figure C.20 Top Flange Vertical Displacement



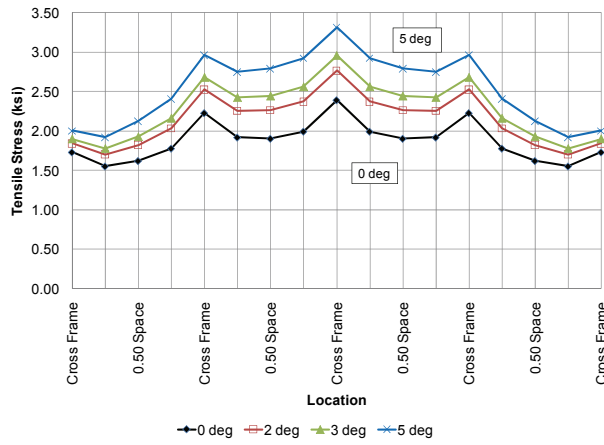
a) Bottom Flange



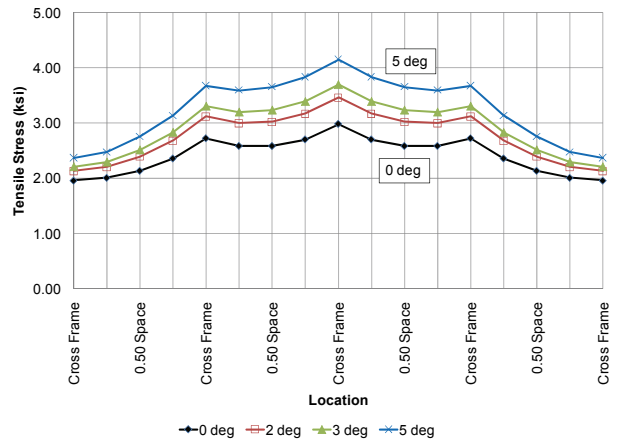
b) Top Flange

Figure C.21 G2 Flange Lateral Displacement

### C.1.7 Flange Stresses (R=909.3 ft)

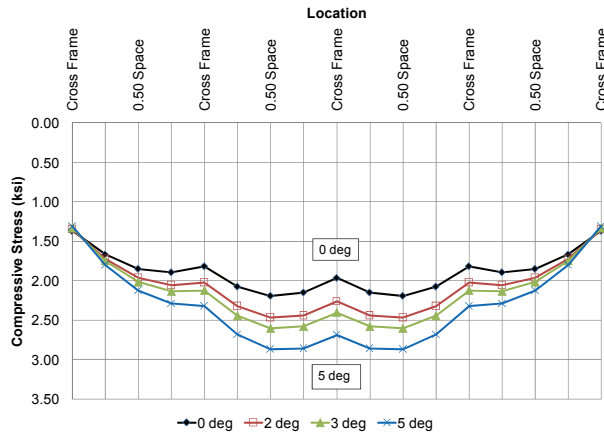


a) Girder G1

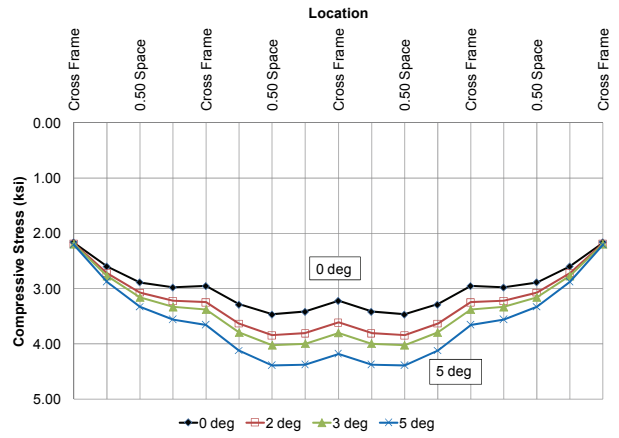


b) Girder G2

**Figure C.22** Outer-Edge Bottom Flange Tip Stresses at 0.5L of Center Span

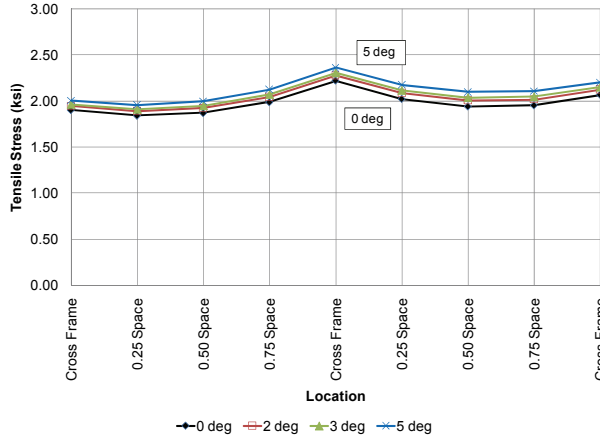


a) Girder G1

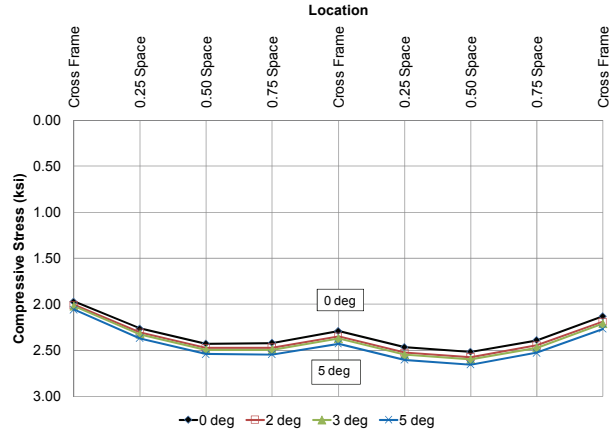


b) Girder G2

**Figure C.23** Inner-Edge Top Flange Tip Stresses at 0.5L of Center Span

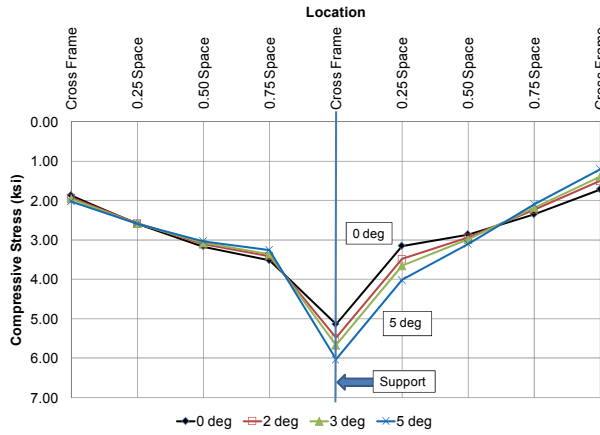


a) Outer-Edge Bottom Flange

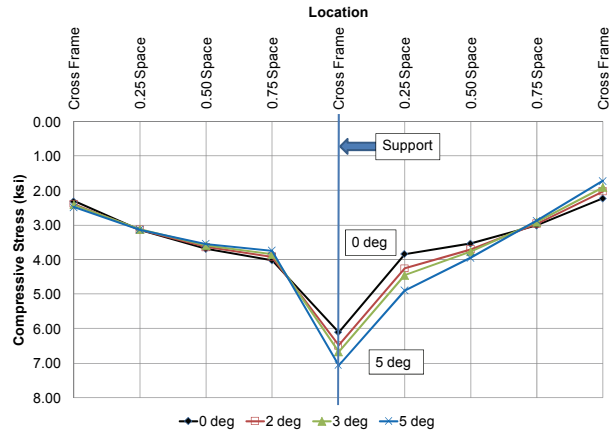


b) Inner-Edge Top Flange

Figure C.24 G2 Flange Tip Stresses at 0.4L of End Span

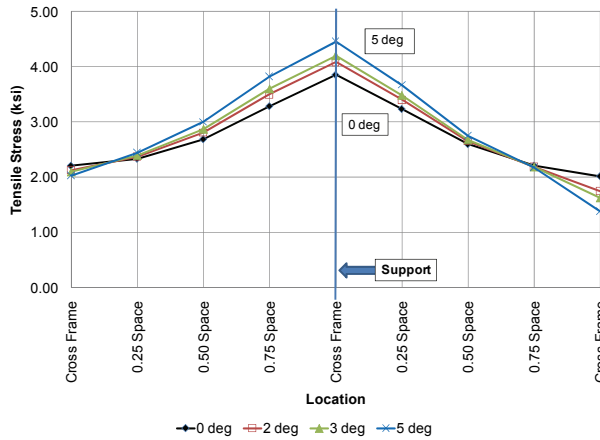


a) Girder G1

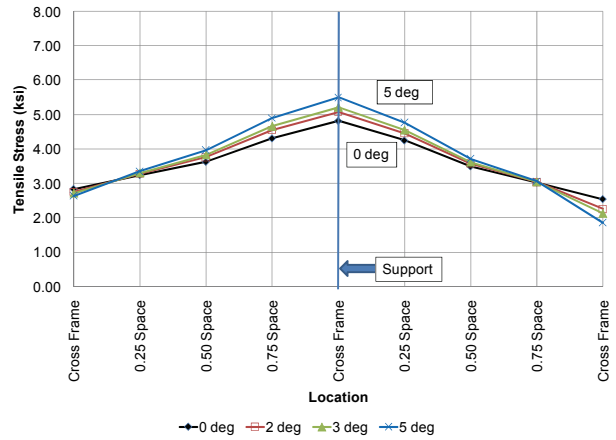


b) Girder G2

Figure C.25 Inner-Edge Bottom Flange Tip Stresses at 0.0L of Center Span



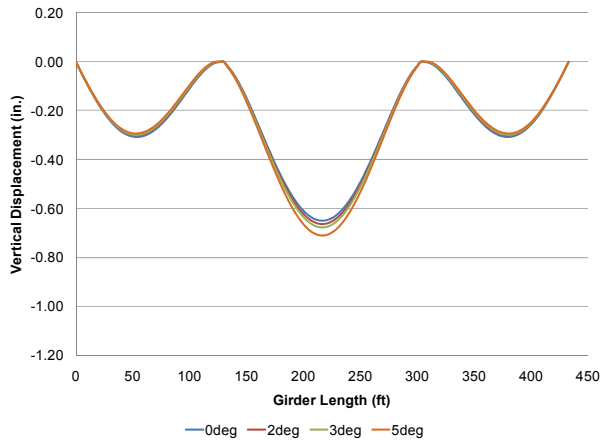
a) Girder G1



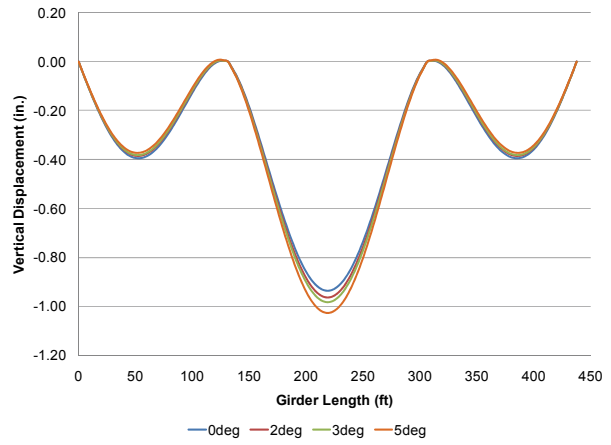
b) Girder G2

Figure C.26 Outer-Edge Top Flange Tip Stresses at 0.0L of Center Span

### C.1.8 Girder Displacements (R=909.3 ft)

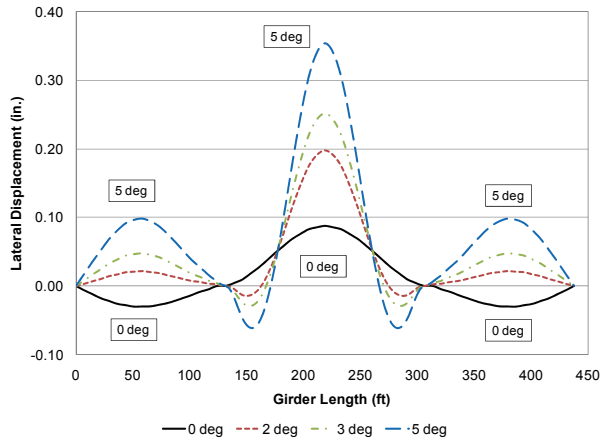


a) Girder G1

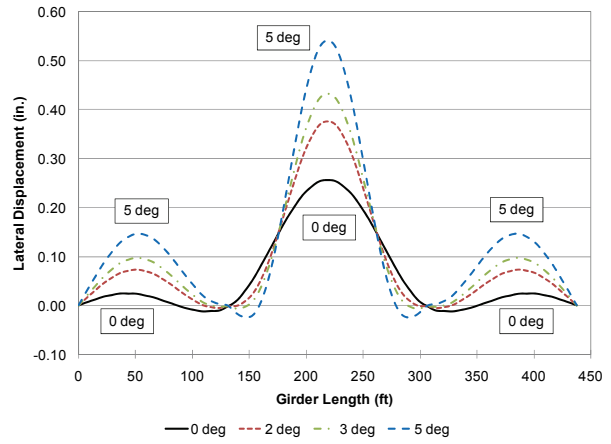


b) Girder G2

Figure C.27 Top Flange Vertical Displacement



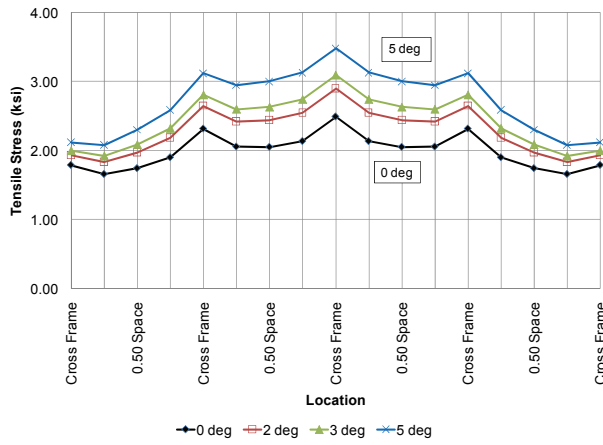
a) Bottom Flange



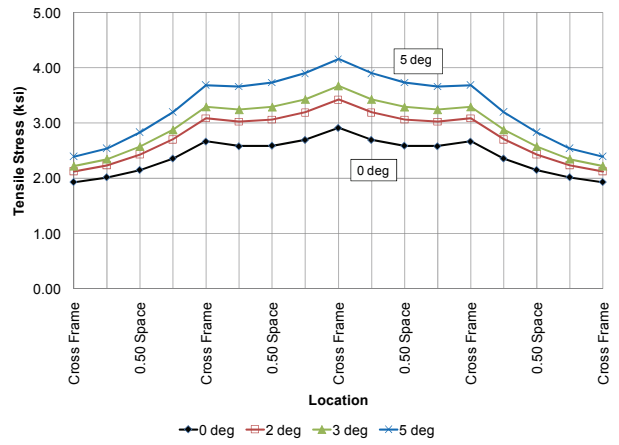
b) Top Flange

Figure C.28 G2 Flange Lateral Displacement

### C.1.9 Flange Stresses (R=1109.3 ft)

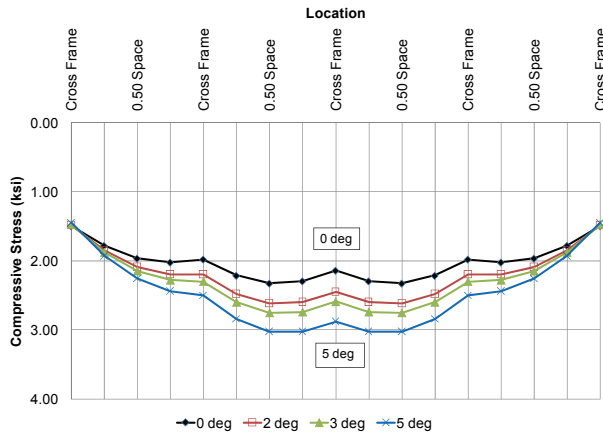


a) Girder G1

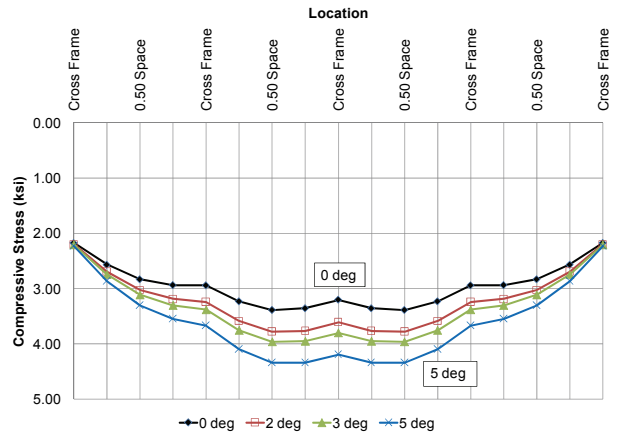


b) Girder G2

**Figure C.29** Outer-Edge Bottom Flange Tip Stresses at 0.5L of Center Span

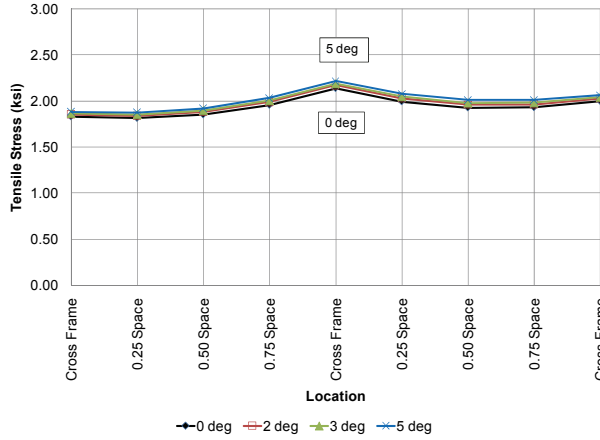


a) Girder G1

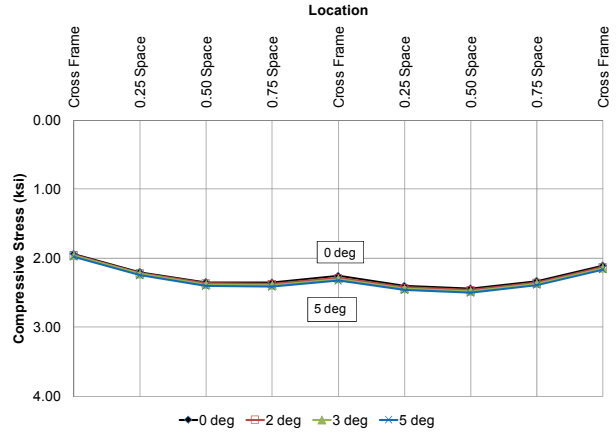


b) Girder G2

**Figure C.30** Inner-Edge Top Flange Tip Stresses at 0.5L of Center Span

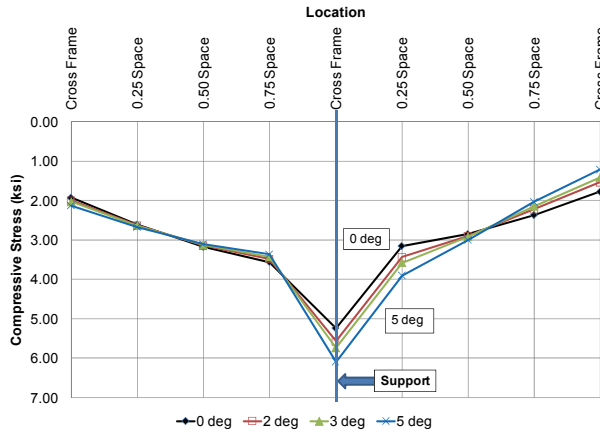


a) Outer-Edge Bottom Flange

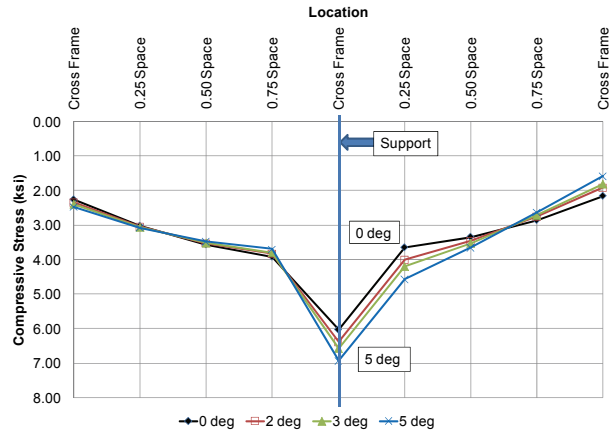


b) Inner-Edge Top Flange

**Figure C.31 G2 Flange Tip Stresses at 0.4L of End Span**

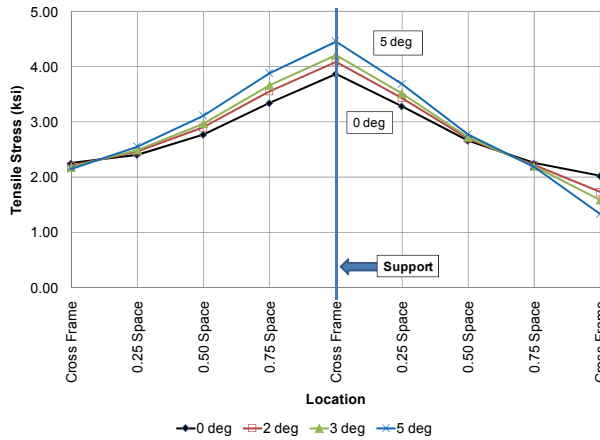


a) Girder G1

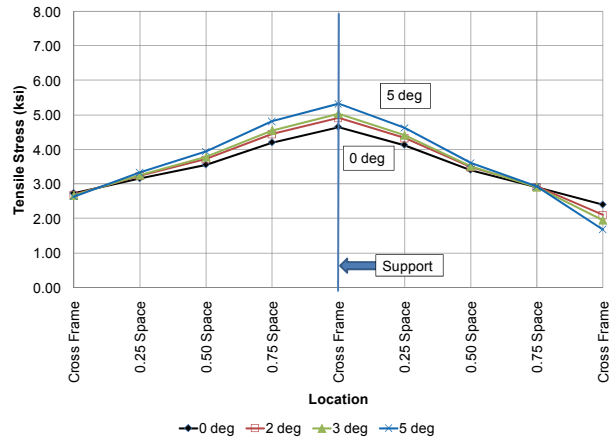


b) Girder G2

**Figure C.32 Inner-Edge Bottom Flange Tip Stresses at 0.0L of Center Span**



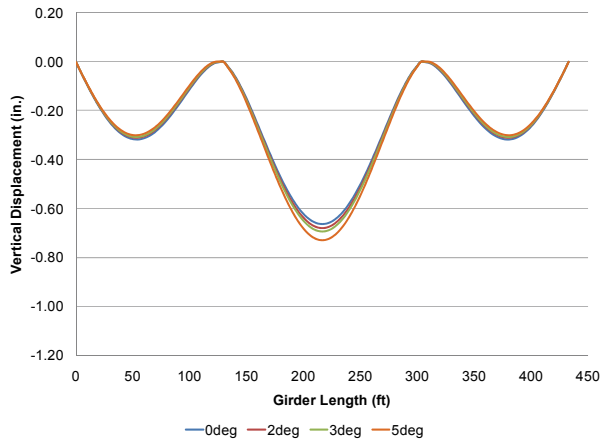
a) Girder G1



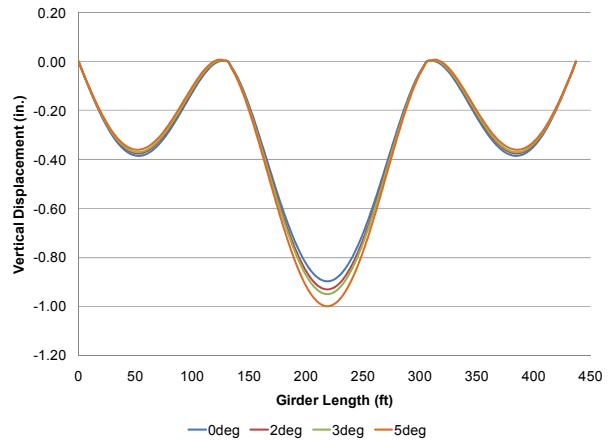
b) Girder G2

**Figure C.33 Outer-Edge Top Flange Tip Stresses at 0.0L of Center Span**

### C.1.10 Girder Displacements (R=1109.3 ft)

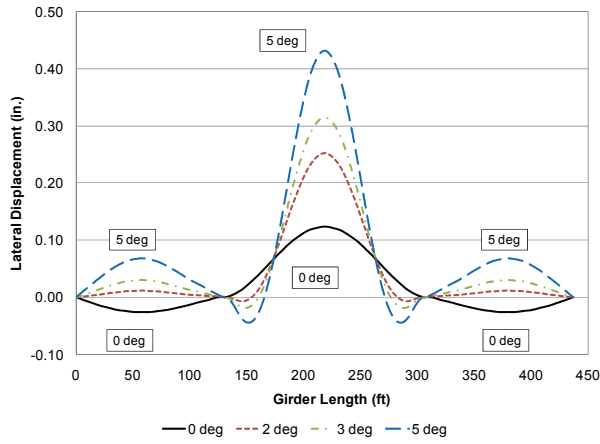


a) Girder G1

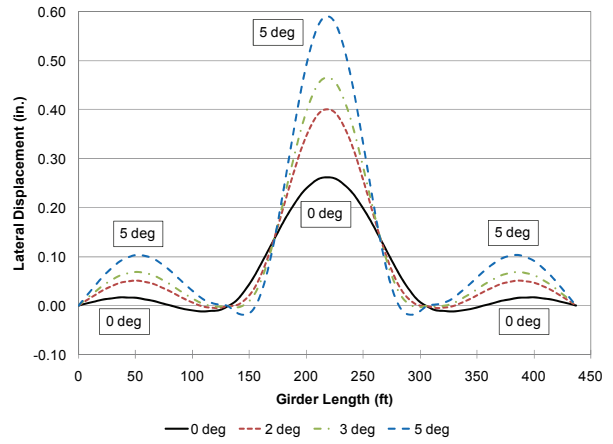


b) Girder G2

Figure C.34 Top Flange Vertical Displacement



a) Bottom Flange



b) Top Flange

Figure C.35 G2 Flange Lateral Displacement

## C.2 GIRDER SPACING PARAMETER

### C.2.1 Flange Stresses (Girder Spacing = 8.21 ft)

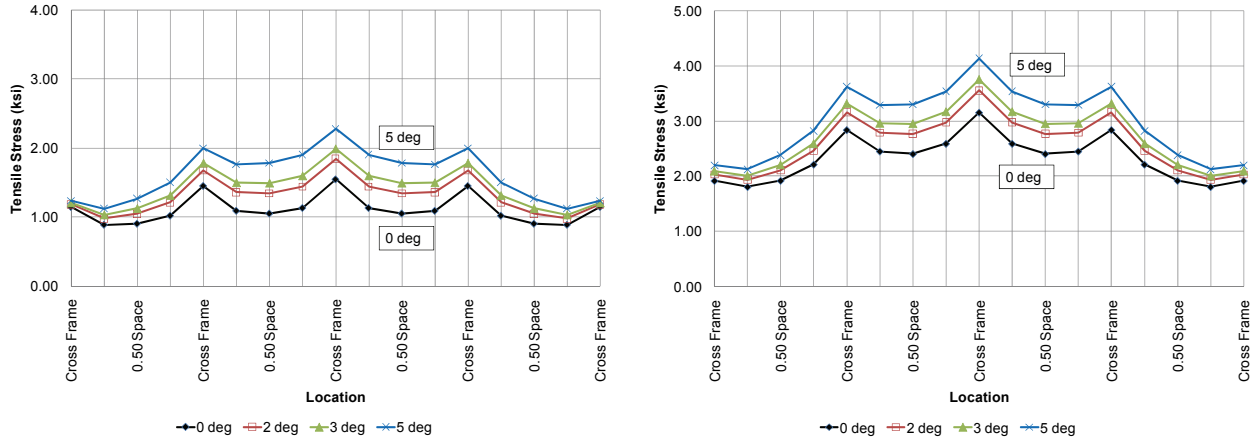


**Figure C.36** Outer-Edge Bottom Flange Tip Stresses at 0.5L of Center Span

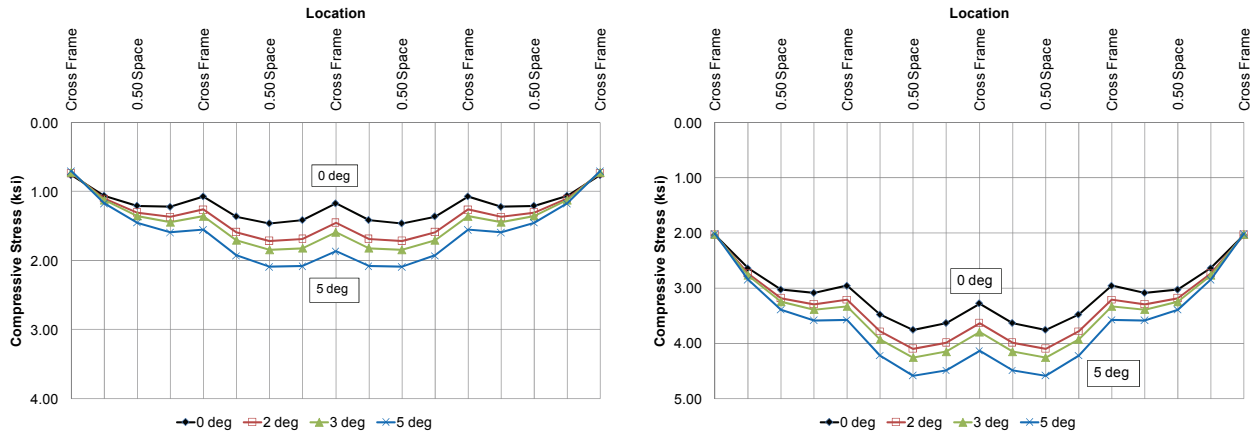
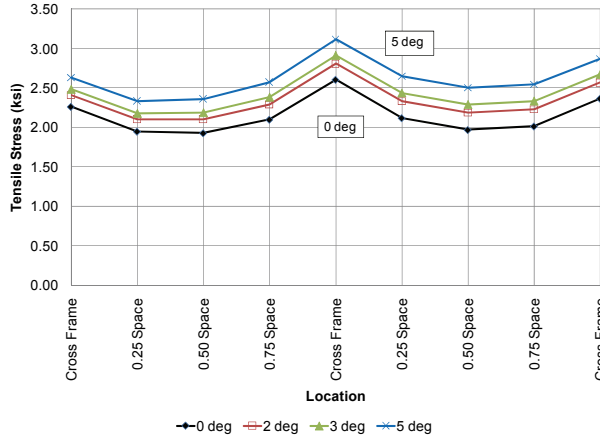
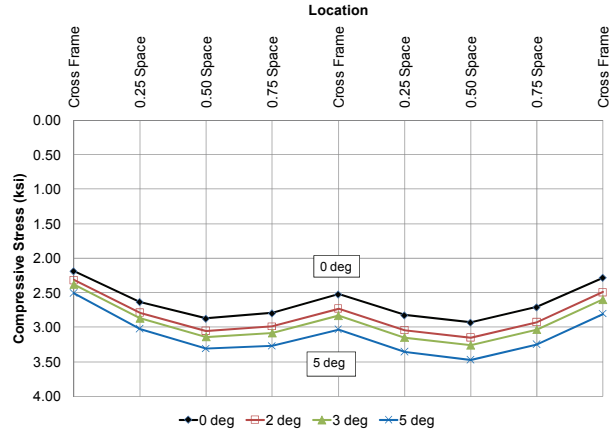


**Figure C.37** Inner-Edge Top Flange Tip Stresses at 0.5L of Center Span

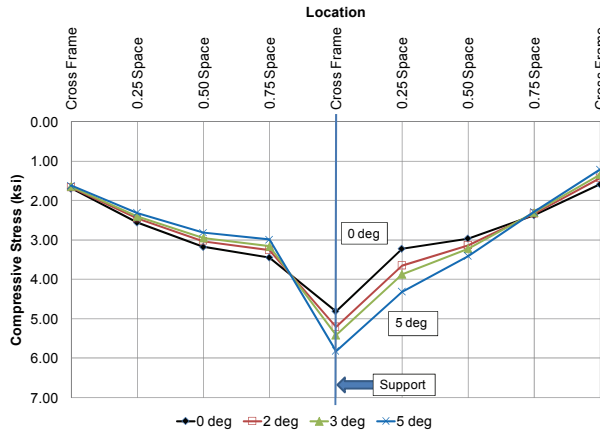


a) Outer-Edge Bottom Flange

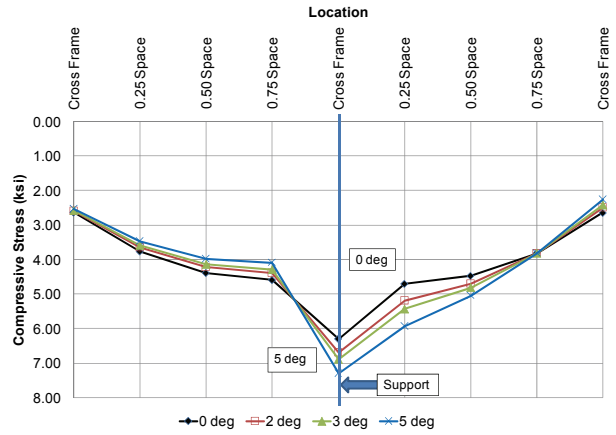


b) Inner-Edge Top Flange

Figure C.38 G2 Flange Tip Stresses at 0.4L of End Span

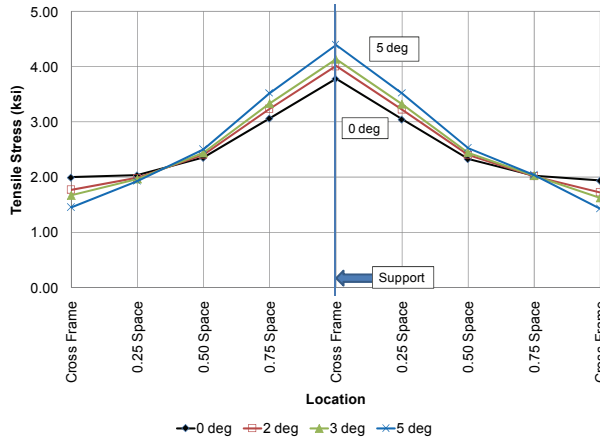


a) Girder G1

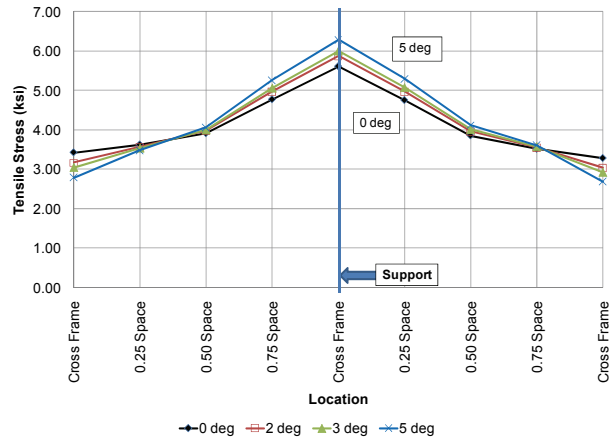


b) Girder G2

Figure C.39 Inner-Edge Bottom Flange Tip Stresses at 0.0L of Center Span



a) Girder G1



b) Girder G2

Figure C.40 Outer-Edge Top Flange Tip Stresses at 0.0L of Center Span

## C.2.2 Girder Displacements (Girder Spacing = 8.21 ft)

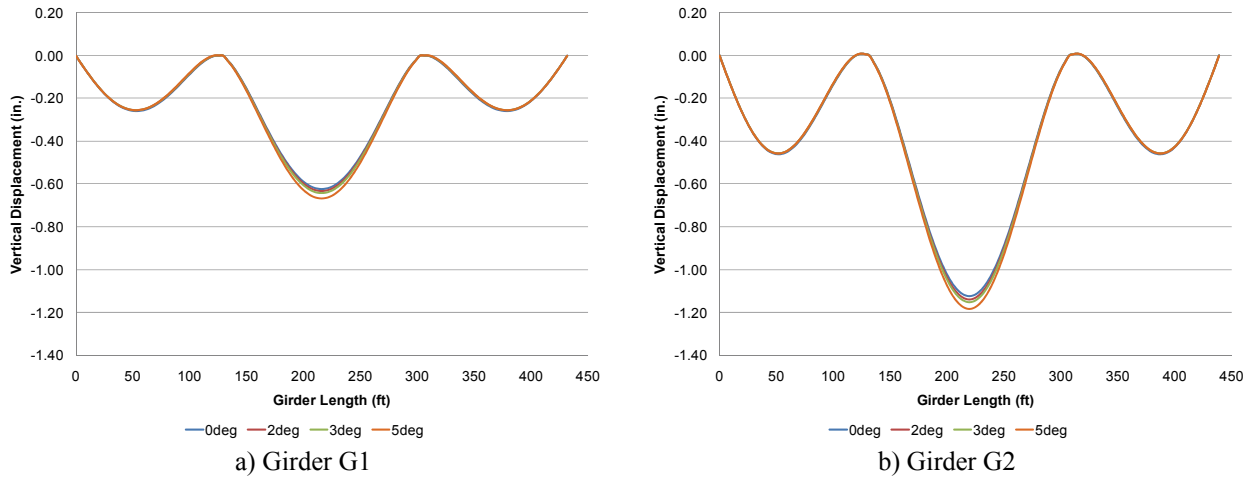


Figure C.41 Top Flange Vertical Displacement

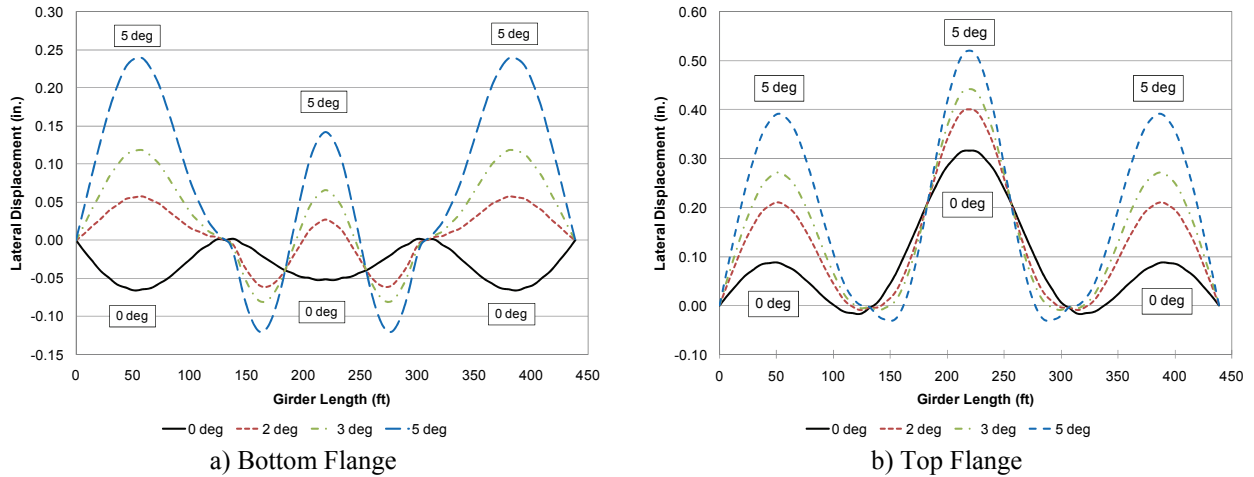


Figure C.42 G2 Flange Lateral Displacement

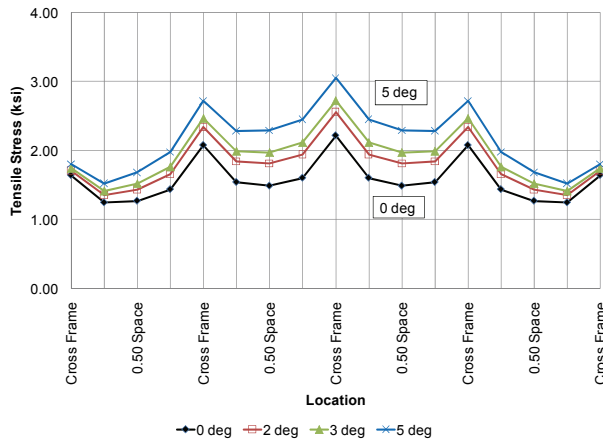
### **C.2.3 Flange Stresses – Base Model (Girder Spacing = 10.21 ft)**

See section C.1.3, which shows a summary of the results for the Base Model, and employs a 10.21 ft girder spacing.

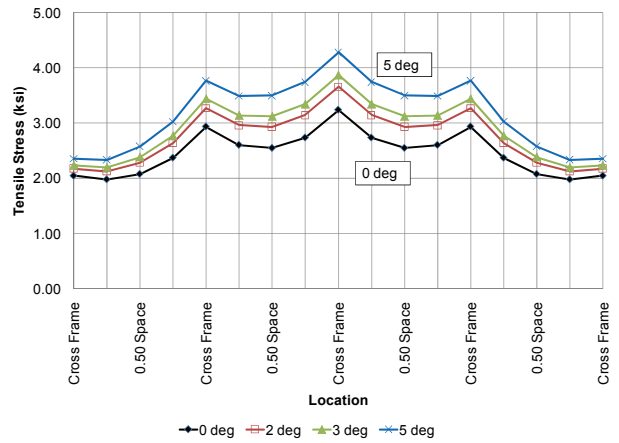
### **C.2.4 Girder Displacements – Base Model (Girder Spacing = 10.21 ft)**

See section C.1.4, which shows a summary of the results for the Base Model, and employs a 10.21 ft girder spacing.

## C.2.5 Flange Stresses (Girder Spacing = 12.21 ft)

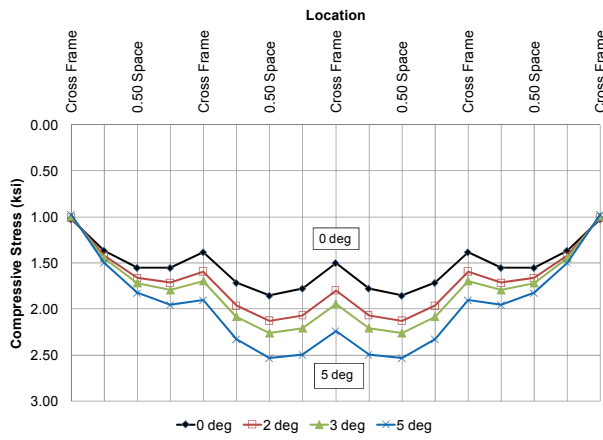


a) Girder G1

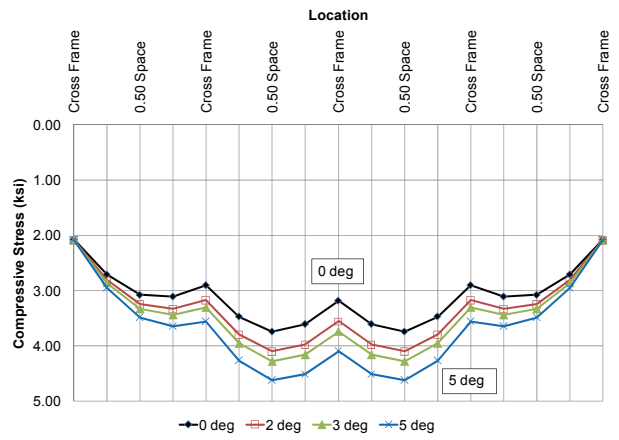


b) Girder G2

**Figure C.43** Outer-Edge Bottom Flange Tip Stresses at 0.5L of Center Span

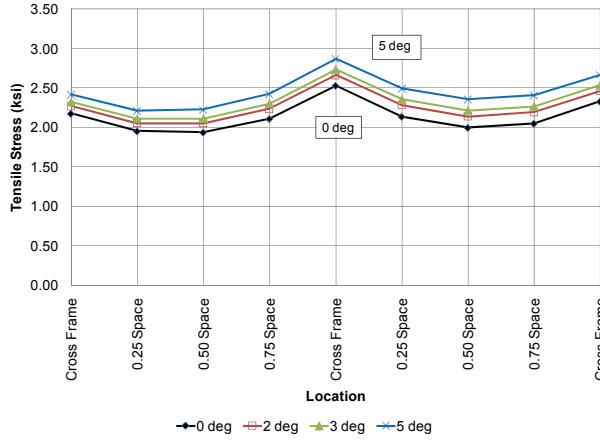


a) Girder G1

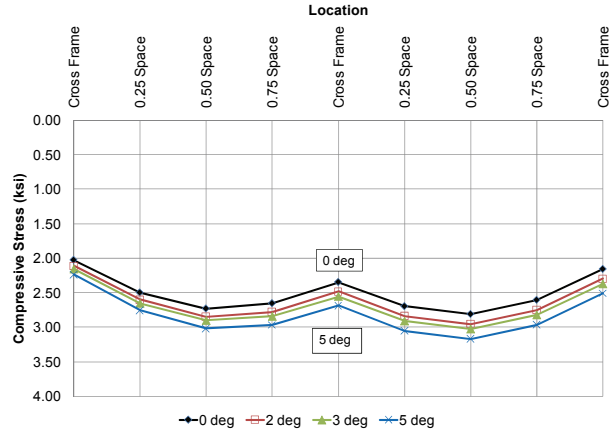


b) Girder G2

**Figure C.44** Inner-Edge Top Flange Tip Stresses at 0.5L of Center Span

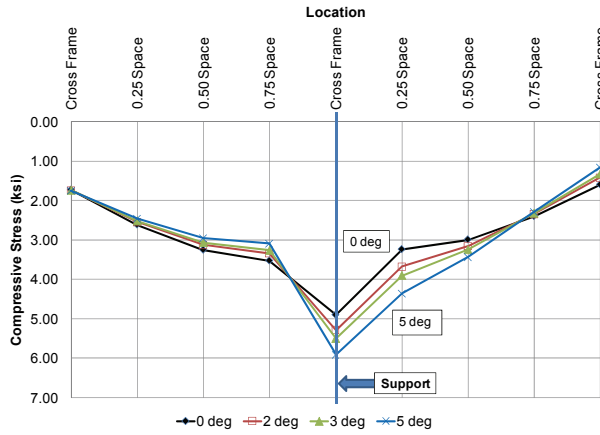


a) Outer-Edge Bottom Flange

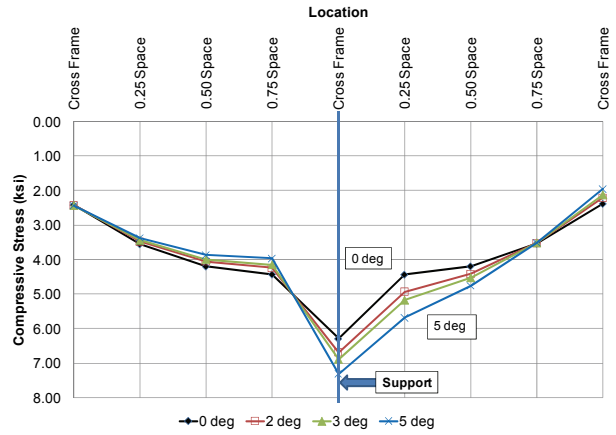


b) Inner-Edge Top Flange

Figure C.45 G2 Flange Tip Stresses at 0.4L of End Span

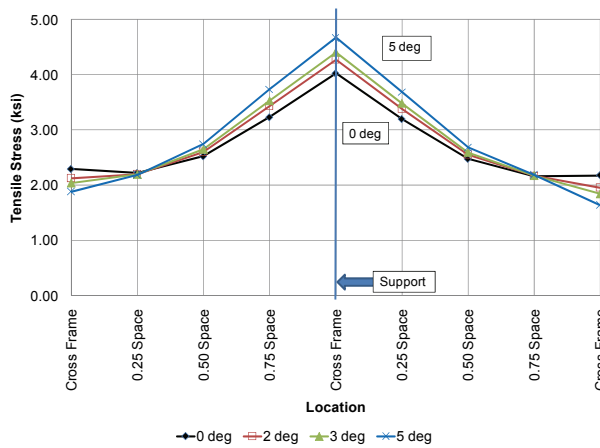


a) Girder G1

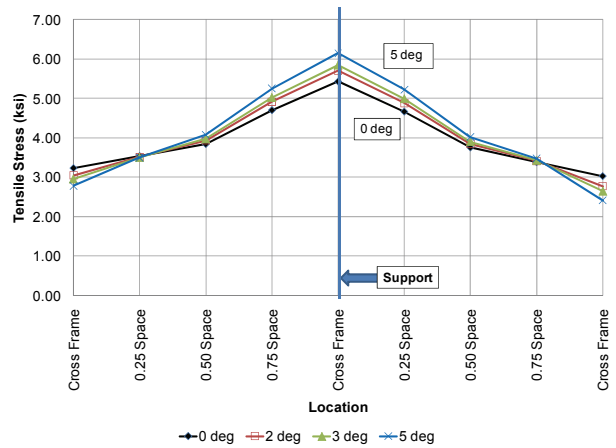


b) Girder G2

Figure C.46 Inner-Edge Bottom Flange Tip Stresses at 0.0L of Center Span



a) Girder G1



b) Girder G2

Figure C.47 Outer-Edge Top Flange Tip Stresses at 0.0L of Center Span

## C.2.6 Girder Displacements (Girder Spacing = 12.21 ft)

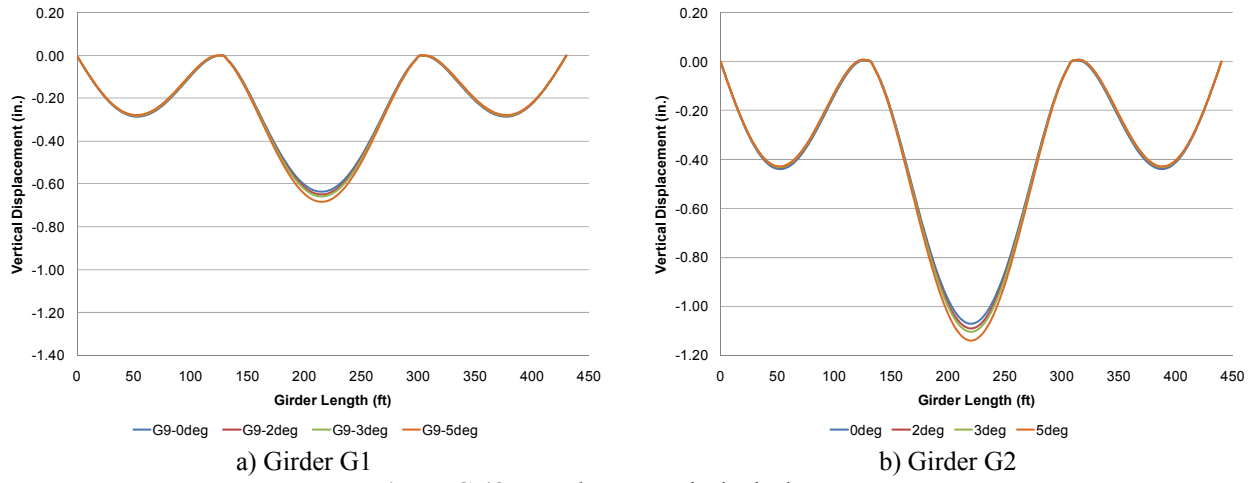


Figure C.48 Top Flange Vertical Displacement

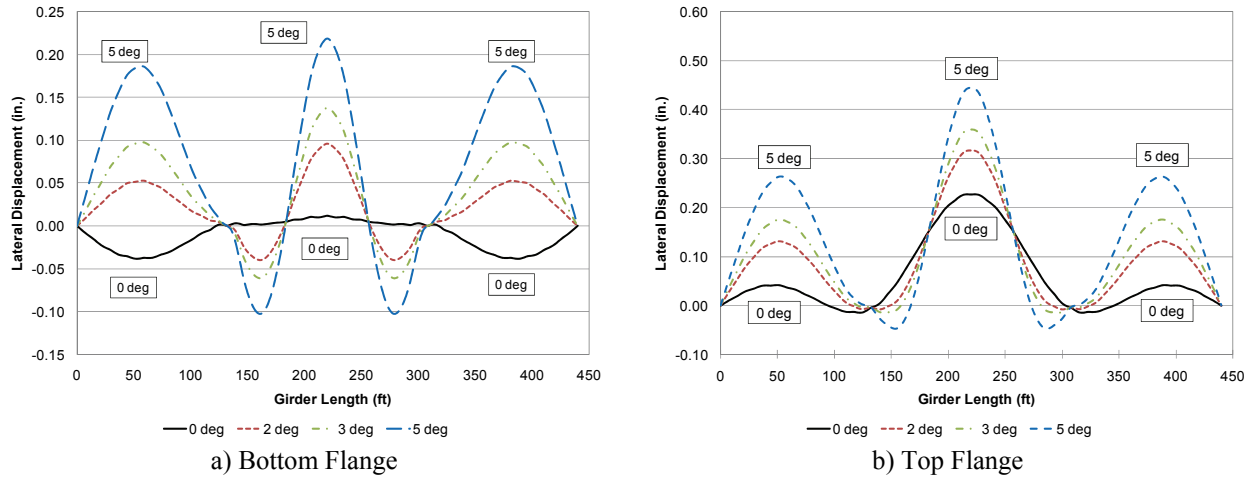
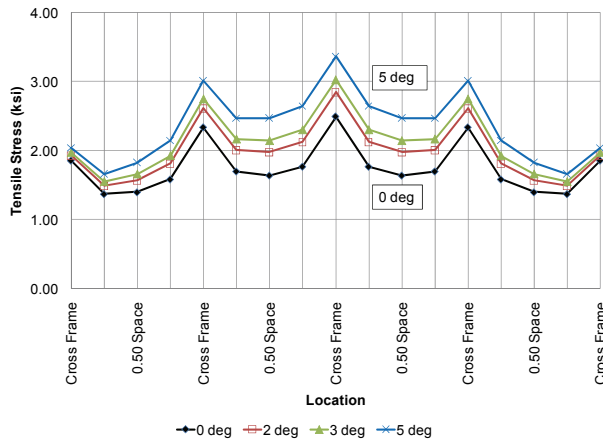
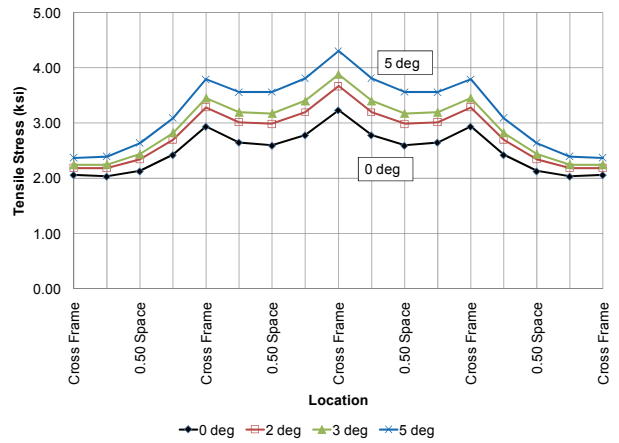


Figure C.49 G2 Flange Lateral Displacement

### C.2.7 Flange Stresses (Girder Spacing = 14.21 ft)

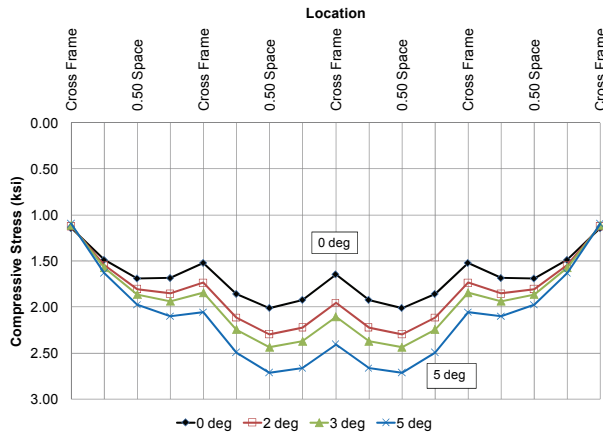


a) Girder G1

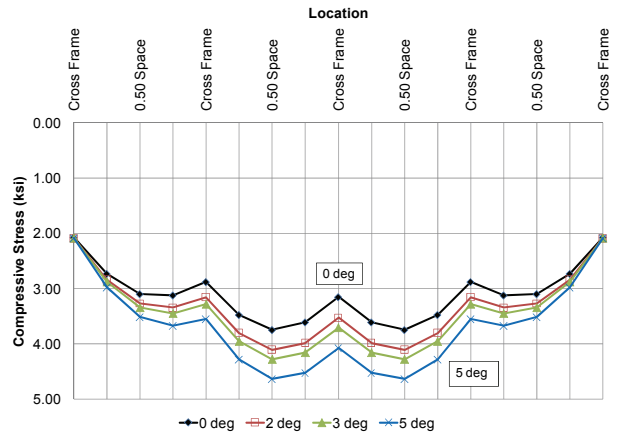


b) Girder G2

**Figure C.50** Outer-Edge Bottom Flange Tip Stresses at 0.5L of Center Span

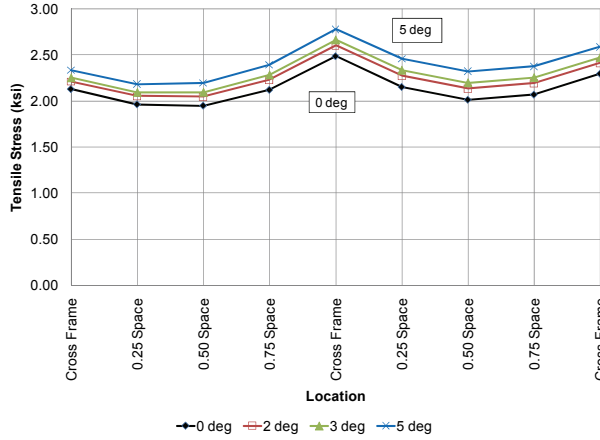


a) Girder G1



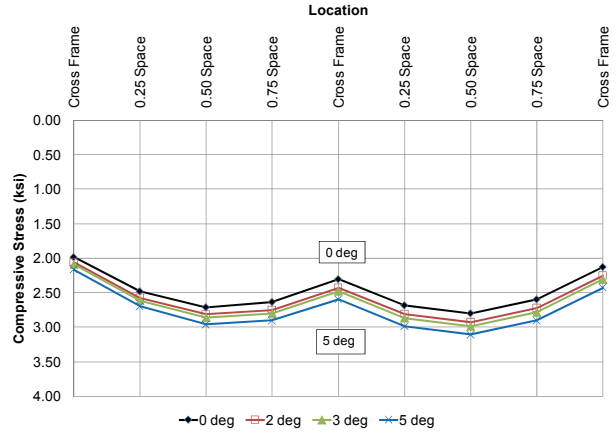
b) Girder G2

**Figure C.51** Inner-Edge Top Flange Tip Stresses at 0.5L of Center Span

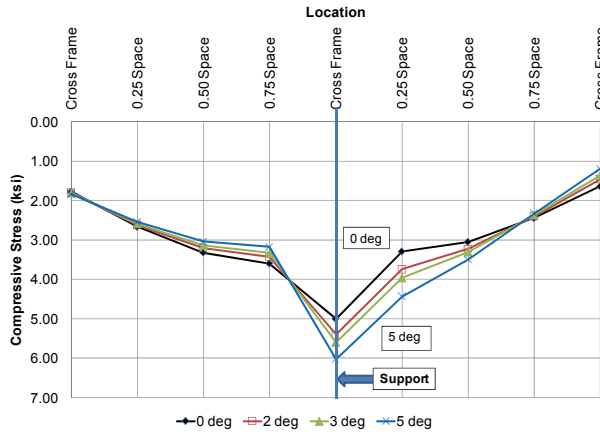


a) Outer-Edge Bottom Flange

**Figure C.52 G2 Flange Tip Stresses at 0.4L of End Span**

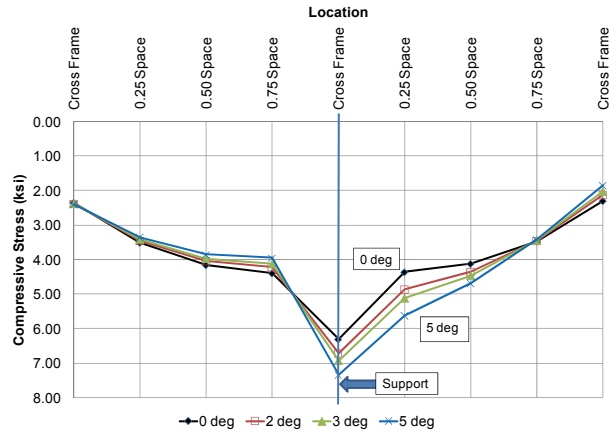


b) Inner-Edge Top Flange

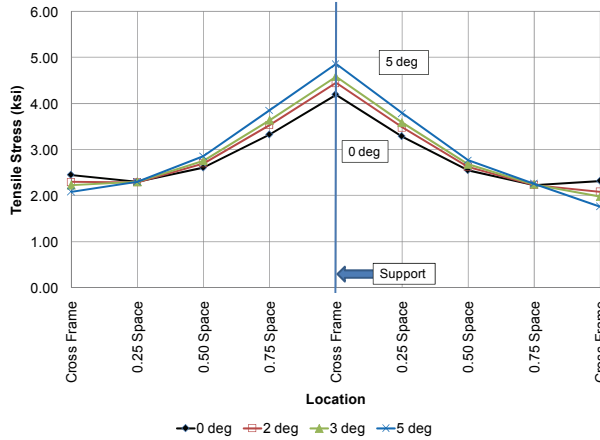


a) Girder G1

**Figure C.53 Inner-Edge Bottom Flange Tip Stresses at 0.0L of Center Span**

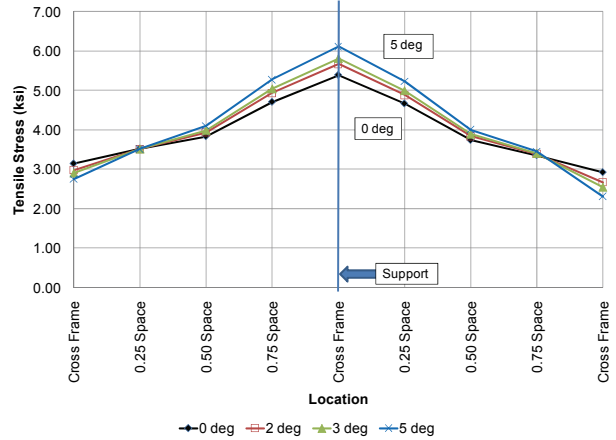


b) Girder G2



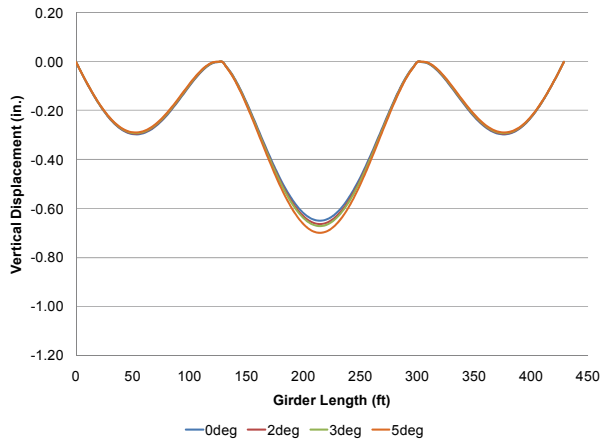
a) Girder G1

**Figure C.54 Outer-Edge Top Flange Tip Stresses at 0.0L of Center Span**

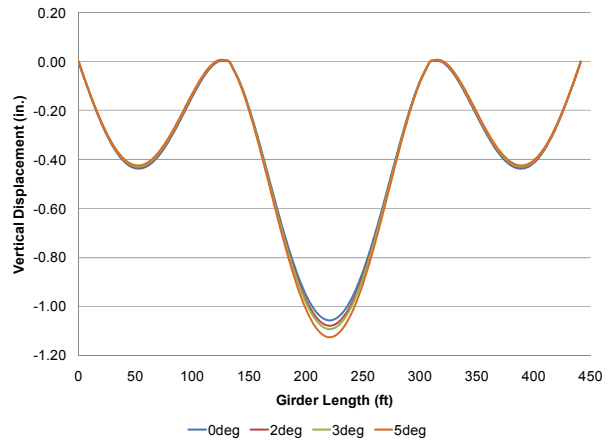


b) Girder G2

### C.2.8 Girder Displacements (Girder Spacing = 14.21 ft)

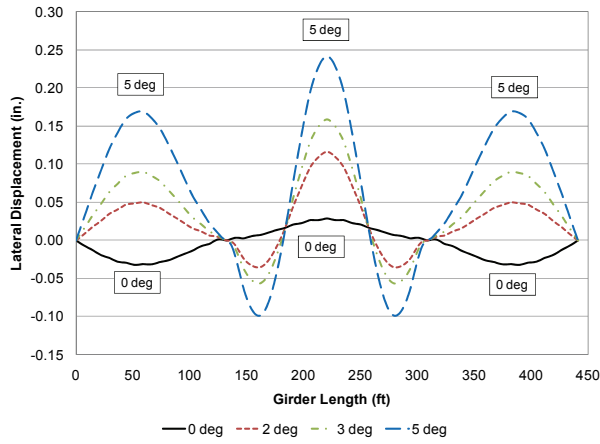


a) Girder G1

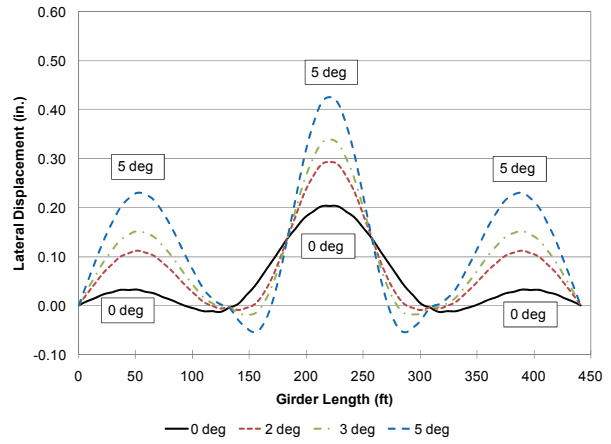


b) Girder G2

Figure C.55 Top Flange Vertical Displacement



a) Bottom Flange

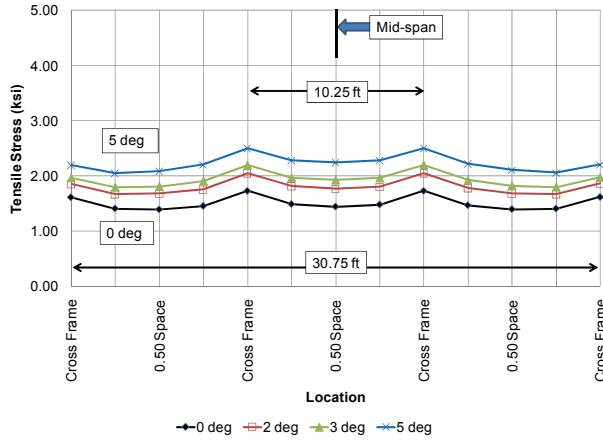


b) Top Flange

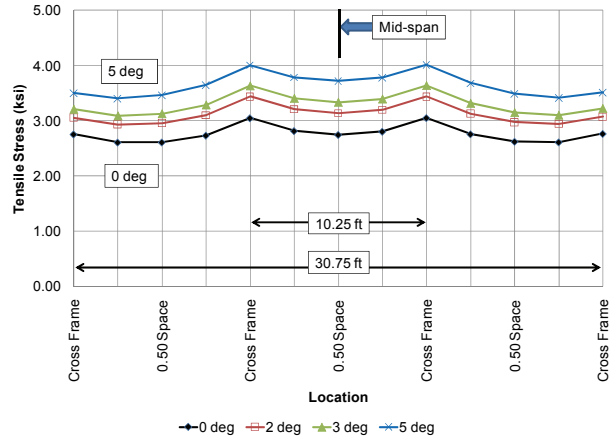
Figure C.56 G2 Flange Lateral Displacement

### C.3 CROSS FRAME SPACING PARAMETER

#### C.3.1 Flange Stresses (Center Span Cross Frame Spacing = 10.25 ft)

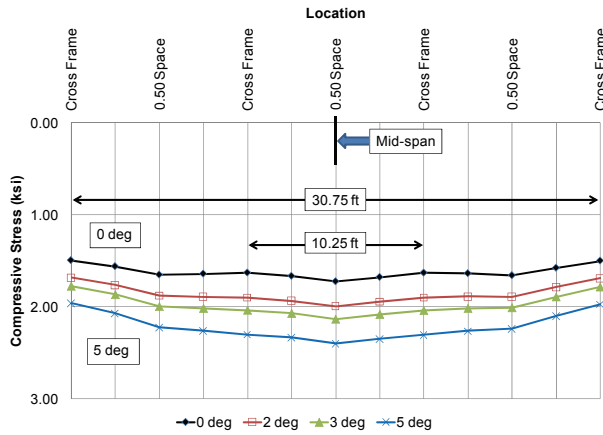


a) Girder G1

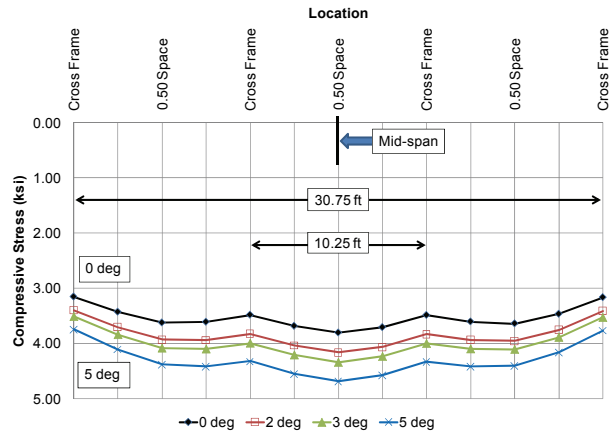


b) Girder G2

**Figure C.57** Outer-Edge Bottom Flange Tip Stresses at 0.5L of Center Span



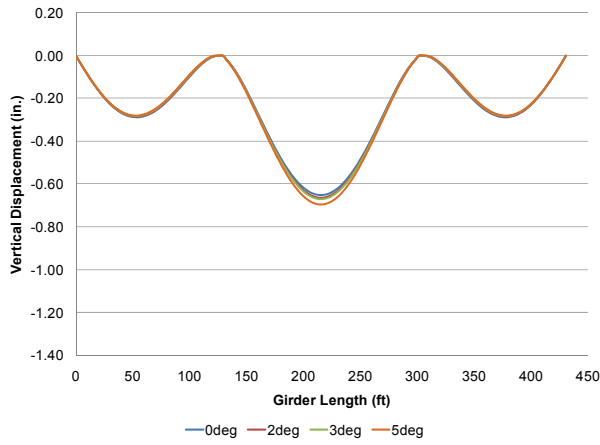
a) Girder G1



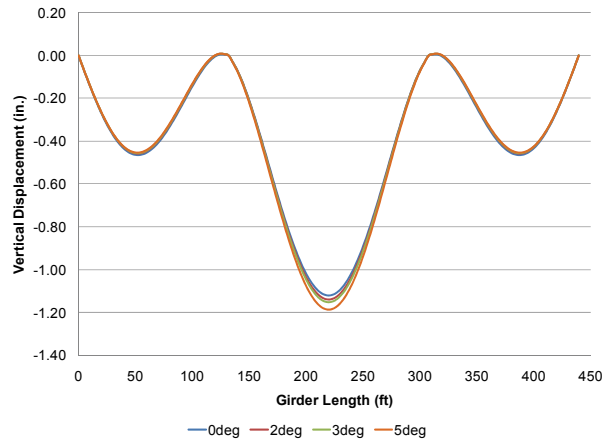
b) Girder G2

**Figure C.58** Inner-Edge Top Flange Tip Stresses at 0.5L of Center Span

### C.3.2 Girder Displacements (Center Span Cross Frame Spacing = 10.25 ft)

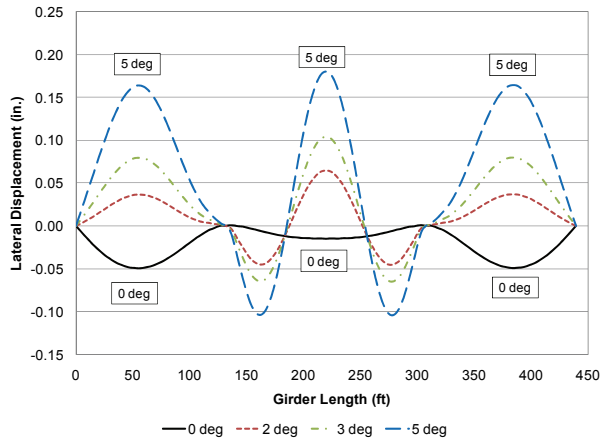


a) Girder G1

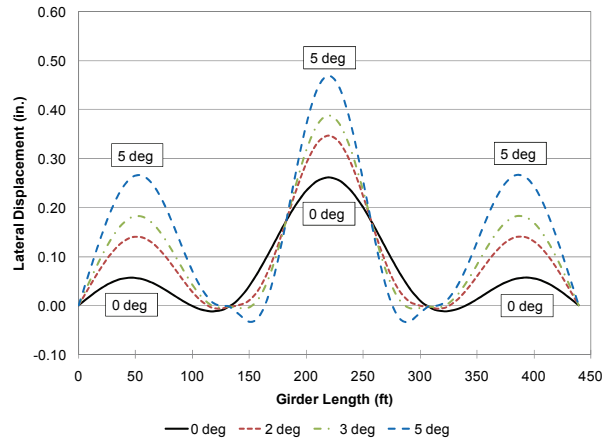


b) Girder G2

Figure C.59 Top Flange Vertical Displacement



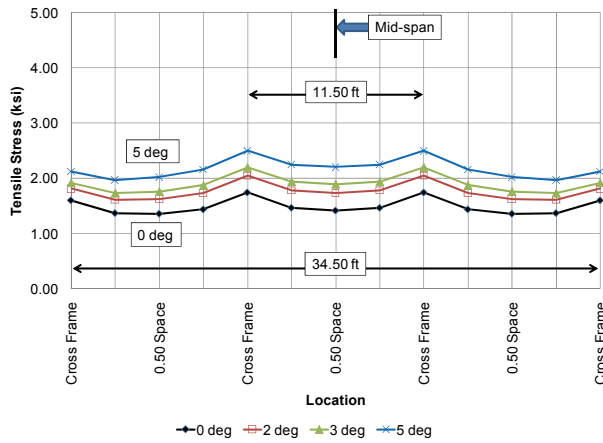
a) Bottom Flange



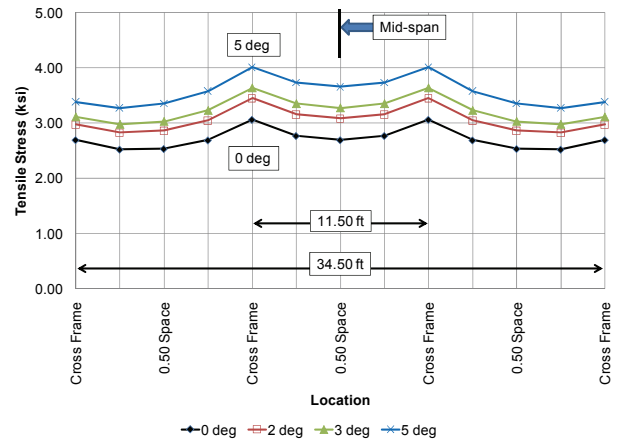
b) Top Flange

Figure C.60 G2 Flange Lateral Displacement

### C.3.3 Flange Stresses (Center Span Cross Frame Spacing = 11.50 ft)

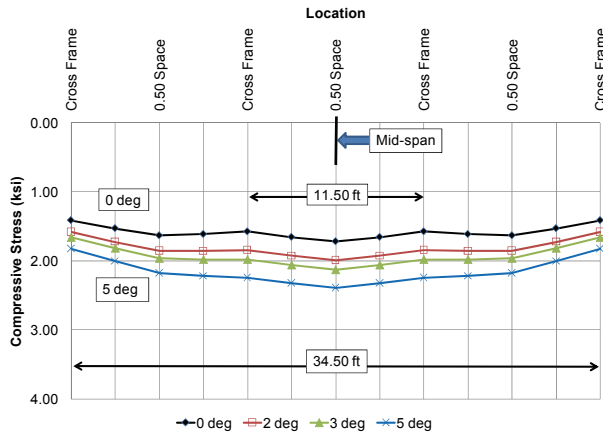


a) Girder G1

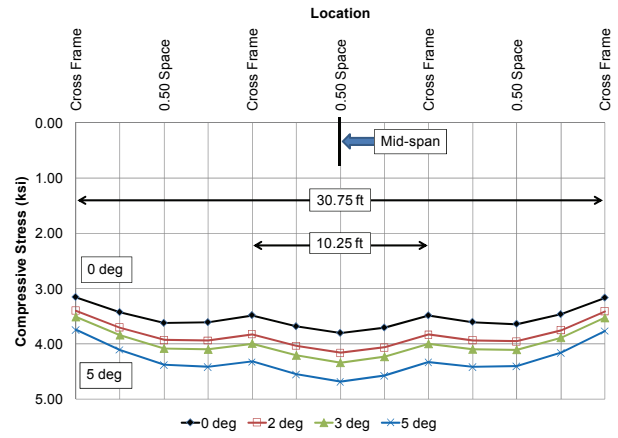


b) Girder G2

**Figure C.61** Outer-Edge Bottom Flange Tip Stresses at 0.5L of Center Span



a) Girder G1



b) Girder G2

**Figure C.62** Inner-Edge Top Flange Tip Stresses at 0.5L of Center Span

### C.3.4 Girder Displacements (Center Span Cross Frame Spacing = 11.50 ft)

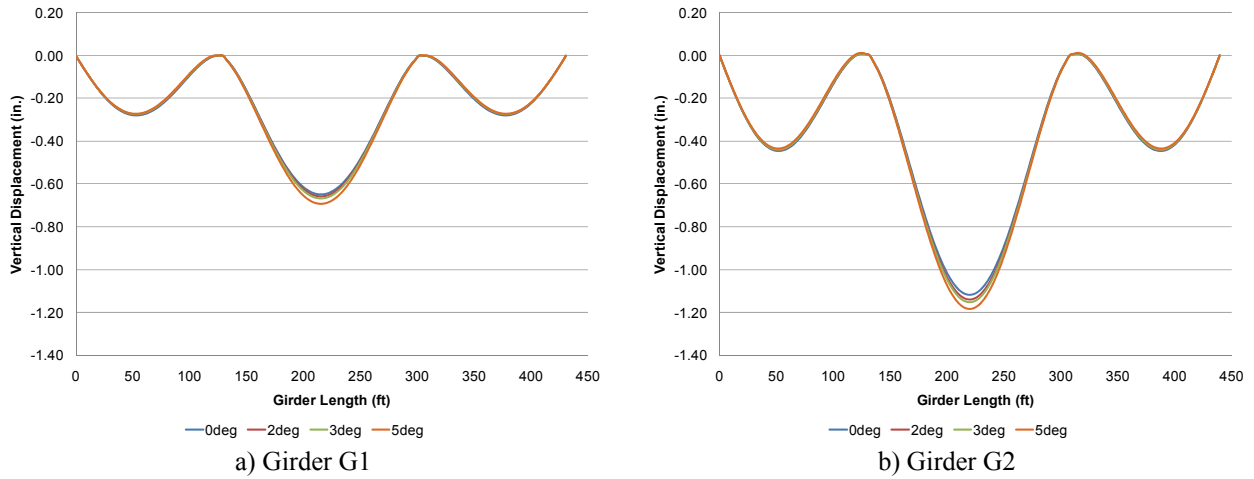


Figure C.63 Top Flange Vertical Displacement

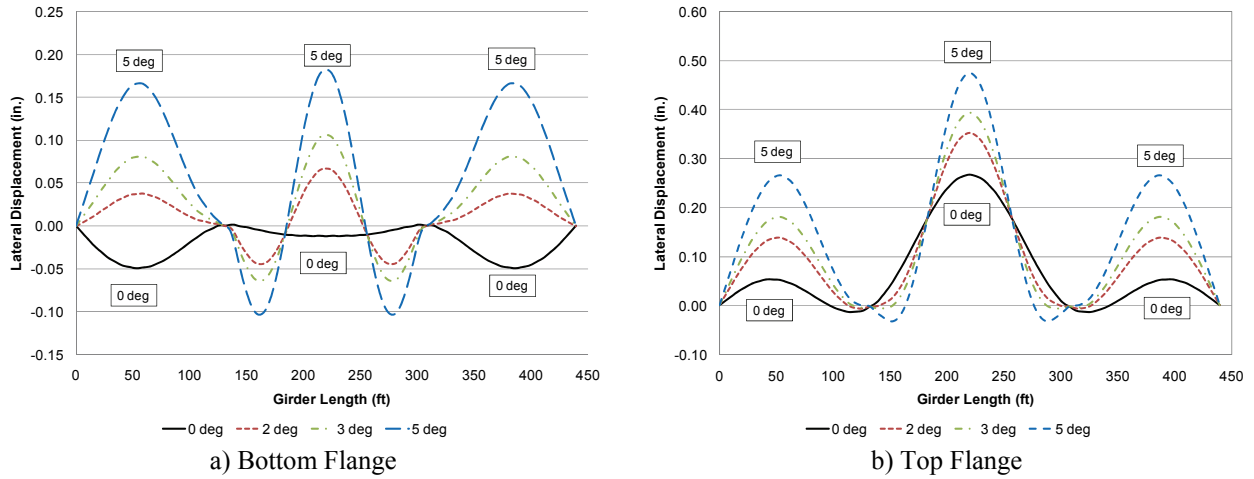


Figure C.64 G2 Flange Lateral Displacement

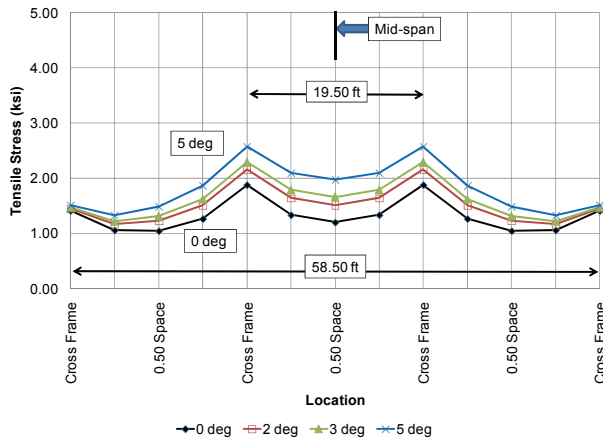
### **C.3.5 Flange Stresses – Base Model (Center Span Cross Frame Spacing = 14.50 ft)**

See section C.1.3, which shows a summary of the results for the Base Model, and employs a 14.50 ft cross frame spacing.

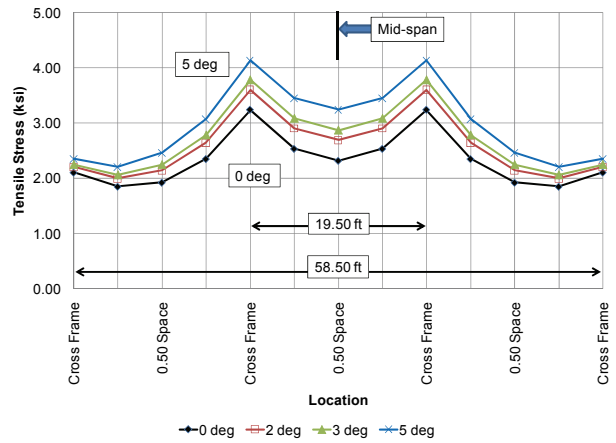
### **C.3.6 Girder Displacements – Base Model (Center Span Cross Frame Spacing = 14.50 ft)**

See section C.1.4, which shows a summary of the results for the Base Model, and employs a 14.50 ft cross frame spacing.

### C.3.7 Flange Stresses (Center Span Cross Frame Spacing = 19.50 ft)

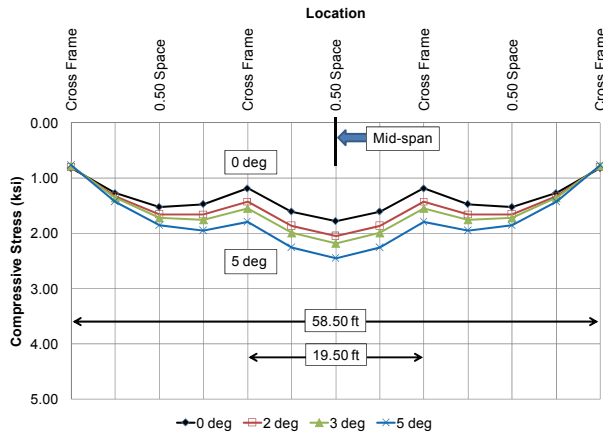


a) Girder G1

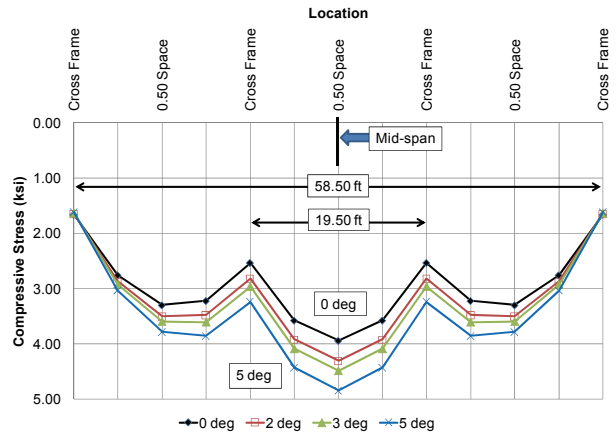


b) Girder G2

**Figure C.65** Outer-Edge Bottom Flange Tip Stresses at 0.5L of Center Span



a) Girder G1



b) Girder G2

**Figure C.66** Inner-Edge Top Flange Tip Stresses at 0.5L of Center Span

### C.3.8 Girder Displacements (Center Span Cross Frame Spacing = 19.50 ft)

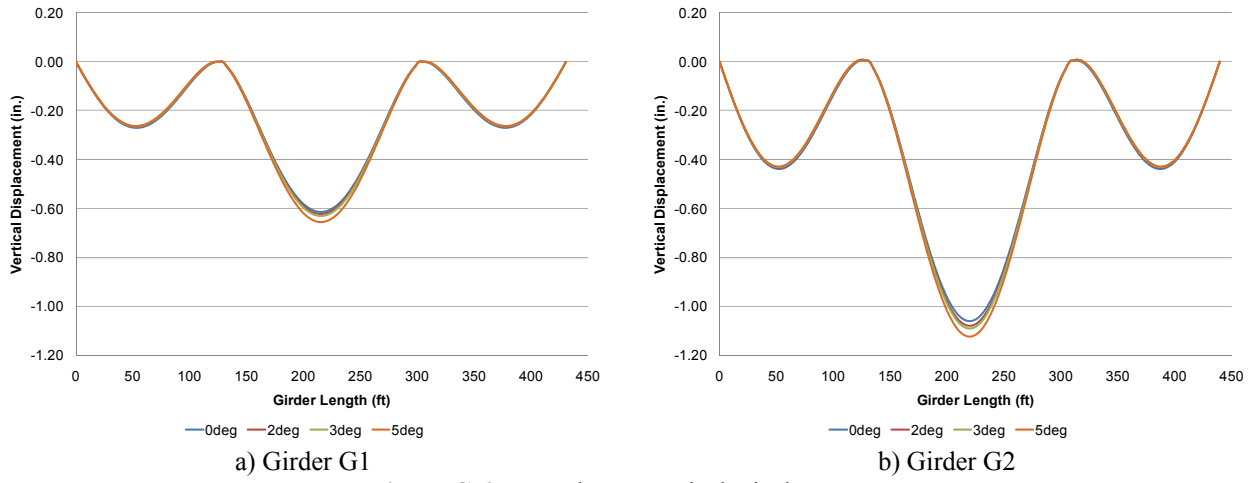


Figure C.67 Top Flange Vertical Displacement

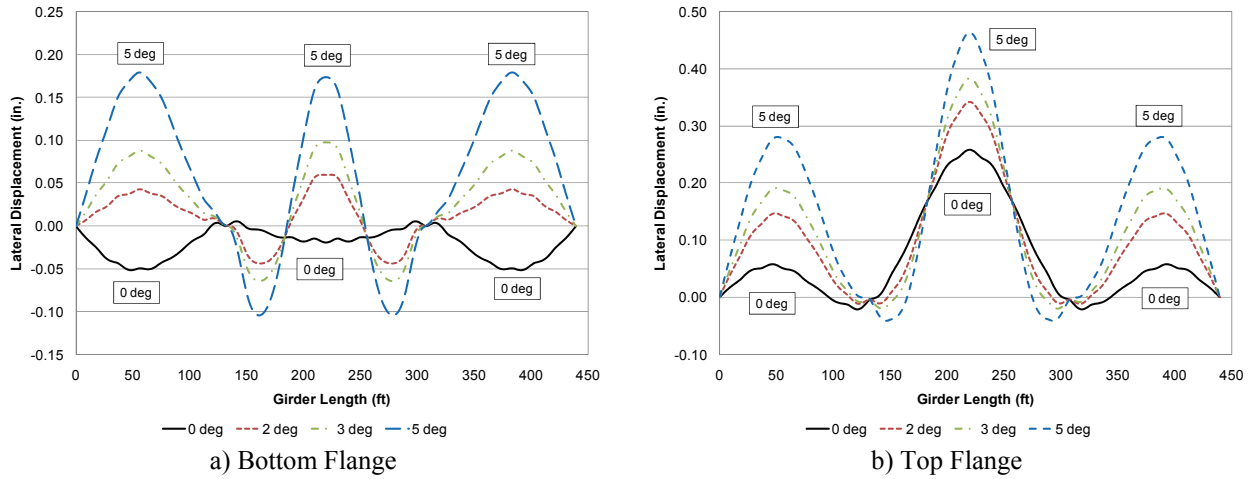
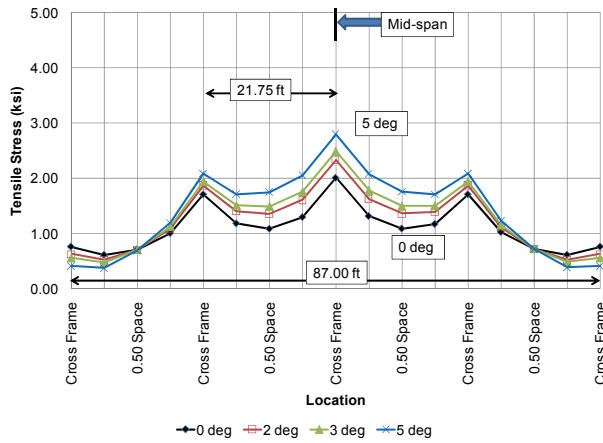
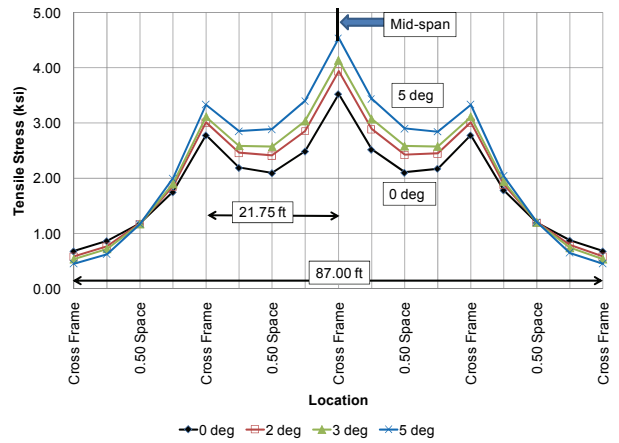


Figure C.68 G2 Flange Lateral Displacement

### C.3.9 Flange Stresses (Center Span Cross Frame Spacing = 21.75 ft)

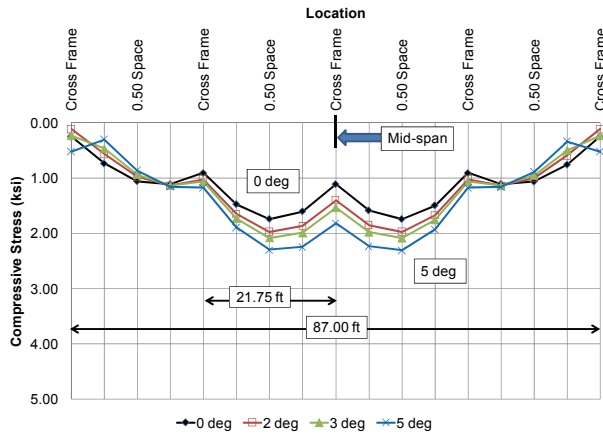


a) Girder G1

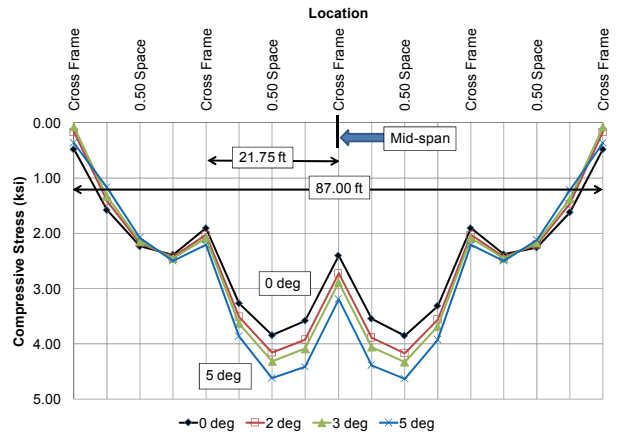


b) Girder G2

**Figure C.69** Outer-Edge Bottom Flange Tip Stresses at 0.5L of Center Span



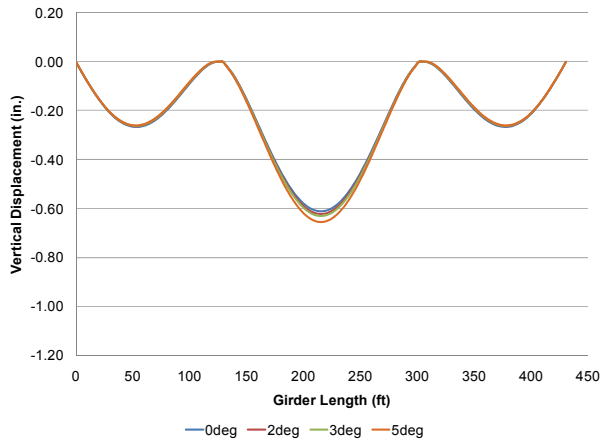
a) Girder G1



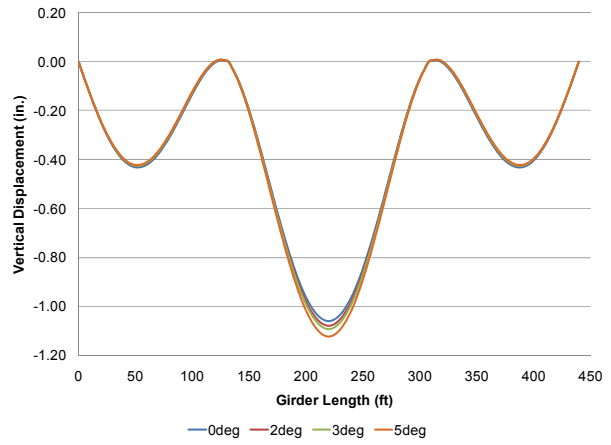
b) Girder G2

**Figure C.70** Inner-Edge Top Flange Tip Stresses at 0.5L of Center Span

### C.3.10 Girder Displacements (Center Span Cross Frame Spacing = 21.75 ft)

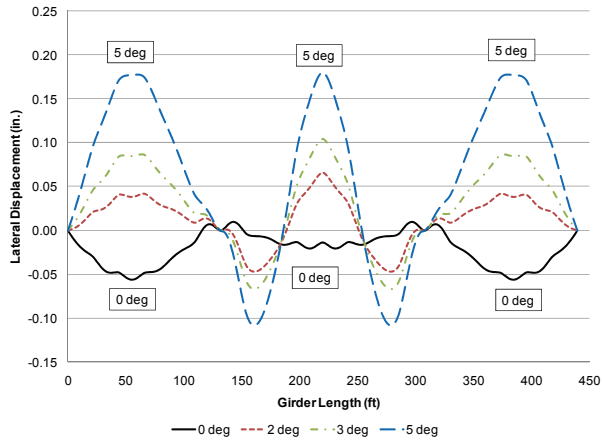


a) Girder G1

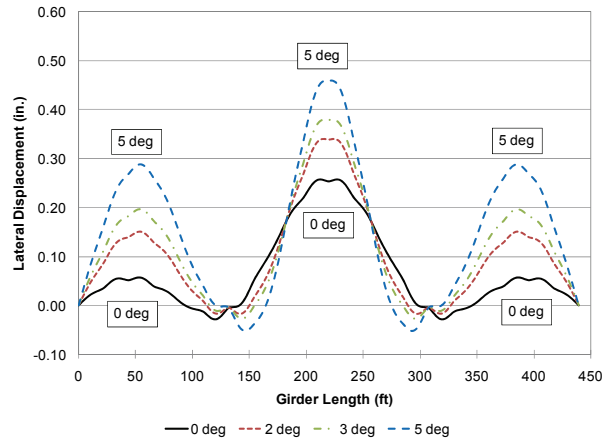


b) Girder G2

**Figure C.71 Top Flange Vertical Displacement**



a) Bottom Flange

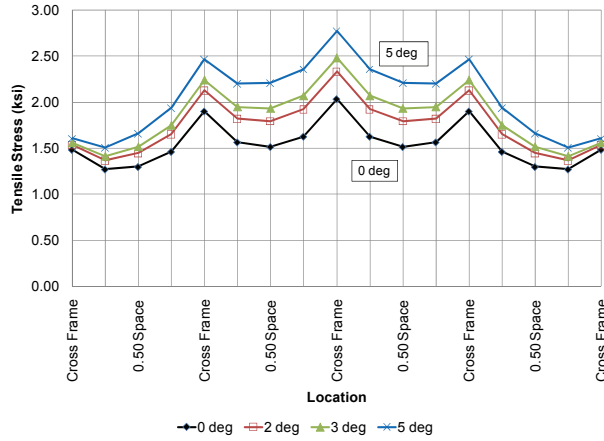


b) Top Flange

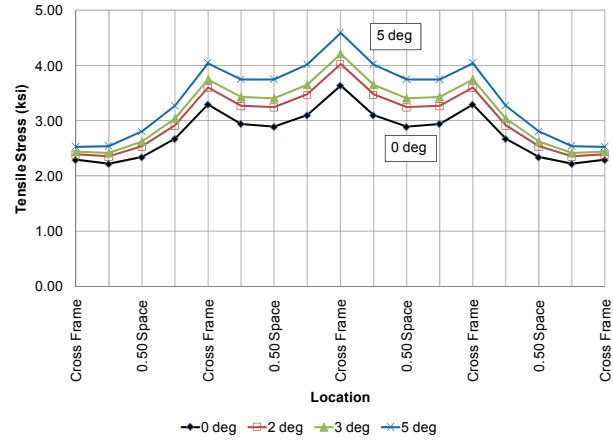
**Figure C.72 G2 Flange Lateral Displacement**

## C.4 WEB DEPTH PARAMETER

### C.4.1 Flange Stresses (Web Depth = 60 in.)

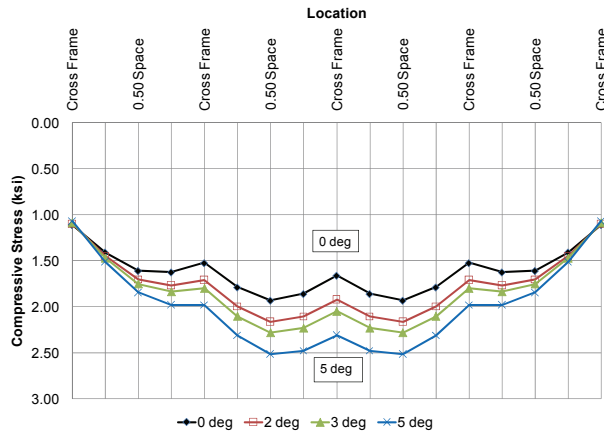


a) Girder G1

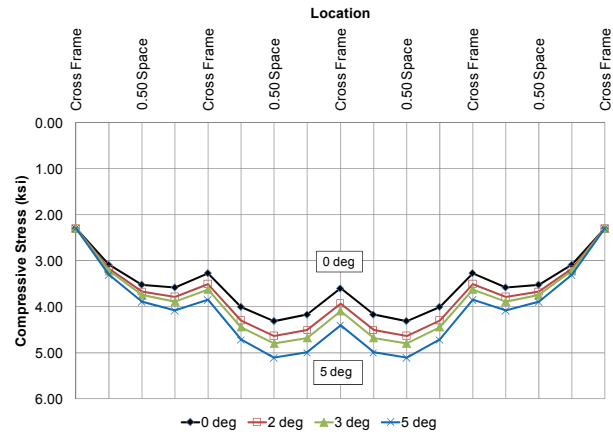


b) Girder G2

**Figure C.73 Outer-Edge Bottom Flange Tip Stresses at 0.5L of Center Span**

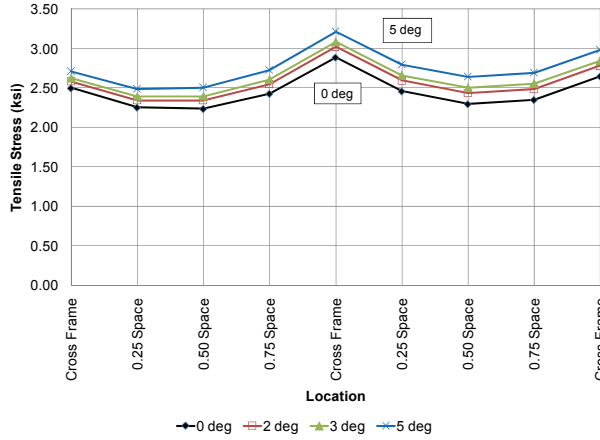


a) Girder G1

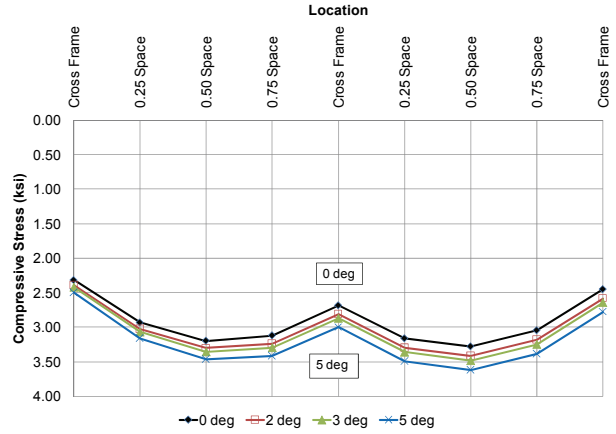


b) Girder G2

**Figure C.74 Inner-Edge Top Flange Tip Stresses at 0.5L of Center Span**

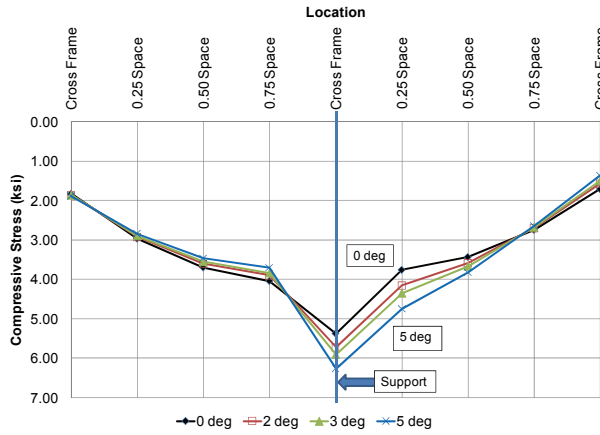


a) Outer-Edge Bottom Flange

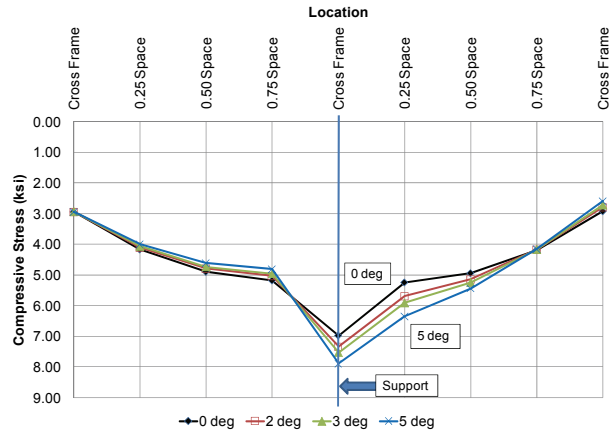


b) Inner-Edge Top Flange

**Figure C.75 G2 Flange Tip Stresses at 0.4L of End Span**

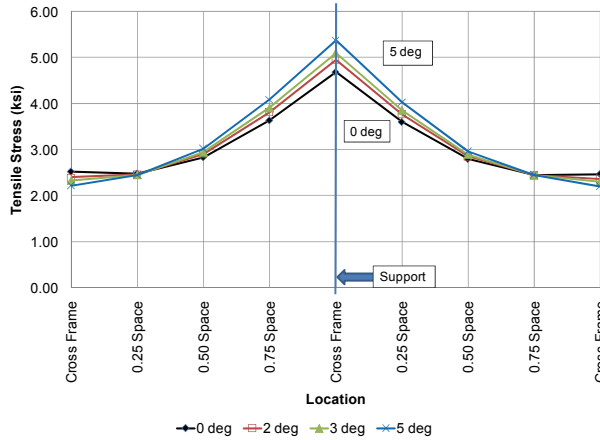


a) Girder G1

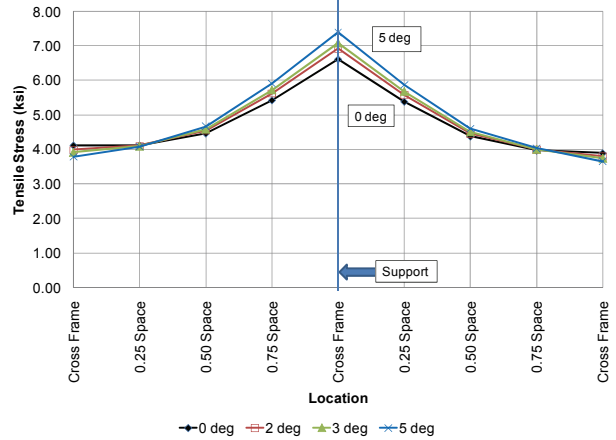


b) Girder G2

**Figure C.76 Inner-Edge Bottom Flange Tip Stresses at 0.0L of Center Span**



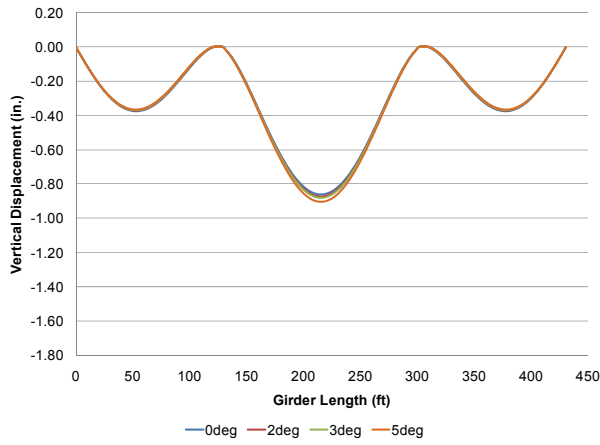
a) Girder G1



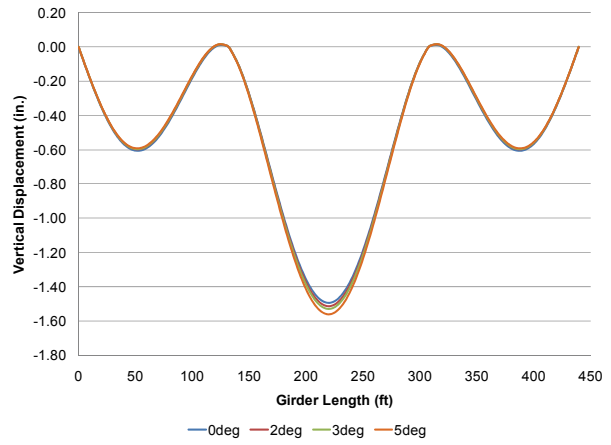
b) Girder G2

**Figure C.77 Outer-Edge Top Flange Tip Stresses at 0.0L of Center Span**

### C.4.2 Girder Displacements (Web Depth = 60 in.)

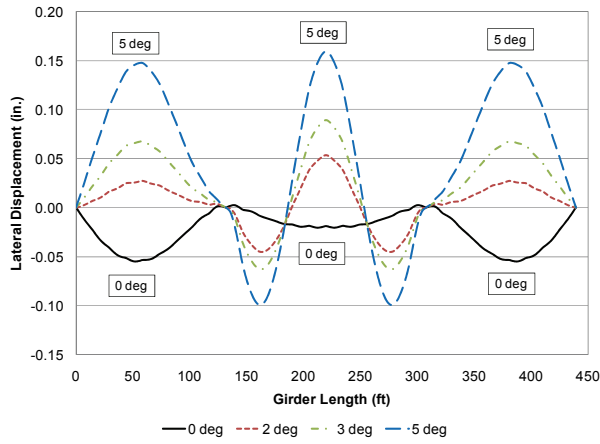


a) Girder G1

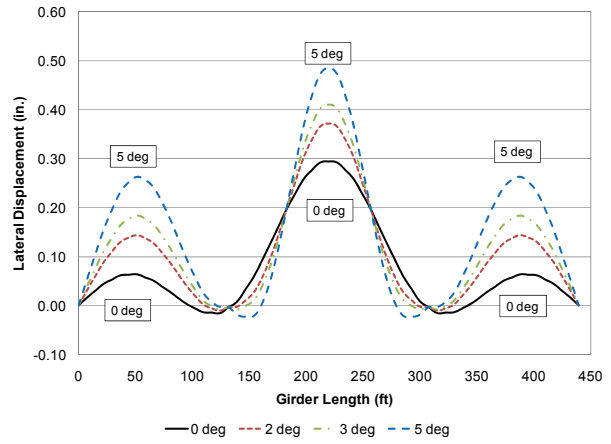


b) Girder G2

**Figure C.78 Top Flange Vertical Displacement**



a) Bottom Flange



b) Top Flange

**Figure C.79 G2 Flange Lateral Displacement**

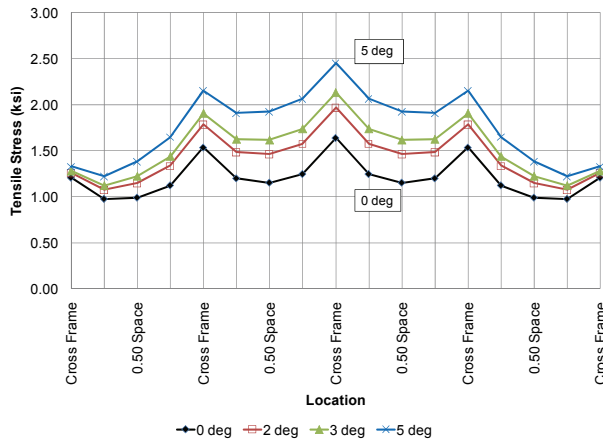
#### **C.4.3 Flange Stresses – Base Model (Web Depth = 72 in.)**

See section C.1.3, which shows a summary of the results for the Base Model, and employs a 72 in. deep web.

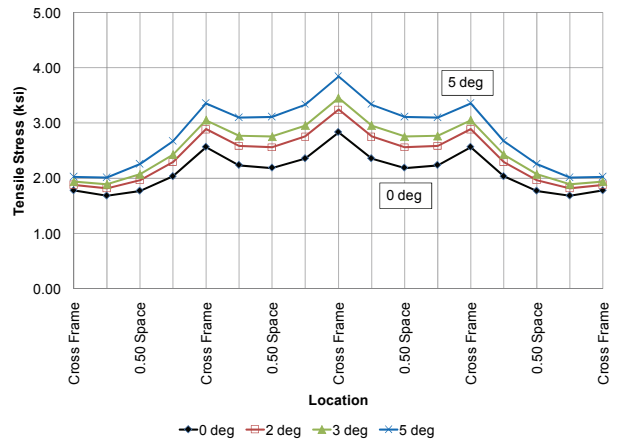
#### **C.4.4 Girder Displacements – Base Model (Web Depth = 72 in.)**

See section C.1.4, which shows a summary of the results for the Base Model, and employs a 72 in. deep web.

### C.4.5 Flange Stresses (Web Depth = 84 in.)

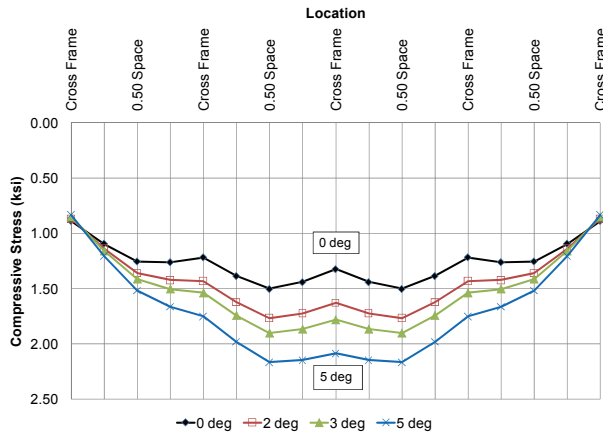


a) Girder G1

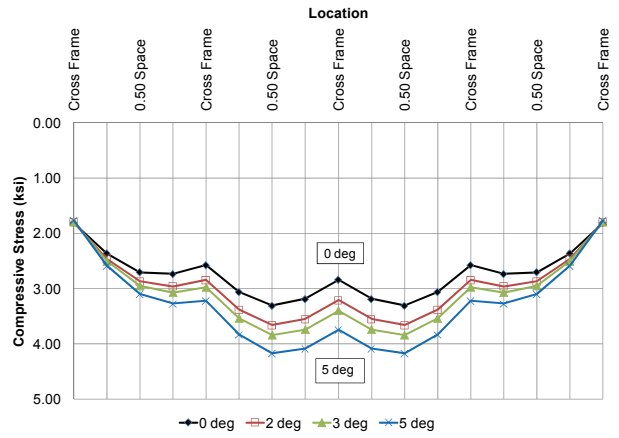


b) Girder G2

**Figure C.80** Outer-Edge Bottom Flange Tip Stresses at 0.5L of Center Span

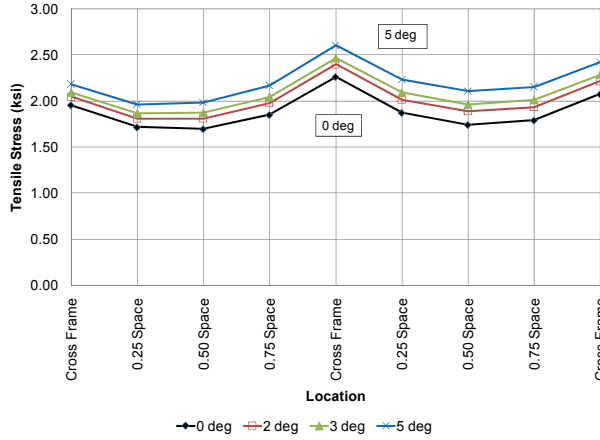


a) Girder G1

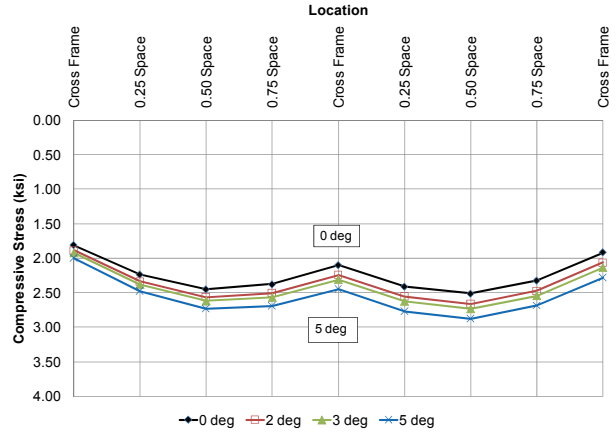


b) Girder G2

**Figure C.81** Inner-Edge Top Flange Tip Stresses at 0.5L of Center Span

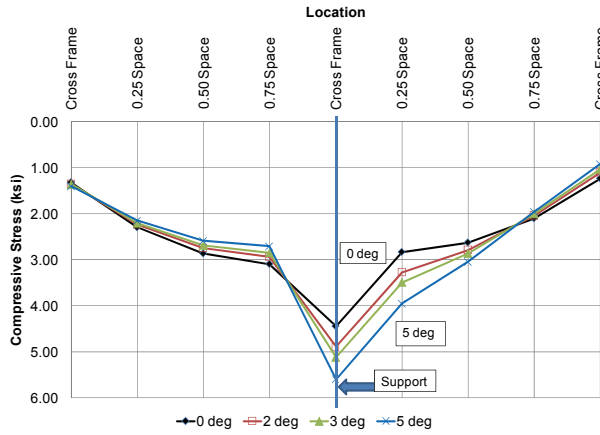


a) Outer-Edge Bottom Flange

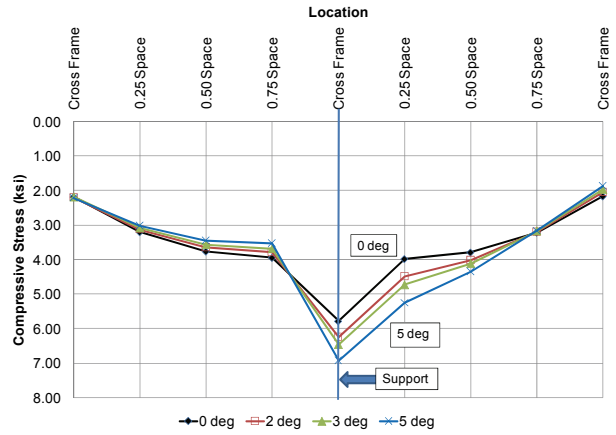


b) Inner-Edge Top Flange

Figure C.82 G2 Flange Tip Stresses at 0.4L of End Span

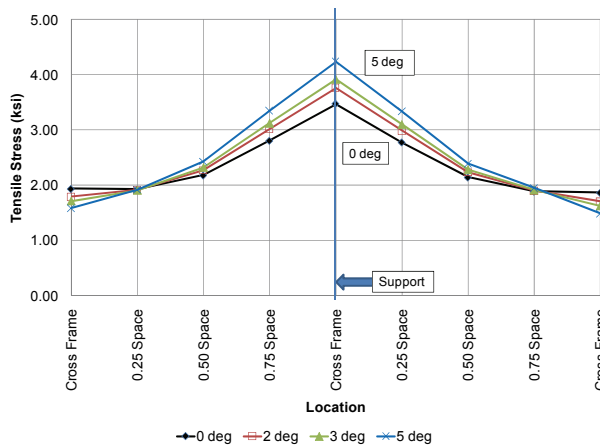


a) Girder G1

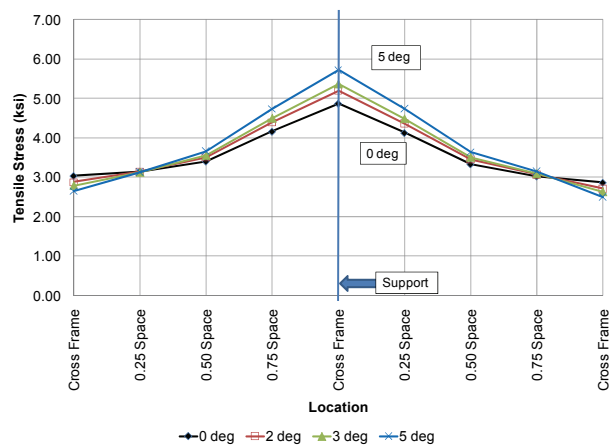


b) Girder G2

Figure C.83 Inner-Edge Bottom Flange Tip Stresses at 0.0L of Center Span



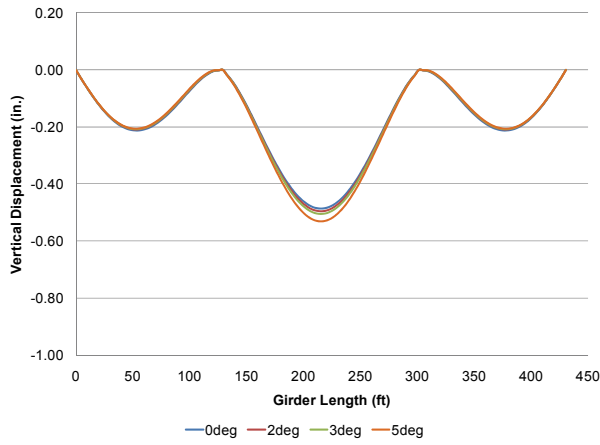
a) Girder G1



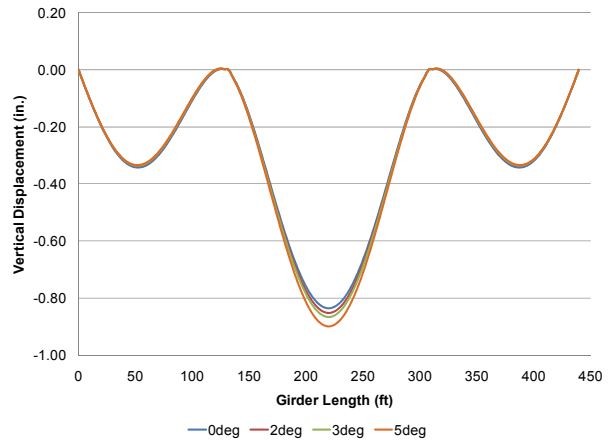
b) Girder G2

Figure C.84 Outer-Edge Top Flange Tip Stresses at 0.0L of Center Span

### C.4.6 Girder Displacements (Web Depth = 84 in.)

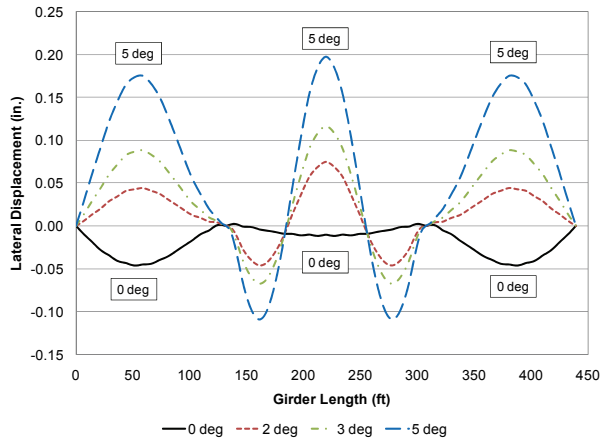


a) Girder G1

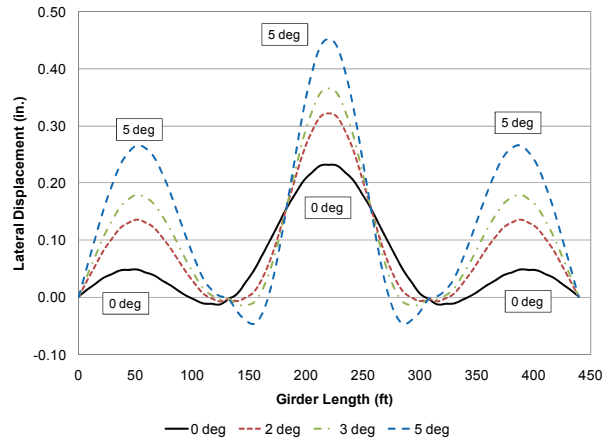


b) Girder G2

Figure C.85 Top Flange Vertical Displacement



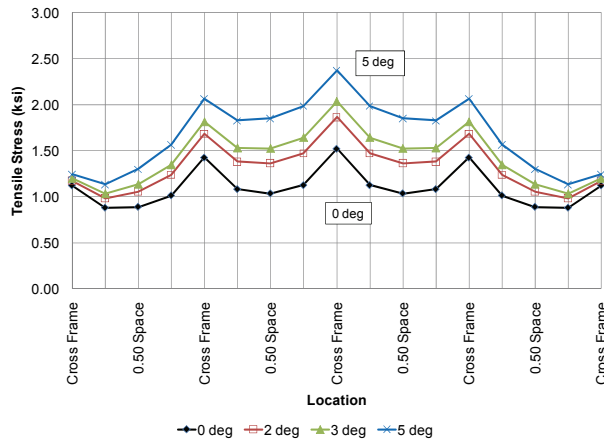
a) Bottom Flange



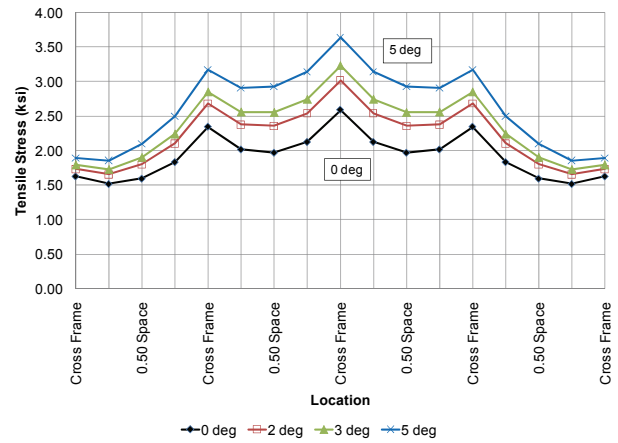
b) Top Flange

Figure C.86 G2 Flange Lateral Displacement

### C.4.7 Flange Stresses (Web Depth = 96 in.)

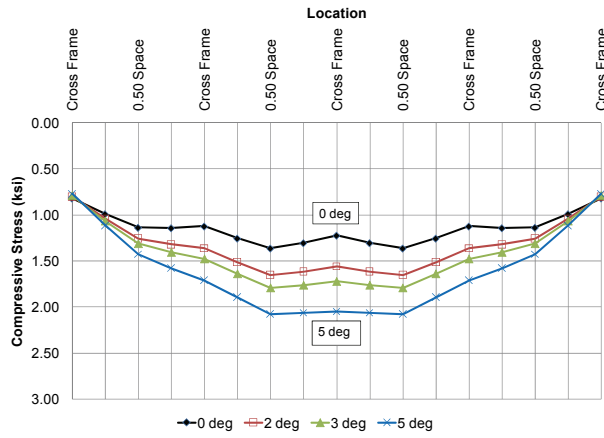


a) Girder G1

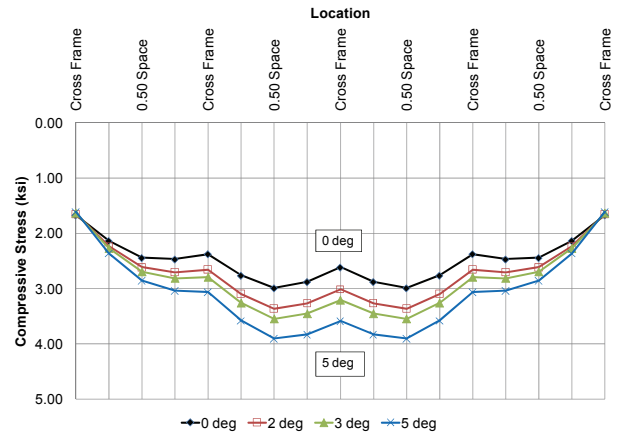


b) Girder G2

**Figure C.87** Outer-Edge Bottom Flange Tip Stresses at 0.5L of Center Span

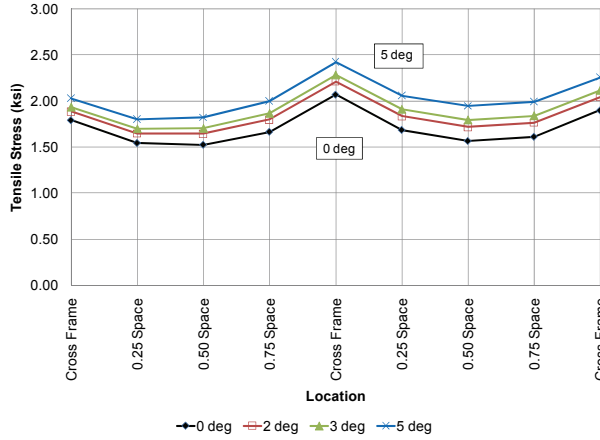


a) Girder G1

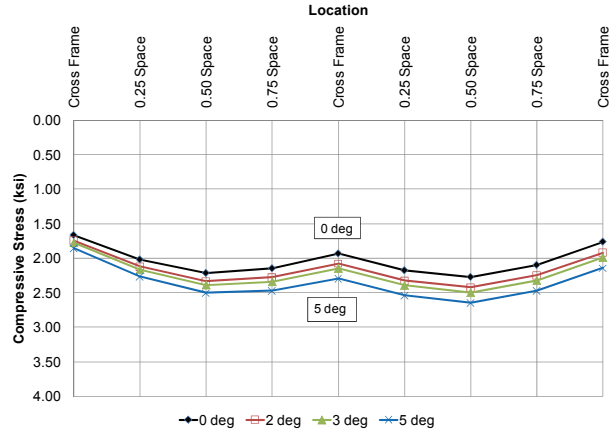


b) Girder G2

**Figure C.88** Inner-Edge Top Flange Tip Stresses at 0.5L of Center Span

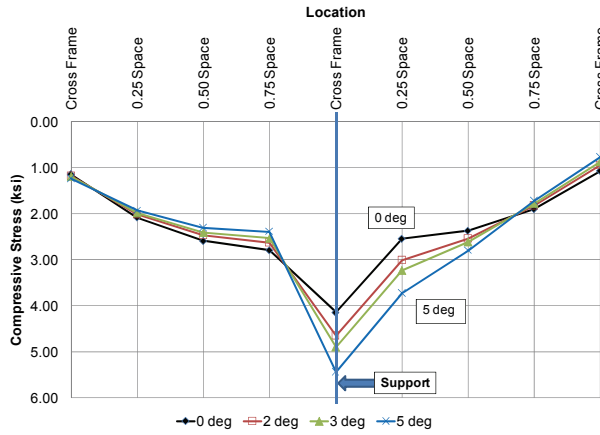


a) Outer-Edge Bottom Flange

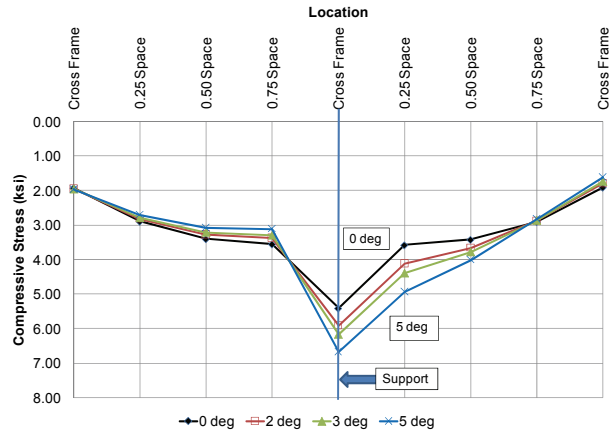


b) Inner-Edge Top Flange

Figure C.89 G2 Flange Tip Stresses at 0.4L of End Span

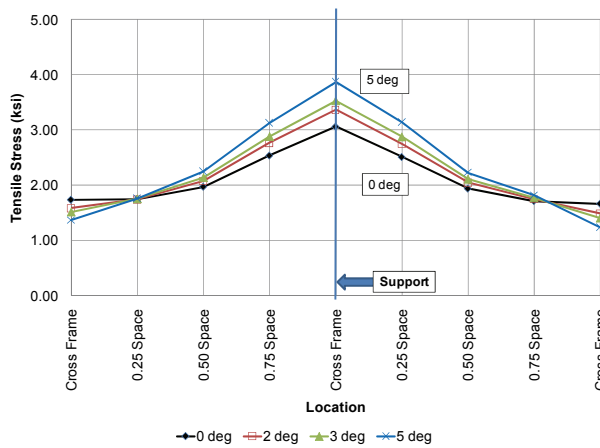


a) Girder G1

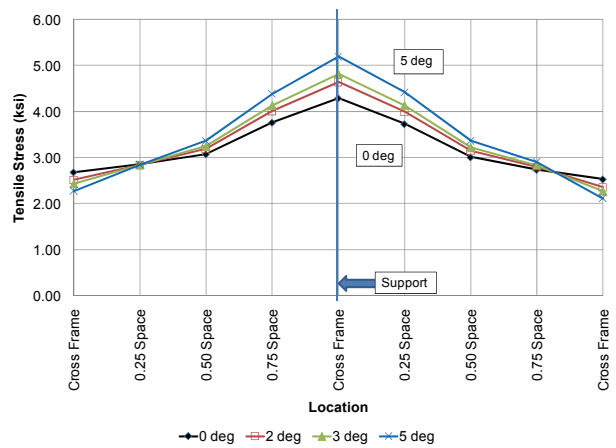


b) Girder G2

Figure C.90 Inner-Edge Bottom Flange Tip Stresses at 0.0L of Center Span



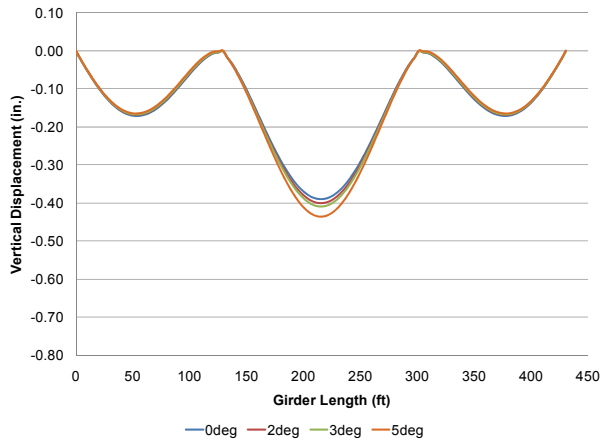
a) Girder G1



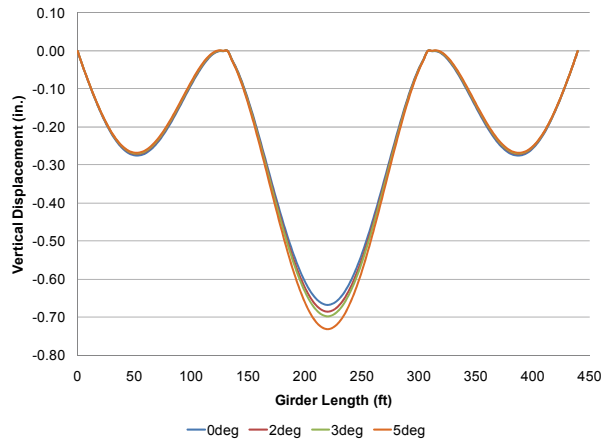
b) Girder G2

Figure C.91 Outer-Edge Top Flange Tip Stresses at 0.0L of Center Span

### C.4.8 Girder Displacements (Web Depth = 96 in.)

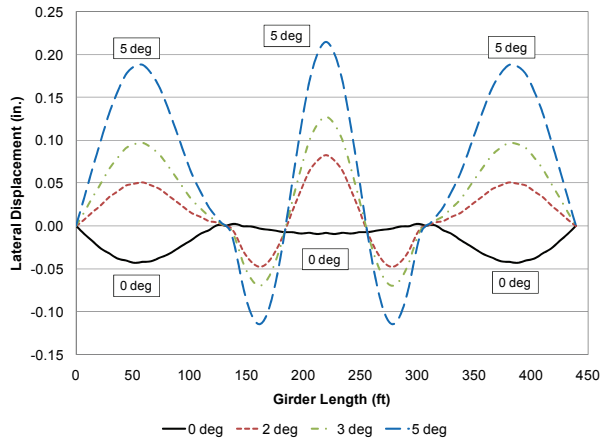


a) Girder G1

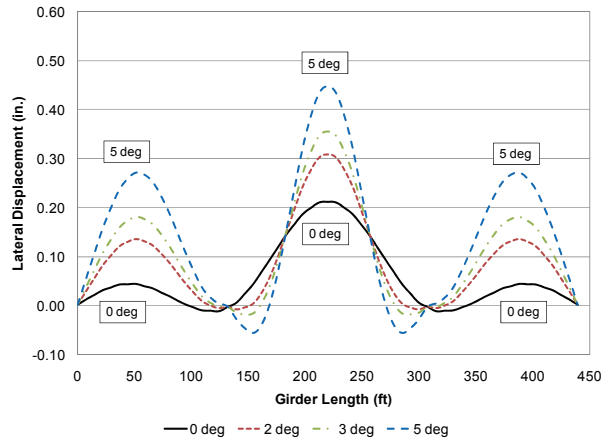


b) Girder G2

Figure C.92 Top Flange Vertical Displacement



a) Bottom Flange



b) Top Flange

Figure C.93 G2 Flange Lateral Displacement

## **APPENDIX D**

### **FINITE ELEMENT MODELING TERMINOLOGY**

#### **D.1 ABAQUS FINITE ELEMENT PROGRAM**

##### **D.1.1 S4R Shell Element**

The finite element models that employ the finite element program ABAQUS, use the S4R shell element to model the girder flanges and webs, and the transverse stiffeners and cross frame connection plates when applicable. The S4R shell element is defined by ABAQUS (2003) as “a 4-node, doubly curved general purpose shell with reduced integration, hourglass control, and finite member strains.” Earls and Shah (2002) considered both the S4R and S9R5 shell elements from the ABAQUS library in their verification work, in which bridge-sized girders were modeled. The verification showed that the S4R element showed better agreement with experimental work used in the verification study by Earls and Shah (2002 ). Given this agreement, and the agreement shown in section 4.1.1 and 4.2.1 of this dissertation, the S4R element is chosen for this current research work.

The S4R element uses thick shell theory as the shell thickness increases and become Kirchhoff thin shell elements as the thickness decreases; the transverse shear deformation

becomes very small as the shell thickness decreases. The S4R is suitable for large-strain analysis involving materials with a nonzero effective Poisson's ratio. The degrees of freedom for a shell element are the displacements and rotations at each node. The active S4R shell element (shown in Figure D.1) degrees of freedom are: 1, 2, 3, 4, 5, 6 ( $u_x, u_y, u_z, \phi_x, \phi_y, \phi_z$ ).

The S4R shell element uses reduced integration to form the element stiffness. In reduced integration techniques, the order of in-plane integration is one integration order less than which would require performing the stiffness matrix exactly. Reduced integration usually provides results that are more accurate and significantly reduces running time, especially in three dimensions, provided the elements are not distorted or loaded in in-plane bending (ABAQUS 2003). The S4R shell element is computationally inexpensive since the integration is performed at one Gauss point per element.

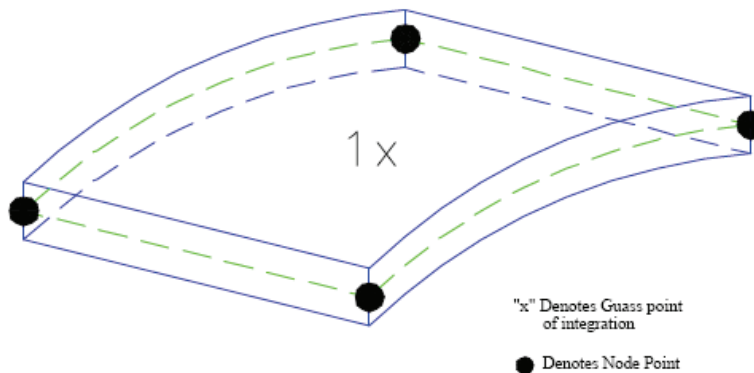


**Figure D.1** S4R Shell Element: 4-Nodes, Reduced Integration (ABAQUS 2003)

## D.2 ADINA FINITE ELEMENT PROGRAM

### D.2.1 MITC-4 Shell Element

The shell elements used in the finite element models that employ the finite element program ADINA are four node ADINA MITC-4 nonlinear shell finite elements. The MITC-4 shell element (shown in Figure D.2) is used to model girder webs and flanges. ADINA automatically assigns five degrees of freedom to each node of the MITC-4, unless loading or mesh compatibility requires six degrees of freedom (ADINA 2003). The elimination of the rotational degree of freedom about the axis normal to the shell surface helps to maintain efficiency with regard to computational time. However, at element intersections, such as web-flange junctions or cross frame connection locations, all six degrees of freedom are utilized.

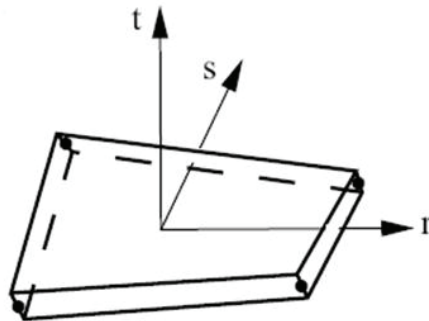


**Figure D.2** General MITC-4 Shell Element (ADINA 2003)

The most effective element for analysis of general shells is the MITC-4 shell element. This element does not lock and has a high predictive capability and hence can be used for effective analysis of thin and thick shells (ADINA 2003). Additional information can be found in Dvorkin and Bathe (1984).

The MITC-4 shell element is an attractive four-node element for which the in-layer strains are computed from the displacement interpolations and the covariant transverse shear strain components are interpolated and tied to the displacement interpolations; since the element is not curved and membrane locking is not present in the displacement-based element (Bathe 1996). The MITC-4 shell element performs quite well in out-of-plane bending, such as plate bending (Bathe 1996). An in-depth treatment regarding the basic formulation of the MITC-4 shell element can be found in sections 5.4.2 and 6.5.2 of Bathe (1996).

## BIBLIOGRAPHY

- ABAQUS, (2003), ABAQUS Standard User's Manual, Version 6.2, Volumes 1 to 3, Hibbit, Karlsson & Sorensen, Inc., Pawtucket, Rhode Island, USA.
- ADINA, (2003), Theory and Modeling Guide, Volume I: ADINA, *Report ARD 03-7*, ADINA Research and Development, Inc., Watertown, MA.
- American Association of State Highway and Transportation Officials (AASHTO), (1993), *Guide Specifications for Horizontally Curved Highway Bridges*, Washington, D.C.
- American Association of State Highway and Transportation Officials (AASHTO), (2003), *Guide Specifications for Horizontally Curved Steel Girder Highway Bridges*, Washington, D.C.
- American Association of State Highway and Transportation Officials (AASHTO), (2006), *Load and Resistance Factor Design (LRFD) Bridge Specifications, 3<sup>rd</sup> Edition*, Washington, D.C.
- Bathe, K.J., (1996), *Finite Element Procedures*, Prentice-Hall, Inc., Upper Saddle River, New Jersey.
- Beckmann, F.R and Mertz, D.R., (2005), *National Cooperative Highway Research Program Synthesis Report 345: Steel Bridge Erection Practices*, Transportation Research Board, Washington, D.C.
- Bell, B.J., and Linzell, D.G. (2007), "Erection Procedure Effects in Deformations and Stresses in a Large-Radius, Horizontally Curved, I-Girder Bridge," *Journal of Bridge Engineering*, ASCE, Vol. 12, No. 4, July, pp. 467-476.
- Brennan, P.J., Antoni, C.M., Leininger, R. and Mandel, J.A., (1970), "Analysis for Stress and Deformation of a Horizontally Curved Girder Bridge Through a Geometric Structural Model," Research Report Submitted to the New York State Department of Transportation, Engineering Research and Development Bureau, Department of Civil Engineering, Syracuse University, August.
- Chavel, B.W. (2001), "Evaluation of Erection Procedures of the Horizontally Curved Steel I-girder Ford City Bridge," Thesis in Civil Engineering, University of Pittsburgh, Pittsburgh, Pennsylvania.

- Chavel B.W., Earls, C.J., (2004), "Deflection of Horizontally Curved I-Girder Bridge Members Under Construction," Report No. CE/ST 28, Department of Civil Engineering, University of Pittsburgh, Pittsburgh, Pennsylvania.
- Chavel, B.W., and Earls, C.J. (2006a), "Construction of a Horizontally Curved Steel I-Girder Bridge: Erection Sequence," *Journal of Bridge Engineering*, ASCE, Vol. 11, No. 1, January, pp. 81-90.
- Chavel, B.W., and Earls, C.J. (2006b), "Construction of a Horizontally Curved Steel I-Girder Bridge: Inconsistent Detailing," *Journal of Bridge Engineering*, ASCE, Vol. 11, No. 1, January, pp. 91-98.
- Coletti, D. and Yadlosky, J.M., (2005), "Behavior and Analysis of Curved and Skewed Steel Girder Bridges," NSBA, World Steel Bridge Symposium, Orlando, Fla.
- CURT, (1975), "Tentative Design Specifications for Horizontally Curved Highway Bridges, Parts I and II," Consortium of University Research Teams, March.
- Duwadi, S.R., Grubb, M.A., Yoo, C.H., and Hartmann, J., (2000), "Federal Highway Administration's Horizontally Curved Steel Bridge Research Project: An Update," *Transportation Research Record 1696, Vol. 1*, Transportation Research Board, National Research Council, Washington, D.C, pp. 152-161.
- Dvorkin, E. and Bathe, K.J., (1984), "A Continuum Mechanics Based Four-Node Shell Element for General Nonlinear Analysis," *Engineering Computations*, Vol. 1, pp. 77-88.
- Earls, C.J. and Shah, B.J., (2002), "High Performance Steel Bridge Girder Compactness," *Journal of Constructional Steel Research*, Volume 58, Issues 5-8, pp 859-880.
- Galambos, T.V., (1978), "Tentative Load Factor Design Criteria for Curved Steel Bridges, Research Report No. 50," Department of Civil Engineering, Washington University, St. Louis, Missouri.
- Galambos, T.V., Hajjar, J.F., Leon, R.T., Huang, W.-H., Pulver, B.E., and Rudie, B.J., (1996), "Stresses in a Steel Curved Girder Bridge," Report No. MN/RC-96/28, Minnesota Department of Transportation, St. Paul, Minnesota.
- Hall, D. H., (1996), "Curved Girders are Special," *Engineering Structures*, Elsevier Science Ltd., Vol. 18, No. 10, pp. 769-777.
- Hall, D.H., Grubb, M.A., Yoo, C.H. (1999), *National Cooperative Highway Research Program Report 424: Improved Design Specifications for Horizontally Curved Steel Girder Highway Bridges*, Transportation Research Board, Washington, D.C.
- Howell, T.D., (2006), "On the Influence of Web Out of Plumbness on Horizontally Curved Steel I-Girder Bridge Serviceability During Construction," Thesis in Civil Engineering, University of Pittsburgh, Pittsburgh, Pennsylvania.

- Howell, T.D., and Earls, C.J., (2007), "Curved Steel I-Girder Bridge Response During Construction Loading: Effects of Web Plumbness," *Journal of Bridge Engineering*, ASCE, Vol. 12, No. 4, July, pp. 485-493.
- Linzell, D.G., (1999), "Studies of Full-Scale Horizontally Curved Steel I-Girder Bridge Systems Under Self Weight," Ph.D. Dissertation, School of Civil and Environmental Engineering, Georgia Institute of Technology.
- McManus, P.F., (1971), "Lateral Buckling of Curved Plate Girders," Ph.D. Dissertation, Department of Civil Engineering, Carnegie Mellon University.
- Morcos, S. (1998). "Moment-Rotation Tests of Steel Bridge Girders for Autostress Design." MS Thesis, Dept. of Civil and Environmental Engineering, University of Pittsburgh, Pittsburgh, Pennsylvania.
- Mozer, J. and Culver, C., (1970), "Horizontally Curved Highway Bridges – Stability of Curved Plate Girders, Report No. P1," Report Submitted to the Department of Transportation, Federal Highway Administration, Department of Civil Engineering, Carnegie-Mellon University, Pittsburgh, Pennsylvania.
- Mozer, J., Ohlson, R., and Culver, C., (1971), "Horizontally Curved Highway Bridges – Stability of Curved Plate Girders, Report No. P2," Report Submitted to the Department of Transportation, Federal Highway Administration, Department of Civil Engineering, Carnegie-Mellon University, Pittsburgh, Pennsylvania.
- Mozer, J., Cook, J., and Culver, C., (1973), "Horizontally Curved Highway Bridges – Stability of Curved Plate Girders, Report No. P3," Report Submitted to the Department of Transportation, Federal Highway Administration, Department of Civil Engineering, Carnegie-Mellon University, Pittsburgh, Pennsylvania.
- Poellot, W. N., (1987), "Computer-aided Design of Horizontally Curved Girders by V-load Method," *Engineering Journal*, AISC, 1st Quarter, pp. 42-50.
- Schelling, D., Namini, A., Fu, C.C., (1989), "Construction Effects on Bracing on Curved I-Girders," *Journal of Structural Engineering*, ASCE, Vol. 115, No. 9, September, pp. 2145-2165.
- Shanmugam, N.E., Thevendran, V., Richard Liew, J.Y., and Tan, L.O. (1995). "Experimental Study on Steel Beams Curved in Plan." *Journal of Structural Engineering*, Vol. 121, No. 2.
- Stegmann, T.H., (1975), "Load Factor Design Criteria for Curved Steel Girders," M.S. Thesis, Washington University, St. Louis, Missouri.
- Zureick, A., Naqib, R., and Yadlosky, J.M., (1994), "Curved Steel Bridge Research Project, Interim Report I: Synthesis," FHWA-RD-93-129, Federal Highway Administration, U.S. Department of Transportation, December.